



INDIAN AGRICULTURAL
RESEARCH INSTITUTE, NEW DELHI.

L. A. R. I. 6.

MGIPC—S1—6 AR/54—7.7.54—10,000.

The Journal of PHYSICAL CHEMISTRY

(Founded by Wilder D. Bancroft)

Editor

S. C. LIND

Associate Editors

E. J. BOWEN

J. G. KIRKWOOD

G. O. BURR

W. ALBERT NOYES, JR.

C. N. HINSHELWOOD

J. R. PARTINGTON

T. F. YOUNG

Assistant Editor

LOUISE KELLEY

Volume 48

BALTIMORE

1944

CONTENTS

NUMBER 1, JANUARY, 1944

Electrokinetics. XXVI. The Electroviscous Effect. III. In β -Lactoglobulin Systems. An Interpretation of the Meaning of $K\phi$ Values Obtained from Electroviscosity Data. D. R. Briggs and Martin Hanig.	1
The Structure of an Egg Albumin-Detergent Complex. K. J. Palmer.	12
On Some Compounds of Iron Deposited on Both Poles Simultaneously. George Antonoff.	21
The Variation of the Viscosity of Gases and Vapors with Temperature. William Licht, Jr., and Dietrich G. Stechert	23
The Vapor Pressure and Heat of Vaporization of Trichloroethylene. Hugh J. McDonald.	47
The Lewis and the Brønsted-Lowry Definitions of Acids and Bases. I. M. Kolthoff.	51
Minima in Surface Tension-Concentration Curves of Solutions of Sodium Alcohol Sulfates. Gilbert D. Miles and Leo Shedlovsky.	57
Discussion and Interpretation of the Migration Data of Laurysulfonic Acid in Aqueous Solution. Pierre Van Rysselberghe	62
New Books:	
War Gases: Their Identification and Decontamination. By Morris B. Jacobs. Reviewed by E. B. Sandell	66
Encyclopedia of Substitutes and Synthetics. Edited by Morris D. Schoengold. Reviewed by Lee Irvin Smith	66

NUMBER 2, MARCH, 1944

The Uses and Limitations of Membrane Electrodes. C. E. Marshall	67
Note on Antonoff's So-called Rule. H. L. Cupples	75
The Mixture Law for Viscosity. F. Kottler	76
Densities of Liquids and their Temperature Changes. George Antonoff	80
The Solid-Liquid Phase Equilibria of the System <i>p</i> -Toluidine-Acetic Acid. Walter W. Lucasse, Robert P. Koob, and John G. Miller	85
Absorption of Light in Soap Solutions. M. E. Laing McBain	89
Communication to the Editor: On the Definition of a Crystal. George Antonoff	95
New Books:	
Advances in Enzymology and Related Subjects of Biochemistry, Vol. III. Edited by F. F. Nord and C. H. Werkman. Reviewed by Erwin Haas	96
Volumetric Analysis. By I. M. Kolthoff and V. A. Stenger. Reviewed by Hobart H. Willard	97
Textbook of Quantitative Inorganic Analysis. By I. M. Kolthoff and E. B. Sandell. Reviewed by C. H. Shiflett	98
Metallography of Aluminum Alloys. By Lucio F. Mondolfo. Reviewed by F. Keller	98
Papers Presented at the Second Conference on the Corrosion of Metals. Reviewed by S. C. Lind	99
The "Particles" of Modern Physics. By J. D. Stranathan. Reviewed by S. C. Lind	99
Physical Biochemistry. By Henry B. Bull. Reviewed by W. M. Sandstrom	100

NUMBER 3, MAY, 1944

Relative Free Energies and Dissociation Constants of Microscopic Ions. Terrell L. Hill.	101
An Application of the Method of Continuous Variations to Complex-Ion Formation in Copper (II) Salt Solutions Containing Chloride Ion. Therald Moeller.	111

Contact Angles and Adsorption on Solid Surfaces. H. K. Livingston.....	120
A Study of the Colloidal System Carbon Dispersed in Xylene. V. R. Damerell and A. Urbanic.	125
Effect of Surface-active Agents upon Dispersions of Calcium Carbonate in Xylene. Vivian Richard Damerell and Raymond Mattson.	134
Foam Formation in Organic Liquids. E. Gray King	141
A Method of Growing Single Crystals of Sodium Stearate and Sodium Palmitate. A. de Bretteville, Jr., and F. V. Ryer.	154
On Harkins' "Final Spreading Coefficient" and Antonoff's Rule. William Fox.	158
Communication to the Editor: Note on the Interpretation of Distribution Equilibria between Molten Metals and Molten Salts. E. Heymann, R. J. L. Martin, and M. F. R. Mulcahy.	159

New Books:

Electrophoresis of Proteins and the Chemistry of Cell Surfaces. By Harold A. Abramson, Laurence S. Moyer, and Manuel H. Gorin. Reviewed by George W. Schwert, Jr., and L. Earle Arnow.	161
Methoden der mathematischen Physik. By R. Courant and D. Hilbert. Reviewed by E. L. Hill	162
Luminescence of Liquids and Solids and its Practical Applications. By Peter Pringsheim and Marcel Vogel. Reviewed by S. C. Lind.	163

NUMBER 4, JULY, 1944

The Relative Viscosity of Aqueous Solutions of Sulfamic Acid and of Some of its Salts at 25°C. A. F. Schmelzle and J. E. Westfall.	165
The Measurement of Boundary Tension by the Pendent-drop Method. II. Hydrocarbons. Grant W. Smith	168
On the Separation of Oil from the Surface of Water. George Antonoff	173
The System Magnesium Selenate-Selenic Acid-Water at 30°C. H. Furukawa and G. Brooks King.	174
Adsorption Analysis of Colorless Compounds: Method and Application to the Resolution of Stearic and Oleic Acids. Herbert J. Dutton.	179
Protective Colloids in Cancer. L. A. Munro	187
Cluster Formation and Phase Transitions in the Adsorbed State. Hans M. Cassel.	195
The Physical Chemistry of Flotation. X. The Separation of Ergot from Rye. Enid C. Plante and K. L. Sutherland.	203
The Kinetics of the Reaction between Silver Perchlorate and Methyl Iodide. M. F. Redies and T. Iredale	224

New Books:

Abridged Scientific Publications from the Kodak Research Laboratories. Volume XXIV. Reviewed by S. C. Lind.	231
Chemical Engineering. By Charles E. Reed. Reviewed by Charles A. Mann	231
The Physical Chemistry of Electrolytic Solutions. By Herbert S. Harned and Benton B. Owen. Reviewed by F. H. MacDougall.	231
Chemical Process Principles. Part One: Material and Energy Balances. By Olaf A. Hougen and Kenneth M. Watson. Reviewed by F. H. MacDougall	232
Synthetic Resins and Rubbers. By Paul O. Powers. Reviewed by Charles F. Fryling.	232
Principles and Applications of Electrochemistry. Volume I. Principles. By H. Germain Creighton. Volume II. Applications. By W. A. Koehler. Reviewed by I. M. Kolthoff.	233
Magnetochemistry. By P. W. Selwood. Reviewed by J. H. Van Vleck.	234

NUMBER 5, SEPTEMBER, 1944

Diffusion of the Lower Alkyl Sulfonic Acids and Some Large Molecules. M. E. Laing McBain.	237
--	-----

The Ternary System <i>n</i> -Butyl Alcohol-Benzene-Water at 25°C. and 35°C. E. Roger Washburn and Carl V. Strandkov..	241
Particle-size Distributions by Centrifugal Sedimentation. Callaway Brown	246
The Electrochemistry of Baths of Fused Aluminum Halides. III. Bromide Baths. Ralph Wehrmann and L. F. Yntema	259
The Electrochemistry of Baths of Fused Aluminum Halides. IV. Ralph G. Verdieck and L. F. Yntema.	268
Foam Stability of Solutions of Soaps of Pure Fatty Acids. Gilbert D. Miles and John Ross	280
The Catalytic Oxidation of Ethylene to Ethylene Oxide. L. H. Reyerson and Hans Oppenheimer.....	290
The Relation between the Force Constant and the Interatomic Distance of a Diatomic Linkage. C. K. Wu and (in part) Chang-Tsing Yang	295
The Magnesium Tungstate Phosphor. Gorton R. Fonda ..	303
New Books:	
A Text-Book of Inorganic Chemistry. By F. Ephraim. Fourth English edition by P. C. L. Thorne and E. R. Roberts. Reviewed by J. R. Partington	307
Lange's Handbook of Chemistry. Norbert Adolph Lange, <i>Editor</i> . Reviewed by H. H. Barber and H. F. Scobie	308
The Total and Free Energies of Formation of the Oxides of Thirty-two Metals. By Maurice deKay Thompson. Reviewed by Merle Randall ..	309
Natural and Synthetic Fibers. Edited by Milton Harris and H. Mack. Reviewed by L. H. Reyerson	309

NUMBER 6, NOVEMBER, 1944

The Quaternary System $\text{CaO-Al}_2\text{O}_3\text{-CaSO}_4\text{-H}_2\text{O}$ at 25°C. Equilibria with Crystalline $\text{Al}_2\text{O}_3\cdot 3\text{H}_2\text{O}$, Alumina Gel, and Solid Solution. F. E. Jones	311
The Quinary System $\text{CaO-Al}_2\text{O}_3\text{-CaSO}_4\text{-K}_2\text{O-H}_2\text{O}$ (1 per cent KOH) at 25°C. F. E. Jones	356
The Quinary System $\text{CaO-Al}_2\text{O}_3\text{-CaSO}_4\text{-Na}_2\text{O-H}_2\text{O}$ (1 per cent NaOH) at 25°C. F. E. Jones..	379
Observations on the Rare Earths. LI. An Electrometric Study of the Precipitation of Trivalent Hydrrous Rare Earth Oxides or Hydroxides. Therald Moeller and Howard E. Kremers	395
Cation Exchange at High pH. Raymond Nelson and Harold F. Walton.	406
Viscosity and Rigidity of Structural Suspensions. Paul S. Roller and C. Kerby Stoddard	410
Communication to the Editor: On the Definition of a Crystal. A. C. Shuman	425
New Books:	
Plant Viruses and Virus Diseases. By F. C. Bawden. Reviewed by Claude H. Hills	426
Systematic Inorganic Chemistry of the Fifth- and Sixth-Group Nonmetallic Elements. By Don M. Yost and Horace Russell, Jr. Reviewed by F. H. MacDougall.	426
Infrared Spectroscopy: Industrial Applications and Bibliography. By R. B. Barnes, R. C. Gore, U. Liddell, and V. Z. Williams. Reviewed by Bryce L. Crawford, Jr.	428

ELECTROKINETICS. XXVI

THE ELECTROVISCOUS EFFECT. III. IN β -LACTOGLOBULIN SYSTEMS. AN INTERPRETATION OF THE MEANING OF $K\phi$ VALUES OBTAINED FROM ELECTROVISCOSITY DATA¹

D. R. BRIGGS AND MARTIN HANIG

Division of Agricultural Biochemistry, University of Minnesota, St. Paul, Minnesota

Received October 23, 1943

Krasny-Ergen (3), following an earlier treatment of the subject by Smoluchowski (8), has derived an equation which is designed, from a theoretical treatment, to describe the electroviscosity phenomena observed in solutions of colloid electrolytes.

Experimental studies of the electroviscosity effect in aqueous systems containing the colloid electrolytes gum arabic (1) and casein (2) with which this equation was tested quantitatively have indicated that it does not accurately describe the effect, although certain factors of the experimental data do agree, apparently, with the theory as treated by Krasny-Ergen.

When the Smoluchowski-Krasny-Ergen equation is written in a linear form, i.e.,

$$\frac{1}{\eta_{sp}} = \frac{1}{K\phi} - \frac{3\epsilon^2}{8\pi^2 r^2} \cdot \frac{\zeta^2}{\lambda(\eta_s - \eta_0)}$$

where η_s = viscosity of the colloid electrolyte solution,

η_{sp} = specific viscosity of the colloid electrolyte solution,

η_0 = viscosity of the solvent,

λ = specific conductivity of the colloid electrolyte solution,

ζ = electrokinetic potential at the colloid-solvent interface,

ϵ = dielectric constant,

r = radius of the colloid micelle,

ϕ = viscometrically effective percentage volume occupied by the colloid, and

K = a constant dependent on the shape of the micelle (= 2.5 for spherical particles)

and the equation is tested by measuring η_s , ζ , and λ for the solutions of purified colloid (i.e., free of foreign electrolyte) with and without the addition of small quantities of electrolyte, it is found that, for a wide variety of colloid systems, the data give straight-line relationships between $1/\eta_{sp}$ and $\zeta^2/\lambda(\eta_s - \eta_0)$, as is required by the equation. However, the slopes of the lines obtained vary with the concentration of the dispersed phase in such a way that slope/ C is approximately constant and with no readily apparent relationship to the radius of the

¹ Paper No. 2116, Scientific Journal Series, Minnesota Agricultural Experiment Station.

particle, neither of which observations is in accord with the Krasny-Ergen equation. On the other hand, the values of $K\phi$, as obtained from intercept values on the $1/\eta_{sp}$ axis, are always such that $K\phi/C$ is a constant (where C is equal to the concentration of the colloid electrolyte), thereby indicating that these systems of colloid electrolytes, when the ζ -potential is suppressed to zero and the electroviscous effect is thus eliminated, follow the Einstein equation with regard to viscosity changes with concentration of the dispersed phase, i.e., at zero ζ -potential,

$$\eta_{sp} = K\phi \quad \text{and} \quad \frac{\eta_{sp}}{C} \quad \text{is a constant.}$$

Thus, without attempting to account for the failure of the equation to describe the electroviscous effect entirely, it can be said that the $K\phi$ values obtained by use of the equation (by extrapolation of the straight line obtained, as described, to zero electroviscous effect) agree with the Einstein relationships, as is required by the theory.

If we define ϕ in terms of concentration of colloid in grams per 100 cc. of solution (C), the partial specific volume of the colloid in solution (V), and a solvation factor (h) for the colloid as it exists in solution, then

$$\phi = \frac{hCV}{100}$$

The factor h , then, is definable as the ratio of the viscometrically effective volume of the dispersed phase (i.e., 100ϕ) to the volume calculated as occupied by this phase on the assumption of no solvation (i.e., CV).

On the basis of the experimental findings we can write the electroviscosity equation as follows:

$$\frac{1}{\eta_{sp}} = \frac{100}{KhCV} - AC \cdot \frac{m^2}{\lambda(\eta_s - \eta_0)}$$

where m is the electrophoretic mobility of the colloid and A is a factor which is approximately constant for a given colloid but varies from one system to another and which, as yet, cannot be identified in terms of other recognized and measurable factors in the systems. The other terms are as above defined. Since the values of A obtained from the slope do not, as yet, allow for any interpretation in terms of radius of the particle, it seems logical to eliminate the conversion of ζ , λ , and $(\eta_s - \eta_0)$ into E.S.U. and to report these values in terms of the actually measured units, i.e., m in $\text{cm}^2 \text{ sec}^{-1} \text{ volt}^{-1}$, λ in reciprocal ohms, and viscosity in poises. The above equation, then, is one describing the experimental findings with regard to the electroviscosity effect.

Table 1 gives values of $K\phi/C$, V , Kh , h (assuming that K is equal to 2.5), and A for several colloids with which the electroviscous effect has been studied in this manner.

From table 1 it is apparent that the values of $K\phi/C$ vary over wide limits for the various colloid electrolytes while remaining constant for a given system.

Simply changing the kind of gegenion to one of different valence (e.g., sodium *vs.* calcium) causes a change in $K\phi/C$ for certain of the colloid electrolytes. Qualitatively it has been found that, for such colloid electrolytes (e.g., casein or gum arabic), a change in the number (or activity) of the gegenions, such as will accompany a change in the pH of the system, will shift the values of $K\phi/C$ to new values. In such cases, an increase in the number of gegenions will result in an increase in the value of $K\phi/C$, and a decrease in the number of gegenions will result in a decrease in $K\phi/C$. Other colloid electrolytes (e.g., serum albumin and, as will be shown later, β -lactoglobulin) give values of $K\phi/C$ which are essentially independent of the pH of the solution (and thus independent of

TABLE 1
Electroviscosity data on aqueous sols of various colloid electrolytes

COLLOID ELECTROLYTE	pH	$K\phi/C$	V^*	Kh	$h (K = 2.5)$	$\frac{\lambda - \lambda'}{C.C. \text{ SOLVENT} - G. \text{ SOLUTE}}$	$\frac{A}{1 \text{ per cent sols}}$
Gum arabic, sodium salt ...	7.0	0.314	0.65	48.0	19.3	11.8	121 (25°C.)
Gum arabic, calcium salt	7.0	0.171	0.65	26.0	10.5	6.1	58 (25°C.)
Casein, sodium salt	6.6	0.208	0.75	28.0	11.2	7.6	37 (30°C.)
Casein, calcium salt	6.6	0.078	0.75	10.4	4.2	2.4	68 (30°C.)
Alginate, sodium salt	7.0	1.05	0.65	162	65	41	43 (25°C.)
Cow serum albumin, sodium salt	7.0	0.042	0.75	5.6	2.2	0.9	36 (25°C.)
Cow serum albumin, chloride salt	4.0	0.045	0.75	6.0	2.4	1.0	34 (25°C.)

* Values of V , the partial specific volume of the colloid electrolyte in solution, for the proteins are taken as 0.75 for casein and cow serum albumin because this approximates the commonly found values for the many proteins upon which V has been determined. The value of $V = 0.65$ is the experimentally determined value for sodium gum arabate, and it is assumed that the values for the other carbohydrate colloids are the same.

the number of gegenions present per unit of protein) and, presumably, which are independent of the kind of gegenions which are present.

Since the $K\phi$ value is a function of the volume occupied by the dispersed phase and/or the shape of the particles making up this phase, it is to be inferred that there exist two distinct types of colloidal electrolytes, for one of which the viscometrically effective volume, ϕ , and/or the shape of the particle (of which K is a function) is changed reversibly with change in number or kind of gegenions present (e.g. gum arabic), while for the other the shape and size of the particle is not varied by kind or number of its gegenions (e.g., crystallizable proteins).

This conclusion is dependent upon the assumption that the $K\phi$ values obtained by the described electroviscosity studies are reliable.

The question arises, then, whether or not the values of $K\phi$ (or Kh) obtained in this manner have in reality their usual physical significance. For example, the value of Kh obtained (see table 1) for sodium gum arabate would require,

if the particles are rigidly spherical, that the colloid must be swollen to nineteen times its unhydrated specific volume, thus incorporating within the swollen particle about twelve times its dry weight of solvent, or that the particle must be very asymmetric in solution. While it is, admittedly, not possible to choose definitely between these two possibilities, in this or in any other case, it is possible to learn whether or not the values of $K\phi$ (or Kh) obtained by this method will agree with such values obtained by other means. In order to make this comparison, it is necessary to obtain the $K\phi$ values by electroviscosity studies on a material whose frictional ratio has been measured by other methods and where good agreement has been obtained by several methods.

Measurements of the frictional ratios of many crystallizable proteins in aqueous solutions have repeatedly indicated that molecules of these substances may be regarded either as compact particles possessing a spherical shape with a small degree of hydration or as non-hydrated particles having a small degree of asymmetry. Also, within a certain pH range on either side of the isoelectric point (i.e., the so-called stability range of the protein) the protein molecules retain the same shape and size, since their frictional ratios are found to remain constant within this pH range.

Ultracentrifuge, diffusion, and viscosity measurements, from which the frictional ratios have been calculated, have been conducted under circumstances (i.e., at higher ionic strengths of their solutions) in which the Donnan effect is reduced to a minimum. Electroviscosity, under these conditions, can be considered as reduced also to a minimum.

If the values of $K\phi$ (or Kh) obtained for such colloid electrolytes by use of the electroviscosity method agree with those obtained from frictional ratios obtained by these other methods, then it should be reasonable to say that the $K\phi$ (or Kh) values obtained for the other colloid systems by the electroviscosity method (and for which systems frictional ratios by the other methods are not available) would be as significant for these systems as are those for the proteins upon which other methods have given agreement.

The β -lactoglobulin of Palmer (5) is a protein with which a great deal of work has been done which has indicated that it is a monodisperse, electrophoretically homogeneous material. The frictional ratios obtained by sedimentation and diffusion and by viscosity and diffusion studies (4, 6, 9) (in salt solutions) agree well. It is also one of the few proteins which crystallize at very low salt concentrations and seemed, therefore, particularly adaptable to electroviscosity studies where very low original salt concentrations are required in the solutions of the colloids to be studied. β -Lactoglobulin, therefore, was chosen as the protein upon which the value of $K\phi$ obtained by electroviscosity methods was to be compared with those obtained by the other methods.

EXPERIMENTAL

Crystalline β -lactoglobulin was prepared by a modification of the method of Palmer (5) and twice recrystallized. Since this protein crystallizes after long dialysis against distilled water and at its isoelectric point (pH = 5.18), the for-

eign electrolyte concentration of the protein preparation was always so low that electrodialysis was unnecessary preliminary to its use in the electroviscosity studies.

The electroviscous properties of this protein were studied at two pH values (one on the acid and the other on the alkaline side of its isoelectric point) and at varying protein concentrations for each pH. For each of these conditions, solutions were prepared which contained, besides the protein, quantities of

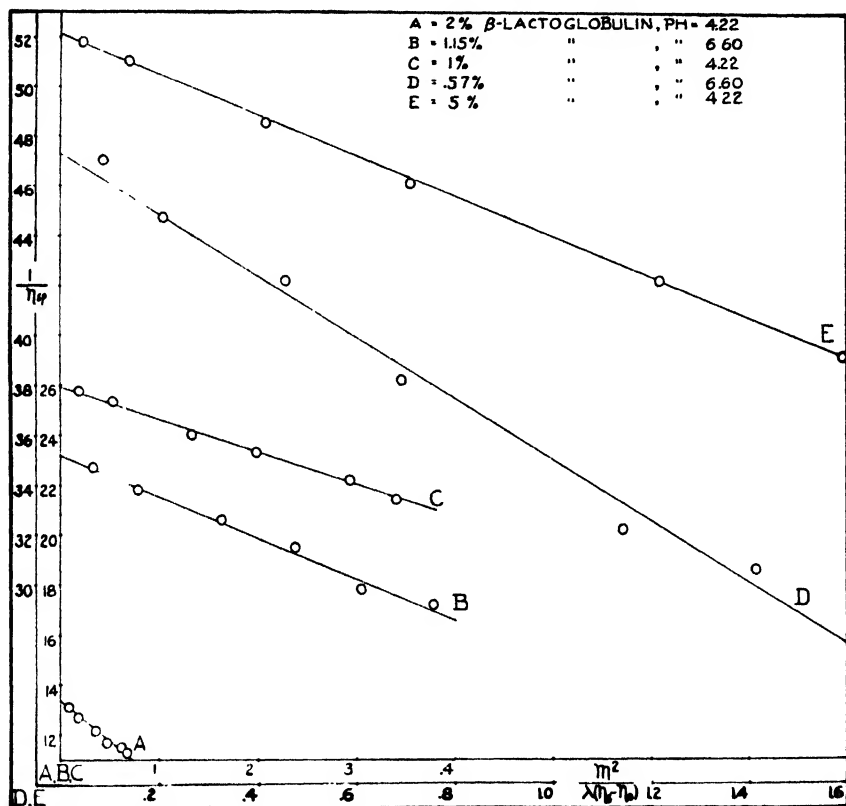


FIG 1. Showing the relationship between $1/\eta_{sp}$ and $m^2/\lambda(\eta_s - \eta_0)$ at various sodium chloride contents for two concentrations of β -lactoglobulin at pH 6.60 and three concentrations of β -lactoglobulin at pH 4.22

sodium chloride varying stepwise from zero amount of added sodium chloride to solutions 0.01 *N* in sodium chloride. The alkaline series was prepared in such a way as to bring the final pH of the solutions to the value 6.60 ± 0.05 and the protein concentrations to 0.57 and 1.15 g. of protein per 100 cc. of solution. The acid series was at pH = 4.22 ± 0.05 and the protein concentrations were 0.5, 1.0, and 2.0 g. of protein per 100 cc. of solution.

On each of these solutions, varying as to pH, protein concentration, and sodium chloride concentration, measurements of viscosity, specific electrical conduc-

tivity, and electrophoretic mobility of the protein were made. Viscosity measurements were made using an Ostwald viscometer which, when charged with 13.0 cc. of water, gave an outflow time at 25.0°C. of 290.1 sec. (approximately 10 cc. flowing). Specific conductivity measurements were made with a standard 1000-cycle A.C. Wheatstone bridge arrangement at 25.0°C. The electrophoretic mobility of the protein was determined in each case by means of the

TABLE 2a

Conductivity, viscosity, and mobility data at 25°C. on solutions of acid β -lactoglobulin ($pH = 4.22 \pm 0.05$) at three concentrations of the protein, without and with the addition of varying quantities of sodium chloride

NaCl	η_{sp}	$\eta_s - \eta_0$	λ	m	$\frac{m^2}{\lambda(\eta_s - \eta_0)}$	$\frac{1}{\eta_{sp}}$
0.5 per cent protein solution						
moles per 1000 cc.	poises	poises	mhos $\times 10^4$	$\left(\frac{cm.^2}{v. sec.} \times 10^4\right)$		
0	0.0256	0.00022 ^s	1.242	2.12	1.59	39.1
0.0005	0.0237	0.00021 ¹	1.466	1.94	1.21	42.2
0.001	0.0217	0.00019 ⁴	2.415	1.82	0.71	46.1
0.002	0.0206	0.00018 ⁴	3.500	1.63	0.41	48.5
0.005	0.0196	0.00017 ^s	6.965	1.30	0.14	51.0
0.010	0.0193	0.00017 ²	12.650	1.01	0.05	51.8
1.0 per cent protein solution						
0	0.0468	0.00041 ^s	2.160	1.75	0.339	21.4
0.0005	0.0451	0.00040 ^s	2.371	1.67	0.292	22.2
0.001	0.0430	0.00038 ^s	3.310	1.58	0.197	23.3
0.002	0.0417	0.00037 ²	4.410	1.47	0.132	24.0
0.005	0.0396	0.00035 ⁴	7.810	1.20	0.052	25.3
0.010	0.0390	0.00034 ^s	13.260	0.95	0.019	25.7
2.0 per cent protein solution						
0	0.0886	0.00079 ¹	3.815	1.41	0.0659	11.3
0.0005	0.0870	0.00077 ^s	4.000	1.38	0.0614	11.5
0.001	0.0847	0.00075 ^s	4.890	1.32	0.0471	11.7
0.002	0.0823	0.00073 ^s	5.940	1.24	0.0352	12.1
0.005	0.0789	0.00070 ⁴	9.160	1.08	0.0181	12.7
0.010	0.0761	0.00067 ^s	14.510	0.89	0.0080	13.1

microelectrophoretic technique wherein the mobility of the protein adsorbed on quartz particles was followed at room temperature (25.0°C. \pm 1.0°).

From these measurements, the values for which are shown in tables 2a and 2b, the factors $1/\eta_{sp}$ and $\frac{m^2}{\lambda(\eta_s - \eta_0)}$ were calculated and plotted as shown in figure 1. From the intercepts, obtained by extrapolating the straight lines, thus formed, to the $1/\eta_{sp}$ axis, the values of $K\phi$, $K\phi/C$, h , and $(hV - V)$ at zero electroviscous

effect, shown in table 3, were calculated. Values of A , obtained from the slopes of these graphs, are also shown in table 3. Table 2c gives the results of viscosity

TABLE 2b

Conductivity, viscosity, and mobility data at 25°C. on solutions of alkaline β -lactoglobulin ($\text{pH} = 6.60 \pm 0.05$) at two concentrations of the protein, without and with the addition of varying quantities of sodium chloride

NaCl	η_{sp}	$\eta_s - \eta_0$	λ	m	$\frac{m^2}{\lambda(\eta_s - \eta_0)}$	$\frac{1}{\eta_{sp}}$
0.57 per cent protein solution						
moles per 1000 cc	poises	poises	$mhos \times 10^4$	$\left(\frac{cm^2}{v \text{ sec.}} \times 10^4\right)$		
0	0.0327	0.00030 ²	0.951	2.01	1.41	30.6
0.0005	0.0310	0.00027 ⁶	1.176	1.92	1.14	32.2
0.001	0.0262	0.00023 ²	2.118	1.84	0.69	38.2
0.002	0.0237	0.00021 ¹	3.205	1.75	0.45	42.2
0.005	0.0224	0.00020 ⁰	6.700	1.67	0.21	44.7
0.010	0.0213	0.00019 ⁰	12.370	1.41	0.08	47.0
1.15 per cent protein solution						
0	0.0582	0.00051 ⁸	1.676	1.81	0.377	17.2
0.0005	0.0561	0.00050 ¹	2.085	1.78	0.303	17.8
0.001	0.0513	0.00045 ⁸	2.826	1.75	0.237	19.5
0.002	0.0486	0.00043 ¹	3.870	1.65	0.162	20.6
0.005	0.0458	0.00040 ⁹	7.296	1.53	0.079	21.8
0.010	0.0440	0.00039 ³	12.880	1.38	0.038	22.7

TABLE 2c

Viscosity data at 25°C. on solutions of varying concentrations of isoelectric β -lactoglobulin ($\text{pH} = 5.20$) with sodium chloride added to minimize the Donnan effect

PROTEIN CONCENTRATION	NaCl	η_{sp}	$\frac{\eta_{sp}}{C}$
grams per 100 cc	moles per 1000 cc	poises	
0.5	0.05	0.019 ⁶	0.039 ²
1.0	0.05	0.036 ⁹	0.036 ⁹
2.0	0.05	0.074 ⁵	0.037 ²
0.195*	0.1†	0.007 ⁴	0.03 ⁸
0.355*	0.1†	0.015 ⁶	0.043 ⁹
0.490*	0.1†	0.020 ⁶	0.042 ¹
0.765*	0.1†	0.031 ⁸	0.041 ⁵
1.775*	0.1†	0.076 ³	0.042 ⁹
1.972*	0.1†	0.084 ²	0.042 ⁷

* Values taken from reference 4.

† In 0.05 M acetate buffer, $\text{pH} = 5.0$.

determinations made on isoelectric β -lactoglobulin at three protein concentrations and in the presence of 0.05 N sodium chloride. Under these conditions any

electroviscous effect is negligible and the values of η_{sp}/C are found to be identical with those values obtained by extrapolation, to zero electroviscous effect, of the data obtained under the conditions described above. Viscosity data of Neurath *et al.* (4) are included in table 2c for comparison.

DISCUSSION

As the salt content of a β -lactoglobulin (salt-free) solution is increased (using in all cases a salt with an ion common with the gegenion of the colloid electrolyte), it is found that the entire change in viscosity of the solution is due to a change in the extent of the electroviscosity effect. The value of $K\phi/C$ obtained by extrapolation of the electroviscosity data coincides accurately with the value of $K\phi/C$ obtained when the electroviscosity effect is totally removed by shifting the pH of the solution to the isoelectric point of the protein and increasing the

TABLE 3
Electroviscosity data on β -lactoglobulin ($V = 0.75$)

EXPERIMENT	PROTEIN CONCENTRATION (C)	INTERCEPT ON $1/\eta_{sp}$ AXIS	$K\phi$ ($\zeta = 0$)	$K\phi/C$	Kh	h ($K = 2.5$)	VOLUME HYDRATION ($hV - V$)	SLOPE	A (SLOPE/ C)
pH = 4.22	0.5	52.1	0.0192	0.0384	5.12	2.05	0.78	8.2	16.4
pH = 4.22	1.0	25.9	0.0386	0.0386	5.14	2.06	0.79	13.0	13.0
pH = 4.22	2.0	13.32	0.0750	0.0375	5.00	2.00	0.75	32.5	16.2
pH = 6.60	0.57	47.3	0.0212	0.0371	4.95	1.98	0.74	12.3	21.5
pH = 6.60	1.15	23.2	0.0431	0.0375	5.00	2.00	0.75	16.8	14.6
pH = 5.20*	0.5		0.0196	0.0392	5.23	2.09	0.82		
pH = 5.20*	1.0		0.0369	0.0368	4.90	1.96	0.72		
pH = 5.20*	2.0		0.0745	0.0372	4.96	1.98	0.74		

* Isoelectric.

salt content to higher ionic strengths. Values for the degree of hydration, or the degree of asymmetry, of β -lactoglobulin in aqueous solution calculated from the value of $K\phi/C$ obtained by either means will thus be the same and are found to agree substantially with those previously reported (4, 7, 9) for the protein.

With this colloid electrolyte, it is apparent that the degree of hydration, or of asymmetry of the molecules, is small (in either case) and it is evident that little change occurs in these values as the pH of the protein solution is changed. Presumably this condition would hold throughout the entire range of pH in which ultracentrifugal studies have already shown a constant value of the molecular dimensions of the protein to exist (i.e., throughout the pH range of the protein's stability).

It is to be concluded that β -lactoglobulin belongs to a group of colloid electrolytes, the molecules of which are compact rigid particles which are not subject to osmotic expansion (swelling) and contraction with a change in the nature and number of their gegenions or with changes in salt concentration of their solutions

within the range of the protein's stability. Presumably all crystallizable proteins and possibly many proteins which have not as yet been crystallized belong to this class of colloid electrolytes. Strong internal forces maintain these molecules compact and relatively unchanging, and this type of structure is probably necessary to crystallizability.

There exists, on the other hand, a great number of colloid electrolytes the molecules of which are not so strongly knit together by internal forces (partial valences). While these molecules cannot be further peptized because of the primary valence chains extending throughout, they appear to be subject to swelling or contraction as the number or activity of their gegenion content is varied.

It may be pictured that the swelling and contraction occurring in the molecular units of this type of colloid is possible through a rearrangement of atomic positions within the molecule by a rotation of valence bonds in the primary valence chains under the osmotic pull of the gegenions. Such distortion could be reversible, and it appears that the forces required to cause such rearrangement would be of an order of magnitude such as to allow the osmotic forces postulated to cause such deformations, provided no high-energy partial valence forces had to be overcome. Certainly no stretching of primary valence bonds can be involved, and probably only weak secondary valence forces must be acting between the various parts of the molecule if it is to be affected by the weak osmotic forces pictured. The swelling so caused must be maintained only against weaker shearing forces involved in viscosity measurements in order that the solvent thus held be retained as part of the viscometrically effective volume of the colloid particles.

Such a colloid electrolyte is gum arabic. Sodium gum arabate placed in water will disperse to molecular particles, but these particles are also highly solvated. Calcium gum arabate will also disperse to molecular particles, but owing to the fact that the osmotic force (swelling force) is much less when two sodium ions are replaced by one calcium ion in the colloid electrolyte, the degree of swelling of the calcium gum arabate must be less than that of the sodium gum arabate. Hence, we find that the viscosity of a calcium gum arabate solution is less than that of the sodium gum arabate solution of the same colloid concentrations, owing not entirely to the fact that the electroviscous effect is lower in the case of the calcium compound, but also to the fact that the viscometrically effective volume (ϕ) is lower for the calcium compound (the swelling force being lower and the force acting counter to the swelling force remaining the same, presumably, for both the calcium and the sodium compounds).

When sodium chloride is added in increased amounts to sodium gum arabate solutions, it is observed, from studies on the electroviscous effect, that up to an ionic strength of about 0.01 a straight line (within experimental error) is obtained when $1/\eta_{sp}$ is plotted against $\frac{m^2}{\lambda(\eta_s - \eta_0)}$, which upon extrapolation to the $1/\eta_{sp}$ axis gives a value of $K\phi/C$ which is relatively much higher than that to be expected from the partial specific volume of the colloid. As the ionic strength is increased

much beyond a value of 0.01 the linearity of the curve is lost (the deviation from linear becoming consistently greater than experimental error), and a fraction of the viscosity change must be interpreted as due to a decrease in the viscometrically effective volume of the micelles. This may be interpreted as due to the fact that the decrease in osmotic activity of the gegenions at higher ionic strengths becomes greater than the error in experiment beyond an ionic strength of 0.01, the decrease in osmotic activity resulting in a decrease in the degree of swelling of the micelle.

A comparison of the $K\phi/C$ values for β -lactoglobulin in table 3 and with the $K\phi/C$ values for sodium gum arabate, as shown in table 4, illustrates the differences in the dependence of these values upon the osmotic activity of the gegenions for these two types of colloid electrolytes. The value of $K\phi/C$ for β -lactoglobulin

TABLE 4
Electroviscosity data for sodium gum arabate with sodium chloride less than 0.01 N

COLLOID CONCENTRATION (C) <i>grams per 100 cc.</i>	INTERCEPT ON $1/\eta_{sp}$ AXIS	$K\phi$ ($\zeta = 0$)	$K\phi/C$
0.25	12.5	0.080	32.0
0.375	8.7	0.115	30.7
0.50	6.4	0.157	31.4
0.75	4.18	0.239	31.8
1.00	3.20	0.312	31.2

Viscosity data for sodium gum arabate with sodium chloride greater than 0.1 N (negligible electroviscous effect)

COLLOID CONCENTRATION (C) <i>grams per 100 cc.</i>	SODIUM CHLORIDE CONCENTRATION <i>moles per liter</i>	$K\phi/C$
1.00	0.1	27.8
1.00	0.5	23.2
1.00	1.0	21.6

at zero electroviscosity effect obtained by extrapolation data according to the electroviscosity equation is identical with the value of $K\phi/C$ obtained for the isoelectric protein and at high salt concentrations. This indicates that no volume change of the protein micelles occurs with changing pH or other conditions of the solution. The values of $K\phi/C$ for sodium gum arabate obtained from electroviscosity data when in solutions of sodium chloride below 0.01 N are consistent (with change in colloid content) but are higher than values of $K\phi/C$ obtained as the sodium chloride content is further increased. This can best be interpreted as meaning that the sodium gum arabate molecule (micelle) is dehydrated and shrinks in volume (the viscometrically effective volume) as the ionic strength is increased in the solution of the colloid. This results, presumably, from a decrease in the osmotic peptizing force (i.e., lowered activity) of the gegenions resulting in a decrease in the volume of solvent pulled into the

micelle thereby. β -Lactoglobulin does not shrink with a decrease in the osmotic activity of its gegenions because it is too strongly knit together intramolecularly by partial valence forces to have been caused, even at the highest activity of its gegenions, to swell by osmotic forces.

SUMMARY AND CONCLUSIONS

The electroviscous equation of Krasny-Ergen has been modified to illustrate the experimentally found relationship between the viscometrically effective volume and the unsolvated volume of the dispersed phase of a colloid electrolyte, to illustrate the dependence of the equation upon the particular colloid electrolyte system to which it is applied, and to eliminate the conversion of the experimental terms of the equation into E.S.U.

Experimental data for the electrokinetic potentials (ζ), the specific conductivities (λ), and the viscosity increments ($\eta_s - \eta_0$) of the systems β -lactoglobulin-sodium chloride and sodium gum arabate-sodium chloride were applied to the modified equation.

It was found for β -lactoglobulin, as the salt content was increased with an ion common to the gegenion, that the entire change in viscosity is due to the electroviscosity effect and that this change is independent of the pH of the solution and of increased salt concentrations to higher ionic strengths. Thus, under these conditions, the values for the degree of hydration, or of asymmetry, for the protein in aqueous solution, as calculated from the values of $K\phi/C$, agree with those found in the literature from viscosity, diffusion, and ultracentrifugal studies at high salt concentrations.

For the system sodium gum arabate-sodium chloride, it was found that as the ionic strength was increased above 0.01, the straight line of the plot of $1/\eta_{sp}$ against $\frac{m^2}{\lambda(\eta_s - \eta_0)}$ departs from linearity, the rise in the curve being interpreted as a decrease in the viscometrically effective volume of the colloid.

The $K\phi/C$ values for the two systems β -lactoglobulin and sodium gum arabate are compared. Those for β -lactoglobulin were found to be constant throughout the range of ionic strengths, protein concentration, and pH employed; those for sodium gum arabate were found to decrease with high ionic strengths.

A theory is proposed to explain the differences between these two systems as representative of two distinct classes of colloids.

β -Lactoglobulin is pictured as a strong, internally well knit micelle, incapable of changing either in size, or shape, under the relatively weak, osmotic forces of its gegenions; sodium gum arabate is pictured as an internally weakly knit colloid, fully capable of undergoing large changes in size, or shape, under the relatively weak osmotic influence of its gegenions.

REFERENCES

- (1) BRIGGS, D. R.: J. Phys. Chem. **45**, 866 (1941).
- (2) HANKINSON, C. L., AND BRIGGS, D. R.: J. Phys. Chem. **45**, 943 (1941).
- (3) KRASNY-ERGEN, W.: Kolloid-Z. **74**, 172 (1936).

- (4) NEURATH, H., COOPER, G. R., AND ERICKSON, J. O.: *J. Biol. Chem.* **138**, 411 (1941).
- (5) PALMER, A. H.: *J. Biol. Chem.* **104**, 359 (1934).
- (6) POLSON, A.: *Kolloid-Z.* **87**, 149 (1939).
- (7) POLSON, A.: *Kolloid-Z.* **88**, 51 (1939).
- (8) VON SMOLUCHOWSKI, M.: *Kolloid-Z.* **18**, 194 (1916).
- (9) SVEDBERG, T., AND PEDERSEN, K. O.: *The Ultracentrifuge*. Oxford University Press, London (1940).

THE STRUCTURE OF AN EGG ALBUMIN-DETERGENT COMPLEX

K. J. PALMER

Western Regional Research Laboratory, Albany, California
Bureau of Agricultural and Industrial Chemistry, Agricultural Research Administration,
U. S. Department of Agriculture

Received July 12, 1948

At the present time very little is known about the internal arrangement of the peptide chains in the native state of corpuscular proteins (6). Direct evidence which would result from a complete x-ray structure determination of one of the crystalline proteins is not available at present, although notable progress has been made in this direction, particularly by Bernal and his collaborators (8). As a result of this lack of direct evidence, several structures have been postulated for the corpuscular proteins (1, 9, 11, 16, 20, 25) to account for the available physical and chemical data. Of these structures, the layer structure originally proposed by Astbury (1) for native egg albumin and somewhat modified and extended by Pauling (20) has the advantage of being in agreement with the structural data accumulated from a study of simple molecules (16, 20). In this paper it will be shown that this layer structure when slightly modified is also capable of accounting for the recently determined combining capacity of native egg albumin for Nacconol NRSF, a detergent of the alkyl aryl sulfonate type. The structure of the heat-denatured egg albumin-detergent complex is also discussed.

Lundgren, Elam, and O'Connell (14) studied the soluble complex which forms between both native and heat-denatured egg albumin and Nacconol NRSF at pH 6.5. They mixed 1 per cent solutions of protein and Nacconol NRSF in various proportions and studied their electrophoretic behavior. Following their notation the ratio of the volume of protein solution to that of Nacconol solution will be called the mixing ratio. Their results of interest in the following discussion can then be briefly summarized as follows:

(1) When native egg albumin is used, two components are present if the mixing ratio is equal to or greater than 75:25. The components are protein-detergent complex and free protein.¹ The composition of the complex remains constant throughout this range at 75 per cent protein and 25 per cent detergent.

¹ There must also always be a small amount of free detergent. The composition of the complex calculated by Lundgren, Elam, and O'Connell in the region of low detergent concentration was based on the assumption that all of the detergent was in the form of

(2) When the mixing ratio is less than 75:25, complex and free detergent are present, the concentration of free detergent being approximately proportional to the amount of detergent in excess of 25 per cent.

(3) When egg albumin which has been heat denatured at pH 8.0 and then brought to pH 6.5 is used, the composition of the complex varies continuously from zero to about 68 per cent detergent.

(4) The mobility of the complex lies between that of pure protein and that of pure detergent and is approximately proportional to the detergent content.

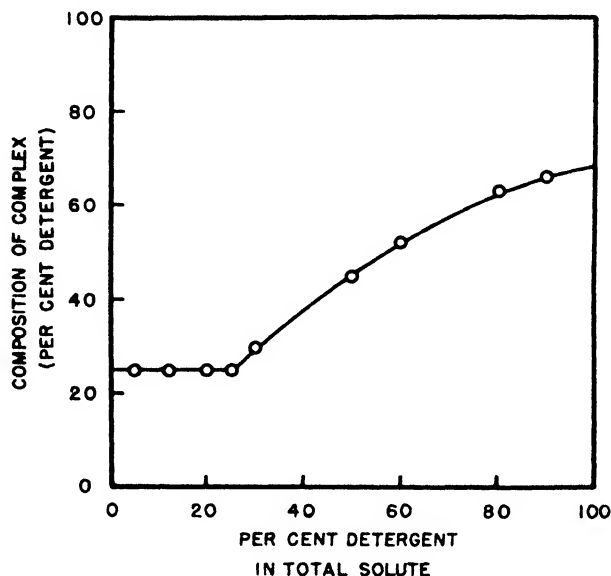


FIG. 1. Plot of composition of the egg albumin-Nacconol NRSF complex against per cent detergent in total solute. Total solute equals 1 per cent in all cases. Data taken from the paper of Lundgren, Elam, and O'Connell (14).

(5) When the mixing ratio is less than 70:30, the complexes formed from native and from heat-denatured egg albumin are indistinguishable electrophoretically.

(6) A plot of the composition of complex (when native egg albumin is used) against percentage of total solute as detergent is shown in figure 1. This shows that the composition of the complex approaches an upper limit of about 68 per cent detergent.

STRUCTURE OF DENATURED EGG ALBUMIN-DETERGENT COMPLEX

Since the electrophoretic behavior of the complex containing 30 per cent or more detergent is the same when made from either native or heat-denatured egg

complex. Actually, the error due to this assumption is probably not large, but the fact that the mobility of the complex was observed to change while its composition remained "constant" may be due to a small change in the concentration of free detergent.

albumin, and since Nacconol, like many other detergents, is known to denature native egg albumin, it is probable that when the mixing ratio is less than 70:30, the protein molecules have a similar unfolded configuration regardless of their initial condition. The structure of the complex is probably also the same in all cases where the composition of the complex exceeds 30 per cent detergent.

At pH 6.5 the protein and detergent are both negatively charged. This suggests that the cohesive forces acting between the protein and detergent are non-polar van der Waals forces, rather than polar attractions. This is further substantiated by the following facts: (a) The complex made with egg albumin heat-denatured at pH 8.0 is more soluble (in solutions of low inorganic ion concentration) than the denatured protein alone, indicating that hydrophobic groups have been covered up. (b) The detergent is easily extracted from the dry residue resulting from either vacuum drying of the solution containing complex or from precipitation with magnesium sulfate. (c) The mobility of the complex has been found (14) to be approximately proportional to the detergent content (indicating that the polar groups of the detergent are free to ionize). (d) X-ray studies of the precipitates obtained by addition of magnesium sulfate indicate that the complex breaks up into two phases on drying (18). This latter fact suggests that the complex results from the mutual attempt of the detergent and denatured protein to cover up their hydrophobic groups, and that the complex is stable only because of the presence of the polar solvent water. (e) Finally, it is well known that, in general, when the detergent and protein have opposite charges a complex involving polar interactions is formed which is insoluble. This reaction has been suggested by McMeekin as a convenient means for removing proteins from solution (15).

On the basis that the molecules in the complex under discussion are held together by non-specific, non-polar forces, it seems likely that the factor determining the upper limit (~68 per cent) for detergent adsorption is a geometrical one. Polarized light (22) and x-ray diffraction (23) studies of the naturally occurring protein-lipide complexes in the myelin sheath of nerve have revealed that in this case the protein exists in the form of thin concentric layers (probably monolayers) and that the lipid molecules are arranged with their long axes perpendicular to the protein layers. It appears probable that the denatured egg albumin-Nacconol NRSF complex may have a similar structure; i.e., the protein exists as a monolayer and the detergent molecules are arranged with their long axes perpendicular to the plane of this layer. The upper limit of detergent adsorption may then be determined by the number of detergent molecules that can be adsorbed on a single egg albumin molecule when the latter is in the form of a monolayer.² The area per molecule of an egg albumin monolayer is approxi-

² The word "monolayer" is used in this paper to designate a flat protein sheet made up of approximately parallel peptide chains. The chains are separated by the "backbone" spacing (4.7 Å.). The side chains of the amino acids project above and below the plane of the sheet. The thickness of such a protein monolayer would be about 10 Å. The area calculated for this monolayer using x-ray data is somewhat less than that observed by Gorter (10) for protein monolayers on the surface of water. This we attribute to the difference in environment of the non-polar side chains.

mately $384 \times 3.3 \times 4.7 = 5950 \text{ \AA}^2$, where 384 is the recently calculated value for the number of amino acids in egg albumin (7) and 3.3 and 4.7 are the x-ray values for the two dimensions lying in the plane of the monolayer.

Since Nacconol NRSF is essentially dodecyl benzene sodium sulfonate, we can assume that when close packed each detergent molecule will occupy about 20 \AA^2 . (this is the approximate cross-sectional area observed for all straight-chain hydrocarbons). The number of detergent molecules which can be packed on *one* side of the protein monolayer is then $5950/20$, or ~ 298 . Taking 323 for the molecular weight of the detergent and the average (approximately 43,000) of the results recently reported for the molecular weight of egg albumin obtained by the rate and equilibrium ultracentrifugation (24), the osmotic pressure (5),

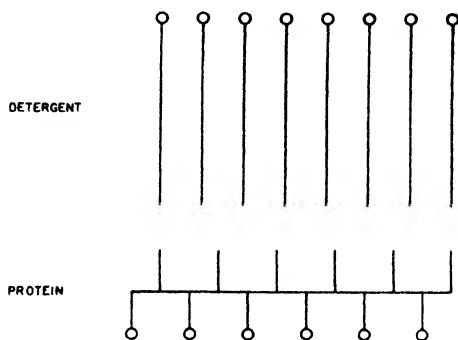


FIG. 2. Schematic drawing of structure of an egg albumin-Nacconol NRSF complex containing 68 per cent detergent. The polar groups of the detergent and the polar side chains of the protein are represented by circles.

and the amino acid analysis (7) methods, the per cent of detergent by weight in this complex is

$$\frac{(298)(323)(100)}{(43,000) + (298)(323)} \sim 69 \text{ per cent}$$

This is in excellent agreement with the observed value for the upper limit of detergent adsorption of about 68 per cent (figure 1). A complex with the postulated structure would be expected to have a mobility lying between that of the protein and the detergent, in agreement with observation (14).

Two plausible deductions follow from the above structure: First, accepting the postulate that the forces of adsorption are of the non-polar type and the conclusion that the detergent molecules occupy just one side of the protein monolayer, it follows that the protein monolayer probably consists of a polar and a non-polar surface. That is, the side chains of the polar amino acids project out on one side of the monolayer and the non-polar side chains on the other. Such a configuration requires about an equal number of polar and non-polar amino acids. This actually appears to be the case for egg albumin (7, 21). A schematic drawing illustrating the polar protein monolayer with the adsorbed detergent molecules is shown in figure 2.

Secondly, if we accept the above deduction, then since the peptide chains in denatured egg albumin are known to have the β -keratin configuration (4, 19), it is probable that the polar amino acids occupy alternate positions along the peptide chain as this would lead simply and directly to a polar and a non-polar surface. The occurrence of polar amino acids in alternate positions has been postulated previously (17) and more recently by Dervichian (9). Astbury (2, 3) has also suggested that the polar amino acids occupy alternate positions in wool keratin and myosin.

STRUCTURE OF NATIVE EGG ALBUMIN

Following the suggestion of Astbury (1) and Pauling (20), we assume that the native egg albumin molecule consists of four superimposed layers. However, whereas Astbury has postulated that the layers are circular, we accept Pauling's suggestion that they are rectangular, the layers being composed of a continuous peptide chain having an extended β -keratin-like configuration. Pauling (20, page 2651) has also suggested that in a corpuscular protein the size of egg albumin, each layer probably contains about eight peptide chain segments, of about twelve residues each. This gives a total of 384 amino acids for egg albumin, a value which is in excellent agreement with the recent analytical results of Chibnall (7). Such a layer would be almost square and measure about 40 Å. on a side. Since the layers are approximately 10 Å. thick and there are four of them, this structure has dimensions in approximate agreement with the results calculated from ultracentrifugal and diffusion data (24) for the egg albumin molecule.

In addition to the above, the postulate is made in this paper that the layers in the native egg albumin molecule are polar. This follows from the assumption that the polar amino acids occupy alternate positions and that the peptide chain has an extended β -keratin-like configuration in the native egg albumin molecule. A schematic drawing of the postulated structure for native egg albumin is shown in figure 3.

This polar grid structure appears to have all of the advantages of the originally postulated layer structure and, in addition, can more readily account for the following three observations: (1) Complex formation with detergents, as will be discussed below. (2) The denaturation of native proteins by detergents as well as hydrogen-bond-forming compounds. The former act on the non-polar interface; the latter on the hydrogen bonds which occur in the polar interface and also between the carboxyl and amino groups within the grid. (3) The dissociation of egg albumin into two components as observed by Longworth, Cannan, and MacInnes (12) which, according to Chibnall (7), are probably "somewhat similar in composition and net ionic charge." This would occur if the molecule dissociated along the polar interface (figure 3).

Dervichian (9) has recently proposed that corpuscular proteins in general consist of only two polar layers. However, the ultracentrifugal and diffusion data on egg albumin appear to be in better agreement with the four-layer structure, as do the electrophoretic results of Longworth, Cannan, and MacInnes

(12) on egg white (see above). Actually, the mechanism of complex formation between native egg albumin and detergent discussed below is more or less independent of the shape of the protein molecule and would be just as applicable to the two-layer structure of Dervichian as to the more symmetrical four-layer model.

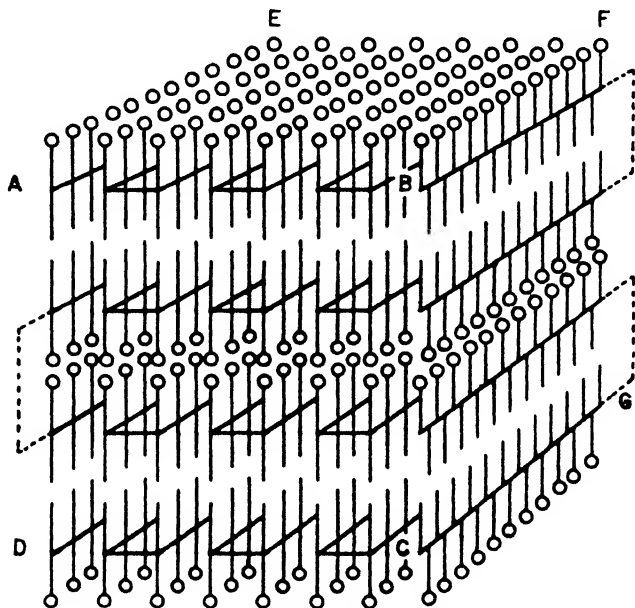


FIG. 3. Schematic drawing of the native egg albumin molecule. The native egg albumin molecule possesses three interfaces, one polar and two non-polar

NATIVE EGG ALBUMIN-DETERGENT COMPLEX

Two facts with respect to complex formation between native egg albumin and Nacconol NRSF need to be accounted for. One is the occurrence of free native protein in equilibrium with complex containing 25 per cent detergent. The other is that the complex formed from native egg albumin never contains less than 25 per cent of Nacconol NRSF at pH 6.5.

A plausible explanation of these facts can be given with the aid of the layer structure discussed above for native egg albumin. The first of these two facts is almost certainly due to a potential barrier. Since we are presumably dealing with non-polar adsorption, the initial process probably involves penetration of the two non-polar interfaces of the protein by the long hydrocarbon chains of the detergent. The potential barrier results from the difficulty that the first detergent molecules have in wedging into the non-polar interface. Once penetration has commenced, however, more detergent molecules follow readily. Adsorption then proceeds until the interface has been covered with a monolayer of the detergent molecules.

The most stable configuration for such a complex would be expected to be

that in which the long hydrocarbon chains of the detergent molecules are lying in the plane of the protein grids, with their polar groups projecting into the solution as shown schematically in figure 4. Such a structure is compatible with the mobility measurements made on this complex (14), which require that the polar groups of both the protein and the detergent be free to ionize.

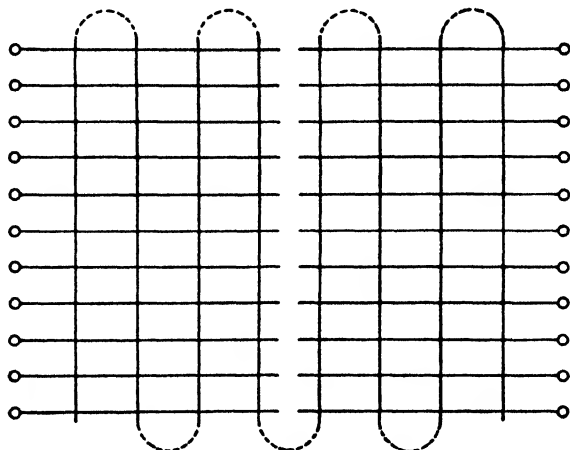


FIG. 4. Schematic drawing showing the structure of the native egg albumin-Nacconol NRSF complex containing 25 per cent detergent. Top view, looking perpendicular to the *ABEF* face (figure 3). Top protein layer removed.

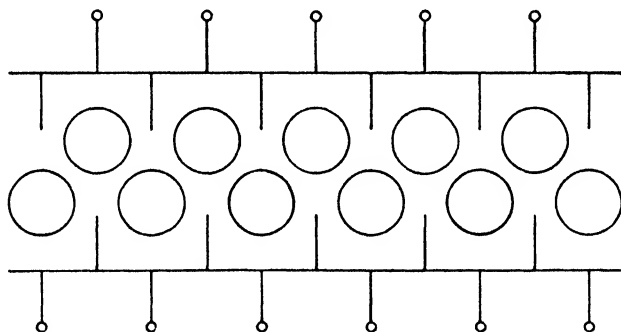


FIG. 5. Schematic drawing showing the structure of the egg albumin-Nacconol NRSF complex containing 25 per cent detergent. Side view, looking perpendicular to the *BCFG* face (figure 3). Just the two top protein layers are shown. The detergent molecules are represented by the large circles.

In a direction parallel to the length of the peptide chain segments there are no open spaces. Their absence is due to the fact that on the average the diameters of the side chains and of the backbone spacing in the grid are about equal (4.7 Å.). However, in a direction perpendicular to this and in the plane of the grid, openings do occur, because the side chains are about 6.6 Å. apart. This results from the fact that only every other side chain projects into the non-polar

interface. The detergent molecules, therefore, will probably enter this side and would tend to arrange themselves as shown schematically in figure 5. That is, there would be about one detergent molecule per amino acid in the peptide chain segment running parallel to this face of the protein molecule. Actually, the number would probably be somewhat less than this because the peptide chain must bend back at each end of the grid. If we assume that eleven detergent molecules will just cover the interface, then since the grid is of the order of 40 Å. (8×4.7 Å.) and the dodecyl benzene sodium sulfonate molecule only about 23 Å. long, two opposed detergent layers per interface will occur (figure 4). Or, since there are two such non-polar interfaces in the molecule, there will be a total of forty-four detergent molecules adsorbed per protein molecule. The per cent of detergent by weight in such a complex is:

$$\frac{(44)(323)(100)}{(44)(323) + (43,000)} \sim 25 \text{ per cent}$$

in agreement with the observed value (figure 1).

When the amount of detergent exceeds 25 per cent, the non-polar interfaces are forced open still farther. The protein molecule eventually unfolds and then has essentially the same configuration as a heat-denatured molecule. The detergent molecules then take up a position like that shown schematically in figure 2. The occurrence of the two highly charged layers due to the polar groups of the detergent in the native egg albumin-detergent complex containing 25 per cent of detergent would be expected to cause the native protein molecule to separate at the polar interface. This may account for the increase in availability of the sulfhydryl groups occurring in the mixing range 0 to 25 per cent detergent as solute (14). This also accounts for the fact that below a mixing ratio of 70:30 the electrophoretic behavior of the complex made from either native or heat-denatured protein is the same.

The structure of the egg albumin-detergent complex proposed in this paper is also in accord with the observation that this complex is much more sensitive to the presence of inorganic ions (13) than either the protein or the detergent alone. This is evidently due to the high concentration of negative charges brought about by the close packing of the detergent molecules on the protein.

It would be desirable to have more quantitative data on the combining capacity of various native and denatured proteins for different types of molecules, particularly at low concentrations of the adsorbed molecule. Such information should lead to more definite conclusions regarding the mechanism of complex formation with native proteins, and enable a decision to be made on the merits of the hypothesis that corpuscular proteins possess both polar and non-polar interfaces in their native configuration.

SUMMARY

A structure for a denatured egg albumin-detergent complex is postulated which appears to be in agreement with the published results of an electrophoretic investigation of this system. It consists of a polar protein monolayer with the

detergent molecules adsorbed on one side only and with the long axes of the detergent molecules perpendicular to the protein layer.

From this structure it is suggested that the polar amino acids probably alternate along the peptide chain in egg albumin. On the basis of this hypothesis it follows that if the layer structure for native egg albumin postulated by Pauling is acceptable, the layers in the native configuration are polar. By use of this model a plausible structure is postulated for the complex which forms between native egg albumin and detergent. This structure appears to account for the observed facts that the complex formed from native egg albumin never contains less than 25 per cent of Nacconol NRSF (whereas that formed from denatured egg albumin does), and that the complex containing 75 per cent "native" egg albumin and 25 per cent detergent can exist in equilibrium with free native protein.

The author wishes to express his gratitude to Dr. H. P. Lundgren, who very kindly permitted him to see the manuscript of his paper describing the results of the electrophoretic behavior of the egg albumin-Nacconol NRSF complex before publication, and to both Dr. Lundgren and Dr. R. C. Merrill, Jr., for many helpful and stimulating discussions. He also wishes to thank Mr. J. A. Galvin for preparing the drawings.

REFERENCES

- (1) ASTBURY, W. T.: *Nature* **137**, 803 (1936).
- (2) ASTBURY, W. T.: *J. Chem. Soc.* **1942**, 337.
- (3) ASTBURY, W. T., AND BELL, F. O.: *Nature* **147**, 696 (1931).
ASTBURY, W. T.: *Chemistry & Industry* **60**, 491 (1941), Jubilee Memorial Lecture.
- (4) ASTBURY, W. T., DICKINSON, S., AND BAILEY, K.: *Biochem. J.* **29**, 2351 (1935).
- (5) BULL, H. B.: *J. Biol. Chem.* **137**, 143 (1941).
- (6) BULL, H. B.: *Advances in Enzymology*. Interscience Publishers, Inc., New York (1941).
- (7) CHIBNALL, A. C.: *Proc. Roy. Soc. (London)* **B131**, 136 (1942), Bakerian Lecture.
- (8) CROWFOOT, D.: *Chem. Rev.* **28**, 215 (1941).
- (9) DERVICHIAN, D. G.: *J. Chem. Phys.* **11**, 236 (1943).
- (10) GORTER, E.: *Ann. Rev. Biochem.* **10**, 619 (1941).
- (11) HUGGINS, M. L.: *J. Chem. Phys.* **8**, 598 (1940); *J. Am. Chem. Soc.* **61**, 755 (1939).
- (12) LONGSWORTH, L. G., CANNAN, R. K., AND MACINNES, D. A.: *J. Am. Chem. Soc.* **62**, 2580 (1940).
- (13) LUNDGREN, H. P.: *J. Am. Chem. Soc.* **63**, 2854 (1941).
- (14) LUNDGREN, H. P., ELAM, D. W., AND O'CONNELL, R. A.: *J. Biol. Chem.* **149**, 183 (1943).
- (15) McMEEKIN, T. L.: *Proc. Fed. Am. Soc. Exptl. Biol.* **1**, 124 (1942).
- (16) MIRSKY, A. E., AND PAULING, L.: *Proc. Natl. Acad. Sci. (U. S.)* **22**, 439 (1936).
- (17) NEUBATH, H., AND BULL, H. B.: *Chem. Rev.* **23**, 391 (1938); *J. Phys. Chem.* **44**, 296 (1940).
- (18) PALMER, K. J., AND GALVIN, J. A.: In preparation.
- (19) PALMER, K. J., AND GALVIN, J. A.: *J. Am. Chem. Soc.* **65**, 2187 (1943).
- (20) PAULING, L.: *J. Am. Chem. Soc.* **62**, 2643 (1940).
- (21) SCHMIDT, C. L. A.: *The Chemistry of the Amino Acids and Proteins*. C. C. Thomas, Springfield, Illinois (1938).
- (22) SCHMITT, F. O., AND BEAR, R. S.: *Biol. Rev.* **14**, 27 (1939).

- (23) SCHMITT, F. O., BEAR, R. S., AND PALMER, K. J.: *J. Cellular Comp. Physiol.* **18**, 31 (1941).
- (24) SVEDBERG, T., AND PEDERSEN, K. O.: *The Ultracentrifuge*. The Clarendon Press, Oxford (1940).
- (25) WRINCH, D. M.: *Nature* **150**, 270 (1942); and many other articles.

ON SOME COMPOUNDS OF IRON DEPOSITED ON BOTH POLES SIMULTANEOUSLY

GEORGE ANTONOFF

Chemistry Department, Fordham University, New York, New York

Received September 28, 1943

When finely divided natural ores containing iron were suspended in acidified water and a current applied, a deposit appeared on the platinum anode (1). In thin layers, this deposit had the appearance of gold. Although not soluble in dilute acids, the deposit could be stripped by a mixture of dilute acid and hydrogen peroxide with an evolution of gas. Besides iron, there were large quantities of calcium, sodium, and other metals present in the deposit. It contained no traces of the anion of the acid used for acidifying the bath. The deposit had a variable composition. The amount plated out was not proportional to the current, i.e., it did not follow Faraday's law.

Pure precipitated iron hydroxide suspended in acid solution gave no anodic deposit. However, ignited ferric oxide gave deposits similar to the ones described above. When the ferric oxide was heated to red heat and quenched in water, larger amounts of anodic deposits were obtained.

It was thought at first that high temperature is necessary in order to produce these results, but further experiments indicated that if the precipitate is simply dried, it acquires the property of giving the same effects. For example, if one takes crystals of commercial aluminum sulfate, dissolves them in water, and filters the solution, an insoluble powder of some sort of iron oxide remains on the filter. This oxide suspended in acidulated water may give effects similar to those described above.

A sample of ferric oxide may contain only minute traces of impurities but by this procedure, lead, manganese, and other metals were extracted in appreciable quantities. For one series of experiments ferric oxide was made from material which contained no manganese (Merck analysis: manganese, 0.000 per cent). However, qualitative tests of the anodic deposit showed traces of manganese.

These phenomena are easily reproducible. The procedure was as follows: 30 g. of ferric oxide was suspended in 2 liters of water and 2 cc. of concentrated sulfuric acid added. The mixture was stirred mechanically and heated to 60°C. The degree of acidity of the bath was of no importance; it was only necessary to keep it acid. Platinum electrodes (2 in. x 2 in.) were inserted and

a current passed. There was no set voltage. Some of the experiments were performed with 60 volts, some with 150 volts, and in some cases 6 volts was sufficient. In most of the experiments the current was about 2 amperes, but this also varied. For stripping, a mixture of equal volumes of dilute hydrochloric acid and 3 per cent hydrogen peroxide was used. At times it was necessary to change the amounts of acid or hydrogen peroxide, owing to the variable composition of the deposit.

In this process a similar deposit was noticed on the cathode, but it was usually masked by large quantities of other matter which was deposited cataphoretically. However, when the cathode was inserted in a porous cup, a deposit was obtained which was similar to the anodic deposit and which also decomposed hydrogen peroxide. When the current density was increased by decreasing the size of the cathode, the deposit became grayish in spots. When the electrode was reduced to the size of wire, the entire deposit was gray and was easily recognizable as metallic iron. On the inner wall of the porous cup there was a brown deposit which was scraped off. It was different from the substances found on the anode or cathode, for it did not decompose hydrogen peroxide.

It was difficult to do a satisfactory analysis of the non-metallic content of the deposit, because it could not be easily detached mechanically from the platinum anode. For the metallic analysis, strippings were accumulated from many depositions in order to have sufficient material. The weight of the material deposited was obtained by weighing the platinum before and after deposition. The platinum itself lost no weight.¹ Because of the variable nature of the deposit, the analysis gave only a rough indication of its composition. In all cases, the weight of the metals present in the deposit was less than the total weight of the material stripped. The difference can only be oxygen or possibly hydrogen. There was no evidence of water of hydration. The deposit was stable up to the beginning of red heat. In a stream of hydrogen, the deposit was reduced and a gray mass resulted which evidently was iron. This iron would not dissolve in acids quantitatively.

It is the belief of the author that these deposits are of the nature of peroxides which, as a rule, decompose hydrogen peroxide. They are of complex and variable composition and may be deposited on either the anode or the cathode according to conditions.

This can be explained by assuming that the particle of a fairly complex matter has a certain dipole moment, the position of which may be not the same in different configurations. Thus in one case the negative pole may be nearer the periphery, and the particle will stick to a positive ion of the acid used and will go the cathode, and *vice versa*. On the basis of chemical analysis of various deposits, it was not possible to conclude whether they consist of any new substance or of a mixture of substances, in view of their variable composition. At this point, without seeing what else could be done under the circumstances, the author communicated with the late Dr. H. Freundlich. The latter found these

¹ It is therefore improbable that the ion of platinum participated in the formation of these deposits, as some people may think.

results extremely interesting and suggested that x-ray method might throw some light on the subject. The author thought that Dr. Freundlich might be the suitable man to carry through this piece of work, but his sudden and unexpected death interrupted the correspondence.

The author then took advantage of the kindness of the General Electric Company, which expressed a willingness to perform these experiments. Samples of both cathodic and anodic deposits were submitted to them. The results obtained, however, did not explain anything. They were examined by Dr. C. J. Davisson of the Bell Telephone Co., to whom the author wishes to express thanks, but he could not draw any conclusion from them.

In view of the great interest attached to this problem the author wishes to publish these results as they are, with the hope that investigators having suitable facilities will want to work in this field.

REFERENCE

- (1) ANTONOFF, G.: *Kolloid-Z.* **79**, 331 (1937).

THE VARIATION OF THE VISCOSITY OF GASES AND VAPORS WITH TEMPERATURE¹

WILLIAM LICHT, JR., AND DIETRICH G. STECHERT

Department of Chemical Engineering, University of Cincinnati, Cincinnati, Ohio

Received July 26, 1948

Fruitful studies of the viscosity of substances in the gaseous state have been carried out for the past century. The results of these studies have been of both theoretical and practical importance. Experimental determinations of the coefficient of viscosity of pure substances as a function of temperature, pressure, and the nature of the molecules making up the substance have led to elaboration and modification of the classical kinetic theory of gases and to a more

¹ The symbols used in this paper are given below:

- a = characteristic constant in the exponential equation,
- b = characteristic constant in Trautz's equation,
- C = characteristic constant in Sutherland's equation,
- C' = characteristic constant in Reinganum's equation,
- D = characteristic constant in Sutherland's modified equation,
- d = characteristic constant in Trautz's equation,
- G = constant characteristic of a substance, dependent upon molecular weight, critical temperature, and pressure,
- J = characteristic constant in Jones' equation,
- K = characteristic constant in Sutherland's equation,
- K' = characteristic constant in Reinganum's equation,
- k = constant in universal viscosity equation,
- \log = logarithm to the base 10,
- M = molecular weight,
- m = characteristic constant in Hassé and Cook's equation,

detailed understanding of intermolecular forces. The numerical value of the coefficient of viscosity plays an important rôle in numerous applications of the unit operations of heat transfer, fluid flow, filtration, classification, absorption, etc.

From the practical viewpoint it is desirable to know quantitatively how the coefficient of viscosity depends upon the factors mentioned above and, when necessary, to be able to estimate its value when no experimental data are at hand for the particular substance or condition in question. Since it has been found that the viscosity of many gases is practically unaffected by variations in pressure below 30 to 50 atmospheres, as is indeed predicted by the kinetic theory, the functional relationship between viscosity and temperature at low or moderate pressures may be considered separately, and is the subject of this study.

A large number of such viscosity-temperature relationships of widely varying nature have been proposed. A study of these was undertaken by the authors in the light of comprehensive experimental data with a view to determining their general applicability and validity, and in the hope of finding a simple function which could be used over wide ranges of temperature to represent the data accurately. It was also hoped that a method of estimating viscosities when no experimental data were available could be found. The extent to which these hopes have been realized is described below.

THE FORM OF μ *vs.* T CURVES FOR GASES

The general form of plots of the coefficient of viscosity, μ , as a function of the absolute temperature, T , at atmospheric pressure is illustrated by sample plots in figure 1. An inspection of such plots reveals several facts. The viscosity of gases is very small and of the order of 100 to 900 micropoises. Without exception it increases with temperature; the rate of increase, however, varies widely from case to case. Some of the plots are curved upward, having an increasing slope, others are curved downward with a decreasing slope, and some are practically straight lines. Occasionally both types of curvature appear in the same plot; then a point of inflection is noted, as in the cases of bromine and sulfur dioxide. In general, for one definite temperature the more complex the structure of the molecule, the lower is the viscosity. Hydrogen is an ex-

- n = characteristic constant in exponential equation,
- P = pressure,
- Q = characteristic constant in Hassé and Cook's equation,
- R = gas constant in perfect gas law,
- S = characteristic constant in Jones' equation,
- s = characteristic constant in Hassé and Cook's and Jones' equations,
- T = absolute temperature,
- U = characteristic constant in Hassé and Cook's equation,
- α = characteristic constant in modified Reinganum equation,
- μ = coefficient of viscosity,
- μ_c = coefficient of viscosity at atmospheric pressure and the critical temperature.

Subscript c refers to the critical point; subscript 0 refers to some reference state or condition; subscript r refers to a reduced quantity, *viz.*, $T_r = T/T_c$.

ception in this as well as in many other respects, as will be noted subsequently. Substances of high molecular weight usually have steeper curves, such as those shown by mercury and bromine. There is no indication of any maximum or minimum values appearing on these curves.

A peculiar property of these curves was stated by Trautz (15). He claimed that for many substances the slope of the curve, $d\mu/dT$, at the critical tempera-

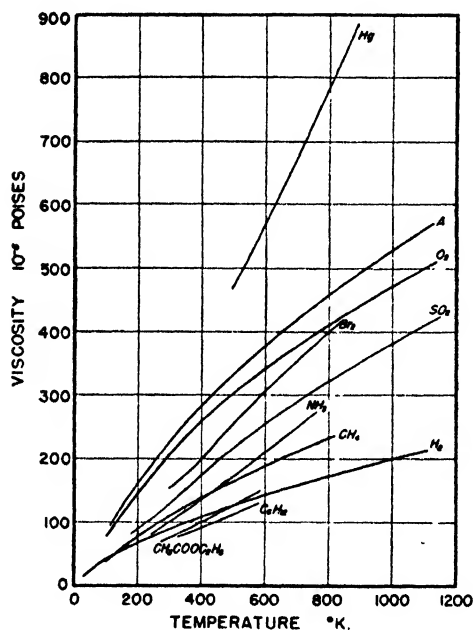


FIG. 1

FIG. 1. Typical viscosity-temperature curves for gases and vapors at atmospheric pressure

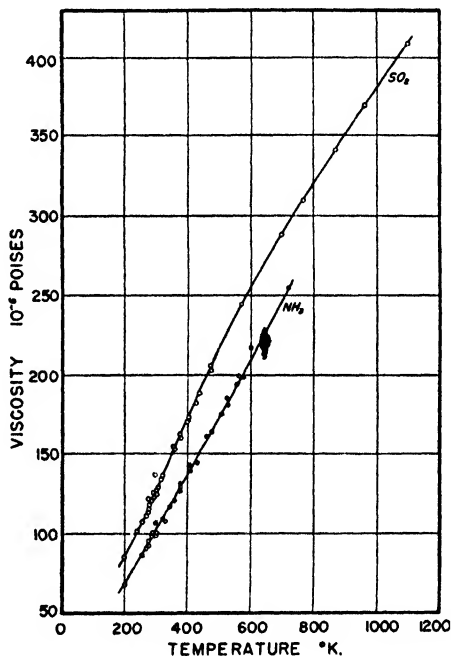


FIG. 2

FIG. 2. Illustrations of the consistency of the experimental data

ture, T_c , is equal to the value of the viscosity at the critical temperature, μ_c , divided by the critical temperature, i.e.

$$\left. \frac{d\mu}{dT} \right|_c = \frac{\mu_c}{T_c}$$

That is, a line drawn from the origin of the μ - T axes to the point on the curve having the coordinates (μ_c, T_c) will be found to be tangent to the curve at that point. This may be expressed in still another way by saying that the value of μ/T is a maximum at T_c . As will be seen, however, this property is only approximately true. It is made the basis for the development of Trautz's equation, which is described below.

For the purposes of this study experimental data were selected for the twenty-six elements and compounds listed in table 1. These substances were chosen

because of their chemical and structural differences, and as being representative of various types of gases. The inert gases, the halogens, the hydrogen halides, the oxides, the hydrides, and the alkyl hydrocarbons of various types as well as aromatic and cyclic hydrocarbons, all are represented. It was felt that conclusions obtained from a study of these substances would be of general ap-

TABLE 1
Characteristic constants for various viscosity-temperature functions
Based upon μ in poises and T in $^{\circ}\text{K}$.

SUBSTANCE	TEMPERATURE RANGE	SUTHERLAND'S EQUATION			TRAUTZ'S EQUATION			EXPONENTIAL EQUATION		
		C	$K \times 10^8$	Average error	$b \times 10^8$	d	Average error	$a \times 10^8$	n	Average error
	$^{\circ}\text{C}$.			per cent			per cent			per cent
Acetone.....	0- 306	530	11.79	1.5	0.449	0.806	2.1	0.272	0.990	0.9
Acetylene.....	0- 120	206	10.07	0.4	1.754	2.340	0.6	0.546	0.919	0.4
Ammonia.....	-77- 441	472	15.42	2.4	0.446	0.361	2.9	0.274	1.041	1.0
Argon.....	-183- 827	133	19.00	0.3	1.197	0.552	0.7	2.782	0.766	3.9
Benzene.....	0- 313	403	10.33	1.2	0.271	0.0890	0.9	0.299	0.974	0.9
Bromine.....	13- 594	517	23.33	1.3	0.649	0.348	1.5	0.664	0.956	1.6
Carbon dioxide.....	-98-1052	233	15.52	1.0	0.791	0.654	1.2	1.057	0.868	4.5
Carbon tetrachloride.....	23- 487	335	12.17	0.9	0.437	0.436	3.8	0.525	0.921	1.2
Cyclohexane.....	46- 306	319	8.41	0.7	0.246	0.0883	1.6	0.408	0.907	0.6
Diethyl ether.....	0- 309	349	9.43	0.4	0.440	0.766	3.6	0.296	0.971	0.9
Ethyl acetate.....	0- 314	425	10.60	0.6	0.267	0.674	0.3	0.226	1.020	0.4
Ethyl alcohol.....	0- 309	400	11.67	0.9	0.394	0.439	2.1	0.449	0.930	0.5
Ethylene.....	-79- 303	232	10.54	1.1	0.504	0.569	1.9	0.493	0.934	1.5
Helium.....	-258- 817	97.6	15.13	9.5	2.790	0.470	0.8	4.894	0.653	1.5
Hydrogen.....	-258- 825	70.6	6.48	5.1	0.653	0.464	1.2	1.860	0.678	5.4
Hydrogen chloride.....	0- 251	359	18.66	0.2	0.568	0.212	0.3	0.572	0.973	0.6
Mercuric chloride.....	255- 587	996	31.29	0.3	0.690	0.471	0.5	0.253	0.110	0.3
Mercury.....	218- 610	996	63.00	0.4	1.225	0.249	0.5	0.573	1.082	0.5
Methane.....	18- 499	155	9.82	0.4	0.578	0.585	1.3	1.360	0.770	5.2
Methyl chloride.....	-20- 300	390	14.45	1.4	0.463	0.337	1.6	0.328	1.016	2.0
Nitrogen.....	-191- 825	102	13.85	0.4	0.993	0.571	0.9	3.213	0.702	4.4
Nitrous oxide.....	-21- 414	273	16.36	0.3	0.745	0.597	0.6	0.977	0.881	0.9
Oxygen.....	-191- 829	110	16.49	0.8	1.138	0.607	1.6	3.355	0.721	4.2
Sulfur dioxide.....	-75- 823	362	16.53	1.1	0.729	0.731	1.5	0.608	0.940	2.8
Toluene.....	61- 251	365	9.09	0.7	0.267	0.175	1.4	0.286	0.968	0.9
Water vapor.....	0- 407	659	18.31	1.0	0.453	0.364	0.9	0.170	1.116	0.9

plicability. In that connection hydrogen and helium were included because of their well-known exceptional behavior with respect to viscosity.

Inasmuch as constants quoted in handbooks and the literature for various viscosity-temperature equations are usually valid only for narrow ranges of temperature for each substance and in the vicinity of room temperature, and in order to study conditions such as might be encountered in industrial practice,

it was desired to include data over as wide a temperature range as possible. Accordingly *all* reliable data obtained by various investigators between 1876 and 1934, as published in the Landolt-Börnstein Tables (7), were employed in this study.

For many substances, the experimental data that have been obtained by various investigators using different experimental methods are quite consistent, but for a few the data are very poor in this respect. Of course the accuracy of any viscosity-temperature function tested by means of experimental data will be no greater than the accuracy of those data. An idea of good and poor data may be obtained by referring to figure 2. The experimental data for sulfur dioxide are very good; those for ammonia are very poor. For most of the twenty-six substances studied, the data are consistent. For the following substances, the data are relatively poor in this sense: water vapor, ammonia, carbon dioxide, ethylene, methyl chloride, and carbon tetrachloride.

TWO-CONSTANT EQUATIONS

Among the many viscosity-temperature relationships proposed by various investigators, four involve only two characteristic constants for each gas. These are known as the exponential, Sutherland, Reinganum, and Trautz equations. Since the simplicity inherent in a relationship involving few constants is so desirable for computational purposes, these equations were examined in detail. More complex equations are discussed later in this article.

The accuracy of the relationships was tested with the experimental data in the following manner: The relationship was first written in such a form that a straight line would theoretically be obtained by plotting two different functions of the viscosity and temperature. Values of these functions computed from the actual experimental data (not from "smoothed" data) were plotted, and the resulting plots were observed. The best straight line was drawn through the points, and the slope and intercept of this line were determined. From these, in turn, the two constants of the relationship were found. With these two constants the equation being tested was used to compute values of the viscosity at various temperatures and these were compared with the experimental values. The discrepancies here observed are a direct measure of the extent to which the equation deviates from the data. The average per cent error so found was determined for each equation as the overall measure of its accuracy.

The exponential equation

The exponential equation is of the form

$$\mu = aT^n \quad (1)$$

where a and n are constants characteristic of each gas. This results from a slight modification of the classical kinetic theory, which predicts that μ should be proportional to $T^{1/2}$ (8). It is the familiar parabolic-hyperbolic type of function which passes through the origin and may represent curves which are

concave upward or downward, according to whether n is greater than or less than 1, but which possess no point of inflection. It may also be written as:

$$\mu = \mu_0 \left(\frac{T}{T_0} \right)^n$$

where μ_0 and T_0 designate some standard reference condition such as 273°K. The constant a is then obviously equal to

$$\mu_0 \left(\frac{1}{T_0} \right)^n$$

Since from equation 1,

$$\log \mu = n \log T + \log a \quad (2)$$

a plot of $\log \mu$ vs. $\log T$ should be a straight line of slope equal to n and ordinate intercept equal to $\log a$. Several $\log \mu$ vs. $\log T$ plots are shown in figure 3.

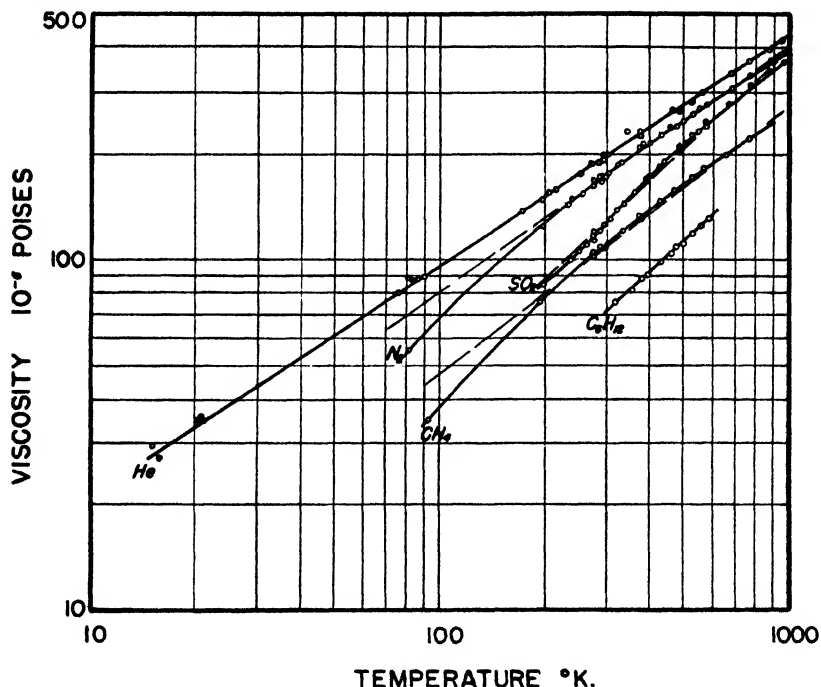


FIG. 3. Rectification of data for the exponential equation

For a few substances, such as helium and cyclohexane, perfectly straight lines were obtained. For most gases, such as nitrogen, sulfur dioxide, and methane, the lines were somewhat curved. For these gases the constants were evaluated as from the dashed straight lines shown in the figure. The values of the constants so obtained are tabulated in table 1, together with the range of tempera-

ture investigated for each gas. These ranges are much wider than those commonly given in handbooks when values of a and n are quoted.

It is to be noted that values of n range from 0.65 to 1.1 and that many of them are very nearly equal to 1.0. This is in accord with Trautz's property which, when applied to the exponential equation, predicts that $n = 1$.

For

$$\left. \frac{d\mu}{dT} \right|_{T_c} = anT_c^{n-1}$$

and

$$\frac{\mu_c}{T_c} = aT_c^{n-1}$$

whence for

$$\left. \frac{d\mu}{dT} \right|_{T_c} = \frac{\mu_c}{T_c}$$

$n = 1$.

The average accuracy of the exponential equation was found to be within 1.8 per cent overall, with the values for the individual gases ranging from 0.4 per cent for acetylene to 5.4 per cent for hydrogen. For those gases for which it is sufficiently accurate, the exponential equation may be used for computation in the form of the simple alignment chart proposed by Generaux (3) and published on page 791 of the second edition of Perry's *Chemical Engineers' Handbook* (10).

Sutherland's equation

Sutherland (13) realized that molecular forces of attraction play an important part in molecular phenomena and cannot be neglected as is done in the simple kinetic theory. By taking into account the increased rate of collision between molecules due to these forces, he derived an expression of the form:

$$\mu = \frac{KT^{3/2}}{T + C} \quad (3)$$

where K and C are constants characteristic of each gas. This may also be written in the alternate forms:

$$\mu = \frac{KT^{1/2}}{1 + \frac{C}{T}} \quad (4)$$

and

$$\frac{\mu}{\mu_0} = \left[\frac{T_0 + C}{T + C} \right] \left[\frac{T}{T_0} \right]^{3/2} \quad (5)$$

where again μ_0 and T_0 designate a reference point, which may be 273°K. In this latter form (5) the equation is usually given in the handbooks, together with values of μ_{273} and C for various gases. Here K is obviously replaced by

$$\frac{\mu_0(T_0 + C)}{T_0^{3/2}}$$

The general form of the function may best be demonstrated by choosing T_0 in equation 5 as the critical temperature T_c and μ_0 as the viscosity at the critical

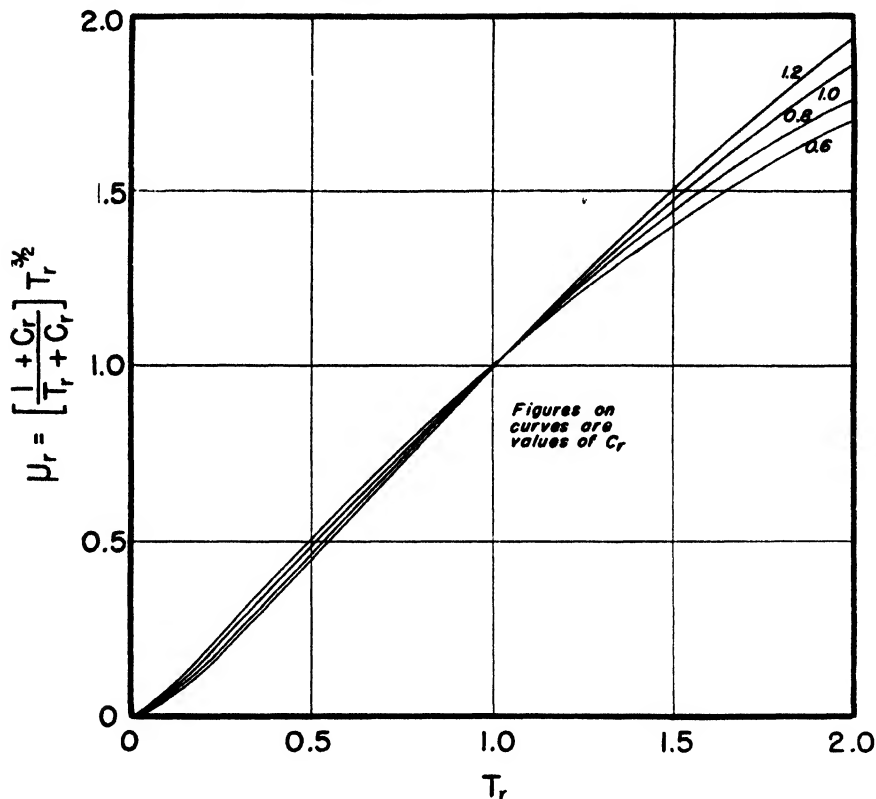


FIG. 4. The general reduced form of Sutherland's equation

temperature and 1 atmosphere pressure, μ_c . Note that this is not the viscosity at the critical point. The form of expression 5 then becomes

$$\frac{\mu}{\mu_c} = \left[\frac{T_c + C}{T + C} \right] \left[\frac{T}{T_c} \right]^{3/2}$$

and, using the familiar designation of subscript r for a "reduced" quantity, we may then write:

$$\mu_r = \left[\frac{1 + C_r}{T_r + C_r} \right] T_r^{3/2} \quad (6)$$

where $C_r = C/T_c$. Figure 4 shows a family of curves for this function for various values of the parameter C_r .

It is evident from equation 3 that C has the dimension of an absolute temperature and as such should be limited to positive values. Detrick (1) has shown, however, that under condition of higher pressure C may take on negative values and the function will represent certain experimental data quite well.

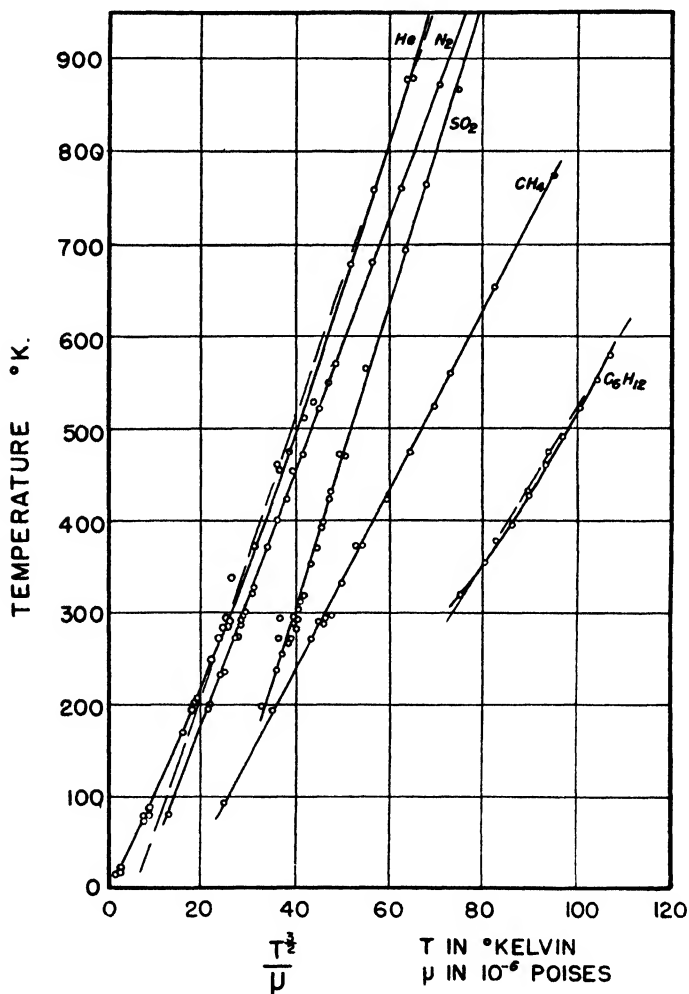


Fig. 5. Rectification of data for Sutherland's equation

The form of equation 3 is such that it possesses a minimum point and a point of inflection. Setting the first derivative equal to zero yields $T = 0$ and $T = -3C$ as minimum points. The first value is of trivial significance and the second important only when C is negative. Setting the second derivative equal to zero shows that a point of inflection is present at $T = C(-3 \pm 2\sqrt{3})$, or

at $T = 0.464C$ and $T = -6.464C$. It has been noted that such a point of inflection is actually observed in the experimental data for some substances.

To evaluate the constants K and C , equation 3 may be written as

$$T = K \left[\frac{T^{3/2}}{\mu} \right] - C \quad (7)$$

and values of T vs. $\frac{T^{3/2}}{\mu}$ plotted. A straight line should result, having a slope K and an ordinate intercept $-C$. Sample plots of this type are shown in figure 5.

TABLE 2
Values of critical constants

SUBSTANCE	M	T_c	P_c	G	SUTHERLAND'S CONSTANTS	
					C	$C_r = \frac{C}{T_c}$
		^{°K.}	atmospheres			
Acetone.....	58.08	508	47	35.2	530	1.043
Acetylene.....	26.04	309.2	61.6	30.6	206	0.668
Ammonia.....	17.03	405.6	111.5	35.1	472	1.164
Argon.....	39.94	151.2	48	36.1	133	0.881
Benzene.....	78.11	562	47.7	40.2	403	0.718
Bromine.....	79.92	575	98.3*	65.9	517	0.900
Carbon dioxide ..	44.01	304.1	73.0	44.6	233	0.766
Carbon tetrachloride..	153.84	556	45.0	54.3	335	0.602
Cyclohexane ..	84.16	554	40.4	37.9	319	0.575
Diethyl ether.....	74.12	467	35.5	33.4	349	0.746
Ethyl acetate.....	88.10	523	37.8	37.5	425	0.813
Ethyl alcohol.....	46.0	516	63.1	37.9	400	0.775
Ethylene.....	28.05	283	50.9	28.2	232	0.821
Helium.....	4.00	5.3	2.26	2.60	97.6	18.4
Hydrogen ..	2.02	33	12.8	4.34	70.6	2.12
Hydrogen chloride.....	36.46	324	81.6	43.4	359	1.107
Mercuric chloride.....	271.52	976			996	1.021
Mercury.....	200.61	1600			996	0.623
Methane.....	16.04	190	45.8	21.3	155	0.813
Methyl chloride.....	50.49	416	65.8	42.4	390	0.938
Nitrogen.....	28.02	126	33.5	24.6	102	0.809
Nitrous oxide.....	44.02	309.5	71.7	43.9	273	0.881
Oxygen ..	32.00	154	49.7	32.8	110	0.712
Sulfur dioxide.....	64.06	430	77.7	52.6	362	0.842
Toluene.....	92.13	593	41.6	39.9	365	0.614
Water vapor.....	18.02	647	217.7	52.2	659	1.018

* Value estimated by the method of Meissner and Redding (9).

For most substances—e.g., nitrogen, sulfur dioxide, and methane—very good straight lines were obtained. For a few, such as hydrogen, helium, and cyclohexane, the lines connecting the points were more or less curved. For hydrogen and helium this curvature was very marked at low temperatures. The nearest straight line was drawn, however, similar to the dashed lines in figure 5, and the best constants were evaluated. The values of the constants K and C

obtained are tabulated in table 1. In addition, values of C_r for use in connection with equation 6 are tabulated in table 2. Again it is to be noted that these constants are based upon as wide a temperature range as experimental data could be found to cover. Their applicability is for much greater ranges than for the constants usually quoted in handbooks.

The values of C_r found all lie within a range of 0.6 to 1.0 (with the exception of those for hydrogen and helium), with an average value of about 0.8. This suggested the possibility of the "universal" viscosity equation which is described below. These values of C_r (and C) are roughly in accord with Trautz's property, for when it is applied to equation 3 a value of $C_r = 1$ is predicted. For

$$\left. \frac{d\mu}{dT} \right|_{T_c} = \frac{KT_c^{1/2}}{T_c + C} \left[\frac{3}{2} - \frac{T_c}{T_c + C} \right]$$

and

$$\frac{\mu_c}{T_c} = \frac{KT_c^{1/2}}{T_c + C}$$

so that in order for

$$\left. \frac{d\mu}{dT} \right|_{T_c} \text{ to equal } \frac{\mu_c}{T_c}, \quad \frac{3}{2} - \frac{T_c}{T_c + C} \text{ should equal 1 and}$$

$$T_c = C \quad \text{or} \quad \frac{C}{T_c} = C_r = 1$$

Sutherland stated that the assumptions on the basis of which he derived his equation were such as to limit its validity to pressures at which Boyle's law holds, and to temperatures above the critical. Since all data studied were for atmospheric pressure the first condition is fulfilled, but for almost all of the substances the wide temperature range investigated includes values both above and below the critical temperature. This, however, proved to be no restriction on the applicability of equation 3, for it was found to possess an average overall error of only 1.3 per cent. Individual average errors varied from 0.2 per cent for hydrogen chloride to 9.5 per cent for helium. If hydrogen (error 5.1 per cent) and helium, the notorious exceptions, are excluded, the overall average error is only 0.8 per cent with the maximum individual error being 2.4 per cent for ammonia.

Quantitatively the agreement for the points of inflection is not good. As nearly as can be determined, this experimental point for bromine occurs at about 450°K., while the value of $0.464C$ is 240°K. For sulfur dioxide the experimental value is about 350°K., while the value of $0.464C$ is 168°K.

Reinganum's equation

Reinganum (11) derived a viscosity-temperature function upon the same basis as Sutherland, arriving at an expression:

$$\mu = \frac{K'T^{1/2}}{e^{C'/T}} \quad (8)$$

which he believed to be a more accurate form of Sutherland's equation. His reason for this belief lay in the fact that the denominator of his equation may be expanded in a series

$$e^{C'/T} = 1 + \frac{C'}{T} + \frac{C'^2}{2!T^2} + \frac{C'^3}{3!T^3} + \frac{C'^4}{4!T^4} + \dots$$

The first three terms of this series may be written:

$$1 + \frac{C'}{T} + \frac{D'}{T^2}$$

where it is evident that C' and D' are positive constants, since μ increases with T for all gases and D' is replacing a term in C' squared. However, Vogel (17) showed in fitting data to the three-constant equation:

$$\mu = \frac{KT^{1/2}}{1 + \frac{C}{T} + \frac{D}{T^2}}$$

which may be regarded as a simplification of equation 8, that C is inherently positive and D inherently negative. This was also observed by Stechert (12) for hydrogen and helium. Hence the terms in the series in the denominator would seem to have alternating signs, when applied to actual data. This would not be the exponential series given above, then, since there the first three terms are all positive, indicating that Reinganum's equation could not be a more accurate form of Sutherland's, i.e., that the denominator in Sutherland's equation is not merely the beginning of the exponential series. This was found to be the case when Reinganum's equation was actually tested.

The general form of equation 8 may be shown to be similar to equation 3. It has a minimum point only at $T = 0$, and a point of inflection at $T = C'(-2 \pm 2\sqrt{2})$ or $0.828C'$ and $-4.828C'$. Again, however, the prediction of the point of inflection is only qualitative, the agreement with actual data being about as good as in the case of Sutherland's equation.

To determine the constants K' and C' , equation 8 may be written:

$$\log \frac{T^{1/2}}{\mu} = \frac{C'}{2.303} \left[\frac{1}{T} \right] - \log K' \quad (9)$$

A plot of $\log \frac{T^{1/2}}{\mu}$ vs. $\frac{1}{T}$ should be a straight line having a slope of $C'/2.303$ and ordinate intercept of $-\log K'$. Plots of this type were made as for the other relationships. In all cases the points scattered badly, but again the best lines were drawn and the constants determined. Since the results were so poor, none of the constants is tabulated nor sample plots shown.

The average overall error was found to be 2.6 per cent, with individual errors ranging from 0.2 per cent for acetylene to 12.3 per cent for helium. Again, hydrogen and helium were by far the worst exceptions. If they are omitted

from consideration the average error is 1.8 per cent, the maximum individual error being 3.3 per cent for methane.

Trautz's equation

Trautz (15) attacked the problem of a viscosity-temperature function from a so-called thermodynamic viewpoint rather than that of the kinetic theory. He made use of the property that

$$\left. \frac{d\mu}{dT} \right|_c = \frac{\mu_c}{T_c}$$

based his work on the properties of ideal gases, and assumed that all states of a gas between $T = \infty$ and $T = 0$ may be represented as equilibrium mixtures of forms existing at these limiting temperatures. Using the results of Trautz's work, Stechert (12) derived the following simplified expression

$$\mu = bT(T_r^{3/4} + T_r^{-3/4})^{-d} \quad (10)$$

hereafter referred to as Trautz's equation.

The quantities b and d are constants characteristic of each gas. It is evident that they are related by

$$b = \frac{2^d \mu_c}{T_c}$$

when equation 10 is considered at the critical temperature. Substituting this expression for b leads to an alternate form of Trautz's equation:

$$\mu_r = 2^d T_r (T_r^{3/4} + T_r^{-3/4})^{-d} \quad (11)$$

in which the variables appear in the reduced form. The Law of Corresponding States does not apply in equation 11, however, for d is still a characteristic constant of the gas.

The general form of equation 11 is displayed in figure 6 in the form of a family of curves for various values of the parameter d . It would seem from Trautz's derivation that d must be inherently positive, but Detrick (1) has shown that on occasion negative values of d are found which permit the function to fit certain data at higher pressures very well. At atmospheric pressure, however, the values of d are positive and small, and generally less than 1. The wide variety of curve forms which this versatile function may represent, as illustrated in figure 6, is truly amazing.

The unique points of equation 11 are found in the usual manner. Setting the first derivative equal to zero yields

$$T_r = \left[\frac{3d + 4}{3d - 4} \right]^{2/3}$$

which is a maximum or minimum point according to whether d is positive or negative. Note that when $d = 4/3$ this maximum occurs at infinity. The

points of inflection are given by

$$T_r = \left[\frac{5 + 3d}{(7 + 3d) \pm \sqrt{16 + 9d}} \right]^{2/3}$$

obtained by setting the second derivative equal to zero. There are two such points on the curve provided $d > -16/9$; otherwise they are imaginary. The curves in figure 6 also show these various possibilities in regard to the unique points.

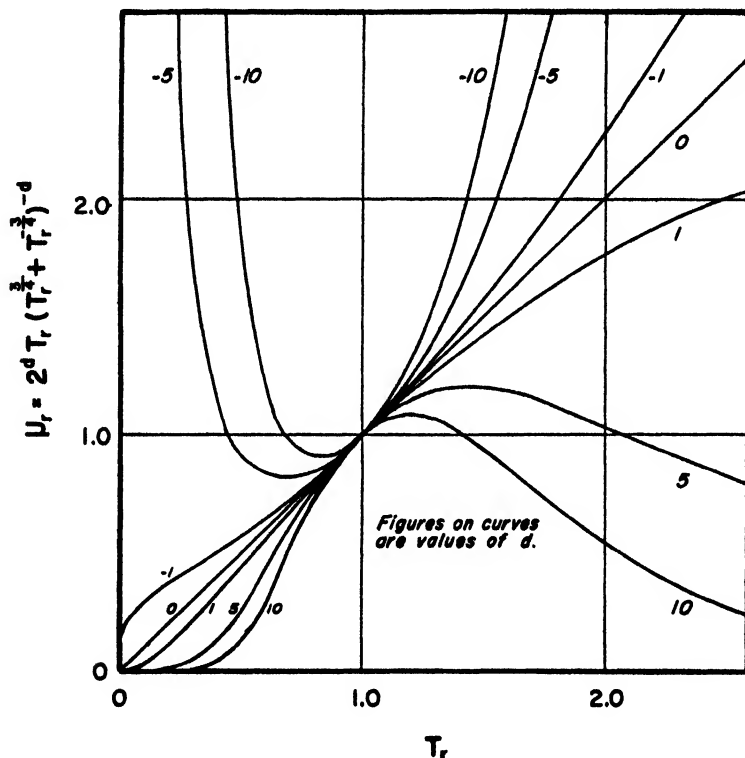


FIG. 6. The general reduced form of Trautz's equation

For purposes of determining b and d , equation 10 may be written

$$\log \frac{\mu}{T} = -d \log (T_r^{3/4} + T_r^{-3/4}) + \log b \quad (12)$$

A plot of $\log \frac{\mu}{T}$ vs. $\log (T_r^{3/4} + T_r^{-3/4})$ should be linear with a slope of $-d$ and an ordinate intercept of $\log b$. Owing to the properties of the function $(T_r^{3/4} + T_r^{-3/4})$, this is a rather peculiar type of plot. This function has a minimum value of 2 when $T_r = 1$, i.e., at the critical temperature; consequently its logarithm has a minimum value of $\log 2$ or 0.3010 at this point. Either above or

below $T_r = 1$ the function increases to infinity at $T_r = 0$ and $T_r = \infty$, the logarithm doing likewise. Hence any plot of actual data covering the range on both sides of the critical temperature must "double back" on itself if Trautz's equation is followed. That is, on the same straight line at a given point for a given value of the function $(T_r^{3/4} + T_r^{-3/4})$, two points of values to T_r and μ must be represented.

For all of the gases investigated plots of this type were made. As samples, the plots for a few of the gases are shown in figure 7. The points scattered more

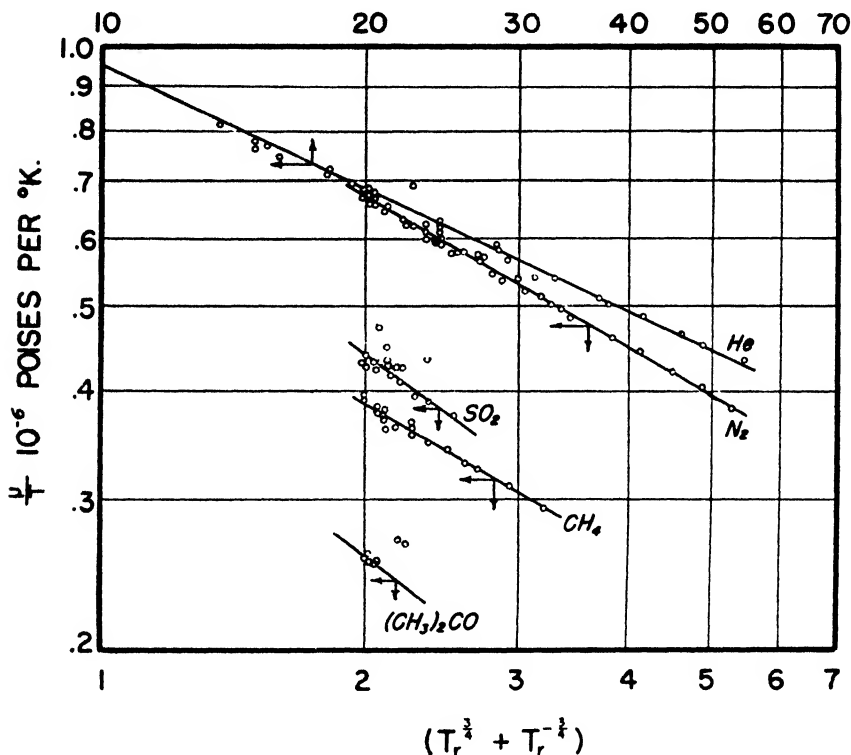


FIG. 7. Rectification of data for Trautz's equation

or less for all substances, and the line did not double back upon itself exactly, as described above. The best straight lines were drawn, however, and the constants determined. These are given in table 1, being valid for the same wide range of temperatures as the constants determined for the other equations investigated.

The average overall error found for Trautz's equation was 1.4 per cent, with individual errors ranging from 0.3 per cent for ethyl acetate to 3.8 per cent for carbon tetrachloride. For hydrogen and helium, it fits the data within an average of 1.2 per cent and 0.8 per cent, respectively. The agreement on points of inflection is not too good, although it is closer than any of the other equations

tested: for bromine 355°K. as against 450°K. actually observed, and for sulfur dioxide 276°K. as against 350°K. observed.

COMPARISON OF RESULTS

A comparison of the general overall percentage error figure shows:

Equation	Per cent error
Exponential.....	1.8
Sutherland's.....	1.3
Reinganum's.....	2.6
Trautz's.....	1.4

from which it would seem that Sutherland's equation is a shade better than Trautz's for representing the actual data. However, it must be borne in mind that hydrogen and helium are outstanding exceptions in the case of all the equations but Trautz's and that when they are not included the average errors are:

Equation	Per cent error
Exponential.....	1.7
Sutherland's.....	0.8
Reinganum's.....	1.8
Trautz's.....	1.4

Hence for the large majority of substances, Sutherland's equation is far and away the most satisfactory. The percentage error for Trautz's equation is not altered by omitting hydrogen and helium, a fact which indicates that it fits the data for all the other substances to about the same accuracy as it does for these two. Reinganum's equation is clearly shown to be a more inaccurate rather than a more accurate form of Sutherland's equation and not worthy of further consideration. These conclusions are valid only for low pressures, however. Some work by Detrick (1) would seem to indicate that at higher pressures they no longer hold and that Trautz's equation may be more generally suitable than the above figures would indicate.

The constants tabulated in table 1 may be used with confidence in computing the viscosity of any of the substances over a wide range of temperatures. Although they have been determined by a graphical method, the small errors found between computed and experimental data and the great extent of the actual data used to construct the plots would seem to insure that they cannot be far wrong. It is recommended that Sutherland's equation be used for all the gases except hydrogen and helium, and that Trautz's equation be used for them.

There have been a number of investigations in the past concerned with viscosity-temperature relationships of gases and vapors (2, 14, 18). All of these have been of limited scope, both as to the data used and as to the range

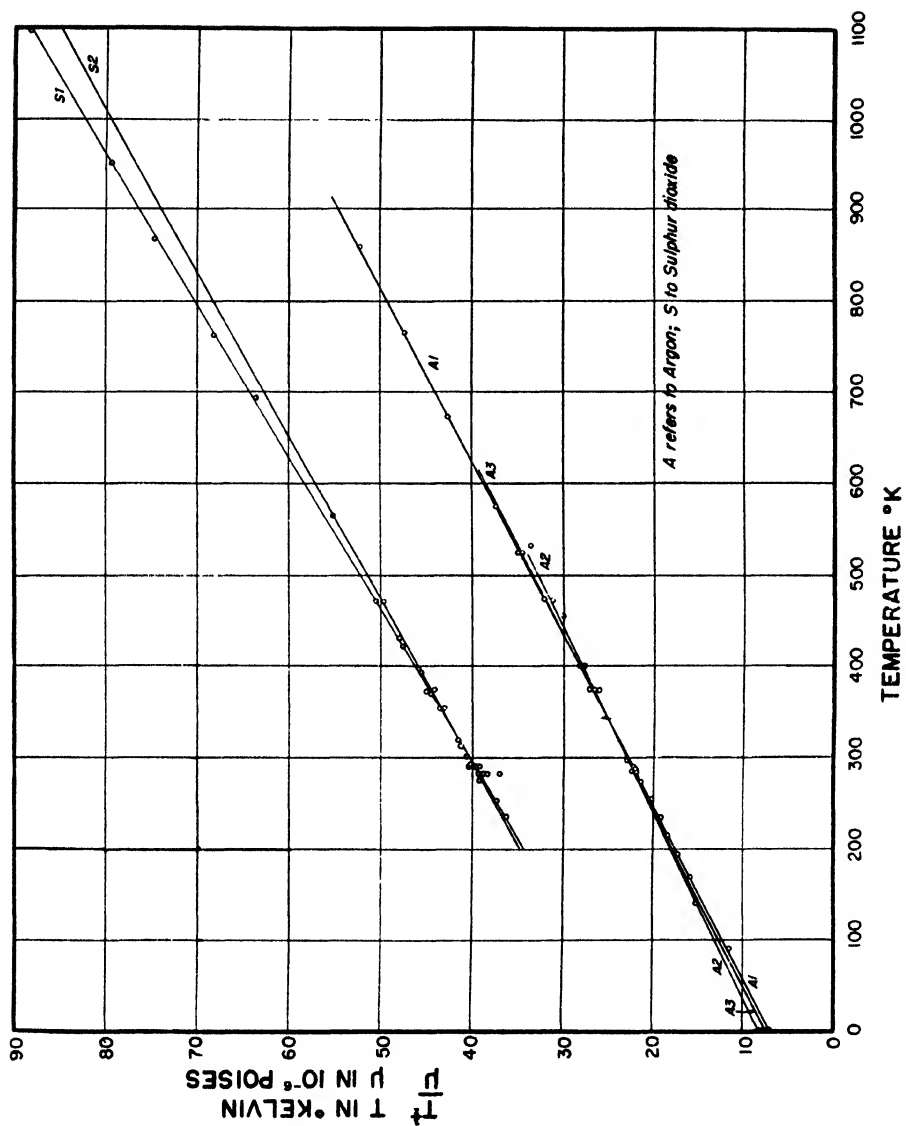


FIG. 8 The agreement with experimental data of the rectified form of Sutherland's equation, using various sets of constants

of temperature considered. Usually they have been based upon the data of a single experimenter working in the region of room temperature. Those quoted in the second edition of Perry's *Chemical Engineers' Handbook* (10), for example, are for the most part limited to the range of 15°C. to 100°C. In some cases two different values of constants are given for somewhat different temperature ranges for the same substance. It is unnecessary to use more than a single value of the constants: Sutherland's constants have been shown to apply very closely over the entire range investigated except in the cases of hydrogen and helium. For these two substances Trautz's equation may be used with similar confidence.

The values of the Sutherland constants K and C given in this article are thought to be more generally applicable than any heretofore published. This is illustrated by a comparison with some of the values given in Perry's *Chemical Engineers' Handbook* as cited above, in figure 8. The comparison is made by plotting the actual data in the linear form of Sutherland's equation (7)—namely, T vs. $\frac{T^{3/2}}{\mu}$ —and then drawing the straight lines of this form as specified by the values of the constants under consideration. For example, in the case of argon the line obtained by the authors has the equation

$$T = 19.0 \times 10^{-8} \frac{T^{3/2}}{\mu} - 133$$

(marked A1 in figure 8) valid for -183°C. to 827°C. The line obtained using one set of constants quoted by Perry, valid from 15°C. to 184°C., has the equation

$$T = 20.6 \times 10^{-8} \frac{T^{3/2}}{\mu} - 170$$

(marked A2) and the line obtained from the other set of values quoted by Perry, valid from 20°C. to 100°C., has the equation:

$$T = 19.5 \times 10^{-8} \frac{T^{3/2}}{\mu} - 147$$

(marked A3). As may be seen from the figure, the line marked A1 gives excellent agreement with the data throughout the entire range. The lines marked A2 and A3 seem to fit fairly well in the range of 0°C. to 100°C., but no better than A1. Outside this range their agreement is poor. In fact, A3 is better than A2 in the range up to 184°C. for which A2 is supposed to hold.

In the case of sulfur dioxide, also shown in figure 8, the line marked S1 as obtained by the authors has the equation:

$$T = 16.5 \times 10^{-8} \frac{T^{3/2}}{\mu} - 362$$

valid from -75°C. to 823°C. , and is seen to fit the experimental points very well. However, the line obtained from the constants quoted in Perry's *Handbook* has the equation:

$$T = 17.8 \times 10^{-6} \frac{T^{3/2}}{\mu} - 416$$

and is stated to be valid only from 18°C. to 100°C. It may be seen that it does indeed fit the data in this region but that at higher temperatures the disagreement becomes very marked.

Similar results were obtained when others of the list of substances were tested. It must be borne in mind, however, that in some cases the data are not too good, i.e., they scatter somewhat about the best straight line which may be drawn. However, the precision of measurements was felt to be such that application of the method of least squares to find the constants of the lines was not warranted.

Similar comparisons were made for the exponential constants and it was also found that those given in this article are more generally applicable than any heretofore published.

ESTIMATION OF VISCOSITY WITHOUT EXPERIMENTAL DATA

Since Sutherland's equation was found to fit actual data so well, it seemed that an analog of the Law of Corresponding States² might be applied to it in the hope of finding a universal equation which could be applied to substances for which there is little or no experimental viscosity data available. Using equation 6 in the form

$$\mu = \mu_c \left[\frac{1 + C_r}{T_r + C_r} \right] T_r^{3/2} \quad (13)$$

where

$$C_r = \frac{C}{T_c}$$

the value of C_r should be a universal constant if the pseudo Law of Corresponding States² applies. Values of C_r are tabulated in table 2. It may be seen that almost all of these values lie between 0.6 and 1.0, with the exception of hydrogen and helium, and further the average value is about 0.8. The important point, however, is not the constancy of C_r but the effect of variations in it upon the function

$$F(T_r) = \left[\frac{1 + C_r}{T_r + C_r} \right] T_r^{3/2}$$

It was found that for values of T_r from 0.0 to 5.0, values of $F(T_r)$, with C_r ranging from 0.6 to 1.0, agree within 8 per cent at the extremes with values when

² This is not really the Law of Corresponding States, because μ_c is not at the critical point but is the viscosity at atmospheric pressure and the critical temperature.

C_r is taken at 0.8. In the range of T_r from 0.6 to 2.0, which is usually of most interest, the maximum deviation is 4 per cent. Hence the function $F(T_r)$ with $C_r = 0.8$ may be used with a good degree of accuracy for any of the gases tested, always excepting hydrogen and helium.

It remains to be able to compute μ_c from readily available data. Trautz has shown that μ_c may be represented as a function of the molecular weight M , the critical pressure P_c , the critical temperature T_c , and the gas constant R . Dimensional analysis indicates that the form of the function should be

$$\mu_c = \text{constant} \left[\frac{M^3 P_c^4}{T_c R} \right]^{1/6}$$

which may be written more compactly as

$$\mu_c = k \left[\frac{M^3 P_c^4}{T_c} \right]^{1/6} = kG \quad (14)$$

where k is a dimensional constant including R , and G is a constant characteristic of the substance as defined by equation 14.

Values of G and K were computed for twenty-three of the twenty-six gases on the list, data for the critical values of bromine, mercury, and mercuric chloride not being available. Values of G are given in table 2 and are based upon viscosity in poises, pressure in atmospheres, and absolute temperatures in degrees Kelvin. With the aid of these and experimental values of μ_c , the value of k was computed from the data for each gas, and the values were compared for universality. With the exception of four substances—ethyl alcohol, water, ammonia, and helium (here hydrogen is *not* an exception)—the values clustered very closely around an arithmetic mean of 3.50×10^{-6} . This value is also in agreement with Trautz's data. If the values for the above four substances are included, the average is 3.61×10^{-6} . It would seem advisable, however, to use the former value for any other gas to be encountered, since the exceptions are notorious non-conformists to most laws.

Using equation 14 as

$$\mu_c = 3.50 \times 10^{-6} G$$

the computed and experimental values of μ_c were compared. Of the twenty-three gases tested, eight agree within 2 per cent, seventeen within 5 per cent, nineteen within 10 per cent, and all within 21 per cent. These results would indicate, then, that equation 13 may be considered fairly reliable when written in the form:

$$\mu = 3.50 \times 10^{-6} G f(T_r)$$

or, gathering up all the constants,

$$\mu = 6.30 \times 10^{-6} G f(T_r) \quad (15)$$

where

$$f(T_r) = \frac{T_r^{3/2}}{T_r + 0.8}$$

which is independent of the substance. This may be regarded as a universal viscosity equation, which may be used for estimating the viscosity of any gas provided only that its critical temperature and pressure and its molecular

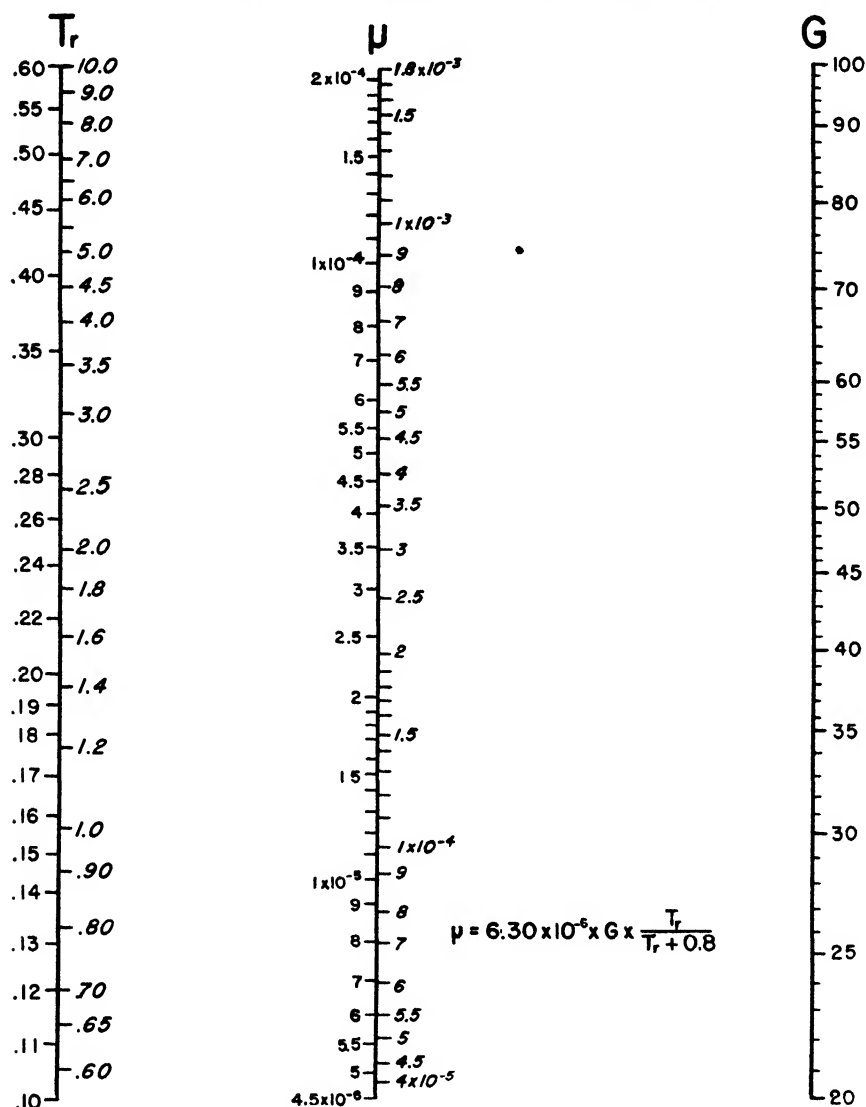


FIG. 9. Nomograph for solving the universal viscosity equation. For $0.10 < T_r < 0.60$, use left side of T_r and μ scales. For $0.60 < T_r < 10.0$, use right side of T_r and μ scales. μ in poises. G determined from table 2.

weight be known. Even if critical data are lacking, they may be estimated by methods such as those described by Meissner and Redding (9). The equation is readily adapted to computation by means of a nomograph which is

presented in figure 9. Note that this is only valid for values of the various quantities when expressed in the specified units.

Since the errors introduced by taking the average values of C_r and k as universal may happen to compensate one another, the final accuracy of equation 15 may be better than the above discussion would lead one to believe. This was found to be the case when it was tested. In general it is reliable within 5 to 10 per cent, with the outstanding exceptions mentioned above, and in some cases to better than 2 per cent. It is therefore offered as a means for estimating viscosity data when no experimental data can be found, or when it is inconvenient to make actual determinations.

OTHER EQUATIONS

In addition to the four two-constant equations discussed above, there have been proposed several of a more complex nature involving three or more constants. These equations were not submitted to the same general test as the others for several reasons. In general, ease in using an equation for computation is very desirable; if a simple equation will reproduce data accurately, there is little need (except in some special cases) for a more complicated equation which may represent the data only slightly better. Further, in an equation of greater complexity it is often quite difficult to evaluate the constants, and when such an equation contains three or more constants, these are frequently dependent on each other, making it impossible to determine them uniquely. For the sake of completeness, however, several other equations are reviewed briefly.

In the discussion under Reinganum's equation it was indicated that a modified form of Sutherland's equation, containing three constants, was

$$\mu = \frac{KT^{1/2}}{1 + \frac{C}{T} + \frac{D}{T^2}}$$

when the denominator was regarded as the beginning of an infinite series. Vogel (17) found that this formula represents data for many gases more accurately than Sutherland's two-constant equation, but the data he used were of limited extent.

Similarly, through the introduction of a third constant, Reinganum's equation may be made to represent experimental data with greater accuracy in the form:

$$\mu = \frac{K' T^{1/2}}{e^{\frac{C'}{T+a}}}$$

Vogel (17), however, claims that this is no more accurate than the modified Sutherland equation.

Hassé and Cook (4) derived an expression for the viscosity-temperature function on the basis of an assumption of a rather general type of intermolecular force field. It was assumed that molecules repel one another according to an

inverse s -power law and attract one another according to an inverse m -power law. The resulting expression is:

$$\mu = \frac{QT^{\left(\frac{1}{2} + \frac{2}{s-1}\right)}}{1 + UT^{\left(\frac{m-s}{s-1}\right)}}$$

where s , m , Q , and U are characteristic constants. The choice of numerical values for m and s is largely a matter of trial and error. For hydrogen, argon, nitrogen, carbon dioxide, and mercury vapor, good agreement with experimental data was obtained with $m = 5$ and $s = 9$, so that the general formula becomes:

$$\mu = \frac{QT^{5/4}}{T^{1/2} + U}$$

For neon the constants $m = 5$ and $s = 3$ were found to be best, so that:

$$\mu = \frac{QT^{4/3}}{T^{2/3} + U}$$

Hassé and Cook found that their equation represents the data for hydrogen and argon from 20°K. to 460°K. with a possible error of about 1 per cent.

The generality of this equation is remarkable. By putting U , the attractive force constant, equal to zero the exponential equation is obtained; by making s tend to infinity so that the repulsive field vanishes, Sutherland's equation is obtained. By setting $m = 3$, an equation first proposed by Jones (5) results:

$$\mu = \frac{JT^{3/2}}{T^{\left(\frac{s-3}{s-1}\right)} + S}$$

wherein s , J , and S are characteristic constants. Again, it is not possible to determine the values of either s or S uniquely. In the case of argon equally good agreement is obtained for $s = 21$ and $S = 62.44$ as for $s = 14.33$ and $S = 38.62$. The only way of determining the constants is by trial and error. For hydrogen and helium this equation is no more accurate than the exponential equation $\mu = aT^n$.

Trautz and Binkele (16) empirically combined the exponential equation and Sutherland's equation to obtain the formula

$$\mu = \frac{aT^n}{1 + \frac{C}{T}}$$

It is claimed (6) that this formula can be made to fit data more accurately than either of the original formulas, or over a much wider range. The constants must be found by trial and error. The equation can be fitted to within 1 per cent over the entire range of experimental data for helium, neon, hydrogen, and

nitrogen, but it cannot be fitted satisfactorily to the data for argon and carbon dioxide.

Of all these more complicated functions, that of Hassé and Cook would seem to be the most promising for future study. It may be that some correlation between values of the constants m and s and the structure of the molecule exists. In this way it might be possible to predict these values without having experimental data. Until the objections to these more elaborate equations have been overcome, however, there seems to be no advantage to using any equation other than Sutherland's (except for hydrogen and helium, for which Trautz's equation is suitable), since it has been found to hold so well.

SUMMARY

This study has led to the following conclusions:

For twenty-four representative gases and vapors at atmospheric pressure Sutherland's equation has been found to fit extensive experimental data with an average error of less than 1 per cent and to be valid over as wide a range of temperature as has been employed in these measurements.

Only two exceptions have been found to this statement: hydrogen and helium. For representing data in these two cases, Trautz's equation has been found to hold with an accuracy comparable to that of Sutherland's equation.

Methods of treating experimental data to evaluate the constants in the various two-constant equations have been developed. It is only necessary to have two experimental points on the viscosity-temperature curve in order to determine these constants.

For practical use, values of the constants K and C in Sutherland's equation and b and d in Trautz's equation have been determined. These are based upon extensive data of many investigators and covering wide ranges of temperature. They are believed to be the most generally applicable set of constants yet offered in the literature.

For estimating values of viscosity when no experimental data are available, a universal viscosity-temperature function has been developed. It is capable of being used in the form of a nomograph, which is presented.

Other more complicated viscosity-temperature functions have been reviewed and found not to warrant detailed investigation insofar as evaluating a set of constants for substances is concerned.

The charts and nomograph were constructed for publication by Mr. Charles J. Boegli. The authors wish to express their appreciation of his assistance.

REFERENCES

- (1) DETRICK, J. K.: "The Variation of the Viscosity of Gases with Pressure", M. S. Thesis, University of Cincinnati, 1942.
- (2) FISHER, W. J.: *Phys. Rev.* **24**, 385-401 (1907).
- (3) GENERAUX, R. P.: *Ind. Eng. Chem.* **22**, 1382 (1930).
- (4) HASSÉ, H. R., AND COOK, W. R.: *Proc. Roy. Soc. (London)* **A125**, 196 (1929).
- (5) JONES, J. E.: *Proc. Roy. Soc. (London)* **A106**, 441 (1924).

- (6) KENNARD, E. H.: *Kinetic Theory of Gases*, p. 157. McGraw-Hill Book Co., Inc., New York (1938).
- (7) LANDOLT-BÖRNSTEIN: *Physikalisch-Chemische Tabellen*, 5th Edition. Julius Springer, Berlin, Volume I, p. 171 (1923); Volume I, Supplement 1, p. 143 (1927); Volume I, Supplement 2, p. 1137 (1931); Volume I, Supplement 3, p. 173 (1935).
- (8) LOEB, L. B.: *Kinetic Theory of Gases*, 2nd Edition, p. 215. McGraw-Hill Book Co., Inc., New York (1934).
- (9) MEISSNER, H. P., AND REDDING, E. M.: *Ind. Eng. Chem.* **34**, 521 (1942).
- (10) PERRY, J. H.: *Chemical Engineers' Handbook*, 2nd Edition, p. 792. McGraw-Hill Book Co., Inc. (1941).
- (11) REINGANUM, M.: *Physik. Z.* **2**, 241 (1900).
- (12) STECHERT, D. G.: "Variation of the Viscosity of Gases with Temperature", M. S. Thesis, University of Cincinnati, 1941.
- (13) SUTHERLAND, W.: *Phil. Mag.* **36**, 507 (1893).
- (14) TITANI, T.: *Bull. Chem. Soc. Japan* **8**, 255 (1933).
- (15) TRAUTZ, M.: *Ann. Physik* **11**, 190 (1931).
- (16) TRAUTZ, M., AND BINKELE, H. E.: *Ann. Physik* **5**, 561 (1930).
- (17) VOGEL, H.: *Ann. Physik* **43**, 1235 (1914).
- (18) WOBSE, R., AND MUELLER, F.: *Kolloid-Beihefte* **52**, 165-276 (1942).

THE VAPOR PRESSURE AND HEAT OF VAPORIZATION OF TRICHLOROETHYLENE

HUGH J. McDONALD

Department of Chemistry, Illinois Institute of Technology, Chicago, Illinois

Received September 15, 1943

The vapor pressure of trichloroethylene was needed in this laboratory for an investigation of liquid-vapor compositions of mixtures of organic liquids and for a study of the rate of oxidation of the material in the vapor phase. A graphical study of the data in the literature showed considerable disagreement in the numerical values of many of the physical properties of trichloroethylene. It was decided to redetermine the vapor pressure over the range 20°C. to the boiling point.

Herz and Rathmann (3) measured the vapor pressure over the temperature range 25°C. to the boiling point (87.15°C. at 760 mm. of mercury) by distillation under vacuum, but the difficulties inherent in securing reliable data by this method, partly due to superheating of the liquid, are such that it is well to have the values checked by an independent procedure. Other determinations of the boiling point have given values of 86.95 (8), 86.7 (1), 87.0-87.2 (5), 87.4 ± 0.1 (10), and 86.60°C. (at 758 mm.) (9).

Values of the heat of vaporization reported include 57.24 ± 0.03 cal. per gram, determined calorimetrically by Mathews (5) at 85.69°C., 58 cal. per gram determined by Carlisle and Levine (1), and 7436 cal. per mole calculated by Herz and Rathmann (3) from their vapor-pressure data between 77° and 87°C.

Weissberger and Proskauer (11), Mellan (6), and Churchill (2) list some of the key references to the physical constants of trichloroethylene.

MATERIAL

The best grade of trichloroethylene obtainable from the Eastman Kodak Co., having a boiling range of 86–87°C., was distilled through a Ewell fractionating column having an equivalent of twenty theoretical plates. The middle portion of the material distilling over, amounting to about 40 per cent of the total and having a boiling range within 0.1°C., was used for the experimental work. The test for acidity with 0.01 *N* sodium hydroxide and phenolphthalein, as recommended by Carlisle and Levine (1), was negative. The refractive index of the liquid as determined by an Abbe refractometer was found to be 1.4767 at 21.4°C., 1.4764 at 22.2°C., 1.4761 at 22.8°C., and 1.4750 at 24.6°C. These values check other refractive-index measurements on the compound, and from them an average molar refractivity of 25.57 over the range 18–27°C. may be calculated in agreement with the value of 25.38 reported by Leithe (4). The variation of the refractive index of trichloroethylene with temperature (°C.) over the range covered by the experimentally determined values (17–27°C.) can be represented by the equation

$$n_D = - 0.0005675t + 1.4890$$

with an accuracy of ± 3 in the fifth significant figure.

APPARATUS

The isoteniscope of Smith and Menzies (7) was used in the vapor-pressure determination. The apparatus was immersed in a water bath fitted with an electrical stirrer. With the system open to the atmosphere, the water bath was heated until the trichloroethylene began to boil and until any dissolved or adhering air was expelled from the space between the main body of the liquid and the trap, and the temperature of the bath was read. For pressures of less than 1 atmosphere, taken as the water bath cooled down, the manometer could be shut off from the system by a stopcock, so that only the temperature reading had to be taken at the moment when the liquid levels in the two arms of the trap were at the same height. The manometer levels were then read by means of a Cenco universal-type cathetometer, which could be read to 0.01 mm.

The thermometer, which was standardized against Bureau of Standards thermometers, could be read directly to 0.05°C., and proper corrections were made in the barometer readings to reduce them to centimeters of mercury at 0°C. and 45° N. latitude.

EXPERIMENTAL DATA

Several preliminary runs were made to improve the design of the equipment and to develop a good technique; then two runs were made carefully. The vapor pressure-temperature data are given in table 1.

When $\log p$ was plotted against $1/T$, the curve was found to be nearly linear, and could be represented by the equation

$$\log p = 30.482609 - 2936.227/T - 7.999975 \log T$$

where p is the vapor pressure in centimeters of mercury and T is the temperature in $^{\circ}\text{K}$.

Over the range of vapor pressure from 5 to 30 cm. of mercury, the vapor pressures calculated from the equation are lower than the values taken from the

TABLE 1
Vapor pressure of trichloroethylene

RUN 1		RUN 2	
t	p	t	p
$^{\circ}\text{K.}$	cm.Hg	$^{\circ}\text{K.}$	cm. Hg
86.32	74.20	86.47	74.25
81.27	63.32	85.82	72.77
79.22	59.31	84.22	69.49
77.95	56.99	81.31	63.18
74.27	50.54	80.38	61.48
71.44	45.84	79.28	59.27
67.19	39.41	78.26	57.44
65.07	36.67	76.93	54.74
57.55	28.06	75.49	52.47
55.86	26.41	72.93	48.22
51.78	22.51	68.05	40.81
46.44	18.24	64.94	36.69
42.41	15.41	63.27	34.65
38.49	12.98	60.50	31.41
34.39	10.72	54.82	25.47
31.20	9.32	51.05	21.95
27.48	7.74	44.51	16.82
24.40	6.61	39.29	13.52
20.99	5.63	30.20	9.00
17.80	4.68	25.50	7.16
		19.85	5.42

smooth curve through the experimental points by an average value of approximately 0.05 cm. of mercury, while over the range of vapor pressure from 40 to 70 cm. of mercury, the vapor pressures calculated from the equation are greater than the values taken from the smooth curve through the experimental points by an average of approximately 0.1 cm. of mercury.

The average deviation between Run 1 and Run 2 over the whole course of the vapor pressure curve is approximately ± 0.03 cm. of mercury.

On extrapolating the curve to a pressure of 76.0 cm. of mercury, the boiling point was found to be 360.37°K. or 87.19°C. By differentiation and substitution in the Clapeyron equation, the expression

$$\Delta H = \frac{p(v_v - v_L)}{T} \cdot (2153.351 - 2.547,992T)$$

is obtained, where ΔH is the heat of vaporization of trichloroethylene, in calories per mole, at the absolute temperature, T ; v_v and v_L are the equilibrium molal volumes of vapor and liquid, respectively, at that temperature; and p is the vapor pressure of the liquid in centimeters of mercury.

Using values of v_L calculated from the density data of Mellan (6) and values of v_v ¹ calculated from the perfect gas laws, the value of the heat of vaporization at 87.19°C., the normal boiling point, was computed to be 7680 cal. per mole, which differs from the calorimetric value of Mathews (5) by 180 cal.

The variation of the density of trichloroethylene with temperature (°C.) over the range covered by the experimentally determined values reported in the literature (0–60°C.) can be represented by the expression

$$d_4^t = -0.001618t + 1.4980$$

with an accuracy of ± 3 in the fourth significant figure.

SUMMARY

The vapor pressure of trichloroethylene was determined over the range 18–86°C. and expressed in the form of an equation, and the heat of vaporization at the boiling point (87.19°C.) and 1 atmosphere pressure was found to be 7679 cal. per mole, with an estimated mean error of ± 100 cal. Equations are given for the variation of density and refractive index with temperature.

REFERENCES

- (1) CARLISLE AND LEVINE: *Ind. Eng. Chem.* **24**, 1164 (1932).
- (2) CHURCHILL: *Refrig. Eng.* **26**, 85 (1933).
- (3) HERZ AND RATHMANN: *Chem.-Ztg.* **36**, 1417 (1912).
- (4) LEITHE: *Z. Elektrochem.* **37**, 623 (1931).
- (5) MATHEWS: *J. Am. Chem. Soc.* **48**, 562 (1926).
- (6) MELLAN: *Industrial Solvents*. Reinhold Publishing Corporation, New York (1939).
- (7) SMITH AND MENZIES: *J. Am. Chem. Soc.* **32**, 1412 (1910).
- (8) TIMMERMANS: *Bull. soc. chim. Belg.* **27**, 334 (1914).
- (9) TREW AND WATKINS: *Trans. Faraday Soc.* **29**, 1310 (1933).
- (10) VELEY: *Proc. Roy. Soc. (London)* **82**, 217 (1910).
- (11) WEISSBERGER AND PROSKAUER: *Organic Solvents*. Clarendon Press, Oxford (1935).

¹ Awbery and Griffiths (*Proc. Roy. Soc. (London)* **44**, 115 (1932)) determined the density of the saturated vapor from 0° to 36.7°C., but suitable analytical testing of their results seems to show that they are in error.

THE LEWIS AND THE BRÖNSTED-LOWRY DEFINITIONS
OF ACIDS AND BASES

I. M. KOLTHOFF

*School of Chemistry, University of Minnesota, Minneapolis, Minnesota**Received September 15, 1943*

When the properties of substances become known and it appears that several substances have properties in common, they are usually classified as a group. A definition based upon the composition or the common properties of the substances is then given to characterize such a group.

In the *interpretation* of the properties of such a group of substances it is usually necessary to develop another definition which is based not upon *facts* but upon *conceptions* or *theories*.

Most definitions are usually more or less limited in scope and sometimes ambiguous. This is especially true of definitions which have been given to characterize the categories of acids and bases.

In the early days of chemistry as an experimental science the terms "acid", "base," and "salt" were used in a vague way (6). Still, in the middle of the seventeenth century acids and bases were already characterized by the fact that upon interaction of the two a salt is formed. It is of interest to note that the Dutch scientist Johann Baptist Van Helmont (1577-1644) made the observation and the interpretation that free silicious earth is precipitated from a potassium silicate solution upon addition of a sufficient quantity of acid to "saturate" the alkali.

The formation of a salt as the result of the interaction of an acid and a base has been the basis of a definition of acids and bases for several centuries. In 1648, Rudolph Glauber (1604-1670) stated that alkalies and the alkali carbonates are "opposed" to the acids, and that salts are made up of two different components: "Thus sal ammoniacum is derived from sal acidum commune (hydrochloric acid) and the sal volatile urinae (ammonia)."

About a century later (1744, 1754), Rouelle clearly defined a salt as a substance which is formed by the union of an acid with an alkali. At about the same time Wm. Lewis (1746) gave a more elaborate characterization of acids, bases, and salts which in many respects is similar to a more modern definition: Acids are substances which (upon proper dilution) taste sour, which effervesce with chalk and alkali carbonates, and which form salts with such substances. Acids turn syrup of violets red, while alkalies turn this syrup blue (7).

We note that the classification of acids and bases, up to this point, has been based upon their mutual interaction and not upon a property related to their composition. The matter of composition was first brought up by Lavoisier (1777), who considered oxygen as the substance which imparts acidity or acid character to all acids. This view was conclusively disproved by Davy (1810) when he showed that hydrochloric acid is composed entirely of hydrogen and chlorine.

Contrary to the views of Berzelius, who defined an acid as an oxide with certain properties, Davy (1815) rejected the view that iodine pentoxide is an acid and maintained that it becomes an acid only by combination with water. In the same year, Dulong expressed the view that oxalic acid contains hydrogen, and that the formation of anhydrous salts from metallic oxides gives water as a result of the union of the hydrogen of the acid with the oxygen of the oxide.

Thus, Davy and Dulong may be considered as the forerunners of Liebig, who in 1838 defined acids as "compounds containing hydrogen, in which the hydrogen can be replaced by metals." This definition, in a somewhat extended form, became generally accepted. It is based upon *experimental facts* referring to *composition* (acids contain hydrogen) and *reactivity* (hydrogen replaced by metals; acid and base react with formation of salt and water).

In the qualitative and quantitative *interpretation* of acidity and basicity it appeared that the classical definition was too limited. In order to account for the properties of acids and bases it was necessary to formulate certain *conceptions*. This was done by Arrhenius, whose definition of acids and bases is based on the *theory* that acids when dissolved in water dissociate into hydrogen (hydronium) ions and anions, and that bases when dissolved in water dissociate into hydroxyl ions and cations. This important definition, which has contributed so much to the quantitative understanding of acidity and basicity, appeared too limited when phenomena of acidity and basicity were studied in non-aqueous solvents. This led Lowry and Brønsted to the more general definition which is based upon the conception that an acid may be considered as a combination product of a proton with a base, while a base is defined as a substance which can combine with a proton to form an acid. This definition limits the group of acids to substances which contain a transferable proton.

G. N. Lewis was the first to point out that many substances which do not contain a proton react in aprotic media with bases with the formation of compounds which have some properties similar to those of a salt formed by interaction of a neutral molecule (Brønsted) acid and a base. Lewis, quite rightly, considers the Brønsted definition too narrow and bases his definition upon the view that a base is a substance which can donate an electron-pair to form a conjugate bond and that an acid is a substance which can accept an electron-pair from a base to form a coördinate bond. Neutralization occurs when an acid and a base combine.

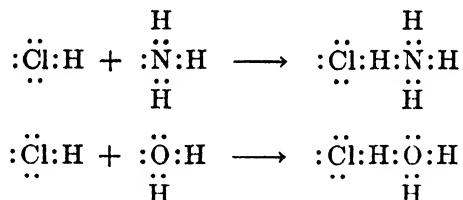
Much has been written¹ during the last decade concerning the conceptions and terminology regarding acids and bases. Unfortunately, the impression has been established that there is a controversy between the Lewis theory on the one hand and the Brønsted-Lowry theory on the other. This contradiction is not real; it merely appears to exist through confusion in the terminology and nomenclature used. By adopting an appropriate terminology it will be seen that it is possible and even advantageous to adopt and teach both definitions or conceptions, even though the Brønsted definition is admittedly more limited in scope than the Lewis definition as far as acids are concerned.

¹ For a review and literature references see "Acids and Bases," published by the Journal of Chemical Education, Easton, Pennsylvania (1941).

Lewis (1) himself states: "The recognition of Brönsted and his school of such ions as the halide ions and acetate ion as true bases, together with the development of the concept of organic bases, tends to make the present recognized list of bases identical with my own. On the other hand, any similar valuable and instructive extension of the idea of acids has been prevented by what I am tempted to call the modern cult of the proton."

Many chemists, however, quite rightly are reluctant to give up the extremely useful and simple Brönsted definition. This definition leads to a simple and adequate description of the behavior of all the common acids, both qualitatively and quantitatively. It is possible to arrange, for a given solvent, all the substances meeting Brönsted's definition of acids and bases in the order of their acid and basic strengths. Furthermore, in all protic solvents, protons enter strongly into any consideration of acid-base properties. But it is not only upon the basis of its practical usefulness that the Brönsted definition deserves general adoption.

In order to explain the acid properties of Brönsted acids like perchloric, sulfuric, hydrochloric, and acetic acids in the Lewis terminology we must consider the proton as a dibasic acid (8). Hydrochloric acid can be considered as the product obtained upon neutralization of a chloride ion with a proton, the proton and the chloride ion forming a coördinate bond. In order to consider hydrochloric acid as an acid, it is assumed that it reacts with a base by the formation of a hydrogen bond.



This hydrogen bonding results in such great electrical stress that practically all of the molecules thus formed split into ions (4). Thus, the product obtained by interaction of hydrochloric acid with water yields the "neutralization product" $\text{ClH} \cdot \text{H}_2\text{O}$, which in water as a solvent breaks down into hydronium ions (H_3O^+) and chloride ions.

The hydrogen-bond product obtained by interaction of one molecule of perchloric acid with one molecule of water is not stable, even in the solid state, and rearranges into hydronium perchlorate, which has the same crystal structure and lattice dimensions as ammonium perchlorate. Thus the acids containing replaceable protons distinguish themselves from other (Lewis) acids by the fact that upon reaction with a base a hydrogen bond is formed first. If the hydrogen bond could be considered as an ordinary coördination bond there would be no difficulty in interpreting the acid properties of acids which contain a proton on the basis of the Lewis definition.

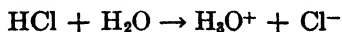
The hydrogen bond was formerly believed to result from the formation of two covalent bonds by the hydrogen atom. This view is no longer held. Pauling (5), for example, says: "It is now recognized that the hydrogen atom, with one

stable orbital (the $1S$ orbital), can form only one covalent bond and that the hydrogen bond is largely ionic in character and is formed only between the most electronegative atoms." Lewis also recognizes that the hydrogen bond differs from an ordinary coördination bond.

Lewis, Magel, and Lipkin (2) made the following statement: "Evidently what has become known as the hydrogen bond differs not only in degree but in *kind* from a true chemical bond." They refer to experiments made by Lewis and Seaborg (3), who noted that trinitrotriphenylmethide ion seems to form complexes with substances like alcohol, phenol, or acetic acid by attachment of hydrogen through the nitro groups, without causing any marked change in color. However, when hydrogen ion was similarly attached to a nitro group the color changed from blue to orange. Probably other strong (Lewis) acids such as stannic chloride or sulfuric trioxide will have a similar effect. Thus we have an example in which the addition compound through the formation of a hydrogen bond between, say, acetic acid and a base has optical properties similar to those of the base, indicating no significant change in the bond structure of the base. On the other hand, the neutralization product of the base with a proton or another Lewis acid has entirely different optical properties.

A strict application of Lewis' definition to acids containing a proton (Brönsted acids) would make it questionable whether such substances should be called acids. In the first place, in their reaction with bases the first reaction ("neutralization") product formed should be considered as a compound with the hydrogen doubly coördinated. This is not correct according to Pauling. The primary product formed in the interaction of a Brönsted acid with a base differs in the nature of its bonding from the neutralization compound of all other Lewis acids with bases. The fact that Brönsted acids need special consideration in the Lewis terminology contributes an urgent argument for classifying the Brönsted acids as a special group.

The Brönsted definition is not concerned with the *mechanism* of acid-base reactions. In this respect it is strictly analogous to the definition of oxidants and reductants. A Brönsted acid in the sense of Lewis is a "neutralization product" of a proton and a base (Cl^- , H_2O , etc.). In such a compound the acid (proton) may be replaced by a stronger acid and the base by a stronger base. In the Brönsted terminology we consider only the replacement of the base by a stronger base. The chloride ion, for example, is a very weak base. Upon reaction of hydrochloric acid with water the stronger base, water, takes the proton from the weaker base, chloride ion:



From the above it is evident that for practical and theoretical reasons there is a place for both the Lewis and the Brönsted definitions of acids and bases. In order to have a place for both classifications the following terminology is suggested.

Acids which satisfy the Lewis definition are called Lewis acids or proto-acids. (Proto is the Greek word for primary.) Substances like the proton, boron trichloride, etc., are proto-acids.

The Brönsted definition remains unchanged. An acid consists of a proton and a base, or of several protons with a base.

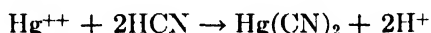
When a distinction is made between a proto-acid and an acid, there is no conflict between the Lewis and the Brönsted classifications of acids and bases.

It has been mentioned already that a great advantage obtained in maintaining (Brönsted) acids as a separate group of acids is that in a given solvent the quantitative expression of the strength of acids and bases is unambiguous. It is the affinity of a base for a proton or the tendency of an acid to give off a proton which determines acidic and basic strength. In the Lewis terminology, acidic and basic strengths become ambiguous expressions. The strength of a given base depends upon the particular proto-acids with which it combines and the strength of a given acid depends on the particular base with which it reacts.

Lewis (9) recognizes this limitation of his generalized treatment and states: "So in studying acids and bases we find that the relative strength depends not only upon the chosen solvent but also upon the particular base or acid used for reference."

Luder (4), an ardent proponent of the Lewis concept, does not agree with this statement and believes that proto-acids and bases can be grouped quite generally in the order of acid and base strength. He tries to show, for example, that the silver ion behaves as a stronger acid toward hydroxyl ions than toward ammonia. However, he bases his argument on the fact that silver ions precipitate with hydroxyl ions without considering whether the silver forms an ionic or a coordinate bond with the hydroxyl. Moreover, it is well known that in dilute aqueous solution silver ions do not combine with hydroxyl ions (silver hydroxide is a strong electrolyte), whereas they do combine with ammonia.

Many examples can be given which substantiate Lewis' statement (3). For instance, upon addition of mercuric ions to a hydrogen cyanide solution the following reaction takes place almost quantitatively:



Regarding its affinity toward the cyanide ion the proto-acid mercuric ion is a stronger acid than the proton. Even in its reactivity toward the extremely weak bases iodide, bromide, and chloride the mercuric ion behaves like a strong acid, or the halide ions behave like strong bases with regard to the proto-acid mercuric ion. Qualitatively, several other cations behave like mercuric ions.

If we consider mercuric iodide as a "neutralization compound" of the strong proto-acid mercuric ion with the base iodide ion, the iodide ion is a much stronger base than, for example, the acetate ion (referred to mercuric ion). The "acid strength" then of the mercuric ion is not determined by the properties of this ion alone, but is also determined by the properties of the base with which it reacts. In the Brönsted system the difficulty is eliminated, because the strength of bases always refers to their affinity for the proton.

Objections have been raised to the Brönsted terminology by pointing out that several metal cations are called acids although they do not contain one or more protons in the anhydrous state. This objection is valid. In the sense of Lewis

several of the inorganic anhydrous cations are proto-acids. They can react, for example, with the base water, with the formation of an acid. The aluminum ion, for instance, is not an acid, but it is a proto-acid. Upon reaction with the base water it forms the hexaaquo aluminum ion, which is an acid. In this respect the formation of the acid hexaaquo aluminum ion is comparable to the formation of sulfuric acid by the interaction of the proto-acid sulfur trioxide with the base water.

The following example is illustrative of the usefulness of the simultaneous application of both the Brönsted and the Lewis concepts.

A solution of sulfur dioxide in water contains the proto-acid SO_2 , part of which has reacted with water with the formation of the acid H_2SO_3 . When the properties of such a solution are studied we have to consider that the proto-acid SO_2 , and the acids H_2SO_3 , HSO_3^- , and H_3O^+ may exhibit acid properties. Whether the proto-acid SO_2 contributes to the acid catalysis of the inversion of sugar in aqueous medium has not been investigated to my knowledge. Indicator bases of suitable strength in aqueous medium seem to react only with the acid constituents and not with SO_2 . Recently, Dr. L. S. Guss and the author have been investigating the behavior of sulfur dioxide dissolved in ethanol toward the indicator thymol blue. A quantitative study revealed that the red color imparted to the thymol blue is due partly to the interaction of the acid $\text{C}_2\text{H}_5\text{OSO}_2\text{OH}$ (or $\text{C}_2\text{H}_5\text{OHH}^+$) with the indicator and partly to that of the "neutralization product" of the proto-acid SO_2 with the indicator. The results of this study will be communicated in a subsequent publication.

In conclusion the following statements are made:

1. The Brönsted acids should be represented as a special class in the group of substances which are acids according to the Lewis concept.
2. The Brönsted acids deserve special designation, because this class comprises the great number of inorganic and organic acids which contain replaceable protons.
3. For a general understanding of the properties of chemical compounds, the Lewis concept of proto-acids and of bases should be adopted.
4. From a qualitative and quantitative viewpoint the Brönsted definition yields an unambiguous expression of acidic and basic strengths of various substances, and of the effect of solvent upon acid and basic strength.
5. There is no pedagogical difficulty involved in presenting both concepts as a harmonious pair.

SUMMARY

1. The proposal is made that acids in the sense of G. N. Lewis be called proto-acids, while the Brönsted-Lowry definition of acids be left unchanged.
2. It is pointed out that the Lewis and Brönsted concepts are not contradictory and that both should be adopted.

The author acknowledges his appreciation to Dr. D. N. Hume for a discussion of the contents of this paper.

REFERENCES

- (1) LEWIS, G. N.: J. Franklin Inst. **226**, 293 (1938).
- (2) LEWIS, G. N., MAGEL, T. T., AND LIPKIN, D.: J. Am. Chem. Soc. **64**, 1774 (1942), especially footnote 7.
- (3) LEWIS, G. N., AND SEABORG, G. T.: J. Am. Chem. Soc. **61**, 1894 (1939).
- (4) LUDER, W. F.: Chem. Rev. **27**, 547 (1940), especially p. 571.
- (5) PAULING, L.: *The Nature of the Chemical Bond*, 2nd Edition, p. 284. Cornell University Press, Ithaca, New York (1940).
- (6) WALDEN, P.: *Salts, Acids and Bases; Electrolytes, Stereochemistry*. McGraw-Hill Book Company, Inc., New York (1929).
- (7) Reference 6, page 48.
- (8) Reference 6, page 297.
- (9) Reference 6, page 299.

MINIMA IN SURFACE TENSION-CONCENTRATION CURVES OF
SOLUTIONS OF SODIUM ALCOHOL SULFATES

GILBERT D. MILES AND LEO SHEDLOVSKY

*Colgate-Palmolive-Peel Company, Jersey City, New Jersey**Received September 28, 1948*

The observation of minima in the surface tension-concentration curves for aqueous solutions of various surface-active materials has been the cause of considerable conjecture. Powney and Addison (12), in particular, found well-defined minima in the surface tension of solutions of sodium salts of primary alcohol sulfates containing from twelve to eighteen carbon atoms. The minima are as much as 5 dynes per centimeter lower than the value reached at higher concentrations. These "anomalous" results have presented apparent disagreement with Gibbs' adsorption equation. The hypotheses proposed to reconcile such incongruities have been frequently discussed (1 to 12).

Usually the explanations proposed fall into two groups: First, it has been claimed that there are experimental difficulties which result in errors in the methods used for measuring surface tension (3, 4, 7). On the other hand, the possible existence of abrupt changes in colligative properties of solutions of certain surface-active substances has been emphasized (12) and this could lead to minima in the surface tension-concentration curves. The data which we present here deal with solutions and procedures not covered by either of the above explanations.

PROCEDURE

The sulfated alcohols used in this work were of a particularly high degree of purity. The details of the methods used in their preparation are given in a report entitled "Some Properties Involving Surface Activity of Sodium Salts of Primary and Secondary Alcohol Sulfates" (5). Particular care was exercised in

preparing the solutions and measuring the surface tension, in order to avoid accidental contamination. From the point of view of speed and ease of maintaining clean surfaces, the best procedure of those used is as follows: A Du Noüy tensiometer was placed upon a flat plate placed on top of a screw-jack. This permitted the uniform elevation of the instrument with respect to the surface of the solution. The material to be tested was weighed and placed in a 1000-ml. Erlenmeyer flask which had been carefully cleaned, rinsed with distilled water, and paraffined inside and out around the neck. The solutions were diluted by stepwise addition of measured volumes of distilled water from an automatic buret of 100-ml. capacity to the flask. During the measurement, the flask rested on the bench top next to the screw-jack. An extension of glass rod approximately 1 mm. in diameter connected the platinum-iridium ring with the torque arm of the tensiometer so that the ring rested upon the surface of the solutions inside the flask. The neck of the flask was covered with a slotted sheet of suitable material, and the measurement was made by gradually pulling the ring away from the surface of the solutions. By the addition of more water, the surface-tension curve was obtained for a concentration range of ten to one before it was necessary to weigh a fresh sample. All the measurements reported here were made at room temperatures (25–30°C.). A calibration curve was employed in which dial readings were plotted against the surface tension of pure liquids given in *International Critical Tables*. This method gave a precision of about ± 0.15 dyne per centimeter.

RESULTS

The results of the measurements are given in figures 1, 2, and 3. In figure 1, curve A for pure sodium dodecyl sulfate which had been extracted with ethyl ether for 36 hr. in a Soxhlet apparatus does not show any minimum. Curve D shows a marked minimum for solutions of the same material before the final extraction with ether. Curves B and C show progressively more pronounced minima as larger amounts of dodecanol are added. If the material extracted with ether was dodecanol, the sample before extraction contained between 0.1 and 0.5 per cent dodecanol.

In figure 2, curve A for pure ether-extracted sodium tridecane-2-sulfate (13-2) (a typical sodium salt of a secondary alcohol sulfate), no minimum is apparent. In curves B and C successive amounts of the homolog containing two more carbon atoms were added. When 10 per cent of sodium pentadecane-2-sulfate (15-2) is added (curve C), a perceptible minimum appears in the curve. In order to demonstrate the more pronounced minimum obtained by the addition of a higher member of the homologous series, 5 per cent of sodium heptadecane-2-sulfate (17-2) was added to (15-2), (curve D). Only the portion of the curve at concentrations above 0.002 molal are shown in figure 2, curve D. Below this concentration, the curve rises steeply.

In figure 3 the effect of the addition of a higher homolog of the sodium salt of a primary alcohol sulfate (16-1) to sodium dodecyl sulfate is shown in curves A and B. As with the sodium secondary alcohol sulfates (figure 2), so for the sodium

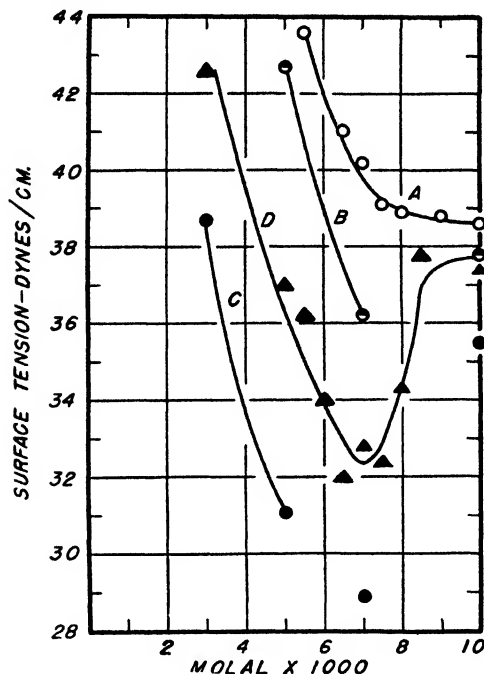


FIG. 1. Effect of dodecanol upon the surface tension of solutions of sodium dodecyl sulfate (12-1). Curve A, pure sodium dodecyl sulfate (12-1); curve B, pure (12-1) + 0.1 per cent dodecanol of the amount of (12-1); curve C, pure (12-1) + 0.5 per cent dodecanol of the amount of (12-1); curve D, (12-1) before final 36-hr. Soxhlet extraction with ethyl ether.

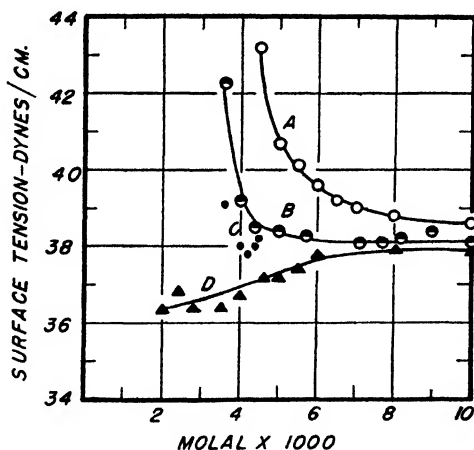


FIG. 2. Effect of sodium pentadecane-2-sulfate (15-2) and sodium heptadecane-2-sulfate (17-2) on the surface tension of solutions of sodium tridecane-2-sulfate (13-2). Curve A, pure sodium tridecane-2-sulfate (13-2); curve B, pure (13-2) + 5 per cent (15-2) of the amount of (13-2); curve C, pure (13-2) + 10 per cent (15-2) of the amount of (13-2); curve D, pure (13-2) + 5 per cent (17-2) of the amount of (13-2).

primary alcohol sulfate addition of the higher homolog (16-1) gives a curve with a measureable minimum. Curve C in figure 1 substitutes sodium chloride for the (12-1) compound in curve B.

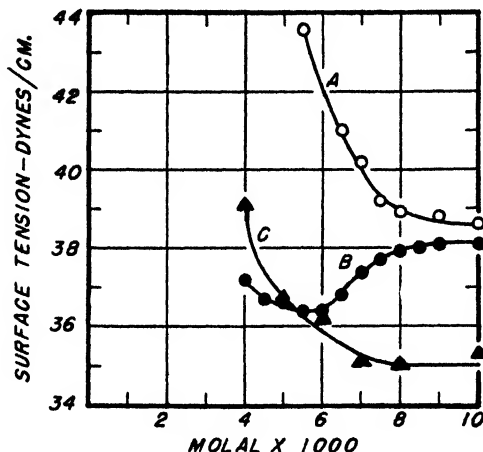


FIG. 3. Effect of sodium hexadecyl sulfate (16-1) and of sodium chloride upon the surface tension of sodium dodecyl sulfate (12-1). Curve A, pure sodium dodecyl sulfate (12-1); curve B, (12-1) + 1 per cent sodium hexadecyl sulfate (16-1) of the amount of (12-1); curve C, sodium chloride + 1 per cent (16-1) of the amount of sodium chloride.

DISCUSSION AND CONCLUSION

The results indicate two ways in which minima can be produced in surface tension-concentration curves. Figure 1 illustrates the effect obtained when two surface-active materials, one of which is only slightly soluble in water, are present in the solution. From other work involving surface viscosity which has been done in these laboratories, we have reason to believe that dodecanol is adsorbed at higher concentrations than corresponds to that for the minimum in surface tension of solutions shown in figure 1, curves B and C, but we have no explanation for the rise in the surface-tension curves of these solutions. Soap solutions are analogous to the above mixture in so far as they also contain a water-soluble surface-active material and a slightly soluble surface-active material which is strongly adsorbed. In the case of soap solutions, we consider that the minima in surface tension reported in the literature are probably due to selective adsorption of the relatively insoluble fatty acid or acid soap. Owing to hydrolysis, soap solutions are not two-component systems (9, 11) and therefore Gibbs' theorem cannot be applied in the usual way.

Figures 2 and 3 exemplify a second means of obtaining minima, which may be obtained by mixing two anionic surface-active electrolytes. This effect should be most pronounced when the material present in the smaller proportion is a homolog of higher molecular weight, or another more surface-active analog of the principal ingredient. From the data shown in figure 3, we may consider these

phenomena as special cases of the salt effects comparable to those which have been observed with added inorganic salts (5). At concentrations below 0.0075 molal, pure sodium dodecyl sulfate begins to lose much of its surface activity. On the other hand, sodium hexadecyl sulfate at one-hundredth of this concentration is still highly adsorbed in the presence of a strong uni-univalent electrolyte such as sodium chloride whose concentration is 0.0075 molal; whereas in distilled water the surface tension of such a solution would be above 40 dynes per centimeter. It has been shown elsewhere (5) that the salt effects for anionic surface-active materials such as the sodium alcohol sulfates are a function of the valence of the cation. The salt effect of sodium dodecyl sulfate on sodium hexadecyl sulfate (figure 3, curve B) seems to be a function of the sodium-ion concentration up to concentrations of 0.0075 molal for the mixture. However, above 0.008 molal, the observed surface tension is approximately 6 dynes per centimeter above the curve for sodium hexadecyl sulfate plus sodium chloride (figure 3, curve C). This may be explained if we take into account the dynamic nature of the equilibria which maintain the surface properties of such solutions. At the air-liquid interface there is a constant exchange of ions between the interface and the interior of the solution. In the mixture which we have studied, the concentration of sodium dodecyl sulfate is one hundred times that of sodium hexadecyl sulfate. Therefore, the chances are roughly one hundred to one that a hexadecyl sulfate ion leaving the interface will be replaced by a dodecyl sulfate ion. For this reason, the surface concentration of hexadecyl sulfate ions will be lower in such solutions at concentrations where sodium dodecyl sulfate is highly surface active, than it would be in solutions where sodium chloride was used instead of the sodium dodecyl sulfate. This displacement of hexadecyl sulfate ions from the surface should result in an increase in surface tension compared to the surface tension of solutions of sodium hexadecyl sulfate plus sodium chloride.

Our work on this subject has been limited to the data presented here, but we suspect that minima may be expected to appear in the surface tension-concentration curves of cationic surface-active materials if the proper materials and concentrations are chosen.

Adam (1) notes that where the surface tension passes through a minimum as the concentration increases it is possible that such cases will be explained by there being more than one capillary-active component in the system, or by the presence of small amounts of an impurity which greatly increases the adsorption of the solute at certain concentrations. It has been seen that our data suggest that minima in surface tension-concentration curves are the direct result of the presence in the solutions of more than one type of surface-active material. This agrees with part of the view given by Adam (1), but his suggestion that the presence of small amounts of an impurity might greatly increase the adsorption of the solute at certain concentrations does not concur with our concepts. A reëxamination of the purity of materials for which minima have been reported is indicated before the necessity arises of reconciling the data with Gibbs' adsorption theorem.

REFERENCES

- (1) ADAM, N. K.: *The Physics and Chemistry of Surfaces*, 2nd Edition, pp. 113, 115. Oxford University Press, London (1938).
- (2) ALEXANDER, A. E.: *Nature* **148**, 752 (1941); *Trans. Faraday Soc.* **38**, 54 (1942).
- (3) CASSEL, H. M.: 105th Meeting of the American Chemical Society, held in Detroit, Michigan, April, 1943.
- (4) CLAYTON, W.: *The Theory of Emulsions and their Technical Treatment*, 4th Edition, pp. 6-12, 53-55. The Blakiston Co., Philadelphia (1943).
- (5) DREGER, E. E., KEIM, G. I., MILES, G. D., SHEDLOVSKY, L., AND ROSS, J.: To be published.
- (6) KRAEMER, E. O.: *Advances in Colloid Science*, pp. 111, 395, 402-5. Interscience Publishers, Inc., New York (1942).
- (7) LONG, F. A., NUTTING, G. C., AND HARKINS, W. D.: *J. Am. Chem. Soc.* **59**, 2197 (1937); **62**, 1496 (1940).
- (8) LOTTERMOSER, A., AND STOLL, F.: *Kolloid-Z.* **63**, 49 (1933).
- (9) MCBAIN, J. W., AND DAVIES, G. P.: *J. Am. Chem. Soc.* **49**, 2230 (1927).
- (10) MCBAIN, J. W., AND MILLS, G. F.: *Report on Progress in Physics* **5**, 30 (1939).
- (11) MCBAIN, J. W., AND WILSON, D. A.: *J. Am. Chem. Soc.* **58**, 379 (1936).
- (12) POWNEY, J., AND ADDISON, C. C.: *Trans. Faraday Soc.* **33**, 1243 (1937).

DISCUSSION AND INTERPRETATION OF THE MIGRATION DATA OF LAURYL SULFONIC ACID IN AQUEOUS SOLUTION

PIERRE VAN RYSSELBERGHE

*Department of Chemistry, University of Oregon, Eugene, Oregon**Received September 15, 1943*

A few years ago, on the basis of the then available data, we gave (4) an interpretation of the osmotic coefficients, the conductivities, and the diffusion coefficients of the typical colloidal electrolyte laurylsulfonic acid in aqueous solution. An average negatively charged micelle H_zL_x , changing with concentration, was calculated. The values of x and z and the concentrations (H_zL_x) and (H^+) were obtained by solving, for each concentration, a system of four simultaneous equations: namely, two stoichiometric conditions, the freezing-point equation in which the experimental van't Hoff i coefficients were introduced, and a conductivity equation based on the use of Stokes' law according to the suggestions of J. W. McBain (3). The latter equation (equation 11 of our previous paper) is

$$350(H^+) + 22 \frac{(x - z)^2}{x^{1/3}} (H_zL_x) = \Delta C \quad (1)$$

The values of x and z so obtained were then introduced into the Nernst formula for the diffusion coefficient, written for an unsymmetrical electrolyte whose molecule dissociates into $(x - z)/x$ hydrogen ions and $1/x$ micelles H_zL_x . The calculated diffusion coefficients were found to be in satisfactory agreement with the experimental data of E. L. McBain (1). In particular, the interesting minimum in the diffusion curve was reproduced by the calculations based upon the average

micelle. Furthermore, in the absence of transference data, we made some predictions by means of the following formula (formula 22 of our previous paper) for the transference number of the laurylsulfonate radical:

$$T = \frac{(H_s L_s) \frac{x - z}{x^{1/3}} x \cdot 22}{\Delta C} \quad (2)$$

We mentioned that these predictions would probably be considerably altered by viscosity corrections. It was, moreover, implicitly assumed in formula 2 that

TABLE 1

Measured and calculated transference numbers of laurylsulfonic acid in aqueous solution

CONCENTRATION <i>m</i>	<i>T</i> (MEASURED)	<i>T</i> (CALCULATED)	"DEGREE OF IONIZATION" OF MICELLES
0	(0.059)	0.059	(1.0
0.005	0.065	0.060	1.0
0.01	0.090	0.065	1.0
0.02	0.130	0.118	1.0
0.03	0.180	0.172	1.0
0.04	0.250	0.226	1.0
0.05	0.320	0.320	1.0
0.055	0.350	0.360	1.0)
0.06	0.330	0.404	0.815
0.07	0.290	0.510	0.569
0.08	0.275	0.669	0.411
0.09	0.270	0.935	0.288
0.1	0.255	1.243	0.206
0.2	0.230	1.396	0.165
0.4	0.220 (extrapolated)	1.517	0.145

the averaging process which had led to the conductivity equation was also valid in the description of electrolytic migration. To what extent this is justified and what alterations should be introduced in the treatment are questions which can now be answered, thanks to the migration data recently published by E. L. McBain (2).¹

¹ Dr. E. L. McBain has asked us to indicate the following corrections in table 2 of her paper (2), the data below replacing the corresponding ones in the table:

<i>N</i>	EQUIVALENTS CHANGE	TRANSFERENCE NUMBER
0.00116	A +0.00001071 M No change C -0.00000362	0.044
0.1164	(correct in paper)	0.239
0.3475	A +0.000485 M -0.000011 C -0.000436	0.223

When the measured transference numbers are plotted against concentration, the values at round concentrations read from the curve are those in the second column of table 1. Using formula 2 with the values of x and z in table 1 of our previous paper we find the transference numbers given in the third column of the present table. We notice that, up to the maximum in the experimental transference curve at concentration $0.055\ m$, the agreement between calculated and measured values is, all things considered, excellent. Above $0.055\ m$, however, our calculated values keep on increasing, the ratio $T_{\text{calcd.}}/T_{\text{measd.}}$ reaching the value 6.895 at the concentration $0.4\ m$. Obviously, some effect not taken into account in formula 2 is appearing around the concentration $0.055\ m$ and becomes increasingly more important as concentration rises. As pointed out above, formula 2 is based upon the same averaging process as the conductivity equation: namely,

$$(H_s L_s) \frac{(x - z)^2}{x^{1/3}} = \sum_{i,j} (H_i L_i) \frac{(i - j)^2}{i^{1/3}} \quad (3)$$

in which $H_i L_i$ designates any particular micellar species, positive or negative, and the summation is extended to all pairs of values of i and j present in the solution. Actually, the transference number of the laurylsulfonate radical should be

$$T = \frac{\sum_{i,j} (H_i L_i) \frac{i - j}{i^{1/3}} i \cdot 22}{\Delta C} \quad (4)$$

and it is not necessarily true that

$$\sum_{i,j} (H_i L_i) \frac{i - j}{i^{1/3}} i = (H_s L_s) \frac{x - z}{x^{1/3}} x \quad (5)$$

The experimental data, however, show that this is true up to the maximum in the transference curve. Now, marked departure from equation 5 would occur if, in the migration process, there is a certain compensation between the movements in opposite directions of negative and positive micelles. All micelles, regardless of sign, contribute a positive amount to the conductivity: namely,

$$\frac{1}{C} (H_i L_i) \frac{(i - j)^2}{i^{1/3}} \cdot 22$$

for the species $H_i L_i$, while this same species contributes

$$\frac{1}{\Delta C} (H_i L_i) \frac{i - j}{i^{1/3}} i \cdot 22$$

to the transference number of the radical, and this contribution will be positive or negative according to the sign of $i - j$. The compensating effect of opposite migrations is particularly likely to occur with positive and negative micelles of similar size and mobility, i.e., when their net charges are small numbers like ± 1 , ± 2 , etc. and the i values of oppositely charged micelles are exactly or nearly equal to each other. The mass action effects would cause such micelles to be present in fairly equal amounts. When $i - j = +1$ and $i' - j' = -1$, with

($H_i L_i$) equal to ($H_j L_j$) and i equal to j , the contributions of these two species to the transference number of the radical would cancel each other. The rather large values of the ratios $T_{\text{calcd.}}/T_{\text{measd.}}$ above the maximum suggest that this type of compensation is important, and hence that an appreciable amount of micelles are nearly neutral. Below the maximum the micelles would be preponderantly negative and their composition would be somewhat concentrated around the average micelle $H_x L_x$. We have

$$\frac{T_{\text{measd.}}}{T_{\text{calcd.}}} = \frac{(H_i L_i) \cdot (i - j) \cdot i^{2/3}}{(H_x L_x) \cdot (x - z) \cdot x^{2/3}} \quad (6)$$

and this ratio is, in a way, a measure of the "degree of ionization" of the micelles. The smaller this ratio, the greater is the compensating effect of the opposite migrations of micelles much closer to neutrality than the average micelle $H_x L_x$. The numerical values of this ratio are given in the fourth column of table 1.

A possible alternative to the foregoing explanation of the transference data is a consideration of the effect of the hydration of the micelles. In determining our $H_x L_x$ average micelle it has been implicitly assumed that the size of the micelles and the application of Stokes' law to the calculation of their mobilities and conductivities are only negligibly affected by hydration. If, however, we make a hydration correction in the transference number, assuming that the migration is due to the single species $H_x L_x$, we arrive at the conclusion that all the water in the solution, and at the higher concentrations even more than the total amount of water, would be water of hydration of the micelles. It may be that the true picture would be a compromise between hydration and nearly neutral micelles with compensating migrations. The latter effect, however, is no doubt present and this is a most important piece of information furnished by E. L. McBain's migration data.

SUMMARY

E. L. McBain's recent migration data for laurylsulfonic acid in aqueous solution are shown to indicate the probable presence of rather large amounts of nearly neutral micelles with compensating migrations at concentrations above the maximum in the transference curve. Below the maximum the transference numbers are in excellent agreement with the values calculated on the basis of a previously calculated average micelle whose composition and size change continuously with concentration.

REFERENCES

- (1) MCBAIN, E. L.: Proc. Roy. Soc. (London) **A170**, 415 (1939).
- (2) MCBAIN, E. L.: J. Phys. Chem. **47**, 196 (1943).
- (3) MCBAIN, J. W.: Trans. Faraday Soc. **9**, 99 (1913).
- (4) VAN RYSSELBERGHE, P.: J. Phys. Chem. **43**, 1049 (1939).

NEW BOOKS

War Gases: Their Identification and Decontamination. By MORRIS B. JACOBS. xiii + 180 pp. New York: Interscience Publishers, Inc., 1942.

This book is a compilation covering the following topics: classification of chemical warfare agents, their physical characteristics and physiological response, effect on food, water, and other materials, sampling, analysis, and methods of decontamination. Approximately one-half of the treatment is devoted to the detection, identification, and determination of the war gases. This section includes organoleptic analysis, field and laboratory chemical tests, determination by various methods, and confirmatory tests.

According to the preface, the book is written primarily for the gas identification officer, the war gas chemist, and decontamination and health officers. Some of the chapters should be of value to the air raid warden. This book gives a large amount of information in a relatively small space and should prove useful to those concerned with the identification of war gases and their decontamination.

E. B. SANDELL.

Encyclopedia of Substitutes and Synthetics. Edited by MORRIS D. SCHOENGOLD. 382 pp. New York: Philosophical Library, Inc., 1943. Price: \$10.00.

This book contains an alphabetical list of many technical products, in which properties and uses are given, together with substitute materials, where such are known. Acknowledgement is made to some seventy-five firms and four Government Agencies who have furnished information. As might be expected, the entries are drawn rather heavily from the fields of plastics and solvents. There is an index of trade names with information as to manufacturers, and a brief subject index which is chiefly a "uses" index.

In spite of the title and the price, however, this book is no encyclopedia. The reviewer asked some of his colleagues to suggest names of common commercial products which could be classed as synthetics; from a list of thirty-one such names, only eleven were found in this book. The list of entries is much smaller than one has a right to expect, the paper is not of the best quality, the work shows evidences of hasty writing, and the book is grossly overpriced.

LEE IRVIN SMITH.

RELATIVE FREE ENERGIES AND DISSOCIATION CONSTANTS OF MICROSCOPIC IONS

TERRELL L. HILL

Morley Chemical Laboratory, Western Reserve University, Cleveland, Ohio

Received December 10, 1943

I

Microscopic dissociation constants have been used frequently (1, 4) and complete sets of microscopic constants have been calculated (1) for substances with two (or more, in the case of extreme symmetry; see below) dissociating groups. Some microscopic constants have also been evaluated for more complicated cases (1), but apparently not the complete set for any particular compound. In this paper a simple mathematical procedure for accomplishing this will be presented and applied to glutamic acid. These constants for glutamic acid are to be used elsewhere (5) in a study of the electrostatic contribution to hindered rotation in microscopic ions of this substance.

In order to extend the method in an approximate manner to compounds for which not all of the necessary experimental dissociation constants are available, electrostatic charge effects are considered.

In connection with the development of the general procedure, certain analogies, which may be instructive, between the relative free energies of microscopic ions and spectroscopic energy levels, and between the microscopic dissociation constants and spectral lines, will be pointed out.

II

In the following discussion we shall speak only of the dissociation of protons, so that a single treatment will apply equally well to substances usually classified separately as acids, bases, and ampholytes.

In considering a particular ampholyte (we shall use the term "ampholyte" to include the three classes mentioned above), let $n + m$ be the maximum number of dissociable protons, where n is equal to the number of uncharged acid groups (e.g., $-\text{COOH}$) and m is equal to the number of cationic acid groups (e.g., $-\text{NH}_3^+$). Then there are 2^{n+m} microscopic ions and $(n + m)2^{n+m-1}$ microscopic dissociation constants to be taken into account (4). These ions and constants will all be different in unsymmetrical molecules such as those of most amino acids. But, at the other extreme, if all the acidic groups are identical (e.g., in $\text{P}(\text{OH})_4^+$ (6)), there will be only $n + m + 1$ different ions and $n + m$ different dissociation constants (either n or m is equal to zero). For cases where there is some symmetry, but not of such a high order, the number of different ions and equilibrium constants will be intermediate (e.g., in dithionic (7) and pyrophosphoric (7) acids).

Writing $p = n + m$, only $2^p - 1$ of the $p2^{p-1}$ microscopic dissociation constants mentioned above are independent (4). Hence, when there is no symmetry,

there must be $2^p - 1$ experimentally determined relationships between the microscopic constants in order to find them all. They have been so found for a number of cases (1) in which $p = 2$, using the gross dissociation constants and making the good approximation that the groups $-\text{COOH}$ and $-\text{COOC}_2\text{H}_5$ have the same effect on the dissociation of the group $-\text{NH}_3^+$. In those compounds in which the symmetry is such that all acidic groups are in equivalent positions, the complete set of gross dissociation constants is adequate by itself.

The notation to be used will be that of earlier papers (4, 7), but writing $p = n + m$. The acidic groups are numbered 1 to p , the order being immaterial. However, it is convenient for certain purposes to list the uncharged groups first (e.g., in studying the state of maximum charge). We shall write a_{125} , say, for the activity of the species (A_{125}) with protons dissociated from positions 1, 2, and 5 only; etc. The subscripts of a and A are written in increasing order. For dissociation constants, we use the notation exemplified by the equations

$$K_{125} = \frac{a_{125}x}{a_{12}} \quad K_{152} = \frac{a_{125}x}{a_{15}} \quad K_{251} = \frac{a_{125}x}{a_{25}}$$

(all subscripts of K other than the last one are written in increasing order). These are equilibrium constants for the dissociation of protons 5, 2, and 1, respectively, from A_{12} , A_{15} , and A_{25} , respectively, to form, in all cases, A_{125} .

Let the k protons numbered, in increasing order, r_1, r_2, \dots, r_k dissociate from A_0 (the completely undissociated ion), in any particular sequence, the final product of the dissociation being $A_{r_1 r_2 \dots r_k}$. Let the successive microscopic equilibrium constants be $K(1), K(2), \dots, K(k)$. Then

$$K(1)K(2) \dots K(k) = \frac{a_{r_1 r_2 \dots r_k} x^k}{a_0} \quad (1)$$

where x is the hydrogen-ion activity. Now the right-hand member of equation 1 is independent of the sequence chosen; hence the product of microscopic dissociation constants on the left side of equation 1 has the same value for all possible sequences leading from A_0 to $A_{r_1 r_2 \dots r_k}$ (clearly the same is true of any pair of microscopic ions). In fact,

$$-RT \ln K(1)K(2) \dots K(k) = F_{r_1 r_2 \dots r_k}^0 - F_0^0 \quad (2)$$

where F^0 is a standard free energy. The right-hand side of equation 2 will be referred to as the relative standard free energy of the microscopic ion $A_{r_1 r_2 \dots r_k}$. Further,

$$\begin{aligned} pK(1) + pK(2) + \dots + pK(k) &= \frac{F_{r_1 r_2 \dots r_k}^0 - F_0^0}{2.303RT} \\ &= f_{r_1 r_2 \dots r_k} \end{aligned} \quad (3)$$

in which f gives the relative free energy in pK units. Incidentally (4),

$$pK(1) + pK(2) + \dots + pK(p) = pK_{(1)} + pK_{(2)} + \dots + pK_{(p)} \quad (4)$$

where $pK_{(j)}$ is the j^{th} gross or macroscopic dissociation constant starting with A_0 .

Evidently, by way of analogy, we can arrange the relative free energies of the microscopic ions in an "energy level" diagram (figure 1). The corresponding "spectrum" is a plot of the microscopic equilibrium constants along a pK axis. Each "line" in the "spectrum" corresponds to an "allowed transition" between "energy levels." That is, pK for the equilibrium between a pair of microscopic ions, one of which may be obtained from the other by the dissociation of a proton, is equal to the difference in f for the two ions. Moreover, from equations 1 and 2,

$$\frac{a_{r_1 r_2 \dots r_k}}{a_{s_1 s_2 \dots s_j}} = x^{j-k} \exp \left(- \frac{F_{r_1 r_2 \dots r_k}^0 - F_{s_1 s_2 \dots s_j}^0}{RT} \right) \quad (5)$$

so that under certain conditions there will be a Boltzmann distribution (*using free energies*) among the different "energy levels." For example, if the solution is sufficiently dilute so that the activities of the two microscopic ions in equation 5 may be set equal to their concentrations (or if the two activity coefficients may be set equal to each other), and if either (a) $j = k$ or (b) $x = 1$, then a Boltzmann distribution will obtain and the relative concentrations of the two ions may be

TABLE 1*

	$pK(1)$	$pK(2)$	$pK(3)$
Glutamic acid	2.155	4.324	9.960
α -Ethyl hydrogen glutamate	3.846	7.838	
γ -Ethyl hydrogen glutamate	2.148	9.19	
Ethyl glutamate	7.035		

* Data from reference 10.

calculated directly from the difference in their free energies (i.e., from the difference in their "energy levels"). In other words, if we can write activity ratios as concentration ratios, (a) there will be a Boltzmann distribution among each set of ions having the same net charge (e.g., the various isoelectric forms); or if (b) the hydrogen-ion activity is unity, the Boltzmann distribution will include *all* microscopic ions. Evidently, when there is a Boltzmann distribution among any set of ions, a difference of q units in f (q pK units) between two ions of the set corresponds to a concentration ratio of 10^q , the ion with the lower value of f having the higher concentration. The relative concentrations of the microscopic ions in these cases may thus be estimated by inspection of the "energy level" diagram. Finally, in symmetrical compounds where some or all of the "different" microscopic ions of a given net charge are indistinguishable, we have the analogue of spectroscopic degeneracy, and such an "energy level" must be given the proper statistical weight.

Glutamic acid serves as an excellent example, inasmuch as the data available are more than sufficient. Since $p = 3$, seven experimental relations are necessary. Eight are available so that we can make a check on the assumptions to be used. It should be remarked that the dissociation constants of glutamic acid

have been discussed before in some detail by Neuberger (10), but certain extensions will be made here.

We shall number the acidic groups as follows: (1) α -COOH; (2) γ -COOH; and (3) $-\text{NH}_3^+$. Using Neuberger's data in table 1 and making the usual assumptions about esters (see above), we have $\text{p}K_3 = 7.035$. Also, since we can neglect the dissociation of $-\text{NH}_3^+$ compared to $-\text{COOH}$ in the same ion,

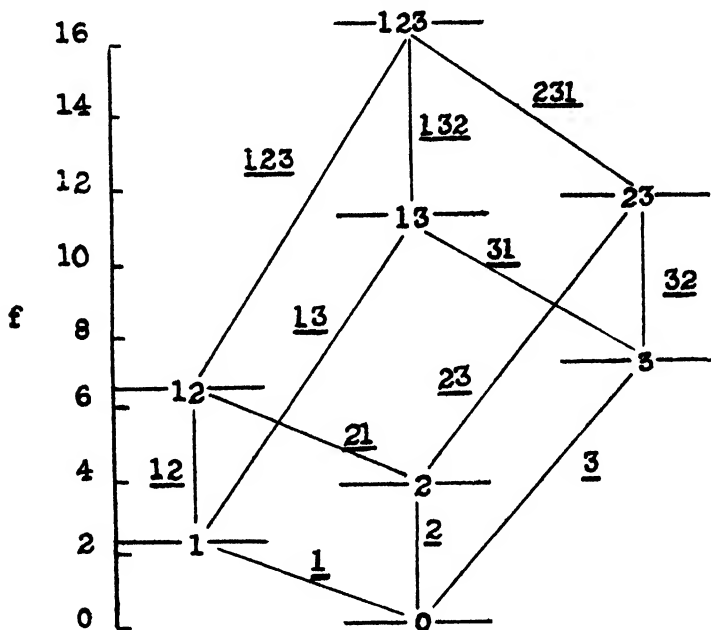


FIG. 1. Relative free-energy levels and dissociation constants of microscopic ions of glutamic acid. Numbers underlined refer to dissociation constants, which are given in the table below:

	$\text{p}K$		$\text{p}K$
1	2.148	23	7.838
2	3.846	31	4.303
3	7.035	32	4.649
12	4.315	123	9.960
13	9.190	132	5.085
21	2.617	231	4.739

$\text{p}K_1 = 2.148$, $\text{p}K_2 = 3.846$, $\text{p}K_{13} = 9.19$, $\text{p}K_{23} = 7.838$, and $\text{p}K_{123} = 9.960$. The values of $\text{p}K_1$, $\text{p}K_2$, and $\text{p}K_{(2)}$ allow the calculation of $\text{p}K_{12}$ and $\text{p}K_{21}$ (see figure 1). The remaining microscopic $\text{p}K$'s may be easily filled in using the fact that the sum of the $\text{p}K$'s along all paths (figure 1) between any two microscopic ions is a constant. $K_{(1)}$ has not been used but it serves as a check. From K_1 , K_2 , and K_3 , $\text{p}K_{(1)} = 2.139$, compared with the experimental value of 2.155. This is within the experimental error, for the individual values in table 1 have

a probable error of ≥ 0.01 pK unit (10). The relative free energies of the microscopic ions may now be found by addition of the microscopic pK's. The results are given in table 2 and plotted in figure 1. Lysine, which is also included in table 2, is discussed in Section III.

TABLE 2
Relative standard free energy, f (in pK units)

MICROSCOPIC ION	GLUTAMIC ACID	LYSINE
A ₀	0.000	0.00
A ₁	2.148	2.18
A ₂	3.846	6.99
A ₃	7.035	9.59
A ₁₂	6.463	11.17
A ₁₃	11.338	12.17
A ₂₃	11.684	17.08
A ₁₂₃	16.423	21.66

One pK unit = $2.303RT$ = 1365 cal. per mole at 25°C.

Assuming activity and concentration ratios to be equal, we may calculate the approximate relative concentrations of some microscopic ions. For any hydrogen-ion activity,

$$c_3:c_2:c_1 = 1:10^{3.189}:10^{4.887} = 1:1,540:77,000$$

and

$$c_{23}:c_{13}:c_{12} = 1:10^{0.346}:10^{5.221} = 1:2.22:166,000$$

For a solution in which the hydrogen-ion activity is unity, the same type of calculation applies to *all* microscopic ions, and the relative concentrations of all species may therefore be estimated by inspection of the free-energy-level diagram. In fact, the concentration of a given microscopic ion is proportional to 10^{-f} .

Edsall (1) gives the microscopic dissociation constants for a number of amino acids in which $p = 2$, such as glycine. The relative free-energy levels may be easily calculated from these constants.

For compounds such as oxalic acid, $H_4PO_4^+$, and ethylenediammonium ion, in which all acidic groups are equivalent (6),

$$K_{(j)} = (p - j + 1)K_{12\dots j/j}$$

since all microscopic dissociation constants for the j^{th} step are equal. Thus the microscopic constants may be calculated quite simply from the macroscopic (gross) dissociation constants¹ (2). The "degeneracy" of the ion with k protons dissociated is (4) $p!/k!(p-k)!$, so that in the presence of a hydrogen-ion activity of unity the concentration of $H_2PO_4^-$ ($k = 2$) is approximately six times that of

¹ The four constants for phosphoric acid are available in the summary in reference 6. Related compounds are also included. $K_{(1)}$ is an estimated value from electrostatic considerations.

$P(\text{GH})_4^+$ ($k = 0$), inasmuch as the relative free energies of the two *microscopic* ions are found to be practically equal. The macroscopic relative free energies of ordinary interest may be calculated from the microscopic relative free energies in these completely symmetrical cases from

$$f_{(k)} = f_{12\dots k} - \log \frac{p!}{k!(p-k)!} \quad (6)$$

III

It is now interesting to compare those microscopic dissociation constants of glutamic acid that refer to the dissociation of the same proton, since the substituent groups in such a set of ions are all identical but the charge distributions differ. Thus, the differences between pK_1 , pK_{21} , pK_{31} , and pK_{231} may be thought of as arising primarily from charge effects (all of these constants relate to the dissociation of proton number 1), since other first-order influences are held constant.

TABLE 3
 ΔpK (*microscopic*), charge effects

	$d = 1$	$d = 2$	$d = 3$	$d = 4$	$d = 5$	$d = 6$	$d = 7$	$d = 8$
2.00/ d	2.00	1.00	0.67	0.50	0.40	0.33	0.29	0.25
Dicarboxylic acids (2)	2.36	2.26	0.69	0.48	0.39	0.34	0.28	0.26
Diamines (13)	2.40	1.44	0.44	0.66			0.27	
Glutamic acid	2.15		0.80	0.47				
	2.12		0.77	0.44				
Glycine (1)	1.99							
α -Alanine (1)	1.92							
α -Aminobutyric acid (1)..	1.89							
Leucine (1)	2.01							
β -Alanine (1)		1.06						
γ -Aminobutyric, δ -amino- valeric, and ϵ -amino- caproic acids (1)			0.72	0.62	0.38			

The study of the influence of charges and their location within molecules on dissociation constants is, of course, not new, and the approach here will not be unrelated to earlier treatments. However, the method has apparently not been previously applied to a complete set of microscopic dissociation constants for $p > 2$.

In this paper we shall merely relate charge effects to the number of intervening carbon atoms between charges and dissociating groups, as has been done, for example, by MacInnes (9), Schmidt (12), Greenstein (3), and Edsall (reference 1, pp. 96-104). A more refined treatment may be carried out employing actual interchange distances (5, 7, 8). Using experimental dissociation constants for a series of dicarboxylic acids (2) and a series of diamines (13), both with substituent groups on terminal carbon atoms, and the data for glutamic acid and

a number of other simpler amino acids given by Cohn and Edsall (1), microscopic equilibrium constants may be calculated as illustrated in reference 1 and Section II, and differences taken between those microscopic constants of a given compound which refer to the dissociation of the same proton. These differences may then be assigned to the influence of a charge or charges located, say, on the α , β , etc., carbon atom or atoms, counting from the dissociating group. Table 3 contains these differences for the substances mentioned above. They are also distances between "spectral lines" in the "spectrum" of microscopic pK values discussed previously. Indeed, an inspection of the three sets of four constants each (see figure 1) in the pK "spectrum" of glutamic acid shows qualitatively the expected effects of positive and negative charges in this molecule. Two sets of differences (table 3) may be obtained from the glutamic acid data in Section II.

Table 3 shows that, except for oxalic acid², malonic acid², and the diamines², the charge effects may be represented quite well by $\Delta pK = 2.00/d$. Plotting ΔpK against $1/d$, this is a straight line passing through the origin. In view of the success of approximate equations of the type³

$$pK_d = pK_\infty + C/d$$

this result is not surprising. For, if we consider, say, carboxylic acids and let the substituent be $-\text{NH}_3^+$, then

$$pK_d - pK_\infty = C_1/d \quad (7)$$

Now, for the same series of acids, let the substituent be $-\text{NH}_2$, and we have

$$pK_d^0 - pK_\infty^0 = C_2/d \quad (8)$$

Combining these equations,

$$(pK_d - pK_d^0) - (pK_\infty - pK_\infty^0) = (C_1 - C_2)/d = C_3/d \quad (9)$$

The differences in parentheses in equation 9 represent charge effects. Further, the second difference should be approximately equal to zero, so that

$$pK_d - pK_d^0 = C_3/d \quad (10)$$

The left member of equation 10 is, to a first approximation, a pure charge effect and hence is more or less independent of the particular group upon which the charge resides and of the dissociating group. Equation 10 should therefore have some degree of generality, as an approximate equation, and this is verified by table 3.

IV

The significance of the values in table 3 representing dicarboxylic acids may be better understood after examining curves for the two microscopic constants $pK_1 = pK_2$ and $pK_{12} = pK_{21}$ (table 3 gives their difference). Such curves are

² See figure 2 and the discussion of this figure below.

³ See reference 9. pK_d and pK_∞ are the pK values of the acid with the substituent at d and at ∞ , respectively. C is a constant.

given in figure 2, where pK_1 and pK_{12} are plotted against $1/d$ for the dicarboxylic acids and also for the diamines of table 3. For the dicarboxylic acids, the negative slope of the pK_1 line is equivalent to the fact that ΔF_1^0 is lower the closer the second carboxyl group is to the dissociating carboxyl group. The points for oxalic and malonic acids fall below the line. One possible explanation of this is that hydrogen bonds are formed in the intermediate ions (A_1 and A_2) of these two acids, thus lowering the free energies of the ions and also ΔF^0 beyond

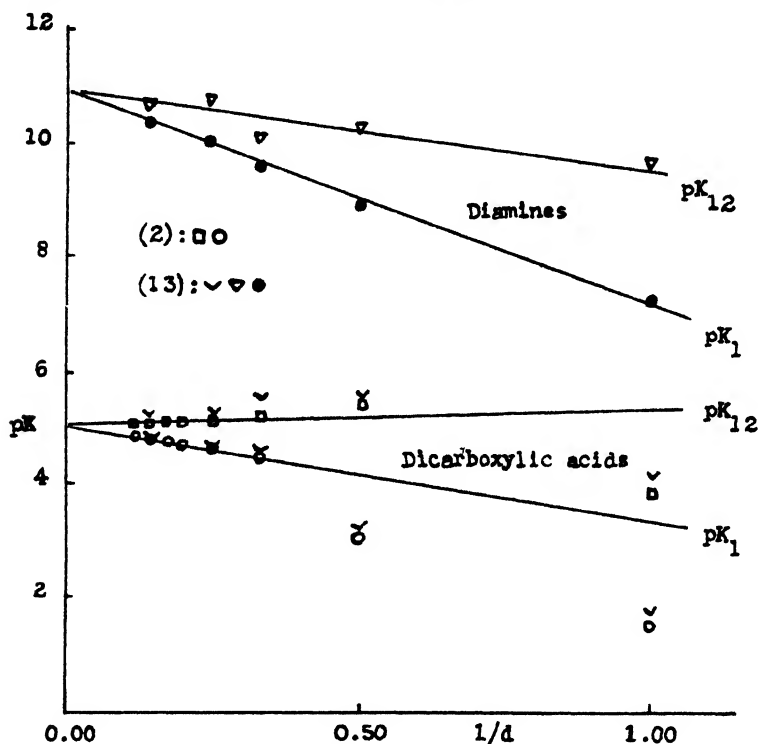
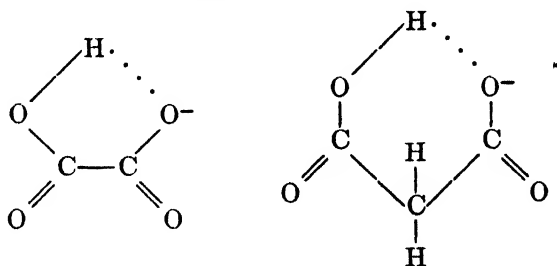


FIG. 2. Microscopic dissociation constants of the diamines and dicarboxylic acids (see references 2 and 13).

what would otherwise be expected. The rings would be five- and six-membered for oxalic and malonic acid, respectively:



Fisher-Hirschfelder models seem to confirm this possibility, even for the five-membered ring. The slight upward slope of the pK_{12} line indicates that a negative charge near a dissociating carboxyl group tends to increase ΔF^0 slightly more than a carboxyl group tends to lower it. If hydrogen bonds exist in the ions suggested above, the points for oxalic and malonic acids should fall above this second line. This is found to be the case for malonic acid. However, in connection with oxalic acid, there is evidence (11) of an additional resonance in the oxalate ion (double bond between the carbon atoms) which would tend to lower the point. Since the experimental point actually falls below the line, this latter effect is apparently more important. We may recall that oxalic acid appears in table 3 to be less anomalous than malonic acid. This is merely because the discrepancies in pK_1 and pK_{12} for oxalic acid are in the same direction and therefore partially cancel. Taking the average deviation of the two malonic acid points from the straight lines, one calculates a hydrogen-bond energy of about 0.9 kcal. per mole in the microscopic ions A_1 and A_2 of this acid. Finally, it may be noticed that the values of pK_1 from Schwarzenbach (13) (20°C.) agree well with those of Gane and Ingold (2) (25°C.), but the pK_{12} values from Schwarzenbach seem to be less consistent.

The pK_1 points for the diamines (13) (20°C.) fall rather near a straight line which has considerable negative slope, corresponding to a lower ΔF^0 the closer the second amine group is to the dissociating $-\text{NH}_3^+$ group and the closer the positive charge (which happens to reside on the second amine group) is to the dissociating $-\text{NH}_3^+$ group. That is, both effects act in the same direction. There are no indications of hydrogen bonds, as above, which is not very surprising since nitrogen forms hydrogen bonds with less ease than oxygen. The points for pK_{12} are quite variable, as they were for the dicarboxylic acids (13), but an approximate straight line is drawn. The slope of this second line results from the influence of an amine group with no charge; hence the difference in slopes between the two lines represents, approximately, the charge effect. Because of the uncertainties in the pK_{12} points, the differences between pK_1 and pK_{12} (with much greater relative uncertainties) for the diamines should not be given much weight in table 3.

Lastly, in connection with figure 2, it may be pointed out that, on the basis of this simplified approach, one might expect the pK_1 and pK_{12} lines for either group of compounds to intersect on the pK axis where $d = \infty$ (see equations 9 and 10).

V

As an example of an approximate calculation using the charge effects discussed above, we may now estimate the microscopic dissociation constants of lysine from $\Delta pK = 2.00/d$ and the apparent gross dissociation constants (reference 1, p. 85), $pK_{(1)} = 2.18$, $pK_{(2)} = 8.95$, and $pK_{(3)} = 10.53$. Number the carboxyl group first, the α -amino group second, and the ϵ -amino group third. Then $pK_1 = 2.18$, as before. It should be remarked that this experimental value is larger than expected in comparison with pK_1 for glycine, etc. Now

$$K_{(2)} = K_{12} + K_{13} \quad (11)$$

and

$$2.18 + pK_{12} + pK_{123} = pK_{(1)} + pK_{(2)} + pK_{(3)} = 21.66 \quad (12)$$

From $\Delta pK = 2.00/d$, we estimate

$$pK_{123} = pK_{13} + 0.50$$

whence equation 12 becomes

$$pK_{12} + pK_{13} = 18.98 \quad (13)$$

Equations 11 and 13 allow the calculation of pK_{12} and pK_{13} provided we know which is larger. The effect of a $-\text{COO}^-$ group on the dissociation of a neighboring carboxyl group is indicated by the pK_{12} line for the dicarboxylic acids in figure 2. The positive slope of this line would lead to the expectation that $pK_{12} > pK_{13}$. However, the effect of a $-\text{COO}^-$ substituent on the dissociation of an $-\text{NH}_3^+$ group leads quite definitely to the opposite conclusion (see the pK_2 line in figure 2, p. 101, reference 1). Therefore, as is conventional, we choose $pK_{13} > pK_{12}$. From equations 11 and 13, $pK_{12} = 8.99$ and $pK_{13} = 9.99$. From equation 12, $pK_{123} = 10.49$. Similarly, using a different path from A_0 to A_{123} , $pK_{132} = 9.49$. Again from $\Delta pK = 2.00/d$, we estimate

$$pK_{21} = pK_1 + 2.00 = 4.18$$

$$pK_{31} = pK_1 + 0.40 = 2.58$$

$$pK_{231} = pK_1 + 2.00 + 0.40 = 4.58$$

Taking appropriate sequences or paths from A_0 to A_{123} (see equation 12), we find with no further approximations, $pK_2 = 6.99$, $pK_3 = 9.59$, $pK_{23} = 10.09$, and $pK_{32} = 7.49$. The data for lysine in table 2 are based on the above approximate calculations. The values given above for pK_{123} , pK_{132} , and pK_{231} may be compared with those estimated by Edsall (reference 1, p. 103): 10.54, 9.8, and 4.3, respectively. As for glutamic acid above, the concentration ratios here are

$$c_3:c_2:c_1 = 1:400:26,000,000$$

and

$$c_{23}:c_{13}:c_{12} = 1:81,000:810,000$$

SUMMARY

Microscopic dissociation constants and relative standard free energies of microscopic ions may be calculated from experimental dissociation constants for a number of compounds. These results may be used to estimate average effects of charges, in different positions within molecules, on microscopic dissociation constants. Microscopic constants may then be approximated for other compounds for which the experimental data are incomplete. Examples are given.

In this connection, the anomalous dissociation constants of oxalic and malonic acids are discussed.

Certain analogies between the relative free energies and spectroscopic energy levels, and between the microscopic dissociation constants and spectral lines, are pointed out.

The author is grateful to Professor John T. Edsall for his helpful comments.

REFERENCES

- (1) COHN, E. J., AND EDSALL, J. T.: *Proteins, Amino Acids and Peptides as Ions and Dipolar Ions*, Chapter 4 (especially p. 99). Reinhold Publishing Corporation, New York (1943).
- (2) GANE, R., AND INGOLD, C. K.: *J. Chem. Soc.* **1931**, 2153.
- (3) GREENSTEIN, J. P.: *J. Am. Chem. Soc.* **58**, 1314 (1936).
- (4) HILL, T. L.: *J. Am. Chem. Soc.* **65**, 2119 (1943).
- (5) HILL, T. L.: *J. Chem. Phys.* **12**, 56 (1944).
- (6) HILL, T. L.: *J. Am. Chem. Soc.* **65**, 1564 (1943).
- (7) HILL, T. L.: *J. Chem. Phys.* **11**, 545, 552 (1943).
- (8) KIRKWOOD, J. G., AND WESTHEIMER, F. H.: *J. Chem. Phys.* **6**, 506 (1938). for example.
- (9) MACINNES, D. A.: *J. Am. Chem. Soc.* **50**, 2587 (1928).
- (10) NEUBERGER, A.: *Biochem. J.* **30**, 2085 (1936).
- (11) ROBERTSON, J. M., AND WOODWARD, I.: *J. Chem. Soc.* **1936**, 1817.
- (12) SCHMIDT, C. L. A., *et al.*: *J. Biol. Chem.* **81**, 723 (1929).
- (13) SCHWARZENBACH, G.: *Helv. Chim. Acta* **16**, 522 (1933).

AN APPLICATION OF THE METHOD OF CONTINUOUS VARIATIONS TO COMPLEX-ION FORMATION IN COPPER(II) SALT SOLUTIONS CONTAINING CHLORIDE ION

THERALD MOELLER

Noyes Chemical Laboratory, University of Illinois, Urbana, Illinois

Received January 21, 1944

INTRODUCTION

Although the familiar color changes produced by addition of excess chloride ion to copper(II) salt solutions and by concentration of copper(II) chloride solutions have in the past been ascribed variously to dissociation, hydrolysis, and solvation (summarized in 3, 4, 9, 13), the more acceptable modern explanation is in terms of the formation of complex chlorine-containing ions (2, 3, 11, 13). But little agreement exists, however, among statements as to the compositions of such chloro complexes, most postulations as to the existence of such ions as CuCl^+ , CuCl_2^- , and CuCl_4^{--} being either unsupported or based upon the preparation of compounds containing copper and chlorine in these ratios. Energy considerations do, however, indicate the CuCl_4^{--} ion to be the most probable one (10).

The colors of such systems have been extensively investigated. Getman (3), in a comprehensive study of the effects of hydrochloric acid and several metal

chlorides upon the absorption spectra of copper(II) chloride solutions, noted displacements of the region of maximum transmittancy toward longer wave lengths with increasing chloride content. This he ascribed to a displacement of an equilibrium between $\text{Cu}(\text{H}_2\text{O})_4^{++}$ and CuCl_4^{--} ions toward the yellow CuCl_4^{--} , although the composition given for the chloro complex was apparently based only upon a consideration of the well-known four-coördinate character of copper(II). Spectrophotometric investigations upon similar systems led Spacu and Murgulescu (11) to the conclusion that Beer's law could be applicable at short and long wave lengths only if the presence of CuCl_4^{--} and CuCl^+ , respectively, were assumed. The general inapplicability of Beer's relation to copper(II) chloride solutions has also been attributed to the presence of mixtures of Cu^{++} , CuCl^+ , CuCl_2^- , and CuCl_4^{--} ions (1).

In view of the uncertainty existent relative to the compositions of these complex ions, it was felt that some further clarification, particularly in terms of the characteristic colors of the systems, was desirable. Recent successes in application of the absorption of monochromatic light to determination of the compositions of complex ions (5, 6, 12) through a modification of Job's method of continuous variations (7) suggested a suitable experimental approach. Although Job was apparently unsuccessful in applying his method to copper(II)-chloride ion systems (8), the modified procedure has been found to be entirely applicable under the conditions here employed.

EXPERIMENTAL

A. Apparatus and materials used

With the exception of the values plotted in figure 5, all absorption data were obtained with a General Electric recording spectrophotometer. Data given in figure 5 were obtained with a Cenco-Sheard spectrophotometer. With both instruments, a slit width of 10 m μ and a cell depth of 1 cm. (± 0.5 per cent) were employed. In some further unreported experiments, both instruments were used upon the same system with identical results.

All chemicals were of analytical reagent quality and were used without further purification. The copper(II) salt solutions were analyzed for copper by the usual iodide-thiosulfate procedure, the sodium and potassium chloride solutions were prepared by direct weighing of the dried halides, the lithium and calcium chloride solutions were analyzed for chloride by the Volhard procedure, and the hydrochloric acid was standardized against pure sodium carbonate. The concentrations of most of the solutions employed are given in table 1. Solutions in a given horizontal line of this table were used in combination with each other. In the discussions to follow, rounded concentrations have been used rather than the exact ones, but the necessary corrections have been made in the construction of the graphs. The concentrations of some solutions not mentioned in table 1 are given in the text.

B. Application of the method of continuous variations

In conformity with the procedure of Vosburgh and Cooper (12), absorption spectra of solutions 1.00 M in copper(II) nitrate and containing sodium or

lithium chloride in varying mole ratios ($\text{Cu}^{++}:\text{Cl}^-$) were measured over the wave length range 400 to 700 $\text{m}\mu$. Data for the lithium chloride systems are plotted in figure 1. Data for solutions containing sodium chloride were exactly similar, except that the limited solubility of this halide precluded measurements at ratios much above 1:5.

Further absorption measurements were then made upon solutions obtained by mixing variable volumes of copper(II) nitrate solutions ($1 - x$) with variable volumes of chloride solutions (x) of like concentrations, the total volumes in a given series all being the same (12). Plotted in figure 2 as deviation (Y) of observed optical density from the theoretical against solution composition (x) are data at several representative wave lengths for the 4 M system containing lithium chloride. In figure 3 are given similar data obtained at 450 $\text{m}\mu$ for systems containing sodium (4 M), lithium (4 M), hydrogen (3 M), potassium

TABLE 1
Concentrations of solutions used

ROUNDED CONCENTRATIONS IN MOLES PER LITER	EXACT CONCENTRATIONS IN MOLES PER LITER					
	$\text{Cu}(\text{NO}_3)_2$	LiCl	NaCl	KCl	HCl	CaCl_2
4	4.03	4.09	4.00	2.00	2.99	1.00
4	3.89					
3	3.20					
2	1.93					
2(1)	2.16					

(2 M), and calcium (1 M , i.e., 2 M in Cl^-) chlorides, the ordinates in some instances being multiplied by the indicated factors. Since other measurements in the copper(II) ion concentration 2 to 4 M were in exact agreement with the values given, they are not included.

Some similar measurements were also made upon copper(II) sulfate solutions containing added chloride. The resulting data, while in agreement with those for the nitrate solutions, were limited in scope by the lesser solubility of the sulfate. Nitrate solutions are also to be preferred because of the negligible coördinating tendency of the anion.

C. Absorption spectra of copper(II) chloride solutions

Absorption spectra of copper(II) chloride solutions were measured for the concentration range 0.05 to 3.0 M . These data are plotted in figure 5.

DISCUSSION

The marked effects of chloride ion upon the absorption spectra of copper(II) nitrate solutions shown in figure 1 are indicative of the formation of at least one new ionic species differing in color from that of the hydrated copper(II) cation. Coincidence or near coincidence at longer wave lengths of all curves regardless of the $\text{Cu}^{++}:\text{Cl}^-$ ratio suggests the presence of but a single colorimetrically detectable complex ion. Since at shorter wave lengths all deviations from the

curve for pure copper(II) nitrate are of the same type, a color contribution by but a single new factor is indicated.

As pointed out by Vosburgh and Cooper (12), a plot of the difference between observed optical density and the theoretical (calculated on the assumption of

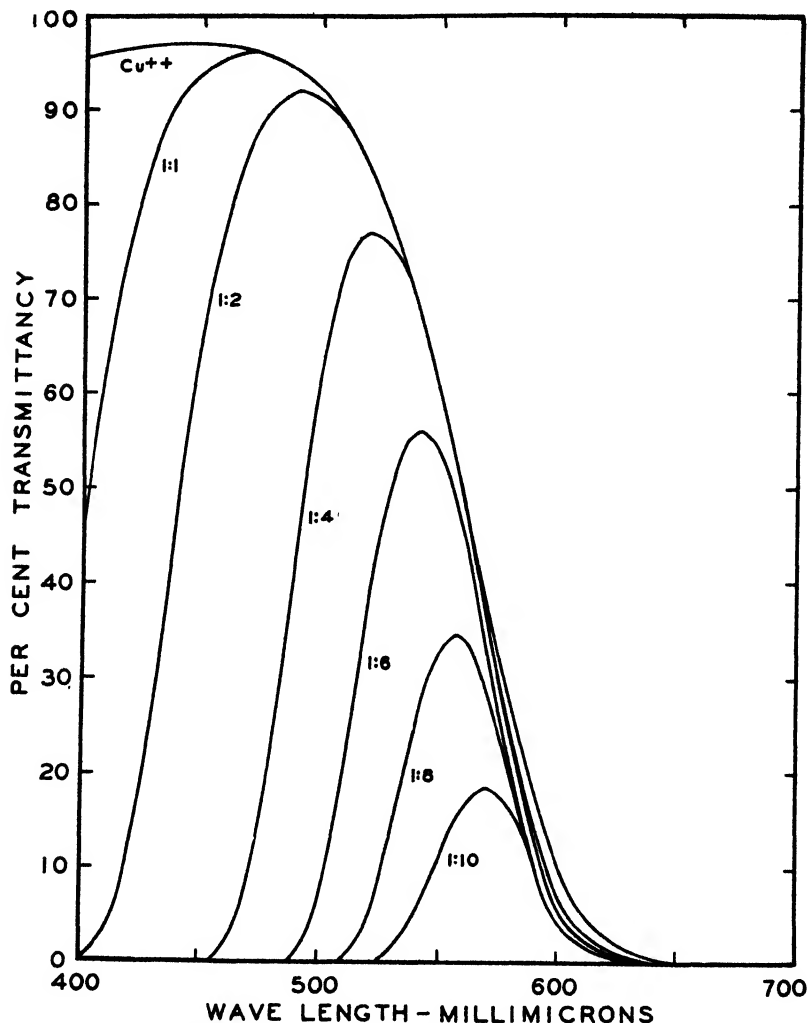


FIG. 1. Absorption spectra of solutions containing copper (II) nitrate and lithium chloride in varying mole ratios ($\text{Cu}^{++}:\text{Cl}^-$).

the existence of a straight-line relation between the optical densities of the component solutions) against the solution composition (x) should show a maximum (or minimum) at some solution composition related to the constitution of the complex ion. Furthermore, if but a single complex be formed, all maxima should fall at the same x value regardless of the wave length selected, providing

the spectra of the mixture and the colored component differ at that wave length (5).

As is apparent from a consideration of figure 1, application of this second criterion to copper(II)-chloride solutions is limited to the shorter wave lengths. However, representative data given in figure 2 for the 4 *M* copper(II) nitrate-lithium chloride system indicate the presence of but a single chloro complex, since all maxima fall at $x = 0.82$ regardless of the wave length selected.

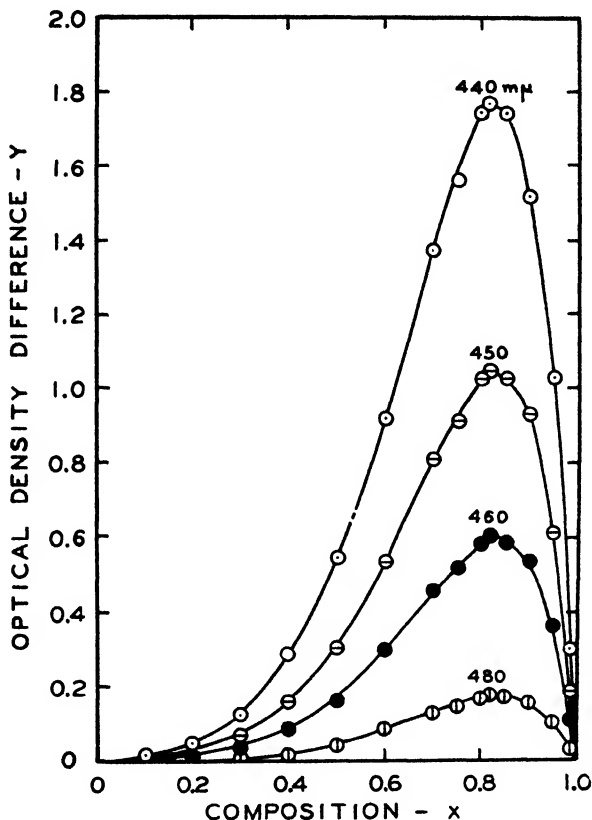


Fig. 2. Variation of optical density difference (Y) with solution composition (x)

Further data plotted in figure 3 are given at the arbitrary wave length 450 $m\mu$, this wave length giving the best coverage for the variety of concentrations employed and still providing measurable optical density differences at lower concentrations. Regardless of the concentration employed or the chloride used, maximum deviation is noted at the same solution composition, the average for the five systems being at $x = 0.80$. Since the Cl:Cu ratio in the complex ion is then given by the ratio of x to $(1 - x)$ (12), it is apparent that the CuCl_4^{--} ion is present.

Although in figure 1 coincidence of all curves occurred at longer wave lengths,

some displacement toward the longer wave lengths with increasing chloride concentration was noted in solutions of varying compositions. This is shown by the solid-line curves in figure 4, where data for the 4 *M* copper(II) nitrate-lithium chloride system are plotted at *x* values of 0.2 and 0.6. Even though deviations between observed and calculated optical densities which thus arise at longer wave lengths might attain maximum values, the effect is probably due only to dilution and cannot be regarded as indicative of the presence of other

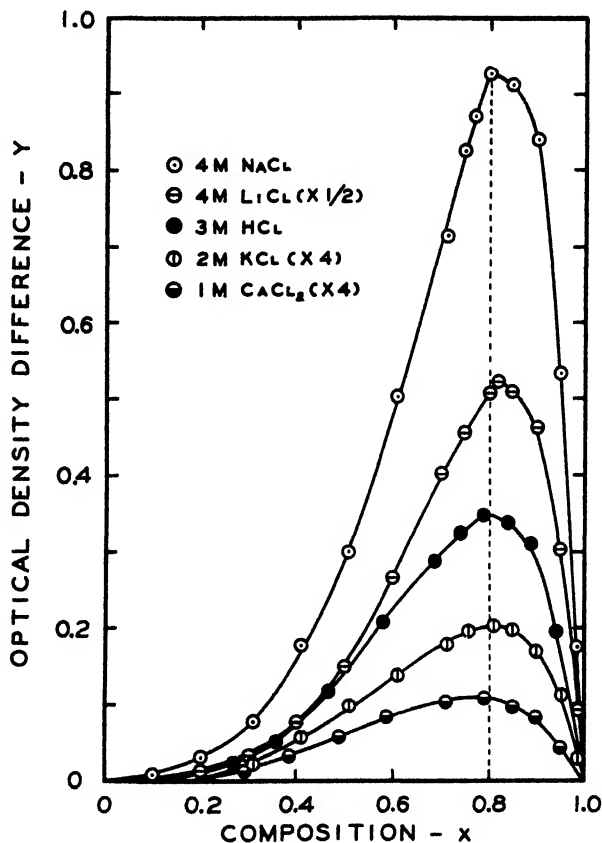


FIG. 3. Variation of optical density difference (*Y*) with solution composition (*x*). Some ordinates have been multiplied by the factors indicated.

complex ions. This is shown in figure 4 by the exact agreement between the experimental points for 4.11 *M* copper(II) nitrate solutions (diluted with water to the same copper contents as the chloride-containing solutions) and the descending branches of the solid curves. The expected deviation at shorter wave lengths is very apparent.

While the method of continuous variations can be regarded as demonstrating definitely the presence of certain ionic species, it does not necessarily prove the

presence or absence of all possible combinations. Thus, although the existence of the CuCl_4^{--} ion is definitely established by the data given, it is impossible to state conclusively that this is the only chloro complex present in these systems. However, the nature of the curves in figure 1 and the analysis in figure 2 are

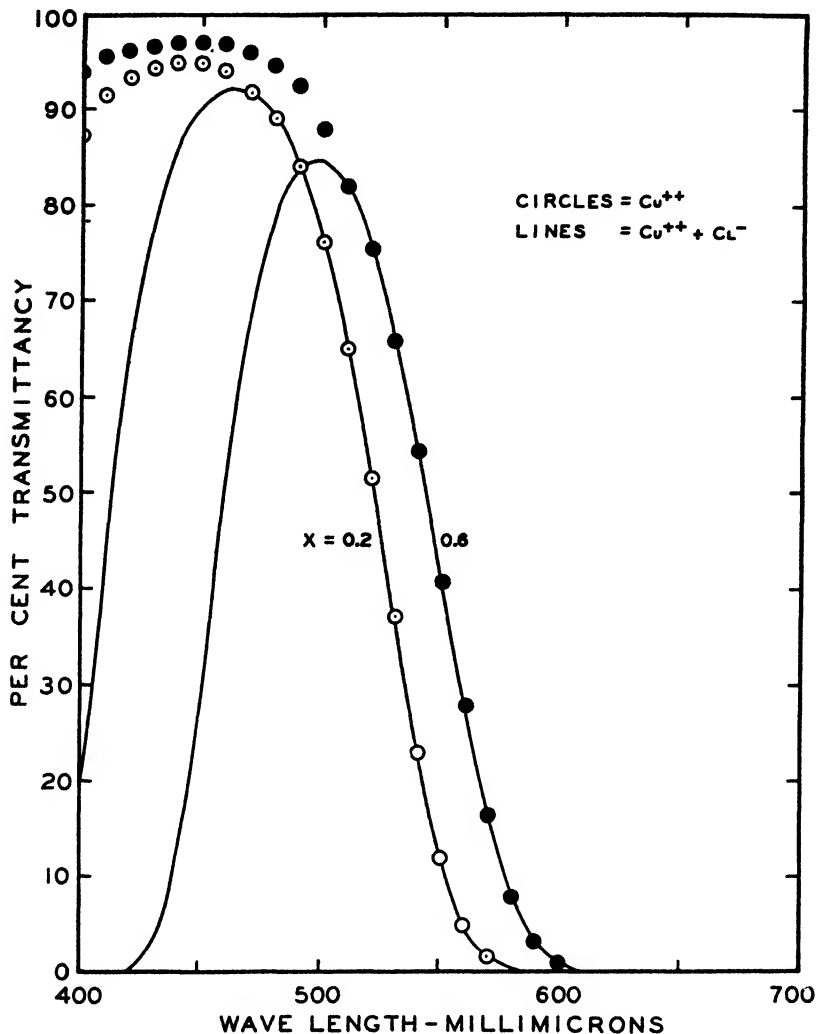
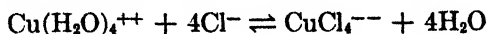


FIG. 4. Dilution effect in solutions of varying composition

strongly indicative that alteration in color in these solutions is associated with the appearance and disappearance of the CuCl_4^{--} ion. From the colorimetric point of view, no other complex is indicated, and no information relative to the CuCl^+ ion (11) is obtainable by this method.

We may then reasonably conclude, in agreement with the postulation of

Getman (3), that color changes in copper(II) salt solutions containing chloride ion are dependent upon displacements of the equilibrium



Data in figure 1, coupled with the impossibility of obtaining measurable absorption differences in solutions of varying compositions derived from copper(II)

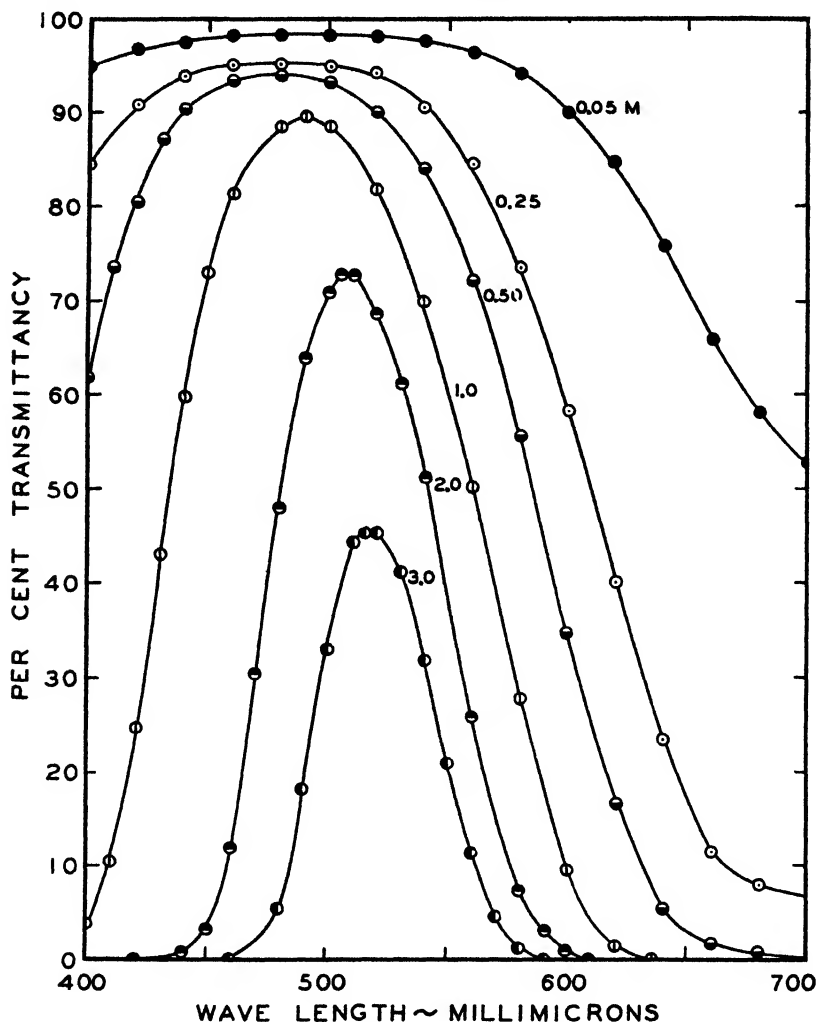


FIG. 5. Absorption spectra of copper(II) chloride solutions of several concentrations

nitrate less concentrated than 2 M, are indicative of the relative instability of the CuCl_4^{--} ion in aqueous solutions. Only under conditions of relatively high copper and chloride concentrations can the above equilibrium be displaced appreciably toward the chloro complex.

The true color of the CuCl_4^{--} ion can only be approximated. The shift in absorption maximum with increasing chloride content shown in figure 1 and the formation of brownish yellow solutions upon the addition of excessive quantities of chloride ion (e.g., in the form of the highly soluble chlorides of calcium or hydrogen) to copper(II) salt solutions (2) suggest a probable yellowish color for this ion. Green solutions containing intermediate amounts of chloride can then be regarded, in terms of the above equilibrium, as containing mixtures of the aquo and chloro complexes, the shade of color being a function of the quantity of chloride. That sodium chloride produces only green solutions when added to copper(II) salts is due to the lesser solubility of this halide, the same being true for the chlorides of potassium and ammonium.

Absorption data for copper(II) chloride solutions plotted in figure 5 are in essential agreement with similar data presented by Getman (3) but encompass somewhat greater wave length and concentration ranges. The similarities existent between these curves and those in figure 1 are indicative of the presence of CuCl_4^{--} ions in the more concentrated solutions. Since this is a case of autocomplex formation, some unaltered $\text{Cu}(\text{H}_2\text{O})_4^{++}$ ions must always be present, and aqueous solutions of copper(II) chloride can never possess the color of the chloro anion alone.

SUMMARY

1. Alterations in the absorption spectra of copper(II) salt solutions produced by addition of chloride ion are ascribed to the formation of chlorine-containing complex ions.
2. Application of the method of continuous variations clearly indicates the presence of the CuCl_4^{--} ion but gives no information relative to the presence or absence of other complexes.
3. Equilibria between $\text{Cu}(\text{H}_2\text{O})_4^{++}$ and the relatively unstable CuCl_4^{--} ions account for variations in color in such systems.
4. Color changes produced by concentration of copper (II) chloride solutions are due to the appearance of CuCl_4^{--} ions as a result of an autocomplexing process.

REFERENCES

- (1) BHAGWAT: J. Indian Chem. Soc. **17**, 52 (1940).
- (2) DONNAN AND BASSETT: J. Chem. Soc. **81**, 939 (1902).
- (3) GETMAN: J. Phys. Chem. **26**, 217 (1922).
- (4) GMELIN-KRAUT: *Handbuch der anorganischen Chemie*, Band V, Abteilung 1, p. 904. Carl Winter's Universitätsbuchhandlung, Heidelberg (1909).
- (5) GOULD AND VOSBURGH: J. Am. Chem. Soc. **64**, 1630 (1942).
- (6) HAENDLER: J. Am. Chem. Soc. **64**, 686 (1942).
- (7) JOB: Ann. chim. [10] **9**, 113 (1928).
- (8) JOB: Ann. chim. [11] **6**, 97 (1936).
- (9) MELLOR: *A Comprehensive Treatise on Inorganic and Theoretical Chemistry*, Vol. III, p. 173. Longmans, Green and Co., London (1923).
- (10) REMY AND LAVES: Ber **66B**, 401 (1933).
- (11) SPACU AND MURGULESCU: Z. physik. Chem. **A170**, 71 (1934).
- (12) VOSBURGH AND COOPER: J. Am. Chem. Soc. **63**, 437 (1941).
- (13) YAJNIK, CHAND, KAPUR, AND JAIN: J. Indian Chem. Soc. **19**, 357 (1942).

CONTACT ANGLES AND ADSORPTION ON SOLID SURFACES

H. K. LIVINGSTON¹*Kent Chemical Laboratory, University of Chicago, Chicago, Illinois**Received February 24, 1944*

Doss and Rao (6) have presented an equation which expresses the relation between adsorption and contact angles as follows:

$$\cos \theta = 2\sigma - 1 \quad (1)$$

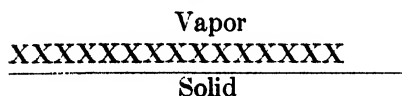
θ = the thermodynamic contact angle between solid, liquid, and vapor, and σ = the fraction of the solid surface covered by adsorbed molecules. This equation was developed from theoretical considerations, and the authors made no attempt to compare it with experimental data. In the following discussion, it will be shown that equation 1 is in agreement with the known facts.

DERIVATION OF EQUATION 1

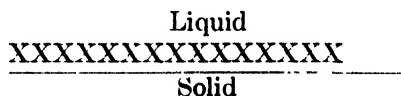
Doss and Rao consider the free-energy change on the immersion into a liquid of a solid which is in equilibrium with the saturated vapor from the liquid. The free-energy change (per unit area) is given by

$$\Delta F = \gamma_{SL} - \gamma_{SV} \quad (2)$$

The condition of the solid surface before and after immersion is given below, where X indicates an adsorbed molecule.



(a) Before immersion



(b) After immersion

Two assumptions have been made to complete the derivation: Assumption I—On immersion, the interface between adsorbed molecules and vapor (which occupies σ area units) is replaced by an interface between adsorbed molecules and liquid (process 1), and an interface (which occupies $(1 - \sigma)$ area units) is established between the free space in the adsorption region and the liquid (process 2).

Assumption II—The free-energy change of process 1 is represented by a decrease in energy equal to the surface tension of the liquid, and the energy change of process 2 is represented by an increase in energy equal to the surface tension of the liquid. That is,

$$\Delta F = -\gamma_{LV}\sigma + \gamma_{LV}(1 - \sigma) \quad (3)$$

Thus,

$$\gamma_{SL} - \gamma_{SV} = \gamma_{LV}(1 - 2\sigma) \quad (4)$$

¹ Present address: Jackson Laboratory, E. I. du Pont de Nemours and Co., Inc., Wilmington, Delaware.

But the fundamental thermodynamic equation of solid-liquid-vapor interfaces is

$$\gamma_{SV} - \gamma_{SL} = \gamma_{LV} \cos \theta \quad (5)$$

Therefore,

$$\cos \theta = 2\sigma - 1 \quad (1)$$

The assumption that the free energy at the surface of an adsorbed molecule is identical with the free energy of molecules at the surface of the liquid is similar to the assumption which Langmuir has made in applying his principle of independent surface action (11). Also, Brunauer, Emmett, and Teller (5) have assumed that the energy of adsorption of vapor molecules on the first or later adsorbed layers is equal to the energy of condensation of the vapor to liquid. If the adsorbed molecules contain groups with different surface energies, such as the hydrocarbon and hydroxyl groups in propyl alcohol, assumption II would not be valid. Doss and Rao have recognized this; they state that their treatment is limited to isotropic molecules.

CONTACT-ANGLE DATA

The most extensive compilation of contact-angle data available is that of Young and Harkins (15), in which an attempt was made to select only those data which were obtained for clean solid surfaces. All the contact angles which they report are equal to zero, except those for water on azobenzene and paraffin and for mercury on glass and similar solids.

The contact angle can be measured by several simple geometric methods. For any given system, values may vary widely depending on the state of the solid surface, whether the liquid is advancing or receding, the presence of vapors of a third component, etc. The *thermodynamic* contact angle is the angle defined by equation 5. This equation applies to a system of solid, liquid, and vapor phases, containing two components, one primarily in the solid phase and the other primarily in the liquid phase. The two components are distributed in their equilibrium condition through the three phases. The terms γ_{SV} , γ_{SL} , and γ_{LV} refer to the free surface energies at the three interfaces between solid (S), liquid (L), and vapor (V). The thermodynamic contact angle therefore is an exact quantity for any thermodynamically defined set of conditions. Inasmuch as Doss and Rao used equation 5 in deriving equation 1, it is the thermodynamic contact angle to which the equation of Doss and Rao refers.

It is apparent that the true thermodynamic contact angle can be obtained only by rigorously outgassing the solid surface so that only molecules of the solid component are present, introducing the pure liquid in sufficient quantity so that some bulk liquid remains, and allowing the liquid to adopt the equilibrium position. Contact angles measured in air are not thermodynamic contact angles. There are many indications that adsorbed molecules from air act to diminish the wetting of the solid surface. For example, Bartell and Cardwell (2) found that the contact angle of water on freshly formed gold and silver surfaces increased

with increasing exposure to air. Adam (1) has reported that air or possibly a greasy material deposited from air increases the difference between the advancing and receding contact angles. It is frequently observed that a solid exhibits a finite advancing contact angle but a zero receding contact angle. The receding contact angle is, of course, the equilibrium contact angle. It would be expected that the thermodynamic contact angle would be equal to or smaller than the receding contact angle determined by careful measurement in air. This means that solid-liquid-vapor systems which exhibit zero contact angles in air have thermodynamic contact angles equal to zero.

ADSORPTION DATA

Multilayer adsorption is characterized by adsorption isotherms which are either sigmoid or concave to the pressure axis, as opposed to Langmuir-type isotherms which are convex to the pressure axis. The existence of multilayer adsorption can be demonstrated by the use of the adsorption equation of Brunauer, Emmett, and Teller (5) to determine whether the pressure at which a complete monomolecular layer is formed is less than the saturation pressure. As far as is known, all experimental isotherms which represent the formation of less than a complete monomolecular layer at saturation obey the Langmuir equation (10). Brunauer (4) reports that only charcoals and chabasite were found to give isotherms of this type up to saturation pressure.

Presumably if the surface is not completely covered, Γ , the number of molecules adsorbed per unit area at saturation pressure, will be less than $(1/A)$. A is the area which an adsorbed molecule occupies on the solid surface, at the closest possible molecular packing. This is essentially the cross-sectional area of the adsorbed molecule, as discussed by the writer elsewhere (12), and is very similar to the area as estimated from x-ray diffraction data. Thus, when the surface is not completely covered,

$$\sigma = 1/\Gamma A \quad (6)$$

CONSIDERATION OF EXPERIMENTAL DATA

Table 1 presents a summary of the available experimental data regarding σ and θ for solid-liquid-vapor systems. Consideration has been limited to non-porous solids and to liquids which have the symmetrical structure required by assumption II (i.e., isotropic liquids). For a number of the systems, experimental contact-angle data are not available. When this is the case, reference has been made to the generalizations of Boyd and Livingston (3), which state that the contact angle is zero for polar and non-polar organic liquids and water on polar solids, or for non-polar liquids on non-polar solids, but is finite for polar liquids on non-polar solids.

Two generalizations can be made, based on the data of table 1: (1) the contact angles for liquids on solids are generally zero; (2) the fraction of the solid surface covered by adsorbed molecules from the vapor at saturation pressure is generally

unity. That is, for most two-component solid-liquid-vapor systems, $\theta = 0$ and $\sigma = 1$. If either one of the generalizations were established, the other would follow according to the equation of Doss and Rao.

TABLE 1
Adsorption and contact-angle data for solid-liquid-vapor systems

SOLID	LIQUID-VAPOR	TYPE OF ADSORPTION	REFERENCE	FRACTION OF THE SOLID SURFACE COVERED AT SATURATION (σ)	CONTACT ANGLE IN AIR	REFERENCE	THERMODYNAMIC CONTACT ANGLE (θ)
Glass	Water	Multilayer	(4, 8, 13)	1	0°	(15)	0°
Glass	Benzene	No data; see glass-toluene			0°	(15)	0°
Glass	Toluene	Multilayer	(4, 8)	1	No data; see glass-benzene		
Glass	Mercury	No data		?	$128-148^\circ$	(15)	?
Silica	Water	Multilayer	(3, 9)	1	0°	(3)*	0°
Silica	Acetone	Multilayer	(1, 14)	1	0°	(3)	0°
Silica	Benzene	Multilayer	(9, 14)	1	0°	(3)	0°
Silica	Heptane	Multilayer	(3)	1	0°	(3)	0°
Anatase	Water	Multilayer	(3, 9)	1	0°	(3)	0°
Anatase	Heptane	Multilayer	(3)	1	0°	(3)	0°
Barium sulfate	Water	Multilayer	(3)	1	0°	(3)	0°
Barium sulfate	Heptane	Multilayer	(3)	1	0°	(3)	0°
Graphite..	Water	†		?	86°	(7)	?
Paraffin	Water	No data		?	106°	(15)	?

* Contact-angle data obtained from reference 3 were obtained from theoretical considerations rather than experimental data (see text).

† The data in reference 3 are not considered, because it has since been determined that the sample of graphite which was used (Dixon 0708) has a high ash content.

SOLID SURFACES COMPLETELY COVERED BY ADSORBED MOLECULES

The derivation of equation 1 should be reexamined for the special case where the surface is completely covered. Then, assumption I involves only the replacement of adsorbed layer-vapor interface by adsorbed layer-liquid interface. Assumption II indicates that the adsorbed layer possesses the energy relations of the bulk liquid, so the surface free energy changes from γ_{LV} to zero on immersion. That is,

$$\gamma_{SL} - \gamma_{SV} = -\gamma_{LV} \quad (7)$$

By combination with equation 5,

$$\gamma_{LV} = \gamma_{LV} \cos \theta$$

or,

$$\cos \theta = 1$$

Therefore, the thermodynamic contact angle for solid-liquid-vapor systems will be zero if the vapor is adsorbed in multilayers on the solid at saturation pressure. There seems to be ample experimental evidence in support of this prediction. A corollary is that the free surface energy of the adsorbed layer at saturation pressure is equal to the surface tension of the liquid (saturated with the solid component).

If the adsorbed layer is not complete at saturation, the free energy of the partially covered surface must be less than the surface tension of the liquid. Whether the relation is exactly that predicted by equation 1 remains to be determined. It will be necessary to study systems which give finite contact angles *in vacuo* to complete the verification of the equation of Doss and Rao. It is hoped that experimental investigations of systems such as water on graphite or mercury on silica will be carried out to conclude this investigation.

CONCLUSION

It has been shown that for most two-component solid-liquid-vapor systems, the contact angle is zero ($\theta = 0$) and the solid surface is completely covered with adsorbed molecules from the vapor at saturation pressure ($\sigma = 1$). This is in agreement with the equation of Doss and Rao which states that

$$\cos \theta = 2\sigma - 1$$

There are no experimental data with which to compare this equation when $\theta > 0$ or $\sigma < 1$. Therefore, the verification of the equation can not be considered to be complete.

REFERENCES

- (1) ADAM: *The Physics and Chemistry of Surfaces*. Oxford University Press, London (1941).
- (2) BARTELL AND CARDWELL: J. Am. Chem. Soc. **64**, 494, 1530, 1641 (1942).
- (3) BOYD AND LIVINGSTON: J. Am. Chem. Soc. **64**, 2383 (1942).
- (4) BRUNAUER: *The Adsorption of Gases and Vapors*, Vol. I. Princeton University Press, Princeton (1943).
- (5) BRUNAUER, EMMETT, AND TELLER: J. Am. Chem. Soc. **60**, 309 (1938).
- (6) DOSS AND RAO: Proc. Indian Acad. Sci. **7**, 113 (1938).
- (7) FOWKES AND HARKINS: J. Am. Chem. Soc. **62**, 3377 (1940).
- (8) FRAZER, PATRICK, AND SMITH: J. Phys. Chem. **31**, 897 (1927).
- (9) GANS, BROOKS, AND BOYD: Ind. Eng. Chem., Anal. Ed. **14**, 396 (1942).
- (10) LANGMUIR: J. Am. Chem. Soc. **40**, 1361 (1918).
- (11) LANGMUIR: In Alexander's *Colloid Chemistry*, Vol. I, p. 524. The Chemical Catalog Co., Inc., New York (1926).
- (12) LIVINGSTON: J. Am. Chem. Soc., April, 1944.
- (13) McHAFFIE AND LENHER: J. Chem. Soc. **127**, 1559 (1925).
- (14) PALMER AND CLARK: Proc. Roy. Soc. (London) **A149**, 360 (1935).
- (15) YOUNG AND HARKINS: *International Critical Tables*, Vol. IV, p. 434. McGraw-Hill Book Co., Inc., New York (1928).

A STUDY OF THE COLLOIDAL SYSTEM CARBON DISPERSED IN XYLENE

V. R. DAMERELL AND A. URBANIC

*Morley Chemical Laboratory, Western Reserve University, Cleveland, Ohio**Received October 23, 1943*

In spite of the great industrial importance of lyophobic organosols in the field of protective coatings, fundamental research in this branch of colloid chemistry is considerably behind that dealing with aqueous systems. In particular, very little fundamental work has been published on organosols of carbon, and the authors have accordingly undertaken an investigation of sols obtained when this substance was dispersed in xylene. The research consisted mainly of a study, by sedimentation and ultramicroscopic analysis, of the effect of twenty-four surface-active agents upon various carbon-xylene systems. In addition adsorption measurements, cataphoresis measurements, and studies of highly dried carbon-xylene systems were carried out.

EXPERIMENTAL

Materials

The xylene used was distilled over fresh barium oxide; its boiling point was 137–138.5°C. A 150-ml. portion gave no weighable residue upon evaporation. Xylene was used as the dispersion medium because of its relative chemical simplicity and its availability in the large amounts (80 liters) required for the research. Three types of carbons were used, and will be referred to hereafter as carbons A, B, and C. Information on them is given in table 1. These carbons, and the analyses for adsorbed oxygen, were furnished by the Columbian Chemical Company of New York City.

The surface-active chemicals used are listed in table 2. These were all pure chemicals except the soaps, tripalmitin, the fatty acids, oleic amine, and lecithin, which were of the best grade obtainable but were not chemically pure.

Preparation of sols

One-half gram of the dried colloidal carbon was added to 500 ml. of xylene containing 0.001 gram mole of surface-active agent. This small concentration was found to be sufficient if the agent was effective, a fact also noted by Harkins and Gans (4). The suspension was then stirred in an 800-ml. beaker for 45 min. with an electric stirrer (667 R.P.M.). To prevent loss by splashing or evaporation a copper plate, containing two holes for the stirrer shaft and a thermometer, was used as a cover. The temperature of the suspension was held at 25°C., either by momentarily cooling the beaker with dry ice or by warming it with the hands. The temperature of the room was also held at 25°C. \pm 2°.

TABLE 1
Properties of carbons used

TYPE OF CARBON	PERCENTAGE OF ADSORBED OXYGEN	DENSITY	SURFACE AREA*, IN SQUARE METERS PER GRAM
A.	0.5	1.85	26.7
B.	6.0	1.97	546
C.	15.3	1.97	600

* Determined by Emmett method.

TABLE 2
The relative effect of surface-active agents on dispersions of carbon A in xylene

NO.	ACTIVE COMPONENT	AMOUNT OF COMPONENT	ORDINATE AT 100 MIN	PARTICLE COUNT OF STANDARD VOLUME
		<i>grams</i>		
1	Lecithin	0.789	0.050	1200
2	Lecithin	0.822	0.053	1350
3	Copper oleate	0.400	0.049	394
4	Cobalt naphthenate	0.714	0.042	189
5	Aerosol OT*	0.446	0.063	73
6	Aerosol OT*	0.434	0.068	60
7	Aerosol MA†	0.403	0.065	59
8	Dicyclohexylamine	0.352	0.070	36
9	Triisoamylamine	0.469	0.070	24
10	Magnesium oleate	0.543	0.070	30
11	Lead naphthenate	0.724	0.076	4
12	Zinc naphthenate	0.751	0.078	3
13	Benzidine	0.201	0.080	5
14	Oleic amine	0.553	0.084	3
15	Diamylamine	0.322	0.085	4
16	Amylamine	0.299	0.086	3
17	Blank		0.088	1
18	Blank		0.089	1
19	Tripalmitin	0.773	0.087	1
20	Stearic acid	0.280	0.086	1
21	Oleic acid	0.578	0.087	1
22	Dibutyl phthalate	0.566	0.087	1
23	Octadecanol	0.540	0.090	1
24	Octadecane	0.471	0.089	1
25	Octadecyl chloride	0.557	0.089	1
26	Stearanilide	0.356	0.088	1
27	Octadecyl acetate	0.321	0.090	1
28	Alpha pinene	0.286	0.092	1

* Sodium dioctyl sulfosuccinate.

† Sodium dihexyl sulfosuccinate.

Sedimentation analysis

The dispersed suspension was poured into a silver Dewar vacuum flask, of 19 cm. length and 8 cm. inside diameter, which contained the pan of the sedi-

mentation balance. The Dewar was immediately put inside the balance, the pan was attached to the balance beam, and the weight of solid depositing with time was observed. The balance was similar to that used by Calbeck and Harner (1). To prevent loss of the xylene by evaporation, a transite cover was used on top of the Dewar and a beaker containing xylene was kept inside the balance case. A temperature within 2° of $25^\circ\text{C}.$ was maintained in the balance case. This had to be watched carefully during sedimentations, and changes corrected for, as a difference of $1^\circ\text{C}.$ caused the buoyancy of the balance pan to change by 5 mg. Each sedimentation analysis took 14 hr. to run.

Sedimentation curves were made by plotting time in minutes against weight of sediment in grams. From these, particle-size distribution and relative degree of dispersion were calculated in the usual manner by drawing tangents to the curve, using a tangentiometer which consisted of a small mirror glued to a straight

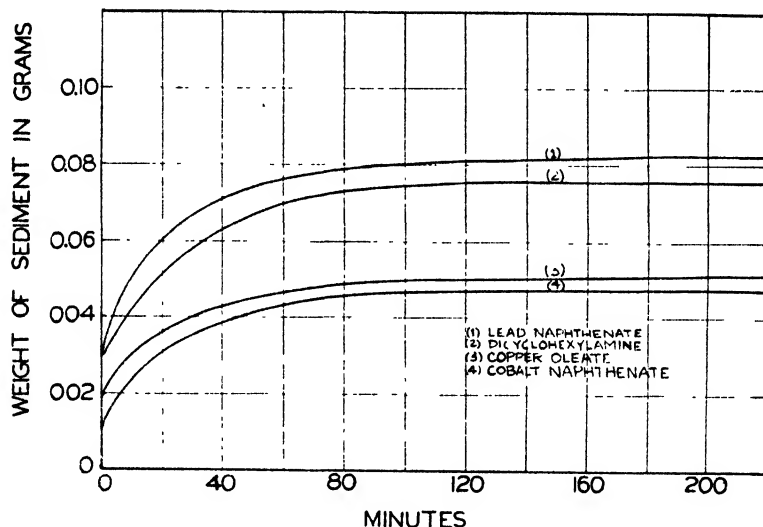


FIG. 1 Sedimentation curves for carbon A

edge. For substitution in Stokes' law the following values were used: density of xylene, 0.855; viscosity of xylene, 0.00631 poise; density of carbon, 1.85 or 1.97, depending upon the type used (see table 1). The constants for xylene were corrected when the temperature varied from $25^\circ\text{C}.$ Typical sedimentation curves for various suspensions are given in figures 1, 2, and 3.

The lower the horizontal part of these curves, the greater the amount of unsettled material and thus the greater the degree of dispersion. Accordingly, as an index of the degree of dispersion the length of the ordinate at an abscissa of 100 min. has been used to summarize results, as the printing of this many sedimentation curves is not practicable. A list of ordinates at 100 min. for the various surface-active agents is given in tables 2, 3, and 4.

It was found that for any given system the sedimentation results could be duplicated, in separate experiments, to within ± 0.003 g., or about 3 per cent.

Ultramicroscopic analysis

The supernatant suspension of the dispersion standing for 36 hr. was called the organosol, as it fulfilled the size specification of such a colloid. A representative sample of this was examined in the quartz cell of a Bausch and Lomb slit

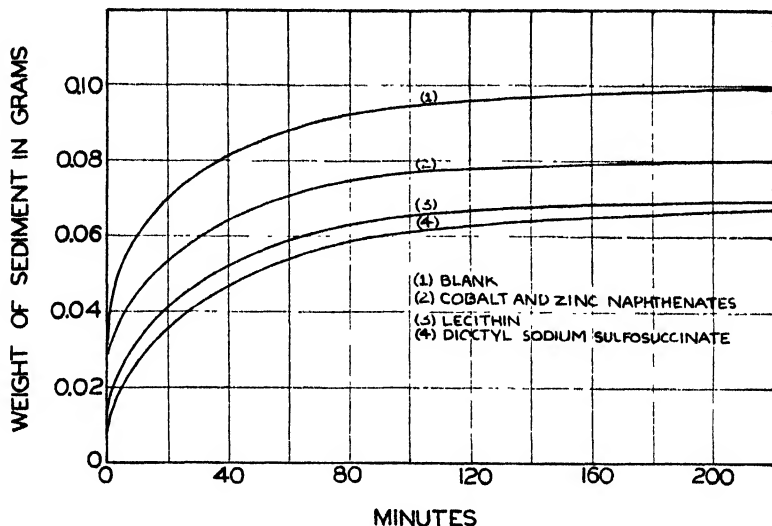


FIG. 2. Sedimentation curves for carbon B

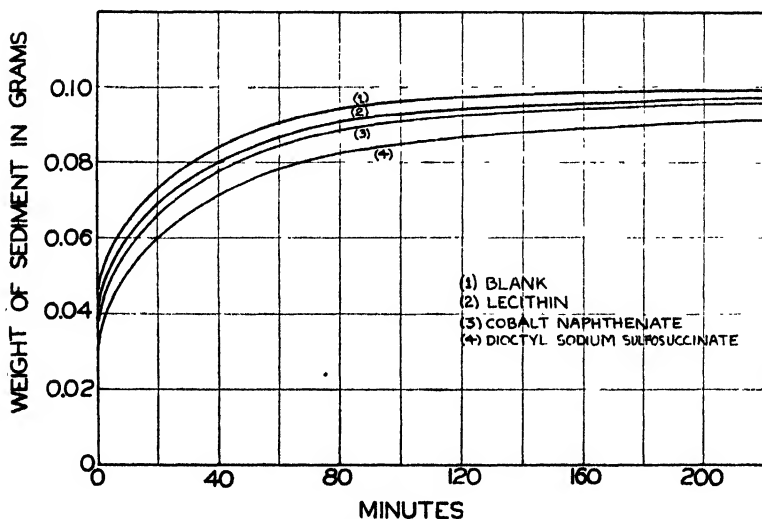


FIG. 3. Sedimentation curves for carbon C

ultramicroscope (Catalog No. 31-28-28). The number of particles in the volume illuminated by five slit divisions and enclosed by eighteen squares of an ocular micrometer was determined. This volume was 9.5×10^{-8} cc. If the sample had many particles, the count was made in a volume of one square and one slit.

This, multiplied by 90, gave the number in the larger volume. In a few cases the sample had to be diluted, because of the very large number of particles present, but this procedure gave considerable error, as a sol which had 74 particles per standard volume before dilution gave 100 particles after dilution, taking the dilution into account.

The particle counts for various suspensions that had been standing for 36 hr. are given in tables 2, 3, and 4. These results are thought to be accurate to 15 per cent.

TABLE 3

The relative effect of surface-active agents on dispersions of carbon B in xylene

NO	ACTIVE COMPONENT	AMOUNT OF COMPONENT	ORDINATE AT 100 MIN	PARTICLE COUNT OF STANDARD VOLUME
		<i>grams</i>		
1	Lecithin	0.841	0.063	538
2	Aerosol OT*	0.449	0.058	135
3	Cobalt naphthenate	0.335	0.074	29
4	Zinc naphthenate	0.756	0.074	30
5	Cobalt oleate	0.230	0.081	4
6	Blank		0.095	1
7	Oleic acid	0.573	0.099	1

* Sodium dioctyl sulfosuccinate.

TABLE 4

The relative effect of surface-active agents on dispersions of carbon C in xylene

NO	ACTIVE COMPONENT	AMOUNT OF COMPONENT	ORDINATE AT 100 MIN	PARTICLE COUNT OF STANDARD VOLUME
		<i>grams</i>		
1	Lecithin	0.720	0.090	252
2	Cobalt naphthenate	0.720	0.089	93
3	Aerosol OT	0.430	0.086	90
4	Dicyclohexylamine	0.445	0.091	4
5	Blank		0.095	0.5
6	Oleic acid	0.642	0.094	0.5

Effect of water on the dispersions

Sedimentation curves are given in figure 4 for three dispersions, each containing 0.500 g. of carbon A, 0.440 g. of sodium dioctyl sulfosuccinate, and 500 cc. of xylene. The three systems varied in water content. In system a the carbon used was saturated with water vapor (30 mg. adsorbed). System b contained normally dry chemicals, while system c was made with exceptionally dry chemicals in a dry box. For this latter experiment the xylene was redistilled over barium oxide, and then put in a 2-liter bottle stoppered with a cork covered with tin foil. It was then further dried by adding 2 g. of sodium every day for 10 days till the last portion retained its metallic luster. This mixture was allowed to stand with occasional shaking for a month.

The carbon was dried in an oven at 120°C . for 48 hr. and both it and the Aerosol OT were dried in a vacuum desiccator over phosphorus pentoxide for a week at 70°C . The drying was then continued in the desiccator at room temperature for 3 weeks. At the end of that time the desiccator, flask of dry xylene, beakers, Dewar, etc. were placed inside a dry box similar to that described by Harkins (4). The air in the box was dried with portions of phosphorus pentoxide renewed daily. At the end of 10 days the powder remained dry. As an added precaution a fresh portion was put in for another 10 days. The box was arranged so that when the carbon was dispersed the suspension could be stirred in the same manner as previously. To do this the motor for the stirrer was above the box and the stirrer was in the box. The hole through which the stirrer went was tightly sealed, except when the stirrer was running.

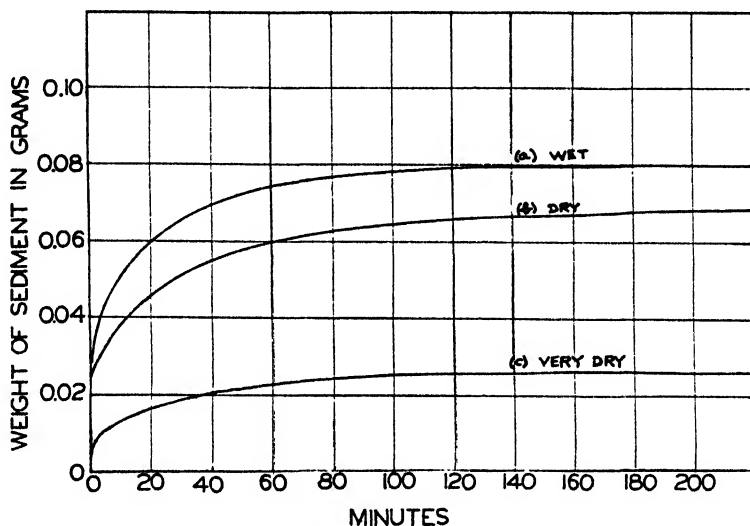


FIG. 4. Effect of moisture on dispersion

To make the drying more effective, the dry box was kept in a small enclosed hood whose air was dried with barium oxide. The method of dispersion was the same as described above. Some moisture had opportunity to get into the system during sedimentation and ultramicroscopic analysis, but it was thought that since dispersion had already taken place this would not have an immediate, pronounced effect.

Effect of concentration of surface-active agents on dispersion

The effect of concentration of surface-active agents was determined with lecithin and sodium dioctyl sulfosuccinate. To measure this effect an ultra-microscope count was made on portions of the dispersions. These are shown as curves in figure 5. The effectiveness of lecithin is seen to reach a maximum at about 0.5 g. and of sodium dioctyl sulfosuccinate at about 0.01 g.

Adsorption of surface-active agents

The adsorption of three surface-active agents, copper oleate, cobalt naphthenate, and oleic acid, was measured. The first two caused dispersion of carbon, while the latter did not. The adsorption was measured by centrifuging off the carbon particles (30 min. at 2000 R.P.M.), analyzing the clear supernatant liquid, and comparing with the original xylene solution before addition of carbon. Copper oleate and cobalt naphthenate were determined colorimetrically, while oleic acid was titrated with 0.001 *N* sodium hydroxide solution. Results are shown in table 5. Carbon A was used.

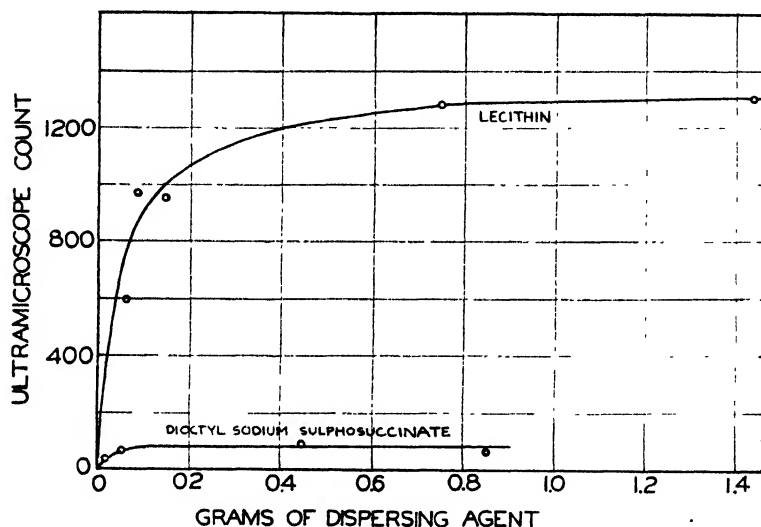


FIG. 5. Effect of amount of dispersing agent

TABLE 5

Adsorption of surface-active agents

SURFACE-ACTIVE AGENT	GRAMS (ORIGINAL) PFR 500 CC XYLENE	GRAMS (FINAL) PER 500 CC XYLENE	GRAMS ADSORBED
Copper oleate	0.230	0.057	0.173
Cobalt naphthenate	0.336	0.272	0.064
Oleic acid	0.58	0.58	0.00

Effect of surface-active agents upon different types of carbon

The three types of carbon described earlier (table 1) gave different and not always predictable results with different surface-active agents, although in general carbon A, with least adsorbed oxygen, gave the best dispersions. The surface area of each carbon was determined by the Emmett low-temperature adsorption method, using helium and nitrogen gas (2, 3). These areas, computed using the assumption that at the beginning of the long, linear part of the adsorption isotherm a monomolecular layer of nitrogen was adsorbed in each case, are

given in table 1. Comparative results for the three carbons are given in tables 2, 3, and 4.

Cataphoresis experiments to determine charge

The charge on the particles was determined by a cataphoresis experiment, using a U-tube, platinum electrodes, and either 110 volts or 900 volts D.C., from a rectifier-filter outfit. For all of the organosols the particles migrated to the positive pole, but with different speeds. Sols containing lecithin or sodium dioctyl sulfosuccinate showed migration at 110 volts, whereas sols containing the soaps required 900 volts before migration could be seen. Dryness or wetness did not seem to affect migration, and even a sol made under the very dry conditions described above showed migration. At 900 volts this latter sol coagulated, although none of the others did.

Properties of the organosols

The unsettled suspension after 36 hr. of standing was regarded as the organosol. The particles remaining in suspension after this period were 0.4 micron or less in diameter, thus fulfilling the size restrictions of a colloid. All the carbon organosols were an intense black and opaque to light. The particles showed Brownian movement and were easily visible in the ultramicroscope. None of the organosols had perfect stability, a fact which agrees with the results of other investigators. Lecithin gave the greatest stability for dispersions made with fairly dry chemicals. The very dry system made with sodium dioctyl sulfosuccinate was, however, by far the most stable sol made.

The very dry system containing sodium dioctyl sulfosuccinate was slightly coagulated when heated to 80°C. for 72 hr., but was not coagulated at all when put in a salt-ice bath at -5°C. for 48 hr. If 0.5 cc. of alcohol or water was added to 10 cc. of this sol and the mixture shaken, the organosol was destroyed completely in 12 hr.

DISCUSSION

The dispersing effect of surface-active additives can be explained by their adsorption, causing (a) formation of a solvated layer and (b) lowering of interfacial tension. The former is indicated by adsorption studies described herein, in which the effective surface-active chemicals copper oleate and cobalt naphthenate were found to be adsorbed, while the ineffective oleic acid was adsorbed, if at all, in too low an amount to be determined.

The explanation of the effect of water in decreasing stability follows also from this, if it be assumed that water goes to the interface, since in that position it would hinder adsorption of the surface-active additives.

It is not necessary to assume a charge in explaining the dispersing effect of surface-active additives, and other organosols have been reported in which no charge was found (5). However, the cataphoresis data indicate without question that the particles in the authors' systems were negatively charged, even in the very carefully dried system. The source of the charge in such systems is difficult

to explain. It could be accounted for by a trace of moisture, which would permit a slight dissociation of the polar-non-polar additive. Even a slight dissociation in pure xylene seems possible in the light of modern views (6).

SUMMARY

The following experimental data have been observed for carbon dispersed in xylene systems:

(a) Certain surface-active chemicals greatly increase the degree of dispersion of carbon in xylene. Lecithin, copper oleate, cobalt naphthenate, and sodium dioctyl sulfosuccinate were most effective, in the order named.

(b) For additions of surface-active materials greater than about 0.001 mole (for 0.5 g. carbon in 500 ml. of xylene), there was no further increase in dispersing ability.

(c) These surface-active agents became more effective as the water content of the system was lowered by extensive drying.

(d) Carbon dispersed in xylene under these conditions is negatively charged.

(e) The effective surface-active chemicals copper oleate and cobalt naphthenate were found to be positively adsorbed by the carbon, while the ineffective oleic acid was not adsorbed.

(f) The dispersed carbon phase could be partially or completely thrown down by the addition of alcohol or water, by heat, or in an electrical field. A low temperature, down to $-5^{\circ}\text{C}.$, had no effect.

(g) The surface area of the three types of carbon used was determined by the Emmett low-temperature adsorption method, using helium and nitrogen gas.

The authors wish to thank the Arco Company of Cleveland for equipment which greatly aided in this research.

REFERENCES

- (1) CALBECK, J., AND HARNER, H.: *Ind. Eng. Chem.* **19**, 58 (1927).
- (2) EMMETT, P., AND BRUNAUER, S.: *J. Am. Chem. Soc.* **59**, 1553 (1937); **59**, 2682 (1937); *Trans. Electrochem. Soc.*, **71**, 383 (1937).
BRUNAUER, S., AND EMMETT, P.: *J. Am. Chem. Soc.* **57**, 1754 (1935).
- (3) EMMETT, P., AND DE WITT, T.: *Ind. Eng. Chem., Anal. Ed.* **13**, 28 (1941).
- (4) HARKINS, W., AND GANS, D.: *J. Phys. Chem.* **36**, 86 (1932).
- (5) HUMPHREY, R., AND JANE, R.: *Trans. Faraday Soc.* **22**, 420 (1926).
- (6) LOWRY, T.: *J. Soc. Chem. Ind.* **44**, 970 (1925).

EFFECT OF SURFACE-ACTIVE AGENTS UPON DISPERSIONS OF CALCIUM CARBONATE IN XYLENE

VIVIAN RICHARD DAMERELL AND RAYMOND MATTSON

*Morley Chemical Laboratory, Western Reserve University, Cleveland, Ohio**Received February 9, 1944*

Little scientific work has been done on the dispersion of powders in organic media, in spite of their industrial importance in such fields as paints and lacquers. Harkins and coworkers (4) have studied the dispersion of metallic oxides in organic media. Reh binder and coworkers (5) have studied the dispersion of metallic oxides, chromates, and other powders. A study of carbon dispersed in xylene has been made by Damerell and Urbanic (2).

The purpose of this investigation was to study the effect of various surface-active agents upon dispersions of calcium carbonate in xylene. The method of study was similar to that used with carbon-xylene systems, reported in an earlier paper (2), and for greater detail in the explanation of experimental work the reader is referred to that paper. Calcium carbonate was chosen as the disperse phase because of its availability in aggregated colloidal form, its purity, its relatively low specific gravity, and its polar nature, which contrasted with the non-polar material previously studied.

The systems were made by stirring very finely divided calcium carbonate with xylene in the presence of surface-active agents. The degree of dispersion was measured by a combination of sedimentation and ultramicroscopic analysis. The effect of heat, cold, extreme dryness, and the addition of other liquids was studied also; in addition, cataphoresis experiments were carried out and the surface area of the dispersed phase was measured.

CHEMICALS

The calcium carbonate was a colloidal product used commercially as an extender for paint pigments. It was further broken up by grinding in xylene in a porcelain pebble mill for 96 hr. The ground material was found by analysis to contain 97.7 per cent of calcium carbonate, 0.5 per cent of silica, and small amounts of the sulfides of iron and antimony. The impurities were largely picked up during the pebble-mill grind.

The xylene was a commercial grade which was purified by distilling from barium oxide. The fraction boiling between 136° and 138.5°C. was retained.

The surface-active agents used are listed in table 3. These were all pure chemicals except the soaps, tripalmitin, oleic amine, lecithin, and the fatty acids, which were of the best grade obtainable but were not chemically pure.

PREPARATION OF CALCIUM CARBONATE-XYLENE SYSTEMS

Five hundred milliliters of redistilled xylene was measured out in a volumetric flask and transferred to an 800-ml. beaker. An accurately weighed amount of dispersing agent, usually about 0.4 g., was dissolved in the xylene. Then a

sample of calcium carbonate ($0.5000 \text{ g.} \pm 0.0005 \text{ g.}$) was added to this solution and the mixture stirred for 45 min. at 1000 R.P.M. The suspension was then quickly transferred to a silvered Dewar flask containing the pan from a sedimentation balance, and a sedimentation analysis was run on the suspension.

The stirring apparatus consisted of a variable-speed laboratory motor attached to a four-bladed stirrer. The dispersion beaker was fitted with a copper lid held in place by three prongs soldered to the under side of the lid in such a fashion that they fitted snugly against the beaker walls and thus held the lid firmly in position. The stirring rod passed through a hole in the center of the lid, as well as through a bushing soldered to the lid. This held the rod steady and prevented vibration. Attached to the under side of the lid was a baffle plate, 1 in. in width and extending to the bottom of the beaker. This plate prevented the liquid from slopping over at the high stirring speed used. The temperature was maintained at $25^{\circ}\text{C.} \pm 0.5^{\circ}$ during the dispersion by cooling the beaker with pieces of dry ice or ice, or by warming it with the hands.

DETERMINATION OF DEGREE OF DISPERSION

The dispersed suspensions were poured into a silver Dewar vacuum flask which contained the pan of a sedimentation balance. A sedimentation analysis was run on each, using the method and precautions described in an earlier paper (2). Typical data for such an analysis are given in table 1, in which 0.4 g. of sodium dioctyl sulfosuccinate was used as the dispersing agent. Figure 1 shows the sedimentation curve drawn from these data. The results obtained by a tangenti-meter analysis of this curve are shown in table 2, and the summarized result is given in the first line of table 3. The remainder of table 3 gives the summarized results for the other dispersing agents studied.

After 16 hr. on the sedimentation balance the remaining suspension, which now contained particles of less than 0.6 micron radius, was examined in a Bausch and Lomb slit ultramicroscope. The number of particles in $1 \times 10^{-4} \text{ cm.}^3$ was determined by the average of fifteen to twenty particle counts; the values obtained are listed in the last column of table 3. The error involved in making these counts is thought not to exceed 15 per cent. The reproducibility of the sedimentation analyses is illustrated in table 3 by the two values in which no dispersing agent was present.

EFFECT OF CONCENTRATION OF SURFACE-ACTIVE AGENT

In table 4 are data showing the effect of varying the concentration of the surface-active agent sodium dioctyl sulfosuccinate (Aerosol OT). It is seen that the amount of dispersion remained fairly constant until a low concentration of 4.8 mg. of dispersing agent was used.

EFFECT OF WATER ON DISPERSION

Several dispersions were made with carefully dried chemicals. For these experiments redistilled xylene was dried in a bottle with metallic sodium for several months, and the calcium carbonate and dispersing agents were dried in a vacuum

desiccator over phosphorus pentoxide for over a month. The dispersion was carried out in a dry box, as described in an earlier paper (2). Results of sedimen-

TABLE 1
Typical sedimentation data
0.4 g. of sodium dioctyl sulfosuccinate used

TIME IN MINUTES AND SECONDS	TEMPERATURE	WEIGHT ON BALANCE PAN	UNCORRECTED WEIGHT OF SEDIMENT ON BALANCE PAN	WEIGHT OF SEDIMENT CORRECTED FOR TEMPERATURE
	°C.	grams	grams	grams
0	25.0	5.0800*		
1:10		5.1400	0.0600	0.0600
1:45		5.1500	0.0700	0.0700
3:00		5.1600	0.0800	0.0800
4:05		5.1650	0.0850	0.0850
6:30		5.1700	0.0900	0.0900
9:00	25.0	5.1730	0.0930	0.0930
14:00		5.1760	0.0960	0.0960
21:00	25.0	5.1780	0.0980	0.0980
34:00		5.1800	0.1000	0.1000
49:00	25.0	5.1810	0.1010	0.1010
67:00		5.1820	0.1020	0.1020
97:00	25.1	5.1830	0.1030	0.1028
1357	22.2	5.1840	0.1040	0.1096

* Weight of empty pan.

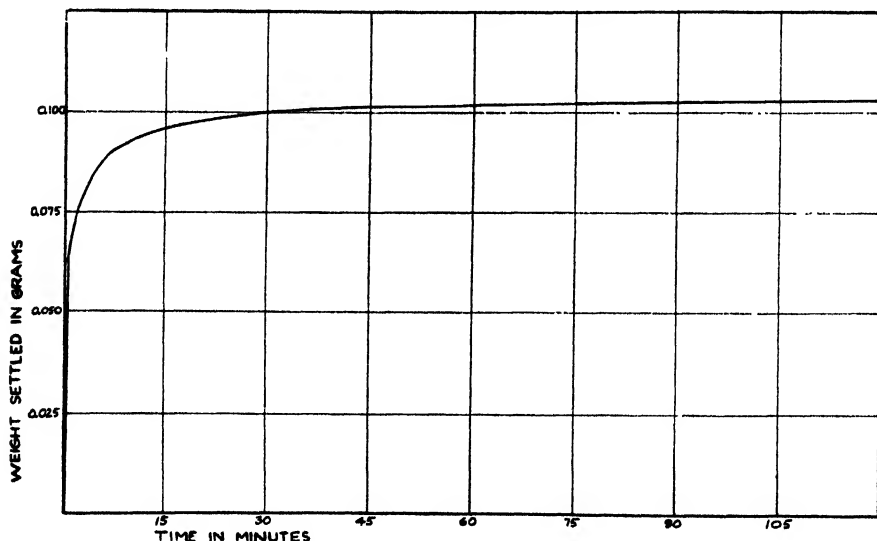


FIG. 1. Sedimentation curve from data in table 1

tation and ultramicroscopic analysis are given in table 5. With no dispersing agent present the dry conditions resulted in a poorer dispersion than when disper-

sions were made in the usual fashion. This was corroborated by visual observation while the dispersion was being made. The calcium carbonate appeared to be more flocculated and tended to stick to the walls of the dispersion beaker. With the surface-active agents there was a considerable decrease in the amount of large material, compared to dispersion under usual conditions, but on the other hand the amount of colloidal material dropped from about 10 per cent to 6 per cent.

DETERMINATION OF THE SURFACE AREA OF CALCIUM CARBONATE

The surface area of calcium carbonate was determined, using the Emmett low-temperature nitrogen-adsorption apparatus (3). From the characteristic break in the adsorption isotherm of nitrogen and the determination of the dead space in the apparatus with helium, it was found that the surface area per gram was

TABLE 2
Data obtained from sedimentation curve in figure 1

PARTICLE-SIZE RANGE	SEDIMENTATION TIME	WEIGHT MATERIAL FOR THIS INTERVAL	PERCENTAGE MATERIAL FOR THIS INTERVAL
<i>microns</i>	<i>minutes</i>	<i>grams</i>	
12 and greater	2.4	0.0532	43.4
11-12	2.8	0.0064	5.2
10-11	3.4	0.0044	3.6
9-10	4.2	0.0080	6.5
8-9	5.4	0.0045	3.7
7-8	7.0	0.0045	3.7
6-7	9.6	0.0047	3.8
5-6	13.8	0.0038	3.1
4-5	21.5	0.0044	3.6
3-4	38.2	0.0027	2.2
2-3	86	0.0033	2.7
0.6-2	960	0.0097	7.9
Below 0.6		0.0131	10.6

21.4 square meters in one experiment, and 21.6 square meters in a second, making the assumption that a monomolecular layer of nitrogen was adsorbed.

ADSORPTION OF SURFACE-ACTIVE AGENTS

Adsorption of surface-active agents was determined gravimetrically by weighing the agent remaining from a known volume of xylene after adsorption had taken place and the xylene had been separated and evaporated. Solutions of the dispersing agent in 500 ml. of xylene were analyzed before and after adding about 5 g. of calcium carbonate. The suspension remaining after adding calcium carbonate was filtered through a glass filtering crucible, if it was necessary to remove suspended material. The results are summarized in table 6. If the cross-sectional area of sodium dioctyl sulfosuccinate is taken as 49 square Ångström units, after Caryl (1), then the 0.0314 g. adsorbed per gram of calcium carbonate

would occupy 21 square meters as a close-packed unimolecular layer. This correlates rather strikingly with the surface area of the calcium carbonate of 21.5 square meters, as determined by the Emmett method described above.

TABLE 3
The effect of surface-active agents

SURFACE-ACTIVE AGENT	WEIGHT USED	PERCENTAGES OF CALCIUM CARBONATE IN DIFFERENT PARTICLE-SIZE GROUPS				ULTRAMICROSCOPE PARTICLE COUNT IN 1×10^{-8} CC. OF DISPERSION
		Over 12 microns radius	2-12 microns radius	0.6-2 microns radius	Under 0.6 micron radius	
	<i>grams</i>					
Sodium dioctyl sulfosuccinate†	0.3980	43.4	38.1	7.9	10.7	36
Zinc dioctyl sulfosuccinate . .	0.5107	42.1	39.6	3.8	14.6	67
Barium dioctyl sulfosuccinate	0.5015	42.1	38.3	8.8	10.7	44
Sodium dihexyl sulfosuccinate‡	0.3468	45.4	43.4	5.6	5.6	25
Phenyl <i>p</i> -toluenesulfonate . .	0.3073	56.0	27.9	16.1	None	None
Ethyl <i>p</i> -toluenesulfonate	0.3219	50.5	42.1	7.4	None	None
Magnesium oleate	0.1500	28.8	47.9	10.8	12.5	31*
Copper oleate	0.1531	44.8	34.7	20.6	None	None
Lecithin	0.4008	44.9	37.1	9.8	8.2	31
Lead naphthenate . . .	0.3033	48.0	35.0	17.0	None	None
Zinc naphthenate . .	0.4306	57.1	34.8	8.1	Trace	5*
Cobalt naphthenate . .	0.1050	58.5	33.0	8.5	Trace	6*
Manganese naphthenate	0.3600	54.7	32.1	13.2	None	None
Triisoamylamine . .	0.4011	49.4	41.8	8.8	Trace	2*
Benzidine . .	0.0600	34.0	45.4	20.6	None	None
Monoamylamine . .	0.4208	43.8	40.7	15.6	None	None
Dicyclohexylamine	0.3281	51.0	37.9	11.1	None	None
Diamylamine	0.4226	56.1	33.7	10.2	None	None
4-Aminodiphenyl . .	0.4000	55.7	39.1	5.2	None	None
Oleic amine . .	0.3734	55.0	36.9	8.1	None	None
<i>n</i> -Octadecyl chloride .	0.3248	61.5	26.5	12.0	None	None
<i>n</i> -Octadecyl acetate	0.4145	49.5	32.6	17.9	None	None
<i>n</i> -Octadecyl alcohol	0.3726	53.4	37.8	8.8	Trace	9*
Stearic acid	0.2010	45.0	44.3	10.8	None	None
Tripalmitin . .	0.4018	62.9	31.2	5.9	None	None
None	None	59.1	33.9	7.0	None	None
None	None	60.1	33.2	6.7	None	None

* Unstable; settled out after a few weeks.

† Aerosol OT.

‡ Aerosol MA.

CATAPHORESIS EXPERIMENTS

Cataphoresis experiments were run on the colloidal suspensions prepared by means of the following dispersing agents: Aerosol OT, Aerosol MA, magnesium oleate, lecithin, and barium and zinc salts of Aerosol OT. A potential of 900 volts was applied for times varying from 8 to 36 hr. Migration was towards the cathode, except when lecithin was used as dispersing agent. With lecithin migration towards both electrodes was observed.

In none of these experiments was a sharp line of demarcation observed between clear liquid and colloidal suspension as a result of migration of particles. Migration was slow, and even after 36 hr. the anode portion of the liquid still contained colloidal material, as shown by ultramicroscopic observation. Migration was

TABLE 4
The effect of concentration of sodium dioctyl sulfosuccinate

GRAMS OF SODIUM DIOCTYL SULFO- SUCCINATE	PERCENTAGES OF CALCIUM CARBONATE IN DIFFERENT PARTICLE-SIZE GROUPS				ULTRAMICROSCOPE PARTICLE COUNT IN 1×10^{-8} cc.
	Over 12 microns radius	2-12 microns radius	0.6-2 microns radius	Under 0.6 micron radius	
0.3980	43.4	38.1	7.9	10.7	36
0.0498	46.1	38.6	4.5	10.9	
0.0208	49.1	32.4	8.0	10.5	
0.0116	51.9	33.3	4.1	10.7	
0.0048	59.4	33.0	6.7	1.0	2

TABLE 5
Dispersion under dry conditions

DISPERSING AGENT	GRAMS USED	PERCENTAGES OF CALCIUM CARBONATE IN DIFFERENT PARTICLE-SIZE GROUPS				ULTRAMICRO- SCOPE PARTICLE COUNT IN 1×10^{-8} cc. OF DISPERSION
		Over 12 microns radius	2-12 microns radius	0.6-2 microns radius	Under 0.6 micron radius	
Sodium dioctyl sulfosuc- cinate	0.3989	28.4	58.1	7.4	6.1	22
Lecithin	0.4738	31.6	37.1	15.6	5.7	16
None	None	71.6	20.0	8.4	None	None

TABLE 6
Adsorption of surface-active agents

WEIGHT OF CaCO_3	WEIGHT OF DISPERSING AGENT	WEIGHT OF DISPERSING AGENT ADSORBED	x/m	DISPERSING AGENT
<i>grams</i>	<i>grams</i>	<i>grams</i>		
4.8490	0.5085	0.1520	0.0314	Aerosol OT
5.7192	0.1420	0.0500	0.0088	Cobalt naphthenate
5.1232	0.1380	0.0870	0.0169	Copper oleate

determined by making an ultramicroscopic count on the suspension before cataphoresis, and on anode and cathode portions after cataphoresis.

Precipitation was observed during the electrolysis of a very dry system dispersed with Aerosol OT in a dry box. After a 26-hr. cataphoresis experiment,

the particles had "plated out" on the cathode. The deposited material could be shaken from the electrode in a coagulated form which settled rapidly.

PROPERTIES OF CALCIUM CARBONATE SOLS IN XYLENE

The sols were milky white and opalescent in appearance, and with the most effective dispersing agents (aerosols, lecithin) were stable for many months. They were partially coagulated by heating for 24 hr. on a steam bath. Cooling to 0°C. had no effect. Precipitation took place within 2 hr. when 95 per cent ethyl alcohol was added, but absolute alcohol had no effect. Diethyl ether caused precipitation within 4 hr., and a small amount of water caused precipitation within 2 hr. When a sol of carbon in xylene (negatively charged) was added to a calcium carbonate dispersion (positively charged), almost complete precipitation of both dispersed phases took place.

MECHANISM OF DISPERSION

The adsorption data indicated that the surface-active agents were positively adsorbed by the calcium carbonate. They evidently aided dispersion by going to the xylene-calcium carbonate interface and forming a protective coating. This process itself can be thought of as having some effect on the breaking up of aggregates, in the same way that water molecules are thought to cause solution by forcing their way between ions of a crystal in the process of hydration. In addition, the dispersed phase was further stabilized by being positively charged. The charge is difficult to explain in a xylene system. A trace of water, going to the interface, might permit some ionization of the dispersing agent, but this does not explain the positive charge in the systems prepared in the dry box, unless it be assumed that enough water was still present to permit a dissociation.

SUMMARY

1. Dispersions of calcium carbonate in xylene have been made in the presence of a number of surface-active agents.
2. These dispersions have been analyzed for particle-size distribution by use of a sedimentation balance and a slit ultramicroscope.
3. The most effective surface-active agents in this system were the zinc, barium, and sodium salts of dioctyl sulfosuccinate, sodium dihexyl sulfosuccinate, lecithin, and magnesium oleate.
4. The calcium carbonate organosols had a milky white, opalescent appearance, and were coagulated by water, 95 per cent ethyl alcohol, and diethyl ether. Heat partially coagulated them, but cooling (to 0°C.) did not. The colloidal particles were positively charged in these systems except when lecithin was used as a dispersing agent, in which case both positively and negatively charged particles were present.

The authors wish to express their thanks to the Arco Company of Cleveland for the fellowship and the use of equipment which made this research possible.

REFERENCES

- (1) CARYL, C. R.: *Ind. Eng. Chem.* **33**, 731 (1941).
- (2) DAMERELL, V. R., AND URBANIG, A.: *J. Phys. Chem.* **48**, 125 (1944).
- (3) EMMETT, P. H., DEWITT, T., AND THOMAS, J.: *Ind. Eng. Chem., Anal. Ed.* **13**, 28 (1941).
- (4) HARKINS, W., AND DAHLSTROM, R.: *Ind. Eng. Chem.* **22**, 897 (1930).
HARKINS, W., AND GANS, D.: *J. Phys. Chem.* **36**, 86 (1932).
HARKINS, W., RYAN, L., AND GANS, D.: *Ind. Eng. Chem.* **24**, 1288 (1932).
- (5) REHBINDER, P.: *Z. physik. Chem.* **146A**, 63 (1930).

FOAM FORMATION IN ORGANIC LIQUIDS¹E. GRAY KING²*Mellon Institute of Industrial Research, Pittsburgh, Pennsylvania**Received January 21, 1944*

The investigations reported in this paper were conducted to determine whether foams comparable in volume and stability to aqueous foams could be produced in organic liquids. Numerous questions presented themselves concerning these subjects. Could such foams be formed, and, if so, what conditions were necessary? What types of compounds would be surface active in organic liquids, and which of them could be used as foaming agents? How did the many physical factors said to be involved in the formation of aqueous foams affect organic foams? Could any relationship between foamer and solvent be discerned? The relevant answers set forth here are preliminary and empirical in nature. These findings indicate, however, the possibilities of this relatively untouched field, and it is hoped that more attention will be given to it in consequence.

Surprisingly little work has been recorded in the literature on either the measurement of the surface tension of solutions in organic solvents or the production of foams in organic liquids. Adam (1) has pointed out that no great amount of positive adsorption can be expected in organic liquids, because the field of force around the hydrocarbon parts of molecules is less than that around most other groups, and that a negative adsorption at the air-liquid interface is perhaps more probable. Gilbert (9) has shown that long-chain fatty acids produce a slight diminution of the surface tension of heavy hydrocarbons. More recently McBain and Perry (12) have demonstrated that lauryl sulfonic acid appreciably decreases the surface tension of Nujol, a liquid petrolatum, and of tetraisobutylene and hydrogenated tetraisobutylene, whereas the same solute scarcely lowers the surface tension of isoöctane, xylene, benzene, and heptane. Numerous other substances of widely different character have little influence on the surface tension

¹ Presented before the Division of Colloid Chemistry at the 106th Meeting of the American Chemical Society, Pittsburgh, Pennsylvania, September 10, 1943.

² Senior incumbent of the Multiple Industrial Fellowship on Cork Technology, sustained at the Mellon Institute by the Armstrong Cork Company, Lancaster, Pennsylvania.

of the hydrocarbons. Taubman (17) has indicated that adsorption in the interfaces of organic liquids can be vertical or horizontal, advancing the thesis that differences in the orientation of the adsorbed molecules are a result of variations in the degree of structure symmetry of those molecules rather than of differences in polarity. Several workers have measured the surface tensions of organic solutions (4).

Research on organic foams has been restricted almost entirely to hot oils and fats (11). Tickell (18) has prepared petroleum-natural gas foams. Numerous references occur in the literature to difficulties with foams during organic preparations, but no effort has been made to assemble this information. Most of the foams probably occurred on the gelation of the product with the simultaneous evolution of a gas, or in complex systems containing large quantities of water. No studies appear to have been made on polar compounds with the specific intention of correlating their surface activity with their propensity to form stable and voluminous foams in organic liquids.

MATERIALS AND PRELIMINARY TESTS

As no information was available concerning the nature of compounds which might be surface active in organic liquids, advantage was taken of that large class of readily obtainable polar compounds known as detergents, emulsifiers, and wetting agents. While there was no reason to assume that these colloidal electrolytes would show surface-active properties in organic liquids, several factors suggested their examination in preliminary experiments. These synthetic compounds include a large number of different combinations of hydrophobic and hydrophilic groups, thus providing ample scope for observation of the effect of different structures. In a few instances families or series of compounds of similar structure but containing substituents of different chain length are procurable,—for example, the Aerosols. In addition, some of these substances are used for dispersing pigments in paint vehicles, while others are proposed for water-in-oil emulsions. Some of these proprietary compounds contain large quantities of inorganic salts, but this fact did not appear to be too objectionable, inasmuch as the inorganic fraction would in most cases be insoluble. Many of the compounds contain water, but the quantity is negligible considering the concentration in which the reagents were used. The grade of solvent employed throughout this work was, for the most part, that usually supplied commercially by the manufacturer.

Forty-seven commercial surface-active agents were examined in the first qualitative tests. These substances represented most of the structural types of colloidal electrolytes commercially available. An indication of the structure of most of these products can be had by referring to several lists (5, 6, 7, 8, 10). To facilitate the discussion in this paper, however, the general chemical structures of several of these reagents, found to be the most interesting in connection with this study, are given in figures 1 and 2.

Initial tests were made to determine which of the substances showed tendencies to foam in three solvents of different chemical nature,—namely, methyl alcohol,

acetone, and benzene. Preliminary experiments revealed that the foams would, in the main, be transient, and that the tendency to foam was greater at concentrations higher than those commonly assumed to be required for foam formation. This finding may have resulted from the stabilizing action of the increased viscosity of the more concentrated solutions. The tests were first made at a concentration of 5 per cent; then the solutions were diluted to 0.2 per cent for further examination. In the majority of cases there was little or no activity at the lower concentration. To determine the foaming tendency, 10 to 15 cc. of the solution was shaken in a glass-stoppered 100-ml. graduate. The foams produced were so transitory that the time of expiration of the foam produced on the surface of the

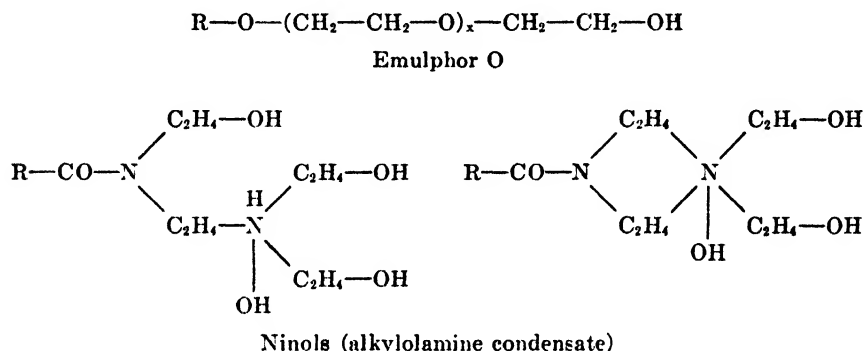


FIG. 1

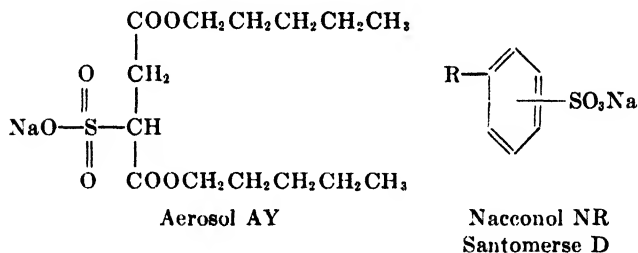


FIG. 2

solution was taken as a measure of its foaming capacity and stability. This observation was apparently unaffected by the volume of liquid or the violence of the agitation. In a few instances a substantial head of foam was obtained.

The greatest tendency to foam was displayed by the agents listed in table 1. The following substances showed little or no foaming tendency in the three solvents investigated: Albatex PO, calcium stearate, diethanolamide of castor oil, Emulphor EL, Flotation Aldol A, Maprimol, Maprofix, Mapromin, Naccolene F, Peregol O, Sapamine FL, Sapamine MS, saponin, and Triton W30.

It appears from the results of these qualitative tests that voluminous foams in volatile solvents are unlikely. Certain general tendencies, however, were

evident. More compounds gave an indication of foam formation in methyl alcohol than in acetone or benzene. The greater activity in methyl alcohol might

TABLE 1

Foaming tendency at 5 per cent concentration as indicated by time of expiration in seconds

SUBSTANCE	METHYL ALCOHOL	ACETONE	BENZENE
Aerosol AY....	7	None	7 cc. of foam stable for some hours
Aerosol MA.	7	3	35
Aerosol OT...	9	5	9
Aquaresin	9	None	None
Areskap 100	15	11	None
Areskelene 400	15	11	None
Aresket 300.	11	Very slight	None
Atlas G 759	15	9	Some tendency at lower concentrations
Atlas G 720	10 at 10 per cent	10 at 10 per cent	None at 10, 2, and 0.5 per cent
Emulphor A	20	9	Extremely slight
Emulphor O	20-25	17	None
Flotation Aldol B	11	None	None
Glyceryl abietate	17	8	4
Glyceryl oleate	10	5	None
Glyceryl phthalate	29	15	None
Igepon AP	9	None	4 cc. of foam; no collapse in 10 min.
Igepon T.	8	None	Slight
Ivory soap	10	None	None (25 sec. in kerosene)
Nacconol NR	None	None	Slight
Nekal A	9	Slight	None
Nekal BX	10	Slight	None
Ninol 313	10	Slight	None
Ninol 400	11	Slight	None
Ninol 466	15	None	None
Ninol 555 base	8	Slight	None
Ninol 700	6	None down to 0.1 per cent	None down to 0.1 per cent
Ninol 967	10	4	Very slight
Prestabit oil V	9	Very slight	None
Santomerse D	12	4	7 cc. of foam; stable at 0.2 per cent
Sapamine KW	10	4	None
Triton K60	None	None	Slight
Ultravon K	18	4	None
Ultravon W...	14	3	None

be accounted for by the fact that this solvent has a higher dielectric constant than the other two solvents. Substances with the greatest tendency to foam in methyl alcohol produced little or no effect in benzene, while those materials which

gave several cubic centimeters of foam in benzene exhibited considerably less activity in methyl alcohol. The results seem to indicate some physical relation between the solvent and the effective foamer. Surface-tension measurements³ were made on some of the solutions which showed the greatest tendency to foam. In no case was the surface tension decreased more than 1.7 dynes; in some cases it was increased slightly.

EFFECT OF PHYSICAL PROPERTIES

Foam formation has been attributed to combinations of high viscosity, low vapor pressure, and low surface tension (3). Undoubtedly these physical properties affect the stability of foams, but they are not the determining factors in foam initiation. That this situation is true of organic as well as of aqueous solutions is indicated by the behavior of Aerosol AY in a series of hydrocarbon solvents (table 2). Over a wide range, the viscosity and vapor pressure had relatively little effect on the volume of foam produced. The volatility of the solvent would obviously affect the stability of the foam if the vapor were not confined. It is plain from the data that the viscosity of the solution has a stabilizing effect on whatever foam is formed. High viscosity undoubtedly inhibits the aeration of liquids; it also decreases the rate at which equilibrium in the interface is set up, thus affecting foam formation. But foams have already been prepared from extremely viscous media, so that viscosity does not seem to be the limiting factor. Nor does low surface tension in itself appear to be a determining characteristic. Although the surface tensions of the majority of hydrocarbons are low, foam formation in their solutions, as already noted, was neither voluminous nor stable. A significant observation was made, however, in the case of a Cumar resin dissolved in benzene. The resultant surface tension of this combination was somewhat higher than that of the hydrocarbon solvents. The addition of Aerosol AY produced a substantial decrease in the surface tension and the solution, for an organic system, foamed voluminously.

CHEMICAL BALANCE OF FOAMER AND SOLVENT

Balance between the polar and non-polar portions of the molecule has been considered an essential factor governing the detergent and wetting properties of colloidal electrolytes in water (6, 8, 10, 16). Caryl (5) has pointed to several conditions which alter balance and contends that they do so by their effect on solubility. The data in table 1 indicate that balance also affects foam formation in organic liquids. In this case the adjustment of balance becomes more complex because of the variations in chemical structure possible with organic compounds.

It would also appear that foaming in organic solutions, just as in aqueous ones, is accompanied by a decrease in surface tension. In order to attain such a decrease more readily, it would seem necessary to start with liquids having surface tensions higher than those of most hydrocarbons. Experiments were therefore

³ All surface-tension measurements were made with a Model No 70520 Cenco du Noüy ring tensiometer, using the method of correction suggested by Macy (14).

extended to include careful attention to the result of using solvents with higher initial surface tension and also a study of the chemical nature of the foamer.

The tendencies of Emulphor O and Aerosol AY to foam in a number of organic

TABLE 2

Relation of physical properties of hydrocarbon solvents to foam formation with 5 per cent Aerosol AY

SOLVENT	PHYSICAL PROPERTIES OF SOLVENT				EFFECT OF ADDITION OF 5 PER CENT AEROSOL AY	
	Boiling point at 760 mm.*	Vapor pressure at 30°C.*	Viscosity*	Surface tension at 30°C.	Surface tension at 30°C.	Foaming tendency
	°C.	mm. Hg	cps.	dynes	dynes	
Benzene.....	80	118	0.56 at 30°C.	27.6	27.4	Very tenacious foam, stable for some hours; only $\frac{1}{2}$ in. of foam on surface of liquid
Xylene.....	137-143	11	0.66 at 20°C.	26.2	26.2	Slightly larger volume of foam than in benzene; expired in 45 sec.
Cumene.....	154	16.5	0.73 at 25°C.	28.4	27.7	Slightly more voluminous foam than in benzene; approximately 1 in., but less stable
Neville 2-50 W.	150-190	Low	0.8 at 20°C.	26.7	26.5	Volume slightly greater than in benzene, approximately $\frac{1}{2}$ in. to $\frac{3}{4}$ in; expired in 75 sec.
Kerosene..	150-300	Low	About 2	24.5	24.2	Very tenacious but less stable foam than that in benzene— $\frac{1}{2}$ in. in height
White mineral oil	200-250 at 1 mm.	Low	About 90	30.0	30.0	No foam—fine dispersion of bubbles throughout the liquid; very slightly soluble
Cumar Resin G, 50 per cent by weight in benzene.				30.7	26.2	Quite voluminous foam; about 100-150 per cent overrun and moderately stable; not all of the liquid entered into the foam
Water	100	31.8	0.8 at 30°C.	71.2	27.4	Voluminous but only moderately stable foam

* Values taken from the literature.

liquids of widely different chemical structure are summarized in table 3. The foaming properties were evaluated by shaking the solution, noting the tendency

TABLE 3

Relation of surface tension and surface-tension change to foam formation with 5 per cent Emulphor O and with 5 per cent Aerosol AY

	SURFACE TENSION OF SOLVENT AT 30°C.	DECREASE IN SURFACE TENSION	FOAMING PROPERTIES OF SOLUTION
Effect of addition of 5 per cent Emulphor O			
Glycerol (Baker's C.P.)	dynes 65.0	dynes 31.1	Too viscous to shake; agitator produced merely emulsion of air bubbles, about 50 per cent overrun
Ethylene glycol	47.5	13.3	Marked tendency to form films; agitator produced 350 per cent overrun
Diethylene glycol	44.3	10.8	Film formation less pronounced; air readily and stably dispersed, but overrun small
Furfural	42.2	0.5	Slight amount of foam; 90 per cent expired in 1 min.; expired completely in 2 min.
Nitrobenzene	42.2	0.0	No tendency to foam
Methyl Carbitol	35.1	0.3	Slight amount of foam; 90 per cent expired in 1 min.; expired completely in 2 min.
1,4-Dioxane	31.6	0.0	Cloudy solution with no tendency to foam
Cellosolve	32.0 at 25°C.		Slight foam which expired in 30 sec.
Butyl acetate	27.6 at 27°C.		Slight foam which expired in 25 sec.
Butyl alcohol	24.6 at 27°C.		Slight foam which expired in 30-60 sec.
Diacetone alcohol			Slight foam which expired in 30-60 sec.
Effect of addition of 5 per cent Aerosol AY			
Ethylene glycol	47.5	9.8	Only slight tendency to foam when agitated rapidly
Furfural	42.2	2.5	Foam volume small; 15 cc. increased to 25 cc.; foam stable for more than 24 hr.
Nitrobenzene	42.2	11.5	Voluminous foam; 15 cc. increased to 97 cc.; equivalent to the best aqueous foams
Propylene glycol	35.1	0.9	Air dispersed, but little tendency to foam
1,4-Dioxane	31.6	0.5	Foam volume small; 15 cc. increased to 22 cc.; 80 per cent expired in 30 sec; remainder tenacious
Ethylene dichloride	30.9	2.0	Considerable foam; 15 cc. increased to 40 cc., but 95 per cent expired in 1 min.; remainder stable several hours

to form bubbles or films, measuring the volume of foam if it was appreciable, and observing the time of expiration if the foam was unstable.

As expected, Emulphor O gave the greatest tendency to produce foam in hydroxylic solvents. With glycol an overrun of several hundred per cent was obtained, and a bubble 2 in. in diameter was blown from the solution. There was decidedly less tendency for the diethylene glycol and methyl Carbitol solutions to foam. A marked decrease in surface tension occurred on dissolving Emulphor O in the diethylene glycol, but no decrease was observed in the case of methyl Carbitol.

It is interesting that nitrobenzene, furfural, and 1,4-dioxane, in spite of their relatively high surface tensions and other properties conducive to foam formation, did not tend to foam with Emulphor O, and that the latter compound caused no appreciable decrease in their surface tensions. As was the case with the solvents of low surface tension listed in table 1, Cellosolve, butyl acetate, butyl alcohol, and diacetone alcohol showed little tendency to foam in conjunction with Emulphor O, but they had a somewhat greater tendency to propagate foam than did methyl alcohol or acetone.

Nitrobenzene containing Aerosol AY afforded a foam which was equivalent to the average aqueous foam. The decrease in surface tension was 11.5 dynes. Furfural, on the other hand, although it has approximately the same surface tension as nitrobenzene, showed only a slight tendency to foam with Aerosol AY. While the surface-tension decrease was only 2.5 dynes in the latter case, this fact does not explain entirely the lack of foaming power. The surface tension of ethylene glycol was decreased 9.8 dynes by the addition of Aerosol AY, that of diethylene glycol 10.8 dynes by Emulphor O, and that of glycerol 31.1 dynes by Emulphor O, without the development of the capacity to form voluminous foams. These observations lead to the inference that, together with positive adsorption, a structural balance between the solvent and the foamer is needed to bring about frothing. It has yet to be ascertained whether this balance increases the abruptness of the change from the body of the liquid to the film, affects the solvation of the solute, or actually determines the degree of effective orientation in the film.

In a further series of experiments to extend the information on types of compounds surface active in organic liquids, six of the most promising foamers were chosen from table 1: namely, Ninol 555 base, Santomerse D, Aerosol AY, Nacconol NR, Nekal BX, and Emulphor O. These compounds vary rather widely in chemical structure (see figures 1 and 2). Their foaming tendency and surface activity were measured in glycol, dibutyl phthalate, tricresyl phosphate, and Halowax No. 1000, liquids of relatively high surface tension and of varied chemical structures. The evaluation was made at 1 per cent concentration of the surface-active material, and the foaming tendency was noted at room temperature, as in the previous experiments, and also at 90°C. In a few cases a slight separation of the solute occurred on standing.

In connection with this series of experiments, it was also noted that the foaming capacity of some of the surface-active agents, Nacconol NR and Santomerse D, for example, was considerably diminished after the samples had been stored for several years.

Glycol

As previously brought out, Emulphor O is an effective foaming agent in glycol. The foaming capacity of the other compounds was very much less; their tendency to foam at 90°C. was in the following order:

Santomerse D \geq Nacconol NR \geq Nekal BX \geq Aerosol AY > Ninol 555 base

The cold solutions were in much the same order.

Dibutyl phthalate

No very substantial foams were obtained in dibutyl phthalate, either at 90°C. or at room temperature. Santomerse D was largely insoluble, and the filtered solution had no tendency to foam, although the unfiltered liquid had given about 0.5 in. of tenacious foam. Aerosol AY caused about the same amount of foam. The other compounds showed little or no tendency to produce foams.

Tricresyl phosphate

Both Aerosol AY and Santomerse D yielded about 0.5 in. of foam, stable for several hours. Santomerse D was not soluble to the extent of 1 per cent, but the filtered solution retained its ability to foam. Some of the Aerosol AY crystallized from the 1 per cent solution after standing several days. The order of the tendency to foam at 90°C. was as follows:

Aerosol AY \geq Santomerse D > Nekal BX > Nacconol NR > Ninol 555
base > Emulphor O

The cold solutions were viscous and their foaming tendencies were difficult to evaluate, but the order appeared to be about identical. Ninol 555 base and Emulphor O exhibited practically no inclination to foam. Aqua Rex, Igepon AP, and Atlas G 720 were also ineffective.

Halowax No. 1000

Voluminous stable foams comparable with aqueous saponin foams were obtained in this liquid with Santomerse D. Although the Santomerse was not soluble to the extent of 1 per cent, the filtered solution foamed hot or cold. The bubble structure of this foam was extremely fine. Aerosol AY was only about 50 per cent as effective as Santomerse D at 90°C., and the bubbles in the foam were larger and less stable. The foam produced with Nacconol NR was only slightly less voluminous, but it was more stable than the Aerosol AY foam. Nekal BX gave a viscous stable foam of about the same volume as the Aerosol AY foam. The foaming capacities of these solutions were slightly less at room temperature and in about the same order. The Nekal BX foam was unusually stable. Ninol 555 base produced only 0.5 to 0.75 in. of foam at 30°C., and it evinced little or no tendency to foam in the hot solution. Emulphor O was ineffective.

Little further comment can be made regarding these results. They seem to

bear out the previous conception that there must be some chemical structural relationship between the solvent and the solute for effective foam propagation. Additional liquids will have to be examined before it can be determined whether some liquids have a greater propensity for foaming than others with comparable properties such as viscosity, surface tension, vapor pressure, and dielectric constant.

Surface-tension measurements were made on the solutions used in the previous series of experiments. The decreases in surface tension on the addition of 1 per cent solute are given in table 4. As expected from the previous observations, Ninol 555 base and Emulphor O showed considerable surface activity in glycol and glycerol but little activity in the other solvents. There is no apparent relation between foamability and the surface activity of the other solutes in the solvents examined.

TABLE 4
Changes in surface tension at 30°C. produced by addition of 1 per cent of several colloidal electrolytes

SOLVENT	SURFACE TENSION OF SOLVENT	DECREASE IN SURFACE TENSION					
		Aerosol AY	Santo- merse D	Nekal BX	Na'conol NR	Ninol 555 base	Emulphor O
	<i>dynes</i>	<i>dynes</i>	<i>dynes</i>	<i>dynes</i>	<i>dynes</i>	<i>dynes</i>	<i>dynes</i>
Glycerol (U.S.P.)	65.0	<u>25.8</u>	<u>30.7</u>	20.3	<u>31.6*</u>	<u>37.2</u>	<u>30.5*</u>
Glycol	47.5	<u>3.4</u>	<u>4.5</u>	5.4	<u>5.8*</u>	<u>15.5</u>	<u>13.7</u>
Halowax No. 1000	41.8	<u>11.4</u>	<u>11.4*</u>	<u>5.6*</u>	<u>11.3*</u>	6.5	+0.4
Tricresyl phosphate	40.5	<u>13.7†</u>	<u>9.1*</u>	<u>2.9†</u>	<u>9.9†</u>	0.0	+1.0
Dibutyl phthalate	32.3	<u>2.6†</u>	<u>0.0*</u>	0.0†	0.0†	+0.2	0.0

* Centrifuged or filtered.

† Some separation of solute on standing.

All the solutions which foamed (underlined in table 4) had a decrease in surface tension which varied from 5.6 to 37.2 dynes. Very few observations of increased surface tension have been made, so that the increases produced by Emulphor O and Ninol 555 base are unusual, especially at 1 per cent concentration. It is inferred that foam formation is accompanied by a decrease in surface tension, but that the converse is not true, and that the degree of change is not too important.

Some divergence from the principle that the degree of foaming induced in any particular solvent is dependent on the structure of the foaming agent was noted in the case of glycerol. Compounds found empirically to be effective in hydrocarbons and slightly oxygenated solvents proved most effective, while Emulphor O, which was extremely efficacious in glycol, showed little tendency toward foam formation in glycerol. If the solutions were merely shaken, the high viscosity of glycerol might account for this behavior. In order to investigate this question and to place the evaluation on a quantitative basis, the foaming capacity of several glycol and glycerol solutions was determined by a beating technique.

TABLE 5

Foaming capacity and foam stabilities of several glycerol and glycol solutions

FOAMER	SURFACE- TENSION DECREASE	FOAM DENSITY	PER- CENT- AGE OVER- RUN*	DRAINAGE FROM 100-G. SAMPLE					REMARKS	
				0.5 hr.	1 hr.	1.5 hr.	2 hr.	3 hr.		
With glycerol										
	<i>dynes</i>	<i>grams per cc.</i>		<i>cc.</i>	<i>cc.</i>	<i>cc.</i>	<i>cc.</i>	<i>cc.</i>		
Ninol 555 base: 1.0%. . .	37.2	0.297	325	0	0	2	3	6	Stiff foam with very fine stable bubbles	
0.5%		0.447	182	0	2		15		More fluid, but fairly stable foam	
Santomerse D: 1.0%	30.7	0.329	285	0	0	2		8	Very fine bubbles, but not as stiff as 1 per cent Ninol foam	
0.5%		0.433	191	1	3		9		Very fluid with fine cells	
Aerosol AY: 1.0%	25.8	0.364	246	0	0	2	4	9	Fairly stiff with fine bubbles; could be poured	
Nacconol NR: 1.0%	31.6	0.476	165	2	3	6			Very fluid foam	
Emulphor O: 1.0%	30.5								No tendency to foam at 0.1, 0.5, or 1 per cent; the few bubbles formed were stable. Gelati- nous solution	
With glycol										
Emulphor O: 1.0%	13.7	0.123	818	50	78				Almost com- pletely col- lapsed in 1 hr.	
0.5%		0.174	550	58	77				Medium-sized bubbles, fairly stiff	
Nacconol NR: 1.0%	5.8								Slight foam; col- lapsed almost immediately	
Santomerse D: 1.0%	4.5								Less than Nac- conol; collapsed as soon as beat- ers stopped	
Ninol 555 base: 1.0%	15.5								Similar to Santo- merse	

* Per cent increase in volume over original volume of solution.

One hundred grams of the solution to be foamed was conditioned at 30°C. in a small mixing bowl and aerated for 30 sec. (with air injected by means of a blow-pipe). The mass was then agitated slowly with a Mixmaster for another 30 sec., and finally beaten on No. 6 speed for 5 min. Air was injected continuously. The density was determined immediately by weighing 100 cc. of the foam. The foam was transferred to a glass jar for drainage observations.

In table 5 the volume of foam produced for each solution is indicated by the foam density as well as by the calculated overrun, which is the percentage increase in volume over the original volume of foam. An aqueous gelatin solution of the same viscosity as ethylene glycol under the same conditions gave a foam with a density of 0.230, corresponding to an overrun of 425 per cent. The organic systems, where capable of foaming, are therefore comparable with aqueous systems in foaming capacity. The drainage figures reveal that the organic foams are extremely stable. The effect of viscosity on stability of foams is brought out by the more rapid drainage from the glycol than from the glycerol foams. The reasons why Ninol 555 base should produce effective foams in glycerol and not in glycol, while Emulphor O is effective in glycol and not in glycerol, might be clarified by a study of the behavior of a larger number of similar compounds of known structure in these solvents.

Apparently differences in molecular structure have an important bearing on the relative efficacy of detergents and wetting agents, and a similar situation seems to apply to foamers for both aqueous and organic liquids. In this connection the examination of a series of colloidal electrolytes in various organic solutions by the technique of Taubman (17), to determine the nature of the orientation in each case, might lead to an understanding of why some of the solutions foam while others do not.

No simple correlation between surface viscosity, surface tension, and foaming power of aqueous soap solutions was found by Preston and Richardson (15). As these authors examined only one system, soap and water, a revision of the possible rôle of surface viscosity in foam formation in other systems might merit research, especially in view of improvements recently suggested for the measurement of surface viscosity (2).

SUMMARY

Partial answers to the questions posed in the introduction to this paper are as follows:

1. Foams comparable in volume and stability to aqueous foams can be produced in organic liquids. It appears that liquids with surface tensions higher than those of the common volatile solvents are more susceptible to foam propagation. There are some indications that certain solvents have a greater tendency to support foam formation than other solvents of comparable surface tension. On the other hand, it is possible that diligent search will reveal for every solvent a chemical structure which is an efficient foaming agent.

2. Foaming is usually accompanied by a decrease in surface tension, but the

converse is not necessarily true. The extent of the decrease in surface tension is apparently not too important. In some instances stable voluminous foams were obtained with surface-tension decreases of 5.6 to 37.2 dynes, while in other cases changes of the same range of magnitude gave no foam formation. While it is true that the least voluminous of these foams occurred where the surface-tension change was small, there is not sufficient evidence that effective foams could not be produced in conjunction with even smaller changes.

3. Physical properties such as vapor pressure and viscosity do not seem to be factors in foam initiation, but they do influence the stability of foams once they are formed.

4. Several types of colloidal electrolytes have been proved to be surface active in organic liquids. The extent of their surface activity and also their propensity for foam formation may reside in a structural balance between the solute and the solvent.

McBain and Spencer (13) have said, "... it is evident that but little is known of the properties of surface layers of solutions"; a similar situation exists in regard to a thorough understanding of the mechanism of foam propagation. The possibility of producing stable foams in organic liquids extends the boundaries of foam studies hitherto limited to the use of aqueous media. The present information supplies a springboard for the development of foaming agents for organic liquids.

REFERENCES

- (1) ADAM, N. K.: *The Physics and Chemistry of Surfaces*, 2nd edition, p. 137. Clarendon Press, Oxford (1938).
- (2) BERGAMI, G.: *Roll soc. ital. sper.* **8**, 1276-8 (1933).
HARKINS, W. D., AND MYERS, R. J.: *J. Chem. Phys.* **5**, 603 (1937).
- (3) BERKMAN, SOPHIA, AND EGLOFF, GUSTAV: *Emulsions and Foams*, 1st edition, pp. 116-21. Reinhold Publishing Corporation, New York (1941).
- (4) CAMPBELL, A. N.: *Can. J. Research* **19B**, 143-9 (1941).
KROTOVA, N. A.: *Caoutchouc and Rubber (U.S.S.R.)* **8**, 28-37 (1940).
PAMFILOV, A. V., AND STAROBINETS, G. L.: *J. Gen. Chem (U.S.S.R.)* **11**, 501-6 (1941).
- (5) CARYL, C. R.: *Ind. Eng. Chem.* **33**, 731-7 (1941).
- (6) CARYL, C. R., AND ERICKI, W. P.: *Ind. Eng. Chem.* **31**, 44-7 (1939).
- (7) CUPPLES, H. L.: U. S. Department of Agriculture, Bureau of Entomology and Plant Quarantine, E504, 56 pp., June, 1940
DE NAVARRE, M. G.: *Wetting Agents*, Bulletin No. 9, Am. Perfumer, New York (1939).
- DUEMLING, W. W.: *Arch. Dermatol. Syphilol* **43**, 264-78 (1941).
- KRITCHEVSKY, W.: U. S. patent 2,089,212 (August 10, 1937).
- VAN ANTWERPEN, F. J.: *Ind. Eng. Chem.* **35**, 126-30 (1943).
- (8) DEAN, H. K.: *Wetting and Detergency*, pp. 25-39. Chemical Publishing Company, Inc., New York, and A. E. Harvey, London (1937).
- (9) GILBERT, E. C.: *J. Phys. Chem.* **31**, 543 (1927).
- (10) GOLDTHWAIT, CHARLES F.: *Am. Dyestuff Repr.* **26**, 569-80 (1937)
- (11) I. G. Farbenindustrie: German patent 704,233.
KAUFMANN, H. P., AND KIRSCH, P.: *Fette u. Seifen* **47**, 196-201 (1940).
ROBINSON, H. E., BLACK, H. C., AND MITCHELL, H. S.: *Oil & Soap* **17**, 208 (1940).
VON HARTNER-SEBERICK, R.: *Ges. Abhandl. Kenntnis Kohle* **11**, 628-9 (1934).

- (12) McBAIN, M. E. L., AND PERRY, L. H.: J. Am. Chem. Soc. **62**, 989-91 (1940).
- (13) McBAIN, J. W., AND SPENCER, W. V.: J. Am. Chem. Soc. **62**, 243 (1940).
- (14) MACY, R.: J. Chem. Education **12**, 573-6 (1935).
- (15) PRESTON, W. C., AND RICHARDSON, A. S.: J. Phys. Chem. **33**, 1142-50 (1929).
- (16) SLUHAN, C. A.: Paper Trade J. **111**, No. 8, 26-31 (1940).
SNELL, FOSTER DEE: Ind. Eng. Chem. **35**, 108 (1943).
- (17) TAUBMAN, A. B.: Compt. rend. acad. sci. U.R.S.S. **29**, 22-6, 103-7, 210-15 (1940) (in English).
- (18) TICKELL, F. G.: Oil Gas J. **27**, N22, 175 (1928).

A METHOD OF GROWING SINGLE CRYSTALS OF SODIUM STEARATE AND SODIUM PALMITATE

A. DE BRETTEVILLE, JR.

64 Terrace Road, Medford, Massachusetts

AND

F. V. RYER

114 Farnham Street, Belmont, Massachusetts

Received February 4, 1944

Although single crystals of sodium stearate have been grown for x-ray work (6) in a gel, the procedure described proved unsuitable for use by the authors. Another technique of growing sodium stearate crystals is offered. In addition, the authors show for the first time how to grow sodium palmitate crystals. An easier method of synthesizing the soap without the additional work involved in the method of Thiessen and Stauff (6) proved feasible.

EXPERIMENTAL

The first samples of sodium stearate were made by a method similar to that of Thiessen and Stauff (6). The ethyl ester was prepared from Eastman stearic acid (No. 402), and was fractionated in a vacuum at 1-mm. pressure, the first fraction being rejected. The ester was then saponified with caustic, and the solution evaporated to dryness at 105°C.

Subsequently it was discovered that the above method was not necessary, since adequate crystals of sodium palmitate and sodium stearate could be grown by a shorter method by saponifying the acid material with caustic soda.

The sodium stearate single crystals were prepared by adding 0.32 g. of anhydrous material to 100 cc. of 95 per cent alcohol (unneutralized). The material was then heated in a refluxing flask by a gentle gas flame. After the solution had cooled to room temperature it was poured into a 250-ml. round-bottomed flask. The flask was suspended in an oil bath at 25°C. by rubber bands, with a hole in the stopper to allow slow evaporation. The oil and rubber bands were used because they damp out vibration that might adversely affect the growth of the

crystals. However, this is not imperative because good crystals grown without the bath were observed in the case of sodium stearate.

The temperature of crystallization is critical and should be observed within a few degrees, otherwise a different concentration is necessary. Crystals of sodium stearate appear from the solution after a few days.

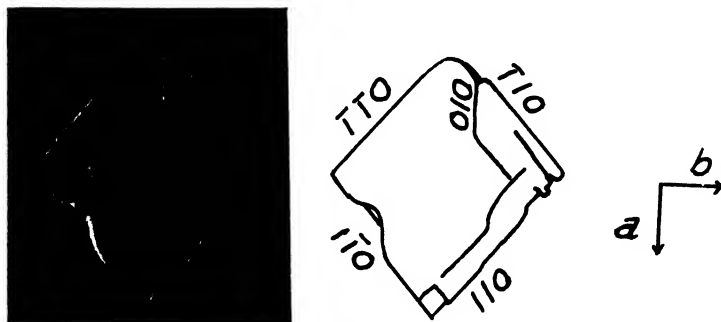


FIG. 1 Sodium palmitate crystal ($60\times$)

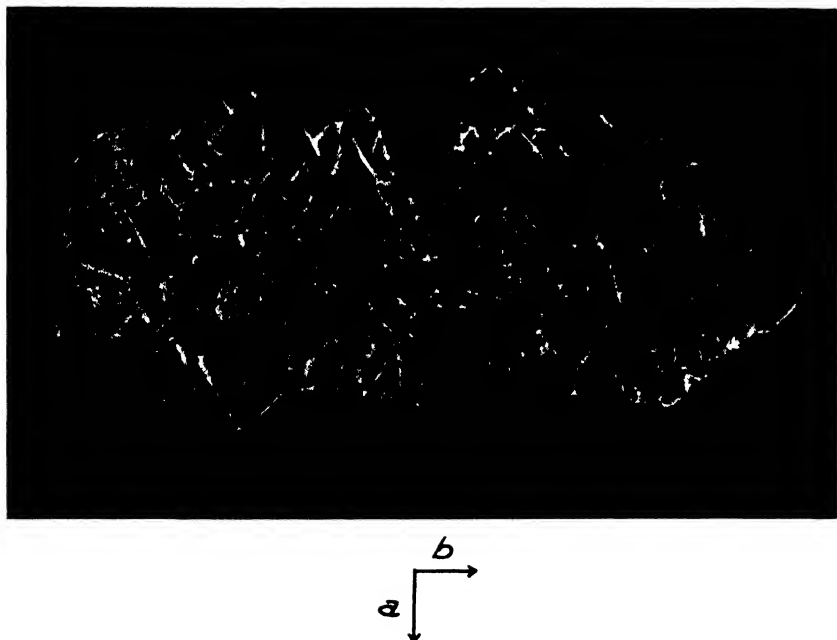


FIG. 2 Sodium palmitate crystals showing imbricated lineage structure ($60\times$)

In the case of sodium palmitate the concentration was raised to 0.62 per cent and a pinch of sodium chloride about the grain size of table salt was added to the solution in the 250-ml. round-bottomed flask at 25°C . Crystals of sodium palmitate grow up from the sodium chloride crystals.

RESULTS AND DISCUSSION

Sodium stearate forms a gel at high concentration in alcohol, and when the concentration is lowered just below that of the gel the crystals appear at the critical concentration. A further reduction in concentration produces no crystals.

For sodium palmitate there was no concentration below the gel concentration which gave crystals. A concentration close to that of the gel point was used, as



FIG. 3. Sodium stearate crystals showing arborescent growth ($60\times$). The b -axis deviates only slightly from the plane of the paper.

in the case of sodium stearate, and a pinch of sodium chloride was added to act as the nucleus from which the sodium palmitate crystals might grow.

The exact function of the sodium chloride is not known. Perhaps the electrical field of the sodium chloride lowers the potential barrier for crystal formation. Once started, the crystals build out from this nucleus.

The common-ion effect may also be responsible. Sodium hydroxide pellets cause the sodium palmitate to crystallize, but have the disadvantage of forming a gel from which crystals are difficult to extract.

Water may be concentrated at the initial point of growth, since the crystals of sodium palmitate and stearate are in the alpha form, as shown by Thiessen and Stauff (6), and these forms are known to be hydrated (2).

The habit of the transparent sodium palmitate crystals is tabular with a diamond shape; the crystals do not exceed 0.5 mm. in over-all dimensions, as shown in figure 1. The a - and b -axes of the crystal lie in the plane of the crystal flake, while the c -axis is nearly perpendicular to the crystal leaflet (4, 6).

The sodium palmitate and sodium stearate crystals both appear to have grown in the direction of the b -axis. Both crystals cleave along the (010) plane. The sodium palmitate crystals have an imbricated or overlapping structure, as shown in figure 2. The sodium stearate crystals are usually longer, and have an arborescent or dendritic appearance, as shown in figure 3. Both crystals exhibit line-age structure (3). The photograph in figure 3 was taken at right angles to the

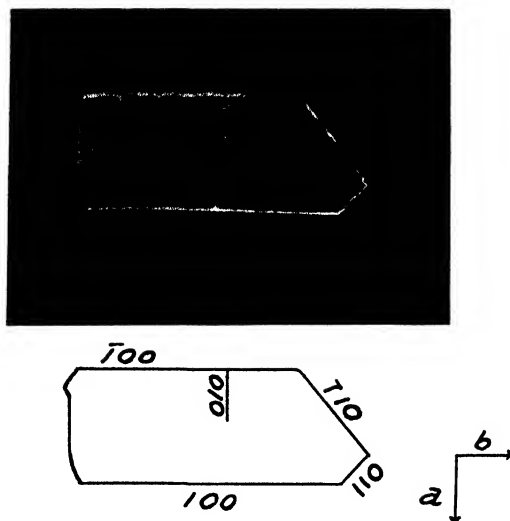


FIG. 4 Sodium stearate crystal cleaved at one end (60 \times)

direction of growth. Sodium stearate crystals, because they grow to longer lengths than sodium palmitate crystals, are more easily separated. Figure 4 shows a single crystal of sodium stearate.

The task of obtaining single crystals of either substance is not made any easier by their plastic deformation.

Surface charges which appear to accumulate on the insulating (001) faces make it easy to pick up the crystals and transfer them with an insulated metallic needle.

SUMMARY

1. Sodium stearate can be crystallized only at a critical concentration below the gel point in an alcohol solution.

2. Sodium palmitate cannot be crystallized below the gel point, but does give crystals on the addition of a pinch of sodium chloride, which appears to act as a nucleus for crystal growth.

The authors wish to thank Professor M. J. Buerger for initiating the above work, and for his helpful discussions. They wish to thank Mr. E. C. Fillmore for photographing the crystals.

The senior author also wishes to thank Professor R. D. Vold, Dr. M. J. Vold, and Dr. J. W. McBain for previous help in this field (1, 5).

REFERENCES

- (1) DE BRETTEVILLE, A., JR., AND MCBAIN, J. W.: *Science* **96**, 470 (1942).
- (2) BUEGER, M. J., SMITH, L. B., DE BRETTEVILLE, A., JR., AND RYER, F. V.: *Proc. Natl Acad. Sci. (U. S.)* **28**, 528 (1942).
- (3) BUEGER, M. J.: *Z. Krist.* **A89**, 195 (1934).
- (4) BUEGER, M. J.: *Proc. Natl. Acad. Sci. (U. S.)* **28**, 530 (1942).
- (5) MCBAIN, J. W., DE BRETTEVILLE, A., JR., AND ROSS, S.: *J. Chem. Phys.* **11**, 181 (1943).
- (6) THIESSEN, P. A., AND STAUFF, J.: *Z. physik. Chem.* **A176**, 397 (1936).

ON HARKINS' "FINAL SPREADING COEFFICIENT" AND ANTONOFF'S "RULE"

WILLIAM FOX

Department of Chemistry, Columbia University, New York, New York

Received February 4, 1944

Recent discussions (1, 6) involving Harkins' "spreading coefficient" and Antonoff's "rule" prompt this communication.

Harkins has pointed out (4) that when Antonoff's "rule" is expressed in terms of the "final spreading coefficient," a relation is given which is "an extremely peculiar one," and states (the italics are Harkins') "*that if the relation were true the phenomena of the spreading of liquids on liquids would be restricted in an extremely remarkable way.*"

It has been shown (2) that Antonoff's "rule" is applicable to a number of liquid-liquid-gas systems, a fact which from Harkins' statements would seem to establish the lack of validity of the theory of the "spreading coefficients" which he supports.

For the systems for which it has been shown (2) that Antonoff's "rule" is applicable, the defined "final spreading coefficient" of Harkins for the liquid with the lower surface tension is equal to zero. Harkins has concluded (5) that the "final spreading coefficient" is (the italics are Harkins') "*always negative*," a conclusion which indicates the lack of general reliability of the experimental tools previously utilized for the study of these relationships.

What is evident therefore is that the objections of Antonoff (1) to much of the criticism of his "rule" have some justification.

Antonoff, however, has neglected to consider recent investigations (2, 3) which

show that while his "rule" may be applied to a number of liquid-liquid-gas systems, the relationship expressed by it is not general.

REFERENCES

- (1) ANTONOFF, G.: J. Phys. Chem. **47**, 709 (1943).
- (2) FOX, W.: J. Chem. Phys. **10**, 623 (1942).
- (3) FOX, W.: "A Semimicro Method for the Study of the Action of Fluid Interfaces", delivered at the Symposium on the Research Tools of the Colloid Chemist before the Division of Colloid Chemistry at the 106th Meeting of the American Chemical Society, Pittsburgh, Pennsylvania, September 10, 1943.
- (4) HARKINS, W. D.: Colloid Symposium Monograph **6**, 20 (1928).
- (5) HARKINS, W. D.: J. Chem. Phys. **9**, 552 (1941).
- (6) YOFFE, A., AND HEYMANN, E.: J. Phys. Chem. **47**, 409 (1943).

COMMUNICATION TO THE EDITOR

NOTE ON THE INTERPRETATION OF DISTRIBUTION EQUILIBRIA BETWEEN MOLTEN METALS AND MOLTEN SALTS¹

Nelson W. Taylor has recently criticized some points in the theoretical treatment in our paper on "Distribution Equilibria between Molten Metals and Molten Salts (J. Phys. Chem. **47**, 473 (1943)). Unfortunately, he has misunderstood our reasoning and the object of our investigation. He states that "one cannot calculate the activity curve for sodium in the *salt phase* from the given data. . . ." However, we do not attempt to do this. Our experiments are directed to estimate activities in the *metal phase*. We have stated in the introduction that "by investigating the deviations of such distribution equilibria from ideality, it is possible to obtain qualitative information about the activities in *binary metallic mixtures* and about the existence of intermetallic compounds in the molten state." In the systems lead-sodium-sodium bromide and cadmium-sodium-sodium bromide, the distribution curves of sodium between molten sodium bromide and the molten metal phase are regarded as a qualitative representation of the activity of sodium in the metal phase (although a note of caution is sounded). This treatment is permissible because the solutions of sodium in the molten salt phase are very dilute (maximum molar fraction = 0.023), and the partial vapor pressure of sodium in the salt phase can therefore be assumed to be approximately proportional to the molar fraction of sodium in the salt phase (Henry's law). As a consequence, Raoult's law as applied to the metal phase and Nernst's law of solubility decrease (W. Nernst: Z. physik. Chem. **6**, 573 (1890)) become virtually identical,² and the distribution curve

¹ Received February 25, 1944.

² Or, $\alpha_{\text{salt}} = \text{const.} \times N_{\text{salt}}$ (Henry's law). Hence $\alpha_{\text{metal}} = \text{const.} \times N_{\text{salt}}$, where a and N are the respective activities and molar fractions of sodium in the salt and metal phase.

can be interpreted in terms of deviations from Raoult's law in the metal phase (cf. E. Heymann and E. Friedlaender: *Z. physik. Chem.* **A148**, 177 (1930)). Hence, measurement of the concentration of sodium in the salt phase takes the place of the measurement of the partial vapor pressure of sodium in the metal phase.

In the system lead-sodium-sodium bromide, the distribution curve shows a very strong negative deviation, suggesting that sodium-lead compounds are stable in the molten state at 780°C. On the other hand, the distribution curve in the system cadmium-sodium-sodium bromide shows a positive deviation. From this we have concluded that cadmium-sodium compounds are not stable at that temperature, which is about 400°C. above the melting point of any one of the known cadmium-sodium compounds. As this last conclusion has been described by Nelson W. Taylor as being on an "erroneous basis," we should like to give another piece of evidence in its favor: whether the salt phase is quite ideal or not, we are dealing with the *same salt phase* in the two systems lead-sodium-sodium bromide and cadmium-sodium-sodium bromide, as lead and cadmium are insoluble in the salt phase. Hence the difference between the two distribution curves must be due to a difference in the constitution of the molten metal phases (*viz.*, lead-sodium and cadmium-sodium).

The other systems under investigation, *viz.*, bismuth-cadmium-cadmium chloride, bismuth-cadmium-cadmium bromide, and antimony-cadmium-cadmium chloride, are complicated because the concentrations of the metallic solutes cadmium and antimony in the salt solvent are high and *both* metallic components show partial solubility in the molten salt phase. No attempt has, therefore, been made to treat the distribution curves in these systems as activity curves, except in the case of bismuth which is present in the salt phase in very low concentration (maximum molar fraction = 0.006). It may be artificial to describe deviations from linearity of the distribution curves in these more complicated systems as "deviations from Raoult's law," and we appreciate Nelson W. Taylor's criticism on this point of terminology, which does not, however, affect in any way our theoretical treatment and the conclusions therefrom.

E. HEYMAN.

R. J. L. MARTIN.

M. F. R. MULCAHY.

Chemistry Department
University of Melbourne
Melbourne, Australia

NEW BOOKS

Electrophoresis of Proteins and the Chemistry of Cell Surfaces. By HAROLD A. ABRAMSON, LAURENCE S. MOYER, AND MANUEL H. GORIN. 6 x 9 in.; 341 pp.; 155 fig. New York: Reinhold Publishing Corporation, 1942. Price: \$6.00.

Dr. Abramson is Assistant Professor of Physiology in the College of Physicians and Surgeons, Columbia University, and Associate in Medicine in the Mount Sinai Hospital, New York. Dr. Moyer, until his untimely death in the service of his country in the late spring of 1942, was Assistant Professor of Botany at the University of Minnesota. Dr. Gorin is Chemical Research Supervisor in the Field Research Department of the Magnolia Petroleum Company, Dallas. Although the immediate interests of these men have differed, they have collaborated on occasion, and many of the numerous references in the book bear their names. The diversity of the training and backgrounds of the authors has given them an unusual opportunity to write an authoritative treatise dealing with all phases of electrophoresis. The haste with which a book devoted to such a rapidly developing field of knowledge must be assembled in order that it not be too far out of date at the time of publication probably explains why this opportunity has not been fully utilized.

The topics discussed by the authors are indicated by the chapter headings: general principles of electric migration in liquids; experiments in the nineteenth century; methods; dissolved and adsorbed proteins and related surfaces; electrokinetic theory and migration of charged particles; electric mobility and the calculation of the net charge; serum and plasma; antibodies, antigens and their reactions; interactions of proteins in mixtures; interactions of proteins at surfaces; enzymes and hormones; miscellaneous electrophoretic investigations of biological interest; latex; and surface chemistry of cells.

The early chapters of the book are well written, and bear evidence of logical and critical thinking on the part of the authors. The discussion of methods includes an excellent description of the special theory and use of the flat type of microelectrophoresis cell, a brief description of other types of microcell, and a discussion of the moving-boundary technic. The latter discussion, while helpful, is neither as clear nor as complete as some of the descriptions published by other authors. The excellent chapter on electrokinetic theory is devoted largely to an outline of the Debye-Hückel-Henry theory and to Gorin's interesting extension of this theory for particles of different shapes and for ions of finite size. A review of the authors' work on the relation of electrophoretic mobility to titration curves is presented in the following chapter.

The latter half of the book is a review of the numerous electrophoretic studies to be found in the literature. This portion is difficult to read, partly because of the great diversity of the systems considered, and partly because many of the electrophoretic results reported have no known correlation with the other properties of the system under study. This section would have been improved had the authors differentiated those studies that were carried out with great care in order to demonstrate the abilities and limitations of the electrophoretic method from those that were carried out incident to the broader investigation of a particular substance or mixture. At worst, however, this portion of the book contains a fairly complete list of references up to the middle of 1941.

Proof reading apparently was done hastily, and numerous obvious errors will be evident to the reader. One of the most unfortunate of these is the omission of a diagram of the Philpot-Svenson optical system, which is almost essential for an understanding of the principles of the method.

The binding is red cloth with gold lettering. The typography and paper are good. Most of the one hundred fifty-five illustrations are graphs or line drawings. Author and subject indices are included.

Since no volume written about a rapidly changing and expanding field of knowledge can be definitive, some of the faults noted above probably should be overlooked. Undoubtedly this book will be welcomed by those who have had no firsthand experience with electrophoretic methods, and who would like to become acquainted with the field. Most workers

in the field probably will find fault with portions of this book, but, at the same time, most of them will have copies within easy reach.

GEORGE W. SCHWERT, JR.
L. EARLE ARNOW

Methoden der mathematischen Physik. By R. COURANT AND D. HILBERT. Published and distributed with the consent of the Alien Property Custodian. Vol. I, second edition; Vol. II, first edition. New York: Interscience Publishers, Inc. Price: \$8 per volume; \$14 for both volumes.

Among the numerous German mathematical books recently made available by action of the Alien Property Custodian, this issue of Courant-Hilbert will be considered a highlight by many. Volume I is well known to many physicists and physical chemists as a basic reference for the mathematical background of quantum mechanics; Volume II is of more recent issue and has not yet attained to such currency.

To those who may be entirely unfamiliar with the work, it may be said that it takes as its field of study the mathematical equations and procedures of theoretical physics; more particularly, those arising from mechanics, optics, the theory of vibrations, potential theory, heat conduction, and wave propagation. In no sense a textbook of the usual type, it studies these problems from the "function-theoretical" point of view, rather than from the method so necessary and so precious to the physicist and chemist, of working out innumerable special cases in order to learn the "go" of the thing. The discussion is on a high plane, and will tax the powers of even mathematically sophisticated readers, so that its study is not to be undertaken lightly. Whosoever would enter the forest at this point must grasp the axe firmly and hew to the line; in recompense, he will be repaid by finding it a lucid and informative study of a wide body of mathematical work of the highest importance in physical theory.

Considering the technical character of the contents, and the level of mathematical achievement presupposed on the part of the reader, it would be difficult, and indeed unprofitable, to give a detailed review of the material here. In general terms, Vol. I is concerned with matrix theory, the expansion of functions (Fourier series and integrals and similar expansion forms), variation principles, integral equations, and a preliminary study of particular partial differential equations coming for the most part from the theory of vibrations of elastic media, and the functions arising therefrom (Bessel functions, Laguerre functions, etc.). A comparison with the first edition shows that the revision has improved the readability, notably in the first chapter on matrix theory. In the opinion of the reviewer, this volume will probably be the more useful of the two to most physicists and chemists, and can be used separately. It constitutes a most valuable adjunct to a serious study of that still classic, if neglected, book—*Theory of Sound*, by Lord Rayleigh—in which can be found a wealth of physical data and discussion to leaven the purity of the mathematics.

Volume II is concerned with the general theory of partial differential equations, and can be studied independently of Volume I. The emphasis in the discussion centers around the method of characteristics and of fundamental solutions. The treatment of Hadamard's methods for the solution of the general wave equation is of especial value now, since Hadamard's books are no longer readily available. If, as seems probable to the reviewer, this volume is less likely to be of immediate appeal and usefulness to chemists and physicists, it is in no wise a reflection on the character of the work itself; it is simply that in the study of actual physical problems the analysis of special cases and their reduction by the method of separation of variables still is often the most practicable procedure, when indeed an explicit solution is obtainable at all. And this is even more the case when it is taken into account that not unusually the differential equation which is used is itself recognized as being only a partial expression of the physical facts, and so does not justify the labor of full solution. For reasons such as these many readers will find that the paucity of specific applications to simpler problems of physical interest makes the high level of the discussion difficult to

follow. On the other hand, it is not unlikely that the current intensive study of important problems arising out of the war effort may well lead to developments in which the more general methods stemming from the work of Riemann, Volterra, Hadamard, and others, among whom must be counted Professor Courant himself, will play a more important rôle. There is reason to think, also, that some of the difficulties facing the further development of relativistic quantum mechanics will demand a thoroughgoing examination of these same mathematical questions. In any event, it seems fairly certain that the next generation of theoretical physicists will be called upon to exert itself still more strenuously in the broadening of its command of mathematical techniques, in which endeavor the present volumes should play a leading part.

In closing, we may pause to pay a word of tribute to the memory of Professor David Hilbert, who died on February 14, 1943. His position in pure mathematics during the last generation has been of the highest order, and in mathematical physics scarcely less, even if more indirect, through his influence on mathematical physicists in Germany, as well as by his own work in integral equations, relativity theory, and other topics. It may not be inappropriate to end our review of this masterly work by his former colleague Professor Courant, by quoting a remark attributed to Hilbert, if only apocryphally: "Die Physik—ja die ist für die Physiker doch viel zu schwer." (Obituary notice by W. Heisenberg in *Physikalische Zeitschrift*, August, 1943).

E. L. HILL.

Luminescence of Liquids and Solids and its Practical Applications. By PETER PRINGSHEIM AND MARCEL VOGEL. 200 pp. New York: Interscience Publishers, Inc., 1943. Price: \$4.00.

This treatise has but little resemblance to the one published by Pringsheim about twenty-five years ago. Both the theory and the practice of fluorescence have changed enormously since that time. It is the purpose of this work to present both of these in their present status of development and to elucidate the connection between the two as far as possible.

It is in the last objective that most difficulty is encountered. While the theory of luminescence is now quite highly developed within the concepts of modern spectroscopy and while the application of luminescence is now in a period of lively interest and activity, the connection between the two is still loose and in many respects remains unexplored. The phenomena of luminescence, as influenced by various factors such as impurities, temperature, crystal structure, and lattice deformation, are so complicated as to render their subjection to theory extremely difficult.

Much scientific work of most exacting character remains to be done. The work of Pringsheim and Vogel is a most welcome aid and guide. The end will not be reached in a day, but its accomplishment will bring rich rewards both to science and to practice.

S. C. LIND.

THE RELATIVE VISCOSITY OF AQUEOUS SOLUTIONS OF SULFAMIC ACID AND OF SOME OF ITS SALTS AT 25°C.

A. F. SCHMELZLE¹ AND J. E. WESTFALL²

Department of Chemistry, The Creighton University, Omaha, Nebraska

Received March 18, 1944

The solubility in water of the barium, calcium, and magnesium salts of sulfamic acid has recently been reported by King and Hooper (3). In view of the increased use of sulfamic acid and of its salts, it seems desirable that more data concerning the physical properties of its solutions be available. It is the purpose of this investigation to determine the viscosity and the density of solutions of sulfamic acid and of the ammonium, barium, calcium, and magnesium salts of this acid.

EXPERIMENTAL

Sulfamic acid of reagent grade, purchased from the G. Frederick Smith Chemical Company, was recrystallized from water, dried in air, and stored over Anhydron. The barium, calcium, and magnesium salts were prepared by treatment of a solution of the reagent-grade acid with a slight excess of a c.p. grade of the carbonate of the desired metal (3). The ammonium sulfamate was prepared by two recrystallizations of a technical grade of the salt from water.

Two viscometers of the Ostwald type were employed for each determination. They were rigidly suspended in a constant-temperature water bath regulated at $25.00^{\circ}\text{C.} \pm 0.04^{\circ}$. A pipet was used to introduce the same volume of solution into each viscometer for the different trials. All solutions were prepared with water filtered through sintered-glass filters. An interval of 15 to 30 min. was allowed for temperature equilibrium. The rate of flow was timed with a stop watch reading to 0.2 sec. From three to six readings were taken for each trial, and the average of these readings was recorded as the time of flow. After each run, the viscometers were cleaned with chromic acid cleaning solution and then rinsed successively with filtered water, alcohol, and ether. They were dried by a current of filtered air.

Calibrated pycnometers were used to determine the densities. All weights were corrected for the buoyancy effect of air.

RESULTS AND DISCUSSION

The data for the various solutions are given in tables 1, 2, 3, 4, and 5, in which the first column gives the concentration, C , in gram-equivalents of solute per liter of solution, the second column gives the density, d , in grams per milliliter of solution relative to that of water at 4°C. , and the third column lists the relative viscosity, η/η_0 .

¹ Present address: Minnesota Mining and Manufacturing Company, St. Paul, Minnesota.

² Present address: Glenn L. Martin-Nebraska Company, Omaha, Nebraska.

TABLE 1
Viscosity of sulfamic acid solutions

C	d	η/η_0	C	d	η/η_0
0.1303	1.0034	1.0161	0.6736	1.0319	1.0644
0.1788	1.0064	1.0163	0.7331	1.0331	1.0707
0.2579	1.0103	1.0280	0.9693	1.0466	1.0902
0.3773	1.0166	1.0349	1.1951	1.0587	1.1145
0.4676	1.0214	1.0450	1.6445	1.0811	1.1668
0.4974	1.0229	1.0551	2.0724	1.1025	1.2214

TABLE 2
Viscosity of magnesium sulfamate solutions

C	d	η/η_0	C	d	η/η_0
0.0422	0.9995	1.0139	0.6582	1.0479	1.2003
0.0866	1.0034	1.0210	0.8042	1.0571	1.2393
0.1696	1.0099	1.0487	1.0238	1.0728	1.3160
0.2506	1.0158	1.0643	1.5082	1.1072	1.4940
0.3992	1.0258	1.1059	2.7160	1.1917	2.1960
0.5366	1.0372	1.1551	4.4960	1.3106	4.4660

TABLE 3
Viscosity of barium sulfamate solutions

C	d	η/η_0	C	d	η/η_0
0.0588	1.0052	1.0116	0.7622	1.0931	1.1501
0.1012	1.0107	1.0186	0.9654	1.1179	1.2024
0.1980	1.0220	1.0370	1.2334	1.1299	1.2334
0.3992	1.0480	1.0788	1.5850	1.1936	1.3775
0.5866	1.0715	1.1166			

TABLE 4
Viscosity of calcium sulfamate solutions

C	d	η/η_0	C	d	η/η_0
0.0529	1.0014	1.0140	0.7029	1.0529	1.1580
0.0826	1.0051	1.0275	0.7258	1.0594	1.1711
0.1618	1.0169	1.0448	1.0130	1.0740	1.2310
0.2209	1.0148	1.0502	1.4611	1.1207	1.4060
0.3432	1.0248	1.0826	2.0876	1.1690	1.6674
0.4657	1.0336	1.0991	2.6746	1.2188	1.9616
0.4718	1.0372	1.0982	3.4820	1.2771	2.5946
0.6014	1.0454	1.1378			

Grüneisen (1) noted that a plot of $(\eta/\eta_0 - 1)/C$ against C passed through a minimum at a low concentration for solutions of electrolytes. Jones and Dole

TABLE 5
Viscosity of ammonium sulfamate solutions

C	d	η/η_0	C	d	η/η_0
0.1185	1.0030	1.0054	1.8263	1.0902	1.1198
0.2074	1.0091	1.0054	1.9127	1.0946	1.1226
0.2958	1.0125	1.0185	3.4105	1.1659	1.3136
0.4765	1.0218	1.0244	5.0832	1.2435	1.6708
0.6863	1.0310	1.0334	6.3656	1.3011	2.1874
0.8254	1.0404	1.0426	7.1813	1.3402	2.7543
1.0245	1.0504	1.0513	8.1696	1.3830	3.8298
1.2778	1.0632	1.0734			

TABLE 6
Constants of the Jones and Dole equation

SOLUTE	A	B	DEVIATION
			<i>per cent</i>
HSO_3NH_2	-0.0087	-0.0801	0.215
$\text{Mg}(\text{SO}_3\text{NH}_2)_2$	-0.0130	-0.2265	0.378
$\text{Ba}(\text{SO}_3\text{NH}_2)_2$	-0.0126	-0.1541	0.507
$\text{Ca}(\text{SO}_3\text{NH}_2)_2$	-0.0380	-0.1484	0.371
$\text{NH}_4\text{SO}_3\text{NH}_2$	+0.0051	-0.0556	0.202

TABLE 7
Constants of the Root equation

SOLUTE	K_1	K_2	DEVIATION
			<i>per cent</i>
HSO_3NH_2	0.0501	+0.000863	0.263
$\text{Mg}(\text{SO}_3\text{NH}_2)_2$	0.0716	+0.000769	0.205
$\text{Ba}(\text{SO}_3\text{NH}_2)_2$	0.1390	-0.0176	0.324
$\text{Ca}(\text{SO}_3\text{NH}_2)_2$	0.0918	-0.00787	0.339
$\text{NH}_4\text{SO}_3\text{NH}_2$	0.0540	-0.00238	0.058

(2) found that this relation can be expressed in terms of the fluidity of the solution by an equation which may be written in the following straight-line form:

$$\frac{\varphi - 1}{\sqrt{C}} = A + B\sqrt{C}$$

where A and B are constants characteristic of the electrolyte. A plot of $\varphi - 1/\sqrt{C}$ against \sqrt{C} for a number of solutions yielded a straight line for concentrations up to about 1 normal. This equation was applied to the data obtained for

the sulfamic acid and sulfamate solutions to a concentration of 1 normal, and the constants evaluated by the method of least squares. Table 6 lists the values of these constants and also the average percentage deviation of the calculated fluidities from the observed values.

The densities of the solutions studied may be expressed in terms of the Root (4) equation, which may be written

$$\frac{d - d_0}{C} = K_1 + K_2\sqrt{C}$$

in which d_0 is the density of pure water, and K_1 and K_2 are constants. The values of these constants, together with the average percentage deviation between the calculated densities and those observed for the sulfamic acid and sulfamate solutions, are given in table 7.

SUMMARY

1. The relative viscosity and the relative density of solutions of sulfamic acid and of the ammonium, barium, calcium, and magnesium salts of sulfamic acid have been studied over the range of the solubility of these substances in water.

2. The results may be expressed by the Jones and Dole equation for fluidities up to 1 normal and by the Root equation for densities over the entire concentration range studied.

REFERENCES

- (1) GRÜNEISEN, E.: *Wiss. Abhandl. physik-tech. Reichsanstalt* **4**, 237 (1905).
- (2) JONES, GRINNELL, AND DOLE, MALCOLM: *J. Am. Chem. Soc.* **51**, 2950 (1929).
- (3) KING, G. B., AND HOOPER, J. F.: *J. Phys. Chem.* **45**, 938 (1941).
- (4) ROOT, W. C.: *J. Am. Chem. Soc.* **55**, 850 (1933).

THE MEASUREMENT OF BOUNDARY TENSION BY THE PENDENT-DROP METHOD. II

HYDROCARBONS

GRANT W. SMITH¹

Department of Chemistry, The University of Kansas City, Kansas City, Missouri

Received January 15, 1944

The pendent-drop method of measurement of the surface tension of a liquid has been adequately described in the literature. Briefly, it involves the determination of certain critical dimensions of a drop of the liquid hanging from a suitable support, such as a glass capillary tip. The dimensions to be determined are the maximum diameter of the drop, D_e , and the diameter, D_s , of a selected cross-

¹ Present address: Research Laboratories, The B. F. Goodrich Company, Akron, Ohio.

sectional plane located at a distance equal to D_c along the axis from the apex of the drop. By employing the table of " H - S functions" which was derived experimentally by Andreas, Hauser, and Tucker (1), the boundary tension of the liquid may be calculated readily.

In the first paper (2) apparatus was described which was used to measure the surface tensions of several calibrating liquids and a series of aliphatic alcohols. The apparatus has been improved notably since this previous work was done, and the result has been higher precision of measurement and greater convenience and speed of operation. These improvements will be briefly described.

The present study was undertaken to determine the surface tensions of a number of highly purified hydrocarbons in the range from C_5 to C_8 .²

EXPERIMENTAL METHOD

Certain important changes in apparatus and technique of measurement have been made since the earlier work (2). A Leitz Mikro-Summar f4.5 microscope objective of 35-mm. focal length, equipped with an iris diaphragm, was used as camera lens. The camera system was rebuilt so that the distance from lens to focal plane was constant, roughly 45 cm. A Korelle Reflex camera, minus lens and lens mount, was used as before to furnish the shutter, focusing, and film-rewinding mechanism. The camera, thus assembled, was of fixed focus, and focusing was achieved by manipulating the object to be photographed. The advantage of this system was that the magnification was constant for all measurements.

The thermostat which housed the cell was also rebuilt. The glass syringe with special tip, which supported the drops of liquid, was mounted vertically on a microscope mechanical stage. With this arrangement, the drop of liquid could be moved in a horizontal plane either along the optical axis or at right angles to it, and focusing was accomplished quickly and accurately. Drops were expelled from the tip of the syringe by simply turning a screw which acted upon the plunger. Both the syringe and the glass compartment in which the liquid was suspended for photographing were completely enclosed in a double-walled housing through which water from a constant-temperature bath was circulated.

A new device for measurement of the photographs of the drops was used. The photograph was fixed in place by means of tape on a piece of heavy plate glass 25 cm. square, illuminated by diffuse light from below. The pictures were measured with the aid of a special microscope mechanical stage, equipped with scales and verniers which could be read directly to 0.05 mm. On this stage was mounted a sharp needle point and nine-power doublet magnifier, so that the point was in focus and could be observed as it traversed the picture during the measuring process. A peephole 1 mm. in diameter over the magnifier served to eliminate parallax.

² The hydrocarbons used in this work were prepared under the direction of Professor C. E. Boord of the Department of Chemistry of the Ohio State University as part of the American Petroleum Institute Hydrocarbon Research Project in the Industrial Research Foundation of the University.

The magnification obtained with the camera was 12.78 times, compared to 8.273 times with the earlier equipment. The magnification was determined by photographing an eyepiece micrometer scale and measuring the image on the

TABLE 1
Surface tensions of hydrocarbons at 20.0°C.

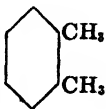

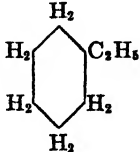
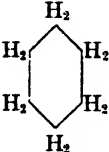
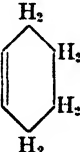

HYDROCARBON	FORMULA	NUMBER OF OBSERVATIONS	MEAN DEVIATION	SURFACE TENSION IN DYNES PER CENTIMETER
Octane.....	$\text{CH}_3\text{CH}_2\text{CH}_2\text{CH}_2\text{CH}_2\text{CH}_2\text{CH}_3$	4	0.05	21.7
2-Methylheptane	$\begin{array}{c} \text{CH}_3\text{CHCH}_2\text{CH}_2\text{CH}_2\text{CH}_3 \\ \\ \text{CH}_3 \end{array}$	4	0.04	20.7
3-Methylheptane	$\begin{array}{c} \text{CH}_3\text{CH}_2\text{CHCH}_2\text{CH}_2\text{CH}_3 \\ \\ \text{CH}_3 \end{array}$	4	0.04	21.2
4-Methylheptane	$\begin{array}{c} \text{CH}_3\text{CH}_2\text{CH}_2\text{CHCH}_2\text{CH}_3 \\ \\ \text{CH}_3 \end{array}$	4	0.04	21.2
2,5-Dimethylhexane	$\begin{array}{c} \text{CH}_3\text{CHCH}_2\text{CH}_2\text{CHCH}_3 \\ \qquad \qquad \\ \text{CH}_3 \qquad \qquad \text{CH}_3 \end{array}$	4	0.01	19.8
2,2,4-Trimethylpentane	$\begin{array}{c} \text{CH}_3 \\ \\ \text{CH}_3\text{CCH}_2\text{CHCH}_3 \\ \quad \\ \text{CH}_3 \quad \text{CH}_3 \end{array}$	4	0.04	18.9
<i>o</i> -Xylene		4	0.01	30.1
<i>p</i> -Xylene		4	0.04	28.5
Ethylcyclohexane.		5	0.03	25.8

TABLE 1—*Concluded*

HYDROCARBON	FORMULA	NUMBER OF OBSERVATIONS	MEAN DEVIATION	SURFACE TENSION IN DYNES PER CENTIMETER
Heptane	$\text{CH}_3\text{CH}_2\text{CH}_2\text{CH}_2\text{CH}_2\text{CH}_2\text{CH}_3$	4	0.05	19.7
Cyclohexane		4	0.01	25.2
Cyclohexene		5	0.04	26.6
Benzene		4	0.05	29.2
Pentane	$\text{CH}_3\text{CH}_2\text{CH}_2\text{CH}_2\text{CH}_3$	4	0.04	16.3
Isopentane	$\begin{array}{c} \text{CH}_3\text{CHCH}_2\text{CH}_3 \\ \\ \text{CH}_3 \end{array}$	4	0.06	15.5

negative by means of a measuring microscope. A correction factor for shrinkage of the negatives during development or storage was obtained as follows: As part of the measuring routine, the length of the camera aperture image on the negative was determined, and this was compared with the known corresponding value on the calibrating negatives mentioned above. The correction for shrinkage proved to be small, but variable. The maximum deviation from the adopted standard was about ± 0.4 per cent. The average deviation, however, was only 0.013 per cent.

It was felt that a high degree of precision was attained with the experimental methods and apparatus used in this study.

RESULTS AND DISCUSSION

The values for the surface tension of fifteen hydrocarbons at 20.0°C . are presented in table 1. To indicate the reproducibility of these values, the number of independent observations on which each value is based is shown, and the mean

deviation of these values from the mean is given. Each observation was made on a single 10-sec.-old drop in equilibrium with air saturated with the vapor.

The surface-tension values given in table 1 are shown only to the first decimal place. Although it is felt that the precision attained in the present study would justify the recording of another figure, it is not justifiable in the face of the limitations of the table of H - S values of Andreas, Hauser, and Tucker by means of which these results were calculated. The need for a refinement of the table of H - S values is clearly indicated.

The following basic trends of the surface tension with configuration of the hydrocarbons are readily noted from the table: (a) The surface tension increases with increasing molecular weight of the straight-chain hydrocarbons. (b) The surface tension decreases with increased degree of branching of the aliphatic hydrocarbons. This is observed in the case of the two pentanes and also the six aliphatic octanes. In both cases, the normal compound has the highest surface tension. In the case of the methylheptanes, the methyl side chain has the greatest effect when near the end of the long chain; the actual value obtained for 3-methylheptane was 21.17, and for 4-methylheptane, 21.23. (c) The surface tensions of cyclic hydrocarbons are, in general, higher than those of the corresponding straight-chain types. Also, the surface tension decreases with increasing saturation of corresponding cyclic hydrocarbons. Both of these trends are indicated by the two sets of three cyclic compounds containing six and eight carbon atoms, respectively. In the case of the six-membered rings, the effect of unsaturation on the surface tension is especially noteworthy.

SUMMARY

Improved technique and apparatus for the precise measurement of boundary tensions by the pendent-drop method have been briefly described.

The surface tensions of fifteen pure hydrocarbons have been measured at 20.0°C. The effects of configuration, molecular weight, and degree of saturation of the molecule on the surface tensions have been indicated for the systems studied.

REFERENCES

- (1) ANDREAS, J. M., HAUSER, E. A., AND TUCKER, W. B.: *J. Phys. Chem.* **42**, 1001-19 (1938).
- (2) SMITH, G. W., AND SORG, L. V.: *J. Phys. Chem.* **45**, 671-81 (1941).

ON THE SEPARATION OF OIL FROM THE SURFACE OF WATER

GEORGE ANTONOFF

*Department of Chemistry, Fordham University, New York, New York**Received March 12, 1943*

When two immiscible liquids are placed in contact with one another, the lighter liquid will not spread and float in the form of a lens on the heavier liquid if its surface tension is substantially higher than that of the lower liquid, for example, in the case of a drop of water on carbon tetrachloride. If, however, a drop of oil is placed on the surface of water, the oil in most cases will spread on the surface of the water and form such a thin layer that its removal will be difficult. This takes place because the oil has a lower surface tension than water. This problem gains in importance at the present time in view of the fact that enormous amounts of oil are being spilled on the surface of the seas. Pollution of water in harbors is quite a problem in itself.

Considerations such as the above show that oil could be easily collected if it were possible to increase its surface tension substantially. Such a possibility suggests itself as a result of observations on the behavior of powders in a medium brought into a state of rotation. Thus, if one rotates a saturated solution of ammonium chloride in which some finely divided ammonium chloride is distributed, the latter concentrates itself into a planetary body¹. This can be done in a cylindrical glass vessel, in which the liquid is stirred by circular movements of a glass rod. It is thus obvious that, as a result of rotation, an attractive force has been generated which caused the collection of suspended matter into a planetary system. Similar effects have been observed with finely divided carbons suspended in liquids.

A similar experiment has been performed with water and oil spread over its surface in the form of a thin layer (see figure 1). In this case, the experiment was done in a large basin. The stirrer, driven electrically, was inserted into it; the speed was controlled by means of a slide rheostat. The blades of the stirrer were bent so as to give a gentle pull inward.

At moderate stirring speed the oil collected around the axis in the form of a planetary body. Increase in speed at first favored the formation of the planetary body, but afterwards the sphere began to flatten out and showed a tendency to form a Saturnian ring. However, the condition not being ideal, further increase in the speed of rotation resulted in the formation of moons, and finally the system disintegrated.

Thus it is seen that rotation causes such an increase of the inward pressure and surface tension that the oil which normally spreads on the surface of the water will organize itself into a planetary body. In such cases, the oil can be sucked off by means of a pipet, as is shown in figure 1.

¹ The body will become spherical if the specific gravity of the solution is not much different from that of the solid. This can be attained by adding, say, zinc chloride to the solution.

This experiment has been carried out also with a variety of light oils and particularly with gasoline used for driving motors.

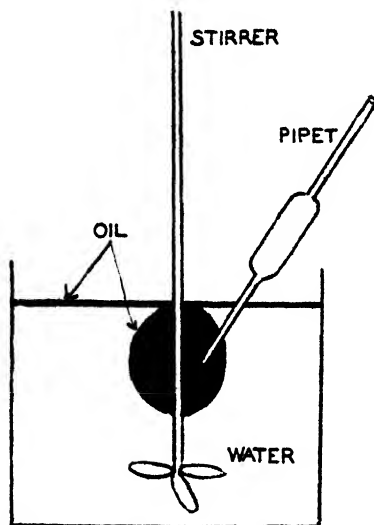


FIG. 1

The author had difficulty in explaining the observed phenomenon. He therefore approached Professor A. Einstein, who was kind enough to explain that no special hypothesis is needed, because the whole phenomenon can be attributed to currents created within the liquid.

THE SYSTEM MAGNESIUM SELENATE-SELENIC ACID-WATER AT 30°C.

H. FURUKAWA¹ AND G. BROOKS KING

Department of Chemistry, State College of Washington, Pullman, Washington

Received March 18, 1944

Continuing the study of ternary systems of the type selenate-selenic acid-water (3), the authors have determined the solubility relations in the system magnesium selenate-selenic acid-water at 30°C. Several hydrates of magnesium selenate have been reported (6), but as far as the authors are aware, no solubility determinations of magnesium selenate in selenic acid solutions have been made and no acid selenates of magnesium have been reported.

¹ This paper is an abstract of a thesis presented by H. Furukawa in partial fulfillment of the requirements for the degree of Master of Science at the State College of Washington.

EXPERIMENTAL

Preparation and purification of materials

Selenic acid² was prepared by a previously described method (1). Magnesium selenate was prepared by treating analytical reagent quality magnesium carbonate with a moderately concentrated selenic acid solution, filtering, concentrating, and recrystallizing the salt twice. The recrystallized salt proved to be the hexahydrate, as evidenced by analyses which showed a deviation of not more than 0.1 per cent from the theoretical composition of this hydrate.

Apparatus and method of procedure

Magnesium selenate hexahydrate was dissolved in solutions of selenic acid of various concentrations at an elevated temperature, and the solutions were then cooled to 30°C. On the basis of preliminary experiments, the proportions of components were so regulated as to cause the formation of a considerable excess of solid phase when the solution was cooled to 30°C. A temperature of 30°C. $\pm 0.05^\circ$, as measured by a calibrated thermometer, was maintained with a large electrically controlled water thermostat. In most cases the stable solid phase in equilibrium with the saturated solution separated spontaneously, but in some instances it was necessary to seed the solution with the expected phase. The mixtures were agitated frequently, and, in the lower acid concentrations, equilibrium was attained in from 48 to 72 hr. Solutions of higher acid concentrations required longer periods of time to reach equilibrium.

For equilibrium mixtures in which the solutions contained more than 60 per cent selenic acid, additional samples were prepared, using the indirect analysis method of Hill and Miller (2). Calculated quantities of selenic acid and magnesium selenate hexahydrate of known composition were weighed into test tubes and stirred with a mercury-sealed glass stirrer for several days in the thermostat. The solutions were analyzed for selenic acid and magnesium.

Methods of analysis

From equilibrium mixtures containing less than about 50 per cent selenic acid, samples of the solutions were withdrawn by means of a pipet, transferred to weighing bottles, and weighed. The solid phase was drained of excess solution and weighed in weighing bottles. Solutions which contained acid concentrations in excess of 50 per cent were very viscous, and separation of the solid phase from the solution was a difficult operation. It was found necessary to employ a sintered-glass filter and reduced pressure in order to effect the separation. During the filtration the temperature was maintained at 30°C. by surrounding the tube containing the equilibrium system with a water bath.

The weighed portions of solids and solutions were dissolved in small amounts of distilled water and diluted to 100 ml. Aliquots were taken for analyses for magnesium selenate and selenic acid. Magnesium selenate was determined by precipitation as magnesium ammonium phosphate and subsequent ignition to the

² The hydrogen peroxide used in the preparation of the selenic acid was furnished by E. I. du Pont de Nemours and Company. This kindness is gratefully acknowledged.

pyrophosphate. Selenic acid was determined by titration with standard alkali, using *p*-nitrophenol as indicator. Water was determined by difference.

TABLE 1
The system $\text{MgSeO}_4\text{-H}_2\text{SeO}_4\text{-H}_2\text{O}$ at 30°C .

SOLUTION		RESIDUE		SOLID PHASE
MgSeO_4	H_2SeO_4	MgSeO_4	H_2SeO_4	
weight per cent	weight per cent	weight per cent	weight per cent	
36.60*	0.0			$\text{MgSeO}_4 \cdot 6\text{H}_2\text{O}$
34.02	4.61	52.62	1.53	
28.33	14.65	46.50	6.53	
23.78	24.85	43.85	11.54	
22.94	29.20	47.42	10.36	
22.57	34.55	45.95	13.44	$\text{MgSeO}_4 \cdot 6\text{H}_2\text{O} + \text{MgSeO}_4 \cdot 4\text{H}_2\text{O}$
22.86	35.40	54.02	11.57	
23.10	35.60	49.55	13.40	
Av. = 22.98	35.50			$\text{MgSeO}_4 \cdot 4\text{H}_2\text{O}$
23.01	37.77	48.72	17.10	
22.93	39.22	49.80	17.11	
22.60	41.30	56.70	11.02	
22.63	41.87	39.96	26.04	
22.22	43.08	42.10	28.86	$\text{MgSeO}_4 \cdot 4\text{H}_2\text{O} + \text{MgSeO}_4 \cdot \text{H}_2\text{SeO}_4 \cdot 6\text{H}_2\text{O}$
22.28	43.06	39.61	29.39	
22.16	43.10	53.43	18.23	
Av. = 22.22	43.08			$\text{MgSeO}_4 \cdot \text{H}_2\text{SeO}_4 \cdot 6\text{H}_2\text{O}$
21.09	44.32	38.36	35.21	
17.50	48.99	37.32	36.44	
16.06	50.90	35.29	37.89	
15.13	52.63	40.03	34.51	
12.68	56.86	43.36	32.10	$\text{MgSeO}_4 \cdot \text{H}_2\text{SeO}_4 \cdot 6\text{H}_2\text{O} + \text{MgSeO}_4$
12.68	56.73	43.40	33.48	
12.62	56.77	41.95	34.57	
Av. = 12.66	56.79			MgSeO_4
10.10	59.60			
7.28†	63.47			
3.24†	70.29			
1.98†	74.09			
1.68	76.11			
1.28	77.69			

* From data of Lawrence and King: J. Am. Chem. Soc. **60**, 1987 (1938).

† Determinations made by indirect method.

RESULTS AND CONCLUSIONS

The compositions of the solutions and residues are recorded in table 1 and plotted graphically in figure 1. Except in the cases of the samples made up for the indirect determination of the solid phase, the compositions of the solid phases in equilibrium with the solutions were determined graphically by the method of Schreinemakers (7).

Four solid phases were found to exist in equilibrium with solutions of selenic acid at 30°C. From 0 to 35.50 per cent selenic acid the stable phase is magnesium selenate hexahydrate. This phase separates as medium thick, granular crystals. Between 35.50 per cent and 43.09 per cent selenic acid, the solid phase in equilibrium with the solution is magnesium selenate tetrahydrate. This phase is composed of fine long needles. While it sometimes crystallized spontaneously, it was usually necessary to seed the solution with the expected phase. Both

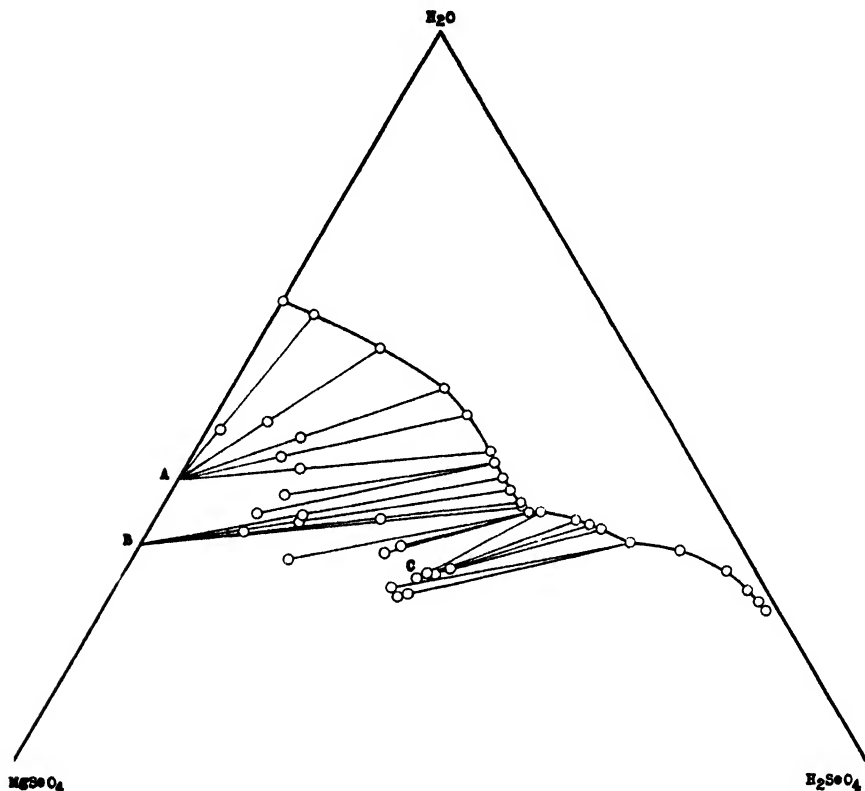


FIG. 1. Solubility relationships in the system $\text{MgSeO}_4\text{-H}_2\text{SeO}_4\text{-H}_2\text{O}$ at 30°C. The compositions of the two hydrates are represented on the diagram by A and B. The composition of the acid salt is represented by C. A has the composition $\text{MgSeO}_4 \cdot 6\text{H}_2\text{O}$, B the composition $\text{MgSeO}_4 \cdot 4\text{H}_2\text{O}$, and C the composition $\text{MgSeO}_4 \cdot \text{H}_2\text{SeO}_4 \cdot 6\text{H}_2\text{O}$.

the hexahydrate and the tetrahydrate have been reported by Meyer and Aulich (6). The stable solid phase between 43.08 per cent and 56.79 per cent selenic acid is the hexahydrated acid salt, $\text{MgSeO}_4 \cdot \text{H}_2\text{SeO}_4 \cdot 6\text{H}_2\text{O}$. This solid separated in beautiful, large, well-defined plates. No reference to this compound was found in the literature. The solid phase in equilibrium with solutions of more than 56.79 per cent selenic acid is probably anhydrous magnesium selenate, although data obtained in this region were not sufficiently concordant to establish definitely the composition of the solid phase. That equilibrium condi-

tions had been obtained, however, is indicated by the concordance of data on the composition of the saturated solutions. Thus the difficulties of determination of the solid phase would appear to be mechanical in nature. Since most of the projections of the tie-lines center around the composition of the anhydrous salt, the presence of the latter compound is indicated. Preparation of both the monohydrate (6) and the anhydrous salt (4) has been reported. A number of factors influence the accuracy of solubility determinations in this region of high selenic acid concentration. Because the solutions were viscous and the solid phase finely divided, separation of the liquid and solid was accomplished only with difficulty. It was necessary to employ suction in separating the two, and this operation probably caused some evaporation of water. All residues obtained by filtration were very wet, causing the plots of the compositions of the wet solids to fall very close to the solubility curve, so that small errors were magnified considerably in the projection of the tie-lines.

Data obtained by using the indirect analysis method tended to support the belief that the anhydrous salt was the solid phase present in the high acid region, although the presence of a monohydrate was not precluded. In order that the equilibrium mixtures contain enough liquid to permit drawing off of samples for analyses without using prohibitive quantities of selenate and acid, it was necessary to make up the mixtures such that the compositions were located fairly close to the solubility curve. Thus this method did not give an appreciable increase in accuracy in projection of tie-lines over the method of wet residue analysis.

SUMMARY

1. Solubility relationships for the system magnesium selenate-selenic acid-water have been investigated at 30°C.

2. Four solid phases, $\text{MgSeO}_4 \cdot 6\text{H}_2\text{O}$, $\text{MgSeO}_4 \cdot 4\text{H}_2\text{O}$, $\text{MgSeO}_4 \cdot \text{H}_2\text{SeO}_3 \cdot 6\text{H}_2\text{O}$, and probably MgSeO_4 , are in equilibrium with solutions of selenic acid at this temperature.

REFERENCES

- (1) GILBERTSON AND KING: *J. Am. Chem. Soc.* **58**, 180 (1936).
- (2) HILL AND MILLER: *J. Am. Chem. Soc.* **49**, 3 (1927).
- (3) KING: *J. Phys. Chem.* **41**, 6 (1937).
- (4) KLEIN: *Ann. chim.* **14**, 263-317 (1940).
- (5) LAWRENCE AND KING: *J. Am. Chem. Soc.* **60**, 1987 (1938).
- (6) MEYER AND AULICH: *Z. anorg. allgem. Chem.* **172**, 321-43 (1928).
- (7) SCHREINEMAKERS: *Z. physik. Chem.* **11**, 76 (1893).

ADSORPTION ANALYSIS OF COLORLESS COMPOUNDS: METHOD
AND APPLICATION TO THE RESOLUTION OF STEARIC
AND OLEIC ACIDS

HERBERT J. DUTTON

*Western Regional Research Laboratory¹, Albany, California**Received February 26, 1944*

Methods (9, 12) that have been used to locate the bands of colorless compounds upon adsorption columns include the following: empirical sectioning of the column; use of colored indicators; observation of fluorescent bands in ultra-violet light; formation of colored products either before or after adsorption; the use of adsorbents that yield colored products. Another method of adsorption analysis consists of periodic analysis of the percolate by either chemical or physical methods.

The adsorption analysis method recently developed by Tiselius (10) is of the last type. In this method, a solution is passed through an adsorption column and the changes in composition of the percolate are followed by measurement of the rate of change of refractive index (dn/dv) with volume, by use of a Toepler-Schlieren optical system. The composition of the solution leaving the column varies in steps. Each step corresponds to the presence of an additional solute and is revealed by a peak in the dn/dv versus v curve. As Tiselius pointed out, this technique is not adapted to the preparation of pure compounds, since it does not permit development of the adsorption column (separation of bands of adsorbed solutes by the use of increasingly polar solvents). Because of the necessity of boundary formation within the optical cuvette, the method is reported (1, 11) to be not very satisfactory with organic solvents and very dilute solutions where difference in density is slight.

During the course of preparation of this manuscript, an abstract of an unavailable paper by Tiselius and Claesson (11) appeared. This paper reports the application of a "microinterferometer" to adsorption studies with lauric, palmitic, and myristic acids. The procedure apparently obviates many of the limitations of earlier technique.

This paper describes a modification of a highly sensitive differential refractometer by means of which periodic readings of refractive index can be made upon the percolate from adsorption columns. Examples show that the use of this instrument with adsorption columns permits preparative separations as well as qualitative analyses of colorless compounds.

APPARATUS

The refractometer used (figure 1) was adapted from the highly sensitive instrument described by Rau and Roseveare (8), which uses the differential prin-

¹ One of the four regional research laboratories operated by the Bureau of Agricultural and Industrial Chemistry, Agricultural Research Administration, U. S. Department of Agriculture.

ciple of Kettler (4), but differs from it in the following respects: The double slit used to form an interference pattern in the microscope eyepiece is omitted, since the line image of the narrow slit is found to be less confusing than the interference pattern. Monochromatic light (5461 \AA , mercury) rather than poly-

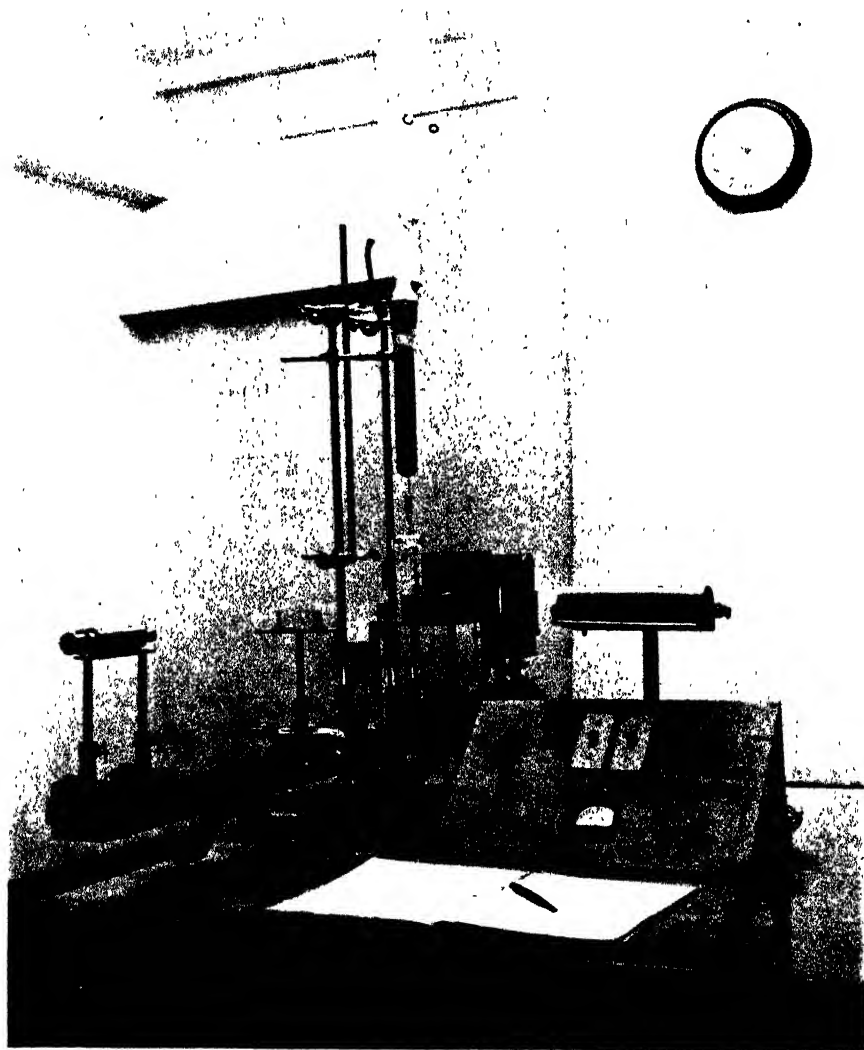


FIG. 1. Apparatus for the adsorption analysis of colorless compounds

chromatic (white) light is used. Since the present refractometer cell (figure 2) is designed for use with organic solvents, the joints are sealed with sodium silicate rather than sealing wax. To permit measurements during continuous flow, the solution prism (upper one) of the refractometer cell is equipped with inlet and outlet tubes and with temperature-control devices.

Preliminary measurements showed that if variations in refractive index of one unit in the sixth decimal place are to be significant, the temperature of the

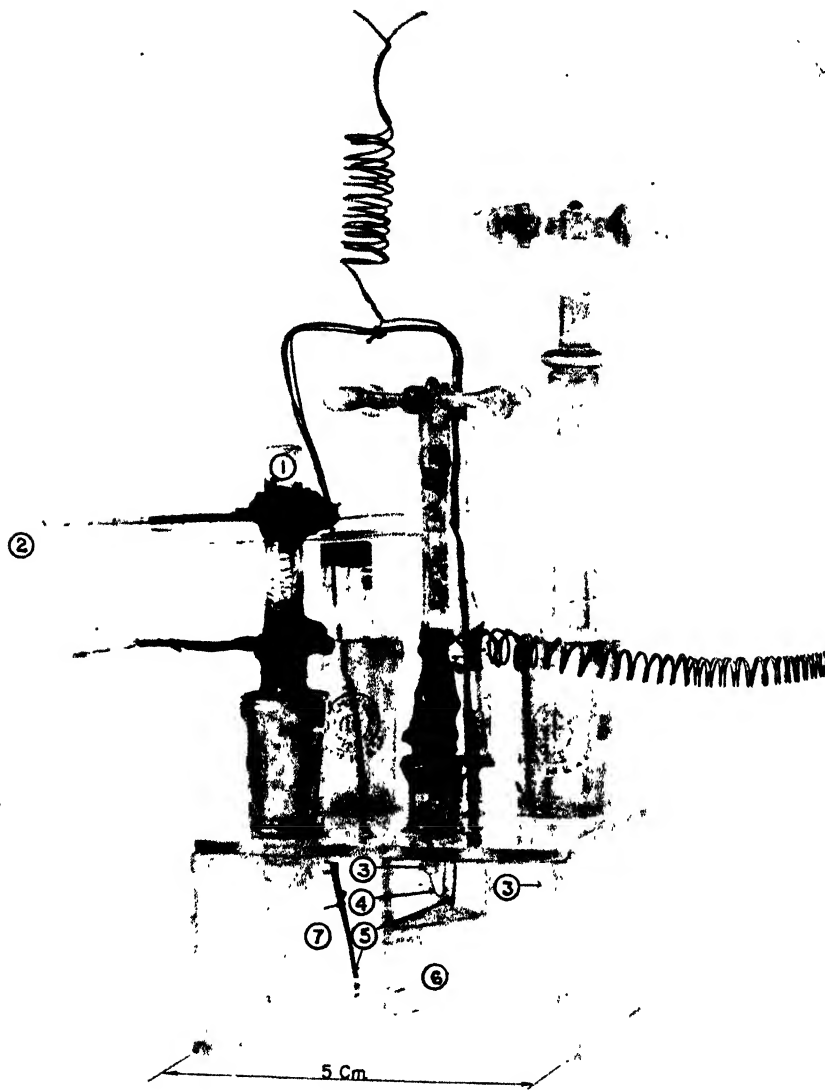


FIG. 2 Refractometer cell equipped with (1) entrance tube and continuous heater; (2) exit tube; (3) stirrers; (4) intermittent heater for upper solution prism; (5) thermocouple junctions; (6) lower prism, (7) outer cell.

liquid in the upper solution prism must not differ from that of the solvent in the lower prism and outer cell by more than 0.01°C .

It has been observed that solvent passing downward through the exit tube of the adsorption column exhibits a tendency to boil as a result of reduction of

pressure in the falling column of liquid. In order to counteract the consequent slight temperature drop in the liquid, a continuous heater was inserted in the entrance tube of the refractometer cell. The additional heat required is supplied by a small intermittent heater sealed into the upper prism and controlled by a differential three-junction thermocouple-galvanometer-photocell-relay system. One set of thermocouple junctions is located in the solvent which fills the lower prism and outer cell and the other set in the solution in the upper prism.

Air-driven stirrers (figure 2) are used to assure uniform temperatures throughout the inner prism and the outer cell compartments. The prism stirrer also serves to eliminate concentration gradients within the 5 ml. of solution contained by the prism.

EXPERIMENTAL RESULTS

The usefulness of the continuous-flow refractometer as a tool in adsorption analysis of colorless compounds was tested upon a mixture of oleic and stearic acids. Previous workers (3, 5, 6, 7) have reported varying degrees of success in separating this pair of acids by adsorption. It was necessary, however, in most of these earlier experiments, to cut the column to recover the acids rather than to elute them successively from the intact columns. In those experiments in which the fatty acids were eluted from the columns, only indications of enrichment of one component were obtained.

Detailed results of two experiments have been selected for presentation here. In each of the experiments, the adsorption column was prepared by packing 40 g. of Darco-G-60² thoroughly mixed with 40 g. of Hyflo Super Cel³ into a tube 3.3 cm. in diameter to form a column 19.5 cm. high. Unless otherwise noted all liquids were forced through the column with air under a pressure of 2 pounds per square inch.

In the first experiment, the steps in washing, adsorption, and development were accomplished by passing the following solvents and solutions through the column in the order listed: 75 ml. of Skellysolve B, 50 ml. of Skellysolve B containing 500 mg. each of oleic acid and stearic acid,⁴ 175 ml. of Skellysolve B, 550 ml. of 1 per cent amyl alcohol⁵ in Skellysolve B and 200 ml. of diethyl ether. The difference in index of refraction (Δn) of the liquid leaving the column and of Skellysolve B was observed at frequent intervals. The results are shown in figure 3a, in which the scale reading of the refractometer (which is directly proportional to Δn and hence also proportional to concentration in the case of a single dissolved solute) is plotted against the volume of percolate, v . The percolate was collected in five fractions, and the solvent was removed from each fraction by evaporation under reduced pressure. The melting point and iodine value of each residue were then

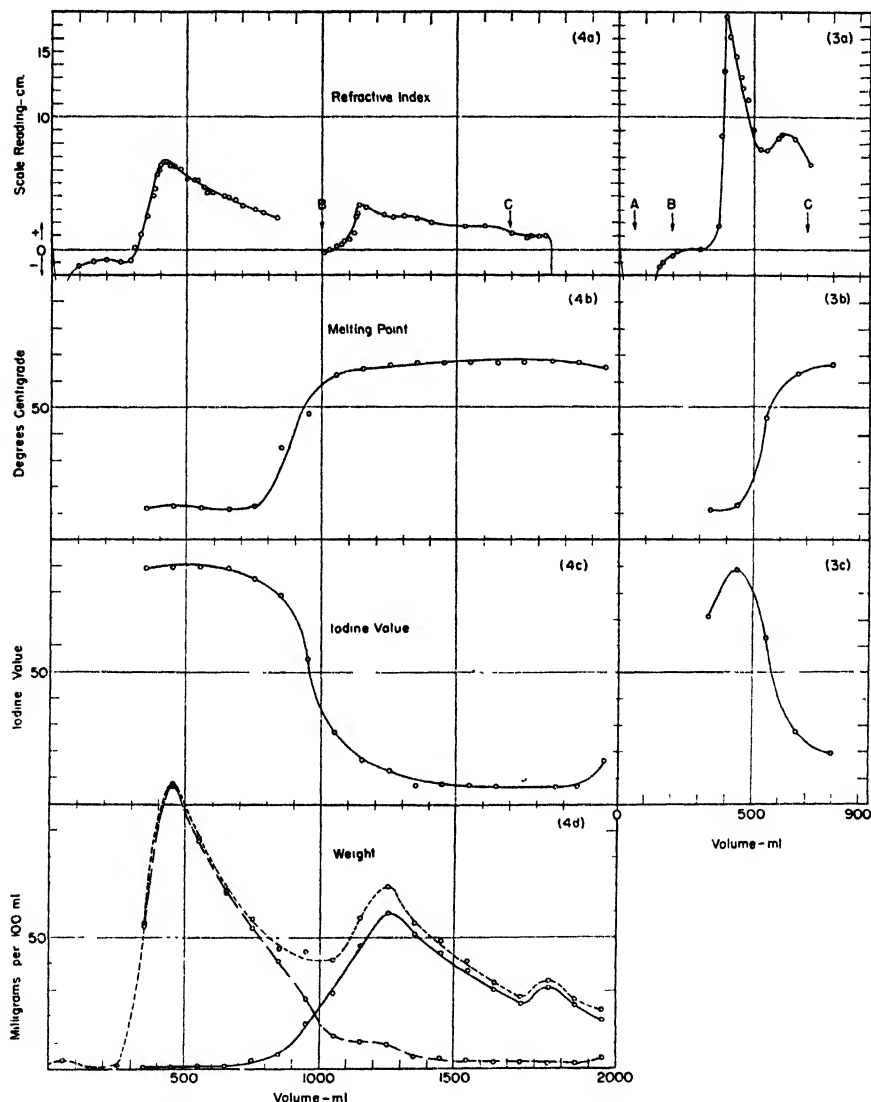
² The Darco-G-60 was obtained from the Darco Corporation, New York, New York.

³ The Hyflo Super Cel was obtained from the Johns-Manville Company.

⁴ The oleic acid, m.p. 12.8°C., was prepared by C. J. Gaiser of this laboratory. The stearic acid, m.p. 69°C. was obtained from the Eastman Kodak Company, Rochester, New York.

⁵ It was found that addition of up to 1 per cent of a 3:1 mixture of normal and tertiary amyl alcohols to Skellysolve B would not give a measurable change in refractive index.

determined and are plotted in figures 3b and 3c, respectively, against volume. Since the melting-point determinations were made upon the total residues contained in test tubes, the values given should be considered as approximate.



FIGS. 3 AND 4. Adsorption analyses of stearic and oleic acids. Letters indicate points of introduction of solvents and solutions upon the top of the column: A, Skellysolve B; B, 1 per cent amyl alcohol in Skellysolve B; C, diethyl ether.

In the second experiment the following sequence of solvents and solutions was used: 50 ml. of Skellysolve B containing 500 mg. each of stearic and oleic acid was poured on the dry column, followed by a developing solvent of 0.5 per cent

amyl alcohol in Skellysolve B. After a total of 840 ml. of liquid had been collected, the air pressure on the column was removed and the solvents allowed to percolate through the column overnight under gravity flow. On the following morning, when a total of 1000 ml. of percolate had been collected, the excess of the 0.5 per cent amyl alcohol solution was siphoned off and the development was continued with a 1 per cent solution of amyl alcohol in Skellysolve B. After a total of 1710 ml. of percolate had been collected, diethyl ether was passed through the column, giving a total volume collected of 2100 ml. The refractometer observations on the liquid leaving the column are shown in figure 4a. The percolate was collected in 100-ml. aliquots.⁶ Again each portion was analyzed as in the first experiment. The results are shown in table 1 and figure 4. The weight of oleic acid in each fraction was calculated from the iodine value and the weight of the residue; it was assumed that the residue contained only oleic and stearic acids. The weight of stearic acid was found by difference.

The recoveries of oleic and stearic acids from all fractions, calculated on the assumption mentioned above, were 99 per cent and 84.8 per cent, respectively, or a total recovery of fatty acids from the column of 91.9 per cent. Sixty-three per cent of the oleic acid originally placed on the column was recovered, with a purity of 99 per cent or more, in fractions 4 to 7. Stearic acid having a purity greater than 90 per cent, recovered in fractions 14 to 20, inclusive, represented 53 per cent of the stearic acid originally placed on the column. The greater purity of the oleic acid, the first solute eluted from the adsorption column, and its persistence in the subsequently eluted stearic acid is in accordance with experience in the chromatography of pigments and the prediction from theory (2). This limitation, inherent in adsorption analysis, may be partially circumvented by repeating the adsorption of the stearic acid fraction.

The refractive index *versus* volume curves for both experiments (figures 3a and 4a) show a great initial depression corresponding to the elution of a small amount of impurity of low refractive index which was originally present in the Darco-G-60. Subsequent to the elution of this impurity, the refractive index rises sharply to a maximum and then falls off more gradually, describing the course of elution of the oleic acid. In the case of the data of figure 3a, a second maximum due to the elution of stearic acid followed close upon the oleic acid maximum and is superimposed upon the oleic acid band. It is apparent from this curve that the use of 1 per cent amyl alcohol in Skellysolve B for developing the column resulted in an unsatisfactory separation of oleic and stearic acids. This conclusion is confirmed by the melting-point and iodine-value curves of figure 3.

In the second experiment, recorded in table 1 and figure 4, in which the column was first developed with 0.5 per cent amyl alcohol followed by 1 per cent amyl alcohol, the separation is considered satisfactory. The stearic acid began to appear during the overnight period when no readings of the refractive index were taken. In a similar experiment, a small maximum was observed during this

⁶ Since 160 ml. was collected overnight, the two 100-ml. aliquots between 800-900 ml. and 900-1000 ml. are in error because of partial mixing.

period. A discontinuity in the refractive-index curve (vertical displacement) occurred during the night and is probably due to some leakage or evaporation from the refractometer cell. The sharp rise in the refractive-index curve beginning at 1115 ml. (the pore volume of the charcoal being 115 ml.) is not to be considered as comparable to the stearic acid maxima of figure 3a, but rather indicates an increased rate of elution due to the increase in polarity of the developing

TABLE 1
Analyses of percolate fractions obtained in experiment 2

FRACTION NUMBER	WEIGHT OF MIXED ACIDS	MELTING POINT OF MIXED ACIDS	IODINE VALUE OF MIXED ACIDS (Wijs)	COMPOSITION OF MIXED ACIDS		WEIGHT OF OLEIC ACID	WEIGHT OF STEARIC ACID
				Oleic acid	Stearic acid		
	mg.	°C.		per cent	per cent	mg.	mg.
1	3.2						
2.	0.0						
3.	1.1						
4.	54.9	12	89.13	99.1	0.9	54.4	0.5
5.	107.6	13	89.65	99.7	0.3	107.3	0.3
6.	87.0	12	89.58	99.6	0.4	86.7	0.3
7.	67.2	12	88.98	99.0	1.0	66.5	0.7
8	56.9	13	84.88	94.4	5.6	53.7	3.2
9	45.8	34	78.67	87.5	12.5	40.1	5.7
10.	44.3	47	54.80	60.9	39.1	27.0	17.3
11.	41.1	62	27.36	30.4	69.6	12.5	28.6
12.	57.3	65	16.28	18.1	81.9	10.4	46.9
13.	68.9	66	12.79	14.2	85.8	9.8	59.1
14.	55.3	67	7.16	8.0	92.0	4.4	50.9
15.	48.3	67	7.94	8.8	91.2	4.3	44.0
16.	40.6	67	7.55	8.4	91.6	3.4	37.2
17.	32.6	67	7.05	7.8	92.2	2.6	30.0
18.	27.7	67	8.90	9.9	90.1	2.7	25.0
19.	33.4	68	6.89	7.7	92.3	2.6	30.8
20.	26.6	67	7.21	8.0	92.0	2.1	24.5
21.	23.0	66	16.67	18.5	81.5	4.3	18.7
Total weight..	919.6					495.9	423.7
Percentage recovery	92.0					99.2	84.7

solvent which was introduced after 1000 ml. of percolate had been collected. The sharp downward break occurring at 1825 ml. is due to the emergence of the diethyl ether, which has a refractive index much lower than that of Skellysolve B.

DISCUSSION

The method herein described for the adsorption analysis of colorless compounds appears to offer a distinct advantage over the previously published method utilizing the Toepler-Schlieren optical system. Development of the column has been accomplished by the method reported here. There is no restriction upon the size of

the adsorption column, and thus the present procedure is applicable to large-scale preparative as well as qualitative and quantitative analytical procedures. Furthermore, the observed readings from this system are directly proportional to the difference between the refractive indices of the solution and the solvent (Δn), and hence are proportional to the concentration where a single solute is involved. In the Toepler-Schlieren methods concentration is determined by measuring areas under the refractive-index gradient curve (dn/dv versus volume).

The differential refractometer method imposes certain restrictions upon the adsorption procedure. Thus it is necessary to choose solvents having refractive indices different from the refractive indices of the dissolved solutes. It is also desirable, if not essential, that solvents employed for development have the same refractive index as the solvent in the outer cell of the differential refractometer. It is probable that the restrictions just stated will also apply to the more recent "interferometric" method of Tiselius and Claesson (11).

The optics of our modified differential refractometer appear to be adapted to automatic photographic recording of refractive index versus volume. This feature and an improved method of temperature control have been incorporated in the design of apparatus now under construction.

SUMMARY

A method for the adsorption analysis of colorless compounds is described which employs a highly sensitive differential refractometer modified for measurement of changes in the refractive index of percolates from adsorption columns during continuous flow. The resolution of stearic and oleic acids has been studied as an example of the application of this general method. Advantages and limitations of the method are discussed.

The author is indebted to G. F. Bailey for assistance and helpful suggestions in the preliminary phases of this study; to W. L. Sylvester for technical assistance in the construction of the refractometer cell; and to G. R. Van Atta for assistance in the preparation of the manuscript.

REFERENCES

- (1) CLAESSON, S. T.: *Arkiv. Kemi. Mineral. Geol.* **15A**, 1 (1942).
- (2) DE VAULT, DON: *J. Am. Chem. Soc.* **65**, 532 (1943).
- (3) GRAF, M. M., AND SKAU, E. L.: *Ind. Eng. Chem., Anal. Ed.* **15**, 340 (1943).
- (4) *Handbuch der Physik*, Vol. XVIII, p. 675. Julius Springer, Berlin (1927).
- (5) KAUFMANN, H. P.: *Angew. Chem.* **53**, 98 (1940).
- (6) KONDO, H.: *J. Pharm. Soc. Japan* **57**, 218 (1937).
- (7) MANUNTO, C.: *Helv. Chim. Acta* **22**, 1156 (1939).
- (8) RAU, D., AND ROSEVEARE, W. E.: *Ind. Eng. Chem., Anal. Ed.* **8**, 72 (1936).
- (9) STRAIN, H. H.: *Chromatographic Adsorption Analysis*. Interscience Publishers, Inc., New York (1942).
- (10) TISELIUS, A.: In *Advances in Colloid Science* (edited by E. O. Kraemer), Vol. I. Interscience Publishers, Inc., New York (1942).
- (11) TISELIUS, A., AND CLAESSON, S. T.: *Arkiv. Kemi. Mineral. Geol.* **15B**, 1-6 (1942); *Chem. Zentr.* **1942**, I, 3123-4; *Chem. Abstracts* **38**, 35 (1944).
- (12) ZECHMEISTER, L., AND CHOLNOKY, L.: *Principles and Practice of Chromatography*. John Wiley and Sons, Inc., New York (1941).

PROTECTIVE COLLOIDS IN CANCER

L. A. MUNRO

The Hendry-Connell Research Foundation, Kingston, Ontario, Canada

Received February 24, 1944

Differences in the protective action of the colloids of spinal fluid in health and disease have been recognized and used for a long time in the Lange gold number technique.

In cancer the constituents of the blood serum differ from normal. F. L. Munro (19), working in these laboratories, obtained the values given below in a study of the sera of one hundred and thirty-five cancer patients:

Serum albumin	3.63 \pm 0.37 grams per cent
Serum globulin	2.52 \pm 0.32 grams per cent
A/G ratio	1.52 \pm 0.41 grams per cent
Total protein	6.41 \pm 0.39 grams per cent

For a group of thirty normals the values were:

Albumin	4.70 \pm 0.21 grams per cent
Globulin	2.45 \pm 0.30 grams per cent
A/G ratio	2.02 \pm 0.20 grams per cent
Total protein	7.04 \pm 0.26 grams per cent

These normal values, although from a relatively small group, are in agreement with the results of Streef and Streef-Spaan (26), who reported the following:

Albumin	4.66 grams per cent
Globulin	2.33 grams per cent
A/G ratio	2.0 grams per cent
Total protein	7.3 grams per cent

Furey (8), from a study of seventy-eight normals, gave slightly higher values: viz., 4.9, 2.4, 2.06, and 7.4 grams per cent, respectively. Gutman *et al.* (12) gave 5.2, 2.0, 2.60, and 7.2 grams per cent as mean values.

Several workers have also noted a decrease in the total protein in cancer serum (4, 5, 6, 7, 10, 14, 15, 18). There is considerable evidence that this lowering is chiefly due to a lower albumin (3, 6, 8, 9, 10, 11, 13, 15, 16, 17, 18, 23, 24, 25). The globulin values are practically unchanged, although some workers have reported an increase in globulin (15, 20). Obviously, if the albumin decreases and the globulin is unchanged or is higher, the A/G ratio will invariably be lower.

Marchal, Paturel, Guerin, and Guerin (18) reported that in hens inoculated with sarcomas a decrease in both albumin and globulin of from 25 to 40 per cent is obtained.

Rabb (21) found that the A/G ratio for carcinomatous dogs was only 0.74, whereas for normals the value was 1.11. Wladasch (27) gave 1.51–2.40 as the normal range,—the average being 1.9 grams per cent.

This marked difference between normals and cancerous individuals should be indicated in the protective action of the sera against the coagulation of a solution by an electrolyte. That such is the case will be seen from the following results.

EXPERIMENTAL

The test used in the experiments reported below is a modification of that used by Asai (1) in an attempt to detect the onset of malaria by such changes in the blood serum. The adaptation of this test was undertaken because the author was using Congo red in other work on the reticulo-endothelial system. Other solutions or dyes could doubtless be used.

To a mixture of 5 cc. of 0.1 per cent Congo red and 0.5 cc. of serum, Asai added 5 cc. of 0.3 per cent quinine hydrochloride. After 1 to 2 hr. at room temperature, the mixture was centrifuged and the supernatant liquid compared in a colorimeter with 0.025 per cent Congo red. The test was reported positive within 4 days of infection.

Various electrolytes, including other alkaloid sulfates and chlorides, have been tried in this laboratory, but so far the quinine hydrochloride seems to give better differentiation between the two groups. Tests are run using three different quantities of sera: 0.075, 0.10, and 0.15 ml. The serum is transferred to conical centrifuge tubes in duplicate with a micropipet. Five-milliliter portions of standard Congo red are then added and the mixture stirred well. Five milliliters of the electrolyte are pipetted into separate tubes. At zero minus 2 min. the electrolyte is dumped into the tube containing the largest amount of serum and mixed by pouring back and forth four times. This has been found to be better than shaking the tubes, probably owing to changes in concentration of serum induced by the frothing which occurs when the mixture is shaken. The tube containing the smallest amount of serum is mixed at zero time and the three tubes placed in a thermostat at 30°C. for 30 min. The three tubes are then centrifuged for 4 min., and the color in the supernatant is evaluated in a Klett photoelectric colorimeter from a standard curve for Congo red, using a green filter No. 59.

The results for seventy-eight cancer sera and for seventy normal sera are given in tables 1 and 2. In column two the values are given in gammas of Congo red per milliliter. In columns three and four the results are grouped to show extent of coagulation: 6+ indicates residual color from 0 to 25 γ ; 5+ from 25 to 50 γ ; 4+ from 50 to 100 γ ; 3+ from 100 to 200 γ ; 2+ from 200 to 350 γ ; 1+ from 350 to 450 γ ; \pm from 450 to 500 γ , the theoretical maximum. Since before flocculation there is an increase in absorption, although the mixture appears clear, such an increase in Klett reading without visible precipitate is denoted as "trace" or tr. If the value = 500, showing no coagulation, the reading is indicated by a minus sign. All sera were prepared from "fasting" bloods.

TABLE 1
Cancer patients

(1) PATIENT NO.	(2) RESIDUAL DYE (0.075 ML. SERUM) <i>γ per milliliter</i>	(3) DYE REMOVED (0.10 ML. SERUM)	(4) DYE REMOVED (0.15 ML. SERUM)
C 1.....	3.4	6+*	tr
C 2.....	26.	2+	tr
C 3.....	13.3	5+	++
C 4.....	5.6	5+	+++
C 5.....	9.0	6+	tr
C 6.....	4.3	6+	+
C 7.....	8.1	2+	tr
C 8.....	6.3	5+	tr
C 9.....	8.1	6+	tr
C 10.....	8.5	4+	+++
C 11.....	2.6	6+	tr
C 12.....	3.1	6+	tr
C 13.....	6.0	5+	tr
C 14.....	6.1	3+	tr
C 15.....	3.5	6+	tr
C 16.....	8.4	5+	tr
C 17.....	7.2	2+	tr
C 18.....	6.3	4+	tr
C 19.....	4.3	6+	++++
C 20.....	4.3	6+	+++++
C 21.....	6.0	6+	tr
C 22.....	7.2	5+	tr
C 23.....	6.7	6+	+++++
C 24.....	3.6	6+	++
C 25.....	6.1	6+	-
C 26.....	15.	2+	++
C 27.....	5.0	6+	+++++
C 28.....	7.8	6+	-
C 29.....	7.5	2+	+++
C 30.....	5.4	4+	++++
C 31.....	4.0	6+	tr
C 32.....	9.5	6+	tr
C 33.....	6.7	5+	tr
C 34.....	10.2	±	tr
C 35.....	7.3	5+	tr
C 36.....	6.0	5+	tr
C 37.....	7.1	6+	tr
C 38.....	11.4	3+	tr
C 39.....	8.2	5+	tr
C 40.....	10.3	3+	++
C 41.....	6.4	6+	tr
C 42.....	4.7	6+	tr
C 43.....	4.6	6+	tr
C 44.....	3.6	6+	tr
C 45.....	4.8	6+	tr
C 46.....	9.3	3+	tr
C 47.....	7.3	5+	+++++

TABLE 1—*Concluded*

(1) PATIENT NO.	(2) RESIDUAL DYE (0.075 ML. SERUM) <i>γ per milliliter</i>	(3) DYE REMOVED (0.10 ML. SERUM)	(4) DYE REMOVED (0.15 ML. SERUM)
C 48.....	4.7	6+	tr
C 49.....	6.3	5+	tr
C 50.....	9.0	3+	tr
C 51.....	10.7	5+	tr
C 52.....	23.0	3+	tr
C 53.....	9.3	5+	tr
C 54.....	17.5	tr	tr
C 55.....	11.6	6+	tr
C 56.....	16.5	6+	++
C 57.....	14.1	6+	+++
C 58.....	11.6	5+	tr
C 59.....	14.0	4+	tr
C 60.....	10.0	6+	±
C 61.....	12.0	5+	tr
C 62.....	4.6	6+	++++
C 63.....	34.	±	tr
C 64.....	14.2	5+	+++
C 65.....	7.4	6+	+++
C 66.....	24.0	4+	tr
C 67.....	14.2	3+	tr
C 68.....	22.2	3+	tr
C 69.....	8.3	6+	tr
C 70.....	11.5	4+	tr
C 71.....	6.0	6+	+++
C 72.....	9.0	5+	tr
C 73.....	12.2	6+	++++
C 74.....	7.5	6+	+++++
C 75.....	10.5	6+	+++++
C 76.....	7.3	6+	+++
C 77.....	10.7	6+	++
C 78.....	11.9	6+	+++

* The significance of the notations used is given below:

NOTATION	γ PER MILLILITER	NOTATION	γ PER MILLILITER
6+	0-25	+	350-450
5+	25-50	±	450-500
4+	50-100	tr	Apparent 500
3+	100-200	—	Original
2+	200-350		

DISCUSSION

The results show that the protective colloids in normal serum are much more effective than in the serum of cancerous individuals. This will be seen from the

averages and from the distribution curves for the first and second tubes (table 4; figures 1 and 2). For the 30-min. incubation, the 0.15 ml. of serum affords protection in all but some of the cancer sera.

TABLE 2
Normal patients

SERUM NO.	SERUM AMOUNTS			SERUM NO.	SERUM AMOUNTS		
	0.075 ml.	0.10 ml.	0.15 ml.		0.075 ml.	0.10 ml.	0.15 ml.
N 1	22 γ	tr		N 36.	18	tr	—
N 2	27	+	tr	N 37.	23	tr	—
N 3.	15	4+	—	N 38.	10	tr	tr
N 4	28	4+	—	N 39.	34	—	—
N 5	48	tr	—	N 40.	30	tr	—
N 6	79	tr	—	N 41.	10	4+	—
N 7.	39	tr	—	N 42.	36	tr	—
N 8.	18	4+	tr	N 43.	24	tr	—
N 9	26	\pm	—	N 44.	31	tr	—
N 10.	17	4+	—	N 45.	31	tr	—
N 11.	41	tr	—	N 46.	26	tr	—
N 12.	15	5+	tr	N 47.	53	tr	—
N 13.	17	tr	—	N 48.	17	tr	—
N 14.	48	tr	—	N 49.	18	tr	—
N 15.	25	2+	tr	N 50.	28	4+	tr
N 16.	22	tr	—	N 51.	56	3+	tr
N 17.	16	6+	tr	N 52.	19	3+	tr
N 18.	15	tr	—	N 53.	68	2+	—
N 19.	82	tr	—	N 54.	26	3+	\pm
N 20.	142	tr	—	N 55.	79	tr	tr
N 21.	33	tr	—	N 56.	20	3+	tr
N 22.	26	tr	—	N 57.	85	tr	tr
N 23.	40	tr	—	N 58.	43	3+	—
N 24.	26	tr	—	N 59.	22	tr	tr
N 25.	37	\pm	—	N 60.	59	2+	tr
N 26.	18	tr	—	N 61.	200	tr	tr
N 27.	10	tr	—	N 62.	140	2+	—
N 28.	80	tr	tr	N 63.	38	tr	—
N 29.	41	+	tr	N 64.	50	tr	—
N 30.	15	tr	tr	N 65.	34	2+	tr
N 31.	24	tr	—	N 66.	40	4+	tr
N 32.	33	tr	—	N 67.	38	4+	—
N 33.	29	tr	—	N 68.	51	\pm	tr
N 34.	31	tr	—	N 69.	49	tr	tr
N 35.	26	tr	—	N 70.	120	tr	tr

An examination of the data for the 0.075 ml. of serum in table 3 shows that the differences between the amounts of residual dye are significant. The difference between means for the cancer patients and group A of the normals is over seven times the standard error, and the difference in the case of group B of the normals is over ten times the standard error.

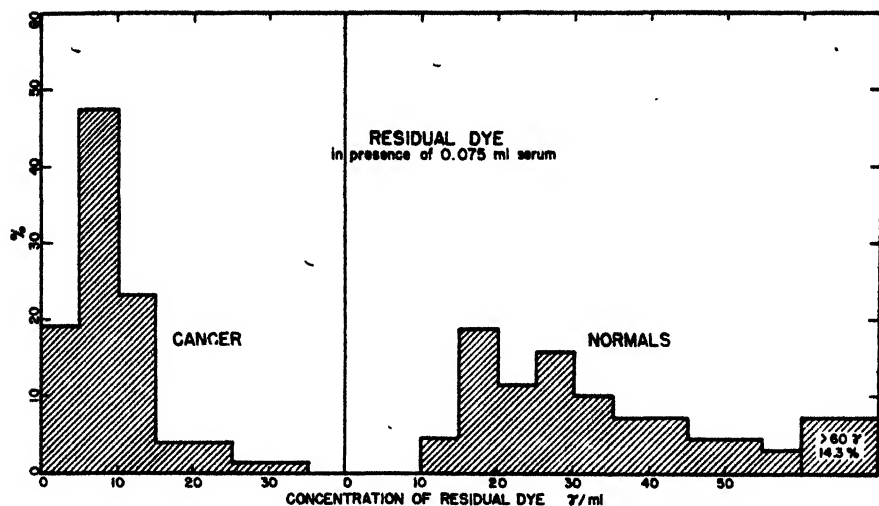


FIG. 1. Distribution curves for residual dye after 30 min. incubation with electrolyte at 30°C. in the presence of 0.075 ml. of serum.

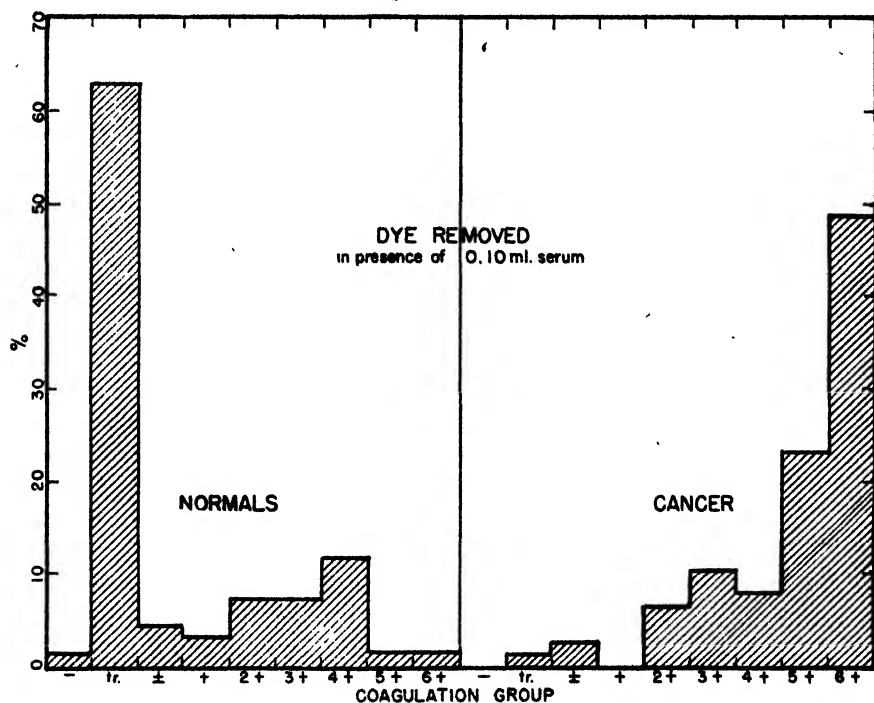


FIG. 2. Distribution curves showing percentage of cases in the different coagulation groups in the presence of 0.10 ml. of serum.

Figure 1 gives the distribution of data in the first column of each half of table 4 arranged in groups differing in concentration of residual color by 5 γ per milliliter. It will be noted that 89.6 per cent of the cancer patients have values less

TABLE 3
Statistical significance of data

	CANCER PATIENTS	NORMALS	
		A	B*
Number of cases.....	78	70	66
Mean.....	9.26	40.52	33.86
Standard deviation.....	5.54	33.19	18.35
Standard error of mean.....	0.63	3.96	2.26
Standard error of the difference between means: (1) cancer and normals A 4.01			
(2) cancer and normals B 2.35			
Difference between means: (3) cancer and normals A 31.26			
(4) cancer and normals B 24.00			

* Omitting the four high values.

TABLE 4
Distribution of cases in the different coagulation groups

CANCER PATIENTS						NORMALS					
0.075 ml. of serum			0.10 ml. of serum			0.075 ml. of serum			0.10 ml. of serum		
Residual dye, γ per milli- liter	Number (78)	Per cent of total	Dye re- moved	Number (78)	Per cent of total	Residual dye, γ per milli- liter	Number (70)	Per cent of total	Dye re- moved	Number (70)	Per cent of total
<5	15	19.2									
<10	37	47.4	6+	38	48.7	<10	0	0.0	6+	1	1.4
<15	18	23.1	5+	18	23.1	<15	3	4.3	5+	1	1.4
<20	3	3.8	4+	6	7.7	<20	13	18.6	4+	8	11.6
<25	3	3.8	3+	8	10.2	<25	8	11.4	3+	5	7.0
<30	1	1.3	2+	5	6.4	<30	11	15.7	2+	5	7.0
<35	1	1.3	+	0	0.0	<35	7	10.0	+	2	2.9
>35	0	0	\pm	2	2.5	<40	5	7.1	\pm	3	4.3
			tr	1	1.3	<45	5	7.1	tr	44	63.0
			—	0	0.0	<50	3	4.3	—	1	1.4
						<55	3	4.3			
						<60	2	3.0			
						>60	10	14.3			
Total...	78	99.9		78	99.9	Total...	70	100.1		70	100.1

than 15 γ per milliliter. Only 4.3 per cent of the normals gave values below this figure.

The plot of residual color in the second tube shows that 63 per cent of the normals gave only the initial increase in opacity and only two, or 3.1 per cent,

gave 5+ and 6+ coagulation. In the cancer group the corresponding figures are 1 and 72 per cent, respectively.

Robinson (22) reported that low albumin and total protein are often found in patients with cardiac edema, pernicious anemia, chronic nephritis, gastric enteritis, and pertussis as well as cancer. To this must be added malaria, active tuberculosis, and active asthma (2). However, in the absence of these diseases, which can be eliminated, the protective colloid test may be of service in diagnosis or in following the patient's clinical progress. In one case (Miss R. O'C.) where cancer was suspected, a "P. C." blood test was made, giving values of 9 γ for the first tube and 4+ for the second tube. An operation was subsequently performed and the biopsy showed malignancy. In another case (Mrs. D.) where cancer was suspected, a value well up in the normal range was obtained. Biopsy proof showed a benign cyst.

While the average total protein and albumin are lower for cancer patients than for normals, the A/G ratio is more consistent. An examination of this ratio on some sixty of the above cancer patients shows that there is only a very rough agreement between the A/G ratio and the protective colloid index.

The protective action indicates more than changes in amounts of the above serum constituents. Induced qualitative variations in the state of aggregation or even in molecular species may possibly occur, owing to differences in protein metabolism.

Further experiments are in progress to adapt this test to micro amounts of serum (0.02 cc.) and to substitute another coagulant for the quinine hydrochloride.

SUMMARY

The protective colloids of seventy-eight cancer sera have been compared with normal sera from seventy individuals. The addition of 0.075 ml. of serum is made to 5 ml. of Congo red and after addition of the coagulating electrolyte and incubation at 30°C. for 30 min., the residual color is determined in a photoelectric colorimeter. Average values of 9.26 and 40.52 γ per milliliter, respectively, were obtained, 89.6 per cent of the cancer patients and 4.3 per cent of normals giving values below 15 γ per milliliter. The A/G ratio shows a rather poor parallel to the protective colloid (P.C.) index. It is suggested that other factors such as molecular dispersity and even molecular species are more important.

The author wishes to acknowledge his debt to Dr. W. C. Kruger of the Toronto Western Hospital and members of his staff for the major number of the cancerous bloods; to Agnes Medley, B.A., who carried out the protein analysis; and to Gwendolyn Daw, B.A., for technical assistance. The work was made possible by a grant from the Province of Ontario through the Department of Health.

REFERENCES

- (1) ASAI, M.: J. Med. Assoc. Formosa **40**, 45-54; Chem. Abstracts **36**, 5541 (1942).
- (2) AUBRY, THRODET, AND RIBÈRE: Compt. rend. soc. biol. **123**, 327-8 (1936).
- (3) BAUER, R.: Wien. med. Wochschr. **81**, 855 (1931).

- (4) BOWMAN, R. O., PITTS, H. C., MICHELL, P. H., AND ERWETZ, E.: *Can. Med. Assoc. J.* **34**, 527-32 (1936).
- (5) BUGNARD, L., COLOMBIES, F. H., MILELSKY, O., AND BOURSIAIC, P.: *Bull. assoc. franç. étude cancer* **20**, 596-600 (1931).
- (6) CODOUNIS, A.: *Paris Med.* **1**, 457 (1932).
- (7) EYTON, W. G., AND ROSE, A. R.: *J. Am. Med. Assoc.* **99**, 1236-9 (1932).
- (8) FUREY, E. D.: *Proc. Staff Meetings Mayb Clinic* **13**, 730-2 (1938); *Chem. Abstracts* **33**, 8734 (1939).
- (9) GREENBERG, D. M.: *J. Biol. Chem.* **82**, 545-50 (1929).
- (10) GUNTHER, R., AND GREENBERG, D. M.: *Arch. Intern. Med.* **46**, 67-71 (1930).
- (11) GUTHMANN, H.: *Arch. Gynäkol.* **132**, 148 (1927).
- (12) GUTMAN, A. E., MOORE, D. H., GUTMAN, E. B., MCCLELLAN, V., AND KABAT, E. A.: *J. Clin. Investigation* **20**, 765-83 (1941).
- (13) KAHN, H.: *Klin. Wochschr.* **3**, 920 (1924); **4**, 178 (1925).
- (14) KENNAWAY, E. L.: *Quart. J. Med.* **17**, 302-11 (1924).
- (15) LEITNER, M.: *Magyar Biol. Kutatóintézet Munkái* **10**, 307-13 (1938); *Chem. Abstracts* **33**, 5058 (1939).
- (16) LEOPER, M., FORRESTIER, J., AND TONNET, J.: *Presse méd.* **29**, 333 (1921).
- (17) LEOPER, M., AND TONNET, J.: *Compt. rend. soc. biol.* **83**, 1032 (1920); **83**, 1139 (1920).
- (18) MARCHAL, S., PATUREL, L., GUERIN, M., AND GUERIN, P.: *Compt. rend. soc. biol.* **131**, 213-16 (1939).
- (19) MUNRO, F. L.: *Bulletin, Hendry-Connell Research Foundation* **III**, 15-25 (1938).
- (20) PURJESZ, B.: *Z. Krebsforsch.* **44**, 1-11 (1936).
- (21) RABB, W.: *Z. ges. exptl. Med.* **97**, 588-609 (1936).
- (22) ROBINSON, H. W.: *J. Med.* **19**, 491-8 (1930).
- (23) RUSZNYAK, S., BARAT, I., AND KURTHY, I.: *Z. klin. Med.* **96**, 337 (1924).
- (24) SCHNEIDER, E., AND ACHELIS, H.: *Klin. Wochschr.* **7**, 1955-8 (1928).
- (25) STARLINGER, W., AND WINANDS, E.: *Z. ges. exptl. med.* **60**, 138, 260, 288, 308 (1938).
- (26) STREEF, G. M., AND STREEF-SPAAN, A. M.: *Acta Brevia Neerland. Physiol. Pharmacol. Microbiol.* **8**, 203 (1938); *Chem. Abstracts* **33**, 1374 (1939).
- (27) WLADASCH, A.: *Biochem. Z.* **287**, 337-41 (1936).

CLUSTER FORMATION AND PHASE TRANSITIONS IN THE ADSORBED STATE

HANS M. CASSEL

1126 East 46th Street, Chicago 15, Illinois

Received March 8, 1944

I. INSUFFICIENCY OF CURRENT MULTILAYER THEORIES

It is well known that in Langmuir's derivation of an isotherm for molecules adsorbed from the gas phase on a plane crystalline surface the interaction of neighboring adatoms is neglected. Consequently, the equation of state of the monolayer corresponds to that of a compressed gas above its critical point. As this holds no matter what the magnitude of the adsorption energy, the question naturally arises: How can extensions of the simple Langmuir mechanism to the treatment of multilayers in the adsorption of vapors account for the final liquefaction of the adsorbates?

Let us combine the (A form of the) Emmett-Brunauer-Teller (4) adsorption isotherm:

$$\Gamma = \Gamma_m c p / (P - p)(P + (c - 1)p)$$

where Γ designates the surface density, Γ_m that of the complete monolayer, p the equilibrium pressure of the adsorbate, and P the saturation pressure of the adsorbate, with Gibbs's equation:

$$-d\sigma = \Gamma R T dp/p$$

where σ designates the sum of the interfacial tension of the adsorbent, as resulting from the presence of the adsorbate, and the surface tension of the multilayer.

By eliminating the surface density, Γ , and integrating over the pressure range from 0 to p , the reduction in surface tension due to adsorption is obtained:

$$F = \sigma_0 - \sigma = \Gamma_m R T \log \frac{P + (c - 1)p}{P - p}$$

In other words, with increasing number of layers the film pressure increases continuously so that the surface tension of the finally built up, presumably liquid layer would become negative and even infinitely so.

This failure is undoubtedly due to the disregard of lateral cohesion forces in the design of the film model.

II. COHESION FORCES IN MONOLAYERS

In the transition from the adsorbed gaseous state to greater surface densities and to the liquid phase in bulk, generally, a discontinuity of the same kind has to be passed as is characteristic of condensation processes in volume phases. The liquid mass may be in equilibrium with a gaseous, an expanded, or a condensed monolayer or, as will be discussed later, with a multilayer. These possibilities are apparently correlated with differences in the wetting angle at the gas-liquid-film boundary.

At any event, without the interaction of neighboring adatoms there are no phase changes. This was early recognized by Frenkel (11), who contemplated double-molecule formation as the first step towards two-dimensional condensation. As the adsorption energy of a cluster-bound adatom increases with the number of closest neighbors, the surface density of polymerized molecules may become many times larger than that of single adatoms. In fact, examples of this nature have been observed in the adsorption of dipole molecules on liquid mercury (7). The adsorption isotherms of the lower alcohols, nitromethane, and water at 50°C. cannot be interpreted but as being indicative of a pronounced polymerization in the adsorbed state—ethyl alcohol forming double molecules, methyl alcohol and nitromethane quadruple molecules, and water probably larger aggregates.

In these instances, even at fairly low pressures, the surface density of single

adatoms is practically negligible and Langmuir's equation is not even approximately correct, i.e., the film-gas equilibrium is not governed by Henry's law

$$\Gamma = kp$$

(line *H* in figure 1), which is the very foundation of Langmuir's isotherm (curve *L*). Instead, the isotherms osculate the pressure axis (curve *N*) to an order which is higher the higher the degree of polymerization, ν ; i.e., the law of distribution is that of Nernst.

$$\Gamma = Kp^\nu$$

This dipole effect in the adsorbed state is in perfect analogy to the behavior of the same class of substances in solutions of non-polar solvents where the association manifests itself in a depolarization (18).

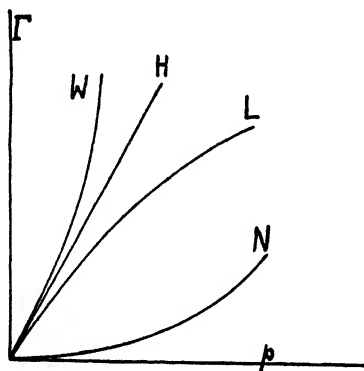


FIG. 1. Low pressure range isotherm types; H, Henry; L, Langmuir; W, van der Waals; N, Nernst.

In noticing deviations from the Langmuir isotherm it was Frumkin (12) who first suggested a van der Waals type equation of the adsorbed state for monolayers formed on water from solutions of fatty acids. As to the adsorption of gas molecules on crystalline surfaces, Fowler (10), Peierls (17), and Band (1) arrived at similar conclusions on the basis of a statistical-mechanical treatment of two-dimensional cluster formation.

If we write the two-dimensional van der Waals equation:

$$F + \frac{\alpha}{A^2} = RT/(A - B) \quad \text{or} \quad F = \frac{RT\Gamma}{1 - \beta\Gamma} - \alpha\Gamma^2$$

we can eliminate $-d\sigma = dF$ in Gibbs's equation and obtain by integration what may be called a "van der Waals adsorption isotherm" in the true sense of the word:

$$p = \frac{K\Gamma}{1 - \beta\Gamma} e^{1/(1-\beta\Gamma)} \cdot e^{2-\alpha\Gamma/RT}$$

Here the first factor on the right-hand side agrees with Langmuir's isotherm, and the second factor accentuates the concave curvature against the pressure axis, while the third factor, representing the effect of the internal film energy, acts in the opposite direction, i.e., the van der Waals isotherm (curve *W* in figure 1) differs from the ordinary Freundlich-Langmuir type (curve *L*) by a partial although sometimes only slight convexity against the pressure axis, depending on the predominance of the attraction over the repulsion forces between adatoms.

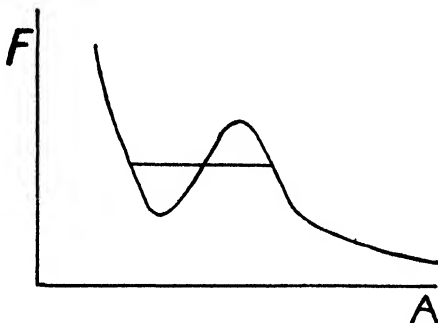


FIG. 2. van der Waals phase transition

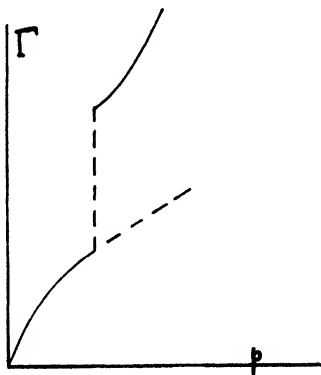


FIG. 3. Adsorption isotherm showing discontinuity corresponding to van der Waals loop.

Since the irregularities of solid surfaces in general prevent an unambiguous interpretation of adsorption measurements, some examples of adsorption isotherms obtained on mercury may be quoted. Here the heavier rare gases (6) represent the simple Henry-Langmuir type, while hexane, cyclohexane, benzene (7), and carbon tetrachloride exemplify the Henry-van der Waals type.

It is obvious that the van der Waals loop in the F - A diagram (figure 2) has its counterpart in the adsorption isotherm (figure 3). However, except for the adsorption of metal vapors (15), no example of a "mono-mono" discon-

tinuity on solids seems to have been established with certainty. Nevertheless, the possibility remains that phase transitions of the first order occur at higher than monomolecular surface densities. The van der Waals loop, in this case, would simply be shifted to smaller A values in the F - A diagram.

If a van der Waals equation of state with constants α and β holds for the monolayer, while the constants of the coexisting volume phase are a and b , the critical temperature for the monolayer discontinuity is:

$$\theta_{\text{ads.}} = \theta_{\text{vol.}} \frac{\alpha \cdot b}{a \cdot \beta}$$

Under the simple assumptions implied in the derivation of the van der Waals equation this expression can be evaluated provided the potential, $u(r)$, between two molecules is known (16). When the potential decreases with the m^{th} power of the distance, one easily obtains:

$$\theta_{\text{ads.}} = \theta_{\text{vol.}} \cdot \frac{2}{3} \frac{m-3}{m-2}$$

so that in the case of London dispersion forces:

$$\theta_{\text{ads.}} = \frac{1}{2} \theta_{\text{vol.}}$$

This relation accounts—in a qualitative way—for the fact that much higher densities can be reached in monolayers without achieving condensation than is possible in volume phases.

III. COHESION FORCES IN POLYLAYERS

Under certain conditions more than one discontinuity may be encountered in the transition from the adsorbed gaseous to the liquid volume phase, and a phase change of the first order may degenerate to a transition of the second or higher order. In a somewhat schematic way the following cases may be distinguished: (1) mono-mono; (2) mono-poly; (3) mono-liquid; (4) poly-poly; (5) poly-liquid; (6) mono-mono-poly; (7) mono-poly-liquid. However, there is no experimental evidence, so far, for the occurrence of two-step condensations.

In the recent work of Frumkin (13), polylayer-liquid phase transitions have been discussed for the first time on the basis of thermodynamic considerations, and the existence of such equilibria has been experimentally substantiated in a number of cases. No attempt seems to have been made, so far, to derive a mathematical expression for the adsorption isotherm of polylayers with laterally interacting molecules. This is, naturally, a very complex problem even if orientation effects are disregarded.

Since the adsorption energies do not explicitly enter into the equation of state in a semiempirical approach, one may develop the film pressure as a power series in the surface density:

$$F = RT\Gamma + A\Gamma^2 + B\Gamma^3 + \dots$$

and, by means of Gibbs's equation, obtain the Γ - p and the F - p isotherms. Here, then, the integration constant and the "virial coefficients" have to be so deter-

mined as to comply with the boundary conditions of Henry's law, the saturation pressure, and the surface tension of the liquefied film, a requirement which in adsorption on solids may not be easily fulfilled. However, one should be aware that with asymmetric molecules the distinction between mono- and poly-layers cannot be based upon the measurement of surface densities alone. The molecules in the second layer may lie flat, while the orientation in the first one is perpendicular to the surface, or *vice versa*.

IV. SUPERSATURATION PHENOMENA IN ADSORBED PHASES

As with phase transitions of the first order in general, so also with condensation processes starting from adsorbed phases supersaturation phenomena have to be expected (5). The existence of highly supersaturated monolayers on water has long been known. Likewise, no matter what the film thickness, on solids supersaturation can result from the compression of the coexisting vapor. It is easy, then, to visualize the collapse of the metastable state when the system is cooled by adiabatic expansion.

In accordance with Gibbs's ideas on the "formation of a fluid of different phase within any homogeneous fluid," Volmer (20) has shown that metastability depends on the free energy of nucleus condensation. Here the term "nucleus" designates a cluster in labile equilibrium with the metastable phase, i.e., the smallest cluster capable of growing by condensation, provided the creation and the growth of nuclei by coalescence are comparatively rare events. The free-energy barrier which has to be overcome by fluctuations in order to produce a Volmer nucleus decreases with increasing supersaturation as the surface area of the nucleus decreases. In two-dimensional transitions the linear tension around condensed patches has to be considered in place of surface tension.

It is very likely that the hysteresis observed in the sorption and desorption of vapors on porous and powdered solids represents a supersaturation phenomenon of this kind.

Supersaturation is necessary to form at the surface nuclei of a condensed monolayer or polylayer or of a lens of condensed liquid before, on the breakdown of the metastable adsorbed phase, the vapor pressure drops to its equilibrium value. Thereupon, the desorption isotherm follows a lower (the equilibrium) course than the adsorption isotherm. In capillary condensation the situation is, naturally, complicated by the interference of different adsorption fields and by the curvature of the adsorbing surfaces.

It is worth mentioning that Coolidge (8) in a very thorough study of the adsorption of vapors on charcoal was much puzzled by the vacillating results he observed when switching from an "in-curve" to an "out-curve," which he correctly took for the equilibrium isotherm; however, he assumed that the alternations were due to unknown impurities.

In principle there should be no difficulty in interpreting hysteresis curves whenever the adsorption isotherms and their discontinuities on plane surfaces are accessible to experimental investigation.

From the present standpoint also the elimination of hysteresis (21) by proper

thermal treatment of the adsorbent seems to find a simple explanation. If such a treatment contributes to a roughening of the surface, one may anticipate a drastic reduction of the activation energy of nucleus condensation in the two- or three-dimensional cavities of the adsorbent.

Ever since hysteresis was established as a definite phenomenon in the adsorption of vapors, most investigators have associated it with the liquefaction of the adsorbate. No doubt we have to deal with supersaturation in the adsorbed state. But which of the above-mentioned phase transitions is involved has not yet been precisely decided. Here the relation between the critical temperatures of the volume phase and the monolayer phase allows a clear-cut conclusion, at least in the case of true van der Waals adsorption. Thus, the hysteresis in the adsorption of nitrogen (9) on glass has been observed at and around 90°K., while the critical temperature of the gas is only 126°K. It can, therefore, fairly safely be said that the transition is not one of the mono-mono type. Since it is hard to imagine that glass should be well wettable by liquid nitrogen, the discontinuity is probably of the monolayer-liquid phase type.

V. ADSORPTION ON POWDERED MATERIALS

After what has been said, the Emmett-Brunauer-Teller deduction of "surface areas" of powdered materials from the occurrence of knee-points in the adsorption isotherms of vapors unfortunately cannot longer be regarded as a satisfactory procedure. The chief argument in favor of their position has been the agreement of "area" values for different adsorbates on the same adsorbent. The fact will not be disputed that knee-points do quite frequently correspond to approximately equal volumes of adsorbed gases, and it therefore needs another interpretation. The simplest assumption is an overwhelming probability for condensation onto active zones before regular monolayers are possibly completed. However, in addition to the effects of surface irregularities double adsorption in the contact areas of adjacent granules seems to deserve more attention. It should be interesting to check the existence of the latter contribution by interrupting the contacts in an appropriate experimental arrangement.

In general, the superposition of Langmuir isotherms resulting from more and less active adsorption fields will tend to produce a concavity against the pressure axis as in the Freundlich type; the superposition of Nernst isotherms will retain the convexity of that type. With this in mind it is interesting that Bangham (2) has drawn attention to a striking parallelism between F - p isotherms found on mercury and swelling isotherms of the same molecules adsorbed on charcoal. In both instances the characteristic difference between polar and non-polar molecules, i.e., the convex and concave type, respectively, is clearly apparent and overshadows any effects of differences in the surface structures. This is, to a certain extent, also true for the Γ - p isotherms. Thus, the adsorption of water on mercury as well as on charcoal is definitely of the osculating (i.e., *Nernst*) type according to a relatively small adsorption energy of the single molecule in comparison with that of the cluster-bound dipoles.

Further progress can certainly be expected from the study of adsorption on

well-defined crystalline surfaces (3). As to the investigation of phase changes of the first or second order the measurement of the specific heat of adsorbed films (19) ought to be of great help. On the whole, a resumption of the work on mercury adsorption appears as promising as ever.

SUMMARY

1. Current multilayer adsorption theories are insufficient to account for the liquefaction of adsorbed vapors.

2. On plane surfaces mutual attraction and cluster formation manifest themselves in the shape of adsorption isotherms as a convexity against and as an osculation of the pressure axis.

3. A van der Waals equation of state for monolayers and the corresponding equation for the coexisting volume phases being assumed, a relation between the critical temperatures of two- and three-dimensional condensation is derived. For London dispersion forces $T_2 = \frac{1}{2}T_3$.

4. The possible discontinuities in the transition from the adsorbed gaseous to the liquid state in bulk are discussed, and the hysteresis in sorption-desorption processes is interpreted as a supersaturation phenomenon.

5. The occurrence of knee-points in adsorption isotherms on powdered materials is reinterpreted as an effect of active areas.

REFERENCES

- (1) BAND, W.: J. Chem. Phys. **7**, 324, 927 (1939); **8**, 178 (1940).
- (2) BANGHAM, D. H.: Proc. Roy. Soc. (London) **A147**, 175 (1934).
- (3) BEEK, O., SMITH, A. E., AND WHEELER, A.: Proc. Roy. Soc. (London) **A177**, 62 (1940).
- (4) BRUNAUER, S., DEMING, L. S., DEMING, W. E., AND TELLER, E.: J. Am. Chem. Soc. **62**, 1723 (1940).
- (5) CASSEL, H.: *Ergeb. exakt. Naturw.* **6**, 114 (1927).
- (6) CASSEL, H., AND NEUGEBAUER, K.: J. Phys. Chem. **40**, 523 (1935).
- (7) CASSEL, H., AND SALDITT, F.: Z. physik. Chem. **A155**, 321 (1931).
- (8) COOLIDGE, A. S.: J. Am. Chem. Soc. **46**, 610 (1924).
- (9) EMMETT, P. H., AND DEWITT, T. W.: J. Am. Chem. Soc. **65**, 1253 (1943).
- (10) FOWLER, R. H.: Proc. Cambridge Phil. Soc. **32**, 116 (1936).
- (11) FRENKEL, J.: Z. Physik **26**, 117 (1924).
- (12) FRUMKIN, A.: Z. physik. Chem. **116**, 466 (1925).
- (13) FRUMKIN, A.: Acta Physicochim. U.R.S.S. **9**, 313 (1938).
- (14) GIBBS, J. W.: *Collected Works*, Vol. I, pp. 252, 260 (1928).
- (15) LANGMUIR, I.: J. Chem. Phys. **1**, 3 (1933).
- (16) MAYER, J. E., AND MAYER, M. G.: *Statistical Mechanics*, p. 268. John Wiley and Sons, New York (1940).
- (17) PEIERLS, R.: Proc. Cambridge Phil. Soc. **32**, 471 (1936).
- (18) POHL, H. A., HOBBS, M. E., AND GROSS, P. M.: Ann. N. Y. Acad. Sci. **40**, 389 (1940).
- (19) SIMON, F., AND SWAIN, R. C.: Z. physik. Chem. **B28**, 189 (1935).
- (20) VOLMER, M.: Z. Elektrochem. **35**, 555 (1929).
- (21) WEISER, H. B., MILLIGAN, W. O., AND HOLMES, J.: J. Phys. Chem. **46**, 582 (1942).

THE PHYSICAL CHEMISTRY OF FLOTATION. X

THE SEPARATION OF ERGOT FROM RYE

ENID C. PLANTE AND K. L. SUTHERLAND

*Officers of the Division of Industrial Chemistry, Council for Scientific and Industrial Research,
Melbourne, Australia*

Received November 24, 1943

I. INTRODUCTION

Though the fungus *Claviceps purpurea* Tulasne, ergot, uses several host plants, commercial ergot is usually obtained from rye (*Secale cereale* Linn.). The individual grains of ergot are black, compact, and similar in shape to rye grains. They may be shorter than or as much as five times as long as an average rye grain. Ergot contains several alkaloids which are important medicinally. Prior to the war Australia imported all her ergot from Europe, but owing to supply difficulties during wartime attempts are being made to produce ergot locally.

The standard methods of separating the rye from the grain are laborious, and the authors were asked to devise a simple method. Preliminary laboratory experiments using an entirely new method were so promising that a pilot plant was constructed with which the greater part of the current year's production of ergot has been recovered without difficulty.

In Europe ergot is separated from rye by one of three processes: (1) The ergots are harvested by hand-picking the standing crop. (2) The whole crop is harvested, the ergot separated from the grain by a density method, using strong solutions of sodium chloride (saturated or 20 per cent solutions), and the product is finally hand-picked. (3) In Central Europe the harvested crop is fed to fowls which eat the grain.

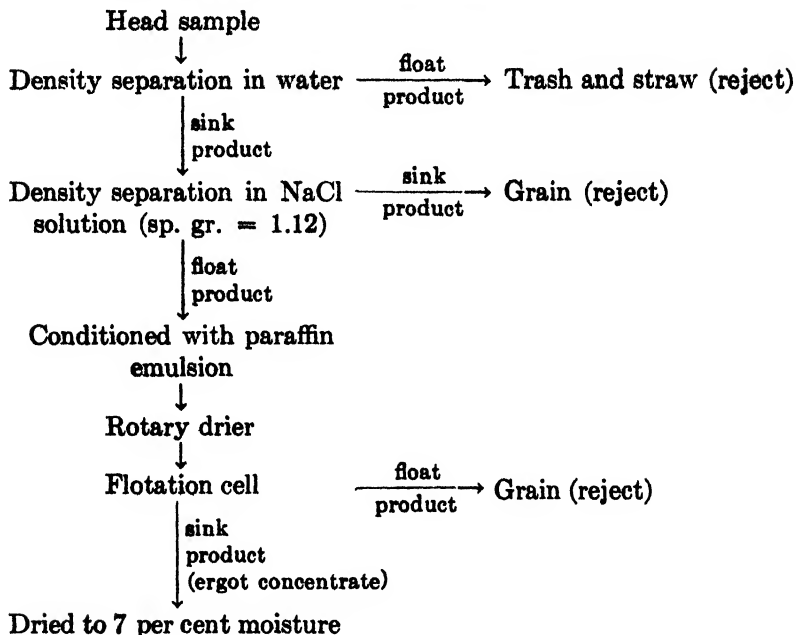
Békésy (2) attempted to separate ergot from rye by density and seed-cleaning methods, but the methods used "gave very unsatisfactory results, involving a minimum loss of two-thirds of the ergot."

Stevens (4), whose opinion is much the same as many others, states that a 20 per cent sodium chloride solution allows all the grain to sink and leaves the ergot floating. With our samples, however, experiments failed to give clean separations because of the overlapping densities of ergot and rye.

Once the limitations of the methods based upon differences in density had been established, it became apparent that further separation would have to depend upon differences in other physical properties. Two properties that seemed worthy of consideration were condition of surface and behavior in an electrostatic field. Only the first property was studied, and upon differences in surface properties of ergot and rye a satisfactory separation has been devised.

II. THE PROCESS

The following flow sheet for the process was adopted:

*A. The density separations*

In the density separation in water, 1 to 4 per cent of the ergot is lost because some ergots are lighter than water. No attempt was made to recover these.

The density separation in saline solution of specific gravity 1.120–1.130 rejected between 96 and 99 per cent of the grain, with a loss of less than 0.1 per cent of ergot. At a specific gravity of 1.112, 5 per cent of the ergots sank and were lost. In practice the specific gravity of the solution should be maintained between 1.120 and 1.130.

The exact amount of grain that can be rejected is dependent upon the time of harvesting of the rye. If the rye is green, only a 96 per cent rejection is obtained, but if it is ripe then 99.9 per cent of the grain may be rejected. The crop is usually harvested green, since the ergots mature before the grain and may drop from the ear unless gathered.

B. The flotation treatment

The ergot surface is much less hydrophobic than that of rye. The contact angle for the grain surface depends upon ripeness at the time of harvesting. If the rye is very green, air bubbles will adhere to a grain immersed in water and buoy it to the surface, whereas if it is ripe or only slightly green, bubbles of air will adhere, but because of the lower contact angle these are smaller and are not able to buoy the grain to the surface. A pneumatic flotation machine must be

used, in which air is forced through a porous medium (canvas, unglazed porcelain) at the bottom. The air bubbles on collision with grains adhere if the bubble does not exceed a size determined by the contact angle and other factors. A small amount of a frothing agent, 20 mg. of pine oil per liter, is added to produce a stable froth.

Air bubbles will also adhere to the ergot, but they are insufficient in number or size to buoy the ergot to the surface. Ripe and near-ripe grain behaves like ergot, so that separation of this grain from ergot required the development of a new method. A theoretical study was then undertaken, the results of which (as set out later) indicated that the surface of the grain had to be so modified that the contact angle should be raised. This led to trial of the addition of paraffin oil which one might expect would spread preferentially over the partly hydrophobic surface of the grain. It was then discovered that if the ergot-rye mixture is treated with a dilute paraffin oil emulsion, the paraffin spreads over the grain surface but not over the ergot surface. The paraffined surface has a sufficiently large contact angle (table 7) to ensure flotation.

The floating grain is removed continuously at the surface, and at the completion of the process the cell is drained of water, leaving a tailing of ergot.

III. THEORETICAL STUDY¹

Two conditions must be fulfilled for the grain to be recovered by flotation. Firstly, air bubbles attached to the grain must provide an adequate buoying

¹ Definition of symbols used in text:

- a = length of equatorial semi-axis of the ellipse,
- b = length of semi-axis of revolution of ellipse,
- d_a = density of air,
- d_g = density of grain,
- d_p = density of paraffin,
- d_w = density of water,
- e = eccentricity of ellipsoid,
- E = tension between grain and air,
- f = acceleration of grain-air system upward,
- F = force required to sink a floating grain,
- g = gravitational acceleration,
- m = direction cosine to y -axis,
- n = number of bubbles attached to the grain,
- n_B = number of bubbles theoretically possible to be attached to a grain,
- p = perimeter of grain at the water-air interface,
- r_0 = equivalent radius of grain,
- S = vertical downward component of stream flow in cell,
- T = surface tension,
- u_0 = velocity of grain on striking the water when dropped from a height y ,
- v = volume of bubble attached to grain,
- v_1 = volume of grain immersed in water,
- v_g = volume of grain,
- v_2 = maximum volume of bubble attached to grain,
- x = x -coordinate,
- x_1 = radius of contact of bubble,

force to lift the grain, and secondly, when the grain reaches the surface it must be able to remain there after the attached air bubbles have collapsed.

In the theoretical study which follows we shall derive (1) the condition for stability at the surface, and its dependence on variations of density and surface tension, and (2) the condition that attached air bubbles be sufficiently large to buoy the grain, and its dependence upon movements of the liquid in the cell.

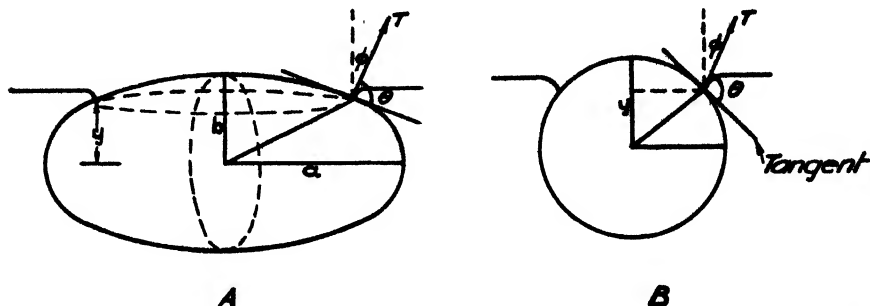


FIG. 1. A grain at the interface air-water. A, longitudinal section; B, transverse section.

A. Stability at the surface

Assume that the grain is a prolate ellipsoid of revolution (figure 1).

Let the force F dynes be applied downward to the grain and at equilibrium we have:

$$F + v_o d_o g - v_i d_w g = T \int \cos \phi \, d\rho \quad (1)$$

where

$$v_i = \frac{\pi a}{3b} (3b^2 y - y^3 + 2b^3) \quad \text{and} \quad v_o = \frac{4}{3} \pi ab^2$$

and the integral is taken around the complete perimeter.

- x_i = number of grains floating when ten are dropped,
- y = y -coördinate,
- y_i = height from which grains are dropped,
- z = z -coördinate,
- z_1 = height of bubble from plane of contact,
- α = angle of normal to tangent plane at point (x, y, z) on ellipsoid,
- β = minor semi-axis of ellipse at water line,
- γ = major semi-axis of ellipse at water line,
- $\Delta F, \Delta T, \Delta d_o$ = increments in F, T , and d_o ,
- θ = angle of contact,
- ϕ = angle between vertical and tensional forces,
- ϕ_1 = angle which normal to surface of bubble makes to axis of revolution,
- ψ = polar coördinate,
- $\xi = \phi_1 + \theta - 180^\circ$,
- η = viscosity,
- σ_x = standard deviation of x_i ,
- σ_y = standard deviation of y_i , and
- ρ = curvature of bubble surface.

The water line of the ellipsoid

$$\frac{x^2}{a^2} + \frac{y^2}{b^2} + \frac{z^2}{b^2} = 1 \quad (2)$$

is described by

$$\frac{x^2}{a^2 \left(1 - \frac{y^2}{b^2}\right)} + \frac{z^2}{b^2 \left(1 - \frac{y^2}{b^2}\right)} = 1 \quad (3)$$

From the equation to the tangent plane the angle which the normal to this plane makes with the y -axis is given by

$$m = \cos \alpha = \frac{y/b^2}{\sqrt{\left(\frac{x}{a^2}\right)^2 + \left(\frac{y}{b^2}\right)^2 + \left(\frac{z}{b^2}\right)^2}} \quad (4)$$

Since ϕ , α , and θ are in the same plane

$$\phi = 90 - \theta - \alpha$$

and hence

$$\cos \phi = m \sin \theta - \sqrt{1 - m^2} \cos \theta \quad (5)$$

Hence equation 1 becomes

$$F = v_1 d_w g - v_2 d_o g + T \int (m \sin \theta - \sqrt{1 - m^2} \cos \theta) d\rho \quad (6)$$

At the water line let

$$\left. \begin{aligned} x &= \gamma \cos \psi \\ z &= \beta \sin \psi \end{aligned} \right\} \quad (7)$$

Then

$$d\rho = \gamma \sqrt{1 - e^2 \cos 2\psi} d\psi \quad (8)$$

where

$$\gamma = a \sqrt{1 - \frac{y^2}{b^2}}$$

$$\beta = b \sqrt{1 - \frac{y^2}{b^2}}$$

and

$$e^2 = 1 - \frac{\beta^2}{\gamma^2} = 1 - \frac{b^2}{a^2} \quad (9)$$

Equation 6 becomes on substitution from equation 8:

$$\begin{aligned} F &= v_1 d_w g - v_2 d_o g + 4T \int_0^{\pi/2} (m \sin \theta - \sqrt{1 - m^2} \cos \theta) \gamma \sqrt{1 - e^2 \sin^2 \psi} d\psi \\ &= v_1 d_w g - v_2 d_o g + 4TA(y) \sin \theta - 4TB(y) \cos \theta \end{aligned} \quad (10)$$

Where

$$A(y) = \int_0^{\pi/2} m \sqrt{1 - e^2 \cos^2 \psi} d\psi$$

$$B(y) = \int_0^{\pi/2} \sqrt{1 - m^2} \sqrt{1 - e^2 \cos^2 \psi} d\psi \quad (11)$$

These integrals were evaluated numerically using the following values:

$$T = 72.7 \text{ dynes cm.}^{-1}$$

$$d_g = 1.10 \text{ gm. cm.}^{-3} \text{ (arithmetic mean, figure 5)}$$

$$d_w = 1.00 \text{ gm. cm.}^{-3}$$

$$g = 980 \text{ cm. sec.}^{-2}$$

$$a = 0.27 \text{ cm., } b = 0.10 \text{ cm. or}$$

$$a = 0.29 \text{ cm., } b = 0.13 \text{ cm.}$$

TABLE 1

EQUATORIAL DIAMETER (2a)	NUMBER OF GRAINS		DIAMETER OF REVOLUTION (2b)	NUMBER OF GRAINS	
	I	II		I	II
0.350-0.400	10		0.100-0.125	1	
0.400-0.450	36	1	0.125-0.150	12	
0.450-0.500	131	14	0.150-0.175	79	
0.500-0.550	119	47	0.175-0.200	174	7
0.550-0.600	131	40	0.200-0.225	154	56
0.600-0.650	48	57	0.225-0.250	57	80
0.650-0.700	17	17	0.250-0.275	14	30
0.700-0.750	4	2	0.275-0.300	4	8
0.750-0.800		3	0.300-0.325	1	
Total number.....	496	181	Total number....	496	181

The values of a and b were determined by direct measurement of two samples of grain which were used in flotation tests. These samples (I, II) give an idea of the variation (table 1) in size. The arithmetic mean value for each sample was used as a suitable statistic for the calculations.

The curves for the functions given by equation 11 could be drawn smoothly if five equally spaced values of ψ were plotted. Equation 10 can be evaluated, and the curves are shown in figures 2 and 3. If $F \geq 0$, then the grain is stable at the interface. For the numerical values selected, these figures indicate that under ideal conditions grains can stay at the surface if θ exceeds 30° , but any small force in the system, e.g., movement of the water, would dislodge them. The angle of 105° was plotted, because it is the angle at a paraffin wax surface and represents the highest angle conceivably obtainable in practice.

Table 2 shows the effect of a variation of density of grain, the other numerical values being constant.

Variation of the surface tension of the water, e.g., by addition of a frothing agent, is described by the following equation:

$$\Delta F = -4 [A(y) \sin \theta - B(y) \cos \theta] \Delta T \quad (12)$$

where ΔT = change in surface tension from water. Table 3 shows the effect on the stability for sample I only and for $\theta = 90^\circ$. These results will be used later.

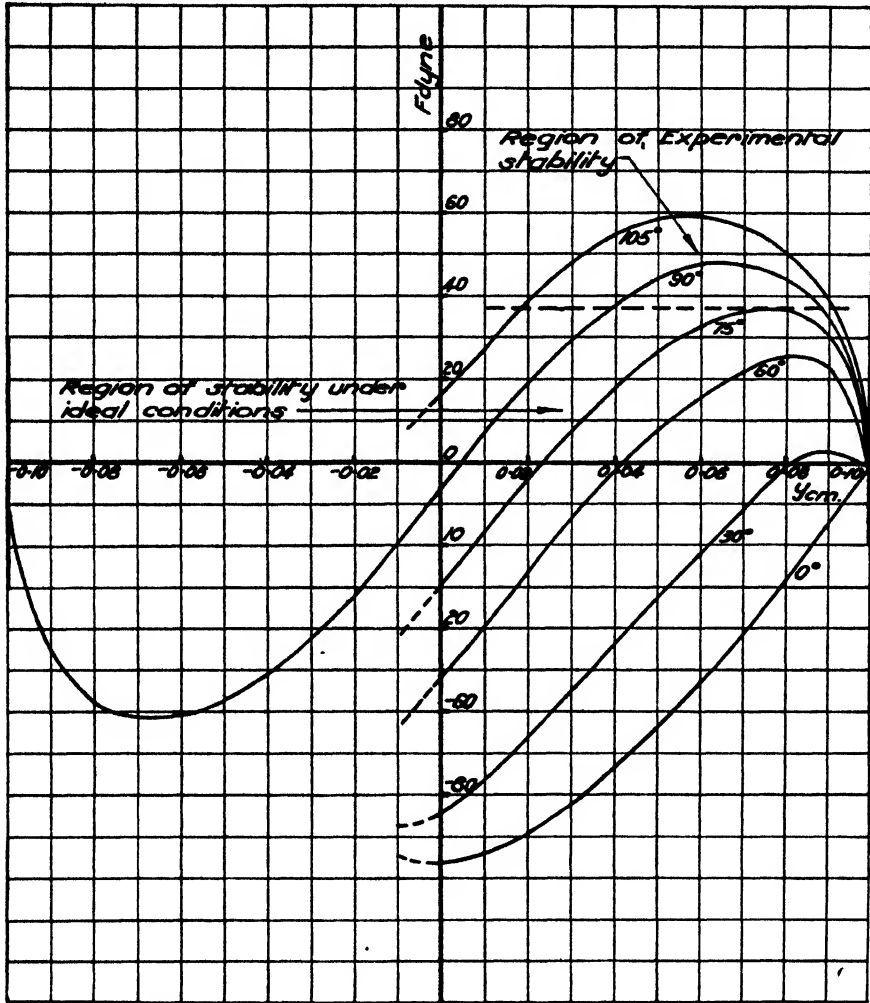


FIG. 2. The relationship between the force F (in dynes) required to sink a rye grain the center of which is immersed to a depth of y cm., for given angles of contact (sample I).

B. Conditions for the grain to be buoyed through the water

Let n bubbles of volume v be attached to the grain. It can be shown that (5)

$$E = g d_w n v v_g \left(\frac{d_g - d_a}{n v_2 d_a + v_g d_g} \right) \quad (13)$$

and

$$f = g \left\{ \frac{(n v + v_g) d_w - (n v d_a + v_g d_g)}{n v d_a + v_g d_g} \right\} \quad (14)$$

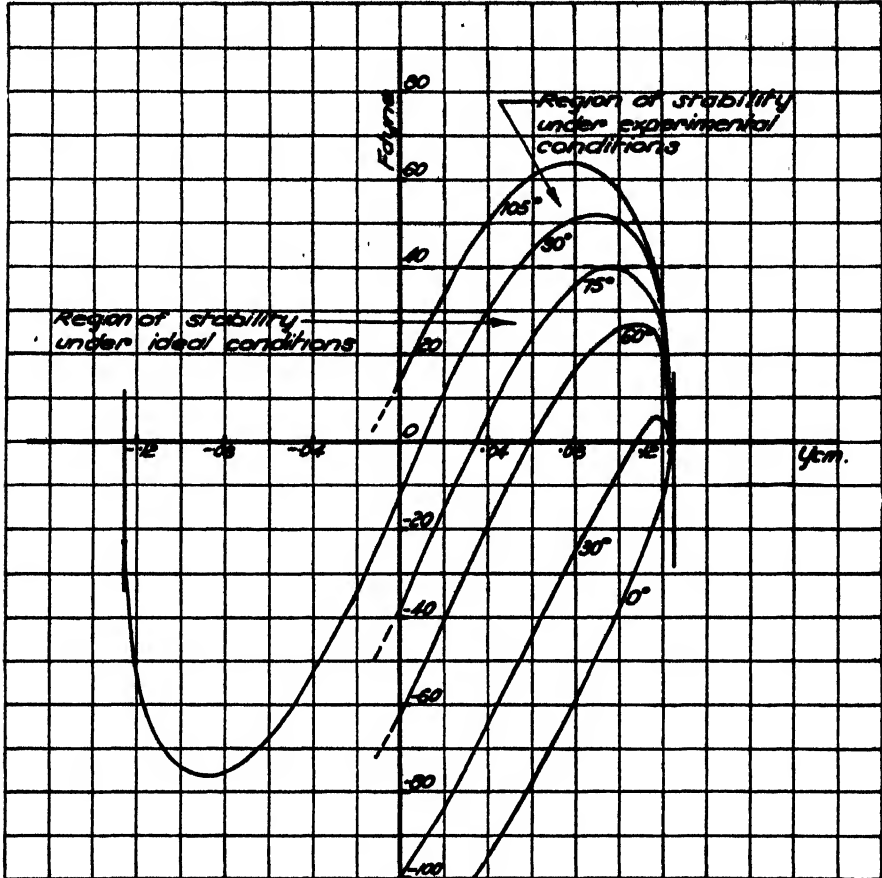


FIG. 3. The relationship between the force F (in dynes) required to sink a rye grain the center of which is immersed to a depth of y cm., for given angles of contact (sample II).

TABLE 2
Effect of density upon region of stability

DENSITY d_g^1	Δd_g	ΔF SAMPLE I	ΔF SAMPLE II
1.05	-0.05	+0.6	+1.0
1.10	0.0	0.0	0.0
1.15	+0.05	-0.6	-1.0
1.20	+0.10	-1.1	-2.0
1.30	+0.20	-2.2	-4.0
1.60	+0.50	-5.5	-10.0

d_g^1 = actual density of grain,

$\Delta d_g = d_g^1 - d_g$,

$\Delta F = F^1 - F$, where F^1 is the stability of grain when the density is d_g^1 .

If d_a is neglected,

$$E = nv gd_w \quad (15)$$

which is equal to the upward thrust due to buoyancy of the air. Wark (5) distinguishes four cases, which in terms of our present problem are:

(1) The bubbles and grain both sink if f is negative, that is, if

$$nv d_a + v_g d_g < (nv + v_g) d_w \quad (16)$$

and the capillary attraction between air and grain is greater than E .

TABLE 3

Effect of a change, ΔT , in surface tension on the force holding the grain at the surface

$-\Delta T$	FORCE ΔF FOR DIFFERENT DEPTHS (y) OF SUBMERGENCE					
	$y = 0.00$	$y = 0.02$	$y = 0.04$	$y = 0.06$	$y = 0.08$	$y = 0.10$
5	0	1.6	2.8	3.4	3.2	0
10	0	3.2	5.6	6.8	6.3	0
20	0	6.4	11.2	13.6	12.6	0
30	0	9.6	16.8	20.4	18.9	0
40	0	12.8	22.4	27.2	25.2	0
50	0	16.2	28.1	34.1	31.5	0

TABLE 4

Number of bubbles (n) of volume (v) which must be attached to raise a typical grain (sample I)

v	n
cm. ³	
0.025	1
0.020	1
0.010	1
0.001	2
0.0001	20

(2) The bubbles and grain both rise if f is positive, that is, if

$$nv d_a + v_g d_g < (nv + v_g) d_w \quad (17)$$

and the capillary attraction between air and grain is greater than E .

(3) The bubbles and grain separate if the capillary attraction is less than E .

(4) Disruption of the bubbles may occur in preference to separation of bubbles and grain. This condition arises when bubbles have reëntrant surfaces (5, page 640).

Table 4 shows the number of bubbles which must be attached to raise a typical grain (sample I). The bubbles which will be attached to the grain will have the

form shown in figure 4. Consider a section of the grain perpendicular to the axis of revolution. We have (1)

$$v_2 = \frac{\pi x_1^2 T}{g(d_a - d_g)} \left(\frac{1}{\rho} - \frac{\sin \phi_1}{x} \right) - \pi b^3 \left(\cos \xi - \frac{\cos^3 \xi}{3} \right) \quad (18)$$

where

$$\rho = \left\{ 1 + \left(\frac{dz}{dx} \right)^2 \right\}^{3/2} / \frac{d^2 z}{dx^2}$$

The second term of the expression corrects for the non-planar surface of the grain and assumes that its radius of curvature is constant and equal to b . Using

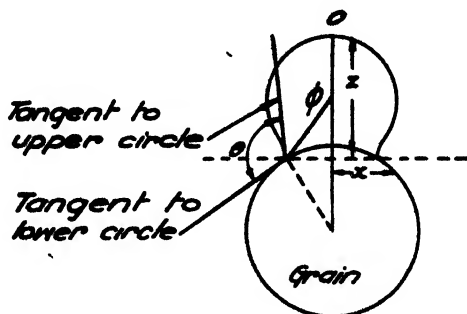


FIG. 4. Attachment of an air bubble to a grain

TABLE 5
Maximum bubble volume obtainable for given contact angle

θ	ξ	x_1 CM.	v_2	n_B
106	45	0.071	0.025	5
85	30	0.050	0.020	5
60	15	0.026	0.010	9

sample I ($b = 0.10$), table 6 shows the maximum bubble volumes (5) which can be obtained for various angles of contact.

The area of a grain (as an ellipsoid) is given by

$$\frac{2\pi ab}{e} (e \sqrt{1 - e^2} + \arcsin e)$$

The area of an average grain in sample I is 0.282 cm.² The last column of table 5 shows the number of bubbles (n_B) which can be accommodated on a grain (sample I). If v_2 is equal to 0.001 cm.³, forty-two bubbles can be accommodated. Comparing tables 4 and 5 it is seen that there is ample room to attach the number of bubbles required to lift a grain. Actually, bubbles of the maximum volume are valueless in flotation because they are readily detached. No informa-

tion is available concerning the size of bubble which can be stable under flotation conditions. This point will be discussed on page 214.

One other factor needs discussion: if conditions in the cell are such that currents of water tend to carry the grains from the surface, then these currents must not exceed a certain value.

Let S cm. sec.⁻¹ be the component of the velocity of flow of the water directly opposed to vertical rise of the grain. The velocity of fall of a free grain through water has been found to be 8.0 cm. sec.⁻¹ From Stokes' law² the equivalent radius of the grain is determined from the equation

$$\text{Velocity of fall} = \frac{2}{9} g r_0^2 \frac{d_g - d_w}{\eta}$$

where $g = 980$ cm. sec.⁻², r_0 = radius (in centimeters), η = viscosity (0.01 poise), d_w = density of water (1.00 gm. cm.³), and d_g = density of grain (1.10 gm.

TABLE 6
The relation between the number of bubbles necessary to buoy the grain against the given stream velocity

S cm. sec. ⁻¹	$6 \eta S r_0$	0.010 cm.	NUMBER OF BUBBLES (n) FOR A BUBBLE VOLUME OF	
			0.001 cm. ³	0.0001 cm. ³
0	0	1	2	20
10	0.113	1	2	22
100	1.13	1	4	32

cm.³). Hence $r_0 = 0.060$ cm. For the grain to rise against the current, S cm. sec.⁻¹

$$d_w n v_g - v_g (d_g - d_w) g \geq 6 \pi \eta S r_0 \quad (19)$$

in which the symbols are defined as previously. Table 6 shows the number of bubbles (n) required to buoy the grain against a stream velocity of S cm. sec.⁻¹

Under the best experimental conditions streams of water carrying grains from the surface appeared to move at rates between 20 and 50 cm. sec.⁻¹ With more turbulent conditions there is an appreciable loss in recovery.

IV. EXPERIMENT AND THEORY

The measured angles of contact for ergot and rye are given in table 7, together with the maximum variation found in the angle.

Experimentally it is found that the grain must have a contact angle greater than 80° before flotation is possible. Preferably the angle should exceed 85°.

² The application of Stokes' law to this system is incorrect, but unfortunately the terminal velocity and size of the grain place it in the region where neither Newton's nor Stokes' law applies. The analysis is sufficiently accurate for the purpose, since the resistance to motion of the grain is smaller than that predicted by Stokes' law.

With contact angles less than 80° air bubbles adhere to a grain, but the number of bubbles adhering is too small. With an increase in the contact angle from 75° to 90° , larger bubbles are observed to be attached to any one grain. Usually

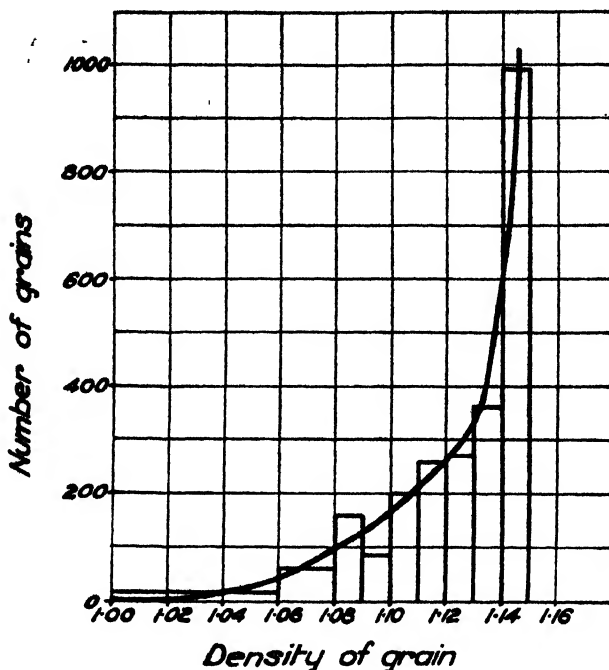


FIG. 5. Distribution of grain densities

TABLE 7

Contact angles for air on rye, corn, and ergot surfaces

SAMPLES	VARIATION IN ANGLE	AVERAGE ANGLE
Ripe grain.....	72° - 80°	75°
Ripe grain (wetted and air-dried).....	32° - 75°	60°
Ripe grain (soaked overnight)	30° - 50°	45°
Ripe grain (washed with paraffin emulsion; dried at 95 - 100°C. or air-dried)	Constant	90°
Green grain (1941 crop)	85° - 90°	87°
Green grain (1942 crop)	70° - 80°	75°
Ergot: (a) dried.	Constant	20°
(b) wetted.....	Constant	20°

when a grain floats, ten to twenty bubbles each of volume $4 \times 10^{-3} \text{ cm.}^3$ are attached. Even for a contact angle of 90° these bubbles never approach the theoretical maximum bubble volume of $2 \times 10^{-2} \text{ cm.}^3$. A reasonable estimate would place the maximum practical bubble volume as $4 \times 10^{-3} \text{ cm.}^3$ for 90° and as $5 \times 10^{-5} \text{ cm.}^3$ for 75° . For the latter size forty bubbles are necessary to

buoy the grain to the surface. This number was never observed on a grain. It is difficult to explain why a decrease of 15° in the contact angle should diminish the maximum practical bubble volume by one hundred fold, whereas the maximum theoretical bubble volume is decreased approximately to one-half by such a change. Obviously the change is connected with dynamic rather than static conditions. Frequently a number of small bubbles adhere to the surface of a grain and larger bubbles are then unable to adhere, since coalescence between bubbles occurs infrequently when a frothing agent is present. Sometimes a froth structure forms on a grain, the bubbles adhering to one another.

Although flotation requires grain with a contact angle of 90° , the fundamental method of separation,—namely, that of holding a grain at the air-water inter-

TABLE 8

The frequency with which x_i grains float when ten grains are dropped from a height of y_i cm. above the surface

y_i	$x_i = 0$	$x_i = 1$	$x_i = 2$	$x_i = 3$	$x_i = 4$	$x_i = 5$	$x_i = 6$	$x_i = 7$	$x_i = 8$	$x_i = 9$	$x_i = 10$
0.1								1		1	1
0.2							2	3	3	2	1
0.3								1	1		1
0.4				1		4	1	1			
0.5							1			1	
0.6			3	3		2			1	2	1
0.7								1			
0.8	1	1	1	1	1	2	2	5	2	1	
0.9					1		1				
1.0	2	4	4		3	1	2	2			
1.1				1							
1.2	2	3	1		1	1					
1.3	1			2	1						
1.4	1	2				1					
1.5	2	2			1			1			
1.6	1	1									
1.7											
1.8	1										

$\sigma_x = 2.95$ grain; $\sigma_y = 0.414$ cm. Correlation coefficient = 0.70.

face, shows that a grain with an angle as low as 45° may be suspended at the interface. The slightest movement of the water immediately dislodges the grain. Not until the angle of contact exceeds 75° is it possible to float grain by launching it. The reason for requiring this comparatively high angle is disclosed if one investigates theoretically the fall of grains on to a water surface.

If u_0 is the downward velocity of the grain as it strikes the water surface then

$$\frac{1}{2}u_0^2 = \int_b^y \frac{F}{v_g d_g} dy \quad (20)$$

The value of the integral is obtained graphically. If and only if θ exceeds 90° is it possible for a grain dropped from *above* the water surface to remain in it. Table 8 shows the number of grains (x_i) floating when ten grains are freely dropped from a height y_i cm. ($\theta = 90^\circ$).

The curve of best fit is

$$y_i = 1.31 - 0.100x_i \quad (21)$$

It is observed that there is considerable variation in behavior of the sample and that if the theory describes stability correctly then θ must exceed 90° . Thus for sample I, if $\theta = 105^\circ$ then the height from which grains can theoretically be dropped is 1.16 cm. From equation 21 only 1.5 grains out of ten grains dropped would float for this height. By assuming a value of θ between 90° and 105° , it is possible to obtain a value of y in agreement with theory. The actual angle



FIG. 6. Rye grain (sample I)

of contact for a grain falling rapidly through a liquid surface is unknown, and as advancing contact angles are greater than equilibrium angles, angles up to 10° larger than normal are to be expected. Equation 20 neglects inertial changes in the water, neglects the fact that the actual angle of contact may originally be 180° (owing to an air film around the grain), and neglects the viscosity of the liquid (water). The results, however, are probably of the right order of magnitude.

Examination of other postulates which were introduced earlier is necessary. Figures 6 and 7 show photographs of grain samples I and II. Obviously the grains are not ellipsoids of revolution, and examination reveals that many are

like triangular prisms with conical ends. The cross section of other grains bears some resemblance to a cardioid. The surface of the grain is wrinkled, and the grain perimeter is much greater than that of a corresponding ellipsoid. Whilst curves of figures 2 and 3 describe a typical grain of samples I and II, sample I contains many grains which have the dimensions of a typical grain of sample II and *vice versa*. The difference in stabilities between these grains is not large.

If the density of the grain is greater than $1.30 \text{ gm. cm.}^{-3}$, no flotation is found possible even for a contact angle of 90° . Table 2 shows that the decrease in stability due to this high density is only 4 dynes. This is negligible compared



FIG 7. Rye grain (sample II)

with the stability of the grain at the surface, which is of the order of 50 dynes. Actually, jostling of grain and water movements will all tend to dislodge grain, but it is difficult to see why a 10 per cent decrease in stability can so markedly affect the behavior.

Behavior in presence of excess paraffin emulsion

In practice, conditioning of the grain with paraffin emulsion is necessary for its flotation. By passing large volumes of air through the cell, much of any excess paraffin is removed with the overflow, but sufficient remains to prevent

satisfactory flotation. This difficulty is overcome by drying the emulsion-treated grain before flotation.

It can be shown theoretically that if a multilayer of paraffin lies between air bubble and grain, the cohesive forces within the paraffin layer are sufficiently large to allow a bubble of the maximum size for a contact angle of 90° to be attached. Grains can therefore be buoyed to the surface by attached bubbles.

The froth at the surface of a pine oil solution covered with paraffin oil is unstable. Hence air bubbles attached to the grain burst immediately they reach the surface, and the grain must be held at the surface if flotation is to be successful. The surface tension of the oil-covered surface is between 20 and 30 dynes cm^{-1} . Table 3 shows that for $T = 72.2 - 22.7$ (say) $= 50$, the region of stability shown in figures 2 and 3 is decreased enormously and only small movements of the liquid are necessary to cause the grains to drop from the surface. This instability at the surface is well illustrated by the following phenomenon: A number of grains may clump together because they share air bubbles, and as they rise to the top of the flotation cell they may be stable there for some time. The upper bubbles in the aggregate burst, but bubbles which are between the grains do not reach the surface and hence continue to buoy the aggregate.

The condition that there is sufficient paraffin oil suspended in the water to form paraffin-grain aggregates with a density less than that of water, is:

$$v_p (d_p - d_w) + v_g (d_g - d_w) \leq 0 \quad (22)$$

where v_p is the volume of the paraffin, d_p is the density of paraffin ($0.80 \text{ gm. cm.}^{-3}$), and the other symbols are defined above: i.e.,

$$v_p \geq 0.5v_g$$

Since only 0.05 g. of paraffin oil per 1000 g. of grain is added, i.e., $v_p = 7 \times 10^{-5}v_g$, the above condition cannot be fulfilled. The grain is not therefore floated under these conditions in the presence of free paraffin. Apparently the spread of paraffin and its absorption by the grain is slow. Drying and/or thorough washing assists this process, with drying as the preferred process, since absorption of oil is thereby greatly hastened.

V. PRACTICAL RESULTS

By gravity separation in a salt solution the grade of ergot may be raised to 80 per cent, but no further. This enriched material was used as a starting point in our work, the major advantages having been firstly, that once the grain had been salt-treated, deterioration of the crop was inhibited and secondly, that a single flotation operation served to raise the grade of the product to the purity required by the specification of the *British Pharmacopoeia*: namely, not more than 2 per cent of foreign organic matter.

A. Preliminary tests

An early observation was that if the ergots and rye grains were thoroughly wetted, then upon panning the material, film flotation of the rye grains occurred and the ergots sank. Tests showed that a 95 per cent recovery of ergot of 98

per cent purity could be obtained by this operation. We then attempted to separate the ergot by a process in which the grain, spread evenly on an inclined travelling canvas belt, was passed through a water surface flowing slowly across the belt. The grain remained in the water surface and the ergot travelled on the belt through the water surface. The belt was 30 cm. wide and travelled at 3-5 cm. per second. It was essential to control the rate of feeding to give a monolayer of grain; otherwise grain sank owing to insufficient space in the surface. Tests showed that at least four operations on the belt were necessary to obtain a 98 per cent ergot product, and the over-all recovery was 90-95 per cent. This process, although successful, was slow.

B. Tests in pneumatic flotation machine with unripe grain

Flotation in a small pneumatic machine was investigated, pine oil (20 mg. per liter) being used as a frother. The following results were obtained:

Test 1: Recovery of ergot.....	99.5 per cent
Grade of ergot.....	98.5 per cent
Test 2: Recovery of ergot.....	98.5 per cent
Grade of ergot.....	99.2 per cent

In a subsequent test with rye grain which appeared mouldy, flotation failed but treatment of the grain with salt solution restored normal flotation. The grain must be either salt-treated or thoroughly dried to prevent fermentation and mould growth. All the above tests were made with rye which had been harvested green and sun-dried.

C. Tests with ripe grain

For further tests a bag of ripe rye grain was used. This grain showed no flotation whatever; moreover, when placed on the moving belt, it would remain in the surface of the water only under ideal conditions.

The difference in behavior between green and ripe rye grain is due to the more hydrophobic nature of the green grain. The ripe grain was treated with liquid paraffin emulsified with sodium oleate in water, but the grain would not float if the emulsion was added to the flotation cell, or if the grain was treated and then placed wet in the cell, either with or without washing. If the paraffin-treated grain was partly dried—until the surface of the grain appeared dry—excellent flotation resulted. Ergots similarly treated did not float, and a preliminary salt treatment of the rye and ergot did not alter the effect of the paraffin treatment. This inability of wet paraffined grains to float is in accordance with theoretical predictions. Measurements of contact angles showed that ripe rye grain had a smaller angle than that required for stable flotation of the grain, while paraffin-treated grain and green rye grain had sufficiently large angles for flotation. Too stringent drying must be avoided: if the paraffin-treated rye grain-ergot mixture was dried at a temperature of 120°C., about 50 per cent of the ergot floated with the grain. If the paraffin concentration was too high, then ergots dried with the grain also floated. A concentration of 0.1 lb. of paraffin per ton of grain was finally adopted.

Small-scale tests on 5-lb. samples of mixtures of ripe grain and ergot were then

conducted. No salt separation was made, the operation consisting of paraffin-treating, drying, and floating the grain as harvested. The final product was analyzed by hand picking. The results are shown below:

TEST NO.	RECOVERY OF ERGOT	ERGOT IN PRODUCT
	<i>per cent</i>	<i>per cent</i>
1.....	100	87
2.....	100	91
3.....	100	86
4.....	100	93
5.....	99	90

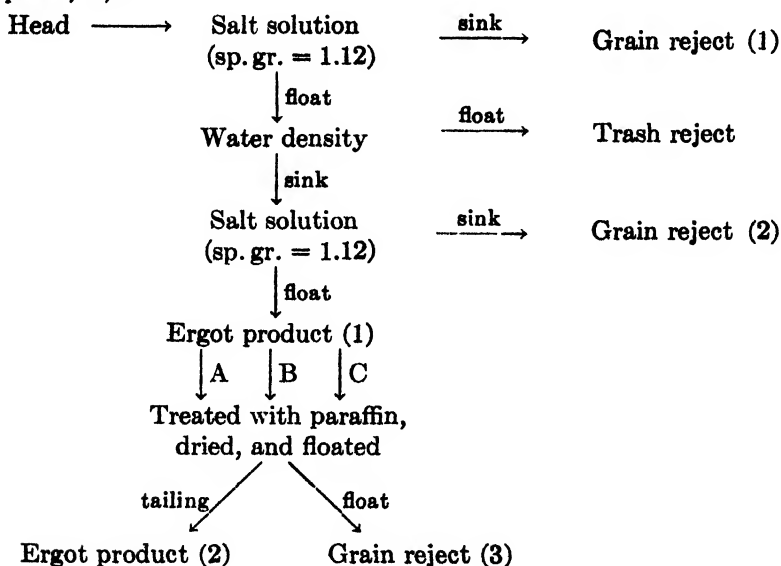
Treatment of this product or of the original head sample in a salt solution of sp.gr. 1.12-1.13 would have brought the ergot product to the required 98 per cent grade, since rye grains of a specific gravity greater than 1.30 will not float, and there is always quite a number of these in any sample.

Tests on a pilot-plant scale were conducted in a larger flotation cell which could handle 35 lb. of material in one operation. Sample I was part of an artificially infected rye crop which had been harvested with a header-winnower and contained very little straw. It had not been subjected to any salt treatment. Sample II had not been winnowed, contained much straw, but had been enriched by a salt treatment.

The general procedure adopted is set out on page 204. The results of a separation of each sample are given below:

(1) *Sample I*: Three bags were treated separately, but in the same manner until the second density separation, which gave an ergot product of about 80 per cent grade in each case. These ergot products were then combined and treated in the flotation cell to give a final ergot product of 99.8 per cent purity.

Sample A, B, C:

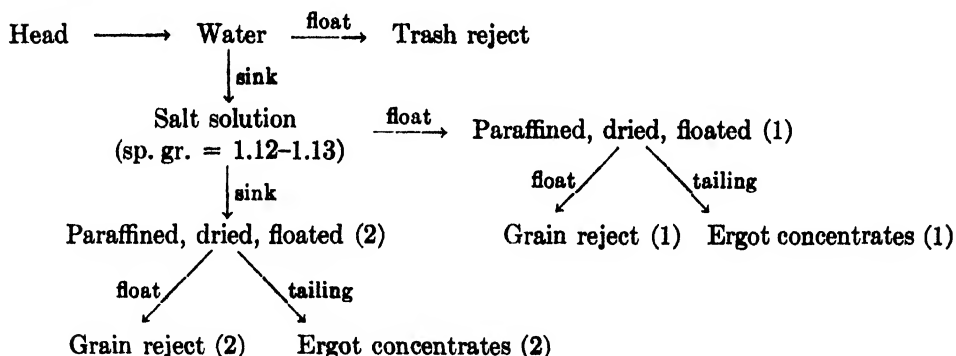


Salt treatment

PRODUCT	WEIGHT PER CENT OF PRODUCT			PER CENT ERGOT IN PRODUCT			PER CENT DISTRIBUTION OF ERGOT		
	A	B	C	A	B	C	A	B	C
Trash reject.....	1.45	1.48	1.40	15.2	5.5	4.3	6.5	2.3	0.2
Ergot product (1).....	4.02	4.09	3.53	78.9	79.4	80.0	93.5	97.7	99.8
Grain reject (1).....	92.0	91.8	91.5	0.0	0.0	0.0	0.0	0.0	0.0
Grain reject (2).....	2.53	2.63	3.53	0.0	0.0	0.0	0.0	0.0	0.0
Composite head.....	100.0	100.0	100.0	3.40	3.32	3.30	100.0	100.0	100.0

Flotation of combined ergot products from tests A, B, and C

PRODUCT	WEIGHT PER CENT OF PRODUCT	PER CENT ERGOT IN PRODUCT	PER CENT DISTRIBUTION OF ERGOT
Ergot product (2).....	78.8	99.8	99.5
Grain reject (3).....	21.2	2.3	0.5
Composite head.....	100.0	79.4	100.0

(2) Sample II:

In the salt density separation some ergot sank; hence the sink product was paraffined, dried, and floated in the small flotation cell in which the grain was floated away and the ergot recovered. This ergot amounted to only 0.8 per cent of the total product.

PRODUCT	WEIGHT PER CENT OF PRODUCT	PER CENT ERGOT IN PRODUCT	PER CENT DISTRIBUTION OF ERGOT
Trash reject.....	31.1	1.09	1.3
Ergot concentrates (1).....	25.5	99.5	96.4
Ergot concentrates (2).....	0.62	31.8	0.8
Grain reject (1).....	23.8	1.6	1.5
Grain reject (2).....	19.0	0.08	0.0
Composite head.....	100.0	26.4	100.0

Hence the main ergot product was of 99.5 per cent purity and contained 96.4 per cent of the total ergot.

The second salt treatment at the same specific gravity (1.12–1.13) as the first treatment was included because it gave a further rejection of grain: *viz.*, grain which had become water-logged in the water treatment and had attained a density greater than that of the salt solution (1.12–1.13). It was later found more satisfactory to carry out this second salt treatment as a final process after flotation, for then grains which became water-logged in the flotation cell and hence did not float were also rejected. If the flotation product contains 98 per cent of ergot, this second salt separation may be omitted.

D. Tests with commercial paraffin oil emulsions

Two commercially available emulsions, one of which was self-emulsifying, were used, and small-scale tests were conducted to determine the effectiveness of these for "oiling" the grain, and the amounts required. Both were satisfactory for the purpose, but it was necessary to use amounts containing 1.0 lb. of paraffin per ton of grain. With lower concentrations of paraffin, the grain would not float. It was still necessary to dry the grain after treatment with these reagents. The emulsion prepared in the laboratory contained 20 per cent paraffin and 3 per cent sodium oleate in water, and amounts to give 0.1 lb. of paraffin per ton of grain were sufficient. The commercial paraffin emulsions contained a higher percentage of an emulsifying agent, and as ten times the amount of paraffin was required, the amount of emulsifying agent in the "oiling" solution was greatly increased. The emulsifier dried on the grain and redissolved in the water of the flotation cell. Consequently if the same water was used for several floats, the emulsifier became sufficiently concentrated to have a detergent effect. Its presence could be identified by the appearance of the froth, which lost the characteristics of a pine oil froth and had the appearance of a soap froth. The flotation of the grain became progressively worse. Hence it was necessary to renew the water in the flotation cell after each float.

E. Tests concerning some commercial conditions

Tests were also conducted to determine factors such as the capacity of the flotation cell, the time required to dry the ergot to 5–7 per cent moisture content in the rotary drier used for the purpose, and the amount of ergot which could be separated in one day. Using the process described, and a flotation cell with a capacity of 35 lb. (50 per cent ergot, 15 per cent moisture), it is estimated that two people can separate 150 lb. of ergot per day. Determination of the alkaloid content of the ergot showed that this is unaffected by the processes described above. Long periods of soaking and/or drying at temperatures exceeding 70°C. may lead to loss.

VI. COSTS

The reagent costs are less than 0.1 d. per pound of ergot and labor costs are between 2 d. and 3 d. per pound. The cost of equipment to handle 150 lb. of

ergot per day would be about A£300. The details for commercial operation of the process will be described in an Industrial Chemistry Circular to be issued by the Commonwealth Council for Scientific and Industrial Research.

VII. SUMMARY

1. A successful process for the separation of ergot (*Claviceps purpurea* Tulasne) from rye (*Secale cereale* Linn.) by flotation is described. The alkaloid content of the ergot was unaffected by the treatment.

2. The variation of stability under surface tension and gravity of an ellipsoid of revolution at an air-water and oil-air interface is examined theoretically. Rye grains approximate to this form and results are in reasonable agreement with theory.

3. The attachment of air bubbles to a rye grain was investigated and it was found that bubbles effective in flotation were many times smaller than those expected on theoretical grounds. This problem is of general interest in flotation.

The authors express their thanks to Mr. H. A. Pittman, Victorian Agriculture Department, for the supplies of ergot-grain mixture, to Mr. G. B. O'Malley for assistance in the design of pneumatic flotation machines, to Mr. W. I. B. Smith, Division of Aeronautics, C.S.I.R., for help with the mathematical presentation of the stability of floating grains, and to Dr. I. W. Wark, Chief of the Division of Industrial Chemistry, Commonwealth Council for Scientific and Industrial Research, Australia, for his helpful criticism of the manuscript.

REFERENCES

- (1) BASHFORTH AND ADAMS: *Capillary Action*. Cambridge (1883).
- (2) BÉKÉSY: Zbl. Bakt., Abt. 2, **99**, 321.
- (3) DE WITT, C. C., AND MAKENS, R. F.: J. Am. Chem. Soc. **54**, 455 (1932).
DE WITT, C. C., AND ROPER, E. E.: J. Am. Chem. Soc. **54**, 444 (1932).
- (4) STEVENS, E. G.: *Diseases of Economic Plants*. Macmillan, New York.
- (5) WARK, I. W.: J. Phys. Chem. **37**, 623 (1933).

THE KINETICS OF THE REACTION BETWEEN SILVER PERCHLORATE AND METHYL IODIDE

M. F. REDIES AND T. IREDALE

*Physical Chemistry Laboratories, University of Sydney, Sydney, Australia**Received March 28, 1944*

In an attempt to compare the reactivities of alkyl iodides by observing their rates of reaction with silver nitrate in alcoholic solution, Burke and Donnan (1) found that the kinetics were somewhat irregular. The investigation of these unusual kinetics formed the subject of two further papers (2, 3). For any particular run a bimolecular constant was obtained, which in some instances showed a slight drift, decreasing during the course of the reaction, whilst in others it remained constant. It was found, however, to be dependent on the initial concentrations of the reactants, especially the silver nitrate. This can be described empirically by $k = ac^{0.68}$ (k = the bimolecular constant, a = a constant, c = initial concentration of silver nitrate).

The concentration-time curves for different reactions when plotted simultaneously from points of similar concentrations were found to coincide for reactions involving silver lactate, but not for those involving silver nitrate. It was concluded that in the case of silver nitrate some catalytic agent was present. It was, however, established that the main products of the reaction had no appreciable effect on its rate. Pearce and Weigle (5) made a systematic study of the reaction between silver nitrate and ethyl iodide in methyl alcohol-ethyl alcohol mixtures, and obtained similar results to those of Donnan and coworkers.

In view of the likely complications caused by the ionization of silver salts in alcoholic solution, it was thought that the reaction between silver perchlorate and alkyl iodides in benzene solution might be simpler, and that a careful study of its kinetics might lead to a better understanding of the previous complications.

Solutions of silver perchlorate in benzene have been studied by Hill (4) who concluded, mainly from freezing-point measurements, that the substance is somewhat associated in this solvent. Conductivity measurements showed that the ionization of the perchlorate was quite negligible, as might be expected in benzene. It was therefore anticipated that the reaction between silver perchlorate and methyl iodide would not go by way of ions, but that association might affect the calculated order of the reaction. Our results, which are in some respects comparable with those of Burke and Donnan, cannot be linked with this factor. They are the consequence of some mechanism which has not yet been elucidated.

EXPERIMENTAL

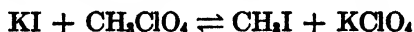
The benzene was purified by treatment with chlorosulfonic acid, freezing, fractionating, drying over phosphorus pentoxide, and redistilling.

The silver perchlorate was made by the method of Hill; it was separated from insoluble matter by extraction with ether in a Soxhlet apparatus, followed by

crystallization from benzene. The salt was kept in the dark in a desiccator over phosphorus pentoxide. Great care was taken in handling the anhydrous silver perchlorate, which is deliquescent.

The other solvents used were the purest obtainable, and were redistilled. The ether was pure anesthetic ether; it was dried over sodium and distilled.

The reaction between solid silver perchlorate and methyl iodide is vigorous. The product of the reaction explodes violently when struck. In dilute solution in benzene the two substances react at a measurable rate, forming methyl perchlorate and silver iodide. The presence of the methyl perchlorate could be inferred from the fact that when a solution of the silver salt was allowed to react to completion with excess methyl iodide, the precipitated silver iodide filtered off, and excess alcoholic potassium iodide added, a precipitate, identified as potassium perchlorate, was slowly formed. This is evidently due to the reaction:



For this reason excess potassium iodide cannot be used to precipitate the silver for back titration during the analysis of the course of the reaction. Potassium chloride was found to react much more slowly with the methyl perchlorate, and was used instead of the iodide.

The precipitation of a double compound between silver perchlorate and silver iodide was not discovered.

The reactions were studied at several temperatures in a thermostat controlled to 0.05°C. Solutions of the reactants were warmed in the thermostat, measured out by pipets, and mixed in Pyrex flasks. The reaction was arrested by the addition of alcoholic potassium chloride, the mixture being chilled, and its course was determined by electrometric titration.

The second-order constant (k_2) was calculated from the integrated form of the equation

$$\frac{dx}{dt} = k_2(a - x)(b - x)$$

namely,

$$k_2 = \frac{2.303}{t(a - b)} \log_{10} \frac{b(a - x)}{a(b - x)}$$

a and b being the initial concentrations of silver perchlorate and methyl iodide, respectively, and x the moles of silver iodide in unit volume formed in time t , computed in seconds. The $2\frac{1}{2}$ -order constant ($k_{2\frac{1}{2}}$) was calculated from the integrated form of the equation

$$\frac{dx}{dt} = k_{2\frac{1}{2}}(a - x)^{3/2}(b - x) = k_{2\frac{1}{2}}(a - x)^{5/2}$$

namely,

$$k_{2\frac{1}{2}} = \frac{1}{\frac{3}{2}t} \left(\frac{1}{(a - x)^{3/2}} - \frac{1}{a^{3/2}} \right)$$

$a = b$ = initial concentration of both the perchlorate and the iodide.

DISCUSSION OF RESULTS

Previous workers have established the existence of two forms of kinetics describing the reaction between silver salts and alkyl iodides, a pseudo-bimolecular (second order) and a $2\frac{1}{2}$ order. The latter was not really recognized as such, but the results of Donnan and Potts for silver lactate appear to be of this type.

Both forms of kinetics were observed for the silver perchlorate-methyl iodide reaction in benzene. The pseudo-bimolecular constant (k_2) was found to be a function of the initial silver perchlorate concentration (a). A constant, independent of a , was obtained by dividing k_2 by $a^{\frac{1}{2}}$ (table 1). Any effect of b on k_2 was within the limits of experimental error. As, however, k_2 frequently showed a drift as the reaction proceeded, it was found more satisfactory to use the value of k_2 obtained during the first 30 min. of the respective run, rather than the mean value.

In the case of the $2\frac{1}{2}$ -order kinetics, it was found that corresponding sections of the concentration-time curves could be superimposed, and the time for half-decomposition when $a = b$ was a linear function of $1/a^{\frac{1}{2}}$. The $2\frac{1}{2}$ -order kinetics

TABLE 1
Temperature, 25°C.; $b = 0.20$; t in minutes

t	$a - x$	k_2	t	$a - x$	k_2	t	$a - x$	k_2
0	0.0121		0	0.0198		0	0.0228	
30	0.0098	289	20	0.0180	392	30	0.0184	399
60	0.0080	286	40	0.0164	392	60	0.0147	412
90	0.0062	306	60	0.0151	384	90	0.0120	410
120	0.0051	299	80	0.0137	389	120	0.0099	404
150	0.0042	299	100	0.0125	392	150	0.0082	395
$k_2/a^{\frac{1}{2}} \dots \dots \dots$		0.0027	$k_2/a^{\frac{1}{2}} \dots \dots \dots$		0.0028	$k_2/a^{\frac{1}{2}} \dots \dots \dots$		0.0027

were also found for certain solvents other than benzene, in which the reaction was given a cursory examination (table 4).

The drift in k_2 mentioned above actually indicates a stage in the kinetics intermediate between the pseudo-bimolecular and the $2\frac{1}{2}$ order. The transition from the one form to the other can be accomplished by altering the initial concentration of the silver salt, and it appears that varying the initial alkyl iodide concentration has the same effect, although this has not yet been adequately established. The higher concentrations favour the $2\frac{1}{2}$ -order reaction, and the low concentrations the pseudo-bimolecular. Thus the reaction in benzene with $a = b = 0.16$ was found to be of the $2\frac{1}{2}$ order, whilst that with $a = 0.020$ and $b = 0.20$ was pseudo-bimolecular. The results of Donnan and Potts for silver lactate and ethyl iodide in acetonitrile show that the reaction is of the $2\frac{1}{2}$ order when the initial concentrations are $N/10$, and pseudo-bimolecular when the initial concentrations are $N/40$ (table 2).

The very good $2\frac{1}{2}$ -order constants obtained with silver perchlorate in benzene

TABLE 2

Results obtained by Donnan and Potts with silver lactate and ethyl iodide

3N/100 ethyl iodide and 3N/100 silver lactate						
<i>t</i> (minutes).....	7	11	16	20	30	40
$k_{2\frac{1}{2}}$ *	2.14	1.99	1.93	1.82	1.99	1.68
3N/200 silver lactate and 3N/200 ethyl iodide						
<i>t</i> (minutes).....	10	25	45	72	105	133
$k_{2\frac{1}{2}}$	1.81	1.50	1.36	1.33	1.39	1.42
N/10 silver lactate and N/10 ethyl iodide						
<i>t</i> (minutes).....	15	36	66	88	115	
$k_{2\frac{1}{2}}$	5.81	5.93	5.98	5.90	5.75	

* $k_{2\frac{1}{2}}$ is in arbitrary units.

TABLE 3

Silver perchlorate and methyl iodide in benzene

<i>t</i>	$\frac{a-x}{b-x}$	$k_{2\frac{1}{2}}$	<i>t</i>	$\frac{a-x}{b-x}$	$k_{2\frac{1}{2}}$	<i>t</i>	$\frac{a-x}{b-x}$	$k_{2\frac{1}{2}}$
Temperature, 25°C.								
0	0.07860		0	0.11730		0	0.15873	
60	0.06534	0.00269	30	0.09882	0.00270	30	0.12372	0.00266
120	0.05748	0.00252	60	0.08628	0.00262	60	0.10494	0.00252
180	0.05220	0.00234	90	0.07860	0.00253	90	0.09210	0.00247
240	0.04722	0.00252	120	0.07194	0.00252	120	0.08262	0.00244
300	0.04272	0.00251	150	0.06642	0.00248	150	0.07440	0.00248
360	0.04026	0.00242	180	0.06222	0.00244			
Temperature, 35°C.								
0	0.08036		0	0.11930				
20	0.07020	0.00549	30	0.08592	0.00535			
40	0.06268	0.00550	45	0.07748	0.00541			
60	0.05748	0.00531	60	0.07032	0.00544			
80	0.05284	0.00534	75	0.06472	0.00540			
100	0.04896	0.00537	90	0.05996	0.00541			
120	0.04608	0.00538	105	0.05616	0.00538			
140	0.04344	0.00528	120	0.05284	0.00538			
160	0.04116	0.00520						
180	0.03912	0.00527						

are shown in table 3. If the reciprocals of the initial concentrations to the power of three-halves be plotted against the times for half-decomposition in each case, a satisfactory straight line is obtained (figure 1). (The dotted line is ob-

tained from a plot of the reciprocals of the squares of the initial concentrations against the times for half-decomposition. A linear relationship would be obtained if the reaction were of the third order, which is not the case.)

The reaction in ether (table 5) presents a new kind of kinetics, a pseudo-bimolecular related to the third instead of the $2\frac{1}{2}$ order. This may yet be another phase of the kinetics observed in other solvents, but no evidence of it is available.

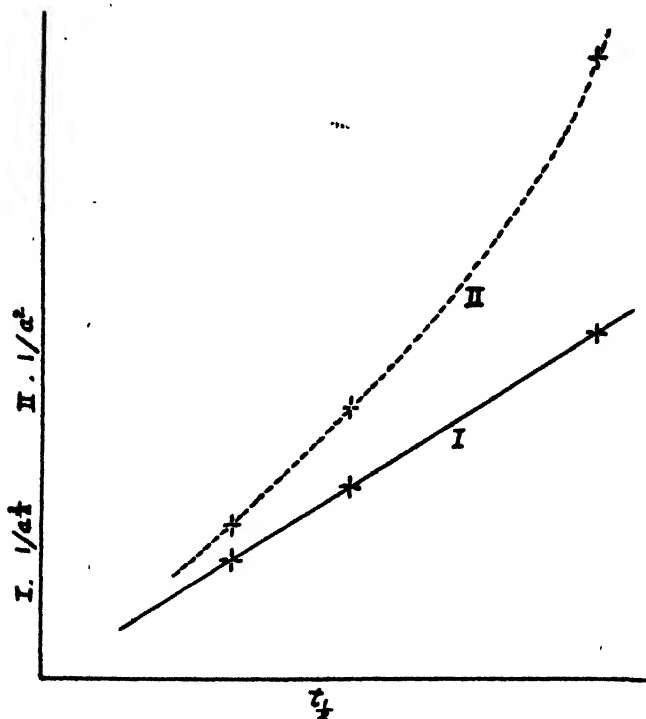


FIG. 1. Reaction of silver perchlorate with methyl iodide in benzene

THE HETEROGENEOUS FACTOR

The presence in the reacting system of precipitated silver iodide suggests that the reaction may be partly heterogeneous. Senter (6) found that the addition of solid silver iodide had some effect in increasing the speed of reaction of silver nitrate and alkyl halides. In the benzene-perchlorate system shaking, and thereby dispersing the silver iodide throughout the solution, had no effect on the reaction velocity. A reaction carried out in the normal way was compared with reactions in which the silver perchlorate solutions were first treated with methyl iodide to form the products of the reaction. When this preliminary treatment was completed the resultant solutions containing colloidal silver iodide were used for reactions carried out in the normal way. No enhancement of the speed due to the presence of excess colloidal silver iodide could be detected. But it is con-

TABLE 4

Silver perchlorate and methyl iodide in solvents other than benzene

SOLVENT	T	$a - b =$	k_2	E
	°C.			calories
Acetic acid.....	15	0.0397	0.0116	12,700
		0.0641	0.0105	
		0.0794	0.0105	
			0.0108 (mean)	
	25	0.0195	0.0220	
		0.0392	0.0229	
		0.0780	0.0237	
			0.0227 (mean)	
Acetone.....	25	0.0395	0.0108	13,000
		0.0605	0.0102	
		0.0807	0.0107	
Ethyl alcohol.....	15	0.0800	0.0197	13,000
	25	0.0197	0.0432	
		0.0397	0.0394	
		0.0786	0.0435	
			0.0422 (mean)	
Benzene.....	25	0.0786	0.00250	13,900
		0.117	0.00253	
		0.159	0.00251	
			0.00251 (mean)	
	35	0.0804	0.00535	
		0.119	0.00540	
			0.00537 (mean)	
Ethyl acetate.....	25	0.0205	0.0664	13,300
		0.0399	0.0664	
		0.0804	0.0604	
Aqueous dioxane (50 per cent).....	15	0.0800	0.0105	13,300
	25	0.0398	0.0244	
		0.0792	0.0227	
			0.0235 (mean)	
Aqueous ethyl alcohol (50 per cent)....	15	0.0396	0.0152	11,400
		0.0791	0.0150	
			0.0151 (mean)	
	25	0.0390	0.0300	
		0.0790	0.0291	
			0.0295 (mean)	

ceivable that this may not be apparent if the mechanism of precipitation is such as to permit the total active service area for catalytic action not to vary greatly throughout the reaction.

THE ENERGY OF ACTIVATION

The energies of activation of the perchlorate-iodide reaction for two different temperatures calculated from the equation

$$E = \frac{2.303RT'' - T'(\log_{10} K''_{24} - \log_{10} K'_{24})}{T'' - T'}$$

are given in table 4. They are approximate values, but the variations for different solvents are real, and within the experimental error. More experimental work will be necessary to determine accurately the true energies of activation.

TABLE 5
Silver perchlorate and methyl iodide in ether

<i>T</i> °C.	<i>a</i> = <i>b</i> =	<i>k</i> ₂	<i>k</i> ₂ / <i>a</i>
15	0.0100	0.0262	2.02
	0.0148	0.0402	2.70
25	0.0051	0.0292	5.78
	0.0049	0.0292	5.91
	0.0100	0.0520	5.20
	0.0099	0.0515	5.21
	0.0151	0.0798	5.30
	0.0199	0.1090	5.47

SUMMARY

The reaction between silver salts and alkyl iodides in various solvents appears to be of the $2\frac{1}{2}$ order, the kinetics assuming a modified, pseudo-bimolecular form, in which k_2 is proportional to $a^{1/4}$ (a = initial silver salt concentration) at lower concentrations.

The energies of activation are of the order 11,000 to 13,000 calories.

REFERENCES

- (1) BURKE, K. A., AND DONNAN, F. G.: J. Chem. Soc. **85**, 555 (1904).
- (2) BURKE, K. A., AND DONNAN, F. G.: Z. physik. Chem. **69**, 148 (1910).
- (3) DONNAN, F. G., AND POTTS, H. E.: J. Chem. Soc. **97**, 1882 (1910).
- (4) HILL, A. E.: J. Am. Chem. Soc. **43**, 254 (1921).
- (5) PEARCE, J. N., AND WEIGLE, O. M.: Am. Chem. J. **48**, 243 (1912).
- (6) SENTER, G.: J. Chem. Soc. **97**, 346 (1910).

NEW BOOKS

Abridged Scientific Publications from the Kodak Research Laboratories. Volume XXIV. 391 pp., and additional author and subject indexes. Rochester, New York: Eastman Kodak Company, 1942.

Condensed accounts of sixty scientific publications (Nos. 783H to 882, not continuous) are included in the present volume.

S. C. LIND.

Chemical Engineering. By CHARLES ELI REED. 20 pp. Boston, Massachusetts: Bellman Publishing Company, Inc. Price: 75 cents.

This booklet is No. 48 of the series entitled "Vocational and Professional Monographs". Of the several publications on vocational guidance in chemical engineering, this is the most comprehensive and instructive. The subject matter is well arranged and lucidly written. The booklet should be in the hands of all vocational counselors in high schools and colleges. The prospective student of chemical engineering can benefit greatly by its continued perusal during his sojourn at college. So much information and advice is included in this monograph that it can be absorbed only by periodic reading.

CHARLES A. MANN.

The Physical Chemistry of Electrolytic Solutions. By HERBERT S. HARNED AND BENTON B. OWEN. American Chemical Society Monograph Series. xxxvi + 611 pp. New York: Reinhold Publishing Corporation, 1943. Price: \$10.00.

Physical chemists who are interested in the properties of solutions of electrolytes will welcome this masterly monograph (or rather, series of monographs) by Harned and Owen. The reviewer is of the opinion that his chief function in the present instance is to give possible readers some adequate idea of the topics discussed and of the comprehensiveness of the treatment.

The first five chapters (pp. 1-134) may be called theoretical. They include a brief but satisfactory thermodynamic introduction, followed by a discussion of the interionic attraction theory in which the authors deal with distribution functions and their change with time, with equations of motion of the ions, with potentials of ions in the absence and also in the presence of external fields of force. Fundamental equations are thus derived to be used in computing activity and osmotic coefficients and in dealing with the theory of viscosity, conductance, and diffusion of electrolytes. In chapter 3, the Debye limiting law is derived as well as the form it assumes when ions are no longer considered to be point charges. The treatment of Gronwall, LaMer, and Sandved is also given in outline. This chapter includes a discussion of Bjerrum's theory of ionic association and of Fuoss and Kraus's theory of the formation of triple ions and of clusters. There is also a derivation of the equation of Debye and McAulay which gives the effect of electrolytes on the activity of a non-electrolyte.

Chapter 4 deals with such irreversible processes as viscous flow, electrical conductance, and diffusion. Here the time of relaxation of the ionic atmosphere (Debye and Hückel), Falkenhagen's theory of viscosity, and Nusager's theory of conductance and related topics are adequately treated. Chapter 5 contains numerical compilations of physical constants and of mathematical functions that are frequently used. It should be noted that the authors adhere to the values of physical constants given in the *International Critical Tables*, Volume I (1930).

Chapters 6 to 10 contain a discussion of experimental methods but no detailed description of apparatus or technique. Included in these chapters is a study of electrical conductance methods, of the effects of high frequencies and high fields, of viscosity and diffusion of electrolytic solutions and of freezing-point, boiling-point, and vapor-pressure measurements.

The remaining portion of the book (chapters 11 to 15) is actually a series of monographs

on the properties of solutions of selected substances or groups of substances. Chapter 11 is devoted to solutions of hydrochloric acid in water and in dioxane-water mixtures; chapter 12 is given over to strong 1-1 electrolytes (chiefly halides of the alkali metals); chapters 13, 14, and 15 deal with electrolytes of higher valence type, with mixtures of strong electrolytes, and with the ionization and thermodynamic properties of weak electrolytes.

The wealth of material, both theoretical and experimental, contained in this volume will make it invaluable to the physical chemist and the graduate student in chemistry whenever adequate information about electrolytic solutions is desired.

Author and subject indexes are satisfactory and, in addition, a detailed table of contents adds greatly to the usefulness of the book.

F. H. MACDOUGALL.

Chemical Process Principles. Part One: Material and Energy Balances. By OLAF A. HOUGEN AND KENNETH M. WATSON. vi + 452 pp. New York: John Wiley and Sons, Inc., 1943. Price: \$4.50.

This excellent text has developed from *Industrial Chemical Calculations* by the same authors. Chapter I to V and chapters VII and VIII cover material given in any good elementary course in physical chemistry, with the addition of many problems (some worked out in detail, others left as exercises to the reader) pertaining directly to the study of chemical engineering. Chapter VI on "Material Balances" is well designed to assist the student in studying operations on a large scale, whether these are merely chemical reactions, counter-current processes, continuous processes, or recycling operations. Chapter IX is an extensive discussion of "Fuels and Combustion." In Chapter X the general methods of calculating material and energy balances are applied to three typical processes in the chemical, metallurgical, and petroleum industries. These are the chamber sulfuric acid plant, the blast furnace, and the petroleum-cracking process.

The reviewer found only two minor errors. On page 57, it is stated that "if a saturated vapor is cooled or compressed, condensation will result and what is termed a *wet vapor* is formed." As a matter of fact, adiabatic compression of saturated water vapor renders it unsaturated. On page 227 the statement is made that "water has a higher specific heat than any other substance with the exception of liquid ammonia and a few organic compounds." The reviewer could add gaseous hydrogen and gaseous helium (at constant pressure) to the list of exceptions.

F. H. MACDOUGALL.

Synthetic Resins and Rubbers. By PAUL O. POWERS. 296 pp. New York: John Wiley and Sons, Inc., 1943. Price: \$3.00.

Synthetic Resins and Rubbers is addressed to young chemists and to students who intend to enter industry. Its purpose, "to describe briefly the chemistry of polymers, particularly those of commercial importance", has been competently achieved. A foundation of knowledge is provided for much of the glue, paint, and rubber chemistry which is so important in practical work. The author, in his capacity as chief of organic research of the Armstrong Cork Company, has had intimate contact with the development and application of the materials whereof he writes.

Short chapters on the economics of the plastics industry and on the principles of resin formation are followed by more detailed considerations of condensation polymers. These include resins prepared from phenol and formaldehyde (Bakelite); urea formaldehyde, best known in pastel-tinted bathroom tumblers, and its improved successor, melamine formaldehyde; the polyester resins used in modern paints and varnishes; and the polyamides, which, as Nylon stockings, conferred glamour on the American girl. The vinyl polymers, including polyvinyl chloride (Koroseal), lustrous polymethyl methacrylate, now used for bomber windows, and polystyrene, are effectively described. The chapter on synthetic rubbers was written by K. H. Weber, a research associate of Powers. It is the best general exposition of this subject that has come to the reviewer's attention. Under "Resins from

Natural Products" are included the various nitrates, esters, and ethers of cellulose, as well as resins derived from *Hevea* rubber. The book is concluded with short chapters on solvents, plasticizers, molding and extrusion operations, and applications of synthetic resins in protective coatings.

This book is the first of its type, although the need for such a treatment has been evident for several years. It is not surprising, therefore, to encounter sins both of omission and of commission. For example, no mention is made of the use, during condensation, of compounds exhibiting a lower degree of functionality to control the properties of polysulfide rubbers, and the treatment accorded this matter under polyesters and polyamides is cursory. It is also the reviewer's opinion that the book would have benefited from inclusion of more information on natural polymers, such as wool and silk, in order to create a unified viewpoint with respect to high polymers of industrial importance. Such statements as "formaldehyde can also be produced by the catalytic oxidation of methane", page 59) and "This diffusion has been attributed to the shape of the molecule, which appears to be rod-shaped in solution and spherical in the emulsion" (page 161) should be taken *cum grano salis*. Minor errors, such as the sentence without a verb (on page 57), and "divinylacetylene" instead of vinylacetylene (on page 192), while unfortunate, are not sufficiently numerous to weaken the book. Despite these aberrations, the book can be highly commended as an introduction to a fascinating branch of technology which is growing rapidly and which is foreordained to play an important rôle in our future economy.

CHARLES F. FRYLING.

Principles and Applications of Electrochemistry. Volume I. Principles. By H. JERMAIN CREIGHTON. 4th edition. 477 pp. New York: John Wiley and Sons, Inc., 1943. Price: \$5.00. *Volume II. Applications.* By W. A. KOEHLER. 2nd edition. 573 pp. New York: John Wiley and Sons, Inc., 1943. Price: \$5.00.

Volume I is the fourth edition of Creighton's well-known and appreciated book on electrochemistry. The mere fact of the publication of the fourth edition nineteen years after the first appearance of the book proves that it has satisfied a definite need and that it has gained many friends.

Even though the added new material makes the text more or less up-to-date, the original character of the book has been maintained. It concentrates on classical electrochemistry and discusses the properties of electrolytes mainly on the basis of the theory of Arrhenius, although two chapters have been devoted to the modern theory of electrolytes. This disregard of the modern theory in the bulk of the text causes a certain inconsistency. For example, on page 38 (Table X) is given the "percentage dissociation" of solutions of various strong electrolytes at different concentrations, but on page 40 the qualitative discussion of the "modern theory of electrolytic dissociation" starts with the statement that "in solution the vast majority of salts and the strong acids and bases exist entirely as ions". The discussion of Table XI (page 53), dealing with the relation between dielectric constant and the dissociating power of solvents, needs a revision on the basis of activities. The classical discussion of "dilution formulas for strong electrolytes" (pages 295-9) might be omitted, while the "explanations of anomaly of strong electrolytes" (pages 299-301) could be substituted by a more modern treatment. The derivation of the equation of the electrode potential is identical with the one originally presented by Nernst. A more modern derivation in which the "osmotic pressure" of the ion is replaced by the activity would be preferable.

There is a certain advantage in the emphasis of the older literature and views. Many facts described in classical papers, and which have not yet been given a quantitative interpretation by the modern theory, might easily be ignored in a treatise based entirely on the modern theory.

The text contains a great deal of scientific and useful information. The problems at the ends of the chapters are well chosen and instructive.

Volume II, entitled "Applications", by Professor W. A. Koehler experiences its second

edition. It is intended as a textbook for students and as a reference work for persons in the industry. It is a unit in itself and could be used independent of Volume I. As a matter of fact, in Chapters II ("Review of theoretical electrochemistry") and XIV ("Electroanalysis") there is considerable overlapping with the material in Volume I. The book is well organized and contains much information of value to those for whom it is written. It gives a concise and well-illustrated description of the many applications of electrochemistry, without entering into the theoretical fundamentals. However, adequate references to journals and books enable the reader to find sources of discussion of the basic principles.

The two volumes together adequately cover the field,—“Principles and Applications of Electrochemistry.”

I. M. KOLTHOFF.

Magnetochemistry. By P. W. SELWOOD. ix + 287 pp.; 80 fig. New York: Interscience Publishing Company, 215 Fourth Avenue, 1943. Price: \$5.00.

This book is what it purports to be: namely, a book on magnetochemistry and not a book on magnetism in general. The author defines magnetochemistry as the “application of magnetic susceptibilities and closely related quantities to the solution of chemical problems.” He explains that he adopts this somewhat restricted definition in order to keep the volume within “reasonable bounds”, and adds that in consequence “No more than mention will be found of several branches of magnetism, particularly of magneto-optical phenomena, of the gyromagnetic effect, and of adiabatic demagnetization. . . . The field of atomic magnetism has been slighted so far as the theoretical side is concerned”. On the other hand, the author says he has tried to omit no major branch of magnetochemistry, as defined, and he has certainly kept his word. It is most illuminating to peruse the book and so realize how tremendously this subject has developed in the last decade. In the preface Professor Selwood notes that from 1934 to the end of 1942 over one thousand papers on magnetochemistry have appeared. These various articles are documented in the numerous footnotes. To workers in the field, the volume, quite apart from its other interests, would be worth while just as a bibliography. It is a truism that writing a volume of this character must have represented an enormously more difficult task than simply collecting one's own investigations in a book, as so many writers do. With such a complete bibliography, it is but natural that there be an occasional misclassification or error. For instance, Jordahl's work on copper is listed among the rare earths. Also, the reference on the measurements of Krishnan and collaborators on the anisotropy of gadolinium salts does not include the revisions they gave in a subsequent paper which reduce the anisotropy by a factor of the order 10 to a magnitude comparable with the theoretical value calculated by W. D. Lewis (*cf.* Phys. Rev. **57**, 1088 (1940); **59**, 770 (1941)).

The first chapter of the book is devoted to the measurement of magnetic susceptibility. Besides the standard classical methods, a discussion is included of determinations of magnetic moment by means of the catalysis of the ortho-para reaction of hydrogen. Chapters II and III treat atomic and molecular diamagnetism, with, naturally, emphasis on the behavior of complicated aromatic compounds. Chapters IV and V follow on atomic and molecular paramagnetism. A very complete discussion is included of paramagnetism as an indicator of free radicals. This is, of course, a field in which magnetic studies have been particularly instructive on moot chemical questions, and is perhaps the particular application which one thinks of first of all when the term “magnetochemistry” is mentioned. Chapter VI is devoted to complex compounds. The discussion is almost entirely on the basis of the Pauling electron pair. It would have been illuminating if more could have been said concerning what this model really means in terms of average electronic charge distribution—possibly with some correlation with molecular orbitals. For instance, $\text{Fe}(\text{CN})_6^{++}$ certainly cannot have as polar a structure as $\text{Fe}^{--} \cdots (\text{CN}^+)_6$, which is what would seem to be indicated by the Pauling model if taken too literally. Also, the author might properly have included some discussion of how the difference in behavior of cobalt and nickel compounds, or of six- and four-coördinated cobalt complexes, can be explained

in terms of inversion of the crystalline Stark pattern. Chapter VII treats metallic dia- and para-magnetism, while chapter VIII is concerned with ferromagnetism. Naturally in a chapter of twenty pages no attempt is made to cover the entire subject of ferromagnetism, and instead, emphasis is properly laid on the relation of ferromagnetism to alloy structure, etc.

Chapter IX, on applied magnetometric analysis, is perhaps the most interesting and unusual of the whole book. It is impressive to see how magnetism can be applied to the analysis of rare earths, metallurgical and mineralogical control, phase ratios and stoichiometry, and especially how it can even be used to provide information on the structure of catalytically active surfaces.

The viewpoint of the book inclines to the empirical rather than theoretical, the chemical rather than the physical, and the encyclopedic rather than the critical. The physicist will be rather terrified at the enumeration of chemical compounds, for instance, on page 70, and will probably not be interested in the magnetic properties of pentaerythritol tetraphenylether, as he will probably feel that the *modus operandi* of magnetism will be more lucid from the study of some less formidable compound. Also, the person interested in "why is ferromagnetism" will find only a sentence stating that the essential condition for it is that the wave functions of electrons in neighboring atoms should only slightly overlap each other near the nuclei. However, this emphasis in viewpoint is proper in view of the avowed purpose of the book. It is perhaps well to caution that theory has not explained completely the magnetic behavior of even such a simple solid as CeF_3 , so that the perfectionist will not get the same comfort from magnetochemistry as he does from spectroscopy. Nevertheless, it is perfectly possible for magnetism to furnish crude but illuminating information on a complicated reaction, even though the details are incomplete. Professor Selwood is to be congratulated on writing a book which fulfills a distinct need not covered by other volumes, and which is devoted to an interesting and growing field, for magnetochemistry has earned its right to stand beside the study of dielectric constant, spectra, and diffraction as a powerful tool for the chemist.

J. H. VAN VLECK.

DIFFUSION OF THE LOWER ALKYL SULFONIC ACIDS AND SOME LARGE MOLECULES

M. E. LAING McBAIN

Department of Chemistry, Stanford University, California

Received April 19, 1944

In a study of the diffusion of the higher paraffin chain sulfonic acids, it was found (3) that a minimum diffusion value occurred in regions below tenth molar for acids containing ten, eleven, twelve, thirteen and fourteen carbon atoms.

The present paper completes the range by reporting diffusion of the lower alkyl acids C_2 , C_5 , C_7 , and C_9 . This group corresponds to the ordinary soaps of shorter carbon chains and shows no minima, but smooth curves dropping from the high values at infinite dilution to values for C_9 comparable to those for sucrose¹.

EXPERIMENTAL

The double-ended diffusion cells pictured by McBain and Dawson (5) were used as described. The cell was wholly immersed in a thermostat at $25^\circ\text{C} \pm 0.02^\circ$. The diffusion constants (D) are integral values, since one compartment was always filled with pure solvent, and are expressed in square centimeters per day. Concentrations for aqueous solutions were in molality, and those in non-aqueous solvents in grams per 100 g. of solvent. The sulfonic acids were those made by McMillan and used in 1939 for the conductivity studies. The small quantity of material available limited the number of experiments. However, each number in table 1 is usually a mean of two duplicate sets of diffusions with any one concentration.

RESULTS AND DISCUSSION

Other high-molecular-weight compounds of obviously complex structure were also used in an endeavor to obtain some correlation between structure and diffusing power. However, the results are disappointing in that the effects noted are not consistent. For example, an increase in carbon chain by the addition of one CH_2 to the plant hormones gives an increase instead of a decrease, but when a second CH_2 group is added there is a decrease. If an acid group is added to taurine, giving cysteic acid, the diffusion is reduced to half. The diffusion of β -phenylpropionic acid is the same as that of the simpler acetic acid. Fastest of all is indolepropionic acid, and slowest is the next homologue, indolebutyric acid.

The results are collected in the following tables, and those obtained with the series of alkyl sulfonic acids are shown in figure 1.

¹ Compare the graph in the paper by McBain and Salmon (Proc. Roy. Soc. (London) **97**, 53 (1920)) and more recently one in a paper by McBain, Dye, and Johnston (J. Am. Chem. Soc. **61**, 3212, graph 2 (1939)).

Table 1 and figure 1 show the family of lower sulfonic acids. It is clearly seen that, as is shown also by the conductivity curves, these acids of lower carbon content behave more like ordinary electrolytes in solution. Their diffusion constants, except in great dilution, lie between those of potassium chloride and sucrose. However, in contrast to the results obtained with strong electrolytes such as hydrochloric acid or potassium chloride, the diffusion coefficients for moderate concentrations lie far below those at infinite dilution (4).

Table 2 shows the diffusion constants of certain plant hormones. These weak acids are not very soluble, and their saturated solutions give the expected high diffusion of dilute solutions. It is seen that the sodium salt of β -indoleacetic acid is not only more soluble, but its diffusion is likewise increased, as in the parallel case of acetic acid and sodium acetate.

Table 3 records the diffusion of some large molecules that promised to be of interest for the development of diffusion theory. The cationic active colloidal electrolyte octyltrimethylammonium bromide has a diffusion (0.75) comparable

TABLE 1
Diffusion of sulfonic acids of chain length C_2 to C_9

C_2		C_4		C_7		C_9	
Concentration	D	Concentration	D	Concentration	D	Concentration	D
0.043	2.40	0.036	1.73	0.020	1.86	0.014	0.852
0.085	2.02			0.09	1.19	0.075	0.846
0.127	1.69	0.111	1.42			0.141	0.699
0.230	1.44	0.187	1.20	0.203	1.01	0.241	0.548
		0.320	1.18	0.313	0.96	0.315	0.509
0.535	1.45	0.566	1.14	0.490	0.762	0.476	0.512
0.993	1.47	1.10	1.15	0.933	0.782	(No more material)	

to that of the colloidal electrolyte laurylsulfonic acid (0.75) over most of its range of concentration. The value of the typical soap, potassium laurate, is 0.70 in 0.5 per cent solution but then falls to a nearly constant value of 0.45 in higher concentrations.

The long chain polymer ω -hydroxydecanoic acid was kindly sent to the author by Drs. Kraemer, van Natta, and Corotias in 1939 (1). Its molecular weight had been determined as 25,000 by direct titration and as 27,000 by centrifugal sedimentation equilibrium. The diffusion was first measured in the single Northrup cell, using carbon tetrachloride as solvent. A 0.392 per cent solution gave two measurements, $D = 0.038$ and $D = 0.068$, in which the amounts diffused in 48 hr. were only 4 to 6 mg., obtained by weight after evaporation to dryness.

For an uncharged sphere the Einstein equation predicts the value $D = RT/N6\pi\eta r$. Assuming a density of 0.85 and viscosity at 25°C. of 0.0090, r of the spherical particle becomes 23 Å. and D becomes 0.092, which is only 2.4 to 1.4 times faster than the two numbers observed.

The diffusion was next taken in chloroform in the double-ended cell, which is more accurate when volatile solvents are used. The two values obtained were $D = 0.219$ and $D = 0.189$. Making a similar calculation, using the viscosity of chloroform at 25°C. as 0.00542, we predict a diffusion of 0.154, which is slower than the observed diffusion, 0.204. Both these results indicate that the re-

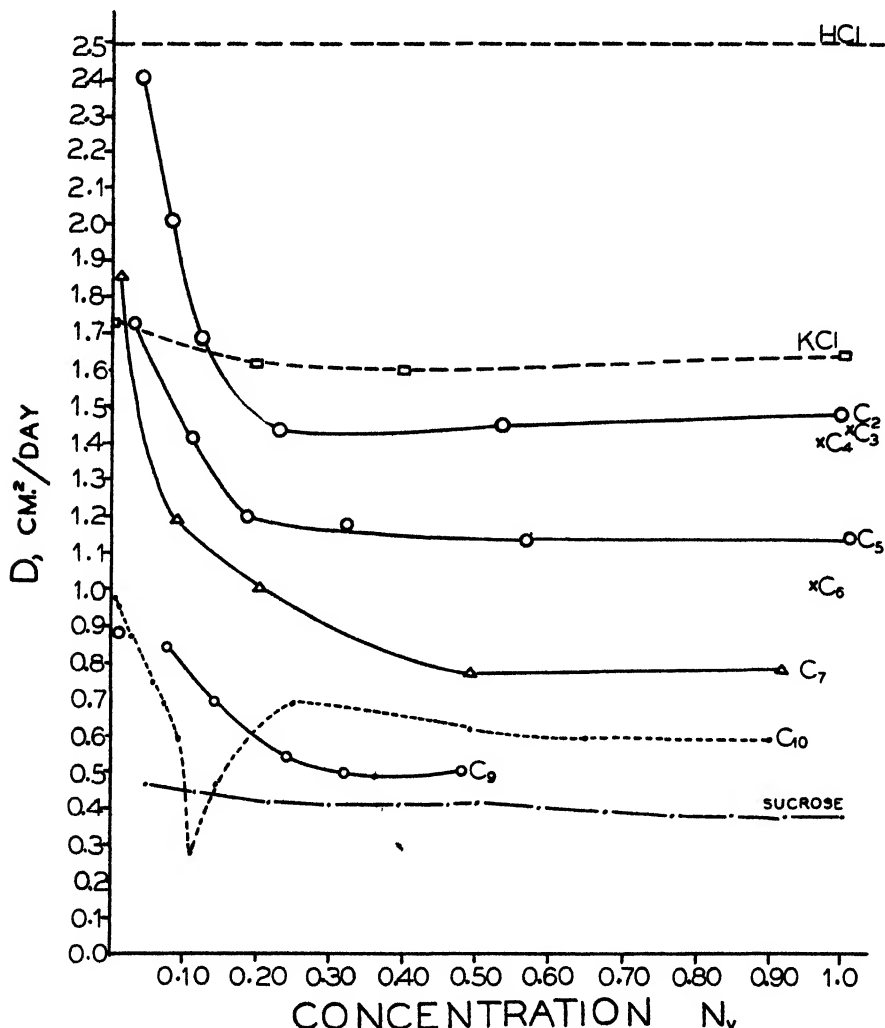


FIG. 1. Diffusion of lower alkyl sulfonic acids

sistence to diffusion of this polymer is much more nearly that of a spherical particle than the long comparatively rigid rods originally postulated by Staudinger.

The long amino acid dipole ξ -trimethylpentadecabetaïne was kindly given to us by Professor R. Kuhn (2), who had shown it to have such an extraordinarily

TABLE 2
Diffusion of saturated aqueous solutions of certain plant hormones

NAME	FORMULA	CONCENTRATION	DIFFUSION*
		<i>per cent</i>	
β -Indoleacetic acid.....	ICH_2COOH	0.051	0.87 0.81
Sodium salt of above.....	ICH_2COONa	0.14	0.99 0.92
β -Indolepropionic acid.....	$\text{ICH}_2\text{CH}_2\text{COOH}$	0.043	1.07 1.08
γ -Indolebutyric acid.....	$\text{ICH}_2\text{CH}_2\text{CH}_2\text{COOH}$	0.029	0.561 0.530
β -Phenylpropionic acid.....	$\text{C}_6\text{H}_5\text{CH}_2\text{CH}_2\text{COOH}$	0.030	0.708 0.727

* That of acetic acid (*International Critical Tables*, Vol. V, p. 69 (1929)) is 0.7; that of sodium acetate 0.74.

TABLE 3
Diffusion of other large molecules

NAME	FORMULA	CONCENTRATION	SOLVENT	DIFFUSION
		<i>per cent</i>		
Taurine.....	$\text{CH}_3\text{SO}_3\text{H}$ CH_2NH_2	1	Water	1.156 1.104 1.200
Cysteic acid.....	$\text{CH}_3\text{SO}_3\text{H}$ $\text{CH}(\text{NH}_2)$ COOH	1	Water	0.567 0.526
Octadecyltrimethylammonium bromide	$(\text{C}_{18}\text{H}_{37}\text{N}(\text{CH}_3)_3)^+\text{Br}^-$	1.232	Water	0.754 0.725 0.765
ω -Hydroxydecanoic acid, (25,000) long-chain polymer	$\text{HO}((\text{CH}_2)_9\text{COO})_{150}\text{H}$	0.39	Carbon tetrachloride	0.038 0.068
		0.75	Chloroform	0.219 0.189
ξ -Trimethylpentadecabetaïne	CH_3 $\text{CH}_3-\text{N}^+(\text{CH}_2)_{15}\text{COO}^- \cdot 3\text{H}_2\text{O}$ CH_3	1.29	Methyl alcohol	0.661 0.667
		1.408	Methyl alcohol	0.621

high dipole moment in alcohol that to account for it the molecule had to be stretched out to a straight zwitter ion of the formula $(\text{H}_3\text{C})_8^+\text{N}(\text{CH}_2)_{14}\text{COO}^-$. The Einstein value for a sphere of betaine would be 0.31, but since methyl alcohol is used as solvent and its molecules are relatively large, the Sutherland value 0.47 should be substituted. Even so, the observed diffusion 0.66 is much *faster*, which must be due to the influence of the free gegen ion accompanying each end of the elongated zwitter ion.

SUMMARY

The diffusion of the lower members of the family of alkyl sulfonic acids is reported. These lower members do not show the characteristic minima of colloidal electrolytes, but resemble half-strong electrolytes.

The diffusion of other large molecules is given, the values indicating that even large long molecules roll into spheres when given an opportunity to diffuse, and that the separated charges on zwitter ions are accompanied in diffusion by free gegen ions.

REFERENCES

- (1) KRAEMER, E. O., AND VAN NATTA, F. J.: *J. Phys. Chem.* **36**, 3175 (1932).
- (2) KUHN, R., AND GEROIL, F.: *Ber.* **67B**, 1130 (1934).
- (3) MCBAIN, E. L.: *Proc. Roy. Soc. (London)* **170**, 415 (1939).
- (4) MCBAIN, J. W.: *J. Phys. Chem.* **43**, 671 (1939).
- (5) MCBAIN, J. W., AND DAWSON, C. R.: *Proc. Roy. Soc. (London)* **A148**, 32 (1935).

THE TERNARY SYSTEM *n*-BUTYL ALCOHOL-BENZENE-WATER AT 25°C. AND 35°C.

E. ROGER WASHBURN AND CARL V. STRANDSKOV

Avery Laboratory of Chemistry, University of Nebraska, Lincoln, Nebraska

Received May 3, 1944

The ternary system made up of benzene, water, and methyl alcohol has been described by J. Barbaudy (1). The related systems containing ethyl alcohol (7) and isopropyl alcohol (4) in place of the methyl alcohol have also been investigated. A rather complete list of other ternary systems made up of similar materials has been compiled by J. C. Smith (5). This report adds to these studies the results of an investigation of the system containing benzene, *n*-butyl alcohol, and water.

MATERIALS AND APPARATUS

Reagent quality benzene from Coleman and Bell was thoroughly dried with sodium and subjected to several fractional crystallizations. The portion which was used had a freezing point of 5.45°C.

The better grade of *n*-butyl alcohol furnished by Eastman Kodak Co. was carefully dried by refluxing over active lime. It was then fractionally distilled through an all-glass apparatus. The fraction which was used had a specific gravity, d_4^{25} , of 0.80649.

Distilled water was redistilled through a tin condenser from an alkaline permanganate solution.

The purified liquids were kept in all-glass storage bottles fitted with burets. Samples were removed by the application of pressure through a side arm protected with soda lime and glass wool.

The solubility measurements were carried out in 50-ml. glass-stoppered volumetric flasks which were mounted in a mechanical shaker in a constant-temperature bath. During the solubility measurements the temperature of the bath did not vary from 25°C. (or 35°C.) by more than $\pm 0.05^\circ\text{C}$. For the measurements of refractive index to be used in the tie-line studies and in the study of the conjugate solutions the temperature was controlled to $\pm 0.01^\circ\text{C}$.

The refractive indices were measured with an Abbe refractometer which was kept at the desired temperature by the circulation of water from the constant-temperature bath.

Calibrated weights and thermometers were employed and experimental precautions were taken to insure that the visual recognition of the end point in the solubility titrations would be the chief factor in determining the accuracy of the measurements.

PROCEDURE AND RESULTS

The experimental procedure was essentially the same as described previously (6). The solubilities were determined by titration of weighed solutions to the appearance of a permanent second liquid phase. The titrant was added from a pipet the stem of which was drawn out as a fine capillary; the amount added was determined by weight. The total weights of the solutions at the end point varied from 18 g. to 25 g. for the different titrations. Benzene was the titrant for the ternary solutions containing less than 1 per cent benzene; water was the titrant in all other ternary solutions. A preliminary study with unpurified materials was made so that in the final study a close approximation to the necessary concentrations could be made at the start of the titration and prolonged dropwise additions could be avoided.

As the appearance of the end point varied somewhat as the concentrations were varied, opportunity was provided to study the solutions with both reflected and transmitted light and with a light or dark background.

The measurements of refractive index were made immediately following the final weighing of the solubility measurement.

The tie-lines were determined by adding alcohol in varying amounts to mixtures of benzene and water. The refractive indices of the conjugate layers were determined after equilibrium at the desired temperature was reached. The concentration of each of the three components in each of the two layers was then read from curves plotted from data obtained in the solubility study. These curves

TABLE 1
Ternary solubility data at 25.0°C.

n-BUTYL ALCOHOL	BENZENE	REFRACTIVE INDEX	n-BUTYL ALCOHOL	BENZENE	REFRACTIVE INDEX
<i>weight per cent</i>	<i>weight per cent</i>		<i>weight per cent</i>	<i>weight per cent</i>	
9.88	89.81	1.4840	56.45	37.20	1.4268
16.56	82.63	1.4758	59.55	33.43	1.4230
21.19	77.55	1.4699	63.97	27.58	1.4171
25.46	72.98	1.4650	69.60	20.11	1.4100
33.06	64.32	1.4557	74.80	11.99	1.4017
40.06	56.58	1.4474	78.40	4.72	1.3938
43.97	51.88	1.4424	3.58	0.30	1.3356
51.08	43.42	1.4336	2.37	0.20	1.3345
n-Butyl alcohol saturated with water			79.73% alcohol (2)		1.3878
Water saturated with n-butyl alcohol			92.65% water (2)		1.3390
Benzene saturated with water			99.93% benzene (3)		1.4958
Water saturated with benzene			99.85% water (3)		1.3322

TABLE 2
Ternary solubility data at 35.0°C.

n-BUTYL ALCOHOL	BENZENE	REFRACTIVE INDEX	n-BUTYL ALCOHOL	BENZENE	REFRACTIVE INDEX	
<i>weight per cent</i>	<i>weight per cent</i>		<i>weight per cent</i>	<i>weight per cent</i>		
6.81	92.90	1.4830	56.26	36.99	1.4226	
11.29	88.25	1.4780	60.71	31.04	1.4168	
16.32	82.96	1.4720	68.29	20.71	1.4072	
23.79	74.67	1.4626	74.06	11.51	1.3978	
33.89	63.62	1.4508	77.47	5.25	1.3918	
40.63	55.76	1.4420	5.08	0.28	1.3362	
46.07	49.13	1.4355	1.90	0.18	1.3329	
n-Butyl alcohol saturated with water			78.94% alcohol (2)			1.3850
Water saturated with n-butyl alcohol			93.17% water (2)			1.3377
Benzene saturated with water			99.90% benzene (3)			1.4915
Water saturated with benzene			99.84% water (3)			1.3313

TABLE 3
Conjugate solutions at 25.0°C.

WATER LAYER			BENZENE LAYER		
Refractive index	n-Butyl alcohol	Water	Refractive index	n-Butyl alcohol	Benzene
	<i>weight per cent</i>	<i>weight per cent</i>		<i>weight per cent</i>	<i>weight per cent</i>
1.3340	1.9 x	97.9	1.4930	2.4 x	97.6
1.3346	2.5	97.3	1.4900	4.9	95.1
1.3350	2.9	96.9	1.4883	6.3	93.6
1.3356	3.5 x	96.2	1.4786	14.2 x	85.2
1.3359	3.8 x	95.9	1.4654	25.2 x	73.4
1.3362	4.1	95.6	1.4565	32.4	65.1
1.3366	4.5 x	95.1	1.4478	39.7 x	56.9
1.3369	4.9	94.8	1.4410	45.1	50.5
1.3371	5.0	94.6	1.4350	50.0	44.8
1.3373	5.3 x	94.4	1.4280	55.6 x	38.3
1.3375	5.5	94.2	1.4226	59.8	33.1
1.3377	5.8	93.9	1.4184	63.0	28.9
1.3379	6.0 x	93.7	1.4150	65.7 x	25.4
1.3383	6.4	93.3	1.4010	75.2	11.3
1.3385	6.7 x	93.1	1.3950	77.9 x	5.8

TABLE 4
Conjugate solutions at 35.0°C.

WATER LAYER			BENZENE LAYER		
Refractive index	<i>n</i> -Butyl alcohol	Water	Refractive index	<i>n</i> -Butyl alcohol	Benzene
	<i>weight per cent</i>	<i>weight per cent</i>		<i>weight per cent</i>	<i>weight per cent</i>
1.3328	1.7	98.1	1.4870	3.6	96.2
1.3338	2.7	97.0	1.4810	8.6	91.0
1.3342	3.1	96.6	1.4732	15.3	84.1
1.3345	3.5	96.3	1.4657	21.3	77.4
1.3348	3.8	96.0	1.4568	28.8	69.3
1.3350	4.0	95.7	1.4500	34.6	62.9
1.3354	4.4	95.3	1.4405	41.9	54.3
1.3356	4.6	95.1	1.4310	49.7	44.9
1.3359	4.9	94.8	1.4248	54.6	39.1
1.3361	5.1	94.6	1.4195	58.7	33.8
1.3363	5.3	94.5	1.4121	64.5	26.0
1.3368	5.8	94.0	1.4054	69.4	19.0
1.3374	6.5	93.5	1.3940	76.4	7.5

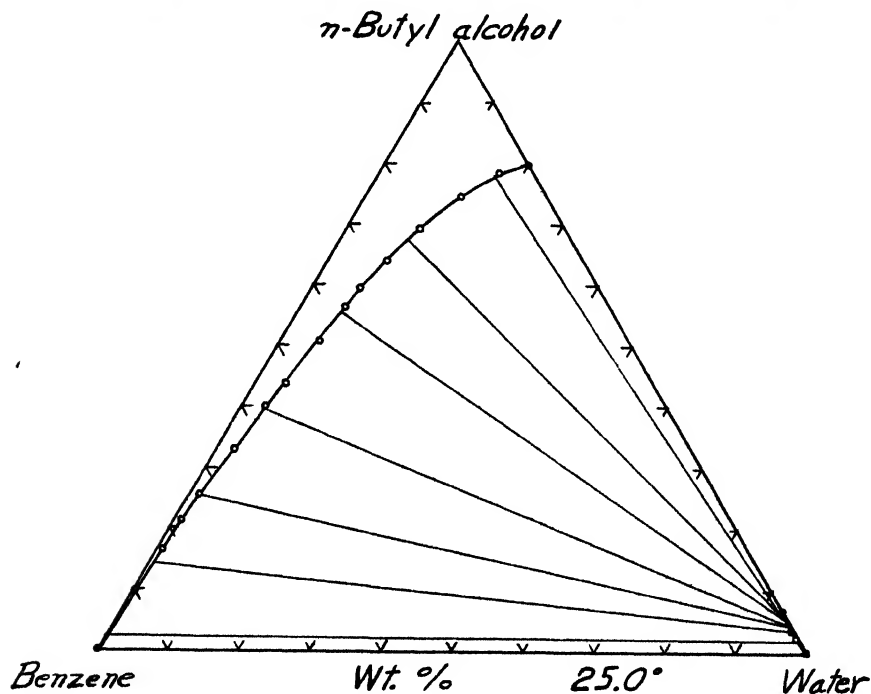


FIG. 1. The System *n*-butyl alcohol-benzene-water at 25.0°C.

were of such a size that 1.0 mm. on the abscissa represented 0.0001 in refractive index and 1.0 mm. on the ordinate represented 0.1 per cent by weight. The sum of the three percentages for any one liquid was 100.0 ± 0.1 .

The results of the solubility determinations are recorded in tables 1 and 2, while the distribution, or tie-line, data are given in tables 3 and 4. In these tables the concentrations are given in per cent by weight. The concentrations in table 1 and those marked x in table 3 (for 25.0°C.) are plotted in figure 1.

This system differs from many of those made up of similar liquids in that the alcohol and water, as well as the hydrocarbon and water, have limited miscibility in each other at the temperatures employed. It represents the opposite of the methyl alcohol-cyclohexane-water system (8), in which the alcohol and the hydrocarbon, cyclohexane, display limited solubility. A study of the concentration of the alcohol in the conjugate solutions shows that as the total amount of alcohol is increased the proportion going into the benzene-rich layer increases continuously. For example, at 25.0°C. the ratio of the concentration of alcohol in the benzene-rich layer to that in the water-rich layer is 1.26 for the first pair, while for the last pair recorded the ratio is 12.4. It suggests that if much smaller total proportions of alcohol had been studied the greater proportion would have entered the water-rich layer, as is usually experienced with the lower alcohols. In other words, the same sort of reversal of slope of tie-lines that was observed for the isopropyl alcohol-benzene-water system (4) probably would be experienced but at much lower concentrations.

SUMMARY

The ternary solubility diagrams, including tie-lines, have been determined for the system *n*-butyl alcohol-benzene-water at 25.0°C. and 35.0°C.

REFERENCES

- (1) BARBAUDY, J.: *Compt. rend.* **182**, 1279 (1926).
- (2) HILL, A. E., AND MALISOFF, W. M.: *J. Am. Chem. Soc.* **48**, 918 (1926).
- (3) *International Critical Tables of Numerical Data*, Volume III, p. 389. The McGraw-Hill Book Company, Inc., New York (1926).
- (4) OLSEN, ALLEN L., AND WASHBURN, E. ROGER: *J. Am. Chem. Soc.* **57**, 303 (1935).
- (5) SMITH, J. C.: *Ind. Eng. Chem.* **34**, 234 (1943).
- (6) WASHBURN, E. ROGER, AND BEGUIN, A.: *J. Am. Chem. Soc.* **62**, 579 (1940).
- (7) WASHBURN, E. ROGER, HNIZDA, V., AND VOLD, R.: *J. Am. Chem. Soc.* **53**, 3237 (1931).
- (8) WASHBURN, E. ROGER, AND SPENCER, H. C.: *J. Am. Chem. Soc.* **56**, 361 (1934).

PARTICLE-SIZE DISTRIBUTIONS BY CENTRIFUGAL
SEDIMENTATION

CALLAWAY BROWN

*Bell Telephone Laboratories, Inc., 485 West Street, New York 14, New York**Received March 28, 1944*

Sedimentation methods for the determination of particle-size distributions are applicable to suspensions of particles ranging in size all the way from molecular dimensions to sieve sizes of 50 microns or more. The theoretical basis for the determination of the particle-size distribution in a suspension of particles settling under gravity according to Stokes' law was established by Odén and a number of efficient applications are available (5). For suspensions containing a large proportion of particles as small as 1 micron, the rate of settling under gravity becomes so slow that use of the stronger settling force afforded by the centrifuge is desirable. The development of the ultracentrifuge (8) and its application to particle-size analysis have opened a whole new field in fundamental chemistry. The ultracentrifuge is a highly specialized tool, however, and it is primarily designed for the study of particles smaller than 0.1 micron.

A variety of centrifugal methods have been applied to the intermediate particle-size range from 0.1 to 2 microns. Continuous sedimentation in the hollow, rotating-cylinder type of centrifuge (1) allows particle-size fractionation as well as analysis (2) to be carried out. Use of the beaker-type centrifuge is more convenient for control tests or in cases where separation of particle-size fractions is not necessary. Analysis of sedimentation data may be simplified by the use of a long-armed centrifuge (4), so that the centrifugal force on all particles is approximately the same and the analysis reduces to that for gravity settling. Another device for simplifying the analysis consists in floating the suspension to be centrifuged on a relatively long column of a denser liquid (3) so that all particles settle essentially the same distance in reaching the bottom of the centrifuge tube.

Direct application of Odén's line of reasoning on gravitational sedimentation to centrifugal sedimentation in a beaker-type or simple cup-type centrifuge has been carried out by Romwalter and Vendl (6). Their analysis apparently solves the problem of calculating the particle-size distribution in a suspension from experimental values of the weight fraction of the suspended particles sedimented by a beaker-type centrifuge running at constant speed, free from vibration, for a series of time intervals. Their treatment, however, appears to involve an incorrect step which renders their solution invalid, as is shown below. The purpose of this paper is to present an alternative treatment which offers a complete solution to the problem in theory. On the basis of the treatment presented, it is proposed that experimental values be determined for the weight fraction of suspended particles sedimented by a beaker-type centrifuge running at constant speed for a suitable *fixed* time interval with varying quantities of suspension in the centrifuge tubes. Particle-size analyses may also be made by determination

of a series of sedimentation-time curves with various quantities of suspension in the centrifuge tubes.

THEORETICAL

The weight fraction sedimented

Particles settling under centrifugal force follow paths radial to the centrifuge axis instead of parallel paths as in gravity settling. For strictly convection-free centrifuging, therefore, sector-shaped centrifuge tubes are essential (8). Figure 1 illustrates the conditions of sedimentation in a sector-shaped tube. The centrifuge rotates free from vibration about its axis, *A*, at constant speed. The suspension fills the sector-shaped tube from the bottom, *R* cm. distant from the axis, to the meniscus, *S* cm. from the axis. A particle *X* cm. from the axis moves outward at a speed determined by the balance between its continually increasing centrifugal force and the Stokes' law force resisting its motion through the dispersion medium.

$$V = \frac{dX}{dt} = \frac{d_1 - d_0}{18\eta} D^2 \omega^2 X \quad (1)$$

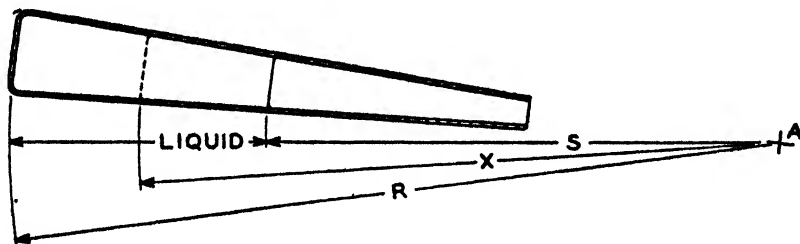


FIG. 1. Centrifugal sedimentation in a sector-shaped tube

where $V = \frac{dX}{dt}$ = outward velocity of particle,

d_1 = density of particle,

d_0 = density of suspension medium,

η = coefficient of viscosity of medium,

D = equivalent spherical diameter of particle, and

ω = speed of rotation of centrifuge in radians per second.

For convenience, let

$$\frac{d_1 - d_0}{18\eta} \omega^2 = b$$

so that

$$\frac{dX}{dt} = bD^2 X \quad (1a)$$

The diameter, D_m , of a particle which starts at the top of the suspension ($X = S$) and just reaches the bottom of the tube ($X = R$) at the end of a fixed time, t

seconds, may be determined by integration of equation 1a between the limits $X = S$ to $X = R$ and $t = 0$ to $t = t$.

$$\ln R/S = bD_m^2 t \quad (2)$$

At the end of t seconds all particles of diameter $D \geq D_m$ have reached the bottom of the tube. In addition, all particles of diameter $D < D_m$ have been partially sedimented. For each particle of diameter $D < D_m$ there exists a starting point, $X = X_0$, such that the particle just reaches $X = R$ at the fixed time, t . The distance X_0 is determined by similar integration of equation 1a:

$$\ln R/X_0 = bD^2 t \quad (3)$$

or

$$X_0 = R e^{-bD^2 t} \quad (3a)$$

Particles of diameter D will be sedimented if at the beginning of the centrifuging they are at a point $X \geq X_0$. The volume to any point X within flat sector-shaped tubes is proportional to $R^2 - X^2$. The sedimented fraction of particles of diameter D is therefore:

$$\frac{R^2 - X_0^2}{R^2 - S^2} = \frac{R^2}{R^2 - S^2} (1 - e^{-2bD^2 t}) \quad (4)$$

Define the particle-size distribution function $F(D)$ so that $F(D) dD$ is the weight fraction of particles with diameters between D and $D + dD$. The weight fraction represented by the sedimented fraction of particles with diameters between D and $D + dD < D_m$ is:

$$\frac{R^2 - X_0^2}{R^2 - S^2} F(D) dD = \frac{R^2}{R^2 - S^2} (1 - e^{-2bD^2 t}) F(D) dD \quad (5)$$

The weight fraction of all particles with diameters $D \geq D_m$ (100 per cent sedimented) is $\int_{D_m}^{\infty} F(D) dD$. The total weight fraction sedimented is:

$$p = \int_{D_m}^{\infty} F(D) dD + \int_0^{D_m} \frac{R^2}{R^2 - S^2} (1 - e^{-2bD^2 t}) F(D) dD \quad (6)$$

Incorrect use of the slope to the sedimentation-time curve

The treatment to this point is identical in principle with that of Romwalter and Vendl (6). At this point they advocate the determination of p , the weight fraction sedimented, after centrifuging for a series of time intervals and use of the slope, $\partial p / \partial t$, of the sedimentation-time curve for calculation of the distribution function. They differentiate equation 6 with respect to time to obtain:

$$\begin{aligned} \frac{\partial p}{\partial t} = & -\frac{\partial D_m}{\partial t} F(D_m) + \frac{\partial D_m}{\partial t} F(D_m) \frac{R^2}{R^2 - S^2} (1 - e^{-2bD_m^2 t}) \\ & + \int_0^{D_m} \frac{R^2}{R^2 - S^2} e^{-2bD^2 t} 2bD^2 F(D) dD \quad (7) \end{aligned}$$

From equation 2, $e^{-2bD_m^2 t} = S^2/R^2$ and therefore

$$\frac{R^2}{R^2 - S^2} (1 - e^{-2bD_m^2 t}) = 1$$

so that the first two terms of equation 7 cancel, leaving:

$$\frac{\partial p}{\partial t} = \int_0^{D_m} \frac{R^2}{R^2 - S^2} e^{-2bD^2 t} 2bD^2 F(D) dD \quad (7a)$$

From equations 3 and 3a it follows that

$$e^{-2bD^2 t} = S^2/R^2 \quad \text{and} \quad 2bD^2 = \frac{1}{t} \ln R^2/S^2$$

when $D = D_m (X_0 = S)$. Romwalter and Vendl substitute these particular values for the two functions in equation 7a, obtaining:

$$\frac{\partial p}{\partial t} = \int_0^{D_m} \frac{R^2}{R^2 - S^2} \frac{S^2}{R^2} \frac{1}{t} \ln R^2/S^2 F(D) dD \quad (7b)$$

Since only $F(D)$ varies with D in equation 7b,

$$\frac{R^2 - S^2}{S^2} \frac{t}{\ln R^2/S^2} \frac{\partial p}{\partial t} = \int_0^{D_m} F(D) dD \quad (7c)$$

apparently gives the distribution function in terms of R , S , t and the slope to the sedimentation-time curve.

Since $e^{-2bD^2 t}$ and $2bD^2$ are functions variable with D , there is no reason for substituting the particular values at $D = D_m$ in equation 7a, and equation 7c is therefore invalid. Equation 7a is the correct expression for the slope of the sedimentation-time curve, but an exact solution for the distribution function seems to be extremely difficult if not impossible to obtain.

Suspension level as a variable for particle-size analysis

The complications arising from differentiation of equation 6 with respect to time may be avoided if, instead of determination of the fraction sedimented after centrifuging for a series of time intervals, the fractions sedimented after a given time interval with the centrifuge tubes filled with suspension to a series of levels are determined; that is, if S instead of t is varied (figure 1). On increasing S , an increasingly large fraction of the suspended particles will be sedimented in a given time.

Differentiate equation 6 with respect to S to obtain:

$$\begin{aligned} \frac{\partial p}{\partial S} = & -\frac{\partial D_m}{\partial S} F(D_m) + \frac{\partial D_m}{\partial S} F(D_m) \frac{R^2}{R^2 - S^2} (1 - e^{-2bD_m^2 t}) \\ & + \int_0^{D_m} \frac{2R^2 S}{(R^2 - S^2)^2} (1 - e^{-2bD^2 t}) F(D) dD \quad (8) \end{aligned}$$

As for equation 7, the first two terms of equation 8 cancel, leaving:

$$\frac{\partial p}{\partial S} = \int_0^{D_m} \frac{2R^2 S}{(R^2 - S^2)^2} (1 - e^{-2SD^2}) F(D) dD \quad (8a)$$

Since $\frac{2S}{R^2 - S^2}$ is independent of D ,

$$\frac{R^2 - S^2}{2S} \frac{\partial p}{\partial S} = \int_0^{D_m} \frac{R^2}{R^2 - S^2} (1 - e^{-2SD^2}) F(D) dD \quad (8b)$$

From equation 6, the right-hand term of equation 8b is

$$p - \int_{D_m}^{\infty} F(D) dD$$

and by definition of $F(D)$,

$$\int_0^{D_m} F(D) dD + \int_{D_m}^{\infty} F(D) dD = 1$$

so that

$$\int_0^{D_m} \frac{R^2}{R^2 - S^2} (1 - e^{-2SD^2}) F(D) dD = -(1 - p) + \int_0^{D_m} F(D) dD \quad (6a)$$

Combining equations 6a and 8b we obtain:

$$\frac{R^2 - S^2}{2S} \frac{\partial p}{\partial S} + (1 - p) = \int_0^{D_m} F(D) dD \quad (8c)$$

Thus, if p is determined for a series of values of S , measurement of the slope of the p vs. S curve allows calculation of $\int_0^{D_m} F(D) dD$, the weight fraction of particles with diameters less than D_m . To each value of S there corresponds a value of D_m (equation 2), so the distribution of particle sizes may be determined in the range of D_m covered by the p vs. S curve.

Just as in gravity sedimentation (5), second derivatives of the fraction sedimented are required to obtain the distribution function itself. To obtain $F(D_m)$ in terms of second derivatives of p , differentiate equation 8c with respect to S :

$$\frac{R^2 - S^2}{2S} \frac{\partial^2 p}{\partial S^2} - \frac{R^2 + 3S^2}{2S^2} \frac{\partial p}{\partial S} = \frac{\partial D_m}{\partial S} F(D_m) \quad (9)$$

From equation 2

$$\frac{\partial D_m}{\partial S} = -\frac{D_m}{2S \ln R/S}$$

so that

$$\frac{\ln R/S}{D_m} \left[\frac{R^2 + 3S^2}{S} \frac{\partial p}{\partial S} - (R^2 - S^2) \frac{\partial^2 p}{\partial S^2} \right] = F(D_m) \quad (9a)$$

Similarly, the distribution function may be obtained in terms of $\partial^2 p / \partial S \partial t$ and $\partial p / \partial t$ by differentiation of equation 8c with respect to time:

$$\frac{R^2 - S^2}{2S} \frac{\partial^2 p}{\partial S \partial t} - \frac{\partial p}{\partial t} = \frac{\partial D_m}{\partial t} F(D_m) \quad (10)$$

From equation 2

$$\frac{\partial D_m}{\partial t} = -\frac{D_m}{2t}$$

so that

$$\frac{2t}{D_m} \left[\frac{\partial p}{\partial t} - \frac{R^2 - S^2}{2S} \frac{\partial^2 p}{\partial S \partial t} \right] = F(D_m) \quad (10a)$$

Three distinct methods are therefore available for calculating the distribution of particle sizes in a suspension if the weight fraction sedimented is determined with sector-shaped centrifuge tubes filled to a series of levels. First, the weight fraction of particles smaller than a known diameter may be calculated from equation 8c and the distribution function determined from the slope of the cumulative weight per cent curve. Second, the distribution function may be calculated directly in terms of the first and second derivatives of the fraction sedimented with respect to the length of the column of suspension centrifuged by use of equation 9a. Or third, from sedimentation-time curves at a series of levels, the distribution function may be calculated by use of equation 10a. In all cases the range of particle sizes covered is that of D_m as calculated from equation 2.

Comparison of equations for centrifugal and gravity sedimentation

The height of the column of suspension containing the particles to be sedimented may also be used as a variable for gravitational sedimentation, although less convenient experimentally than sedimentation-time determinations. It is of interest that analysis similar to the above gives the following equations for gravitational sedimentation:

$$-h \frac{\partial p}{\partial h} + (1 - p) = \int_0^{D_m} F(D) dD \quad (11)$$

$$-\frac{2h}{D_m} \left[2 \frac{\partial p}{\partial h} + h \frac{\partial^2 p}{\partial h^2} \right] = F(D_m) \quad (12)$$

and

$$\frac{2t}{D_m} \left[\frac{\partial p}{\partial t} + h \frac{\partial^2 p}{\partial t \partial h} \right] = F(D_m) \quad (13)$$

where h is the height of the uniform column of suspension containing particles settling under gravity, p is the weight fraction sedimented after time t , and D_m is the size of the smallest particles 100 per cent sedimented. Centrifugal sedimentation reduces to gravitational sedimentation when the length of the cen-

trifuge arm is very great compared with the length of the column of suspension. Reference to equation 8c shows that if $(R + S)/2S$ approaches unity, equation 8c reduces to equation 11, since $R - S = h$ and $dS = -dh$. Similarly, equation 9a reduces to equation 12, since the limit as S approaches R of

$$\frac{R \ln R/S}{R - S} = 1$$

and equation 10a reduces to equation 13.

Cylindrical centrifuge tubes

The use of a simple beaker-type centrifuge with cylindrical tubes is often desirable for particle-size control tests. Many ordinary laboratory centrifuges such as the International clinical centrifuge run remarkably free from vibration when properly balanced, but they are designed for cylindrical centrifuge tubes and require modification if sector-shaped tubes are to be used. In addition, sector-shaped tubes require careful machining for accuracy and are practically impossible to obtain as glass vessels. If cylindrical tubes are used, a fraction of the suspended particles settling under centrifugal force will strike the walls of the tube obliquely, owing to the paths of sedimentation radiating from the axis of rotation. Two effects which partially balance each other may result: (1) Some particles strike the cylindrical walls of the tube before they would reach the bottom of the tube through free sedimentation, agglomerate with similar particles at the wall, and the resulting aggregate is sedimented faster than under free sedimentation; and (2) convection currents result from the oblique force of the suspension on the walls of the tube. Convection currents from this and other sources (temperature gradients, vibration, etc.) may cause some particles to be sedimented faster than under convection-free sedimentation, but it seems probable that the net effect is to decrease the fraction of the suspended particles which are sedimented.

If the length of the column of suspension is kept reasonably small compared to the distance of the bottom of the tube from the axis of rotation,—for example, less than $\frac{1}{2}(S > \frac{1}{2} R$, figure 1),—cylindrical tubes will probably give particle-size analyses of sufficient accuracy for control tests.

The foregoing analysis must be modified slightly for cylindrical centrifuge tubes. At equation 4, the sedimented fraction of particles of size D becomes

$$\frac{R - X_0}{R - S} = \frac{R}{R - S} (1 - e^{-bD^2t}) \quad (4')$$

Carrying this change through to equation 8c we obtain:

$$(R - S) \frac{\partial p}{\partial S} + (1 - p) = \int_0^{D_m} F(D) dD \quad (8c')$$

It is doubtful that calculation of the particle-size distribution function itself is justified if cylindrical tubes are used. However, for cylindrical tubes, equations 9a and 10a become

$$\frac{2S \ln R/S}{D_m} \left[2 \frac{\partial p}{\partial S} - (R - S) \frac{\partial^2 p}{\partial S^2} \right] = F(D_m) \quad (9a')$$

and

$$\frac{2t}{D_m} \left[\frac{\partial p}{\partial t} - (R - S) \frac{\partial^2 p}{\partial S \partial t} \right] = F(D_m) \quad (10a')$$

Another way of using the length of the centrifuge arm as a variable is of possible interest in connection with cylindrical tubes. Instead of centrifuging for a fixed time with the quantity of suspension in the tubes variable, fix the quantity of suspension as well as the time and vary the length of the centrifuge arm (change R with $R - S$ constant, figure 1). With cylindrical tubes this may be readily accomplished by placing in the bottom of the centrifuge cups small blocks of known thickness. The tubes containing suspension may thus be held at a variable distance from the axis of rotation. The analogue of equation 8c' is

$$R \left(\frac{\partial p}{\partial R} \right)_{R-R, t} + (1 - p) = \int_0^{D_m} F(D) dD \quad (14)$$

With sector-shaped centrifuge tubes, use of R as a variable would require a different set of tubes for every change in R , and no advantage over fixing R and varying S is apparent.

It will be noted that equations 8c' and 10a' for centrifugal sedimentation in cylindrical tubes are identical in form with equations 11 and 13, respectively, obtained for gravitational sedimentation, since $R - S = h$ and $dS = -dh$. Equation 9a' reduces to equation 12 as S approaches R . However D_m , the diameter of the smallest particles 100 per cent sedimented, is calculated from equation 2 for the centrifugal case and from the equation

$$h = \frac{d_1 - d_2}{18\eta} D_m^2 g t$$

for the gravitational case.

Assumption of convection-free centrifuging

Schlesinger (7) has developed a method of particle-size analysis in which, instead of the assumption of vibration-free centrifuging, vibrations sufficiently violent to keep the concentration of the suspension uniform during centrifuging are assumed. Continuous sedimentation occurs on a filter paper mat placed at the bottom of the centrifuge tubes. His method is primarily designed for measurement of the particle size in monodisperse sols, but he suggests variation of the length of the column of suspension to determine particle-size distributions.

Precision sedimentation, free from convection currents, is undoubtedly obtained only with the most carefully balanced centrifuge, with sector-shaped tubes, and with precautions to maintain a uniform temperature. However, even without such precautions suspensions in cylindrical tubes in our centrifuge showed very marked concentration gradients after centrifuging. At high speeds and with the tubes filled to a high level, the effect of convection currents was more marked. But it seems likely that the assumption of convection-free sedimentation is adequate for many purposes and much more nearly accurate unless the centrifuging is carried out at high speeds in a deliberately unbalanced centrifuge.

EXPERIMENTAL

Particle-size analyses of suspensions of barium and strontium carbonates in alcohol illustrate the application of equation 8c'. The suspensions analyzed were prepared by adding absolute alcohol to a concentrated carbonate suspension which had been ball milled for 48 hr. in amyl acetate containing 2 per cent of pyroxylin. The resulting suspensions contained 15 g. of carbonates per liter in alcohol mixed with 2.8 per cent amyl acetate and 0.05 per cent pyroxylin.

Cylindrical tubes with flat bottoms were used in an International clinical centrifuge. The centrifuge speed was measured with a General Radio strobatac, and the time of centrifuging was corrected to constant speed by the method of Marshall (3). After centrifuging, the suspension and sediment were carefully separated, and p , the weight fraction sedimented, determined from the volume of 0.1 N hydrochloric acid found equivalent by titration to each of the separated fractions.

The suspensions were centrifuged at 500 R.P.M. for an effective time of 400 sec. with the tubes filled to a series of levels. Figure 2 shows a plot of $1 - p$, the weight fraction remaining in suspension, against $R - S$, the length of the cylindrical column of suspension centrifuged. The slope of the curves was measured with a tangent meter at each experimental point, giving $\partial p / \partial S$ at each point. D_m is calculated at each point from equation 2.

$$D_m = \sqrt{\frac{\ln R/S}{bt}} = \sqrt{\frac{18\eta \cdot 2.303 \log \frac{R}{R - (R - S)}}{(d_1 - d_0)\omega^2 t}}$$

which on substitution for the constants¹ $\eta = 0.0110$ poise, $R = 15.25$ cm., $d_1 - d_0 = 3.64$ for barium carbonate, $d_1 - d_0 = 2.91$ for strontium carbonate, $\omega = 2\pi$ (R.P.M.)/60 = 52.4 radians per second, and $t = 400$ sec., gives

$$\text{For BaCO}_3, D_m \text{ (in microns)} = 3.38 \sqrt{\log \frac{15.25}{15.25 - (R - S)}}$$

$$\text{For SrCO}_3, D_m \text{ (in microns)} = 3.78 \sqrt{\log \frac{15.25}{15.25 - (R - S)}}$$

A convenient method for application of the equation

$$(R - S) \frac{\partial p}{\partial S} + (1 - p) = \int_0^{D_m} F(D) dD \quad (8c')$$

is illustrated in figure 2 at the point $R - S = 3$ on the strontium carbonate curve. The tangent APB is drawn so that the intercept, B , at $R - S = 2 \times 3$ may be read. The intercept B gives the value of $\int_0^{D_m} F(D) dD$, the weight frac-

¹ The viscosity and density of alcohol at 25°C. were used. The viscosity and density data were taken from *Handbook of Chemistry and Physics*, 21st edition, Chemical Rubber Publishing Company, Cleveland, Ohio.

tion of particles with diameters smaller than D_m , since $BC/PC = \partial p/\partial S$ and $PC = R - S$, so that

$$BC = (R - S) \frac{\partial p}{\partial S}$$

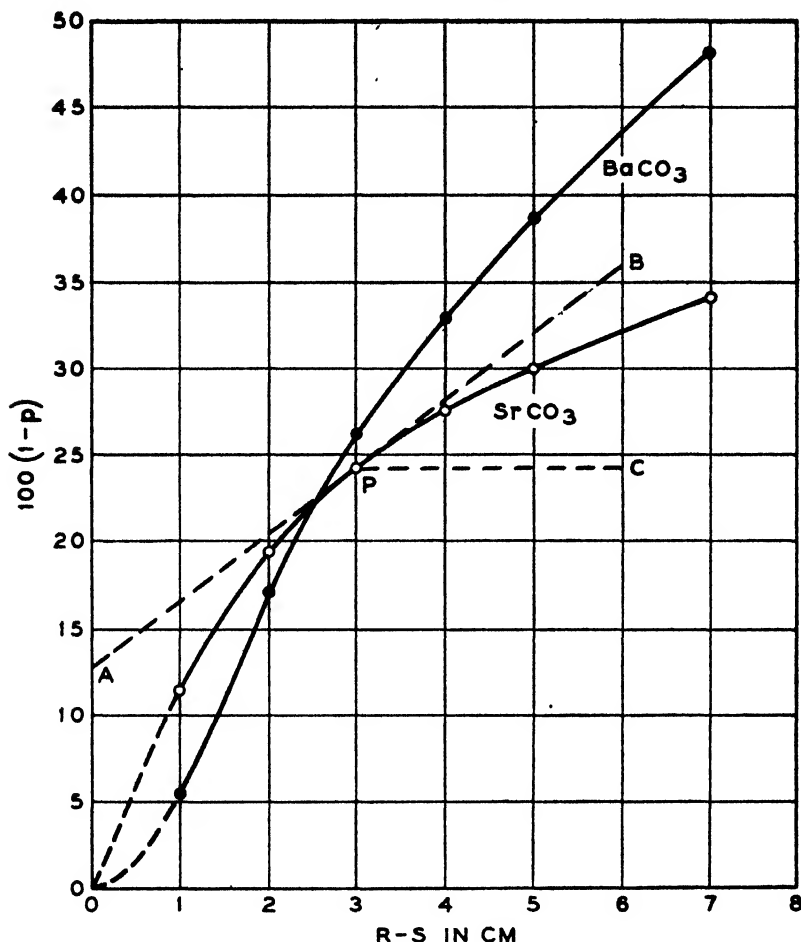


FIG. 2. Sedimentation of barium carbonate and strontium carbonate suspensions in alcohol. $100(1-p)$ is the weight per cent of suspended particles remaining in suspension after centrifuging at 500 R.P.M. for 400 sec.; $R-S$ is the length of the column of suspension in the cylindrical centrifuge tubes.

which is the term added to $1 - p$ to give

$$\int_0^{D_m} F(D) dD \text{ (equation 8c')}$$

If it is not convenient to extend tangents as far as $2(R - S)$,

$$(1 - p) - \text{tangential intercept } A = (R - S) \partial p / \partial S$$

and therefore,

$$2(1 - p) - \text{tangential intercept } A = \int_0^{D_m} F(D) dD$$

Results are summarized in table 1. Column 5 gives the weight per cent of particles with diameters less than D_m , listed in column 6. The resulting cumulative weight per cent curves are shown in figure 3.

A suspension of uniform particles 1 micron in diameter would give a vertical line at $D_m = 1$ in figure 3. Thus the particles of strontium carbonate are distributed over a wider size range than those of barium carbonate; 52 per cent by weight of the barium carbonate particles lie in the size range 0.6–1.6 microns as

TABLE 1
Particle-size distribution

$R - S$	$100(1 - p)$	$100 \frac{\partial p}{\partial S}$	$100(R - S) \frac{\partial p}{\partial S}$	$100 \int_0^{D_m} F(D) dD$	D_m
Barium carbonate suspension					
cm.	per cent	per cent cm. ⁻¹	per cent	per cent	cm. $\times 10^{-4}$
1.00	5.4	13.4	13.4	18.8	0.58
2.00	17.2	10.4	20.8	38.0	0.83
3.00	26.2	7.6	22.8	49.0	1.04
4.00	33.0	6.2	24.8	57.8	1.23
5.00	38.8	5.3	26.5	65.3	1.40
7.00	48.2	4.04	28.3	76.5	1.75
Strontium carbonate suspension					
cm.	per cent	per cent cm. ⁻¹	per cent	per cent	cm. $\times 10^{-4}$
1.00	11.5	11.2	11.2	22.7	0.65
2.00	19.4	5.9	11.8	31.2	0.93
3.00	24.1	4.0	12.0	36.1	1.17
4.00	27.5	2.9	11.6	39.1	1.37
5.00	30.0	2.3	11.5	41.5	1.57
7.00	34.0	2.0	14.0	48.0	1.95

compared with 21 per cent for the strontium carbonate suspension. The difference between these two curves illustrates the superiority of determinations of particle-size distribution over measurements of the average particle size. Any determination of "average" particle size would evidently indicate a larger particle size for the strontium carbonate suspension, yet from the course of the curves in figure 3 it is probable that the strontium carbonate suspension contains a higher proportion of particles of diameter less than 0.5 micron than does the barium carbonate suspension.

Calculation of the distribution function itself from these data, either from the slope of the cumulative weight per cent curves of figure 3 or by application of equation 9a', does not appear to be justified. The approximations introduced by the use of cylindrical centrifuge tubes probably affect the second derivatives

of the fraction sedimented too much to give reliable values of the distribution function. The results on barium carbonate and strontium carbonate suspensions show, however, that the use of cylindrical centrifuge tubes permits effective comparison of suspensions with respect to the range of particle sizes present, and the cumulative weight per cent curves are readily determined.

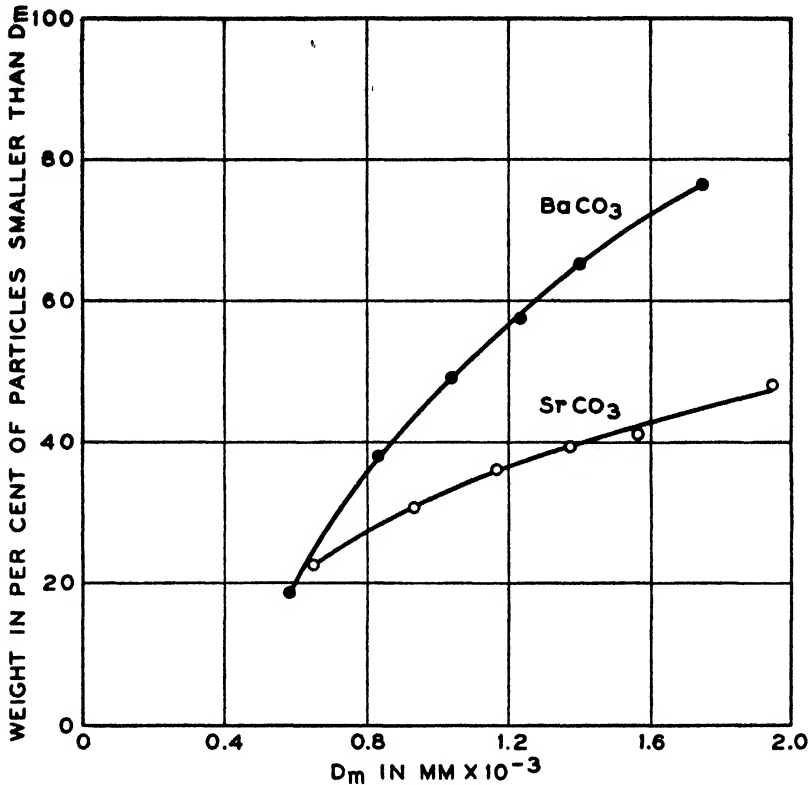


FIG. 3. Cumulative weight per cent curves for barium carbonate and strontium carbonate suspensions.

SUMMARY

1. An analysis is made of the sedimentation of particles from a suspension by a beaker-type centrifuge. Calculation of particle-size distributions is greatly simplified if sedimentation is measured as a function of distance of the suspension from the axis of rotation rather than as a function of the time of centrifuging.

2. The weight fraction of particles with diameters less than D_m , $\int_0^{D_m} F(D) dD$, may be calculated from the equation:

$$\frac{R^2 - S^2}{2S} \frac{\partial p}{\partial S} + (1 - p) = \int_0^{D_m} F(D) dD$$

where R and S are the distances of the bottom and top, respectively, of the suspension from axis of rotation, and p is the weight fraction sedimented in flat sector-shaped tubes. D_m is the diameter of the smallest particles 100 per cent sedimented and is readily calculated from the distance S and various constants.

3. Formulae are derived for the particle-size distribution function in terms of $\partial p/\partial S$ and $\partial^2 p/\partial S^2$ or in terms of $\partial p/\partial t$ and $\partial^2 p/\partial S \partial t$. The latter formula allows calculation of $F(D_m)$ from sedimentation-time curves for centrifuge tubes filled to a series of levels.

4. Approximations introduced by the use of cylindrical centrifuge tubes and the assumption of vibration-free centrifuging are discussed. If cylindrical tubes are used, the sedimentation equations become identical in form with those for gravitational sedimentation.

5. Particle-size analysis of alcohol suspensions of barium carbonate and of strontium carbonate from sedimentation data in cylindrical tubes filled to a series of levels illustrates the method suggested.

This analysis was undertaken at the suggestion of Dr. L. A. Wooten. His advice and criticism are gratefully acknowledged.

REFERENCES

- (1) HAUSER, E. A., AND SCHACHTMAN, H. K.: *J. Phys. Chem.* **44**, 584 (1940).
- (2) HAUSER, E. A., AND LYNN, J. E.: *Ind. Eng. Chem.* **32**, 659 (1940).
- (3) MARSHALL, C. E.: *Proc. Roy. Soc. (London)* **A126**, 427 (1930).
- (4) NORTON, F. H., AND SPEIL, S.: *J. Am. Ceram. Soc.* **21**, 89 (1938).
- (5) ODÉN, S.: In J. Alexander's *Colloid Chemistry*, Volume 1, p. 861. The Chemical Catalog Co., New York (1926).
- (6) ROMWALTER, A., AND VENDL, M.: *Kolloid-Z.* **72**, 1 (1935).
- (7) SCHLESINGER, M.: *Kolloid-Z.* **67**, 135 (1934).
- (8) SVEDBERG, T., AND PEDERSEN, K. O.: *The Ultracentrifuge*, p. 67. Oxford University Press, London (1940).

THE ELECTROCHEMISTRY OF BATHS OF FUSED ALUMINUM HALIDES. III

BROMIDE BATHS^{1, 2}RALPH WEHRMANN AND L. F. YNTEMA³*Department of Chemistry, St. Louis University, St. Louis, Missouri**Received May 28, 1944*

The solubilities of metal bromides in anhydrous aluminum bromide and the high conductivities of the resulting mixtures in the fused state have been reported by a number of investigators (2, 4, 6, 8). These mixtures are characterized by low melting points. Izbekov (5) and others (1, 3, 10) have determined the decomposition potentials of various metal bromides dissolved in aluminum bromide alone or admixed with alkali bromides. Deposition potentials have also been measured.

Various reference electrodes have been used in the measurement of deposition potentials in fused halide melts, among which are the following: a mercurous chloride electrode (1) in an aluminum bromide-potassium bromide bath; a sodium electrode (10) in an aluminum bromide-sodium bromide bath; and a platinum electrode (13) and an aluminum electrode (12) in an aluminum chloride-sodium chloride-potassium chloride bath. The aluminum reference electrode, consisting of a rod of pure aluminum, has been shown to be reversible and reproducible. It cannot be used, of course, to determine the potentials of metals more active than aluminum. Because the absolute value of the potential of this electrode is not known, the potentials obtained by its use are only comparative.

Yntema and coworkers (9, 11, 12, 13) have determined the deposition potentials of most of the heavy metals from solutions of their chlorides in an aluminum chloride-sodium chloride-potassium chloride bath and also the decomposition potentials of such solutions. The present work, also using the aluminum reference electrode, extends the study to analogous bromide baths and to mixed chloride-bromide baths.

APPARATUS AND PROCEDURE

The apparatus and experimental techniques have been described previously (12). The bath used as the solvent for the metal bromides consisted of 58.68 g. of aluminum bromide (66 mole per cent), 6.86 g. of sodium bromide (20 mole per cent), and 5.55 g. of potassium bromide (14 mole per cent). These mole percentages are the same as those of the corresponding chlorides in the previous work.

¹ For earlier papers in this series see *J. Phys. Chem.* **46**, 344-58 (1942).

² This paper constitutes a portion of a dissertation submitted by Ralph Wehrmann to the Faculty of the Graduate School of St. Louis University in partial fulfillment of the requirements for the degree of Doctor of Philosophy.

³ Present address: Fansteel Metallurgical Corporation, North Chicago, Illinois.

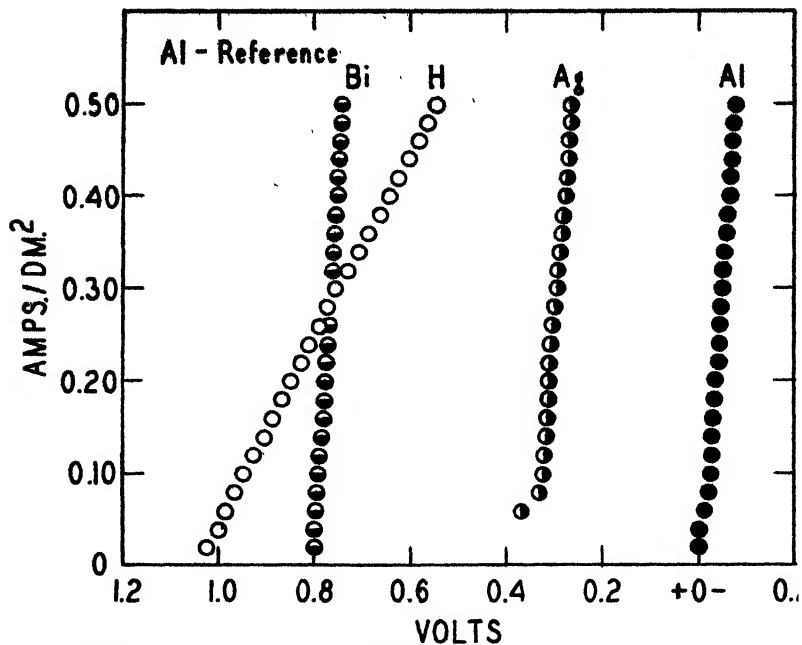


FIG. 1. Deposition potentials. I versus E (measured from aluminum reference electrode to cathode). Aluminum bromide-potassium bromide-sodium bromide bath. Concentration of metals, 1 mole per cent; temperature, 218°C.; lower current densities.

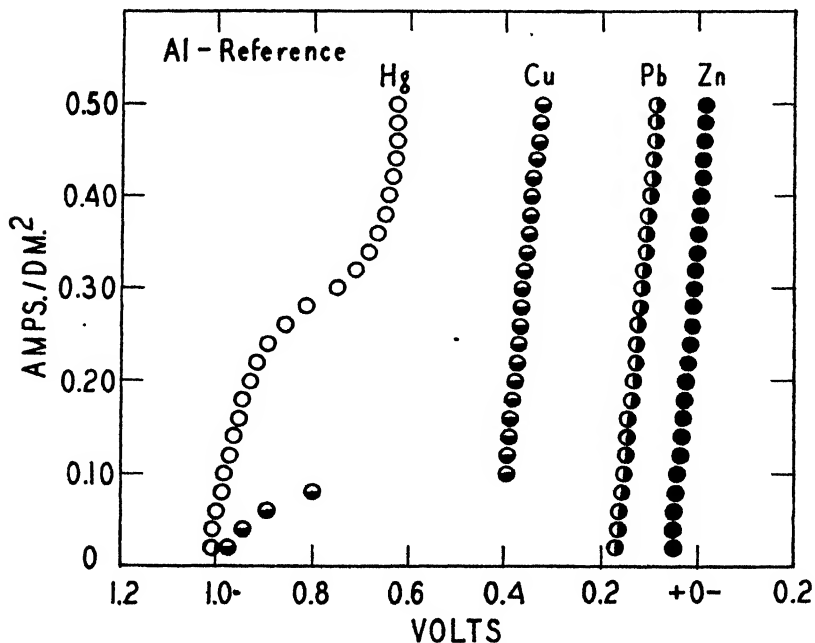


FIG. 2. Deposition potentials. I versus E (measured from aluminum reference electrode to cathode). Aluminum bromide-potassium bromide-sodium bromide bath. Concentration of metals, 1 mole per cent; temperature, 218°C.; lower current densities.

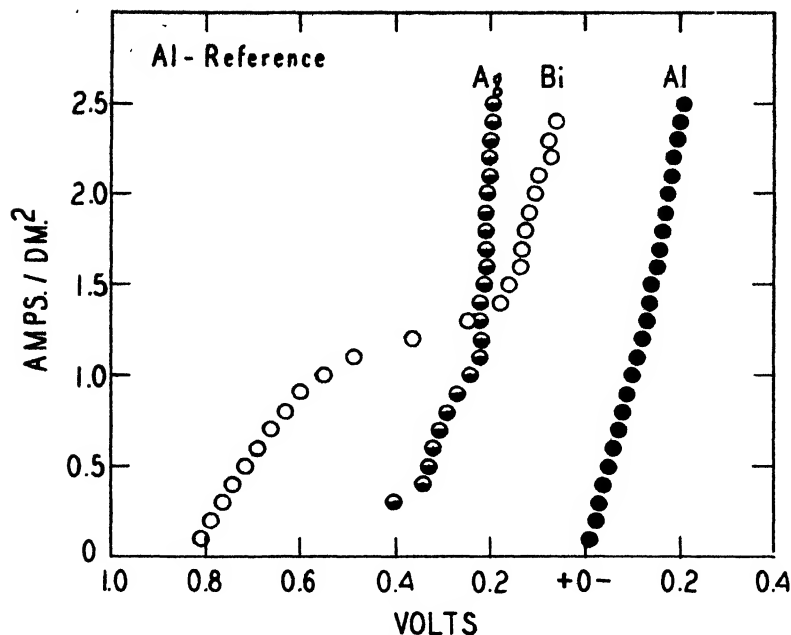


FIG. 3. Deposition potentials. I versus E (measured from aluminum reference electrode to cathode). Aluminum bromide-potassium bromide-sodium bromide bath. Concentration of metals, 1 mole per cent; temperature, 218°C.; higher current densities.

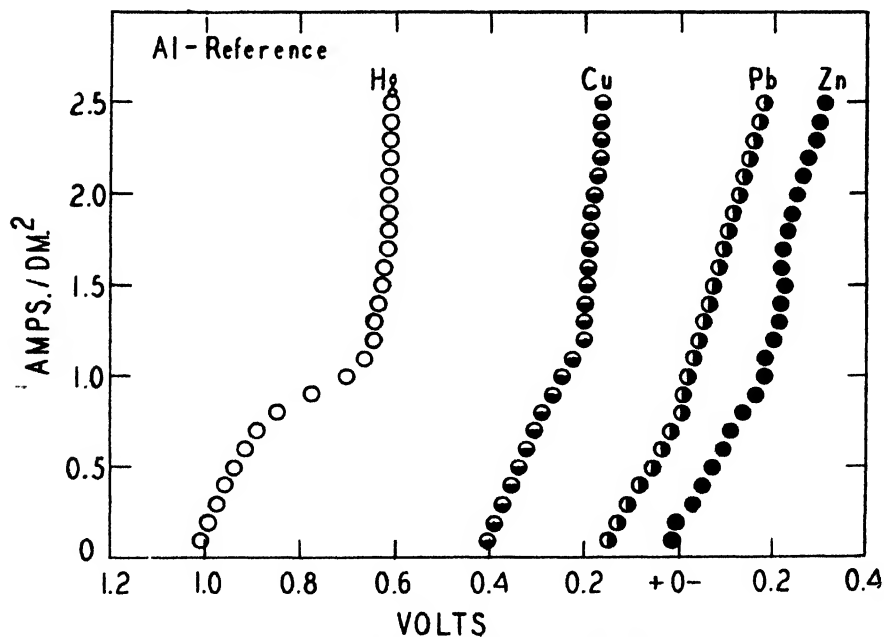


FIG. 4. Deposition potentials. I versus E (measured from aluminum reference electrode to cathode). Aluminum bromide-potassium bromide-sodium bromide bath. Concentration of metals, 1 mole per cent; temperature, 218°C.; higher current densities.

REAGENTS

Anhydrous aluminum bromide was prepared by direct combination of the elements, according to a procedure described by Kaveler and Monroe (7). Bromine, analytical reagent grade diluted with hydrogen or nitrogen, was passed over aluminum at 400°C. The use of the diluent gas facilitated the removal of the product from the reaction zone. After refluxing in a stream of pure nitrogen, the compound was twice distilled. The final distillation yielded a white, crystalline product.

The metal halides of analytical reagent grade were made anhydrous by heating at 110°C. in stream of dry nitrogen.

EXPERIMENTAL PROCEDURE

All the data reported in this paper were obtained at a bath temperature of 218°C., naphthalene being used in the vapor thermostat. The data for the determination of the decomposition potentials were obtained by measuring the potential drop between cathode and anode at various current densities. The deposition potentials were obtained by measuring the potential drop between the cathode and the aluminum reference electrode. The reference electrode is negative with respect to the more noble metal being deposited.

Potentials were obtained by the direct method; the values were taken from I versus E plots by extrapolation to zero current. Measurements were made through two current density ranges. At lower current densities the current was increased by 0.02 ampere per dm.² increments up to 0.5 ampere per dm.² At the higher current densities the increments were 0.1 ampere per dm.² up to 2.5 amperes per dm.²

ALUMINUM BROMIDE-ALKALI BROMIDE BATHS (SEE TABLE 1)

Aluminum: The series of determinations which were made on the bath without the addition of a "foreign" bromide show the reproducibility of the measurements and the reversibility of the aluminum reference electrode. A value of 1.61 volts was found for the decomposition potential. The value of -0.015 volt for the deposition potential is in good agreement with the value of -0.02 volt reported for the corresponding chloride bath. The deviation from zero may be expected as due to polarization effects.

At low current densities smooth adherent deposits were obtained and at higher current densities needle-like crystals were formed.

Hydrogen: The preparation and maintenance of a bath containing 1 mole per cent of hydrogen was difficult. Two procedures were attempted: 0.80 g. of aluminum chloride hexahydrate was added to the melt. A rather violent reaction ensued, liberating considerable quantities of the hydrogen halides so that the actual hydrogen concentration of the solution was less than the calculated 1 mole per cent. In a second experiment anhydrous hydrogen chloride was bubbled into the bath for 2 hr. before potential measurements were taken. The potential values obtained by the two methods agreed quite closely. The average value for the deposition of hydrogen is +1.05 volts. The same value is reported for the

TABLE 1

Deposition potentials and decomposition potentials

Aluminum bromide-sodium bromide-potassium bromide bath; 1 mole per cent solutions; temperature, 218°C.; a, values from measurements at lower current densities; b, values from measurements at higher current densities

ELEMENT	I DEPOSITION POTENTIAL (CATHODE vs. ALUMINUM)	II DECOMPOSITION POTENTIAL (CATHODE vs. ANODE)	SUM OF I AND II
Aluminum.....	-0.02 a 0.01 a 0.02 a 0.01 a 0.02 b 0.01 b 0.01 b* 0.03 b*	1.60 a 1.59 a 1.61 a 1.60 a 1.60 b 1.60 b 1.61 b* 1.65 b*	
Mean	-0.02	1.61	1.59
Hydrogen.....	+1.06 a 1.04 a 1.05 a 1.04 a 1.03 a 1.04 a	0.51 a 0.54 a 0.58 a 0.50 a 0.53 a 0.52 a	
Mean	+1.05	0.53	1.58
Copper.....	+0.41 a 0.41 a 0.41 a 0.40 a 0.41 b 0.42 b 0.43 b	1.17 a 1.19 a 1.17 a 1.17 a 1.13 b 1.15 b 1.17 b	
Mean	+0.41	1.17	1.58
Silver.....	+0.36 a 0.37 a 0.35 a 0.35 b 0.41 b 0.35 b	1.23 a 1.23 a 1.21 a 1.20 b 1.25 b 1.19 b	
Mean	+0.37	1.22	1.59
Zinc.....	+0.04 a 0.06 a 0.05 a 0.04 b	1.56 a 1.54 a 1.54 a 1.58 b	
Mean.....	+0.05	1.56	1.61

TABLE 1—*Continued*

ELEMENT	I DEPOSITION POTENTIAL (CATHODE VS. ALUMINUM)	II DECOMPOSITION POTENTIAL (CATHODE VS. ANODE)	SUM OF I AND II
Mercury.....	+0.66 a 0.66 a 0.65 b 0.66 b	0.99 a 0.98 a 1.00 b 0.99 b	
Mean.....	+0.66	0.99	1.65
(Reduction potential).....	+1.02 a 0.99 a 1.04 b 1.02 b	0.58 a 0.54 a 0.59 b 0.57 b	
Mean.....	+1.02	0.57	1.59
Lead.....	+0.17 a 0.17 a 0.17 b 0.17 b	1.45 a 1.44 a 1.44 b 1.46 b	
Mean.....	+0.17	1.45	1.62
Bismuth.....	+0.32 b 0.30 b 0.32 b	1.24 b 1.28 b 1.30 b	
Mean.....	+0.31	1.27	1.58
(Reduction potential).....	+0.80 a 0.82 a 0.85 a 0.80 b 0.82 b 0.83 b	0.77 a 0.73 a 0.80 a 0.78 b 0.73 b 0.76 b	
Mean.....	+0.82	0.76	1.58

* Values from measurements at 156°C.

deposition potential of hydrogen from an aluminum chloride-alkali chloride melt (12). In view of the fact that hydrogen would not be expected to form complexes in either solution, this agreement is not surprising.

Copper: 0.48 g. of cuprous bromide was used. Bright crystalline deposits of metallic copper were obtained. The current density-potential curves extrapolated to +0.41 volt for the deposition potential and to 1.17 volts for the decomposition potential. The lower portion of the aluminum reference-cathode curve which extrapolates to +1.01 volts is interpreted to represent the reduction of cupric to cuprous ions.

Silver: 0.63 g. of anhydrous silver bromide was readily soluble in the bath. Electrolysis produced a crystalline deposit of silver possessing a bright metallic luster. Silver deposits from this bath at a potential of +0.37 volt, and silver bromide decomposes at a potential of 1.22 volts.

Zinc: Zinc bromide was the most soluble metal bromide studied. 0.75 g. dissolved very rapidly. The measured deposition potential was +0.05 volt and the decomposition potential was 1.56 volts. Since these baths were rapidly depleted of zinc and especially so at higher current densities, potential measurements also were made with solutions containing 2 mole per cent of zinc bromide. These values, within the limits of experimental error, agreed with the results obtained from the more dilute solutions.

Mercury: 1 mole per cent (0.93 g.) of mercurous bromide was readily soluble in the anhydrous salt melt. Globules of metallic mercury were obtained by electrolyzing in both current density ranges. Mercury shows a reduction potential at +1.02 volts and a deposition potential at +0.66 volt; the decomposition potential of mercurous bromide is 0.99 volt.

Lead: A 1 mole per cent solution was obtained by adding 1.20 g. of lead bromide to the solvent. Solution was rapid and electrolysis liberated dark colored deposits of the metal. The average deposition and decomposition potentials were +0.17 and 1.45 volts, respectively.

Bismuth: Bismuth oxide was found to be insoluble in the bath. Potential measurements were made with baths containing 1 mole per cent (0.87 g.) of bismuth oxychloride or 1 mole per cent (1.02 g.) of bismuth oxybromide. The observed deposition and decomposition potentials were +0.31 and 1.27 volts, respectively. It is believed that the lower portion of the aluminum reference-cathode curve which extrapolates to a value of +0.82 volt represents a reduction potential of bismuth. A loosely adherent powder was obtained at the cathode.

ALUMINUM CHLORIDE-ALKALI BROMIDE BATHS (SEE TABLE 2)

In order to determine the effect of large concentrations of chlorides in the solvent, baths consisting of 58.66 g. of aluminum chloride (66 mole per cent), 13.72 g. of sodium bromide (20 mole per cent), and 11.11 g. of potassium bromide (14 mole per cent) were also investigated.

Aluminum: By electrolyzing the solvent containing no foreign metal, smooth adherent deposits were obtained at low current densities. At higher current densities crystalline deposits were obtained. For both current density ranges the average of the extrapolated values for the deposition potential of aluminum and the decomposition potential of the aluminum halide were -0.02 and 1.71 volts, respectively.

Silver: 0.96 g. of silver chloride or 1.25 g. of silver bromide was added to the bath. These salts dissolved rapidly. Small variations in the chloride-to-bromide ratio in the bath had no measurable effect on either the deposition potential of silver or the decomposition potential of the bath. The values found were +0.58 volt and 1.12 volts. Silver was deposited as crystalline metal.

Mercury: Baths were prepared by adding 1.57 g. of mercurous chloride or 1.87

TABLE 2

Deposition potentials and decomposition potentials

Aluminum chloride-sodium bromide-potassium bromide bath; 1 mole per cent solutions; temperature, 218°C.; a, values from measurements at lower current densities; b, values from measurements at higher current densities

ELEMENT	I DEPOSITION POTENTIAL (CATHODE VS. ALUMINUM)	II DECOMPOSITION POTENTIAL (CATHODE VS. ANODE)	SUM OF I AND II
Aluminum:			
AlCl ₃	-0.01 a	1.68 a	
	0.02 a	1.70 a	
	0.02 a	1.70 a	
	0.01 a	1.71 a	
	0.02 b	1.70 b	
	0.02 b	1.73 b	
	0.02b*	1.72b*	
	0.02b*	1.70b*	
Mean.....	-0.02	1.71	1.69
Silver:			
AgCl.....	+0.58 a	1.10 a	
	0.59 a	1.10 a	
	0.58 a	1.11 a	
	0.58 b	1.15 b	
	0.59 b	1.13 b	
Mean.....	+0.58	1.12	1.70
AgBr.....	+0.58 a	1.09 a	
	0.58 a	1.13 a	
	0.59 a	1.12 a	
	0.57 b	1.17 b	
	0.58 b	1.10 b	
Mean.....	+0.58	1.12	1.70
Mercury:			
HgCl.....	+0.84 a	0.87 a	
	0.86 a	0.87 a	
	0.85 b	0.89 b	
	0.85 b	0.88 b	
Mean.....	+0.85	0.88	1.73
(Reduction potential)	+1.03 a	0.62 a	
	1.05 a	0.65 a	
	1.04 a	0.66 a	
Mean.....	+1.04	0.64	1.68
HgBr.....	+0.84 b	0.92 b	
	0.87 b	0.88 b	
	0.85 b	0.85 b	

TABLE 2—*Continued*

ELEMENT	I DEPOSITION POTENTIAL (CATHODE VS. ALUMINUM)	II DECOMPOSITION POTENTIAL (CATHODE VS. ANODE)	SUM OF I AND II
	0.85 b	0.84 b	
Mean.....	+0.85	0.87	1.72
(Reduction potential).....	+1.06 a	0.60 a	
	1.07 a	0.61 a	
	1.09 a	0.62 a	
Mean.....	+1.07	0.61	1.68

* Values from measurements at 156°C.

g. of mercurous bromide. The deposition potential was found to be +0.85 volt and the decomposition potential to be 0.88 volt. There is a reduction potential indicated by the graphs at +1.04 volts.

DISCUSSION

In previous work on aluminum chloride-alkali chloride baths, the anode compartment consisted of a glass tube with a constricted lower end packed with glass wool upon which a layer of granulated aluminum was placed to prevent diffusion of free chlorine into the cathode compartment. When this device was used with bromide baths containing copper or bismuth bromides, the aluminum became coated with the foreign metal. It is probable that both copper and bismuth were present in anion complexes which migrated to the anode compartment.

A correlation pointed out in an earlier paper (12) may also be noted in this work. The decomposition potential of the aluminum bromide-alkali bromide bath was found to be 1.61 volts. The sum of the deposition and decomposition potentials for baths containing other metals is 1.61 ± 0.04 volts. The close agreement among the data also indicates to us that the procedure described and the values reported are trustworthy. The correlation between deposition and decomposition potentials also applies to the reduction potentials and to the potentials observed for the mixed aluminum chloride-alkali bromide baths.

When chloride is substituted for part of the bromide in the bath, values for the potentials are obtained which are intermediate between those obtained with a chloride and a bromide bath.

SUMMARY

1. The aluminum reference electrode is shown to be applicable for the determination of deposition potentials of metals from a fused aluminum bromide-alkali bromide bath.

2. Deposition potentials determined from baths in which the aluminum was introduced as the chloride were considerably higher, of the order of 0.2 volt with mercury and silver, than those obtained from the all-bromide baths.

3. The deposition potentials as measured with the aluminum reference electrode of the metals studied are as follows: aluminum, -0.02 ; zinc, $+0.05$; lead, $+0.17$; bismuth, $+0.31$; silver, $+0.37$; copper, $+0.41$; mercury, $+0.66$; and hydrogen, $+1.05$ volts. This order of deposition is the same as the voltaic series for the aqueous sulfate solutions of these metals, except for the interchanged positions of copper and silver and the location of hydrogen at the noble end of the series.

REFERENCES

- (1) DELIMARS'KII AND IZBEKOV: Mem. Inst. Chem. Ukrain. Acad. Sci. **3**, 541 (1936).
- (2) IZBEKOV AND PLOTNIKOV: Z. anorg. Chem. **71**, 328 (1911).
- (3) IZBEKOV AND YA ZAKHARCHENKO: Mem. Inst. Chem. Ukrain. Acad. Sci. **2**, 121 (1935).
- (4) IZBEKOV: Z. anorg. Chem. **143**, 80 (1925).
- (5) IZBEKOV: Z. physik. Chem. **116**, 304 (1925).
- (6) IZBEKOV: J. Russ. Phys. Chem. Soc. **45**, 1792 (1913).
- (7) KAVELER AND MONROE: J. Am. Chem. Soc. **50**, 2421 (1928).
- (8) KENDALL, CRITTENDEN, AND MILLER: J. Am. Chem. Soc. **45**, 963 (1923).
- (9) MARSHALL AND YNTEMA: J. Phys. Chem. **46**, 353 (1942).
- (10) SKOBETS AND KAVETSKII: J. Gen. Chem. (U. S. S. R.) **10**, 1858 (1940).
- (11) VERDIECK, RALPH G.: Thesis, St. Louis University, 1943.
- (12) VERDIECK AND YNTEMA: J. Phys. Chem. **46**, 344 (1942).
- (13) WADE, TWELLMAYER, AND YNTEMA: Trans. Electrochem. Soc. **78**, 77 (1940).

THE ELECTROCHEMISTRY OF BATHS OF FUSED ALUMINUM HALIDES. IV

RALPH G. VERDIECK AND L. F. YNTEMA¹

Department of Chemistry, St. Louis University, St. Louis, Missouri

Received May 23, 1944

This communication extends previous studies (9, 11) on the deposition potentials of metals from solutions of their chlorides in an aluminum chloride-alkali chloride bath. The data for a number of additional elements are presented to complete the list of those that can be studied by the procedure.

APPARATUS AND PROCEDURE; REAGENTS

The apparatus and experimental procedures used were the same as those previously described. All reagents were of A.R. or C.P. grade. The chlorides were dehydrated, when necessary, by heating in a current of dry hydrogen chloride. Certain compounds were prepared by standard methods, as indicated.

The electrolysis bath consisted of 58.68 g. of anhydrous aluminum chloride (66 mole per cent), 7.78 g. of sodium chloride (20 mole per cent), and 6.96 g. of potassium chloride (14 mole per cent). A bar of pure aluminum served as reference

¹ Present address: Fansteel Metallurgical Corporation, North Chicago, Illinois.

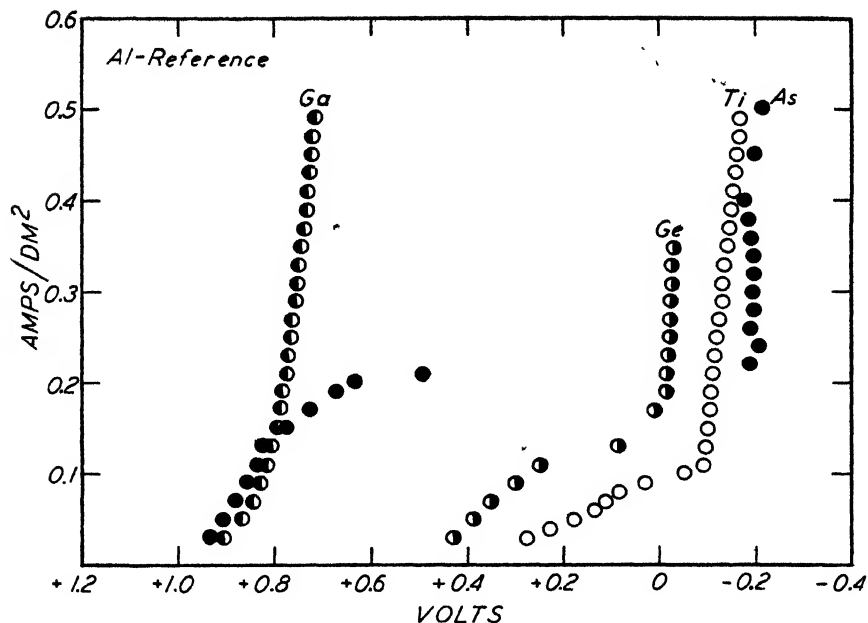


FIG. 1. Deposition potentials. I versus E (measured from aluminum reference (electrode to cathode)). Concentration of metals, 1 mole per cent; temperature, 156°C.; lower current densities.

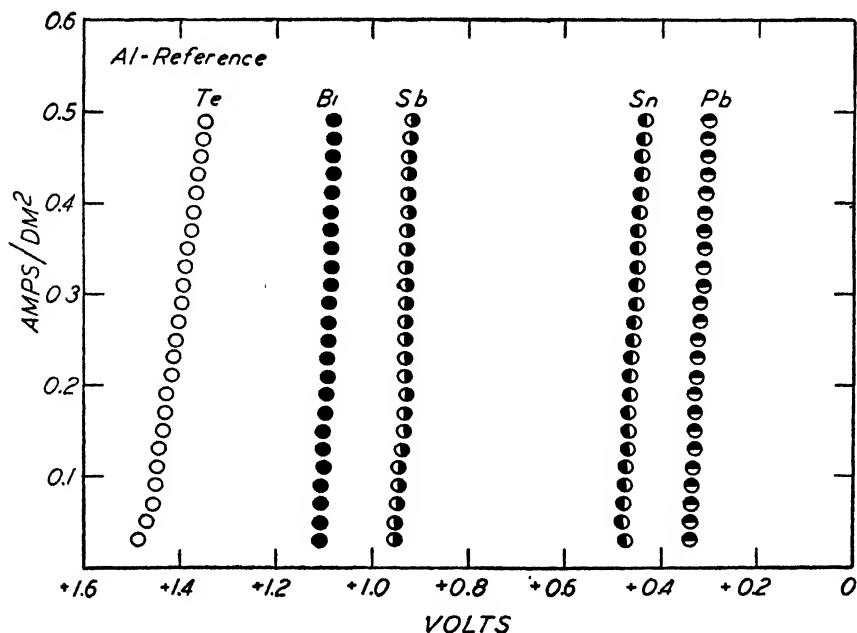


FIG. 2. Deposition potentials. I versus E (measured from aluminum reference electrode to cathode). Concentration of metals, 1 mole per cent; temperature, 156°C.; lower current densities.

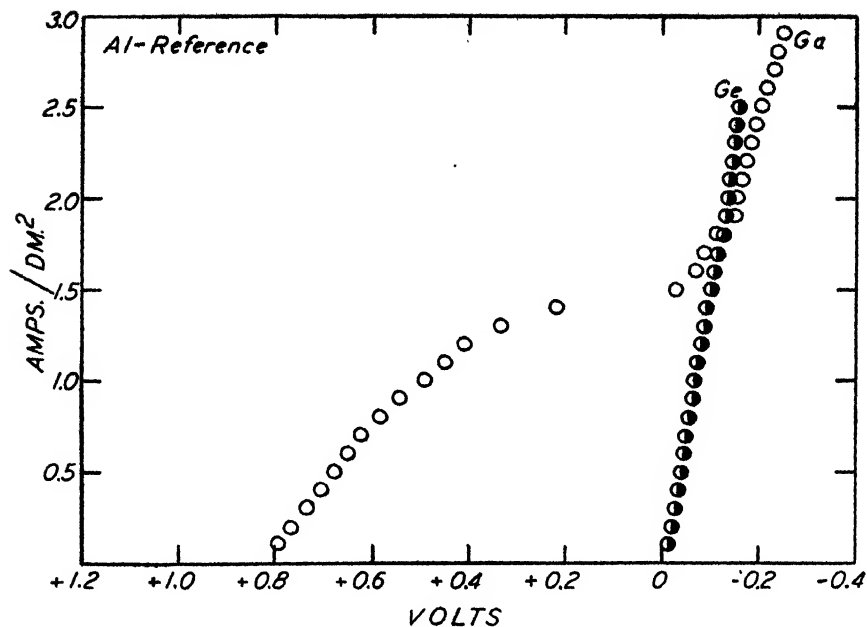


FIG. 3. Deposition potentials. I versus E (measured from aluminum reference electrode to cathode). Concentration of metals, 1 mole per cent; temperature, 156°C. ; higher current densities.

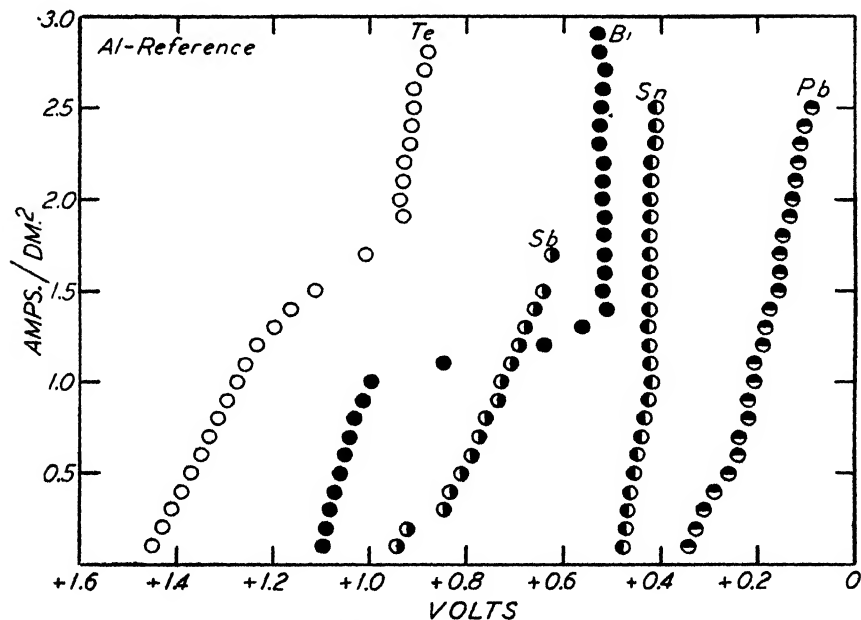


FIG. 4. Deposition potentials. I versus E (measured from aluminum reference electrode to cathode). Concentration of metals, 1 mole per cent; temperature, 156°C. ; higher current densities.

electrode, and the measured deposition potentials represent the potential difference between the cathode and the aluminum reference electrode. Decomposition potentials were found by measuring the cathode to anode voltage drops.

Typical *I versus E* graphs are given in figures 1, 2, 3, and 4.

RESULTS (SEE TABLE 1)

Gallium: A 1 mole per cent solution of gallium was prepared by adding 1.61 g. of gallic oxide, Ga_2O_3 , to the bath. At low current densities a darkening of the cathode occurred, but the deposit contained no gallium. At higher current densities small globules of metallic gallium were deposited.

The extrapolation of the *I versus E* graphs for lower current densities indicates a reduction potential at 0.83 volt. At higher current densities the data do not give regular curves, but a value of approximately 0.2 volt for the deposition potential of the metal is indicated. The decomposition potential appears to be about 2.0 volts.

Thallium: 1.61 g. of thalious chloride was dissolved in the bath. Electrolysis of the solution gave deposits containing aluminum but no thallium. The deposition potential and decomposition potentials were identical with those obtained with a bath without any additions. It is probable that the concentration of free Tl^+ ions in solution is extremely small.

Skobets and Abarbarchuk (10) reported that the deposition potential of thalious chloride in a bath of fused cadmium chloride is the same as that of cadmium chloride, 1.08 volts, indicating that cadmium is deposited at a lower potential than thallium.

Germanium: It was found that germanium dioxide was insoluble in the bath, but that solutions could be prepared by dissolving 1.76 g. of potassium fluogermanate. Electrolysis gave a thin black plate, insoluble in dilute hydrochloric acid. At low current densities there is a reduction potential at 0.50 volt. At higher current densities the deposition potential is -0.01 volt.

The anode to cathode potential is 1.58 volts at low current densities and 2.06 volts at higher current densities.

Tin: Upon electrolysis of a bath containing 1.27 g. of stannous chloride, a bright deposit of metallic tin crystals was obtained. At lower current densities a deposition potential of 0.48 volt was found and at higher current densities a potential of 0.49 volt. At still higher current densities a value of 0.44 volt was found.

The decomposition potential is 1.61 volts at low current densities and 1.62 volts at higher current densities.

Izbekov and Chovnik (4) reported a decomposition potential of 0.74 volt for stannous chloride in a melt of aluminum and potassium chlorides at 250°C . and 0.60 volt at 350°C . Skobets and Abarbarchuk (10) deposited tin from a solution of stannous chloride in molten cadmium chloride and reported the decomposition potential to be 0.56 volt. Drossbach (3) reported the decomposition potential of stannous chloride to be 0.535–0.550 volt at 460°C . Coerver (1), using essentially the same procedure as the authors, found that the deposition potential of tin, referred to metallic aluminum, is 0.47 ± 0.03 volt.

TABLE 1

Deposition potentials and decomposition potentials

1 mole per cent solutions; temperature, 156°C. (except as indicated); a, values from data at lower current densities; b, values from data at higher current densities; potentials marked "R" represent reduction potentials to lower valent forms

ELEMENT	I DEPOSITION POTENTIAL	II DECOMPOSITION POTENTIAL	SUM OF I AND II
Gallium.....	+0.83 a 0.84 a 0.80 a 0.80 a 0.83 a 0.84 a 0.82 a 0.82 a 0.86 a 0.86 a 0.86 a 0.86 a	1.22 a 1.21 a	
Mean.....	0.83 (R)	1.22	2.05
	0.20 b 0.20 b	1.26 b 2.0 b	
Mean.....	0.20	?	
Thallium.....	-0.01 a 0.00 a 0.02 b 0.02 b	2.06 a 2.06 b	
Mean	0.01	2.06	2.07
Germanium	+0.52 0.50	1.58 1.58	
Mean.....	+0.51 (R)	1.58	2.09
	+0.01 a -0.01 a 0.00 b 0.00 b	2.07 a 2.05 a 2.05	
Mean.....	0.00	2.06	2.06
Tin.....	+0.47 a 0.50 a 0.48 a 0.48 a 0.48 a	1.61 a 1.60 a 1.60 a 1.63 a	

TABLE 1—Continued

ELEMENT	I DEPOSITION POTENTIALS	II DECOMPOSITION POTENTIALS	SUM OF I AND II
Tin.....	0.49 a 0.49 a 0.49 a		
Mean.....	0.48 0.43 b 0.43 b 0.44 b 0.44 b	1.61 1.61 b 1.62 b 1.63 b	2.09
Mean.....	0.43	1.62	2.05
Lead.....	+0.37 a 0.36 a 0.35 a 0.37 a 0.36 a 0.36 a 0.36 a 0.36 b 0.37 b 0.36 b	1.76 a 1.74 a 1.72 a 1.74 a 1.52 b (?)	
Mean.....	0.36	1.74	2.10
Titanium.....	-0.04 b -0.05 b -0.04 b -0.04 b -0.04 b -0.07 b	2.11 b 2.10 b 2.12 b	
Mean.....	-0.05	2.11	2.06
Arsenic.....	+1.01 a 0.99 a 0.98 a 0.96 a 0.96 a	1.10 a 1.08 a	
Mean ..	+0.98	1.09	2.07
Antimony ..	+0.96 a 0.94 a 0.95 a 0.94 a 0.95 a 0.94 a 0.96 a	1.08 a 1.10 a	
Mean.....	0.95	1.09	2.04

TABLE 1—Continued

ELEMENT	I DEPOSITION POTENTIAL	II DECOMPOSITION POTENTIAL	SUM OF I AND II
Bismuth:			
(Bi ₂ O ₃).....	+1.10 a	1.00 a	
	1.11 a	1.00 a	
	1.11 a	1.01 a	
	1.11 a	1.00 a	
	1.11 a	1.01 a	
	1.11 a	1.01 a	
	1.11 a	1.01 a	
Mean.....	+1.11 (R)	1.01	2.12
	+0.53 b	1.62 b	
	0.50 b	1.62 b	
Mean.....	0.51	1.62	2.13
(BiOCl)	+1.08 a	1.01 b	
	1.08 a		
Mean.....	+1.08 (R)		
Vanadium:			
K ₂ VO ₂ F ₃	-0.10 a	2.20	
	-0.13 a	2.20	
	-0.12 a		
	-0.10 a		
Mean.....	-0.11	2.20	2.09
V ₂ O ₅	-0.09 a	2.16 a	
	-0.10 a	2.21 a	
	-0.10 a		
	-0.04 b		
	-0.04 b		
Mean	-0.07	2.19	2.12
Columbium:			
(Cb ₂ O ₅).....	+0.03 a	2.08 a	
	0.03 a		
Mean.....	+0.03		
K ₂ CbF ₇	+0.02 a	2.08 a	
	0.02 a	2.14 a	
	0.02 a	2.08 b	
	0.01 b		
	0.00 b		
	-0.02 b		
Mean.....	+0.01	2.10	2.11

TABLE 1—*Concluded*

ELEMENT	I DEPOSITION POTENTIAL	II DECOMPOSITION POTENTIAL	SUM OF I AND II
Tantalum.....	+0.83 a 0.84 a	1.21 a	
Mean.....	+0.84 (R)		
K ₂ TaF ₇	+0.86 a 0.85 a 0.83 a 0.81 a 0.85 a 0.84 a	1.33 a 1.30 a 1.30 a	
Mean.....	+0.84 (R)	1.31	2.15
Ta ₂ O ₅	-0.03 b -0.01 b -0.03 b -0.01 b	2.11 b 2.10 b	
Mean.....	-0.02	2.11	2.09
K ₂ TaF ₇	0.00 b -0.01 b +0.02 b +0.02 b -0.01 b -0.02 b +0.01 b -0.03 b -0.01 b -0.02 b	2.20 b 2.14 b 2.14 b 2.17 b 2.17 b	
Mean ...	0.00	2.16	2.16
Tellurium	+1.46 a 1.48 a 1.47 a 1.47 a 1.47 a 1.46 a 1.48 a 1.48 a	0.60 0.60 0.60 0.59 0.60 0.60 0.57	
Mean	+1.47 (R) +1.15 b 1.02 b 1.08 b 1.04 b	0.60	2.07
Mean	+1.07		

Lead: 1.86 g. of lead chloride was dissolved, and electrolysis at low current densities produced small bright crystals of metal. The deposition potential is 0.36 volt; above 1 ampere cm.² the deposition potential is 0.28 volt. The decomposition potential is 1.74 volts.

Lorenz and Velde (7) measured the E.M.F. in carbon anode-carbon cathode systems at different temperatures and reported a value of $1.2467 - 6.5 \times 10^{-4}(t - 550^\circ)$. Skobets and Abarbarchuk (10) found that the decomposition potential of lead chloride in a melt of cadmium is greater than that of the solvent. Coerver (1), using essentially the same procedure as the authors, found the deposition potential of lead, referred to an aluminum reference electrode, to be 0.34 ± 0.03 volt.

Titanium: The dioxide of titanium is insoluble in the bath. A 1 mole per cent solution was prepared by dissolving 1.59 g. of potassium fluotitanate. No deposits were formed on the cathode at potentials lower than those required for the deposition of aluminum. At higher potentials a black deposit, interspersed with a white non-adherent material, was formed. The black deposit was soluble in hot concentrated sulfuric acid, forming a solution containing titanium ions.

The deposition potential of titanium from the solution is higher than that of aluminum, -0.05 volt, and the decomposition potential of the solution is 2.11 volts.

Arsenic: 0.66 g. of arsenious oxide was used. Metallic arsenic plated out as a jet-black, bright deposit at 0.98 volt at low current densities. At higher current densities, arsenic and aluminum were deposited together. The decomposition potential of the bath was found to be 1.09 volts.

Antimony: 1.16 g. of antimony oxychloride was used. Electrolysis at low current density gave a gray deposit in which small bright crystals were present. At higher current densities the deposit was a dark gray, loose powder. The deposition potential was found to be 0.95 volt and the decomposition potential 1.09 volts.

Izbekov and Chovnik (4) reported the decomposition potentials of solutions of antimony trichloride in a fused aluminum chloride and potassium chloride bath to be 0.85 volt at 250°C. and 0.82 volt at 350°C.

Bismuth: 1 mole per cent solutions were prepared by adding 1.56 g. of bismuth sesquioxide or 1.74 g. of bismuth oxychloride to the bath. On electrolysis at low current densities no metallic bismuth was deposited, but if the cathode was placed in 95 per cent ethyl alcohol to remove the melt, a reddish brown compound was found. It had a low melting point. When the cathode was placed in water, the compound apparently underwent autooxidation and reduction to form a fine black deposit of free bismuth. The reddish brown deposit was formed at a potential of 1.11 to 1.08 volts, which is assumed to represent the reduction potential of trivalent bismuth to a lower valent form, probably bivalent.

By raising the current density metallic bismuth was obtained, but the values for the deposition potential were not consistent, probably because of varying concentrations of the reduced form of bismuth at the cathode surface. The probable value is 0.51 volt. The decomposition potentials are 1.01 volts and 1.62 volts, respectively, for the reduction and deposition reactions.

According to Weber (12) and to Deherain (2), chlorine reacts slowly with bismuth at room temperature, forming bismuth bichloride, a brown oily liquid.

Izbekov and Chovnik (4) obtained 0.64 volt for the decomposition potential of bismuth trichloride dissolved in a melt of aluminum chloride or of aluminum and potassium chlorides at 250°C. Izbekov and Skobets (5) found that the decomposition potential of bismuth trichloride dissolved in stannous chloride was 0.18 volt at 300°C.

Vanadium: 1.45 g. of potassium vanadyl fluoride was added to a bath that contained 1.00 g. less potassium chloride than the usual bath. In another series vanadium pentoxide was used. Because of the low volatility of the halides of vanadium, *n*-butyl alcohol was used in the vapor thermostat to maintain the temperature at 117°C.

At low current densities, the aluminum reference electrode *versus* cathode readings gave values of -0.11 volt when potassium vanadyl fluoride was used and -0.10 volt when vanadium pentoxide was used. At higher current densities the value obtained with the pentoxide solution was -0.04 volt.

The decomposition potential of the bath at lower current densities was 2.20 volts with potassium vanadyl fluoride and 2.19 volts with vanadium pentoxide.

A small amount of vanadium metal was identified on the cathode, but its deposition potential is as high as that of aluminum.

Marshall (8), using essentially the same procedure as the authors, found the deposition potential, as measured against an aluminum reference electrode, to be 0.00 volt and the decomposition potential of the bath to be 2.20 volts.

Columbium: 2.02 g. of potassium fluocolumbate or 0.89 g. of columbium pentoxide was added to the bath. Solution was slow, but at the end of 48 hr. all but a small amount had dissolved.

Electrolysis yielded a dark brown deposit that would drop off when introduced into ethyl alcohol, leaving a dark grey deposit which was insoluble in cold concentrated hydrochloric acid but soluble in hot. Its identity as metal or as a compound containing columbium at a lower valence was not determined.

The deposition potential of the bath was found to be 0.02 volt for the fluocolumbate and 0.03 volt for the pentoxide at low current densities. At high current densities the value was 0.00 volt.

Columbium is not deposited at a lower potential than aluminum.

Marshall (8) obtained values of 0.00 volt for the deposition potential and 2.10 volts for the decomposition potential of columbium solutions by the same procedure as the authors.

Tantalum: 2.62 g. of potassium fluotantalate or 1.42 g. of tantalum pentoxide was used. The former compound is more soluble. Upon electrolysis a loosely adherent, black deposit was formed. When the deposit was washed with ethyl alcohol, a grey adherent plate was exposed. Aluminum was removed by washing with hydrochloric acid, leaving a residue which dissolved in hot concentrated sulfuric acid.

The deposition potential was found to be -0.02 volt. At very low current densities, there was a straight portion of the curve which extrapolated to 0.84 volt. This is apparently the reduction potential of pentavalent tantalum to a

lower valence state. The decomposition potential of the bath is about 2.08 volts at low current densities and 2.17 volts at higher.

Kirk and Bradt (6) reported 1.47 volts as the decomposition potential of a bath containing potassium fluotantalate and potassium chloride at 800°C.

Marshall (8) found the deposition potential to be 0.00 volt and the decomposition potential to be 2.10 volts.

Tellurium: 1.06 g. of tellurium dioxide was used. The bath was colored an intense purple. Electrolysis at low current densities produced no deposit, but when the data were plotted a straight line was obtained, extrapolating to 1.47

TABLE 2

ELEMENT	I DEPOSITION POTENTIAL	II DECOMPOSITION POTENTIAL	SUM OF I AND II
Vanadium	Not deposited at lower potentials than aluminum		
Manganese			
Titanium			
Tantalum			
Germanium			
Columbium			
Chromium	0.16	1.95	2.11
Gallium	0.20 (approx.)	2.0 (approx.)	
Zinc	0.24	1.82	2.06
Molybdenum	0.31	1.87	2.18
Cadmium	0.36	1.74	2.10
Lead	0.36	1.74	2.10
Tungsten	0.39	1.68	2.07
Iron	0.47	1.58	2.05
Tin	0.49	1.62	2.11
Bismuth	0.51	1.62	2.13
Copper	0.62	1.46	2.08
Silver	0.66	1.41	2.07
Cobalt	0.69	1.49	2.18
Nickel	0.80	1.25	2.05
Mercury	0.91	1.16	2.07
Antimony	0.95	1.09	2.04
Arsenic	1.00	1.09	2.09
Hydrogen	1.05	1.03	2.08
Tellurium	1.07		

volts. At higher current densities a loose black deposit appeared at a potential of 1.07 volts. The decomposition potential at low current densities is 0.60 volt. The curves representing data for higher current densities were irregular.

The value of 1.47 volts represents a reduction potential. Since no product of electrolysis adhered to the cathode, it was soluble in the bath. At higher current densities, the irregularities in the curves may be attributed to changes in cathodic surface area as metallic tellurium was being deposited.

A considerable amount of metallic tellurium was prepared by electrolyzing for several hours at 10 volts. The bath was extracted with water, leaving intensely black needles of metallic tellurium.

DISCUSSION

The metals whose deposition potentials have been determined in 1 mole per cent solutions in the aluminum chloride-sodium chloride-potassium chloride melt are given in table 2.

The cell formed by the aluminum reference electrode and the cathode upon which the metal, M, is deposited may be represented as follows:



where MCl_n is the chloride of the metal of valence n . The deposition potentials represent the electrode potentials of the metal in a 1 mole per cent solution as referred to the electrode potential of aluminum in a 66 mole per cent solution.

It was found that most of the deposition potentials of the metals measured were reproducible to within ± 0.02 volt.

The cell formed by the cathode and the anode may be represented as follows:



The measured potentials represent the decomposition potentials of a 1 mole per cent solution of the substance MCl_n .

The numerical sum of the deposition potential and of the decomposition potential should equal the potential of the cell



which was found to be 2.07 volts in a previous study. The experimental values are given in column III and it is assumed that the fairly good agreement with the theory indicates the accuracy of the experimental data.

The series obtained in this study does not conform to the familiar series in a water system. Hydrogen is the most noble element, except for tellurium. Lead, bismuth, copper, and silver are comparatively less noble than cobalt and nickel. The divergences between the aluminum chloride-alkali chloride system and the water system are probably related to differences in solvation of the metal ions and in degrees of association of the solutes.

REFERENCES

- (1) COERVER: Thesis, St. Louis University, 1941.
- (2) DEHERAIN: Bull. soc. chim. [1] **3**, 51 (1861).
- (3) DROSSBACH: Z. Elektrochem. **44**, 288 (1938).
- (4) IZBEKOV AND CHOVIK: Mem. Inst. Chem. Acad. Sci. Ukrain. S. S. R. **4**, 57 (1937).
- (5) IZBEKOV AND SKOBETS: Mem. Inst. Chem. Acad. Sci. Ukrain. S. S. R. **4**, 85 (1937).
- (6) KIRK AND BRADT: Trans. Electrochem. Soc. **70**, 231 (1936).
- (7) LORENZ AND VELDE: Z. anorg. allgem. Chem. **183**, 81 (1929).
- (8) MARSHALL: Dissertation, St. Louis University, 1942.
- (9) MARSHALL AND YNTEMA: J. Phys. Chem. **46**, 353 (1942).
- (10) SKOBETS AND ABARBARCHUK: Mem. Inst. Chem. Acad. Sci. Ukrain. S. S. R., **6**, 71 (1939).
- (11) VERDIECK AND YNTEMA: J. Phys. Chem. **46**, 344 (1942).
- (12) WEBER: Pogg. Ann. **96**, 130, 496 (1855).

FOAM STABILITY OF SOLUTIONS OF SOAPS OF PURE FATTY ACIDS

GILBERT D. MILES AND JOHN ROSS

Colgate-Palmolive-Peet Co., Jersey City, New Jersey

Received May 24, 1944

In order to determine some of the factors which influence the foam stability of solutions of soaps, the authors have applied a comparative method (9) for measuring relative foam stability to solutions of the sodium salts of pure fatty acids.

The work presented in this paper includes the examination of the influence of such variables as pH, temperature, concentration, the presence of calcium and magnesium soaps, and combinations of soaps on the foam stability of soap solutions.

The inadequacy of previous methods for evaluating foams with the high order of stability usually associated with soaps is emphasized by the absence of any directly relevant published work. C. L. Baker (2) has presented some observations on the influence of pH on the foam stability of sodium stearate as part of a study on silicates as detergents. These results with regard to foam stability are too ambiguous to permit detailed discussion here.

We recognize that foam stability is a composite manifestation of several surface phenomena. However, we have learned that changes in foam stability provide exceedingly useful clues to the possible mechanisms involved in certain phases of surface activity.

MATERIALS

The fatty acids used in this work were derived from natural fats and were purified by different methods, according to the nature of the fatty acid. The saturated fatty acids were converted into the methyl esters and these were treated with potassium permanganate in acetone solution in order to remove the unsaturated impurities. The recovered neutral methyl esters were then fractionally distilled through a 5-foot modified Fenske fractionating column.

	BOILING POINT	ESTIMATED PURITY
	°C.	per cent
Methyl stearate	178.5 at 3.0 mm.	} > 98
Methyl palmitate ..	160.5 at 2.9 mm.	
Methyl myristate ..	132.5 at 1.8 mm.	
Methyl laurate	109.8 at 3.2 mm.	
Capric acid	132.5 at 4.3 mm.	
Methyl oleate	148.5 at 0.8 mm.	Approx. 95
Methyl ricinoleate ..	210.0 at 4.0 mm.	Approx. 95
Methyl undecylenate	105.4 at 3.3 mm.	Approx. 98
Elaidic acid	m.p. 43.5°C.	< 95

The oleic acid was purified through fractional crystallization of the lithium salt from 80 per cent alcohol; the elaidic acid by distillation and fractional crystallization of the acid prepared from purified oleic acid by action of selenium; the ricinoleic acid by fractional distillation of the methyl ester made from castor oil; the undecylenic acid by fractional distillation of the methyl ester of the crude acid prepared from castor oil. The purity of these acids was checked by the acid, saponification, and iodine values and by the melting point.

The free fatty acids were obtained from the esters by saponification, acidifying, washing, and drying. The soaps were prepared from the fatty acids by neutralizing exactly in alcohol solution, using phenolphthalein as an external indicator. They were obtained in the solid form (0.5–2.0 per cent moisture) by drying on a laboratory drum dryer. In this way soaps which were substantially neutral and contained only traces (< 0.2 per cent) of free alkali were obtained.

PROCEDURE

The foam stability of the solutions was compared by means of the pour foam test described by J. Ross and G. D. Miles (9). This consists in allowing 200 ml. of solution to fall through an orifice of fixed dimensions into a cylindrical glass column 90 cm. long, which contains 50 ml. of the same solution. The height of foam is measured and this is considered to be directly proportional to its volume. In most cases the height can be reproduced to within ± 3 mm. Since the productive and destructive forces are concomitant, the foam produced is subject to the destructive forces embodied in the action of the falling droplets upon the foam already formed. The design of the apparatus provides means for protecting the foam from evaporation and thermal shock.

The solutions were made by dissolving the soap required in distilled water. No stock soap solutions were employed and no dilutions were made. In dissolving the soaps, care was taken to avoid heating the solutions above the temperature of the test.

Where the effects of the calcium and magnesium soaps were studied, the soaps were always dissolved in distilled water and stock solutions of calcium or magnesium salts were added.

pH adjustments were made by the use of dilute solutions of sodium hydroxide or hydrochloric acid. Foam stabilities were frequently checked by raising and re-lowering the pH to be sure that the observed effects were attributable to pH changes and not to salt effects.

In the course of this work it was observed that the rate of recovery of the foam stability to the original value was influenced by the history of the pH changes made on the solution. If the pH was dropped and then raised, the recovery was slower than in instances where the change was from high to low pH. Therefore, as far as possible the procedure followed involved as few re-elevations of the pH as possible.

Measurements of pH were made using the Beckman Model G pH meter equipped with a type E glass electrode, which is stated to be relatively free from sodium-ion error at high pH values.

RESULTS

The influence of pH on the foam stability

Figures 1, 2, and 3 show the foam stabilities for solutions of soaps of pure fatty acids when the pH was altered by adding hydrochloric acid or sodium hydroxide.

Figures 4 and 5 show the pH range for the maximum foam stability as a function of concentration.

Detailed study of the influence of electrolytes on the foam stability of soap solutions was not made here. Care has been exercised, however, in the examination of other effects to eliminate salt effects as an unknown variable.

TABLE 1

Foam stability of solutions of soaps of the saturated fatty acids in hard water measured at their optimum pH

MATERIAL	CONCENTRATION	P. P. M. HARDNESS ADDED, CALCULATED AS CaCO ₃		CALCULATED FINAL CONCENTRATION OF SODIUM SOAP	MILLI- METERS OF FOAM FOR CALCULATED CONCENTRATION*	OBSERVED FOAM	CALCULATED FINAL PER CENT OF SOAP PRE- SENT AS PRE- CIPITATE	TEMPERATURE
		Ca	Mg					
	<i>per cent</i>			<i>per cent</i>		<i>mm.†</i>	<i>per cent</i>	<i>°C.</i>
Sodium laurate.	0.25	225		0.15	190	190	40	57
	0.25		225	0.15	190	185	40	57
Sodium myristate...	0.20	200		0.10	270	265	50	57
	0.20	300		0.05	235	220	75	57
	0.20	350		0.025	155	165	87	57
	0.20		300	0.05	235	220	75	57
Sodium palmitate . . .	0.05	72		0.01	180	170	80	57
			72	0.01	180	170	80	57

* Salt was added to distilled water solutions equivalent to that formed in the hard water precipitation of soap.

† All foams are reported to the nearest 5 mm.

The effect of calcium and magnesium soaps

Table 1 shows the influence of calcium and magnesium soaps upon the foam stability of solutions of sodium soaps of the saturated fatty acids, and table 2 shows the corresponding effects for soap solutions of the unsaturated fatty acids.

Temperature effects

The influence of temperature on the foam stability was found to be small. All of the soaps showed increases in foam height from 20 to 70 mm. over the range of 27° to 82°C. Details are omitted because of the similarity of the results for all the soaps studied.

The effect of temperature on the pH range for maximum foam stability was measured in some detail for two soaps. The results are shown in table 3.

The pH for maximum foam stability for a mixture of soaps appears in table 4.

TABLE 2

Foam stability of solutions of soaps of the unsaturated fatty acids in hard water measured at their optimum pH

MATERIAL	CONCENTRATION	P.P.M. HARDNESS ADDED, CALCULATED AS CaCO ₃		CALCULATED FINAL CONCENTRATION OF SODIUM SOAP	MILLI-METERS OF FOAM FOR CALCULATED CONCENTRATION*	OBSERVED FOAM	CALCULATED FINAL PER CENT OF SOAP PRESENT AS PRECIPITATE	TEMPERATURE
		Ca	Mg					
	<i>per cent</i>			<i>per cent</i>		<i>mm.†</i>	<i>per cent</i>	<i>°C.</i>
Sodium ricinoleate. .	0.10	78		0.05	170	Nil	50	57
	0.15	78		0.10	200	Nil	33	57
	0.25	37.5		0.226	235	Nil	10	57
	0.10		78	0.05	170	75	50	57
Sodium undecylenate ...	0.40	12.5		0.395	168	40	1	57
	0.40		484	0.20	75	67	50	57
Sodium oleate	0.10	12.5		0.092	205	195	8	24
	0.10	25		0.085	205	197	15	24
	0.10	122		0.025	175	Nil	75	24
	0.10		122	0.025	175	165	75	24
Sodium elaidate	0.10	142		0.015	200	197	85	57

* Salt was added to distilled water solutions equivalent to that formed in the hard water precipitation of soap.

† All foams are reported to the nearest 5 mm.

TABLE 3

The pH range for maximum foam stability as a function of temperature

MATERIAL	TEMPERATURE	pH RANGE	
		0.10 per cent solution	0.50 per cent solution
	<i>°C.</i>		
Sodium laurate	26	7.6-7.7	8.5-8.8
	57	7.1-7.3	8.0-8.8
Sodium caprate	26	6.2-6.3	7.8-8.5
	57	5.9-6.0	7.8-8.3

TABLE 4

Foam stability of mixtures of sodium palmitate and sodium laurate as a function of pH at 57°C.

COMPOSITION OF SOLUTION	pH OF SOLUTION TO NEAREST HALF UNIT									
	7.0	7.5	8.0	8.5	9.0	9.5	10.0	10.5	11.0	11.5
0.1% Sodium laurate	160*	120	80	55	30					
0.01% Sodium palmitate				25	40		110		183	195
0.01% Sodium palmitate } 0.10% Sodium laurate	195		208	185		190	210	185	178	210
0.005% Sodium palmitate } 0.10% Sodium laurate	162		152							175

* Figures represent foam height as measured in millimeters.

DISCUSSION

One of the fundamental distinctions between the properties of soaps and those of other detergents, such as the sodium alkyl sulfates, is that soap solutions hydrolyze, while synthetic detergents which are salts of strong acids do not hydrolyze. This is a complicating feature of any study of the surface-active properties of soap, because at least two of the hydrolysis products in such solutions are surface-active: namely, the undissociated fatty acid and the fatty acid anion.

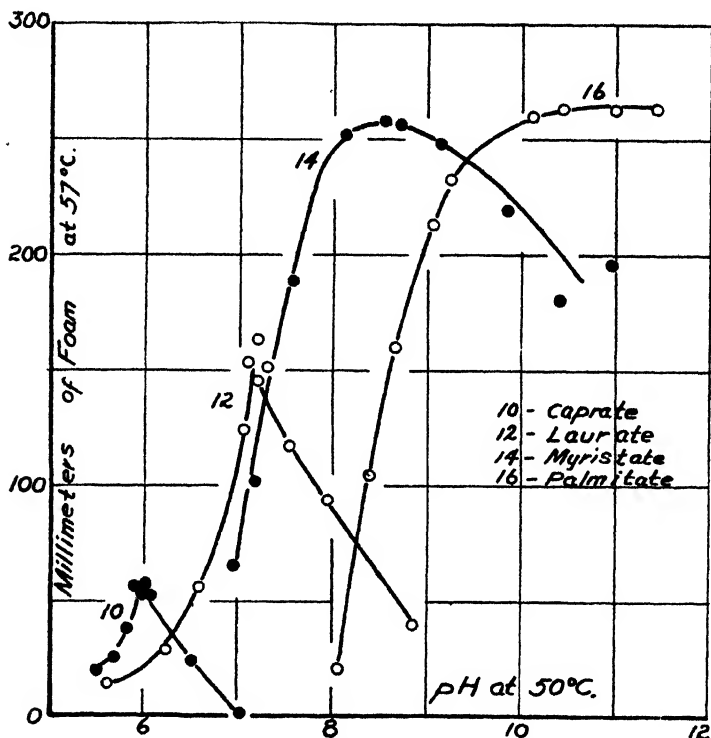


FIG. 1. Foam stability of 0.10 per cent solutions of pure sodium salts of saturated fatty acids as a function of pH at 57°C.

Further complications arise owing to the difference in apparent weakness of the various fatty acids, which is probably a manifestation of differences in their solubility. With this in mind it is clear that pH is a variable of considerable influence in determining the surface-active properties of soap solutions.

This point is illustrated in figure 1, where the pH determines the balance between the relative amounts of the various surface-active components. This is reflected in the changes in stability of the foam as a function of changes in the pH of the solutions.

In comparing the relative foam stability of solutions of soaps of the pure fatty acids, some arbitrary pH must be chosen. Figures 2 and 3 were prepared by comparing the foam stability of the solutions as a function of concentration at

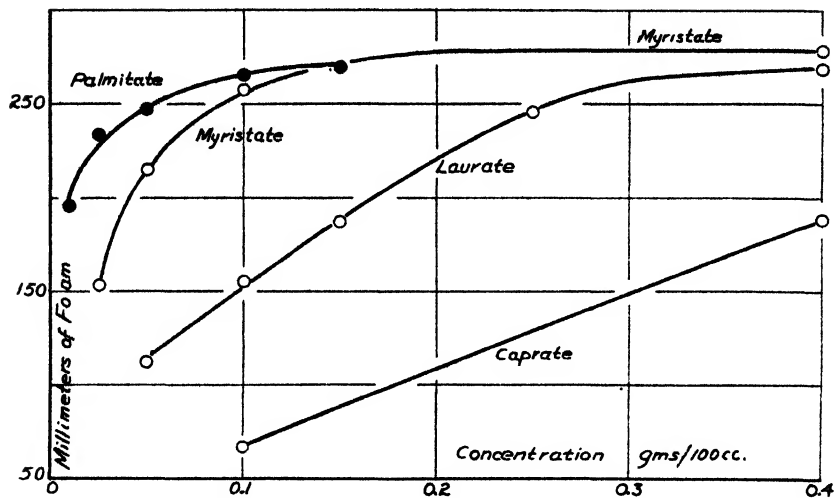


FIG. 2. Foam stability of solutions of pure sodium salts of saturated fatty acids at 57°C. as a function of concentration where each solution was adjusted to the pH for maximum foam stability.

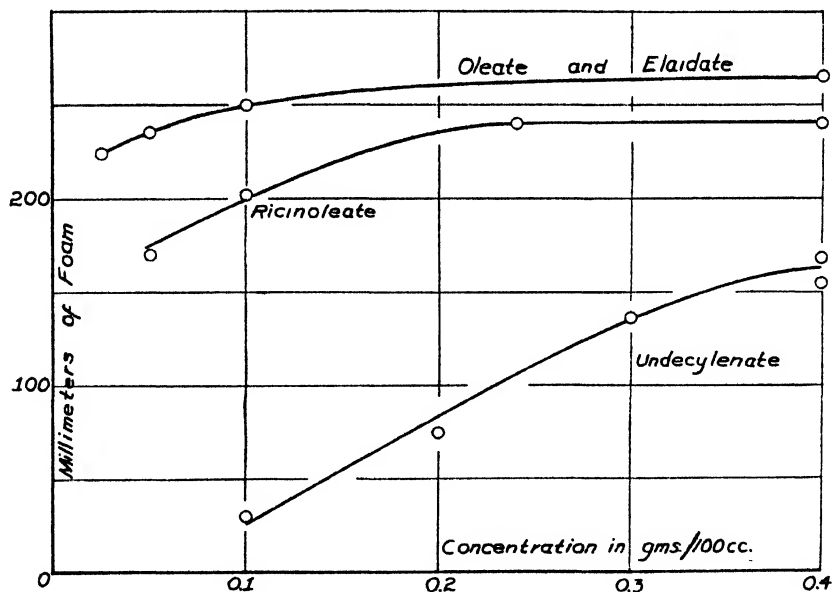


FIG. 3. Foam stability of solutions of pure sodium salts of unsaturated fatty acids at 57°C. as a function of concentration where each solution was adjusted to the pH for maximum foam stability.

the pH which gave the highest foam stability obtainable with such a material. Here we see the customary increase in over-all stability or surface activity usually associated with increasing molecular weight in a homologous series. Figures 4

and 5 show the pH range within which the maximum foam stability was exhibited for each concentration studied and shown in figures 2 and 3. The general trends discernible in these graphs are fairly obvious and a detailed discussion of them serves of little value at this time, owing to our limited knowledge of the exact nature of the hydrolysis of soaps as a function of molecular weight and concentration. Let us return to figure 1, which is a detailed section through figure 4 with particular attention focussed on the foam stabilities observed beyond the

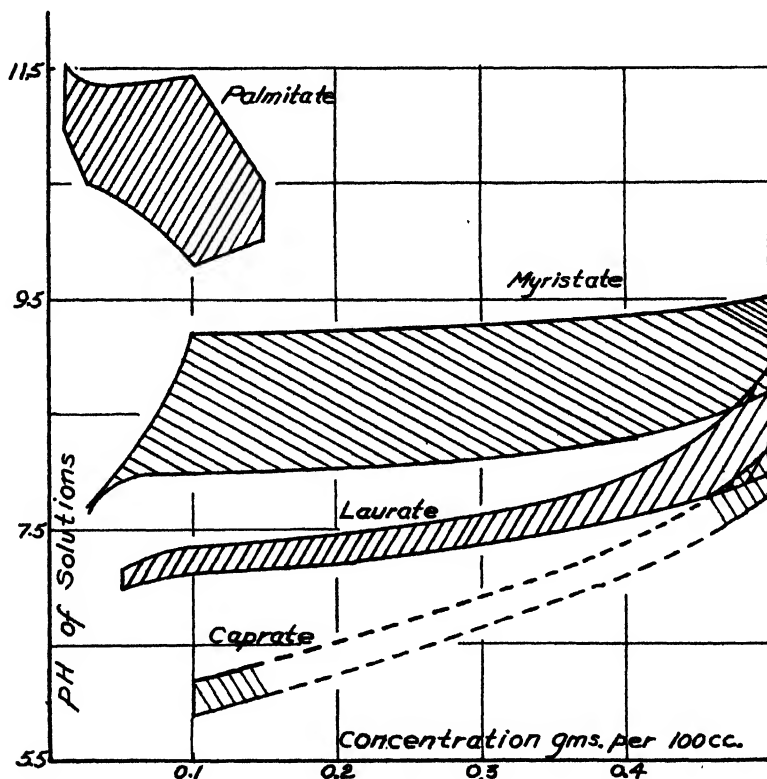


FIG. 4. pH range for maximum foam stability for solutions of sodium salts of the saturated fatty acids at 57°C. as a function of concentration.

limits for maximum foam. A striking feature here is the way the maximum foam stability is obtained with increasing ratios of undissociated fatty acid to fatty acid anion as the number of carbon atoms in the series is decreased. In fact, if the pH of the sodium caprate or sodium laurate solutions was elevated to a point where the concentration of the undissociated fatty acid approached zero, the foam stability was also nearly zero. Powney (7) has observed analogous surface tension behavior for potassium laurate solutions when potassium carbonate was added.

Cupples (3) found related changes in contact angle, interfacial tension, and surface tension for soaps as a function of the pH.

An interesting feature in the behavior of these materials is the important rôle played by the fatty acids in stabilizing the foams of certain solutions. Naturally, we can only guess with regard to the form in which the fatty acid is present at the interface. It seems probable that the films are simple mixtures of the acid anion and the acid. This concept suggests that other combinations of two surface-active materials, neither of which produces stable foams when blended, might yield a relatively more stable foam. The number of surface-active materials

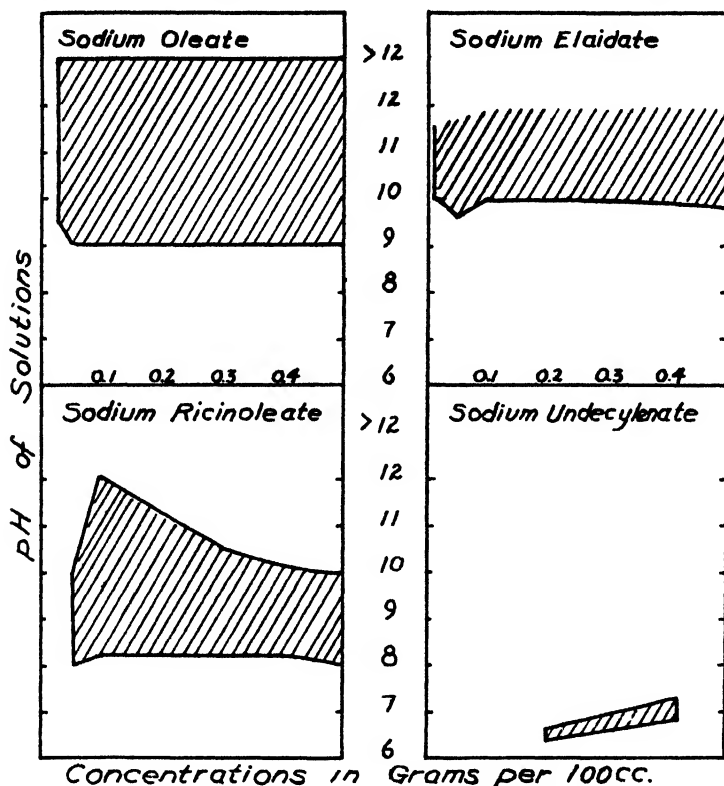


FIG. 5. pH range for maximum foam stability for solutions of sodium salts of the unsaturated fatty acids at 57°C. as a function of concentration.

which do not produce stable foams is fairly large, and therefore a further clue as to the desirable nature of each member of the pair was sought in the prototype mixture of sodium laurate-lauric acid. The laurate anion might be considered as a water-soluble surface-active ion in which the hydrophilic character is so dominant that adsorption is inadequate for production of stable foam. The lauric acid, on the other hand, is a member of a series of homologues in which none exhibit foam-stabilizing properties and those members which are appreciably surface active are only slightly water soluble. With these rough characterizations in mind a few simple experimental tests of this concept were made. It was found that lauryl alcohol would stabilize the foam of 0.1 per cent sodium laurate

solutions at pH 10 and lauric, myristic, or palmitic acid would stabilize the otherwise unstable foam of 0.2 per cent sodium decyl sulfate solution at pH 4. All of these solutions were saturated with respect to the least soluble component. With each of the acids a definite temperature had to be exceeded before any foam could be produced. Washing the stabilized foams with solutions of either one of the components alone inevitably led to foam collapse.

In connection with the properties of mixtures of surface-active materials, others have reported experimental results which may be related to the foam stability data just mentioned. Davis and Bartell (4) reported that the extremely low interfacial tensions observed for partially hydrolyzed sodium laurate solutions and a non-polar organic liquid "are the result of two factors neither one of which, by itself, is sufficient to lower the interfacial tension to the extent observed." Adam (1), referring to the work of Schulman and Hughes, stated that they found that mixtures of 3 moles of oleic acid to 1 mole of hexadecyl alcohol exhibited film areas decidedly larger than the sum of the areas of the constituents. Elsewhere, Adam has stated that vapor-expanded films are also found to be more or less condensed by admixture with cholesterol or tripalmitin.

In our own experience we have observed that lauryl alcohol may increase many-fold the surface viscosity of sodium lauryl sulfate solution.

In figure 1, in contrast to the behavior of sodium laurate, the sodium palmitate solutions could not be acidified below pH 9.5 without loss in foam stability. From a titration curve for a 0.1 per cent sodium palmitate solution, it has been estimated that the fatty acid concentration at pH 9.5 is not less than 0.028 per cent. This is nearly twenty-four times as much palmitic acid as is soluble in water at 60°C., according to Ralston and Hoerr (8). In other words, the concentration of the soluble active ingredient may have been reduced by the formation of some insoluble palmitic acid. It is not surprising, therefore, that some loss in foam stability was observed when this loss in active material occurred in the concentration range studied.

A similar calculation based upon a titration curve obtained with sodium laurate indicates that at pH 7.2, 0.1 per cent sodium laurate contains not less than 0.007 per cent lauric acid. This figure is approximately equal to the reported water solubility of lauric acid.

The solubility of fatty acids in water probably can not serve as a measure of their solubility in a solution of the corresponding sodium soap because of solubilization. In this regard our discussion may be oversimplified. However, it is quite possible that solubilized fatty acids are just as inactive, from a foam stabilizing point of view, as precipitated fatty acids.

It is seen, therefore, that no direct comparisons among soap solutions can be made unless hydrolysis is completely suppressed or suitable corrections are applied. These corrections should include factors which compensate for the difference in solubility of the various fatty acids and its manifestation as apparent differences in the strength of the acids.

Table 3 shows that the effect of temperature on the pH range for maximum foam stability is to lower the pH range as the temperature rises. This suggests

that, as the temperature rises, the fatty acid is apparently stronger because it becomes more soluble.

Variations in pH appear to affect the foam stability of solutions of mixtures of soaps less than solutions of the individual soaps of which they are composed. This is shown in table 4.

Our experiments on the influence of calcium or magnesium soaps on the foam stability of solutions of the corresponding sodium soaps are based upon the use of foam stability as a guide to the effective concentrations of surface-active material. Under the best conditions the concentration can be estimated to within 5–10 per cent, using the pour foam test. Tables 1 and 2 show that, contrary to Frisch and Valko (5), the calcium and magnesium soaps formed, in general, can be considered as compounds of uniform composition. Frisch and Valko have postulated the formation of continuously variable complexes with increasing calcium content up to a final calcium–fatty acid ratio of 1 to 2 at the equivalence point. Within the limits of the precision of our method, this uniform stoichiometric ratio appears to exist for all soaps of saturated fatty acids.

Furthermore, it has been demonstrated that, as a rule, calcium and magnesium soaps are not foam breakers in solutions of sodium soaps. Certain exceptions to this appear among the calcium soaps of the unsaturated fatty acids. Our interpretation of these exceptions is based upon the idea that all of the calcium and magnesium soaps are surface active but only those possessing sufficient solubility can exhibit this property. The fact that calcium elaidate is not a foam breaker, while the isomeric calcium oleate is a foam breaker, is in accord with this viewpoint.

No measurements of surface or interfacial tension have been made for the systems studied in this paper because of their complex nature. It has been shown elsewhere (6) that solutions containing two surface-active species may exhibit "anomalous" surface tensions, and for this reason the usefulness of such data may be questioned. It is clear that surface activity as measured by surface adsorption cannot be correlated directly with foam stability, detergency, wetting, and other complex but highly significant attributes of solutions of this type.

SUMMARY

1. The effect of alterations in pH upon relative foam stability has been examined for 0.1 per cent solutions of sodium caprate, laurate, myristate, palmitate, and stearate.
2. Relative foam stability as a function of concentration has been measured at 57°C. for solutions of sodium caprate, laurate, myristate, palmitate, stearate, undecylenate, oleate, elaidate, and ricinoleate at the pH where each solution showed maximum foam.
3. The pH range associated with the maximum foam stability for these soaps as a function of concentration was determined at 57°C.
4. The influence of calcium and magnesium soaps upon the foam stability of solutions of the corresponding sodium soaps was examined.
5. The composition of the calcium and magnesium soaps was determined indirectly by measurements of foam stability.

6. The effect of temperature upon the relationship of pH to foam stability was studied for sodium caprate and laurate.

7. The effect of temperature on the foam stability of all the soaps mentioned in paragraph 2 above was ascertained for the range 27° to 82°C.

8. The effect of pH on the foam stability of mixtures of sodium laurate and palmitate was determined.

9. Good foam stability was obtained for a few solutions containing two materials neither of which, alone, is a particularly good foam stabilizer.

The authors wish to express their appreciation to Mr. C. W. Jakob for the care which he exercised in performing many of the determinations upon which this paper is based.

- (1) ADAM, N. K.: *The Physics and Chemistry of Surfaces*, 2nd edition, p. 71. Oxford University Press, London (1938).
- (2) BAKER, C. L.: *Ind. Eng. Chem.* **23**, 1025 (1931).
- (3) CUPPLES, H. L.: *Ind. Eng. Chem.* **29**, 924 (1937).
- (4) DAVIS, J. K., AND BARTELL, F. E.: *J. Phys. Chem.* **47**, 40 (1943).
- (5) FRISCH, J., AND VALKO, E.: *Chem.-Ztg.* **50**, 333 (1926).
- (6) MILES, G., AND SHEDLOVSKY, L.: *J. Phys. Chem.* **48**, 57 (1944).
- (7) POWNEY, J.: *Trans. Faraday Soc.* **31**, 1510 (1935).
- (8) RALSTON, A. W., AND HUERR, C. W.: *J. Org. Chem.* **6**, 54 (1942).
- (9) ROSS, J., AND MILES, G. D.: *Oil & Soap* **18**, 99 (1941).

THE CATALYTIC OXIDATION OF ETHYLENE TO ETHYLENE OXIDE

L. H. REYERSON AND HANS OPPENHEIMER

School of Chemistry, University of Minnesota, Minneapolis 14, Minnesota

Received May 5, 1944

A number of years ago the catalytic oxidation of ethylene was studied, using a series of active metallized silica gels as catalysts (4). The results indicated that the oxidation was incomplete over the temperature range then explored. The products of the partial oxidation proved to be largely the oxides of carbon and water. However, at times when the silver-silica gel catalyst was used, a trace of a pleasant odor differing from that of ethylene was detected in the products of reaction. Attempts to identify the substance failed. Since that time less active forms of silver catalysts, giving rise to almost no oxides of carbon, have been successfully used on a commercial scale in the production of ethylene oxide. It therefore seemed desirable to study the oxidation of ethylene, using a series of silver catalysts over a wide temperature range, in an attempt to establish some of the conditions for the successful preparation of ethylene oxide from ethylene.

It was decided to use three different silver catalysts: (1) a silver-silica gel catalyst similar to the one previously used; (2) silver deposited on fused aluminum

oxide, known to be effective in the commercial production of ethylene oxide; (3) finely divided silver produced by the thermal decomposition of silver oxalate. The silver-silica gel catalyst was prepared by shaking 80 g. of purified silica gel in 500 ml. of a solution of 0.5 N $\text{Ag}(\text{NH}_3)_2\text{NO}_3$. The solution was decanted after several hours, the gel was lightly dried, and the adsorbed silver salt was reduced in a slow stream of hydrogen at 200°C . The gel granules usually became black and lustrous. Silver gels containing 8.9, 14.7, and 22.2 per cent of silver were prepared in this way. The dark film coating was proved to be silver. In one of the preparations an interesting product was obtained. The gel was by accident treated with a silver nitrate solution that did not contain ammonium hydroxide. When this was noted the solution was decanted from the gel and ammonium hydroxide added, after which the solution was again poured onto the gel and the treatment carried out as usual. The gel was divided into two parts for reduction in hydrogen. One of them produced the regularly obtained black or gray black silver-coated gel. The other contained granules which were very shiny, and it appeared as though they were covered with silver mirrors. On crushing, the fragments looked black and treatment with strong nitric acid instantly turned the silver mirrors black. Every evidence pointed to a very thin mirror-like film that coated the granules.

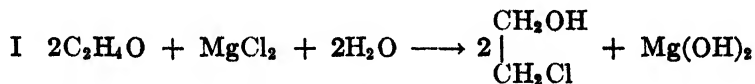
The catalyst consisting of finely divided silver on fused aluminum oxide contained 5 per cent silver and had a yellow appearance. It was a sample of a catalyst used in oxidizing ethylene to ethylene oxide.

Silver oxalate was formed by mixing approximately 1 normal solution of silver nitrate and oxalic acid. The white precipitate was allowed to settle for several hours. It was then filtered, washed with distilled water, and dried at about 80°C . Thermal decomposition began at about 110°C . and became rather violent at 150°C . The residue was very voluminous, had a brownish yellow color, and possessed no structural strength.

Each of these catalysts was used in an electrically heated U-tube having a diameter of 17 mm. By using 10 ml. of the catalyst, the curved part of the U-tube was always filled to the same extent. This catalyst bed was equivalent to one 6 cm. deep. A thermometer was inserted in the tube so that its bulb was always buried in the catalyst. Variable resistances and a lamp bank in the heating circuit made it possible to work in a temperature range of 150° to 350°C . The ethylene used was a commercial product of high purity. It was taken from the tank, mixed with the required amount of air, and stored over water. In the runs without added steam the gas mixture was dried by passing it through tubes of anhydrous calcium chloride. A mixture of 2 per cent ethylene and 98 per cent air, or one of 2 per cent ethylene, 48 per cent air, and 50 per cent steam, was passed over the catalysts at a constant rate and temperature for slightly more than 1 hr. for each run. The rates of flow were measured by calibrated flowmeters and varied from 950 ml. to 3860 ml. per hour. In the earlier study (4) the concentration of ethylene was maintained at more than ten times the amount used in the present study. It has since been learned that low ethylene concentration gives better conversion to ethylene oxide.

When the catalyst tube had reached the desired temperature, the air in the

system was swept out by the gas mixture before the actual run was begun. After passing over the catalyst, the gases were bubbled through three gas-washing bottles. The first two contained solutions of hydrochloric acid saturated with magnesium chloride. The third bottle contained water in order to catch any acid that might be carried over from the first two bottles. The gas was bubbled through the solutions from small orifices. Analytical determinations showed that almost all of the ethylene oxide formed in the reaction was absorbed in the first wash bottle. However, the solutions of the bottles were always analyzed to determine the total ethylene oxide absorbed. Divergent opinions still prevail as to the exact mechanism of the absorption of ethylene oxide by the acid magnesium chloride solution. W. Deckert (2) concludes that the reaction proceeds in two stages:



On the other hand, Lubatti (3) believes that the ethylene oxide adds directly to the hydrochloric acid. The salt is required to control the activity of the acid. J. H. Brønsted and his coworkers (1) have shown that the truth probably lies somewhere between these two viewpoints. For this work, however, the mechanism is not important, since 50 mg. of ethylene oxide in a cubic meter of gas can be detected by this method. The hydrochloric acid used up by the ethylene oxide was readily determined by titration. The percentage of ethylene converted to ethylene oxide was then calculated.

The results of different runs are given in the following tables. The yield of ethylene oxide is the percentage of the ethylene which was converted to the oxide. These results show the very low efficiency of silver-silica gel catalysts in converting ethylene to ethylene oxide. The other catalysts proved effective and both showed a maximum efficiency somewhere between 260°C. and 300°C.

The results shown in table 2 indicate that changes in space velocity within reasonable limits do not appreciably affect the conversion to ethylene oxide. However, there was some evidence that the catalysts lost activity to a slight extent if used for several runs at one temperature. When the catalyst was allowed to stand overnight exposed to air, its activity appeared to be fully restored. This was especially true of the finely divided silver catalyst. Activity appeared to be definitely impaired if the catalyst was heated to 350°C. or above. Heating of the catalyst affected the color of the finely divided silver, so that the surface was undoubtedly altered. The effect of diluting the gas mixture with 50 per cent steam was studied on finely divided silver and on silver-silica gel catalysts (see table 3).

Comparison of these results with those obtained without steam showed that this catalyst lost some efficiency in the presence of steam. Silver-silica gel catalysts seemed to gain some efficiency in the presence of steam, but prolonged use of these catalysts in the presence of steam finally cut down their activity. The

fact that water vapor and ethylene are strongly adsorbed by such silica gel catalysts may partially account for this effect. At any rate each of the later runs

TABLE 1

The effect of temperature on the reaction composition of the gas mixture consisting of 2 per cent ethylene and 98 per cent air

Rate of gas flow through the catalyst, 1930 ml. per hour

TEMPERATURE	YIELD OF ETHYLENE OXIDE	TEMPERATURE	YIELD OF ETHYLENE OXIDE
Catalyst: Silver on fused aluminum oxide		Catalyst: finely divided silver from silver oxalate	
°C.	per cent	°C.	per cent
208	10.6	182	6.7
228	25.1	214	14.3
246	32.6	238	34.7
254	28.9	282	45.1
268	33.5	300	42.6
291	27.2	314	39.7
307	19.3	350	29.1
Silver-silica gel catalyst, 22.3 per cent silver; rate of gas flow, 1820 ml. per hour		Second preparation of finely divided silver	
177	2.2	196	3.3
210	1.1	220	22.3
230	1.0	268	42.5
270	1.5	285	40.1
290	1.1	300	31.1
306	1.8	333	25.6

TABLE 2

The effect of changing space velocity

CATALYST	TEMPERATURE	RATE OF FLOW	YIELD
	°C.	ml per hour	per cent
5 per cent silver on fused aluminum oxide	265	1080	33.2
	261	1620	32.5
	262	2070	31.4
Silver-silica gel, 14.7 per cent silver	289	1020	1.7
	292	1740	2.2
	290	1930	3.0
Finely divided silver from silver oxalate	288	980	39.1
	292	1350	39.5
	291	1820	42.8
	293	2240	38.7

were made using fresh catalysts. The yields obtained with the silver-silica gel catalyst (14.7 per cent silver) and 50 per cent steam were about double those obtained in the absence of steam (see table 4). Since the silver-silica gel catalysts

were known (4) to be effective in oxidizing a portion of the ethylene to the oxides of carbon and water, it seems likely that the steam reduced this activity of the catalyst enough to increase its effectiveness in ethylene oxide formation. Finally, another silver-silica gel catalyst containing 8.9 per cent silver was prepared, and fresh samples of catalyst were used for a series of runs at varying temperatures

TABLE 3

Catalyst, finely divided silver; gas mixture, 2 per cent ethylene, 48 per cent air, 50 per cent steam

RATE OF FLOW	TEMPERATURE	YIELD
<i>ml. per hour</i>	<i>°C</i>	<i>per cent</i>
3860	263	17.7
3860	290	29.9
2180	290	30.4
1960	278	38.2

TABLE 4

Silver-silica gel catalyst, 14.7 per cent silver; gas mixture, 2 per cent ethylene, 48 per cent air, 50 per cent steam

RATE OF FLOW	TEMPERATURE	YIELD
<i>ml. per hour</i>	<i>°C.</i>	<i>per cent</i>
3860	180	4.0
3860	237	4.0
3860	272	6.3
1960	271	7.1

TABLE 5

Silver-silica gel catalyst, 8.9 per cent silver; gas mixture, 2 per cent ethylene, 48 per cent air, 50 per cent steam

TEMPERATURE	YIELD
<i>°C.</i>	<i>per cent</i>
153	2.3
181	3.7
235	3.8
275	4.1
293	2.7
349	1.7

and a constant rate of gas flow (see table 5). The gas mixture was diluted with 50 per cent steam. An optimum yield was obtained at 275°C., which corresponds to the optima obtained for the other two catalysts. However, the efficiency of the silver-silica gel catalysts is much lower than that of the other silver catalysts used in this investigation. The results reported in table 1 for the silver-silica gel catalyst show no such temperature optimum of activity. The presence of steam

appears to make the silica gel catalysts behave more like the other silver catalysts but with a much lower efficiency.

SUMMARY

The finely divided silver and the silver on fused aluminum oxide showed an optimum activity in the conversion of ethylene to ethylene oxide in the temperature range of 260–290°C. Addition of steam lowered the activity of these catalysts slightly. Changes in space velocity of the gases did not greatly affect their efficiency. In the absence of steam the silver-silica gel catalysts showed very low activity and no such temperature optimum. The presence of 50 per cent steam about doubled the efficiency of these catalysts, and they showed an optimum of efficiency in the same temperature range as the other two catalysts. It seems likely that had steam been added to the gas mixtures in the earlier study (4) the investigators might well have found ethylene oxide in the products of the reaction.

REFERENCES

- (1) BRÖNSTED, J. H., KILPATRICK, MARY, AND KILPATRICK, M., JR.: *J. Am. Chem. Soc.* **51**, 428 (1929).
- (2) DECKERT, W.: *Z. angew. Chem.* **45**, 559 (1922); *Z. anal. Chem.* **82**, 297 (1930); **109**, 166 (1937).
- (3) LUBATTI, O. F.: *J. Soc. Chem. Ind.* **51**, 361 (1932); **54**, 424 (1932).
- (4) REYERSON, L. H., AND SWEARINGER, L. E.: *J. Am. Chem. Soc.* **50**, 2872 (1928).

THE RELATION BETWEEN THE FORCE CONSTANT AND THE INTERATOMIC DISTANCE OF A DIATOMIC LINKAGE

C. K. WU AND (IN PART) CHANG-TSING YANG

National Chekiang University, Tsunyi, China

Received March 28, 1944

In recent years many empirical relations have been proposed to connect the vibration frequency, ω_e , or the force constant, K_e , with the internuclear distance, R_e , of a diatomic linkage. Among them, the Clark rule (3)

$$R_e = \frac{K_{gr} - K'_{gr}}{\omega_e \sqrt{N}}$$

the Badger rule (2)

$$R_e = (C_{ij}/K_e)^{1/3} - D_{ij}$$

and the Allen-Longair rule (1)

$$R_e = (K_{ij}/K_e)^{1/6}$$

are relatively successful, where N is the "group number", K_g and K'_g are constants for a given "molecular period" and a given "electron configuration" within the molecular period, and C_{ii} , D_{ii} , and K_{ii} are constants for a given molecular period. Clark and Stoves (4) have analyzed the results of the applications of these rules to seventy states of thirty-three non-hydride diatomic molecules, and have shown that the average error of the calculated R_e is about

TABLE 1

Period.....	00	01	02	11	12	22
m	4	4	4	4	6	6
$b \times 10^{18}$ c.g.s.u.....	0.10	0.602	1.15	0.25	2.38	34.3
$p \times 10^8$ cm.....	0.10	0.131	0.135	0.33	0.065	0.199
Relation:	$K'_g = \frac{A}{R_e^{m+1}} - \frac{B}{R_e^{n+2}} \begin{cases} A \dots\dots & 4.00 & 18.30 & 34.0 & 33.0 & 220 & 1033 \\ B \dots\dots & 2.00 & 12.04 & 23.0 & 5.00 & 110 & 1440 \end{cases}$					

K_g in 10^5 dynes per centimeter; R_e in 10^{-8} cm.

TABLE 2

Period 0,0; $K_g = -2.0/R_e^4 + 4.0/R_e^6$

(K_g in 10^5 dynes per centimeter and R_e in 10^{-8} cm.)

MOLECULE	STATE	ω_e	R_e	K_g	K_g (CALCULATED)	ERROR
		cm. ⁻¹				per cent
H ₂	1s σ 7p $\pi^3\Pi_u$	2293	1.067	1.55	1.54	-0.6
	1s σ 5p $\pi^3\Pi_u$	2309	1.066	1.57	1.55	-1.3
	1s σ 4p $\pi^3\Pi_u$	2336.5	1.065	1.61	1.57	-2.5
	1s σ 4p $\sigma^3\Sigma_u^+$	2184(?)	1.081	1.41	1.46	+3.5
	1s σ 3p $\pi^3\Pi_u$	2372.53	1.059	1.65	1.59	-3.6
	1s σ 3p $\sigma^3\Sigma_u^+$	2197	1.120	1.42	1.26	-14.1
	1s σ 2s $\sigma^3\Sigma_g^+$	2664.61	0.999	2.10	2.01	-4.4
	1s σ 3s $\sigma^3\Sigma_g^+$	2538	1.06	1.90	1.58	-16.8
	1s σ 3d $\sigma^3\Sigma_g^+$	2455.45	1.07	1.78	1.52	-7.8
	1s σ 2p $\pi^3\Pi_u$	2446.5	1.06	1.77	1.58	-12.1
	1s σ 2p $\sigma^3\Sigma_u^+$	1357.23	1.313	0.544	0.640	+18.4
	1s σ^3 1 Σ_g^+	4371	0.749	5.64	5.64	0
Average (\pm)						7.1

1 to 3 per cent with some larger individual errors. Sutherland (6), in an attempt to find a theoretical basis for these relations, has shown that they may be derived semiempirically from a potential function of the form

$$V = -\frac{\alpha}{R^m} + \frac{\beta}{R^n}$$

By $\left(\frac{\partial V}{\partial R}\right)_{R_e} = 0$ and $\left(\frac{\partial^2 V}{\partial R^2}\right)_{R_e} = K_g$, the relations

$$K_g = m\alpha(n-m)/R_e^{m+2} = n\beta(n-m)/R_e^{n+2}$$

TABLE 3
Period 0,1; $K_e = -12.04/R_e^2 + 18.30/R_e^5$

MOLECULE	STATE	ω_e	R_e	K_e (EXPERI- MENTAL)	K_e (CALCU- LATED)	ERROR
						<i>per cent</i>
LiH.....	$G^1\Sigma^+$	1406.1	1.6	1.02	1.02	0
BeH ⁺	$^1\Sigma^+$	1476.1	1.603	1.16	1.02	-12.0
	$G^1\Sigma^+$	2220	1.310	2.62	2.32	-11.0
BeH ⁰	$^2\Pi_{reg.}$	2087.6	1.330	2.32	2.23	-3.6
	$G^1\Sigma^+$	2058.5	1.340	2.25	2.16	-4.0
BH... ..	$^1\Pi$	(2450)	1.213	3.25	3.19	+1.9
	$G^1\Sigma^+$	(2230)	1.226	2.69	3.09	+14.5
CH.....	$^1\Sigma^+$	2675 (ω_1)	1.13 (r_0)	3.90	4.01	+2.9
	$^1\Delta$	2800 (ω_1)	1.20 (r_0)	4.27	4.42	+3.5
	$G^2\Pi_{reg.}$	2851 (ω_1)	1.13 (r_0)	4.43	4.01	-9.5
OH... ..	$^1\Sigma^+$	3182.5	1.009	5.62	6.14	+9.3
	$G^2\Pi$	3568.4 (ω_1)	0.969	7.07	6.88	+0.2
FH... ..	$G^1\Sigma$	4037	0.864	9.14	9.08	-0.7
Average (\pm)						5.3

TABLE 4
Period 0,2; $K_e = -23.0/R_e^2 + 34.0/R_e^5$

MOLECULE	STATE	ω_e	R_e	K_e (EXPERI- MENTAL)	K_e (CALCU- LATED)	ERROR
						<i>per cent</i>
MgH ⁺	$^1\Sigma^+$	1138.4	2.008	0.734	0.691	-6.1
	$G^1\Sigma^+$	1702.2	1.310	1.64	1.66	+1.2
MgH ...	$^2\Pi$	(1700)	1.67	1.63	1.56	-4.3
	$^2\Pi_{reg.}$	1603.45	1.68	1.46	1.52	+4.1
	$G^2\Sigma^+$	1493.45	1.73	1.26	1.33	+5.5
AlH	$G^1\Sigma^+$	1680.6	1.644	1.61	1.67	+3.7
SiH ..	$G^2\Pi_{reg.}$	(2012) (ω_0)	1.527 (R_0)	2.31	2.28	-2.2
HCl ⁺ ...	$^2\Pi$	(2608)	1.313	3.90	4.23	+8.4
HCl ...	$^1\Sigma$	2989.7	1.272	5.13	4.88	-4.8
Average (\pm)						4.5

TABLE 5
Period 1,1; $K_s = -5.00/R_s^4 + 33.0/R_s^6$

MOLECULE	STATE	ω_s	R_s	K_s (EXPERI- MENTAL)	K_s (CALCU- LATED)	ERROR
						<i>per cent</i>
Li ₂	¹ Π _g	269.7 (H)	2.93	0.142	0.145	+2.1
	¹ Σ ⁺	253.2 (H)	3.11	0.125	0.107	-14.4
	G ¹ Σ ⁺	351.6	2.67	0.242	0.229	-5.8
BeO.....	¹ Σ	1370.8	1.358	6.33	6.33	0
	¹ Π	1127.8	1.468	4.28	4.33	+1.2
	G ¹ Σ	1486.9	1.327	7.47	7.08	-5.2
CC.....	¹ Π	1832.5	1.251	11.81	9.45	-19.8
	³ π	1792.6	1.261	11.30	9.09	-10.7
	¹ π	1608.3	1.315	9.09	7.37	-18.9
	G ³ π	1641.6	1.308	9.47	7.61	-19.6
BeF.....	³ π	1172.6	1.390	4.92	5.62	+14.2
	G ³ Σ	1265.6	1.357	5.74	6.35	+10.6
B ¹¹ O.....	³ Σ	1280	1.301	6.26	7.81	+24.6
	³ π	1259.1	1.348	6.05	6.65	+9.9
	G ³ Σ	1885.4	1.199	13.57	11.59	-14.6
B ¹⁰ O.....	G ³ Σ	1940.5	1.199	14.21	11.59	-18.1
CN.....	³ Σ	2164.2	1.148	17.76	14.33	-19.0
	³ π	1788.7	1.236	12.11	10.02	-17.3
	G ³ Σ	2068.8	1.169	16.24	13.10	-19.3
CO.....	¹ Σ	2182.4	1.118	19.14	16.34	-14.6
	¹ π	1516.7 H	1.232	9.24	10.13	+9.6
N ₂	³ π	1037.6	1.201	12.30	11.52	-6.4
	³ Σ	1460.4	1.291	8.74	8.11	-7.2
	G ¹ Σ	2359.6	1.094	22.84	18.14	-20.6
NO.....	³ π	1737.64	1.413	4.71	5.22	+9.8
	³ Σ	2375.6	1.060	24.67	21.77	-11.7
	G ³ π	1906.5	1.146	16.27	14.40	-11.5
O ₂	³ Σ	710.1	1.599	2.36	2.86	+21.2
	¹ Σ	1432.6	1.223	9.62	10.58	+9.1
	G ³ Σ	1584	1.204	11.78	11.38	-3.4
F ₂	¹ π	1139.8 H	1.278	7.23	8.52	+17.8
CO ⁺	³ Σ ⁺	1722.1	1.16	11.92	13.62	+14.3
	³ π	1564.5	1.24	9.83	9.86	+3.0
	G ³ Σ ⁺	2212	1.11	17.92	16.88	-5.9
N ₂ ⁺	³ Σ ⁺	2417.7	1.071	23.77	20.03	-11.5
	G ³ Σ	2206	1.113	19.96	16.71	-16.3
O ₂ ⁺	G ³ Σ	1876	1.14	16.50	14.86	-9.9
Average (±)						12.0

are obtained. If α , n , m are constant for a molecular period, then with $m = 4$, the Allen-Longair rule is obtained. By substituting $(R_e - D_{ij})$ for R_e and with $m = 1$, the Badger rule is obtained. Subsequently, Sutherland (7) has discussed the consequences of this potential function. It seems that such a method of derivation may also be used to find new relations of R_e and K_e by assuming other types of potential functions. It is the purpose of this paper to test such a possibility.

The potential function assumed is of the Born-Mayer form:

$$V = ae^{-R/p} - b/R^m \quad (1)$$

By $\left(\frac{\partial V}{\partial R}\right)_{R_e} = 0$ and $\left(\frac{\partial^2 V}{\partial R^2}\right)_{R_e} = K_e$, we obtain

$$\frac{a}{p} e^{-R_e/p} = \frac{bm}{R_e^{m+1}} \quad (2)$$

and

$$\begin{aligned} K_e &= \frac{1}{e^{R_e/p}} \left[\frac{a}{p^2} - \frac{a(m+1)}{pR_e} \right] \\ &= \frac{1}{R_e^{m+1}} \left[-\frac{bm(m+1)}{R_e} + \frac{bm}{p} \right] \end{aligned} \quad (3)$$

If m , p , a are constant within a molecular period, or if m , p , b are constant, then a plot of $K_e e^{R_e/p}$ in the former case or a plot of $K_e R_e^{m+1}$ in the latter case against $1/R_e$ will yield a straight line for molecules of the same period. If, on the other hand, more than one of the four varies, neither plot will in any case give a straight line.

The plot of $K_e e^{R_e/p}$ against $1/R_e$ was first tried with different values of p . However, all the plots tried failed to give straight lines. The plot of $K_e R_e^{m+1}$ against $1/R_e$ is more successful; with $m = 4$ for diatomic molecules of molecular periods 00, 01, 02, and 11, and with $m = 6$ for molecular periods 12 and 22, good results are obtained. The constants determined from the plots are given in table 1.

From these relations, calculations of K_e are made from R_e for molecules with available data. The results, together with the value of K_e calculated from ω_e and μ , are tabulated in tables 2, 3, 4, 5, 6, and 7. For other molecular periods, the data seem too meagre to justify a plot. All data are taken from Jevons (5). As the present war conditions do not allow the author to consult all original data cited, the points are weighted equal in the plotting of $K_e R_e^{m+1}$ against $1/R_e$.

DISCUSSION

The average percentage error in K_e calculated from R_e for the periods 00, 01, 02, 11, 12, and 22 is 7.1, 5.3, 4.5, 12.0, 13.1, and 19.0, respectively. The error grows larger as the atoms in the linkage become heavier. This is probably due to the accuracy of R_e used, since for lighter molecules the moment of inertia is

smaller and R_e is better known. We did not calculate R_e from ω_e ; however, the error in R_e if calculated should be much smaller and could be estimated by the formula

$$\frac{\delta K_e}{K_e} = \left\{ \frac{(m+1)R_e A - (m+2)B}{R_e A - B} \right\} \frac{-\delta R_e}{R_e} = \left\{ m+1 - \frac{B}{R_e A - B} \right\} \frac{-\delta R_e}{R_e}$$

The value in parentheses is about 3.5 to 5 for $m = 4$, and 6 to 7 for $m = 6$. Then the average error for R_e calculated from K_e in periods 00, 01, 02, and 12 is less than 2 per cent, and less than 3 per cent in periods 11 and 22. This shows that the present relation is at least as good or slightly better than all the existing relations. The individual largest error is about twice as large as the average error and is, in general, less than 5 per cent for values of R_e calculated from ω_e . Since the constants are determined from a plot involving high powers of R_e which may not be accurate enough, the constants tabulated in table 1 are subject to correction when better data are available. There is also a possibility that the values of m may not be integers; however, unless the accuracy of R_e is much increased, this need not be tried.

It may be of considerable interest that there should exist so many different relations between R_e and K_e , and questions may be raised as to whether other relations could also be found. Actually, the Allen-Longair rule is less accurate, particularly for the first few molecules of a period (see Clark and Stoves (4)). The Clark rule does not contain the mass term, and is therefore theoretically weak for isotopic molecules (see Allen and Longair (1)). So there remain only the Badger rule and this present relation, which are relatively more successful. These two rules, though quite different, probably bear a relation to one another similar to that of the van der Waals equation to the Dietereci equation for imperfect gases, and may indeed be approximations of a more complex rule. This complex rule may also be derived by the same procedure as used here from other potential functions; however, ingenious methods for evaluating the constants are required.

One other similarity between the Badger rule and the present relation is that both indicate a lower limit of R_e below which these rules have no meaning. Thus D_{17} is the lowest value of R_e in the Badger rule, while for the present relation R_e should be not less than B/A . Whether there is also an upper limit is not indicated in both relations. However, the author believes that there should be one; otherwise we should be able to predict the dissociation energy correctly from merely a simple potential function with the constant determined only from the curvatures of a limited range of R . To show this, the dissociation energy of H_2 in the ground state is found to be 4.465 volts, while the value calculated from equations 1 and 2 with the constants given is only 0.8 volt. However, molecules within the same molecular period show only a small variation in R_e , usually not over 200 per cent, so these limitations do not seriously impair the usage of these relations. This conclusion, on the other hand, may not exclude the possibilities of establishing empirical or semi-empirical relations between R_e , K_e , and D_e , as Sutherland (7) has done.

Next we come to the all-important applications of these relations to polyatomic molecules. First of all, one must answer the question whether the atoms are bonded in the polyatomic molecules the same way as in the diatomic molecules. It is generally believed that they are bonded in the same way, and calculations made for hydrocarbons do show that the predicted R_e 's are at least not far in error. So these relations could be applied to polyatomic molecules. Next we encounter other difficulties: the number of harmonics known in polyatomic infrared absorption or Raman spectra is usually not enough for the evaluation of anharmonicity constants, so that ω_e is generally used instead of ω_e in the calculation of K_e ; this introduces an error of a few per cent. Moreover, the potential function usually contains more constants than the number of fundamental vibration frequencies; unless the vibration data of isotopic molecules are available the force constants could not be evaluated. Usually some of the "interaction terms" which for physical reasons are probably small are omitted from the potential function, so that the remaining constants could be calculated. This is really an averaging process in which the small interaction energy is averaged over other terms; in this way another small error is introduced, though probably very often of opposite sign to the former one. For these reasons it is only for a very few molecules that the force constants are relatively accurately known and the hope of judging the superiority of one relation over others from data of polyatomic molecules is still out of the question, at least for the present. On the other hand, the value of R_e calculated by these relations from K_e should be within 5 per cent of the real value, provided a complete potential function is used or, as in the case of hydrocarbons, the interaction terms are not unjustifiably omitted. This may not be an over-optimistic statement and preliminary calculations for some molecules show that the error is in general under 3 per cent for lighter molecules or for bonds involving a hydrogen atom. We shall discuss them more fully in a subsequent paper.

SUMMARY

A semi-empirical relation

$$K_e = -b(m)(m+1)/R_e^{m+2} + bm/pR_e^{m+1}$$

between the force constant, K_e , and the internuclear distance, R_e , has been derived from an assumed potential function

$$V = ae^{-x/r} - b/R^m$$

for the diatomic linkage, and found to be satisfactory for a large number of diatomic molecules. The values of b , p , and m are characteristic constants of a molecular period. A graphic method has been devised to evaluate them. The value of m is found to be 4 for periods 00, 01, 02, and 11, and 6 for periods 12 and 22, respectively, while b and p have different values for different periods.

REFERENCES

- (1) ALLEN AND LONGAIR: *Phil. Mag.* **19**, 1032 (1935).
- (2) BADGER: *J. Chem. Phys.* **2**, 128 (1934); **3**, 710 (1935).

- (3) CLARK: *Phil. Mag.* **18**, 459 (1934).
- (4) CLARK AND STOVES: *Phil. Mag.* **22**, 1137 (1936).
- (5) JEVONS: *Report on Band Spectra of Diatomic Molecules*. Cambridge University Press, London (1932).
- (6) SUTHERLAND: *Proc. Indian Acad. Sci.* **8**, 341 (1938).
- (7) SUTHERLAND: *J. Chem. Phys.* **8**, 161 (1940).

THE MAGNESIUM TUNGSTATE PHOSPHOR

GORTON R. FONDA

Research Laboratory, General Electric Company, 1 River Road, Schenectady 5, New York

Received April 19, 1944

One of the component phosphors used in the manufacture of the fluorescent lamp is magnesium tungstate (3, 4, 5, 6). It is prepared by firing a mixture of magnesium oxide with tungstic oxide (WO_3), without the addition of any foreign activator. The writer's attention was brought to it several years ago by T. E. Foulke of the General Electric Company, who had found that the greatest brightness resulted by firing a mixture of about 2 moles of magnesium oxide per mole of tungstic oxide. Such a curious departure from the proportions of the recognized compound, MgWO_4 , led to an investigation in this laboratory with the aim of finding if any unique compound were involved. It developed, however, as will be discussed in this paper, that, when the phosphor was prepared from this most favorable composition or in fact from any other composition by firing at a suitable temperature to render it fluorescent, it yielded an x-ray diffraction pattern identical with that of MgWO_4 . However, when the mixture comprised 2 or more moles of magnesium oxide per mole of tungstic oxide, and was fired for an extended time at 1250°C . or above, another compound was formed which had an entirely different diffraction pattern and which was non-fluorescent.

EXPERIMENTAL

Suitable firing conditions for preparation of the phosphor consisted in heating the mixture at 1100°C . for 1 hr. Firing at lower temperatures produced almost equal brightness of fluorescence, but correspondingly longer times were required—4 hr. at 1000°C ., 15 hr. at 900°C ., and 70 hr. at 470°C . Somewhat higher brightness values, especially at the optimum concentration, would have resulted from following in detail the directions given by Foulke, but even with the simple firing schedule used there was a notable increment in brightness that characterized those mixtures approximating 2 moles of magnesium oxide, as is brought out in the first two vertical columns of table 1.

When the phosphors were refired at 1250°C ., the fluorescence was greatly reduced or destroyed altogether, as is brought out in the table. On an additional

refiring at 950°C., fluorescence reappeared at appreciable brightness values that approached those resulting from the initial firing at 1100°C.

In the case of mixtures containing 1.44 moles of magnesium oxide or less, firing at 1250°C. produced a highly sintered mass, verging on fusion, which was completely fused by firing at 1400°C. There was also a change to a yellowish color, but without loss in weight. For mixtures with 1.93 moles of magnesium oxide or more, the product remained as a white powder at both 1250°C. and 1460°C., with no sintering whatever.

TABLE 1
Effect of composition and firing temperature upon fluorescence brightness

MOLES MgO PER MOLE WO ₃	FLUORESCENCE BRIGHTNESS		
	1 hr. at 1100°C.	1 hr. at 1100°C. + 1 hr. at 1250°C.	1 hr. at 1100°C. + 1 hr. at 1250°C. + 15 hr. at 900°C.
	<i>per cent</i>	<i>per cent</i>	<i>per cent</i>
1.00	89	0	56
1.15	88	0	80
1.44	100	25	
1.93	100	0	73
2.88	79	0	
5.75	66	0	34

TABLE 2
Effect of composition and firing temperature upon crystalline pattern

MOLES MgO PER MOLE WO ₃	CRYSTALLINE PATTERN		
	1 hr. at 1100°C.	1 hr. at 1100°C. + 1 hr. at 1250°C.	1 hr. at 1100°C. + 1 hr. at 1250°C. + 15 hr. at 900°C.
1.00	A	A	A
1.44	A	A	
1.93	A	B	A
2.88	A	B	
5.75	A + MgO	B + MgO	A + MgO

With the assistance of E. T. Asp of this laboratory, x-ray diffraction patterns with molybdenum K_α radiation were obtained for these various products. Two different patterns resulted, A and B, as is disclosed in table 2. For mixtures containing the highest content of magnesium oxide, some lines of the magnesium oxide pattern were found as well. In no case were there any lines of tungstic oxide (WO₃) observable. When phosphors were fired in platinum boats for over 50 hr. at 1100°C., no alterations in fluorescence brightness or in x-ray pattern were observable.

The lattice spacings corresponding to these two types of x-ray pattern are given in table 3.

The lattice spacings of pattern A were found to be identical with those reported by Broch (1) for MgWO₄, having monoclinic structure. Broch reports

also some other lines which were not found in our samples, presumably because they were too weak. Inasmuch as pattern A was found also for precipitated

TABLE 3

Lattice spacings corresponding to the x-ray patterns of the two forms of magnesium tungstate

PATTERN A		PATTERN B	
5.59	s*	5.40	m
4.64	s	4.62	m
3.71	s	3.55	s
3.60	f	3.20	m
2.90	s	3.01	f
2.46	m	2.71	s
2.34	m	2.32	m
2.18	m	2.14	w
1.97	w	2.06	w
1.88	w	1.87	m
1.80	w	1.76	w
1.75	m	1.615	s
1.693	m	1.530	m
1.571	f	1.482	f
1.494	m	1.450	f
1.424	m	1.410	w
1.362	w	1.280	f
1.310	m		
1.259	f		
1.202	f		
1.175	f		
1.112	f		
1.100	f		
1.078	f		

*s = strong; m = moderate; w = weak; f = faint.

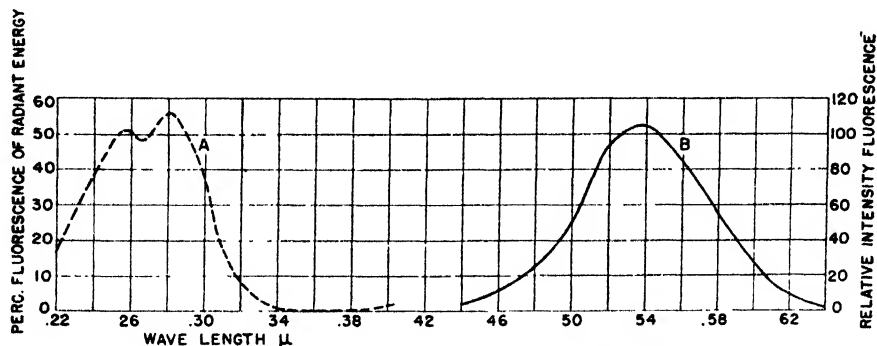


FIG. 1. Excitation and emission spectra of magnesium tungstate phosphor. Curve A, efficiency of excitation; curve B, fluorescence spectrum.

MgWO₄, it seems safe to assume that the phosphor is essentially monoclinic MgWO₄, with which an excess of magnesium oxide may advantageously be associated.

Pattern B bears no relation to any compound of magnesium or tungsten that is on record. It appears therefore to be a unique compound.

The spectral distribution of fluorescence for the phosphor was determined with a spectrophotometer by exciting it with 2537 Å. and measuring the energy emitted by comparison with that from a calibrated tungsten incandescent lamp. With the aid of Frank B. Quinlan, the efficiency of excitation was determined under radiation from a monochromator, measuring the radiant energy of the exciting line with a thermopile and the fluorescence lumens in a 4.5-cm. sphere with a photovoltaic cell and eye-correcting filter (2). The resulting curves are given in figure 1. The breadth of the excitation band yielding high efficiency of conversion is noteworthy. An efficiency very close to the formation of one quantum of fluorescence energy from one quantum of radiant, exciting energy exists throughout the spectral range extending from 2500 Å. to 2950 Å.

DISCUSSION

Normal magnesium tungstate, having the composition MgWO_4 and the monoclinic structure, is itself converted into a phosphor by suitable firing. Although no foreign activator is required for this, it is noteworthy that a higher fluorescence yield results when an excess of magnesium oxide is present during firing. It is difficult to conceive that the presence of MgO groups loosely bound to the MgWO_4 crystal could have any effect upon fluorescence brightness. It seems preferable to assume either that the excess MgO is incorporated in the MgWO_4 lattice, with the O ion replacing a WO_4 ion, despite the absence of any alteration in lattice size, or else that atoms of Mg and of O are introduced interstitially into the MgWO_4 lattice.

The loss of fluorescence that was observed by refiring at 1250°C . those phosphors containing 0.44 mole excess MgO or less can be explained as the result of partial conversion into a colloidal, glassy state, owing to the fact that the melting point of MgWO_4 lies in the neighborhood of this temperature. This view is supported by the appearance of the lines in the x-ray pattern which had become broken and more diffuse. The reconversion into a phosphor that took place on refiring at the reduced temperature of 900°C . is of course due to devitrification that led to recrystallization.

For those phosphors containing 1.93 moles of MgO or more it is evident that a drastic alteration in structure was produced by the firing at 1250°C . Inasmuch as the compound corresponding to pattern B did not appear at this firing temperature until this composition was reached, it can be assumed that it has the formula Mg_2WO_6 . It differs from the monoclinic MgWO_4 , not only in structure but also in being still infusible at 1460°C . and in being non-fluorescent. It is stable only above 1200°C . or thereabouts and is reconverted into the fluorescent, monoclinic form by refiring at 900°C .

An interesting contrast to magnesium tungstate is shown in the behavior of calcium tungstate, the most familiar member of the tungstate group of phosphors. It can be prepared by firing a mixture of the oxides. In crystalline form it belongs to the tetragonal system and has the scheelite structure. Its characteristic x-ray pattern persisted after firing for 60 hr. at 1100°C . and after 3 hr. at 1200°C .

and its fluorescence remained unaltered. At 1400°C. it sintered down in 15 min. to a semi-fused mass, but it still maintained the scheelite pattern and considerable fluorescence.

SUMMARY

The magnesium tungstate phosphor always exhibits the monoclinic structure of MgWO_4 , even in the presence of an excess of magnesium oxide which, at a concentration approaching 1 mole, serves to give a notable increase in fluorescence brightness. When fired for a long period at 1250°C. it loses its fluorescence in one of two ways, depending upon the concentration of magnesium oxide: (a) by conversion into a semi-glassy state, if it contains 0.5 mole or less of excess magnesium oxide; (b) by alteration into another crystalline modification, having presumably the formula Mg_2WO_6 , if it contains 1 mole or more of excess magnesium oxide. Mg_2WO_6 differs from MgWO_4 not only in being non-fluorescent but also in being stable only above 1200°C. or thereabouts and in having a melting point which lies above 1460°C. The quantum efficiency of excitation of the phosphor is near unity for the range 2500–2950Å.

REFERENCES

- (1) BROCH, EINAR: *Z. physik. Chem.* **1B**, 415 (1928).
- (2) FONDA, G. R.: *J. Phys. Chem.* **43**, 574 (1939).
- (3) FOULKE, T. E.: U. S. patent 2,203,682 (June 11, 1940); 2,232,780 (February 25, 1941).
- (4) FRERICHS, R.: *Naturwissenschaften* **26**, 681 (1938).
- (5) THAYER, R. N., AND BARNES, B. T.: *J. Optical Soc. Am.* **29**, 131 (1939).
- (6) UYTERHOEVEN, W.: *Elektrische Gasentladungslampen*. Julius Springer, Berlin (1938).

NEW BOOKS

A Text-Book of Inorganic Chemistry. By F. EPHRAIM. Fourth English edition by P. C. L. Thorne and E. R. Roberts. 24 x 16 cm.; xii + 921 pages. London and Edinburgh: Gurney and Jackson, 1943. Price: 28 shillings net.

This work, now published in the fourth English edition, is probably well known to most readers. It is an advanced text-book in which the treatment follows an order of topics rather than a grouping of individual elements, with chapters on theory. In considering compounds, the order is usually that of valence rather than the periodic law order.

The book is deservedly popular and can be recommended to advanced students. The reviewer has noticed a number of places in the text which seem to call for consideration when a new edition is required. It is impossible to notice all of these in a short review, but some indication may be given of the kind of thing which is meant.

The theoretical side of the book is the least satisfactory, although it has been improved in the English editions as compared with the original. The chapters on atomic structure and valence contain a number of errors and obscure statements; for example, the force between the electron and nucleus is said to be quantized, the uncertainty principle is obscurely stated (page 3), it is said that the outer electron shell of 8 of the inert gases is confined to those of low atomic number, a special parachor value is given for semi-polar double bonds, etc. The short account of the quantum theory of valence on pages 53–57 is good as far as it goes, but the statement of the quantum-mechanical basis on page 53 is defective, and the symbols s , p , d for the electrons are not defined. The assertion on page 56 that

hybridization involves a tendency to form bonds with "the greatest possible energy" is misleading. On page 89 the transuranic elements are first dealt with in some detail, and then it is said that they do not exist. This reluctance to omit obsolete information turns up in other parts of the book. The statement of the second law of thermodynamics on page 92 is not intelligible to the reviewer.

The descriptive part of the book is more successful. The main divisions are into elements, halogen compounds, oxides of hydrogen and metals, compounds of sulfur, selenium, and tellurium; the nitrogen, phosphorus, and arsenic group; and elements of the fourth group and boron. There are appendices, including a very useful short account of the main lattice types. This descriptive part is not free from errors, a few of which may be mentioned. On page 194 it is said that ammonia is "extensively" dissociated into its elements at 200°; on page 224 it is stated that hydrogen chloride is "readily" soluble in benzene; and on page 283 pyridine is described as an "amine." On page 282 it is stated that there are no groups conferring a positive charge on a Werner nucleus, whilst an example of one is given on page 297; on page 319 it is said that there are no compounds of cobalt with one neutral group in the nucleus, whilst one is formulated on the opposite page, and on page 301 $\text{Co}(\text{OH})_3$ is said to be the only simple compound of trivalent cobalt. On pages 358 and 368 the compound OF still appears. The use of the names "hypiodous acid" and "hypiodite" seems objectionable, since the Greek prefix may belong to either "hypo" or "hyper." Several names are incorrectly given, e.g., "Moh's" for "Mohs," "Losenty" for "Lorentz," "Bodländer" for "Bodenstein," "Harbold" for "Hubold"; and the translation is sometimes defective, as when "Austernschalen" is rendered as "ostracite shales" and "gute Leuchtsteine" as "the best minerals," on page 536. Yellow tungstic acid is said to be "colloidal" (page 510), and the statements that there is no direct evidence for the doubled formula for hyposulfurous acid (page 546), that the copper hydride precipitated by hypophosphite is CuH_2 (page 714), and that silver peroxide is precipitated by persulfate (page 594), are incorrect. On page 563 H^+ ions should read OH^+ ions; the CaSO_4 in superphosphate is now regarded as anhydrous and not "gypsum" (page 722); and recent work contradicts the formulae of the metal carbonyls given on pages 793-4. The reviewer failed to find any mention of the important vanadium pentoxide catalyst in the manufacture of sulfur trioxide. The references to four figures given in the preface are all incorrect.

The above examples are given with the object of directing the attention of the editors to some defects in the book which can be removed by more careful attention to the text, and not with the object of presenting an unfavorable criticism of the book as a whole. It is not easy to keep such a large amount of detailed information as is presented in a completely accurate form, but some of the errors should be put right in a new edition.

J. R. PARTINGTON.

Lange's Handbook of Chemistry. NORBERT ADOLPH LANGE, *Editor*. 5th edition. 1777 pp. + 271 pp. of mathematical tables (compiled by Richard Stevens Burlington) + 28 pp. of index. Sandusky, Ohio: Handbook Publishers, Inc., 1944. Price: \$6.00.

The latest edition of this valuable handbook consists of 1777 pages of technical information and data of interest to chemists, chemical engineers, and physicists. Mathematical tables and formulas make up a special appendix of 271 pages. The index of 28 pages is thorough and informative. The general arrangement and subject matter are largely that of the fourth edition, but new tables and revisions have added 174 new pages.

An important revision is in the table of physical constants of organic compounds. This section now includes 6507 compounds with Beilstein references given where possible. Among several new features are a Periodic Chart by Prof. Deming, and additional information on plastics. Properties and limitations of plastics are of increasing interest. Other new tables in the fifth edition are entitled: "Flammable Liquids," "Flame Temperatures," "Fluorescence of Chemicals, Minerals, and Gems," and "Water for Industrial Use." A large table entitled "Composition and Physical Properties of Alloys" is distinguished by being one of the few tables for which no references are given. Reference might have been made to the *National Metals Handbook* and the *Cast Metals Handbook*. Carbon steel and

gray iron are each given a single line, whereas these names are generic and include a wide range of analyses and properties. In contrast, a number of alloy steels of very similar analyses and properties are listed individually and with trade names.

The editor has had the assistance of a number of capable educators and technical men in preparing the handbook. All are to be congratulated on the results of their work. The fifth edition, like earlier editions, has made available a mass of valuable material for the technical library.

H. H. BARBER AND H. F. SCOBIE.

The Total and Free Energies of Formation of the Oxides of Thirty-two Metals. By MAURICE DEKAY THOMPSON. 6 x 9 in.; 89 pp. New York City: The Electrochemical Society, Inc., 1942. Price (paper): \$1.00.

As indicated in the title, this summary reviews, criticizes, and assembles most of the valuable thermodynamic data relating to the heat contents, heat capacities, and free energies of the common metallic oxides. One hundred and fifty-seven references are given, and there is an appendix showing the location of 121 factual equations derived in the text. The author uses G in place of the more familiar F for free energy; otherwise, the nomenclature of Lewis and Randall is used. All empirical heat equations for heat capacity are of the form suggested by Dr. K. K. Kelley of the Bureau of Mines.

The reviewer has not attempted to check the calculations, but merely wishes to point out the omission of the minus sign before 0.6027 in Equation 4 on page 2; 453 should be substituted for 4.35 on page 13; and there are gross errors in the equations on page 14.

In combination of equations, as is constantly the practice in free-energy calculations, one must bear in mind that it is absolutely necessary, if large non-apparent accumulative errors are to be avoided, to utilize the same equations in a given series of calculations, and to avoid rounding off coefficients once these coefficients are chosen. This would have been rendered much easier if the coefficients in T in the heat capacity equations had always been made divisible by 2, and if the author had not inadvertently rounded off the coefficients in his $T \ln T$ term. Again, while the calculations of the author are quite within the experimental error (except for arithmetical errors), great care must be used when combining the author's equations with those of Lewis and Randall. Thompson's work is a valuable and timely addition to our thermodynamic literature.

MERLE RANDALL.

Natural and Synthetic Fibers. Edited by MILTON HARRIS AND H. MACK. An abstract service; issued monthly. 215 Fourth Avenue, New York City 3; Inter-science Publishers, Inc., 1944. Price: \$60.00 per year; binder, \$3.00.

As the editors point out, this is not an abstract service in the usual sense of the word. It is rather a new service which will build up an encyclopedia of contemporary research and progress in the textile field. It proposes a service which makes available on short notice all of the papers and patents published in this field during the year.

In order to accomplish this result a special filing system has been developed. Each of the principal types of fibers heads a main division designated by a capital letter. When necessary the main divisions are broken up into classes. A series of subdivisions follows and these cover all phases of the subject. A numbering system based on units of hundreds with decimals makes it possible to file any subject properly. At the top of each abstract appears the subject and in the upper right-hand corner the key letter and numbers appear. These enable the user to place the abstracts in the proper places in the file. The first abstracts are complete and well illustrated with figures. Necessary tables are also included and the summary of the pertinent information on each patent or paper is good.

The first issue of 64 pages indicates to the reviewer that the service will be reasonably complete, and as a result it should render a valuable service in the textile field. It is proposed to issue about 1000 pages the first year. About fifty journals will be surveyed in addition to the important patents that are issued. The place which the editors occupy in the textile field should assure the subscribers of an excellent service.

L. H. REYERSON.

THE QUATERNARY SYSTEM $\text{CaO}-\text{Al}_2\text{O}_3-\text{CaSO}_4-\text{H}_2\text{O}$ AT 25°C .

EQUILIBRIA WITH CRYSTALLINE $\text{Al}_2\text{O}_3 \cdot 3\text{H}_2\text{O}$, ALUMINA GEL, AND SOLID SOLUTION

F. E. JONES

Building Research Station, Garston, Watford, Herts, England

Received May 27, 1944

Recently (8) the writer has described an investigation of the system $\text{CaO}-\text{Al}_2\text{O}_3-\text{CaSO}_4-\text{H}_2\text{O}$ at 25°C ., which is of particular interest in the chemistry of Portland and aluminous cements. In that work only the gel form of hydrated alumina was considered. In the present work, equilibria involving crystalline $\text{Al}_2\text{O}_3 \cdot 3\text{H}_2\text{O}$ have been determined. The method of investigation was similar to that previously employed. Much of the work involving solutions of higher lime concentrations was carried out with stainless-steel tubes instead of the Pyrex-glass tubes previously used, in order to eliminate the possibility of reaction of lime with the glass of the containing vessel. In addition to the work with crystalline $\text{Al}_2\text{O}_3 \cdot 3\text{H}_2\text{O}$, supplementary data for the system with alumina gel have been obtained, dealing with equilibria in solutions of high lime concentration, and solid solution equilibria have been investigated. As before, a shorthand notation has been used in writing certain formulae: $\text{CaO} = \text{C}$, $\text{Al}_2\text{O}_3 = \text{A}$. For the convenience of the reader, the refractive indices of relevant compounds reported in the literature are collected together in table 9. For the refractive indices of solid solution phases reference should be made to table 7 and the sections dealing with the solid solution curves SW and QU.

PHASE-RULE EQUILIBRIA

It appears desirable, for the sake of clarity, to include some discussion of phase-rule equilibria pertinent to the relations found in this system. Before doing so it is necessary to define the terms stable, metastable, and unstable, as applied to various equilibria. Throughout this paper these are used to accord with the senses given by E. A. Guggenheim (7) and J. S. Marsh (11). The distinction drawn by Guggenheim between the metastable and unstable states is that a metastable state is defined as "stable" compared with all states differing only infinitesimally from the given state, but unstable compared with some other state differing finitely from the given state; while an unstable state is defined as one which is "unstable" compared with all states differing infinitesimally from the given state.

Let us consider the simpler relations to be met with in a ternary system. In the usual way compositions may be represented within an equilateral triangle, and the temperature variable along an axis at right angles as shown in figure 1(a). Such a solid figure gives a complete representation of the condensed (i.e., constant pressure) ternary system. Any isothermal is obtained by a cut through the

temperature axis at right angles, intersecting the solid-liquid equilibrium surfaces in curves which at the temperature of the isotherm give the compositions of liquid in equilibrium with appropriate solid phases. Thus an isotherm may be repre-

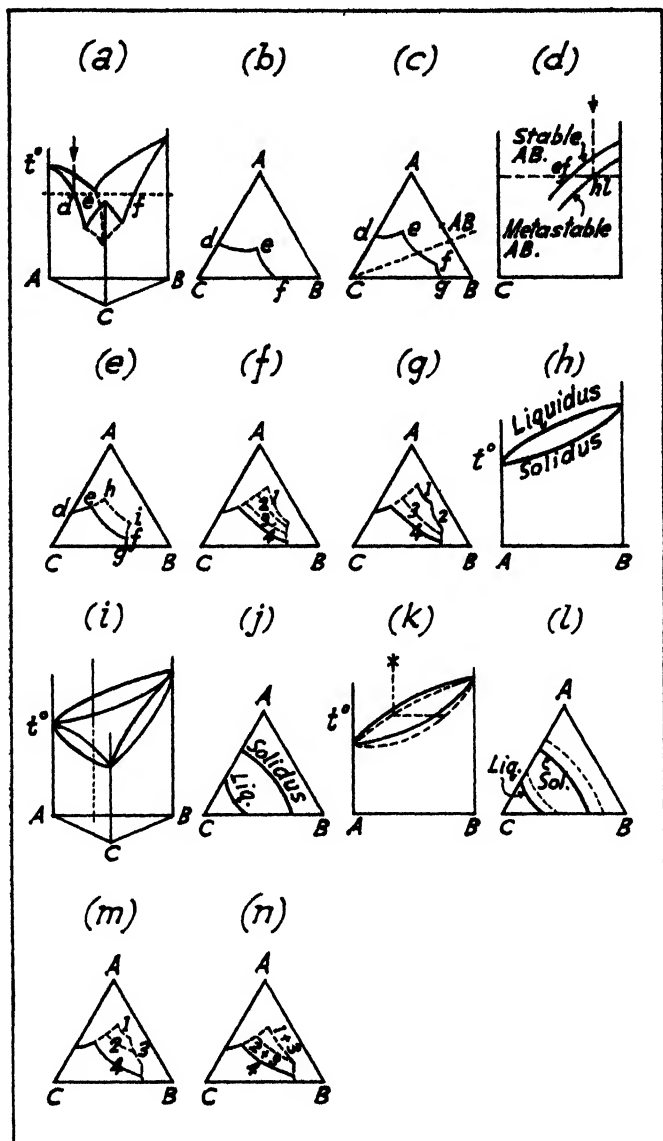


FIG. 1. Phase-rule equilibria

sented quite simply by figure 1(b), where the curve de gives the compositions of liquid in equilibrium with solid A, and curve ef those of liquid in equilibrium with solid B. In this we are so far dealing with stable equilibria. If, for example, we

consider a mix of a composition given by some point along de , but at a higher temperature than the isotherm, the whole mix is liquid. As it is cooled it remains liquid until the temperature of the isotherm is reached, when the *stable* solid phase A begins to separate out along the stable equilibrium curve de . Let us now suppose that compound formation can occur between A and B. The isothermal figure may now be as in figure 1(c), where ef gives the composition of liquid in equilibrium with the compound of composition AB. As before, if we take a mix of composition given by some point along ef , at temperatures above the isotherm it will be wholly liquid, but on cooling to the temperature of ef , the *stable* solid phase AB will begin to separate out. Now let us consider the possibility of some other compound of A and B being formed, *metastable* with respect to the stable compound already considered. In figure 1(c), ef is an isothermal cut across the liquid-solid equilibrium surface of the *stable* AB compound. The *metastable* AB compound will also have its appropriate liquid-solid equilibrium surface. Consider now, as in figure 1(d), a plane through the temperature axis at C (i.e., a vertical plane in which the axis lies) cutting both *stable* and *metastable* surfaces as shown. This plane may be shown in projection by the broken line passing through C in figure 1(c). If we take a mix of composition hi , it is clear that at temperatures above the stable surface AB the mix is wholly liquid. If now the mix is cooled, separation of stable AB should take place as soon as the temperature falls to the intersection with the stable surface AB. If this separation fails to occur, with further cooling the *metastable* surface AB will be reached and separation of metastable AB may occur. It is thus apparent that there exists the possibility of a *metastable* isothermal curve hi being realized at the temperature t° in addition to the *stable* curve ef . The isothermal diagram would then be as in figure 1(e). This is simply figure 1(c) over again, with the addition of a *metastable* curve for the metastable AB compound, and *metastable* prolongations of de and gf . More than one metastable surface and more than one metastable curve may exist, depending on the possibilities of metastable compound formation. Similar considerations apply in relation to the metastable and stable equilibria which may arise when ternary compounds are formed. Thus such isothermal diagrams may arise as are shown in figures 1(f) and 1(g). Here the full curves are for stable compounds and the broken curves for metastable compounds. In figure 1(f) are shown compounds of varying degrees of metastability with respect to the stable compound. The metastable compound corresponding to curve 1 is metastable with respect to 2, 3, and the stable compound 4, 2 is metastable with respect to 3 and 4, and 3 is stable with respect to 4. The metastable compounds formed may, however, be of the same order of metastability, neither lying above the other, as, for example, compounds 1 and 2 in figure 1(g).

We have so far not considered the case of solid solution formation. Let us commence with a simple binary system in which a continuous series of solid solutions is formed. This is represented in the usual way as in figure 1(h) by two curves, one for liquid compositions (the liquidus) and the other for solid compositions (the solidus), giving, respectively, the liquid and solid compositions in equilibrium at any temperature. Now let us suppose that in a ternary system

the three binary systems form such a continuous series of solid solutions, and that all three components are completely miscible. Liquidus and solidus surfaces will be formed as in figure 1(i). An isothermal cut across the solid figure will intersect both liquidus and solidus surfaces in liquidus and solidus curves, as in figure 1(j). Both liquid and solid compositions are varying along the respective curves and for every point on the liquidus there is a corresponding equilibrium point on the solidus.

Hitherto we have dealt with the *stable* liquidus and solidus, and we may note that in the case of solid solution formation *unstable* equilibria appear to be theoretically possible. Thus, consider a mix of the composition given by the broken line and its full continuation in figure 1(i). Above the *stable* liquidus surface shown the mix is wholly liquid. As it is cooled, intersection with the *stable* liquidus should occur and if solid separates out there will be equilibrium with the *stable* solidus. However, just as in the case of compound formation, separation of the stable solid may not occur. With further cooling, separation of solid phase will eventually take place. Since, however, the liquid is at a lower temperature than corresponds to its stable position on the liquidus, it cannot be in equilibrium with a solid of composition given by a point on the *stable* solidus at the temperature of the liquid. The equilibrium solid will have some other composition in the solid solution series and be in *unstable* equilibrium with the *unstable* supercooled liquid. Both liquid and solid are then supersaturated at the temperature under consideration. It may well be, of course, that such an *unstable* equilibrium cannot persist, and that the compositions of both solid and liquid change rapidly to those corresponding to the stable liquidus and solidus at the temperature of the mix. However, the rate at which such a change occurs must depend on the particular system under consideration. This conception will be made clearer by restricting consideration for the moment to a binary system. Thus in figure 1(k) a mix of composition X is considered to be supercooled below the point of intersection with the stable liquidus. The solid which eventually separates out will not lie on the stable solidus, but on an *unstable* solidus corresponding to an *unstable* liquidus. Both *stable* liquidus and solidus curves may be considered to move downwards through unstable areas, eventually reaching liquidus and solidus curves of maximum instability such as are indicated by the broken curves of figure 1(k). Applying this conception to the ternary system of figure 1(i), we must consider that both *stable* liquidus and solidus surfaces may extend downwards through *unstable* liquidus and solidus volumes. The lower limits of these volumes is determined by the possibilities of unstable equilibria inherent in the system. Isothermal intersection of these volumes would give liquidus and solidus *areas* of *unstable* equilibria as in figure 1(l). The liquidus and solidus curves nearest C give the stable liquidus and solidus equilibria, while those furthest away give the extreme limits of the *unstable* solid solution liquidus and solidus areas. For every point in the liquidus area there will be a corresponding equilibrium point in the solidus area. The same considerations will apply to solid solution equilibria between stable or metastable ternary compounds.

The idea of unstable equilibria put forward in the above may be looked at in

another way. Consider an aqueous ternary system in which solid solution equilibria occur. If we start with a supersaturated (i.e., supercooled) solution, we may expect the solid phase which separates out first to be in equilibrium with the unstable solution and therefore itself be unstable and supersaturated with respect to a stable solid solution.

It now remains to consider a combination of compound and solid solution formation. Discussion will be limited to two cases. In figure 1(g), if we assume complete miscibility of compounds 1 and 2, curves 1 and 2 will merge into a single continuous curve. Again, consider the case shown in figure 1(m). Metastable curves are shown for compounds 1, 2, and 3. Curve 1 and part of curve 3 are metastable with respect to 2. Curve 2 and the remaining part of curve 3 are metastable with respect to 4. If however, 1 and 3 and 2 and 3 form separate series of continuous solid solutions, we will have two solid solution curves as in figure 1(n). If unstable supersaturated liquidus-solidus equilibria be possible, the equilibria 2 + 3 will move upwards through an area of increasing instability and will eventually include the curve 1 + 3. Theoretically the area need not be limited by the curve 1 + 3, but the chances are since 1 + 3 is a metastable curve, that it will be. Any tendency which the system may possess for the formation of further supersaturated equilibria beyond curve 1 + 3 in the direction of greater instability will be much less than in position 2 + 3 and may then be balanced by the tendency to revert to the metastable position 1 + 3.

Extending the discussion of the isothermal equilibria to quaternary systems, it is evident that when the fourth component also enters into the solid solution, a solid solution curve in the ternary system passes into a solid solution surface in the quaternary system. Further, areas of unstable solid solution equilibria, should these occur in the ternary system, would become unstable volumes in the quaternary.

In the above there has been discussed, incidentally, the possibility of unstable equilibria arising by virtue of supersaturation in both liquid and solid phases. We have also to distinguish unstable equilibria arising from variations in the physical structure of a particular solid phase. Here we are concerned with conditions in systems such as aqueous systems where a solid may occur in the gel or crystalline state. The equilibria relations for the solid in the gel state may be markedly different from those for the same solid in an obviously crystalline condition. The essential difference between the two conditions is, however, one of crystal size, the size decreasing as the gel state is approached. With the decrease in size of crystal and therefore increase in specific surface area, the specific surface energy increases. It follows that, depending on crystal size, the position of the equilibrium solid-liquid curve moves over an area which is limited by a stable curve for the obviously crystalline material (largest crystals and lowest "solubility"), and an unstable curve for the material in the gel condition (smallest crystals and highest "solubility"). The area is thus one of a continuously varying degree of instability. This kind of unstable equilibrium is specifically exemplified by hydrated alumina in the present work.

A further complication ensues when, in addition to variations in the structure

of the solid phase regarded as a whole, due to variations in crystal size, there may also be changes in the crystal structure of the individual crystal units. This actually happens in the case of hydrated alumina. The crystal unit originally formed in the gel is that of $\gamma\text{-Al}_2\text{O}_3 \cdot \text{H}_2\text{O}$ (böhmite), but this gradually changes over, first to $\alpha\text{-Al}_2\text{O}_3 \cdot 3\text{H}_2\text{O}$ (bayerite), and finally to $\gamma\text{-Al}_2\text{O}_3 \cdot 3\text{H}_2\text{O}$ (gibbsite or hydrargillite).

Attention may be drawn to the fact that in the previous paper (8) by the writer, the distinction between metastable and unstable equilibria now adopted was not used, and the term metastable was applied to the alumina gel equilibria. This equilibria should preferably be described as unstable.

MATERIALS

Crystalline $\text{Al}_2\text{O}_3 \cdot 3\text{H}_2\text{O}$

From the work of several investigators, in particular of Rooksby (13), Fricke (4), Fricke and Severin (5), and Weiser and Milligan (14), it is to be concluded that two closely related but distinct polymorphic forms of crystalline $\text{Al}_2\text{O}_3 \cdot 3\text{H}_2\text{O}$ exist, relatively metastable $\alpha\text{-Al}_2\text{O}_3 \cdot 3\text{H}_2\text{O}$ (named "bayerite" by Fricke) and $\gamma\text{-Al}_2\text{O}_3 \cdot 3\text{H}_2\text{O}$ (gibbsite or hydrargillite). Both forms can be obtained by allowing alkali aluminate solutions to stand in contact with air, and therefore to be acted upon slowly by atmospheric carbon dioxide. According to Fricke (4), the α -form arises under conditions of relatively quick formation in relatively dilute alkali aluminate solutions, while the γ -form is produced by slower action in more concentrated solutions, or by allowing the α -form first produced to stand in contact with alkali. The γ -form appears to be identical with naturally occurring gibbsite.

Preparation of $\text{A} \cdot 3\text{H}_2\text{O}$

Crystalline $\text{A} \cdot 3\text{H}_2\text{O}$ was prepared in a manner similar to that of Goudriaan (6) and the later workers mentioned, by slow crystallization from a solution of sodium aluminate (75 g. per liter). The solution was allowed to stand in an open vessel with access to the air of the laboratory, but with protection against dust. The temperature was maintained at 25°C . by placing the solution within a controlled electric oven. In the course of some weeks, crystalline $\text{A} \cdot 3\text{H}_2\text{O}$ precipitated. After removal from the crystallizing vessel, the preparation was washed with water and dried *in vacuo* over saturated ammonium sulfate solution at room temperature. Two preparations were employed in the course of the work. They were not identical and gave different equilibria data.

Preparation A was obtained after 19 days' standing. Microscopic examination showed coherent clusters of slightly birefringent material, apparently as small plates, though the form could not be clearly distinguished. On edge, the plates appeared as short tapering needles, showing positive elongation and with indices $\gamma = 1.593 \pm 0.003$, mean $\alpha, \beta = 1.583 \pm 0.003$ (gibbsite, monoclinic, has indices $\gamma = 1.587$, $\alpha = \beta = 1.566$). The Al_2O_3 content, determined by solution in hydrochloric acid, precipitation, and ignition was 64.9 per cent and by direct ignition at 1000°C . 64.7 per cent (theory = 65.3 per cent).

Preparation B was obtained after 27 days' standing. It was of a markedly "looser" nature than preparation A. Microscopic examination showed a much higher proportion of single crystals as well as clusters, showing slight birefringence. The short "needles" showed positive elongation with indices $\gamma = 1.583 \pm 0.003$, mean $\alpha, \beta = 1.570 \pm 0.003$. The Al_2O_3 content, by solution in hydrochloric acid, precipitation, and ignition was 64.8 per cent ± 0.2 per cent, and by ignition at 1000°C . was 65.2 per cent ± 0.2 per cent.

X-ray examination

X-ray powder photographs of the two preparations were made by Mr. G. E. Bessey (3), using a large camera of radius 9.2 cm. and CuK_α radiation. The positions of the lines were measured to ± 0.1 mm., and the relative intensities estimated by eye. Photographs showing a considerable number of lines were obtained. The calculated spacings and line intensities are given in table 1 in comparison with data obtained by other workers. Owing to the very large number of lines obtained, spacings less than 1.25 \AA . are omitted in order to save space. In the case of mineral gibbsite all the data reported by Rooksby (13) and Weiser and Milligan (14) are given. The data for mineral gibbsite obtained in the present investigation were obtained (3) with a sample supplied by Thomas Murby & Sons. Refractive indices: $\alpha, \beta = 1.565$, $\gamma = 1.585 \pm 0.003$. Loss on ignition at 1000°C . = 34.5 per cent (theory = 34.7 per cent). It will be seen from the data that the mineral gibbsite obtained from various sources and the artificial gibbsite prepared by Fricke (4) are essentially identical. The photographs obtained by Fricke and especially those obtained by Bessey are clearly a considerable improvement on those obtained by Rooksby and by Weiser and Milligan, with respect both to the number of lines recorded and to their intensities. Fricke (4) has reported that the preparations of bayerite which he obtained could be divided into two groups, which he distinguished as bayerite (a) and bayerite (b). The x-ray data corresponding to these two groups are given in table 1. Fricke points out that bayerite (b) is rather more similar to gibbsite than is bayerite (a). Fricke also states that his results are in line with solubility data, bayerite (a) being more soluble than bayerite (b) and the latter more so than artificial gibbsite. Further, it is noteworthy that Fricke states that in the case of separation from standing potassium aluminate solutions, bayerite (b) and also artificial gibbsite separate as a powder, while bayerite (a) appears as a characteristic crust-like structure. This description might well be applied to the preparations B and A, respectively, (corresponding to bayerite (b) and (a)) of the present work, and suggests a similarity between them. The solubilities are in agreement, since preparation B shows a smaller solubility than A. A sharper x-ray pattern obtained with B indicates a larger crystal size as compared with A, and it is possible that this may have an effect in reducing solubility, though it appears to the writer questionable whether crystal growth has not proceeded sufficiently far to make differences in surface area between preparations A and B insufficient to affect the solubility appreciably. However this may be, the x-ray data for A and B show that A has a pattern similar to that for bayerite, i.e.,

TABLE 1
X-ray data for various preparations of crystalline $A \cdot 3H_2O$

NO.	MINERAL GIBBSITE						ARTIFICIAL GIBBSITE		$A \cdot 3H_2O(A)$		BAYERITE (a)		$A \cdot 3H_2O(B)$		BAYERITE (b)	
	R*		W and M		B		F	I	d	I	d	I	d	I	d	I
	d	I	d	I	d	I										
1	4.83	v.s.	4.85	v.s.	4.83	v.s.	4.84	v.s.	4.64	v.s.	4.82	v.s.	4.83	v.s.	4.84	v.s.
2																
3	4.37	s	4.34	v.s.	4.35	v.s.	4.35	s	4.35	v.s.	4.37	s	4.35	v.s.	4.33	s
4																
5																
6																
7																
8	3.34	v.w.			3.34	m										
9	3.30	v.w.	3.31	v.w.	3.30	m										
10	3.17	w			3.20	m	3.32	m								
11			3.12	v.w.	3.12	w	3.13	w								
12																
13					2.84	v.w.										
14	4.37				2.73	v.w.			2.70	w	2.68	v.w.	2.70	w	2.67	w
15					2.66	v.w.										
16	2.45	m	2.45	s	2.46	s	2.46	s	2.46	w	2.46	m	2.46	m	2.48	m
17					2.43	v.w.										
18	2.38	m	2.38	s	2.39	s	2.38	s	2.36	m	2.37	w	2.39	m	2.37	m
19					2.34	v.v.w.							2.36	v.w.		
20	2.28	v.w.	2.26	v.w.	2.29	w	2.30	m								
21	2.24	v.w.			2.25	m										
22							2.19	m								
23	2.16	w	2.17	w	2.16	m			2.19	v.s.	2.23	v.s.	2.26	m	2.23	s
24					2.08	v.v.w.	2.06	m.s.	2.15	w	2.08	v.w.	2.16	w		
25	2.04	w	2.04	w	2.04	m.s.			2.06	w			2.06	w	2.07	w
26													2.03	w		
27	1.99	w	1.99	v.w.	1.99	m.s.	2.00	m.s.			1.99	v.w.	2.00	m	1.99	v.w.
28	1.91	w	1.91	v.w.	1.96	v.v.w.			1.96	m			1.98	w		
29	1.89	v.v.w.			1.91	m	1.93	m	1.90	w			1.91	w		
30	1.80	w	1.80	m.s.	1.80	m.s.	1.81	m.s.	1.83	w			1.83	v.w.	1.82	v.w.

α -A \cdot 3H₂O, while B appears to be an intermediate step between the structure of α -A \cdot 3H₂O and γ -A \cdot 3H₂O (i.e., B has been partially converted within the original crystal to the structure of γ -A \cdot 3H₂O), but with the α -form predominating. A few weak lines which have not been recorded in either α -A \cdot 3H₂O or γ -A \cdot 3H₂O, notably at spacings $d = 4.18, 3.88, 3.60, 3.40$ Å., are also present in preparation B. A pure γ -A \cdot 3H₂O has not been prepared for examination in the present work.

RESULTS

I. THE TERNARY SYSTEMS

Of the four ternary systems concerned, two involve alumina:

- (1) H₂O-Al₂O₃-CaO
- (2) H₂O-Al₂(SO₄)₃-Al₂O₃

As in the previous work, system 2 has not been considered.

(1) *The ternary system H₂O-Al₂O₃-CaO*

A limited amount of work has been carried out to determine the equilibria with crystalline A \cdot 3H₂O. Relevant curves in the ternary system are shown in figure 2, which may be compared with figure 2 of the previous work. Curves (a) and (b) are those for alumina gel and C₃A \cdot 6H₂O, respectively, as determined by Lea and Bessey (9). The invariant point, crystalline A \cdot 3H₂O(B)-C₃A \cdot 6H₂O as found indirectly in the present investigation, is given by the point D₂. That part of the C₃A \cdot 6H₂O curve represented by D₂D is clearly a metastable prolongation of the C₃A \cdot 6H₂O curve, while the curve H₂O-D for alumina gel is wholly unstable. Stable curves are shown in the figure by full heavily drawn lines, unstable curves and metastable prolongations of stable curves by broken lines. It will be clear from the introductory section on phase-rule equilibria that the area H₂O-D-D₂ is one of unstable equilibria. It might be regarded as an area of supersaturation with respect to γ -A \cdot 3H₂O (gibbsite).

The boundary curve A \cdot 3H₂O(B) (H₂O-P)

The data (table 2) were obtained with preparation B of the crystalline A \cdot 3H₂O, from mixes with lime solutions of different concentrations shaken for 7 or 28 days. Owing to the reluctance of C₃A \cdot 6H₂O to crystallize from solution at 25°C., the metastable prolongation of this curve after meeting the stable curve C₃A \cdot 6H₂O in the invariant point C₃A \cdot 6H₂O-A \cdot 3H₂O is also obtained. The curve H₂O-P in figure 2 shows the stable portion of the crystalline A \cdot 3H₂O curve and its metastable prolongation so far as it can be traced. In higher lime concentrations, other solid phases (metastable) were formed.

The isothermal invariant point A \cdot 3H₂O(B)-C₃A \cdot 6H₂O (D₂)

Theoretically this can be obtained either from mixes of A \cdot 3H₂O, C₃A \cdot 6H₂O, and lime solutions of concentration less than the invariant point value, leading to solution of C₃A \cdot 6H₂O and crystallization of A \cdot 3H₂O, or from mixes of A \cdot 3H₂O and lime solutions containing more lime than corresponds to the invariant point,

leading to crystallization of $\text{C}_2\text{A} \cdot 6\text{H}_2\text{O}$. Neither of these two methods of approach has proved practicable within the shaking periods used. Mixes of the first type have invariably yielded points on the $\text{A} \cdot 3\text{H}_2\text{O}$ curve, the $\text{C}_2\text{A} \cdot 6\text{H}_2\text{O}$ ap-

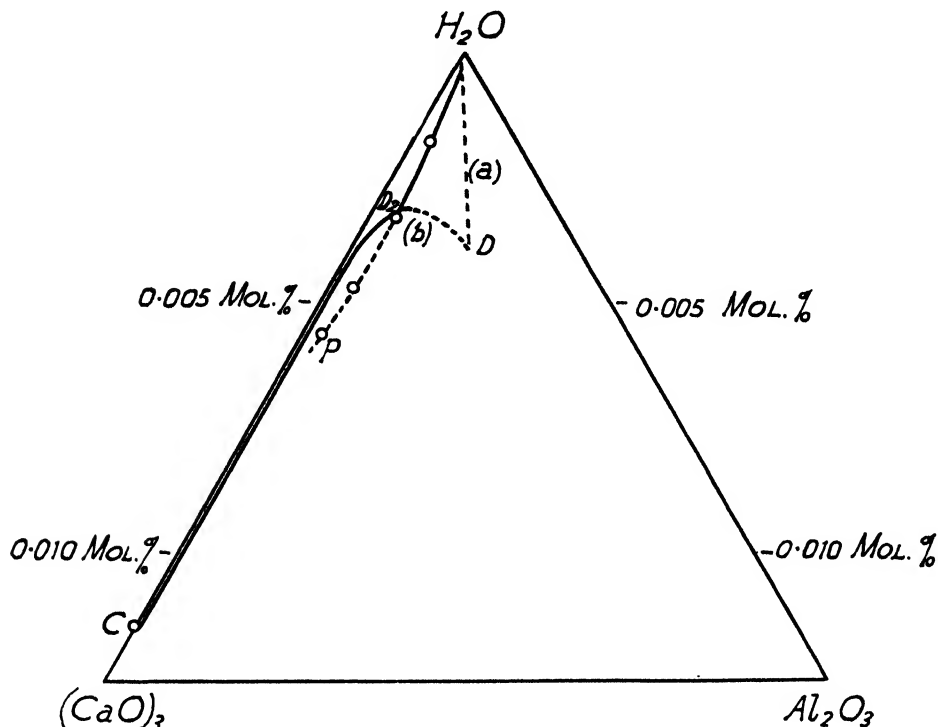


FIG. 2. Ternary system $\text{H}_2\text{O}-\text{Al}_2\text{O}_3-\text{CaO}$

TABLE 2
The ternary system $\text{H}_2\text{O}-\text{Al}_2\text{O}_3-\text{CaO}$
Solubility curve $\text{A} \cdot 3\text{H}_2\text{O}$ (B)

NO.	TIME SHAKEN	GRAM-MOLS $\times 10^4$ PER 1000 G. OF SOLUTION		TOTAL GRAM-MOLS $\times 10^4$ PER 1000 G. OF SOLUTION	$(\text{CaO})_3$	Al_2O_3	TOTAL SALTS IN SOLUTION
		$(\text{CaO})_3$	Al_2O_3				
	days				mole per cent	mole per cent	mole per cent
P24..	7	7.3	1.4	8.7	83.9	16.1	0.00157
P23	28	7.1	1.7	8.8	80.6	19.4	0.00159
P20	28	15.0	2.25	17.25	87.0	13.0	0.00311
P28	7	23.3	2.1	25.4	91.7	8.3	0.00458
P22	7	28.8	1.85	30.65	94.0	6.0	0.00552

parently remaining inert. As mentioned, the second type yields metastable solid phases. Indirectly the invariant point is obtained by the intersection of the $\text{C}_2\text{A} \cdot 6\text{H}_2\text{O}$ and crystalline $\text{A} \cdot 3\text{H}_2\text{O}$ curves (point D_2 in figure 2). The in-

variant point composition in grams per 1000 g. of solution is $\text{CaO} = 0.265$, $\text{Al}_2\text{O}_3 = 0.022$.

II. THE QUATERNARY SYSTEM

Equilibria with crystalline $\text{A} \cdot 3\text{H}_2\text{O}$

The following boundary curves and invariant points have been determined:

(a) Boundary curves:

Stable (1) $\text{CaSO}_4 \cdot 2\text{H}_2\text{O} - \text{A} \cdot 3\text{H}_2\text{O}$ (J_2E_2)¹

(2) $\text{A} \cdot 3\text{H}_2\text{O} - \text{C}_3\text{A} \cdot 3\text{CaSO}_4 \cdot 32\text{H}_2\text{O}$ (E_1H_1 , E_2H_2)

(3) $\text{A} \cdot 3\text{H}_2\text{O} - \text{C}_3\text{A} \cdot 6\text{H}_2\text{O}$ (H_2D_2)

Metastable (4) $\text{A} \cdot 3\text{H}_2\text{O} - \text{C}_3\text{A} \cdot 3\text{CaSO}_4 \cdot 32\text{H}_2\text{O}$ (broken curve $\text{H}_2\text{R}_2\text{L}_2$) (metastable prolongation of E_2H_2)

(5) $\text{A} \cdot 3\text{H}_2\text{O} - [\text{C}_3\text{A} \cdot \text{CaSO}_4 \cdot 12\text{H}_2\text{O} + \text{C}_3\text{A} \cdot \text{Ca}(\text{OH})_2 \cdot 12\text{H}_2\text{O}]$ (solid solution) ($\text{R}_2\text{S}_2\text{Q}_2$)

(b) Invariant points:

Stable (1) $\text{CaSO}_4 \cdot 2\text{H}_2\text{O} - \text{A} \cdot 3\text{H}_2\text{O} - \text{C}_3\text{A} \cdot 3\text{CaSO}_4 \cdot 32\text{H}_2\text{O}$ (E_1 , E_2)

(2) $\text{C}_3\text{A} \cdot 3\text{CaSO}_4 \cdot 32\text{H}_2\text{O} - \text{C}_3\text{A} \cdot 6\text{H}_2\text{O} - \text{A} \cdot 3\text{H}_2\text{O}$ (H_1 , H_2)

Metastable (3) $\text{A} \cdot 3\text{H}_2\text{O} - \text{C}_3\text{A} \cdot 3\text{CaSO}_4 \cdot 32\text{H}_2\text{O} - \text{C}_3\text{A} \cdot \text{CaSO}_4 \cdot 12\text{H}_2\text{O}$ (R_2)

It should be noted that the equilibria E_1H_1 , E_1 and H_1 for $\text{A} \cdot 3\text{H}_2\text{O}(\text{A})$, i.e. for $\alpha\text{-A} \cdot 3\text{H}_2\text{O}$ (bayerite), although conveniently listed as stable in the above, are really fundamentally metastable with respect to the equilibria E_2H_2 , E_2 and H_2 for $\text{A} \cdot 3\text{H}_2\text{O}(\text{B})$. The boundary curve (4) is a metastable prolongation of the stable curve (2) beyond the stable invariant point H_2 . It is metastable with respect to the stable portion of the boundary curve $\text{C}_3\text{A} \cdot 6\text{H}_2\text{O} - \text{C}_3\text{A} \cdot 3\text{CaSO}_4 \cdot 32\text{H}_2\text{O}(\text{H}_2\text{G})$ (figure 3). The metastable curve (5) is shown in figure 3c and as a projection on the $\text{CaO}-\text{Al}_2\text{O}_3-\text{H}_2\text{O}$ face in figure 6. All the equilibria listed are considered in their appropriate sections. As in the previous work (8, Fig. 11a), results have been plotted in figure 3a as a projection onto the base of the pyramidal space figure. Compared with the previous figure, the present one is complicated by the fact that the boundary curves for alumina gel previously determined are drawn as well as the boundary curves for the preparations A and B of crystalline $\text{A} \cdot 3\text{H}_2\text{O}$ now obtained. The original lettering is retained. Thus E is the invariant point with alumina gel $\text{CaSO}_4 \cdot 2\text{H}_2\text{O} - \text{Al}_2\text{O}_3\text{aq.} - \text{C}_3\text{A} \cdot \text{CaSO}_4 \cdot 32\text{H}_2\text{O}$, E_1 and E_2 the corresponding invariant points with $\text{A} \cdot 3\text{H}_2\text{O}(\text{A})$ and $\text{A} \cdot 3\text{H}_2\text{O}(\text{B})$, while EH is the boundary curve with alumina gel $\text{Al}_2\text{O}_3\text{aq.} - \text{C}_3\text{A} \cdot 3\text{CaSO}_4 \cdot 32\text{H}_2\text{O}$, and E_1H_1 and E_2H_2 the corresponding boundary curves with $\text{A} \cdot 3\text{H}_2\text{O}(\text{A})$ and $\text{A} \cdot 3\text{H}_2\text{O}(\text{B})$. A complete set of curves has been obtained only for $\text{A} \cdot 3\text{H}_2\text{O}(\text{B})$. Fundamentally stable curves are shown by full lines. Other curves, including those for $\text{A} \cdot 3\text{H}_2\text{O}(\text{A})$ (metastable with respect to $\text{A} \cdot 3\text{H}_2\text{O}(\text{B})$) are shown by broken or dotted lines. In order to make clear the course of the several boundary curves in the $(\text{CaSO}_4)_3$ corner, and especially in the $(\text{CaO})_3$ corner where the data are crowded, details of these corners are given on an enlarged scale in figures 3b and 3c, which are partly diagrammatic.

¹ The lettering refers to the appropriate curves in figures 3a, 3b, and 3c.

Stable equilibria

The boundary curve $\text{CaSO}_4 \cdot 2\text{H}_2\text{O}-\text{A} \cdot 3\text{H}_2\text{O}(\text{B})$ (J_2E_2):—This curve, because of the low solubility of $\text{A} \cdot 3\text{H}_2\text{O}$, cannot be appreciably different from the solubility curve for $\text{CaSO}_4 \cdot 2\text{H}_2\text{O}$ in the ternary system $\text{H}_2\text{O}-\text{CaSO}_4-\text{Al}_2(\text{SO}_4)_3$ (see previous work (8), Table III and p. 1491, section (iii)). Similar mixes to those previously employed for the ternary system, but with the addition of crystalline $\text{A} \cdot 3\text{H}_2\text{O}(\text{B})$, gave almost identical results (Q_1 , Q_2 , figure 3a). Other mixes were examined in which sufficient sulfuric acid was added to increase the $\text{SO}_3/\text{Al}_2\text{O}_3$ ratio in the

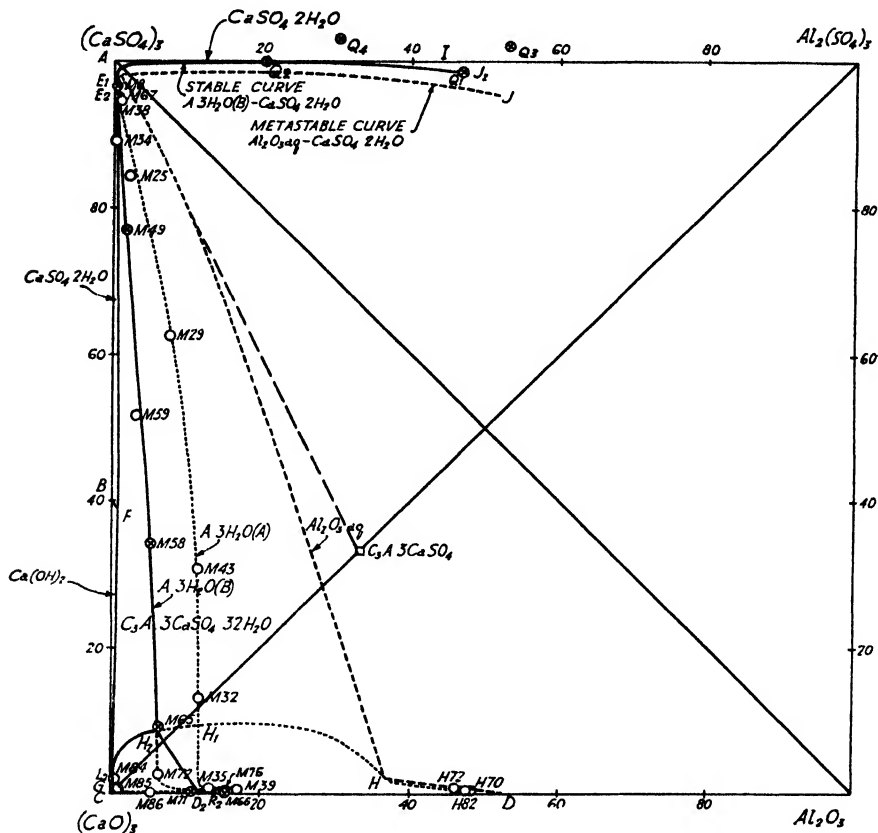


FIG. 3a. Quaternary system: projection on base of pyramid

aluminum sulfate used (16.3 per cent Al_2O_3 , 37.3 per cent SO_3 : $\text{SO}_3/\text{Al}_2\text{O}_3 = 2.91$) to > 3 and hence ensure the necessity for solution of the $\text{A} \cdot 3\text{H}_2\text{O}$ for attainment of equilibrium. After 28 days' shaking, the analytical data showed that solution of $\text{A} \cdot 3\text{H}_2\text{O}$ had occurred, but the solution was still very slightly acid, though barely outside the limits of experimental error (Q_3 and Q_4 , figure 3a). While it is questionable as to how far the divergence of the data shown in figure 3a and which is exaggerated by the projection is due to experimental error, and how far to non-attainment of equilibrium even after 28 days' shaking, it is nevertheless to

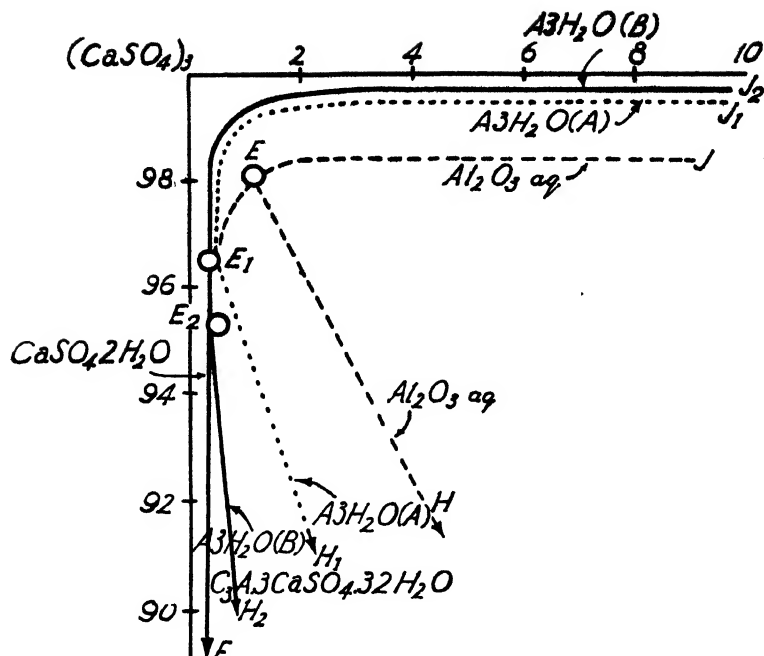


FIG. 3b. Quaternary system: detail of $(\text{CaSO}_4)_3$ corner

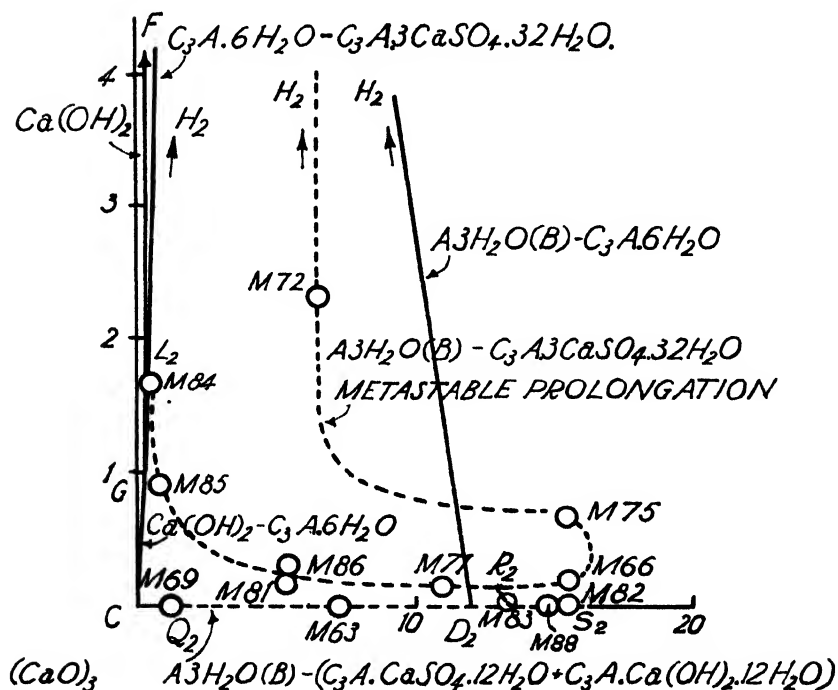


FIG. 3c. Quaternary system: detail of $(\text{CaO})_3$ corner

be concluded that the solubility of crystalline $\text{A} \cdot 3\text{H}_2\text{O}$ in solutions of calcium sulfate and aluminum sulfate is negligible within the range examined, and the boundary curve is essentially identical with that for $\text{CaSO}_4 \cdot 2\text{H}_2\text{O}$ in the ternary system except where it curves to meet the invariant point E_2 . The boundary curve (drawn through Q_1 and Q_2) is shown as curve J_2E_2 in figure 3a. Data are given in table 3.

The isothermal invariant point $\text{CaSO}_4 \cdot 2\text{H}_2\text{O}-\text{A} \cdot 3\text{H}_2\text{O}-\text{C}_3\text{A} \cdot 3\text{CaSO}_4 \cdot 32\text{H}_2\text{O}$ (E_1, E_2):—The 28-day data, M8, M67, given in table 4 are for mixes of $\text{CaO}-\text{CaSO}_4$ solution, $\text{CaSO}_4 \cdot 2\text{H}_2\text{O}$ and $\text{A} \cdot 3\text{H}_2\text{O}(\text{A})$ and $\text{A} \cdot 3\text{H}_2\text{O}(\text{B})$, respectively. They are the points E_1 and E_2 in figures 3a and 3b. Reaction of $\text{A} \cdot 3\text{H}_2\text{O}$ with CaO and CaSO_4 occurs to give $\text{C}_3\text{A} \cdot 3\text{CaSO}_4 \cdot 32\text{H}_2\text{O}$.

The boundary curve $\text{A} \cdot 3\text{H}_2\text{O}-\text{C}_3\text{A} \cdot 3\text{CaSO}_4 \cdot 32\text{H}_2\text{O}$ ($\text{E}_1\text{H}_1, \text{E}_2\text{H}_2$):—Data have been obtained with both preparations A and B of crystalline $\text{A} \cdot 3\text{H}_2\text{O}$. The Jänecke projections (E_1H_1 and E_2H_2) onto the base of the pyramid are shown in figure 3a, and on an enlarged scale at the $(\text{CaSO}_4)_3$ corner in figure 3b. Spacial positions, including metastable prolongations, are shown in figure 4. Selected

TABLE 3
Boundary curve J_2E_2 : $\text{CaSO}_4 \cdot 2\text{H}_2\text{O}-\text{A} \cdot 3\text{H}_2\text{O}(\text{B})$

NO	TIME SHAKEN	GRAM-MOLES $\times 10^4$ PER 1000 G. OF SOLUTION			TOTAL GRAM- MOLES $\times 10^4$ PER 1000 G OF SOLUTION	$(\text{CaSO}_4)_2$	Al_2O_3	$\text{Al}_2(\text{SO}_4)_3$	TOTAL SALTS IN SOLUTION
		$(\text{CaSO}_4)_2$	Al_2O_3	$\text{Al}_2(\text{SO}_4)_3$		mole per cent	mole per cent	mole per cent	mole per cent
	days								
Q1	28	47.0	1.4	42.6	91.0	51.6	1.5	46.9	0.01640
Q2	28	49.2	0.1	12.5	61.8	79.7	0.1	20.3	0.01113
Q3	28	46.8	-2.0	51.1	95.9	48.8	-2.1	53.3	0.01730
Q4	28	49.1	-2.2	20.4	67.3	72.9	-3.2	30.3	0.01213

data sufficient to define the positions of the boundary curves are given in table 4. All available data are plotted in figures 3 and 4.

Boundary curve A (E_1H_1):—Except for the invariant point with $\text{CaSO}_4 \cdot 2\text{H}_2\text{O}$, the data for $\alpha\text{-A} \cdot 3\text{H}_2\text{O}$ (bayerite) were obtained after 7 days' shaking. It was found that for any given concentration of CaSO_4 in the initial mix, it was necessary to reduce the CaO concentration to such a point that excessive formation of $\text{C}_3\text{A} \cdot 3\text{CaSO}_4 \cdot 32\text{H}_2\text{O}$ was avoided, otherwise there was interference with the attainment of equilibrium, apparently owing to the formation of an inhibiting coating on the surface of the $\text{A} \cdot 3\text{H}_2\text{O}$. In practice, for each point a series of mixes was made up, keeping the CaSO_4 constant and decreasing the CaO concentration to the point where no $\text{C}_3\text{A} \cdot 3\text{CaSO}_4 \cdot 32\text{H}_2\text{O}$ formation occurred. That mix containing just sufficient CaO to induce formation of $\text{C}_3\text{A} \cdot 3\text{CaSO}_4 \cdot 32\text{H}_2\text{O}$ was then taken as yielding the equilibrium value. The method of working is made clear in figure 5. Mixes such as 13, 15, 6, 7, and 9 on analysis gave results showing that only a part of the $\text{C}_3\text{A} \cdot 3\text{CaSO}_4 \cdot 32\text{H}_2\text{O}$ formation necessary to reach the boundary curve occurs before further reaction is inhibited. In such mixes the Al_2O_3 concentration was practically nil.

Boundary curve B (E_2H_2):—This is based mainly on 28-day data. In general the same initial mixes were employed as in determining curve A, though in one or two cases increased concentrations of CaO were required to bring about formation of $C_3A \cdot 3CaSO_4 \cdot 32H_2O$.

Figure 3b makes clear the relationship between the curves at the $(CaSO_4)_3$ corner. The most stable curve for $A \cdot 3H_2O(B) - C_3A \cdot 3CaSO_4 \cdot 32H_2O$ (E_2H_2) meets the stable curve $CaSO_4 \cdot 2H_2O - C_3A \cdot 3CaSO_4 \cdot 32H_2O$ (E_2F) in the stable invariant point $CaSO_4 \cdot 2H_2O - A \cdot 3H_2O(B) - C_3A \cdot 3CaSO_4 \cdot 32H_2O$ (E_2). From E_2 there must be a short metastable prolongation of FE_2 to the metastable invariant point E (shown as a broken line in figure 3b), while from E_1 a curve E_1J_1 for

TABLE 4

Invariant points E_1, E_2 : $CaSO_4 \cdot 2H_2O - A \cdot 3H_2O - C_3A \cdot 3CaSO_4 \cdot 32H_2O$ (mixes M8, M67)

Boundary curves: E_1H_1, E_2H_2 : $A \cdot 3H_2O - C_3A \cdot 3CaSO_4 \cdot 32H_2O$ (other mixes)

NO.	TIME SHAKEN	GRAM-MOLES $\times 10^4$ PER 1000 G. OF SOLUTION			TOTAL GRAM-MOLES $\times 10^4$ PER 1000 G. OF SOLUTION	$(CaSO_4)_3$	$(CaO)_3$	Al_2O_3	TOTAL SALTS IN SOLUTION
		$(CaSO_4)_3$	$(CaO)_3$	Al_2O_3					
Crystalline A $\cdot 3H_2O$ (A)									
	days					mole per cent	mole per cent	mole per cent	mole per cent
M8	28	50.3	1.7	0.15	52.15	96.5	3.3	0.3	0.00940
M25	7	15.8	1.75	0.4	18.8	84.1	13.8	2.1	0.00339
M43	7	3.2	6.0	1.2	10.4	30.8	57.7	11.5	0.00188
M32	7	1.45	8.2	1.3	10.95	13.2	74.9	11.9	0.00197
M35	7	0.15	22.2	3.45	25.8	0.6	86.0	13.4	0.00465
Crystalline A $\cdot 3H_2O$ (B)									
M67	28	49.9	2.25	0.25	52.4	95.3	4.3	0.5	0.00945
M49	28	16.9	4.7	0.4	22.0	76.9	21.4	1.8	0.00397
M58	28	5.0	8.85	0.8	14.65	34.1	60.4	5.5	0.00264
M65	28	1.3	11.85	0.9	14.05	9.3	84.3	6.4	0.00253
M72	7	0.45	17.65	1.25	19.35	2.3	91.2	6.5	0.00349
M66	28	0.05	22.1	4.05	26.2	0.2	84.4	15.5	0.00473

$CaSO_4 \cdot 2H_2O - A \cdot 3H_2O(A)$ must proceed. This, while not determined, has been shown in its probable position in figure 3b. From the invariant points E, E_1 , and E_2 the curves for $C_3A \cdot 3CaSO_4 \cdot 32H_2O$ and alumina gel, $A \cdot 3H_2O(A)$ and $A \cdot 3H_2O(B)$ proceed as shown.

The isothermal invariant point $C_3A \cdot 3CaSO_4 \cdot 32H_2O - C_3A \cdot 6H_2O - A \cdot 3H_2O(H_1, H_2)$:—Both boundary curves A and B ($A \cdot 3H_2O - C_3A \cdot 3CaSO_4 \cdot 32H_2O$) meet the boundary curve $C_3A \cdot 6H_2O - C_3A \cdot 3CaSO_4 \cdot 32H_2O$ at invariant points $C_3A \cdot 3CaSO_4 \cdot 32H_2O - C_3A \cdot 6H_2O - A \cdot 3H_2O$ (α - $A \cdot 3H_2O$ (bayerite) and near γ - $A \cdot 3H_2O$ (gibbsite), respectively). The positions of these points and that of the invariant point with alumina gel in relation to the curve $C_3A \cdot 6H_2O - C_3A \cdot 3CaSO_4 \cdot 32H_2O$ are shown in figure 3a. The solution concentrations at the point of intersection

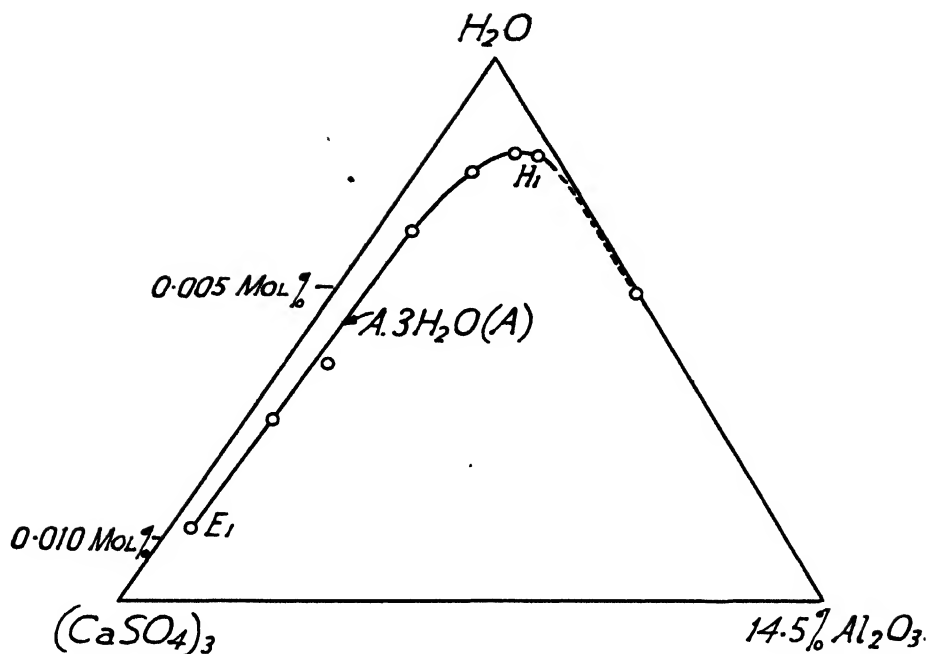


FIG. 4a. Quaternary system. Boundary curve: crystalline $A \cdot 3H_2O(A) - C_3A \cdot 3CaSO_4 \cdot 32H_2O$.

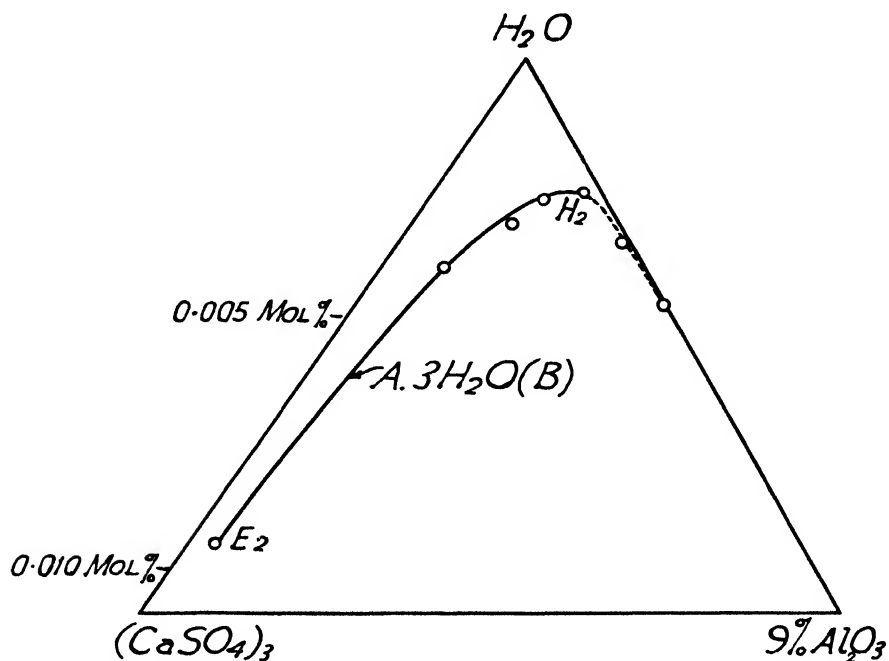


FIG. 4b. Quaternary system. Boundary curve: crystalline $A \cdot 3H_2O(B) - C_3A \cdot 3CaSO_4 \cdot 32H_2O$.

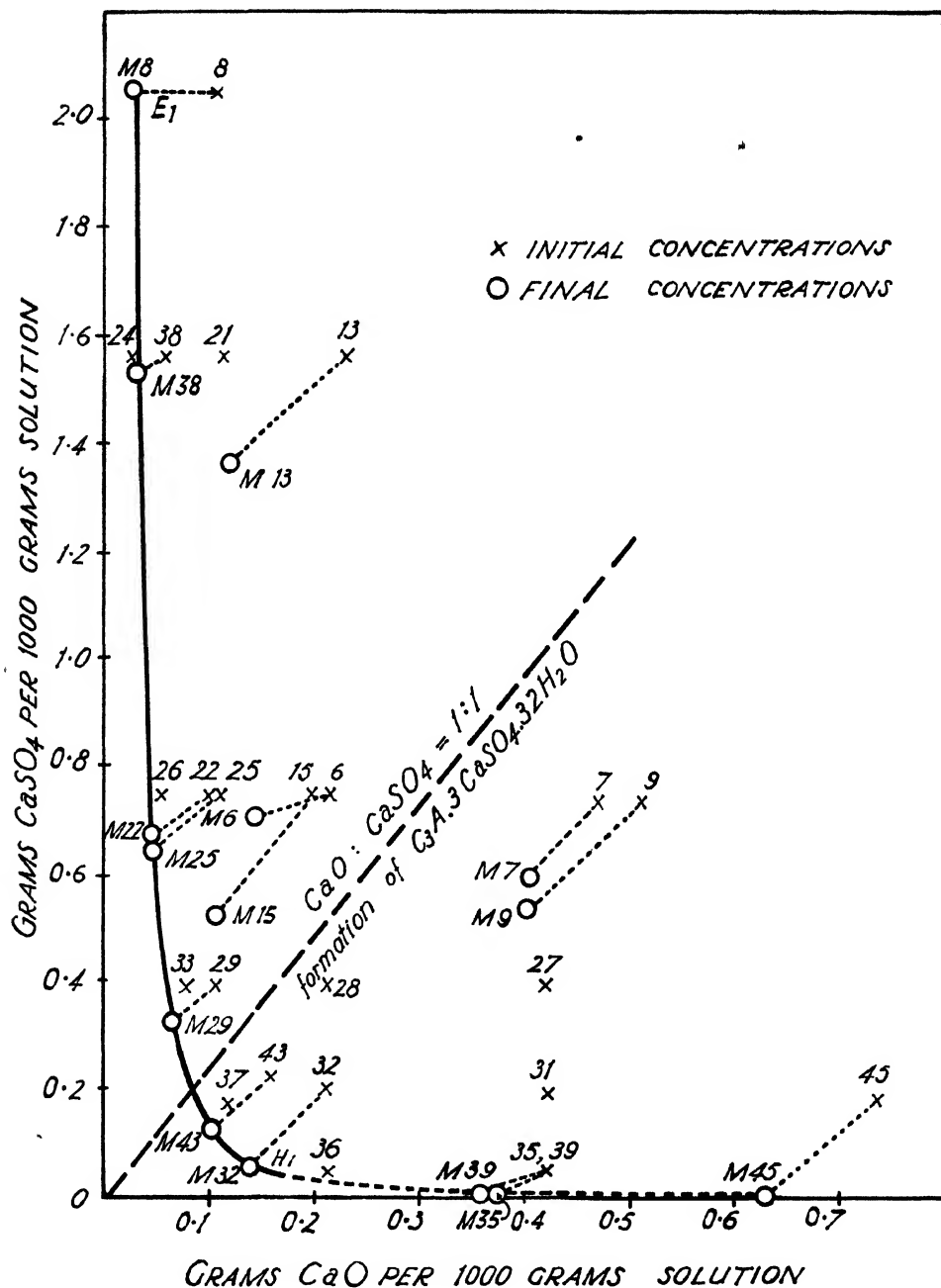


FIG. 5. Quaternary system. Equilibrium concentrations along curve $\text{A} \cdot 3\text{H}_2\text{O}(\text{A}) - \text{C}_1\text{A} \cdot 3\text{CaSO}_4 \cdot 32\text{H}_2\text{O}$.

of the boundary curves (by interpolation) are, respectively, in grams per 1000 g. of solution:

H₁ Curve $\text{A} \cdot 3\text{H}_2\text{O}(\text{A})-\text{C}_3\text{A} \cdot 3\text{CaSO}_4 \cdot 32\text{H}_2\text{O}$: $\text{CaO} = 0.17$, $\text{Al}_2\text{O}_3 = 0.016$, $\text{CaSO}_4 = 0.049$

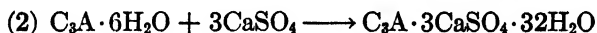
Curve $\text{C}_3\text{A} \cdot 6\text{H}_2\text{O}-\text{C}_3\text{A} \cdot 3\text{CaSO}_4 \cdot 32\text{H}_2\text{O}$: $\text{CaO} = 0.172$, $\text{Al}_2\text{O}_3 = 0.016$, $\text{CaSO}_4 = 0.049$

H₂ Curve $\text{A} \cdot 3\text{H}_2\text{O}(\text{B})-\text{C}_3\text{A} \cdot 3\text{CaSO}_4 \cdot 32\text{H}_2\text{O}$: $\text{CaO} = 0.199$, $\text{Al}_2\text{O}_3 = 0.009$, $\text{CaSO}_4 = 0.0535$

Curve $\text{C}_3\text{A} \cdot 6\text{H}_2\text{O}-\text{C}_3\text{A} \cdot 3\text{CaSO}_4 \cdot 32\text{H}_2\text{O}$: $\text{CaO} = 0.193$, $\text{Al}_2\text{O}_3 = 0.009$, $\text{CaSO}_4 = 0.049$

Mean H₂: $\text{CaO} = 0.196$, $\text{Al}_2\text{O}_3 = 0.009$, $\text{CaSO}_4 = 0.051$

There are a number of difficulties which make the direct determination of the invariant point impracticable. Crystallization of $\text{A} \cdot 3\text{H}_2\text{O}$ from solution is rather improbable in this system at 25°C ., and crystallization of $\text{C}_3\text{A} \cdot 6\text{H}_2\text{O}$ a matter of considerable difficulty. Other difficulties arise in the formation of $\text{C}_3\text{A} \cdot 3\text{CaSO}_4 \cdot 32\text{H}_2\text{O}$. In any mix involving crystalline $\text{A} \cdot 3\text{H}_2\text{O}$, $\text{C}_3\text{A} \cdot 6\text{H}_2\text{O}$, and CaO and CaSO_4 solutions, this compound may arise in two ways:



Either or both reactions may proceed, and both reactions may be inhibited. As previously shown, only a limited amount of $\text{C}_3\text{A} \cdot 3\text{CaSO}_4 \cdot 32\text{H}_2\text{O}$ can be produced by equation 1 before the $\text{A} \cdot 3\text{H}_2\text{O}$ is prevented from reacting further. As regards equation 2, it has been found that this reaction does not always occur where theoretically it should do so. The cause is not clear and may be the presence of a superficial protective coating or an inherent inertia which is not necessarily overcome at some definite CaO and CaSO_4 concentration. Several attempts have nevertheless been made to obtain the invariant point directly, using a variety of methods of approach, but it is hardly surprising that it has not been found possible.

The boundary curve $\text{A} \cdot 3\text{H}_2\text{O}-\text{C}_3\text{A} \cdot 6\text{H}_2\text{O}$ (H_2D_2):—Because of the difficulty of crystallizing $\text{A} \cdot 3\text{H}_2\text{O}$ or $\text{C}_3\text{A} \cdot 6\text{H}_2\text{O}$ directly in this system at 25°C ., it has not been found practicable to obtain data for this curve. Its position, however, is sufficiently defined by the invariant points. The curve for $\text{A} \cdot 3\text{H}_2\text{O}(\text{B})-\text{C}_3\text{A} \cdot 6\text{H}_2\text{O}$ is given by H_2D_2 in figure 3a.

Metastable equilibria

It will be clear from the preceding that the low-sulfate form of calcium sulfoaluminate, " $\text{C}_3\text{A} \cdot \text{CaSO}_4 \cdot 12\text{H}_2\text{O}$ ", does not occur in the quaternary system as a stable phase. Examination of the metastable equilibria shows, however, that it may be formed as a terminal component in a metastable solid solution series.

The metastable equilibria in the region lying between the $\text{C}_3\text{A} \cdot 6\text{H}_2\text{O}-\text{C}_3\text{A} \cdot 3\text{CaSO}_4 \cdot 32\text{H}_2\text{O}$ boundary curve (HG) and the $(\text{CaO})_3-\text{Al}_2\text{O}_3$ edge in figure 3a

were determined almost wholly with the preparation B of crystalline $A \cdot 3H_2O$, since only a limited supply of preparation A was available. The few data obtained with the preparation A are, as is to be expected, not identical with those for the preparation B. Except for a brief interval of rapidly increasing CaO and rapidly decreasing $CaSO_4$ concentrations between the boundary curve $C_3A \cdot 6H_2O - C_3A \cdot 3CaSO_4 \cdot 32H_2O$ (HG) and the plane $H_2O - (CaO)_3 - Al_2O_3$, the data in the $(CaO)_3$ corner lie near to or in this plane, the $CaSO_4$ concentration being either very small, or practically nil. This will be made clear by reference to figure 3c (showing $CaSO_4$ contents on a greatly exaggerated scale) and to table 5. Referring to figure 3c, it will be noted that the metastable prolongation $H_2R_2L_2$ of

TABLE 5

Metastable equilibria with crystalline $A \cdot 3H_2O$ (B)

Boundary curve $H_2R_2L_2$: $A \cdot 3H_2O(B) - C_3A \cdot 3CaSO_4 \cdot 32H_2O$

Invariant point R_2 : $A \cdot 3H_2O(B) - C_3A \cdot 3CaSO_4 \cdot 32H_2O - C_3A \cdot CaSO_4 \cdot 12H_2O$

Boundary curve $R_2S_2Q_2$: $A \cdot 3H_2O(B) - C_3A \cdot CaSO_4 \cdot 12H_2O + C_3A \cdot Ca(OH)_2 \cdot 12H_2O$ —solid solution

NO.	TIME SHAKEN	GRAMS PER 1000 G. OF SOLUTION			NO.	TIME SHAKEN	GRAMS PER 1000 G. OF SOLUTION		
		CaO	Al ₂ O ₃	CaSO ₄			CaO	Al ₂ O ₃	CaSO ₄
Boundary curve H ₂ R ₂ L ₂					Boundary curve R ₂ S ₂ Q ₂				
	days					days			
M65.	28	0.199	0.009	0.0535	M62	28	0.443	0.044	Nil
M72	7	0.297	0.0125	0.0175	M52	28	0.468	0.045	0.001
M75	28	0.319	0.036	0.007	M73	28	0.606	0.0635	0.001
M66	28	0.371	0.0415	0.0015	M88	28	0.621	0.0655	0.001
M71	28	0.521	0.039	0.0015	M82	28	0.672	0.075	0.001
M81, M86	7	0.630	0.022	0.003	M89	28	0.679	0.0705	Nil
M85	3	0.731	0.0035	0.017	M57	28	0.781	0.0415	0.0015
M84	3	0.846	0.0025	0.0345	M63	28	0.802	0.038	Nil
Invariant point R ₂					M70	28	0.913	0.022	0.0015
M83.	28	0.461	0.037	0.002	M69	7	1.000	0.0065	Nil

the $A \cdot 3H_2O(B) - C_3A \cdot 3CaSO_4 \cdot 32H_2O$ curve (E_2H_2) shows an abrupt curvature. The point R_2 is the metastable invariant point $A \cdot 3H_2O(B) - C_3A \cdot 3CaSO_4 \cdot 32H_2O - "C_3A \cdot CaSO_4 \cdot 12H_2O."$ Strictly speaking, it appears that the third phase approaches the composition $C_3A \cdot CaSO_4 \cdot 12H_2O$, and it is written thus as a matter of convenience. From this point there proceeds a solid solution boundary curve $A \cdot 3H_2O(B) - "C_3A \cdot CaSO_4 \cdot 12H_2O + C_3A \cdot Ca(OH)_2 \cdot 12H_2O"$ ($R_2S_2Q_2$) which shows a rapid reduction in the $CaSO_4$ equilibrium value to practically nil. In projection, the curve follows the course R_2 to S_2 and then reverses abruptly in direction along the $(CaO)_3 - Al_2O_3$ edge to Q_2 .

The data for the metastable equilibria are most conveniently plotted in rectangular coördinates, expressing concentrations in grams per 1000 g. of solution.

The data for $A \cdot 3H_2O(B)$ (given in table 5) are plotted thus in figure 6. The limited data available for $A \cdot 3H_2O(A)$ are not tabulated, but are however plotted in figure 6 and are distinguished from those for $A \cdot 3H_2O(B)$ by flagged symbols. It will be clear that the metastable prolongations of the $A \cdot 3H_2O - C_3A \cdot 3CaSO_4 \cdot 32H_2O$ curves are represented partly in projection in this figure. Comparing figure 3c and figure 6, the curves $H_2R_2I_2$ in each case give $A \cdot 3H_2O(B) - C_3A \cdot 3CaSO_4 \cdot 32H_2O$ equilibria, and the curves $R_2S_2Q_2$, $A \cdot 3H_2O(B) - "C_2A \cdot CaSO_4 \cdot 12H_2O + C_3A \cdot Ca(OH)_2 \cdot 12H_2O"$ solid solution equilibria.

Metastable prolongation of boundary curve $A \cdot 3H_2O - C_3A \cdot 3CaSO_4 \cdot 32H_2O$ ($H_2R_2L_2$):—The curve obtained for $A \cdot 3H_2O(B)$ using suitable mixes of $A \cdot 3H_2O$ with $CaO - CaSO_4$ solutions of increasing CaO concentrations is that lettered

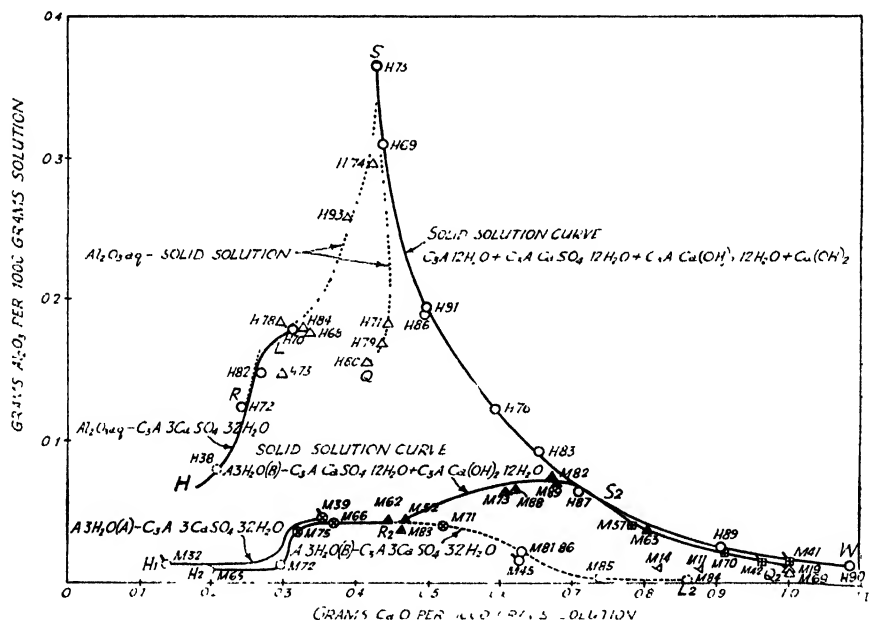


FIG. 6. Quaternary system: equilibria with (a) crystalline $A \cdot 3H_2O$ (b) alumina gel

H₂R₂L₂ in figure 3c and figure 6. The curve is characterized by first an increase and then a decrease in the amount of Al₂O₃ in solution as the CaO concentration increases. This is combined with a decrease to a very small value in the CaSO₄ content, followed by a slight increase. In the basal projection (figure 3c), this behavior is shown by an abrupt curvature near the (CaO)₃-Al₂O₃ line, followed by a reversal of direction towards the (CaO)₃ corner. Corresponding data for A·3H₂O(A), which are limited to very few points, are consistent with a curve similar in form to that for A·3H₂O(B), and showing a slightly increased Al₂O₃ solubility.

Invariant point $A \cdot 3H_2O - C_3A - 3CaSO_4 \cdot 32H_2O - "C_3A \cdot CaSO_4 \cdot 12H_2O" (R_2)$:—One 28-day point was obtained for $A \cdot 3H_2O(B)$, with mix M83 of table 5 and figures 3c and 6.

Solid solution boundary curve $A \cdot 3H_2O$ —“ $C_3A \cdot CaSO_4 \cdot 12H_2O + C_3A \cdot Ca(OH)_2 \cdot 12H_2O$ ” ($R_2S_2Q_2$):—In general, this curve was traced with similar mixes to those employed for the more metastable portion of the $A \cdot 3H_2O$ — $C_3A \cdot 3CaSO_4 \cdot 32H_2O$ curve $H_2R_2L_2$, shown as a broken line R_2L_2 in figure 6, but with much longer periods of shaking. The $C_3A \cdot 3CaSO_4 \cdot 32H_2O$ initially formed undergoes change, the typical “needles” being converted into hexagonal plates, and a new and less metastable equilibrium is set up. The data obtained are almost entirely for $A \cdot 3H_2O(B)$, only three points M19, M41, and M42 (figure 6) being given for $A \cdot 3H_2O(A)$ in the high lime region. It is to be expected that the curve for $A \cdot 3H_2O(A)$ will lie somewhat above that for $A \cdot 3H_2O(B)$. Along the curve $R_2S_2Q_2$ of figure 6, the solid phases consisted of $A \cdot 3H_2O$ and hexagonal plates the refractive indices of which increased towards the high CaO region from those reported previously for “ $C_3A \cdot CaSO_4 \cdot 12H_2O$ ” ($\omega = 1.504$, $\epsilon = 1.488$), until the highest indices found corresponded to those for α - $C_4A \cdot 12$ – $13H_2O$ (1, 12) ($\omega = 1.536 \pm 0.003$; $\epsilon = 1.521 \pm 0.003$). The changing refractive indices are indicative of a changing composition of the hexagonal plate phase and it appears therefore that it may be expressed in terms of $C_3A \cdot CaSO_4 \cdot 12H_2O$ and $C_3A \cdot Ca(OH)_2 \cdot 12H_2O$. As is shown later (figure 8), solid solutions formed in equilibrium with solutions of high lime concentrations reach a C/A ratio in excess of 4. Accepting tentatively that the solid solution is here one of $C_3A \cdot CaSO_4 \cdot 12H_2O$ and $C_3A \cdot Ca(OH)_2 \cdot 12H_2O$ only, it is possible to calculate, from the known initial composition of the various mixes and the final solution concentrations, the changing compositions of the solid solutions along the curve $R_2S_2Q_2$ in terms of these two compounds. Thus, from the known contents of lime and calcium sulfate in the initial mix and in the final solution, the lime and calcium sulfate content of the solid is obtained. The alumina content of the solid solution phase is not in this case known, since crystalline $A \cdot 3H_2O$ is also present. However, the evidence of the refractive indices as R_2 is approached points fairly conclusively to the presence of $C_3A \cdot CaSO_4 \cdot 12H_2O$, and the amount of this compound in the solid solution may therefore be calculated from the calcium sulfate content. Lime in excess of that required for $C_3A \cdot CaSO_4 \cdot 12H_2O$ can only be present as one or possibly more of the hydrated calcium aluminates. The evidence of the rising refractive indices of the solid solution phase as Q_2 is approached, and specifically that of mix M42 ($\omega = 1.536$; $\epsilon = 1.522 \pm 0.003$) points to the presence of $C_3A \cdot Ca(OH)_2 \cdot 12H_2O$. Indirectly, its presence is confirmed by the evidence of other solid solution equilibria, described later, as for example along the curve SW of figure 6, where it is shown that with increasing lime concentrations in the equilibrium solutions above 0.6 g. CaO per 1000 g. of solution, increasing amounts of $C_3A \cdot Ca(OH)_2 \cdot 12H_2O$ must be present. Calculating the lime present in the solid solution in excess of $C_3A \cdot CaSO_4 \cdot 12H_2O$ in terms of $C_3A \cdot Ca(OH)_2 \cdot 12H_2O$, and plotting the ω index of the hexagonal plate phase against the composition, figure 7 is obtained. This figure includes data obtained with both preparations of $A \cdot 3H_2O$. Apart from mix M63 (a duplicate of M57), the data lie on a smooth curve between the indices for the end components. It is probable that a lower hydrated calcium aluminate than the tetra compound,

probably the tricalcium compound, also enters into the solid solution. In this case, figure 7 does not give strictly the true composition of the solid solution, but the form of the curve relating refractive index to solid solution composition will nevertheless be very similar. It is concluded, later, that the curve $\text{R}_2\text{S}_2\text{Q}_2$ is a boundary curve to a solid solution surface.

The further metastable prolongation R_2L_2 of the boundary curve $\text{A} \cdot 3\text{H}_2\text{O}(\text{B})-\text{C}_3\text{A} \cdot 3\text{CaSO}_4 \cdot 32\text{H}_2\text{O}$, shown as a broken line in figure 6, is only a transient stage, the $\text{C}_3\text{A} \cdot 3\text{CaSO}_4 \cdot 32\text{H}_2\text{O}$ initially formed being metastable with respect to $\text{C}_3\text{A} \cdot \text{CaSO}_4 \cdot 12\text{H}_2\text{O}$ or a solid solution containing it. Longer periods of shaking lead to the equilibria defined by the full curve $\text{R}_2\text{S}_2\text{Q}_2$ in figure 6 for $\text{A} \cdot 3\text{H}_2\text{O}(\text{B})$ and solid solution, concluded to be essentially one of $\text{C}_3\text{A} \cdot \text{CaSO}_4 \cdot 12\text{H}_2\text{O}$ and $\text{C}_3\text{A} \cdot \text{Ca}(\text{OH})_2 \cdot 12\text{H}_2\text{O}$. It is of interest to consider the relationship between the various points obtained on the curves $\text{R}_2\text{S}_2\text{Q}_2$ and R_2L_2 , since this throws light on the mechanism of formation of the various compounds. As previously noted, R_2

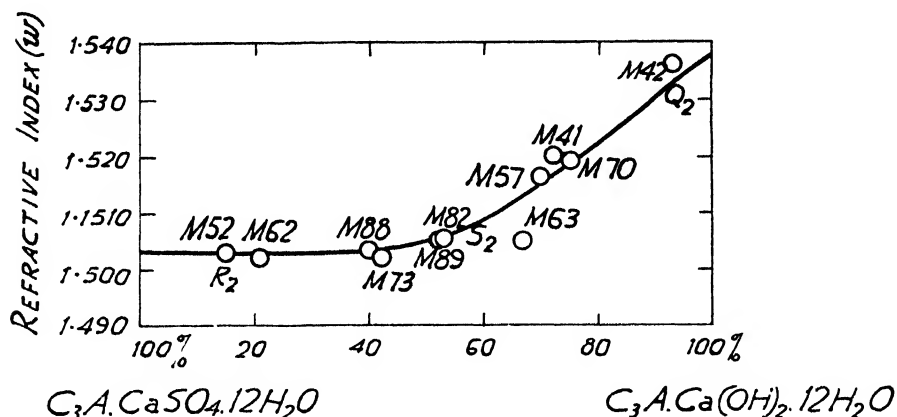


FIG. 7. Boundary curve ($\text{R}_2\text{S}_2\text{Q}_2$) $\text{A} \cdot 3\text{H}_2\text{O}-(\text{C}_3\text{A} \cdot \text{CaSO}_4 \cdot 12\text{H}_2\text{O} + \text{C}_3\text{A} \cdot \text{Ca}(\text{OH})_2 \cdot 12\text{H}_2\text{O})$. Relation between refractive indices and composition of solid solution.

is strictly not an invariant point for pure $\text{C}_3\text{A} \cdot \text{CaSO}_4 \cdot 12\text{H}_2\text{O}$, but for a solid solution approaching this composition. In lime concentrations greater than correspond to the invariant point R_2 , $\text{C}_3\text{A} \cdot 3\text{CaSO}_4 \cdot 32\text{H}_2\text{O}$ becomes metastable with respect to $\text{C}_3\text{A} \cdot \text{CaSO}_4 \cdot 12\text{H}_2\text{O}$ or solid solution. The change is slow in fairly low lime concentrations (thus mix M71 after 28 days gave only $\text{C}_3\text{A} \cdot 3\text{CaSO}_4 \cdot 32\text{H}_2\text{O}$ with $\text{A} \cdot 3\text{H}_2\text{O}(\text{B})$), but occurs more quickly as the lime concentration increases. Mixes M81 and M86, duplicates shaken for 7 days, gave the high-sulfate form only, but mixes M52 and M62 (at R_2) of the same initial composition but shaken for 28 days, gave the solid solution only. It is thus apparent that the $\text{C}_3\text{A} \cdot 3\text{CaSO}_4 \cdot 32\text{H}_2\text{O}$ initially formed has gradually been converted to the solid solution. M85 and M84, 3-day mixes, gave the high-sulfate form only. M73, however, of the same initial composition as H84, gave after 28 days the solid solution. M69 (with solid $\text{Ca}(\text{OH})_2$ present) after 7 days gave hexagonal plates of indices corresponding to the low-sulfate form, and crystalline $\text{Ca}(\text{OH})_2$

still remained as a solid phase, but an identical mix M70 after 28 days gave no solid $\text{Ca}(\text{OH})_2$ and hexagonal plates of refractive indices $\omega = 1.519 \pm 0.003$, $\epsilon = 1.501 \pm 0.003$. There is thus a further slow reaction following formation of $\text{C}_3\text{A} \cdot \text{CaSO}_4 \cdot 12\text{H}_2\text{O}$, more lime and alumina being taken up to give a solid solution of $\text{C}_3\text{A} \cdot \text{CaSO}_4 \cdot 12\text{H}_2\text{O}$ and $\text{C}_3\text{A} \cdot \text{Ca}(\text{OH})_2 \cdot 12\text{H}_2\text{O}$. The few points obtained with $\text{A} \cdot 3\text{H}_2\text{O}(\text{A})$ show a similar behavior.

Equilibria with alumina gel

In addition to the equilibria with crystalline $\text{A} \cdot 3\text{H}_2\text{O}$ described above, equilibria with alumina gel were determined, supplementary to those described in the previous paper. Such equilibria (see phase-rule equilibria section) are regarded as "unstable" as distinct from "metastable." The following boundary curves and invariant points have been examined. Their relation to the corresponding equilibria (a)(4), (a)(5), and (b)(3) for crystalline $\text{A} \cdot 3\text{H}_2\text{O}$ should be noted.

(a) Boundary curves:

Unstable (1) $\text{Al}_2\text{O}_3\text{aq.}-\text{C}_3\text{A} \cdot 3\text{CaSO}_4 \cdot 32\text{H}_2\text{O}$ (HRL) (prolongation of EH)

(2) $\text{Al}_2\text{O}_3\text{aq.}-\text{solid solution}$ (RSQ)

(b) Invariant points:

Unstable (1) $\text{Al}_2\text{O}_3\text{aq.}-\text{C}_3\text{A} \cdot 3\text{CaSO}_4 \cdot 32\text{H}_2\text{O}-\text{solid solution}$ (R)

The data are plotted partly in figure 6 (H mixes), giving a direct comparison with the corresponding data on crystalline $\text{A} \cdot 3\text{H}_2\text{O}$; in figure 8, where the relationship between the final equilibrium solution and the initial complex composition of the mixes is shown, and in figure 10. Mixes were ordinarily prepared as follows: Alumina gel was precipitated in the cold by the addition of a standard amount of a nearly saturated lime solution to a definite amount of aluminum sulfate solution. After filtration and washing with water, the gel was transferred to the reaction tube. The gel so used contained a standard amount of Al_2O_3 , together with definite amounts of CaO and SO_3 . The sulfate was mainly CaSO_4 . Varying amounts of water and lime solution were added to give a total volume of 125 ml. In several cases, varying amounts of crystalline $\text{Ca}(\text{OH})_2$ were also added to the mix. In this way, a series of mixes containing standard amounts of Al_2O_3 and SO_3 but varying amounts of CaO were made up. The initial composition of the complex with respect to Al_2O_3 and CaO (exclusive of CaO equivalent to the SO_3 content) is shown in figure 8, along the constant composition line of 0.620 g. Al_2O_3 per 1000 g. of solution. The sulfate content was equivalent to 0.164 g. CaSO_4 per 1000 g. of solution. Another series of mixes was also prepared with a higher content of Al_2O_3 , equivalent to 0.938 g. Al_2O_3 per 1000 g. of solution, but the same amount of SO_3 . For these, alumina gel was precipitated as described above, transferred to the reaction tube, and made up to 62.5 ml. with water. A metastable solution containing CaO and Al_2O_3 was meanwhile prepared by shaking finely powdered " $5\text{CaO} \cdot 3\text{Al}_2\text{O}_3$ " with water (0.250 g. " C_5A_3 ", passing a 300-mesh sieve, with 125 ml. of water for 4 hr. in a Pyrex-glass tube). After filtration in the absence of carbon dioxide, 62.5 ml. of this solution was added to the mix together with sufficient crystalline $\text{Ca}(\text{OH})_2$ to give the required initial composition of the complex. The mixes were in general shaken for 7 days at 25°C . before filtration.

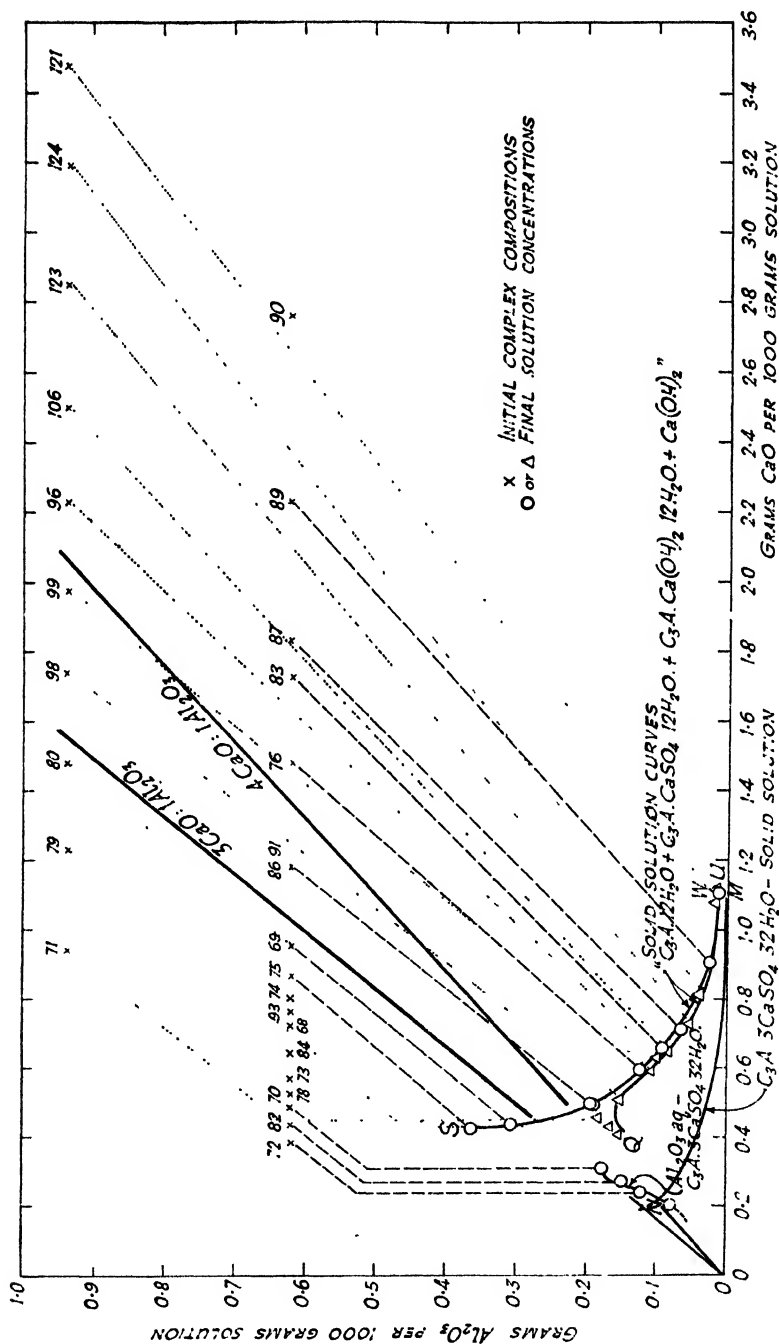


Fig. 8. Quaternary system. Equilibria with alumina gel and solid solution, showing relation between initial complex compositions and final solution concentrations.

Unstable prolongation of boundary curve $\text{Al}_2\text{O}_3\text{aq.}-\text{C}_3\text{A}\cdot 3\text{CaSO}_4\cdot 32\text{H}_2\text{O}(\text{HRL})$:— In figure 3a the boundary curve $\text{Al}_2\text{O}_3\text{aq.}-\text{C}_3\text{A}\cdot 3\text{CaSO}_4\cdot 32\text{H}_2\text{O}$ established in the previous work is shown as the broken line EH, meeting the $\text{C}_3\text{A}\cdot 6\text{H}_2\text{O}-\text{C}_3\text{A}\cdot 3\text{CaSO}_4\cdot 32\text{H}_2\text{O}$ boundary curve GH in the invariant point H ($\text{C}_3\text{A}\cdot 3\text{CaSO}_4\cdot 32\text{H}_2\text{O}-\text{C}_3\text{A}\cdot 6\text{H}_2\text{O}-\text{Al}_2\text{O}_3\text{aq.}$). This curve is of course fundamentally unstable. It has now been traced beyond the point H, the prolongation being given by mixes H72, H82, and H70 in table 6, figure 6, and figure 8. The curve HRL could not be traced further, since at higher lime concentrations than that of the initial H70 mix (0.49 g. CaO per 1000 g. of solution), a hexagonal plate phase also appeared even after short shaking periods (compare similar behavior in the case of crystalline $\text{A}\cdot 3\text{H}_2\text{O}$ at somewhat higher lime concentrations). This prolongation of the $\text{Al}_2\text{O}_3\text{aq.}-\text{C}_3\text{A}\cdot 3\text{CaSO}_4\cdot 32\text{H}_2\text{O}$ boundary curve, as in the case of the equilibria with crystalline $\text{A}\cdot 3\text{H}_2\text{O}$, is characterized by an abrupt increase in the amount of alumina in solution as the CaSO_4 concentration becomes very small. As is to be expected from the greater solubility of the gel, this increase is much greater than with crystalline $\text{A}\cdot 3\text{H}_2\text{O}$, and occurs at rather lower lime concentrations. Neglecting the possibility of adsorption of further lime from solution by the alumina gel phase, the course of the reaction may be represented by the broken lines in figure 8, drawn between the initial complex composition points and final solution concentrations. The lines parallel to the C_3A composition line indicate the extent of $\text{C}_3\text{A}\cdot 3\text{CaSO}_4\cdot 32\text{H}_2\text{O}$ formation, and the vertical line the amount of Al_2O_3 in the gel phase. In so far as lime is adsorbed from solution into the alumina gel phase, the amounts of $\text{C}_3\text{A}\cdot 3\text{CaSO}_4\cdot 32\text{H}_2\text{O}$ and $\text{Al}_2\text{O}_3\text{aq.}$ will be relatively less and greater than that indicated.

Invariant point $\text{Al}_2\text{O}_3\text{aq.}-\text{C}_3\text{A}\cdot 3\text{CaSO}_4\cdot 32\text{H}_2\text{O}-\text{"C}_3\text{A}\cdot \text{CaSO}_4\cdot 12\text{H}_2\text{O}"(\text{R})$

Solid solution boundary curve $\text{Al}_2\text{O}_3\text{aq.}-\text{solid solution}(\text{RSQ})$:— A number of data provide evidence for an invariant point R and solid solution curve RSQ similar to the invariant point R_2 and solid solution curve $\text{R}_2\text{S}_2\text{Q}_2$ found for crystalline $\text{A}\cdot 3\text{H}_2\text{O}(\text{B})$. The data are shown by triangular symbols grouped about the dotted line RSQ in figure 6. They are not tabulated. Examination of mixes of the initial composition of mix H78 (0.52 g. CaO per 1000 g. of solution) showed that there was first rapid solution of part of the alumina gel, followed by rapid precipitation of $\text{C}_3\text{A}\cdot 3\text{CaSO}_4\cdot 32\text{H}_2\text{O}$ and formation of spherulitic clusters of a hexagonal plate phase within alumina gel. It was not possible to determine the refractive index of the hexagonal plate phase, except that it was less than that of the alumina gel (refractive index approximately 1.52-1.53) within which it was embedded. Mix H73, with a slightly higher initial lime content, showed a similar behavior. We have thus in these two mixes some evidence for the existence of an invariant point $\text{Al}_2\text{O}_3\text{aq.}-\text{C}_3\text{A}\cdot 3\text{CaSO}_4\cdot 32\text{H}_2\text{O}-\text{"C}_3\text{A}\cdot \text{CaSO}_4\cdot 12\text{H}_2\text{O}."$ Mixes H84, H68, H93, H74 with increasingly higher initial lime contents gave no $\text{C}_3\text{A}\cdot 3\text{CaSO}_4\cdot 32\text{H}_2\text{O}$, the solid phases present being $\text{Al}_2\text{O}_3\text{aq.}$ and a hexagonal plate phase of refractive indices $\omega = 1.515 \pm 0.003$ and $\epsilon = 1.505 \pm 0.003$. The amount of alumina gel remaining decreased with increase in the initial lime content, and the last two mixes had very little of this phase in the equilibrium mix.

It is clear that these data for the alumina gel equilibria are analogous to those for the invariant point $R_2: \text{A} \cdot 3\text{H}_2\text{O}(\text{B}) - \text{C}_3\text{A} \cdot 3\text{CaSO}_4 \cdot 32\text{H}_2\text{O} - [\text{C}_3\text{A} \cdot \text{CaSO}_4 \cdot 12\text{H}_2\text{O}]$ and solid solution curve $R_2\text{S}_2\text{Q}_2: \text{A} \cdot 3\text{H}_2\text{O}(\text{B}) - [\text{C}_3\text{A} \cdot \text{CaSO}_4 \cdot 12\text{H}_2\text{O} + \text{C}_3\text{A} \cdot \text{Ca}(\text{OH})_2 \cdot 12\text{H}_2\text{O}]$ found for crystalline $\text{A} \cdot 3\text{H}_2\text{O}(\text{B})$. As indicated, it was not found possible to trace the solid solution curve beyond H74 with mixes of the same initial Al_2O_3 content of 0.620 g. Al_2O_3 per 1000 g. of solution, but mixes with the initial Al_2O_3 content of 0.938 g. Al_2O_3 per 1000 g. of solution yielded a group of points H71, H79, and H80 in figures 6, 8, and 12, which appear to form a continuation of this alumina gel-solid solution equilibria. The amount of alumina gel left as a solid phase in these three mixes decreased as the initial amount of lime increased. This is shown in figure 8 by the decrease in the lengths of the vertical dotted tie-lines. As is shown in the next section, the solid solutions formed in equilibrium with lime solutions up to about 0.5 g. CaO per 1000 g. of solution have a $\text{C/A} = 3$ ratio, excluding CaO equivalent to SO_3 present, and this is shown in figure 8 by drawing the H71, H79, H80 tie-lines parallel to the C_3A composition line. The hexagonal plate phase formed had the refractive indices $\omega = 1.515 \pm 0.003$ and $\epsilon = 1.500 \pm 0.003$. In spite of the constancy of the refractive index, it is clear from figure 8 (increasing lengths of tie-lines parallel to C_3A composition line) that this phase is increasingly rich (in the ratio $\text{C/A} = 3$) in CaO and Al_2O_3 as compared with CaSO_4 . Considering the data as a whole it may be tentatively concluded that they are based on a somewhat indefinite curve $\text{RSQ}: \text{Al}_2\text{O}_3\text{aq.} - [\text{C}_3\text{A} \cdot \text{CaSO}_4 \cdot 12\text{H}_2\text{O} + \text{C}_3\text{A} \cdot 12\text{H}_2\text{O}]$ solid solution. The invariant point R in the quaternary system has only been roughly located. The curve lies above the curve $\text{HRL}: \text{Al}_2\text{O}_3\text{aq.} - \text{C}_3\text{A} \cdot 3\text{CaSO}_4 \cdot 32\text{H}_2\text{O}$ and apparently sweeps upward to S and then downward again through points H71, H79, and H80. Since the solid solutions at H71, H79, and H80 are increasingly rich—in that order—in $\text{C}_3\text{Aaq.}$, it seems necessary to conclude that the solid solution along this curve gradually approaches the composition of $\text{C}_3\text{Aaq.}$ and that eventually we have the solid phases $\text{Al}_2\text{O}_3\text{aq.}$ and $\text{C}_3\text{Aaq.}$, i.e., the curve continues to an invariant point T: $\text{Al}_2\text{O}_3\text{aq.} - \text{C}_3\text{A} \cdot 12\text{H}_2\text{O}$ in the ternary system. This point has of course not been reached. While it is possible that there may be an approach to a $\text{C}_3\text{A} \cdot \text{CaSO}_4 \cdot 12\text{H}_2\text{O}$ composition at R, it is clear from the refractive index values that at H84 there is a considerable modification in the solid solution composition. Accepting a C_3A ratio in the solid solution, the composition can be calculated from the known CaO and CaSO_4 contents in terms of $\text{C}_3\text{A} \cdot \text{CaSO}_4 \cdot 12\text{H}_2\text{O}$ and $\text{C}_3\text{A} \cdot 12\text{H}_2\text{O}$, and corresponds to 0.58 mole $\text{C}_3\text{A} \cdot 12\text{H}_2\text{O}$: 1 mole $\text{C}_3\text{A} \cdot \text{CaSO}_4 \cdot 12\text{H}_2\text{O}$. For comparison, at H80 the solid solution composition corresponds to 4.3 moles $\text{C}_3\text{A} \cdot 12\text{H}_2\text{O}$: 1 mole $\text{C}_3\text{A} \cdot \text{CaSO}_4 \cdot 12\text{H}_2\text{O}$.

It is of interest to note that in mixes H79 and H80, where crystalline $\text{Ca}(\text{OH})_2$ was added to an unstable calcium aluminate solution, pseudomorphs of the original $\text{Ca}(\text{OH})_2$ prisms were formed, showing striations perpendicular to the c -axis, and consisting of hexagonal plates with the refractive indices stated packed face to face. It is thus evident that the original $\text{Ca}(\text{OH})_2$ crystal under these conditions takes up Al_2O_3 and CaSO_4 from solution.

Solid solution surface equilibria

The conditions under which a solid solution area or surface can arise in the isothermal quaternary system have been indicated in the section on phase-rule equilibria. It now remains to describe various equilibria involving only one solid phase—the solid solution (and which therefore trace paths across such a surface)—and one involving both solid solution and $C_3A \cdot 3CaSO_4 \cdot 32H_2O$, which therefore marks a boundary curve to the solid solution area. The following curves have been traced:

- (1) Solid solution curve (SW)
- (2) Solid solution curve (QW)
- (3) Solid solution curve I
- (4) Solid solution curve II
- (5) Solid solution curve III
- (6) Boundary curve: $C_3A \cdot 3CaSO_4 \cdot 32H_2O$ —solid solution (RM)

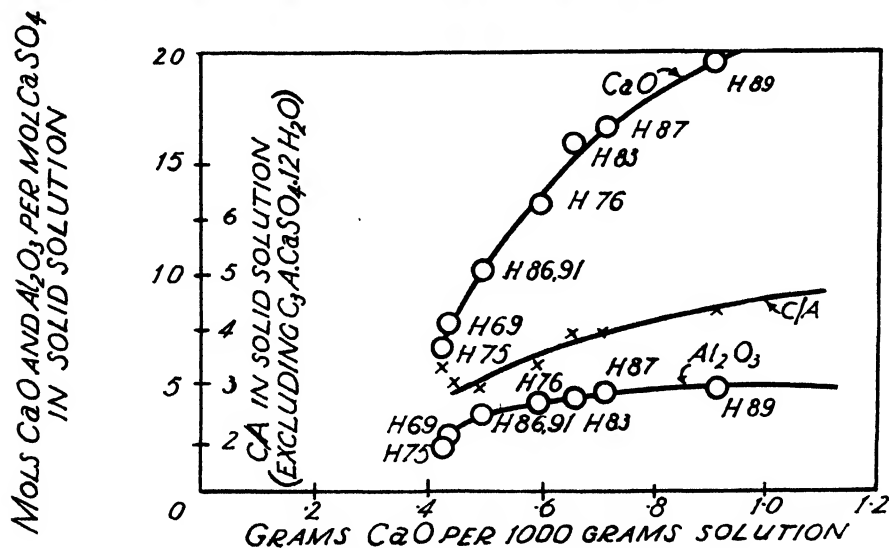
The data are plotted as follows: curve (1) in figures 6 and 8; curve (2) in figures 8 and 10; curves (2), (3), (4), (5), and (6) in figure 10.

Solid solution curve SW (solid solution of " $C_3A \cdot 12H_2O + C_3A \cdot CaSO_4 \cdot 12H_2O + C_3A \cdot Ca(OH)_2 \cdot 12H_2O + Ca(OH)_2$ ") :—Continuing the series of mixes with the initial complex composition corresponding to 0.620 g. Al_2O_3 and 0.164 g. $CaSO_4$ per 1000 g. of solution with increasing lime contents, it was found that at mix H75 there was an abrupt break in the equilibria, marked by the disappearance of the Al_2O_3 aq. solid phase, and the appearance of the solid solution curve SW. This curve is defined by mix H75 (initial lime content = 0.875 g. CaO per 1000 g. of solution) and other H mixes, with the same initial content of Al_2O_3 and $CaSO_4$, but containing higher initial CaO contents in the complex. These gave only a hexagonal plate phase, except for mix H90 which also contained crystalline $Ca(OH)_2$ and therefore marks the upper limit of the curve. In mixes H75, H69, H91, H86, H76, H83 the plates had the refractive indices $\omega = 1.515 \pm 0.003$ and $\epsilon = 1.500 \pm 0.003$, rising in mixes H87, H89, H90 to $\omega = 1.525 \pm 0.003$ and $\epsilon = 1.500 \pm 0.003$. All mixes except H91 were shaken for 7 days. Mix H91, identical in initial composition with mix H86, was shaken for 1 day only and gave the same solution composition as after 7 days' shaking. Equilibrium is thus reached rapidly. Data are given in table 6. It will be seen from figure 8 that the broken lines joining initial complex composition points to final solution composition points are for mixes H75, H69, H91, and H86 essentially parallel to the C_3A composition line, and hence the solid phase must here be of the general composition $C_3A \cdot xCaSO_4$ aq. It may be considered as a solid solution of $C_3A \cdot CaSO_4 \cdot 12H_2O$ and $C_3A \cdot 12H_2O$, or $C_3A \cdot CaSO_4 \cdot 12H_2O$ together with $C_2A \cdot 8H_2O$ and $C_4A \cdot 13H_2O$ in equimolar proportions. The gradual change in slope of the composition tie-lines to parallelism with the C_4A composition line at H89 shows a gradual change in the solid phase composition to one which may be considered as a solid solution of $C_3A \cdot CaSO_4 \cdot 12H_2O$, $C_3A \cdot Ca(OH)_2 \cdot 12H_2O$, and $Ca(OH)_2$, the last-named entering with CaO concentrations above H89. The calculated CaO: $Al_2O_3 \cdot CaSO_4$ molar ratios (from initial complex compositions and final solution concentrations) are shown in figure 9 plotted against the lime

TABLE 6

*Alumina gel and solid solution equilibria*Boundary curve HRL: Al_2O_3 gel- $\text{C}_3\text{A} \cdot 3\text{CaSO}_4 \cdot 32\text{H}_2\text{O}$ Curves SW and QU: solid solution " $\text{C}_3\text{A} \cdot 12\text{H}_2\text{O} + \text{C}_3\text{A} \cdot \text{CaSO}_4 \cdot 12\text{H}_2\text{O} + \text{C}_3\text{A} \cdot \text{Ca}(\text{OH})_2 \cdot 12\text{H}_2\text{O} + \text{Ca}(\text{OH})_2$ "

NO.	TIME SHAKEN	GRAMS PER 1000 G. OF SOLUTION			NO.	TIME SHAKEN	GRAMS PER 1000 G. OF SOLUTION		
		CaO	Al ₂ O ₃	CaSO ₄			CaO	Al ₂ O ₃	CaSO ₄
Boundary curve HRL					Curve SW				
	days					days			
H38.	7	0.208	0.080	0.013	H75	7	0.426	0.365	0.001
H72	7	0.241	0.124	0.008	H69	7	0.435	0.309	0.010
H82	7	0.270	0.150	0.0045	H91	1	0.495	0.194	0.0035
H70	7	0.312	0.179	0.0065	H86	7	0.493	0.189	0.002
Curve QU					H76	7	0.592	0.123	0.001
H98	7	0.511	0.152	0.001	H83	7	0.653	0.093	0.0035
H99	7	0.592	0.112	0.001	H87	7	0.709	0.0635	0.001
H96	7	0.634	0.101	0.0025	H89	7	0.907	0.026	0.0025
H106	3	0.649	0.082		H90	7	1.106	0.012	0.0035
H123	7	0.730	0.052						
H124	7	0.814	0.038						
H121	7	1.08	0.014						
H122	7	1.12	0.011						

Fig. 9a. $\text{CaO}:\text{Al}_2\text{O}_3:\text{CaSO}_4$ along solid solution curve SW

concentration of the solution. Since mix H90 contained crystalline $\text{Ca}(\text{OH})_2$, it was not possible to calculate directly the $\text{CaO}:\text{Al}_2\text{O}_3:\text{CaSO}_4$ ratios in the solid solution in equilibrium with $\text{Ca}(\text{OH})_2$ and solution, but these may be obtained

by extrapolation of the curves in figure 9. At a lime concentration of 1.1 g. CaO per 1000 g. of solution (H90) the ratios are found to be 21.5:4.8:1, respectively, giving the molar ratios $C_2A \cdot CaSO_4 \cdot 12H_2O : C_2A \cdot Ca(OH)_2 \cdot 12H_2O : Ca(OH)_2 = 1:3.8:3.3$. In figure 9a are also plotted the C/A ratios, excluding $C_2A \cdot CaSO_4$, in the solid solution. It is seen that the ratios vary from about 3 to 4.7.

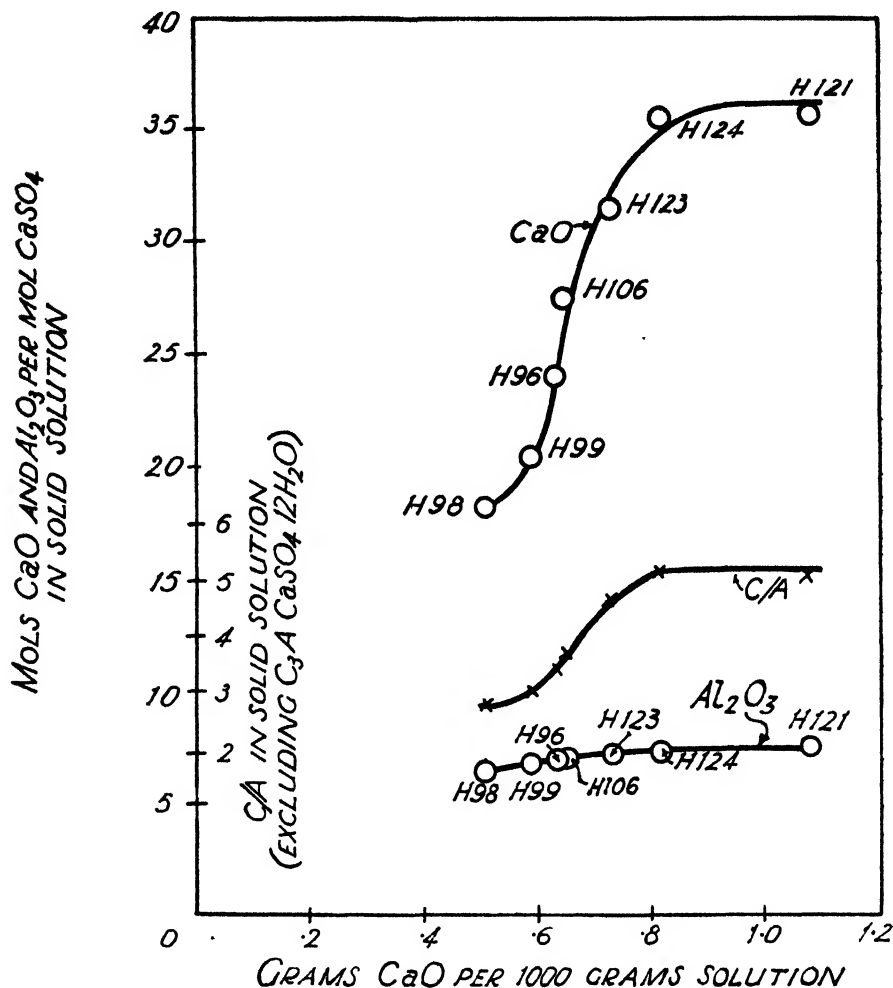


FIG. 9b. $CaO:Al_2O_3:CaSO_4$ along solid solution curve QU

Solid solution curve QU:—A second and similar solid solution curve QU was obtained by continuing the second series of mixes containing the higher content of alumina (and of which mixes H71, H79 and H80 form a part). For the sake of clarity the data (table 6) are plotted in figure 10 along the broken line QU. Figure 10 should be compared with figure 6. Mixes H98, H99, and H96 showed only a hexagonal plate phase of refractive indices $\omega = 1.515$ and $\epsilon = 1.500$. In

mixes H106 and H123 the indices had risen to $\omega = 1.520$, $\epsilon = 1.500$, and in H124 and H121 to $\omega = 1.525$, $\epsilon = 1.500-1.505$. In H122 $\text{Ca}(\text{OH})_2$ remained as second solid phase. Pseudomorphs of the original $\text{Ca}(\text{OH})_2$ prisms, as mentioned previously, were formed throughout this series. Reference to figure 8 again shows, from the increasing slopes of the tie-lines, that the C/A ratios (exclusive of $\text{C}_3\text{A} \cdot \text{CaSO}_4$) increase from about 3 to greater than 4, and figure 9b, comparable with figure 9a, shows that the upper limit of this ratio is approximately 5.

In the previous section dealing with the curve RSQ, it was stated in considering the composition of the solid solutions at H71, H79, H80, that these have a C/A = 3 ratio, excluding CaO equivalent to the SO_3 content. We can now consider the evidence which figure 8 affords for this statement. The mixes H72,

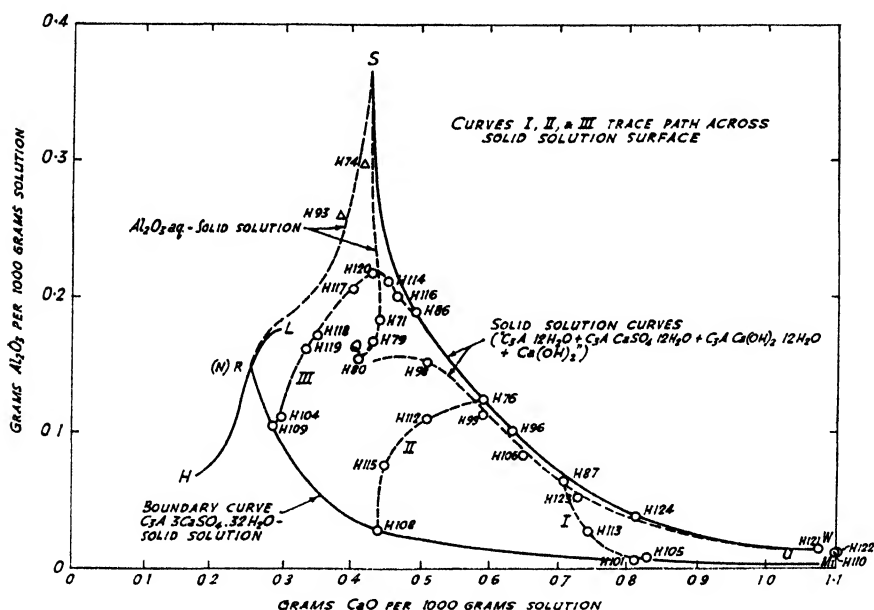


FIG. 10. Quaternary system: equilibria in solid solution surface

H82, and H70 relate to the $\text{Al}_2\text{O}_3\text{aq} \cdot \text{C}_3\text{A} \cdot 3\text{CaSO}_4 \cdot 32\text{H}_2\text{O}$ curve HRL. Since the second solid phase is $\text{C}_3\text{A} \cdot 3\text{CaSO}_4 \cdot 32\text{H}_2\text{O}$, a compound containing C and A in the C_3A ratio, it is evident that the tie-lines corresponding to the formation of this phase must be parallel to the C_3A composition line. In the same series of mixes we have H75, H69, H86, H91, in which the tie-lines directly joining initial mix compositions and final solution concentrations are substantially parallel to the C_3A composition line. Since here there is only one solid phase—the solid solution—it follows that the C and A present in this solid solution must be in the C/A = 3 ratio. As the initial lime concentration of the mixes increases along the curve SW, so the C/A ratio increases from 3 to greater than 4. This is shown in figure 8 by the divergence of the tie-lines corresponding to curve SW from parallelism to the C_3A composition line. It is hardly probable that after

the C/A ratio decreases from a value of greater than 4 to 3 throughout the curve WS, the C/A ratio should increase again at initial lime concentrations less than that of H75. It is concluded that the C/A ratio in those solid solutions formed between H75, and H70 of figure 8 is either 3, or possibly varies, as the initial lime content decreases, from 3 to less than 3, i.e., there is a possibility that $C_2A \cdot 8H_2O$ enters into the solid solution. Substantial confirmation of this conclusion is given by the second series of mixes (to which H71, H79, H80 belong) shown in figure 8, using a higher initial Al_2O_3 content. It is self-evident from the tie-lines of figure 8 that, for example, in the solid solutions of mixes H124 and H121 the C/A ratio in the solid phase is appreciably greater than 4, and that as the initial lime content decreases, so does the ratio C/A in the solid solution until at H98 and H99 the ratio is approximately 3. The points H80, H79, and H71 form a continuation of this series. Moreover, the final equilibrium lime concentrations for these mixes are close to those for mixes H86, H69, and H75 of the first series. It seems reasonable to conclude therefore that the C/A ratio in mixes H80, H79, and H71 is also 3. As suggested above, it is possible that as R is approached the ratio may fall below 3.

The solid solution curves I, II, III

Boundary curve $C_3A \cdot 3CaSO_4 \cdot 32H_2O$ -solid solution (RM):—Before proceeding to describe these curves, it will be well to recall the solid solution equilibria so far dealt with. They are:

Al_2O_3 aq.-solid solution (RSQ)

Crystalline $A \cdot 3H_2O$ (B)-solid solution ($R_2S_2Q_2$)

Solid solution curve SW

Solid solution curve QU

It seems necessary to conclude that the curves RSQ and $R_2S_2Q_2$ mark limits, on the hydrated alumina side, to the existence of a solid solution surface in the quaternary system. They may be regarded as unstable and metastable limits, respectively. The curves SW and QU must be curves across the solid solution surface from the curve RSQ to a limiting curve for solid solution- $Ca(OH)_2$ in the high lime region. It seems likely that SW possesses an additional significance as representing probably the maximum Al_2O_3 in solution in equilibrium with solid solution. From the foregoing it follows that there must be a quaternary boundary curve to the solid solution area passing through R and R_2 and forming a lower limit to the solid solution equilibria. The curve will be that for $C_3A \cdot 3CaSO_4 \cdot 32H_2O$ -solid solution (RM).

It has been found previously by the writer (8) that the compound $C_2A \cdot 8H_2O$, which occurs as a metastable phase in the ternary system, takes up $CaSO_4$ from a calcium sulfate solution to give a solid solution phase of composition $CaO : Al_2O_3 : CaSO_4 = 2 : 0.6-0.7 : 0.26$ throughout a range of concentrations. Above a certain $CaSO_4$ concentration, $C_3A \cdot 3CaSO_4 \cdot 32H_2O$ is formed. The solid solution whose average composition may be expressed by the ratio $CaO : Al_2O_3 : CaSO_4 = 7.7 : 2.5 : 1$ approximates to a molecular composition of 1.5 moles $C_3A : 1$ mole $C_2A \cdot CaSO_4$ and may be regarded as a solid solution of $C_3A \cdot 12H_2O$ and $C_2A \cdot CaSO_4 \cdot 12H_2O$. It has been previously stated (8) that along the metastable

boundary curve MN (figures 9 and 11(b) of previous paper) $\text{C}_3\text{A} \cdot 3\text{CaSO}_4 \cdot 32\text{H}_2\text{O}$ —"C₃A·8H₂O," we are dealing not with pure $\text{C}_3\text{A} \cdot 8\text{H}_2\text{O}$, but with a solid solution. Evidently the curve MN is a boundary curve for a solid solution field in the quaternary system. The invariant point N, which is that for $\text{C}_3\text{A} \cdot 3\text{CaSO}_4 \cdot 32\text{H}_2\text{O}$, $\text{Al}_2\text{O}_3\text{aq.}$ and the solid solution, is here tentatively identified with the invariant point R (only roughly located) of the present work. The position of the curve MN is shown (in projection) in figure 8. M is the invariant point for

TABLE 7
Solid solution equilibria
Equilibria across solid solution area SWMR

NO.	$\text{CaSO}_4 \cdot 2\text{H}_2\text{O}$ ADDED TO INITIAL MIX	REFRACTIVE INDICES OF PLATE PHASE		GRAMS PER 1000 G. OF SOLUTION			TIME SHAKEN
		(± 0.003)	(± 0.003)	CaO	Al_2O_3	CaSO_4	
	<i>grams</i>						<i>days</i>
Curve I, figure 10							
H87		1.526	1.498	0.709	0.0635	0.001	7
H113	0.050	1.514	1.491	0.745	0.0265	Nil	3
H101.	0.100	1.503	1.488	0.812	0.05		7
H105.	0.150	1.503	1.488	0.829	0.0075	0.0015	7
Curve II, figure 10							
H76		1.515	1.500	0.592	0.123	0.001	7
H112	0.050	1.507	1.491	0.510	0.109	0.0015	3
H115.	0.075	1.510	1.490	0.449	0.075	0.0015	3
H108	0.100	1.507	1.490	0.440	0.028	0.005	3
Curve III, figure 10							
H86		1.515	1.500	0.493	0.189	0.002	7
H116	0.015	1.515	1.500	0.467	0.200	0.003	4
H114	0.025	1.512	1.492	0.454	0.211	0.005	3
H120	0.030	1.510	1.493	0.432	0.217	0.0015	3
H117	0.040	1.510	1.495	0.405	0.205	0.0015	3
H118	0.050	1.508	1.492	0.353	0.172	0.001	3
H119	0.050	1.508	1.490	0.337	0.162		3
(Repeat H118)							
H104	0.100	1.503	1.490	0.302	0.111	0.003	7
H109	0.100	1.503	1.488	0.289	0.104	0.0035	3
(Repeat H104)							

$\text{C}_3\text{A} \cdot 3\text{CaSO}_4 \cdot 32\text{H}_2\text{O}$, $\text{Ca}(\text{OH})_2$, and solid solution. The solid solution surface in the quaternary system is to be visualized as extending upwards from the boundary curve MN(R), keeping very close to the $\text{CaO}-\text{Al}_2\text{O}_3-\text{H}_2\text{O}$ face, passing through SW, which is simply a path across the surface and then curling downward to pass through QU to a solid solution curve in the ternary system (VT of figure 11).

Confirmation of the existence and extent of the area SWMR has been secured by tracing the equilibria obtained by starting at selected points on the curve SW

and adding increasing amounts of $\text{CaSO}_4 \cdot 2\text{H}_2\text{O}$ crystals, crossing the area SWMR, and ending on the solid solution- $\text{C}_3\text{A} \cdot 3\text{CaSO}_4 \cdot 32\text{H}_2\text{O}$ boundary curve. Thus to the equilibrium mix represented by point H76 (figure 10, curve II), varying amounts of $\text{CaSO}_4 \cdot 2\text{H}_2\text{O}$ were added and the resulting equilibria found up to the point where $\text{C}_3\text{A} \cdot 3\text{CaSO}_4 \cdot 32\text{H}_2\text{O}$ appeared as a second solid phase. The three curves I, II, and III of figure 10 have thus been traced. Results are given in table 7, which includes the refractive indices found for the hexagonal plate phase. The final mixes in each set, H105, H108, H104 (and H109), contained $\text{C}_3\text{A} \cdot 3\text{CaSO}_4 \cdot 32\text{H}_2\text{O}$ as well as the plate phase. The curve RM of figure 10 has been drawn through the last-named set of points. Calculation, so far as the data permit, of the changing solid solution compositions along the curves I, II, III indicate that the CaO and Al_2O_3 ratios with respect to CaSO_4 are rapidly falling from the high values of curve WS to values which tend to approach 3 and 1 respectively, i.e., the solid solution tends to approach the $\text{C}_3\text{A} \cdot \text{CaSO}_4\text{aq.}$ composition. Thus for mixes H87, H113, and H101 along curve I, the ratios $\text{CaO}:\text{Al}_2\text{O}_3:\text{CaSO}_4$ are approximately 16.6:4.5:1, 5.5:1.7:1, and 3.1:1:1 corresponding, respectively, to $3\text{C}_4\text{A}:\text{1.5C}_3\text{A}:\text{1CaSO}_4$, $0.4\text{C}_4\text{A}:\text{0.3C}_3\text{A}:\text{1CaSO}_4$ and approximately $\text{C}_3\text{A} \cdot \text{CaSO}_4$. The data along curves II and III do not permit a close approach to the curve MR, but it may be noted that the ratios have fallen for curve II from 13.2:4:1 (H76) to 3.9:1.1:1 (H115) and for curve III from 10.1:3.5:1 (H86) to 4.2:1.2:1 (H119).

The space figure and the basal projection:—To the space figure for the quaternary system previously determined must now be added the various additional stable, metastable, and unstable curves established in the present work. For photographs of a space model of the equilibrium relations already established reference should be made to the previous paper. The various boundary curves and invariant points involved in the system are listed below. Since the equilibria with crystalline $\text{A} \cdot 3\text{H}_2\text{O}(\text{B})$ will be closest to those for the most stable structure of hydrated alumina (i.e., the gibbsite structure) they are in the following list, where this is appropriate, termed stable. Invariant point compositions are collected together in table 8.

(a) Ternary system $\text{H}_2\text{O}-(\text{CaO})_3-\text{Al}_2\text{O}_3$ (figure 2):

(i) Boundary curves:

$\text{H}_2\text{O}-\text{D}_2 = \text{A} \cdot 3\text{H}_2\text{O}(\text{B})$ (stable)

$\text{H}_2\text{O}-\text{D} = \text{Al}_2\text{O}_3\text{aq.}$ (unstable)

$\text{D}_2\text{P} = \text{A} \cdot 3\text{H}_2\text{O}(\text{B})$ (metastable prolongation of $\text{H}_2\text{O}-\text{D}_2$)

$\text{D}_2\text{C} = \text{C}_3\text{A} \cdot 6\text{H}_2\text{O}$ (stable)

$\text{D}_2\text{D} = \text{C}_3\text{A} \cdot 6\text{H}_2\text{O}$ (metastable prolongation of D_2C)

(ii) Invariant points:

$\text{D}_2 = \text{A} \cdot 3\text{H}_2\text{O}(\text{B})-\text{C}_3\text{A} \cdot 6\text{H}_2\text{O}$ (stable)

$\text{D} = \text{Al}_2\text{O}_3\text{aq.}-\text{C}_3\text{A} \cdot 6\text{H}_2\text{O}$ (unstable)

$\text{C} = \text{solubility of crystalline } \text{Ca}(\text{OH})_2 \text{ in water}$ (stable)

(b) Ternary system $\text{H}_2\text{O}-(\text{CaO})_3-(\text{CaSO}_4)_3$ (figure 3a; see also figure 3 of previous paper (8))

(i) Boundary curves:

$\text{CB} = \text{crystalline } \text{Ca}(\text{OH})_2$ (stable)

$\text{BA} = \text{CaSO}_4 \cdot 2\text{H}_2\text{O}$ (stable)

TABLE 8
Invariant point compositions

	INVARIANT POINT	GRAM-MOLES $\times 10^4$ PER 1000 G. SOLUTION			TOTAL GRAM- MOLES \times 10^4 PER 1000 G. OF SOLUTION	$(\text{CaSO}_4)_2$ mole per cent	$(\text{CaO})_2$ mole per cent	Al_2O_3 mole per cent	TOTAL SALTS IN SOLUTION mole per cent
		$(\text{CaSO}_4)_2$	$(\text{CaO})_2$	Al_2O_3					
D ₂ ..	$\text{A} \cdot 3\text{H}_2\text{O}(\text{B})-\text{C}_3\text{A} \cdot 6\text{H}_2\text{O}$		15.8	2.2	18.0		87.8	12.2	0.00324
E ₂ ..	$\text{CaSO}_4 \cdot 2\text{H}_2\text{O}-\text{A} \cdot 3\text{H}_2\text{O}(\text{B})- \text{C}_3\text{A} \cdot 3\text{CaSO}_4 \cdot 32\text{H}_2\text{O}$	49.9	2.25	0.25	52.4	95.3	4.3	0.5	0.00945
E ₁ ...	$\text{CaSO}_4 \cdot 2\text{H}_2\text{O}-\text{A} \cdot 3\text{H}_2\text{O}(\text{A})- \text{C}_3\text{A} \cdot 3\text{CaSO}_4 \cdot 32\text{H}_2\text{O}$	50.3	1.7	0.15	52.15	96.5	3.3	0.3	0.00940
E..	$\text{CaSO}_4 \cdot 2\text{H}_2\text{O}-\text{Al}_2\text{O}_3\text{aq}- \text{C}_3\text{A} \cdot 3\text{CaSO}_4 \cdot 32\text{H}_2\text{O}$	52.5	0.45	0.6	53.6	98.1	0.85	1.15	0.00966
F..	$\text{CaSO}_4 \cdot 2\text{H}_2\text{O}-\text{Ca}(\text{OH})_2- \text{C}_3\text{A} \cdot 3\text{CaSO}_4 \cdot 32\text{H}_2\text{O}$	41.1	64.1	0.6	105.8	38.8	60.6	0.6	0.01907
G...	$\text{Ca}(\text{OH})_2-\text{C}_3\text{A} \cdot 6\text{H}_2\text{O}- \text{C}_3\text{A} \cdot 3\text{CaSO}_4 \cdot 32\text{H}_2\text{O}$	0.6	63.3	0.1	64.0	0.95	99.0	0.15	0.01153
H ₂	$\text{C}_3\text{A} \cdot 3\text{CaSO}_4 \cdot 32\text{H}_2\text{O}- \text{C}_3\text{A} \cdot 6\text{H}_2\text{O}-\text{A} \cdot 3\text{H}_2\text{O}(\text{B})$	1.25	10.4	0.9	12.55	10.0	82.8	7.2	0.00226
H ₁	$\text{C}_3\text{A} \cdot 3\text{CaSO}_4 \cdot 32\text{H}_2\text{O}- \text{C}_3\text{A} \cdot 6\text{H}_2\text{O}-\text{A} \cdot 3\text{H}_2\text{O}(\text{A})$	1.2	9.05	1.6	11.85	10.2	76.3	13.5	0.00213
H	$\text{C}_3\text{A} \cdot 3\text{CaSO}_4 \cdot 32\text{H}_2\text{O}- \text{C}_3\text{A} \cdot 6\text{H}_2\text{O}-\text{Al}_2\text{O}_3\text{aq}$	0.3	11.9	7.3	19.3	1.55	61.2	37.2	0.00348
R ₂	$\text{C}_3\text{A} \cdot 3\text{CaSO}_4 \cdot 32\text{H}_2\text{O}-\text{C}_3\text{A} \cdot \text{CaSO}_4 \cdot 12\text{H}_2\text{O}-\text{A} \cdot 3\text{H}_2\text{O}(\text{B})$	0.05	27.2	3.65	30.9	0.15	88.2	11.8	0.00557

TABLE 9
Refractive indices of pure compounds

COMPOUND	SYSTEM	REFRACTIVE INDICES		
		α_e	β	γ_w
$\gamma\text{-Al}_2\text{O}_3 \cdot 3\text{H}_2\text{O}$ (gibbsite)	Monoclinic	1.566	1.566	1.587
$\text{CaSO}_4 \cdot 2\text{H}_2\text{O}$	Monoclinic	1.521	1.523	1.530
$\text{Ca}(\text{OH})_2$	Hexagonal	1.545		1.574
$\text{C}_3\text{A} \cdot 3\text{CaSO}_4 \cdot 32\text{H}_2\text{O}$	Hexagonal	1.458		1.464
$\text{C}_3\text{A} \cdot \text{CaSO}_4 \cdot 12\text{H}_2\text{O}$	Hexagonal	1.488		1.504
$\alpha\text{-C}_3\text{A} \cdot 12\text{-}13\text{H}_2\text{O}$	Pseudo (?) hexagonal	1.521		1.536
$\text{C}_3\text{A} \cdot 11\text{-}12\text{H}_2\text{O}$	Hexagonal	1.506		1.529
$\text{C}_3\text{A} \cdot 8\text{H}_2\text{O}$	Hexagonal	1.505		1.520

- (ii) Invariant points:
 B = crystalline $\text{Ca}(\text{OH})_2\text{-CaSO}_4\cdot 2\text{H}_2\text{O}$ (stable)
 A = solubility of $\text{CaSO}_4\cdot 2\text{H}_2\text{O}$ in water (stable)
 C = solubility of crystalline $\text{Ca}(\text{OH})_2$ in water (stable)
- (c) Ternary system $\text{H}_2\text{O}-(\text{CaSO}_4)_2\text{-Al}_2(\text{SO}_4)_3$
 (i) Boundary curve:
 I = $\text{CaSO}_4\cdot 2\text{H}_2\text{O}$ (stable)
 (ii) Invariant point:
 A = solubility of $\text{CaSO}_4\cdot 2\text{H}_2\text{O}$ in water (stable)
- (d) Quaternary system $\text{H}_2\text{O}-(\text{CaO})_3\text{-Al}_2\text{O}_3\text{-Al}_2(\text{SO}_4)_3\text{-(CaSO}_4)_3$ (figure 3a, 3b, 3c, 4a, 4b, 6)
 (i) Boundary curves:
 $\text{J}_2\text{E}_2 = \text{CaSO}_4\cdot 2\text{H}_2\text{O-A}\cdot 3\text{H}_2\text{O(B)}$ (stable) (figures 3a, 3b)
 $\text{JE} = \text{CaSO}_4\cdot 2\text{H}_2\text{O-Al}_2\text{O}_3\text{aq.}$ (unstable) (figures 3a, 3b)
 $\text{E}_2\text{H}_2 = \text{A}\cdot 3\text{H}_2\text{O(B)-C}_3\text{A}\cdot 3\text{CaSO}_4\cdot 32\text{H}_2\text{O}$ (stable) (figures 3a, 4b)
 $\text{H}_2\text{R}_2\text{L}_2 = \text{A}\cdot 3\text{H}_2\text{O(B)-C}_3\text{A}\cdot 3\text{CaSO}_4\cdot 32\text{H}_2\text{O}$ (metastable prolongation of E_2H_2) (figures 3a, 3c, 6)
 $\text{E}_1\text{H}_1 = \text{A}\cdot 3\text{H}_2\text{O(A)-C}_3\text{A}\cdot 3\text{CaSO}_4\cdot 32\text{H}_2\text{O}$ (metastable) (figures 3a, 4a)
 $\text{EH} = \text{Al}_2\text{O}_3\text{aq.-C}_3\text{A}\cdot 3\text{CaSO}_4\cdot 32\text{H}_2\text{O}$ (unstable) (figure 3a)
 $\text{HRL} = \text{Al}_2\text{O}_3\text{aq.-C}_3\text{A}\cdot 3\text{CaSO}_4\cdot 32\text{H}_2\text{O}$ (unstable prolongation of EH) (figure 6)
 $\text{FE}_2 = \text{CaSO}_4\cdot 2\text{H}_2\text{O-C}_3\text{A}\cdot 3\text{CaSO}_4\cdot 32\text{H}_2\text{O}$ (stable) (figure 3a)
 $\text{E}_2\text{E} = \text{CaSO}_4\cdot 2\text{H}_2\text{O-C}_3\text{A}\cdot 3\text{CaSO}_4\cdot 32\text{H}_2\text{O}$ (metastable prolongation of FE_2) (figures 3a, 3b)
 $\text{BF} = \text{CaSO}_4\cdot 2\text{H}_2\text{O-Ca}(\text{OH})_2$ (stable) (figure 3a)
 $\text{FG} = \text{Ca}(\text{OH})_2\text{-C}_3\text{A}\cdot 3\text{CaSO}_4\cdot 32\text{H}_2\text{O}$ (stable) (figures 3a, 3c)
 $\text{GC} = \text{Ca}(\text{OH})_2\text{-C}_3\text{A}\cdot 6\text{H}_2\text{O}$ (stable) (figures 3a, 3c)
 $\text{GH}_2 = \text{C}_3\text{A}\cdot 6\text{H}_2\text{O-C}_3\text{A}\cdot 3\text{CaSO}_4\cdot 32\text{H}_2\text{O}$ (stable) (figure 3a)
 $\text{H}_2\text{H} = \text{C}_3\text{A}\cdot 6\text{H}_2\text{O-C}_3\text{A}\cdot 3\text{CaSO}_4\cdot 32\text{H}_2\text{O}$ (metastable prolongation of GH_2 (figure 3a))
 $\text{H}_2\text{D}_2 = \text{C}_3\text{A}\cdot 6\text{H}_2\text{O-A}\cdot 3\text{H}_2\text{O(B)}$ (stable) (figures 3a, 3c)
 $\text{HD} = \text{C}_3\text{A}\cdot 6\text{H}_2\text{O-Al}_2\text{O}_3\text{aq.}$ (unstable) (figure 3a)
- (ii) Invariant points:
 $\text{E}_2 = \text{CaSO}_4\cdot 2\text{H}_2\text{O-A}\cdot 3\text{H}_2\text{O(B)-C}_3\text{A}\cdot 3\text{CaSO}_4\cdot 32\text{H}_2\text{O}$ (stable) (figures 3a, 3b)
 $\text{E}_1 = \text{CaSO}_4\cdot 2\text{H}_2\text{O-A}\cdot 3\text{H}_2\text{O(A)-C}_3\text{A}\cdot 3\text{CaSO}_4\cdot 32\text{H}_2\text{O}$ (metastable) (figures 3a, 3b)
 $\text{E} = \text{CaSO}_4\cdot 2\text{H}_2\text{O-Al}_2\text{O}_3\text{aq.-C}_3\text{A}\cdot 3\text{CaSO}_4\cdot 32\text{H}_2\text{O}$ (unstable) (figures 3a, 3b)
 $\text{F} = \text{CaSO}_4\cdot 2\text{H}_2\text{O-Ca}(\text{OH})_2\text{-C}_3\text{A}\cdot 3\text{CaSO}_4\cdot 32\text{H}_2\text{O}$ (stable) (figure 3a)
 $\text{G} = \text{Ca}(\text{OH})_2\text{-C}_3\text{A}\cdot 6\text{H}_2\text{O-C}_3\text{A}\cdot 3\text{CaSO}_4\cdot 32\text{H}_2\text{O}$ (stable) (figures 3a, 3c)
 $\text{H}_2 = \text{C}_3\text{A}\cdot 3\text{CaSO}_4\cdot 32\text{H}_2\text{O-C}_3\text{A}\cdot 6\text{H}_2\text{O-A}\cdot 3\text{H}_2\text{O(B)}$ (stable) (figures 3a, 4b)
 $\text{H}_1 = \text{C}_3\text{A}\cdot 3\text{CaSO}_4\cdot 32\text{H}_2\text{O-C}_3\text{A}\cdot 6\text{H}_2\text{O-A}\cdot 3\text{H}_2\text{O(A)}$ (metastable) (figures 3a, 4a)
 $\text{H} = \text{C}_3\text{A}\cdot 3\text{CaSO}_4\cdot 32\text{H}_2\text{O-C}_3\text{A}\cdot 6\text{H}_2\text{O-Al}_2\text{O}_3\text{aq.}$ (unstable) (figure 3a)

(e) Solid solution area in quaternary system:

(i) Boundary curves:

RSQ = $\text{Al}_2\text{O}_3\text{aq.}$ -solid solution (unstable) (figures 6, 10, 11) $\text{R}_2\text{S}_2\text{Q}_2 = \text{A} \cdot 3\text{H}_2\text{O(B)}$ -solid solution (metastable) (figures 3c, 6, 11)MWUV = Ca(OH)_2 -solid solution (metastable) (figure 11) $\text{MR(N)} = \text{C}_3\text{A} \cdot 3\text{CaSO}_4 \cdot 32\text{H}_2\text{O}$ -solid solution (metastable) (figures 8, 10, 11)

VT = solid solution (ternary; not determined) (metastable) (figure 11)

(ii) Invariant points:

 $\text{R} = \text{Al}_2\text{O}_3\text{aq.}$ -solid solution- $\text{C}_3\text{A} \cdot 3\text{CaSO}_4 \cdot 32\text{H}_2\text{O}$ (unstable) (figures 6, 10, 11) $\text{R}_2 = \text{A} \cdot 3\text{H}_2\text{O(B)}$ -solid solution- $\text{C}_3\text{A} \cdot 3\text{CaSO}_4 \cdot 32\text{H}_2\text{O}$ (metastable) (figures 3c, 6, 11) $\text{M} = \text{Ca(OH)}_2$ -solid solution- $\text{C}_3\text{A} \cdot 3\text{CaSO}_4 \cdot 32\text{H}_2\text{O}$ (metastable) (figures 8, 10, 11) $\text{T} = \text{Al}_2\text{O}_3\text{aq.}$ -solid solution (ternary; not determined) (unstable) (figure 11) $\text{T}_2 = \text{A} \cdot 3\text{H}_2\text{O(B)}$ -solid solution (ternary; not determined) (metastable) (figure 11) $\text{V} = \text{Ca(OH)}_2$ -solid solution (ternary; not determined) (metastable) (figure 11)

(iii) Curves across surface:

SW = solid solution (metastable) (figures 6, 8, 10, 11)

QU = solid solution (metastable) (figures 8, 10, 11)

I = solid solution (metastable) (figure 10)

II = solid solution (metastable) (figure 10)

III = solid solution (metastable) (figure 10)

The spacial relations between the various boundary curves will be made clear by reference to the original space figure and figures 3, 4, 6, 8, 10, 11.

DISCUSSION

In the equilibria involving crystalline $\text{A} \cdot 3\text{H}_2\text{O}$, as in the case of alumina gel (8), only the high-sulfate form of calcium sulfoaluminate, $\text{C}_3\text{A} \cdot 3\text{CaSO}_4 \cdot 32\text{H}_2\text{O}$, occurs as a stable quaternary compound. The examination of the metastable equilibria with crystalline $\text{A} \cdot 3\text{H}_2\text{O}$, however, has shown that the low-sulfate form $\text{C}_3\text{A} \cdot \text{CaSO}_4 \cdot 12\text{H}_2\text{O}$ may occur as a metastable phase as a terminal component of a solid solution series.

Reference to figure 3a shows that, with respect to crystalline $\text{A} \cdot 3\text{H}_2\text{O(B)}$, $\text{C}_3\text{A} \cdot 3\text{CaSO}_4 \cdot 32\text{H}_2\text{O}$ is fundamentally incongruently soluble in any concentration of calcium sulfate or lime up to saturation point. This must also apply to a crystalline $\text{A} \cdot 3\text{H}_2\text{O}$ possessing what is apparently the most stable structure, namely, that of gibbsite ($\gamma\text{-A} \cdot 3\text{H}_2\text{O}$). On treatment with water, decomposition must occur with deposition of some form of hydrated alumina ranging from that in the gel structure to the most stable atomic arrangement of gibbsite, until a solution composition is attained, corresponding to the point of intersection of the prolongation of the $\text{Al}_2\text{O}_3\text{-C}_3\text{A} \cdot \text{CaSO}_4$ line in figure 3a with the appropriate

$C_3A \cdot 3CaSO_4 \cdot 32H_2O$ -hydrated alumina curve, e.g., with the curve EH or E_1H_1 or E_2H_2 in figure 3a.

If the two curves obtained with the different preparations of crystalline $A \cdot 3H_2O$ be compared, it is seen, from figure 3a and figure 4 that curve A for $\alpha\text{-}A \cdot 3H_2O$ (bayerite) lies in a region of less $CaSO_4$ and CaO and greater Al_2O_3 concentration than curve B. The relative position is what is to be expected from the structures shown by the x-ray data. When the two curves are compared with the corresponding curve for alumina gel already reported (8), and traced by the broken line EH in figure 3a, it seems clear that the several curves trace the surface of the $C_3A \cdot 3CaSO_4 \cdot 32H_2O$ field between the limits given by the relatively soluble alumina gel (unstable equilibria) and the most stable $\gamma\text{-}A \cdot 3H_2O$ structure of gibbsite.

It is apparent that, depending on the degree of departure from the most stable crystalline state of aggregation of hydrated alumina, in crystal form and state of subdivision, terminating in the gel structure, a series of invariant points may be obtained as we proceed from left to right in figure 3a along the boundary curve $C_3A \cdot 6H_2O$ – $C_3A \cdot 3CaSO_4 \cdot 32H_2O$. In other words, the position of the invariant point becomes more and more displaced from the stable position (with $\gamma\text{-}Al_2O_3 \cdot 3H_2O$). It seems probable that H_2 is near the most stable invariant point possible, that with $A \cdot 3H_2O$ possessing the gibbsite structure, i.e., $\gamma\text{-}Al_2O_3 \cdot 3H_2O$. The invariant point H_1 , which is that for $\alpha\text{-}Al_2O_3 \cdot 3H_2O$ (bayerite), is to be considered as metastable with respect to the stable invariant point for $\gamma\text{-}Al_2O_3 \cdot 3H_2O$. Between the gel form and crystalline $\alpha\text{-}Al_2O_3 \cdot 3H_2O$ we have to consider two changes, a change from the structure of $\gamma\text{-}Al_2O_3 \cdot H_2O$ (böhmite) to that of $\alpha\text{-}Al_2O_3 \cdot 3H_2O$, and a growth in crystal size. Weiser and Milligan (15) have shown that the gel precipitated from aluminum sulfate solution at $25^\circ C$. gives the electron diffraction pattern of $\gamma\text{-}Al_2O_3 \cdot H_2O$ (böhmite), though with x-rays only a very broad band pattern is obtained. When aged in the cold the $\gamma\text{-}Al_2O_3 \cdot H_2O$ (böhmite) gradually changes over and yields an electron diffraction pattern of $\alpha\text{-}Al_2O_3 \cdot 3H_2O$ (bayerite). These authors quote Baccaredda and Beati (2) as having obtained an $\alpha\text{-}Al_2O_3 \cdot 3H_2O$ (bayerite) electron diffraction pattern from an alumina gel. It thus appears that the change böhmite \rightarrow bayerite may occur while the hydrated alumina is still in the gel stage.

In the metastable equilibria beyond the $C_3A \cdot 6H_2O$ – $C_3A \cdot 3CaSO_4 \cdot 32H_2O$ boundary curve GH (figures 3a, 3c, 6), the data along the metastable prolongation H_2R_2 of the curve E_2H_2 show an abrupt increase in the Al_2O_3 dissolved at a lime concentration of approximately 0.3 g. CaO per 1000 g. of solution, while at the same time the $CaSO_4$ concentration becomes very small. The second solid phase in this region is $C_3A \cdot 3CaSO_4 \cdot 32H_2O$. The association of the rapid diminution of $CaSO_4$ in solution with the increase in Al_2O_3 concentration agrees with the behavior found with alumina gel (boundary curve HR, figure 6). The quaternary equilibria are in fact rapidly approaching the CaO – Al_2O_3 – H_2O face and are linked with the equilibria of the ternary system. In the case of the alumina gel equilibria along the curve HR (figure 6), the increase in the Al_2O_3 solubility occurs at rather lower lime concentrations, and is, as would be expected, much greater than for crystalline $A \cdot 3H_2O$.

At lime concentrations greater than correspond to R' and R_2 , solid solution equilibria first appear. It has been shown that the solid solution along the curves SW and QU has the general formula $x\text{CaO} \cdot y\text{Al}_2\text{O}_3 \cdot z\text{CaSO}_4 \cdot a\text{q.}$, and that the composition varies through such a range that it may conveniently be regarded as comprising $\text{C}_3\text{A} \cdot \text{CaSO}_4 \cdot 12\text{H}_2\text{O}$, $\text{C}_3\text{A} \cdot 12\text{H}_2\text{O}$, $\text{C}_3\text{A} \cdot \text{Ca}(\text{OH})_2 \cdot 12\text{H}_2\text{O}$, and $\text{Ca}(\text{OH})_2$ in varying amounts. However, no evidence of water content is available, and it may be that $\text{C}_2\text{A} \cdot \text{aq.}$ and $\text{C}_4\text{A} \cdot \text{aq.}$ in equimolar amounts are present rather than $\text{C}_2\text{A} \cdot \text{aq.}$ There is definite evidence for the existence of a solid solution surface between the boundary curve MN(R) and the curve WS, the latter not being a boundary curve, but a path across the solid solution surface. Clearly the surface must continue through the path WS as the CaSO_4 content of the solid solution decreases, and it seems that UQ, which is a solid solution curve similar to WS, but with less CaSO_4 present, must also lie in the solid solution surface nearer to the plane $\text{CaO-Al}_2\text{O}_3\text{-H}_2\text{O}$. If this be true, the surface must curl downwards at WS to pass through UQ and finally end in a solid solution boundary curve in the ternary system starting at some point T on a continuation of the curve RSQ and ending at V on a continuation of the curve MWU: $\text{Ca}(\text{OH})_2$ -solid solution. Confirmation of such an abrupt curl in the solid solution surface is obtained by considering the broken curves of figure 10. Thus curves I, II, and III show increasing curvatures directed towards the point S. There is a suggestive curvature in UQ near Q, and finally there is the pronounced curvature of the indefinite curve RSQ. The curvature of $\text{R}_2\text{S}_2\text{Q}_2$ (figure 6) is also in agreement with such a curved surface. Just as RSQ must continue to an unstable invariant point T: $\text{Al}_2\text{O}_3\text{aq.}$ -solid solution in the ternary system, so must $\text{R}_2\text{S}_2\text{Q}_2$ to the ternary invariant point $\text{T}_2\text{:A} \cdot 3\text{H}_2\text{O(B)}$ -solid solution. At the high lime end of the surface there must be a short curve starting from V in the ternary, passing through U and W and continuing to M, the invariant point $\text{Ca}(\text{OH})_2$ -solid solution- $\text{C}_3\text{A} \cdot 3\text{CaSO}_4 \cdot 32\text{H}_2\text{O}$ in the quaternary system. A purely diagrammatic sketch of the solid solution surface equilibria is given in figure 11, showing the relation between the various curves. Here TV represents a solid solution curve in the ternary system. From this curve the solid solution surface extends upwards, reaches its upper limit at WS, and curls over to sweep downward toward the boundary curve MN(R). While there appears to be a considerable upward curl in the surface in the low lime region, this diminishes very rapidly as W is approached, as figure 10 shows. Along the curve MR the solid solution approaches the composition of the low-sulfate form of calcium sulfoaluminate, $\text{C}_3\text{A} \cdot \text{CaSO}_4 \cdot 12\text{H}_2\text{O}$. This curve represents in effect the boundary in the metastable region between the $\text{C}_3\text{A} \cdot 3\text{CaSO}_4 \cdot 32\text{H}_2\text{O}$ field and what would be a field for $\text{C}_3\text{A} \cdot \text{CaSO}_4 \cdot 12\text{H}_2\text{O}$ if solid solution equilibria did not enter. Actually it appears that the $\text{C}_3\text{A} \cdot \text{CaSO}_4 \cdot 12\text{H}_2\text{O}$ immediately enters into solid solution with the metastable hexagonal plate forms of the hydrated calcium aluminates and with $\text{Ca}(\text{OH})_2$. Thus, if from any point along RM we trace a path across the solid solution surface parallel to RST or MWUV, the solid solution becomes richer in lime and alumina and poorer in calcium sulfoaluminate until when the curve TV is reached in the ternary system no sulfoaluminate is present. Again, starting from some point on the boundary curve RST (alumina gel-solid solution of $\text{C}_3\text{A} \cdot \text{CaSO}_4 \cdot 12\text{H}_2\text{O}$ and

centration, no other interpretation appears to fit the available data so well. Since the solid solution surface lies so close to the ternary face $\text{CaO-Al}_2\text{O}_3\text{-H}_2\text{O}$, the precise location of its intersection with this face may well have a wide margin of error. It has been suggested by Mr. G. E. Bessey (private communication) that there are possibly two series of solid solutions. Thus in figure 7, if M63 is not neglected, the data may be interpreted as lying on two curves for separate series of solid solutions of different structures, and it may also be significant that the rapid rise in the indices occurs at S_2 . Further, the curve MR (as drawn through the point H109, figure 10) diverges somewhat from the position of MN

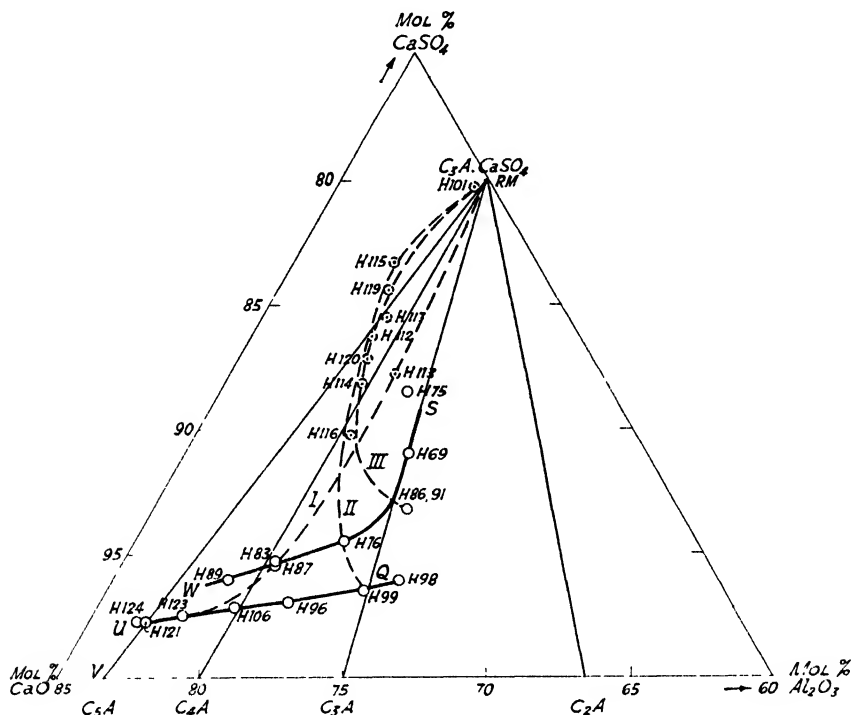


FIG. 12. Calculated solid solution compositions over solid solution surface (excluding water)

in low lime concentrations, and it might be argued that they belong to different series of solid solutions. At any rate it appears possible that the continuous solid solution surface visualized in figure 11 may really be broken into two separate series of solid solutions represented possibly by the "front" and "back" surfaces TVWS and RMWS, respectively. A more closely detailed study of the solid solution equilibria is, however, required with a more precise linking to the equilibria of the ternary system than is at present possible before it can be decided whether the interpretation of the present work must be regarded as only a simplified version to be modified to include separate series of solid solutions.

Returning to figure 6, the metastable curve $H_2R_2L_2 \cdot A \cdot 3H_2O(B) - C_3A \cdot 3CaSO_4 \cdot 32H_2O$ is analogous to the metastable curve $D_2P \cdot A \cdot 3H_2O(B)$ in the ternary system (figure 2). The curves HRL and $H_2R_2L_2$ of figure 6 are simply the metastable prolongations of EH and E_2H_2 , respectively, and the same kind of relationship holds between them, though we are now dealing throughout with metastable equilibria. Thus, according to the state of the hydrated alumina phase varying from the crystalline to the gel condition and varying also in crystal structure, the curve $H_2R_2L_2$ moves gradually upward until it finally reaches the position HRL. The same relation holds between the alumina gel and crystalline $A \cdot 3H_2O$ curves of the ternary system.

As we proceed along the curve $H_2R_2L_2$ towards the high lime region, a point is reached at which solid solution is formed, i.e., we reach the invariant point R_2 . Similarly in passing along the curve HRL, solid solution is eventually formed at R. The same holds good for the equilibria relating any other state of the hydrated alumina and $C_3A \cdot 3CaSO_4 \cdot 32H_2O$. These invariant points—of increasing instability as we proceed from R_2 to R—clearly lie on the lower boundary curve for the solid solution surface, i.e., the curve MN (or MR_2R). Actually R_2 falls close to the previously determined curve MN.

At R_2 , as has been shown, the solid solution formed has a composition close to that of $C_3A \cdot CaSO_4 \cdot 12H_2O$. From this point there proceeds the curve $R_2S_2Q_2$ for $A \cdot 3H_2O(B)$ —solid solution, the latter being simply interpreted as " $C_3A \cdot CaSO_4 \cdot 12H_2O + C_3A \cdot Ca(OH)_2 \cdot 12H_2O$ " in figure 6. The curve clearly lies in the solid solution surface described. Its relation to the alumina gel—solid solution curve RSQ is analogous to that between the several other crystalline $A \cdot 3H_2O$ and alumina gel curves already described, and the curve $R_2S_2Q_2$ must be visualized as moving gradually from the position shown—dependent on the state of the hydrated alumina phase—until with alumina gel it coincides with the position of RSQ. The solid solution surface must then be visualized as of variable extent, the boundary with the hydrated alumina solid phase varying in position according to the state of the hydrated alumina. Both along RSQ and along $R_2S_2Q_2$, as has been shown, the solid solution is changing in composition. At Q, where the solid solution is approaching the invariant point in the ternary system, it appears to have a $C_4A \cdot aq.$ composition. The curve $R_2S_2Q_2$ must also end on the ternary system in an invariant point $T_2 \cdot A \cdot 3H_2O(B)$ —solid solution, and the composition of the solid solution appears to be close to $C_4A \cdot aq.$

The solid solution equilibria of the quaternary system have in this work been considered in relation to a solid solution curve in the ternary system. The possibility has been shown—in the preliminary discussion of phase-rule equilibria—of unstable liquidus and solidus areas in the ternary system rather than curves, and the formation of supersaturated solid solutions in unstable equilibrium with supersaturated liquid solutions. The area thus visualized in the ternary system is really the area swept through by a single solid solution curve between stability and maximum instability limits. This is analogous to the area swept out by the hydrated alumina curves. The liquidus area would in such a case give the concentrations of solutions in equilibrium with a corresponding area of solid solution

concentrations, each point in the area corresponding to an appropriate solid solution composition. The composition of the solid solution and the concentration of the equilibrium solution are then continuously variable within the limits of solid solution formation. This conception depends of course on whether or not an area of solid solution is structurally possible. It does not imply the non-existence of such compounds as $\text{C}_2\text{A} \cdot 8\text{H}_2\text{O}$, $\text{C}_3\text{A} \cdot 12\text{H}_2\text{O}$, or $\text{C}_4\text{A} \cdot 13\text{H}_2\text{O}$, but it is possible (see discussion of figures 1(m) and 1(n)) that these exist as limiting compositions in the solid solution area. Solid solution curves can in this case only be interpreted as relating to a restricted range of compositions of the solid solutions which can be expressed in terms of two specific solid solution compositions. Such compositions may—but not necessarily—be those for pure compounds. Thus, for example, solid solutions whose compositions can be expressed in terms of the compositions $\text{C}_2\text{A} \cdot 8\text{H}_2\text{O}$ (or $\text{C}_3\text{A} \cdot 12\text{H}_2\text{O}$) and $\text{C}_4\text{A} \cdot 13\text{H}_2\text{O}$ (or $\text{Ca}(\text{OH})_2$) would be in equilibrium with solutions whose concentrations fall on a smooth curve. If an unstable solid solution area really exists in the ternary system, this curve may form its unstable upper limit, and a lower stable boundary curve would also exist. The solid solution surfaces described in this work would then constitute an unstable upper limit to a solid solution volume in the quaternary. There would also be a stable lower limit starting from a stable ternary curve. The volume postulated is that swept out by the boundary surface in passing from its stable to its most unstable position. The idea embodied in this paragraph is speculative and its application dependent on the equilibria of the ternary system $\text{CaO-Al}_2\text{O}_3\text{-H}_2\text{O}$. It appears to afford an explanation for the fact that in the ternary system, apparent equilibria resulting from precipitation of solid phases from supersaturated solutions tend to be spread over an area.

The calcium sulfoaluminate in hydrated Portland cement:—In the previous communication (8) dealing with the system $\text{CaO-Al}_2\text{O}_3\text{-CaSO}_4\text{-H}_2\text{O}$, a discussion was included on the nature of the calcium sulfoaluminate formed in hydrated Portland cement. From the present work it is clear that so far as the quaternary system is involved three possibilities exist: namely, the formation of $\text{C}_3\text{A} \cdot 3\text{CaSO}_4 \cdot 32\text{H}_2\text{O}$, of a solid solution containing $\text{C}_3\text{A} \cdot \text{CaSO}_4 \cdot 12\text{H}_2\text{O}$, or of both. It is apparent that a pure $\text{C}_3\text{A} \cdot \text{CaSO}_4 \cdot 12\text{H}_2\text{O}$ could only be formed exceptionally, since it may occur as a pure phase only as a terminal component in a solid solution series. The work so far described affords guidance as to the solid phases formed in a hydrated Portland cement but conclusions are at present restricted to alkali-free and iron-free cements. In such cements treatment with water will lead to dissolution of alumina and lime, either from C_3A or a glass containing alumina or both to give a metastable (or unstable) solution whose lime content will be much increased by lime derived from the tricalcium silicate in the cement. At the same time, calcium sulfate will pass into solution. Since the solution obtained is very rapidly supersaturated with respect to crystalline $\text{Ca}(\text{OH})_2$, it may be expected that so long as solid $\text{CaSO}_4 \cdot 2\text{H}_2\text{O}$ remains in the solid phase, an equilibrium represented by the invariant point F will be maintained, since $\text{C}_3\text{A} \cdot 3\text{CaSO}_4 \cdot 32\text{H}_2\text{O}$ must be formed and crystalline $\text{Ca}(\text{OH})_2$ and $\text{CaSO}_4 \cdot 2\text{H}_2\text{O}$ will be present. If no interfering factors arise, the gypsum should eventually be

entirely used up, and the equilibrium should pass along the boundary curve $FG:Ca(OH)_2-C_3A \cdot 3CaSO_4 \cdot 32H_2O$ towards the invariant point G. It is improbable that $C_3A \cdot 6H_2O$ will be formed at G, and the metastable equilibrium at M or along the curve $MWUV:Ca(OH)_2$ -solid solution will be formed, i.e., either solid solution plus $C_3A \cdot 3CaSO_4 \cdot 32H_2O$ or solid solution alone, depending on the relative available amounts of CaO , Al_2O_3 , and SO_3 . Unless the amount of SO_3 exceeds that necessary to give a solid solution of the maximum SO_3 concentration possible along the boundary curve $MWUV$ (figure 11), i.e., at M, $C_3A \cdot 3CaSO_4 \cdot 32H_2O$ will convert to the solid solution. The solid solution in equilibrium with $Ca(OH)_2$, of maximum SO_3 concentration, obtained in the present work, is that at W. Extrapolation (figure 9) to a lime concentration of 1.1 g. CaO per 1000 g. of solution gives the molar ratios $CaO:Al_2O_3:CaSO_4 = 21.5:4.8:1$. The composition is, however, changing as we proceed along the boundary curve to M, and we need to know the composition at M. The evidence of the present work suggests that it approaches a 3:1:1 ratio. Assuming this, then for 2 per cent SO_3 , equivalent to 3.4 per cent $CaSO_4$ in a Portland cement, the Al_2O_3 content would only need to equal or exceed $3.4 \times 102/136 = 2.6$ per cent before complete conversion of $C_3A \cdot 3CaSO_4 \cdot 32H_2O$ to solid solution becomes possible. The alumina content of British Portland cements including normal and rapid-hardening types varies from 4 to rather more than 8 per cent Al_2O_3 . It thus appears probable that the $C_3A \cdot 3CaSO_4 \cdot 32H_2O$ initially formed may eventually change over completely to the solid solution.

With regard to the attack of calcium sulfate waters on concrete, it should be noted that the equilibria relations to be expected in a freshly hydrated cement are those of point M in figure 11, or some point along the $Ca(OH)_2$ -solid solution curve $MWUV$. So long as the metastable equilibria persist, therefore, formation of $C_3A \cdot 3CaSO_4 \cdot 32H_2O$ can occur in calcium sulfate attack at $CaSO_4$ concentrations in excess of the value at the invariant point M: namely, as previously found (8), 0.004 g. $CaSO_4$ per 1000 g. of solution.

The above considerations have been restricted to alkali-free and iron-free cements. So far as alkalies are concerned, equilibria in the systems $CaO-Al_2O_3-CaSO_4-K_2O-H_2O$ (1 per cent KOH) and $CaO-Al_2O_3-CaSO_4-Na_2O-H_2O$ (1 per cent $NaOH$) at $25^\circ C$. have been examined by the writer, and the results will be communicated.

SUMMARY

In continuance of a previous investigation of the quaternary system $CaO-Al_2O_3-CaSO_4-H_2O$ at $25^\circ C$. further work has been carried out to determine the stable and metastable equilibria involving crystalline $Al_2O_3 \cdot 3H_2O$. The work thus provides the necessary data for the fundamental system involving crystalline $Ca(OH)_2$ and crystalline $Al_2O_3 \cdot 3H_2O$ as solid phases. In addition, equilibria with alumina gel in solutions of high lime concentrations, supplementing those described in the previous paper, have been determined, and solid solution equilibria investigated.

The work with $Al_2O_3 \cdot 3H_2O$ has shown that, as in the case of alumina gel, only

the high-sulfate form of calcium sulfoaluminate, $3\text{CaO} \cdot \text{Al}_2\text{O}_3 \cdot 3\text{CaSO}_4 \cdot 32\text{H}_2\text{O}$, occurs as a stable quaternary compound. With respect to a crystalline $\text{Al}_2\text{O}_3 \cdot 3\text{H}_2\text{O}$ possessing the most stable structure of gibbsite, $3\text{CaO} \cdot \text{Al}_2\text{O}_3 \cdot 3\text{CaSO}_4 \cdot 32\text{H}_2\text{O}$ is incongruently soluble in water and any concentration of calcium sulfate or lime up to saturation point. The extent of the $3\text{CaO} \cdot \text{Al}_2\text{O}_3 \cdot 3\text{CaSO}_4 \cdot 32\text{H}_2\text{O}$ field in the system varies between the limits given by the relatively soluble alumina gel and the most stable $\text{Al}_2\text{O}_3 \cdot 3\text{H}_2\text{O}$ structure of gibbsite. A solid solution curve $\text{Al}_2\text{O}_3 \cdot 3\text{H}_2\text{O}$ —“ $3\text{CaO} \cdot \text{Al}_2\text{O}_3 \cdot \text{CaSO}_4 \cdot 12\text{H}_2\text{O} + 3\text{CaO} \cdot \text{Al}_2\text{O}_3 \cdot \text{Ca}(\text{OH})_2 \cdot 12\text{H}_2\text{O}$ ” has been traced and evidence found for a similar solid solution curve $\text{Al}_2\text{O}_3\text{aq.}(\text{gel})$ —“ $3\text{CaO} \cdot \text{Al}_2\text{O}_3 \cdot \text{CaSO}_4 \cdot 12\text{H}_2\text{O} + 3\text{CaO} \cdot \text{Al}_2\text{O}_3 \cdot 12\text{H}_2\text{O}$.” These curves appear to define the extreme limits of a variation in the extent of a solid solution field dependent, as in the case of the $3\text{CaO} \cdot \text{Al}_2\text{O}_3 \cdot 3\text{CaSO}_4 \cdot 32\text{H}_2\text{O}$ field, upon the nature of the hydrated alumina involved. The so-called low-sulfate form, $3\text{CaO} \cdot \text{Al}_2\text{O}_3 \cdot \text{CaSO}_4 \cdot 12\text{H}_2\text{O}$, occurs only as a terminal component in a solid solution field. The work on the alumina gel equilibria in the quaternary system shows that a similar behavior to that found with $\text{Al}_2\text{O}_3 \cdot 3\text{H}_2\text{O}$ occurs up to a lime concentration of about 0.3 g. CaO per liter, the Al_2O_3 solubility being, however, much increased. The quaternary equilibria are, in fact, rapidly approaching the $\text{CaO-Al}_2\text{O}_3\text{-H}_2\text{O}$ face, and are linked with the equilibria of the ternary system through a solid solution field which extends from a solid solution— $3\text{CaO} \cdot \text{Al}_2\text{O}_3 \cdot 3\text{CaSO}_4 \cdot 32\text{H}_2\text{O}$ boundary curve in the quaternary system to a solid solution curve in the ternary system. The solid solution in equilibrium with $3\text{CaO} \cdot \text{Al}_2\text{O}_3 \cdot 3\text{CaSO}_4 \cdot 32\text{H}_2\text{O}$ approaches the composition of the low-sulfate form of calcium sulfoaluminate, $3\text{CaO} \cdot \text{Al}_2\text{O}_3 \cdot \text{CaSO}_4 \cdot 12\text{H}_2\text{O}$. This curve represents in effect the boundary between the $3\text{CaO} \cdot \text{Al}_2\text{O}_3 \cdot 3\text{CaSO}_4 \cdot 32\text{H}_2\text{O}$ field and what would be a field for $3\text{CaO} \cdot \text{Al}_2\text{O}_3 \cdot \text{CaSO}_4 \cdot 12\text{H}_2\text{O}$ if solid solution equilibria did not enter. The solid solution has the general formula $x\text{CaO} \cdot y\text{Al}_2\text{O}_3 \cdot z\text{CaSO}_4 \cdot \text{aq.}$, and its composition appears to be contained within limits such that it may be considered as being composed of $3\text{CaO} \cdot \text{Al}_2\text{O}_3 \cdot 12\text{H}_2\text{O}$, $3\text{CaO} \cdot \text{Al}_2\text{O}_3 \cdot \text{CaSO}_4 \cdot 12\text{H}_2\text{O}$, $3\text{CaO} \cdot \text{Al}_2\text{O}_3 \cdot \text{Ca}(\text{OH})_2 \cdot 12\text{H}_2\text{O}$, and to a limited extent $\text{Ca}(\text{OH})_2$. It is possible that the compound $2\text{CaO} \cdot \text{Al}_2\text{O}_3 \cdot 8\text{H}_2\text{O}$ also enters into the solid solution, at any rate within the ternary system.

The possibility of unstable solid solution equilibria is advanced and its application to the equilibria of the ternary system $\text{CaO-Al}_2\text{O}_3\text{-H}_2\text{O}$ and the quaternary system $\text{CaO-Al}_2\text{O}_3\text{-CaSO}_4\text{-H}_2\text{O}$ described.

The formation of calcium sulfoaluminates in a hydrated Portland cement is discussed, and it is concluded that in an alkali- and iron-free cement $3\text{CaO} \cdot \text{Al}_2\text{O}_3 \cdot 3\text{CaSO}_4 \cdot 32\text{H}_2\text{O}$ is initially formed, but changes over at least partly, and may eventually change over completely, to the solid solution.

Reference is made to the attack of calcium sulfate waters on concrete.

The writer is indebted to Mr. G. E. Bessey for critical reading and discussion in the course of the preparation of this work for publication. The investigations described in this paper were carried out at the Building Research Station of the Department of Scientific and Industrial Research and the paper is published by permission of the Director of Building Research.

REFERENCES

- (1) ASSARSSON, G.: *Sveriges Geol. Undersökn., Årbok*, Ser. C **30** (6), No. 399 (1936).
- (2) BACCAREDDA, M., AND BEATI, E.: *Atti X° congr. intern. chim.* **2**, 99 (1938).
- (3) BESSEY, G. E.: Private communication.
- (4) FRICKE, R.: *Z. anorg. Chem.* **175**, 249 (1928); **179**, 287 (1929).
- (5) FRICKE, R., AND SEVERIN, H.: *Z. anorg. Chem.* **205**, 287 (1932).
- (6) GOUDRIAAN, F.: *Proc. Acad. Sci. Amsterdam* **23**, 129 (1921).
- (7) GUGGENHEIM, E. A.: *Modern Thermodynamics by the Method of Willard Gibbs*. Methuen & Co., London (1933).
- (8) JONES, F. E.: *Trans. Faraday Soc.* **35**, 1484 (1939).
- (9) LEA, F. M., AND BESSEY, G. E.: Private communication.
- (10) LERCH, W., ASHTON, F. W., AND BOGUE, R. H.: *J. Res. Natl. Bur. Standards* **2**, 715 (1929).
- (11) MARSH, J. S.: *Principles of Phase Diagrams*. McGraw-Hill Book Company, New York (1935).
- (12) MYLIUS, C.: *Acta Acad. Aboensis* **7**, 3 (1933), "The calcium aluminate hydrates and their double salts."
- (13) ROOKSBY, H. P.: *Trans. Ceram. Soc.* **28**, 399 (1928).
- (14) WEISER, H. B., AND MILLIGAN, W. O.: *J. Phys. Chem.* **38**, 1175-82 (1934).
- (15) WEISER, H. B., AND MILLIGAN, W. O.: *J. Phys. Chem.* **44**, 1081-94 (1940).

THE QUINARY SYSTEM $\text{CaO-Al}_2\text{O}_3\text{-CaSO}_4\text{-K}_2\text{O-H}_2\text{O}$
(1 PER CENT KOH) AT 25°C.

F. E. JONES

Building Research Station, Garston, Watford, Herts, England

Received May 27, 1944

The present work is a further contribution to the study of the reactions occurring in the setting and hardening of Portland cements, and the disintegration of such cements on exposure to sulfate waters. Attention has previously been confined to the quaternary system $\text{CaO-Al}_2\text{O}_3\text{-CaSO}_4\text{-H}_2\text{O}$ (8, 9). Since the liquid phase in a setting cement contains much alkali (1, 4, 5, 6, 12, 13), it is necessary to consider how the equilibria found for the quaternary system may be modified in the presence of the additional alkali component. In working out the equilibria in the alkali systems, attention has been confined to concentrations of alkali equivalent to 1 per cent KOH and 1 per cent NaOH, respectively. Since the alkali present in British Portland cements is mainly K_2O , attention has been given first to the K_2O system. The application of the results to the chemistry of cement will be considered in the discussion section. The experimental methods were similar to those previously used. Stainless-steel tubes of 200-ml. capacity were employed for shaking purposes. The potassium sulfate and potassium hydroxide used were of Analar purity. No separate analyses were made for K_2O in the various solutions. Throughout the work there was no evidence of any change in the optical properties of the $\text{CaSO}_4 \cdot 2\text{H}_2\text{O}$, Ca(OH)_2 , $\text{C}_3\text{A} \cdot 6\text{H}_2\text{O}$, or

$\text{C}_3\text{A} \cdot 3\text{CaSO}_4 \cdot 32\text{H}_2\text{O}$ solid phases to suggest the taking up of alkali by these compounds. Specific analyses for alkali on 0.05-g. to 0.2-g. samples of these solid phases from certain of the equilibrium mixes showed only 0.1 or 0.2 per cent ± 0.05 per cent K_2O . In the case of alumina gel, a 0.03-g. sample obtained from a mix containing relatively much KOH gave 0.8 per cent ± 0.2 per cent K_2O , and a similar 0.1-g. sample of crystalline hydrated alumina gave 0.25 per cent ± 0.05 per cent K_2O . The small amounts of K_2O found are probably to be ascribed to some surface adsorption and retention of mother liquor in filtration.

In the study of the quaternary system $\text{CaO}-\text{Al}_2\text{O}_3-\text{CaSO}_4-\text{H}_2\text{O}$ (8, 9), the system was considered as a reciprocal salt-pair. The method of representation

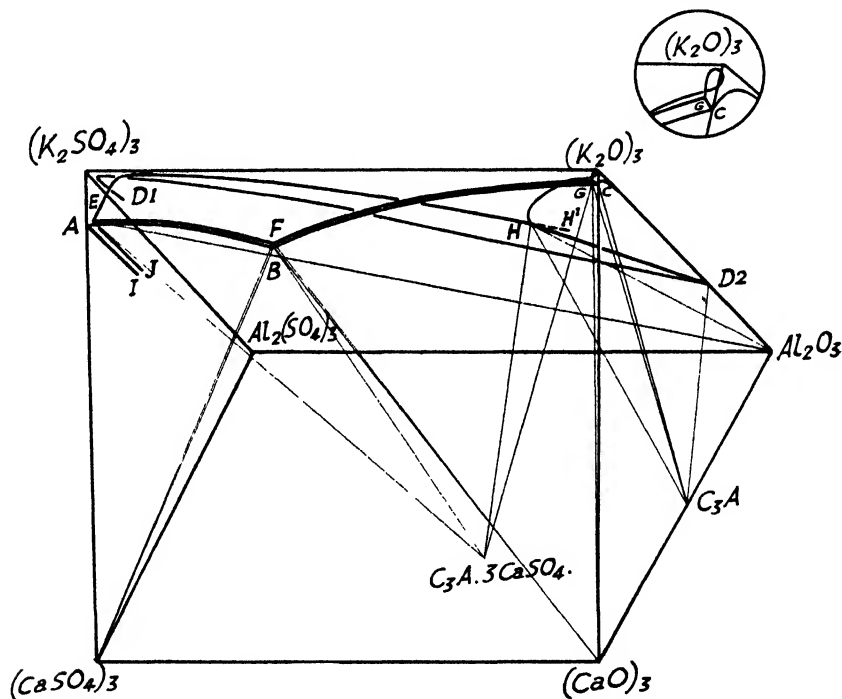


FIG. 1. Quinary system $\text{CaO}-\text{Al}_2\text{O}_3-\text{CaSO}_4-\text{K}_2\text{O}-\text{H}_2\text{O}$ (1 per cent KOH) at 25°C .

adopted for the quinary system is the logical extension of this due to Jänecke though, since the system now shown is a restricted one, there is considerable modification in interpretation. The space figure (figure 1), in which the quinary and quaternary boundary curves are shown, consists of a prism built up of three reciprocal salt-pair systems and two other quaternary systems represented on the triangular end-faces. Only the compositions of the salt mixtures in solution can be expressed by such a figure, the water content not being shown. This may, however, be done by using a projection on to the base $(\text{CaO})_3-\text{Al}_2\text{O}_3-(\text{CaSO}_4)_3-\text{Al}_2(\text{SO}_4)_3$ from the edge $(\text{K}_2\text{O})_3-(\text{K}_2\text{SO}_4)_3$ by lines through this edge and parallel to the end triangles (figure 8). The water content may thus be represented in the usual way within a pyramidal space figure. The composition of the salt

mixture is determinable with the knowledge that the alkali content is always equivalent to 1 per cent KOH. Thus, from the space figure the total content in moles of salt mixture in solution is obtained. This content, less the fixed content of $(K_2O)_3$, gives the molar content of $(CaO)_3$ and Al_2O_3 together; hence, from the projection (figure 8) giving the relative percentage contents of $(CaO)_3$ and $(Al_2O_3)_3$, the actual molar contents of $(CaO)_3$ and Al_2O_3 separately may be calculated. The projection also gives the mole percentage of SO_3 in the total content of salt mixture.

In figure 1, however, as stated, the water content is not shown, though it may be calculated. Moreover, since the alkali concentration is maintained constant in solution and no alkali appears in any solid phase, the figure is essentially a cross section through the complete system for the alkali concentration equivalent to 1 per cent KOH. This involves important differences in interpretation as compared with the same method of representation used for the complete system. Only two solid phases are required to define boundary curves in this restricted quinary system, and stability fields are surfaces, not volumes as in the complete system. The corners of the prism represent pure salt compositions as in the case of the complete system, but the further interpretation differs. While in the complete system the corners are associated with saturated solutions of the respective salts, this is not so in the restricted system. The base corners $(CaSO_4)_3$, $(CaO)_3$, Al_2O_3 , and $Al_2(SO_4)_3$ are to be associated with pure solid phases $CaSO_4 \cdot 2H_2O$, $Ca(OH)_2$, etc., in equilibrium with appropriate solution compositions, while the $(K_2SO_4)_3$ and $(K_2O)_3$ corners represent concentrations of sulfate or hydroxide equivalent to 1 per cent KOH. The point A represents a saturated solution of $CaSO_4 \cdot 2H_2O$ in a K_2SO_4 solution (equivalent to 1 per cent KOH). Points along the edge $(CaSO_4)_3$ – $(K_2SO_4)_3$ between A and the $(K_2SO_4)_3$ corner give the salt compositions of unsaturated solutions of $CaSO_4 \cdot 2H_2O$ in a K_2SO_4 solution (equivalent to 1 per cent KOH), while between A and the $(CaSO_4)_3$ corner complexes of solid $CaSO_4 \cdot 2H_2O$ of saturated solution A are represented. This is the only representation which the system $(K_2SO_4)_3$ – $(CaSO_4)_3$ – H_2O can receive in the figure. The curve AB in the restricted quaternary system $(CaO)_3$ – $(CaSO_4)_3$ – $(K_2SO_4)_3$ – $(K_2O)_3$ – H_2O (1 per cent KOH) gives the compositions of the salt mixtures in solutions saturated with respect to $CaSO_4 \cdot 2H_2O$, while the curve EF in the restricted quinary system is the boundary between the $CaSO_4 \cdot 2H_2O$ and $C_3A \cdot 3CaSO_4 \cdot 32H_2O$ fields and gives the compositions of the salt mixtures in solutions in equilibrium with both $CaSO_4 \cdot 2H_2O$ and $C_3A \cdot 3CaSO_4 \cdot 32H_2O$. Similarly for the other points and curves shown. As shown in figure 1, the tie-lines may be drawn from the various invariant points to the appropriate solid phase compositions, excluding water. It seems desirable to emphasize that in, for example, such a face as $(CaO)_3$ – $(CaSO_4)_3$ – $(K_2SO_4)_3$ – $(K_2O)_3$, the $(CaSO_4)_3$ or $(CaO)_3$ corners are not to be interpreted as representing saturated solutions of $CaSO_4 \cdot 2H_2O$ or $Ca(OH)_2$. This would only be the case if the face represented a projection of the complete quaternary reciprocal salt-pair system through the water point on to the base of the usual pyramidal space figure. The curves shown are, however, not projections. The face is comparable to the simple ternary repre-

sensation of the system $(\text{CaO})_3-(\text{CaSO}_4)_3-\text{H}_2\text{O}$, but instead of representing water, we are representing the alkali concentration in the salt mixture, and since the system forms a reciprocal salt-pair, representation within the usual square figure follows. If, as indicated above, the curves are projected on to the base from the edge $(\text{K}_2\text{SO}_4)_3-(\text{K}_2\text{O})_3$, the $(\text{CaSO}_4)_3$ corner in the projection would then be interpreted as representing the saturated solution of $\text{CaSO}_4 \cdot 2\text{H}_2\text{O}$ in K_2SO_4 solution (equivalent to 1 per cent KOH).

The quinary system involves the following quaternary systems, the first three of which are reciprocal salt-pairs:

- (1) $(\text{CaO})_3-(\text{CaSO}_4)_3-\text{Al}_2(\text{SO}_4)_3-\text{Al}_2\text{O}_3-\text{H}_2\text{O}$
- (2) $(\text{CaO})_3-(\text{CaSO}_4)_3-(\text{K}_2\text{SO}_4)_3-(\text{K}_2\text{O})_3-\text{H}_2\text{O}$
- (3) $\text{Al}_2\text{O}_3-\text{Al}_2(\text{SO}_4)_3-(\text{K}_2\text{SO}_4)_3-(\text{K}_2\text{O})_3-\text{H}_2\text{O}$
- (4) $(\text{CaSO}_4)_3-\text{Al}_2(\text{SO}_4)_3-(\text{K}_2\text{SO}_4)_3-\text{H}_2\text{O}$
- (5) $(\text{CaO})_3-\text{Al}_2\text{O}_3-(\text{K}_2\text{O})_3-\text{H}_2\text{O}$

Except for system (1) $(\text{CaO}-\text{Al}_2\text{O}_3-\text{CaSO}_4-\text{H}_2\text{O})$, which has previously been investigated by the writer, no data appear to be available in the literature on the remaining quaternary systems other than a very limited amount on the system (2) by Herold (7) and D'Ans and Schreiner (3). Accordingly, a limited amount of work has been carried out on these systems, attention being confined to an alkali concentration equivalent to 1 per cent KOH.

RESULTS

I. THE QUATERNARY SYSTEMS

The quaternary system $(\text{CaO})_3-(\text{CaSO}_4)_3-(\text{K}_2\text{SO}_4)_3-(\text{K}_2\text{O})_3-\text{H}_2\text{O}$

The solubility of $\text{CaSO}_4 \cdot 2\text{H}_2\text{O}$ in potassium sulfate solution (K_2SO_4 concentration equivalent to 1 per cent KOH), of crystalline $\text{Ca}(\text{OH})_2$ in 1 per cent KOH solution, the invariant point $\text{Ca}(\text{OH})_2-\text{CaSO}_4 \cdot 2\text{H}_2\text{O}$, and the solubility curves for $\text{CaSO}_4 \cdot 2\text{H}_2\text{O}$ and $\text{Ca}(\text{OH})_2$ have been determined. The value now obtained for the solubility of $\text{CaSO}_4 \cdot 2\text{H}_2\text{O}$ in K_2SO_4 solution (equivalent to 1 per cent KOH) is essentially in agreement with that obtained by Cameron and Breazeale (2). The present work gives 1.450 g. CaSO_4 per 1000 g. of solution (15.5 g. K_2SO_4 per 1000 g. of solution = 1 per cent KOH). It may be noted that in the ternary system $\text{CaSO}_4-\text{K}_2\text{SO}_4-\text{H}_2\text{O}$ no double salt is formed at the concentration of K_2SO_4 here used. Cameron and Breazeale (2) give for the invariant point $\text{CaSO}_4 \cdot 2\text{H}_2\text{O}-\text{CaSO}_4 \cdot \text{K}_2\text{SO}_4 \cdot \text{H}_2\text{O}$ the solution composition at 25°C .: 0.154 per cent CaSO_4 and 3.167 per cent K_2SO_4 (equivalent to 2 per cent KOH). In the quaternary system, D'Ans and Schreiner (3) give for the invariant point $\text{Ca}(\text{OH})_2-\text{CaSO}_4 \cdot 2\text{H}_2\text{O}-\text{CaSO}_4 \cdot \text{K}_2\text{SO}_4 \cdot \text{H}_2\text{O}$ the solution composition in moles per 1000 g. of solution at 25°C .: $\text{K}_2\text{SO}_4 = 0.158$, $\text{KOH} = 0.114$. The lime concentration is not stated. The total equivalent KOH concentration amounts to 2.4 per cent. The data now obtained are given in table 1 and plotted in figure 2, using triangular symbols. The projections of the corresponding boundary curves in the quinary system involving $\text{C}_3\text{A} \cdot 3\text{CaSO}_4 \cdot 32\text{H}_2\text{O}$ as additional solid phase are also plotted in this figure. They are coincident with the quaternary system solubility curves.

The quaternary system $\text{Al}_2\text{O}_3\text{--Al}_2(\text{SO}_4)_3\text{--}(\text{K}_2\text{SO}_4)_3\text{--}(\text{K}_2\text{O})_3\text{--H}_2\text{O}$

In dealing with the quaternary system $\text{CaO--Al}_2\text{O}_3\text{--CaSO}_4\text{--H}_2\text{O}$ (8) the ternary system $\text{Al}_2\text{O}_3\text{--Al}_2(\text{SO}_4)_3\text{--H}_2\text{O}$ was omitted. Similarly here, that part of the equilibria lying within the triangle $\text{Al}_2(\text{SO}_4)_3\text{--Al}_2\text{O}_3\text{--K}_2\text{SO}_4$ of figure 3 has not been

TABLE 1

The quaternary system $(\text{CaO})_3\text{--}(\text{CaSO}_4)_3\text{--}(\text{K}_2\text{SO}_4)_3\text{--}(\text{K}_2\text{O})_3\text{--H}_2\text{O}$

Solubility curve AB: $\text{CaSO}_4 \cdot 2\text{H}_2\text{O}$ (mixes B4, B5)

Invariant point B: $\text{CaSO}_4 \cdot 2\text{H}_2\text{O--Ca}(\text{OH})_2$ (mix A4)

Solubility curve BC: $\text{Ca}(\text{OH})_2$ (mixes B6, B3, B10)

NO.	TIME SHAKEN	GRAM-MOLES $\times 10^4$ PER 1000 G. OF SOLUTION				POSITIVE COMPONENTS = 100 PER CENT			NEGATIVE COMPONENTS = 100 PER CENT	
		$(\text{K}_2\text{O})_3$	$(\text{CaO})_3$	Al_2O_3	$(\text{SO}_3)_3$	$(\text{K}_2\text{O})_3$	$(\text{CaO})_3$	Al_2O_3	$(\text{SO}_3)_3$	$(\text{H}_2\text{O})_3$
	days					mole per cent	mole per cent	mole per cent	mole per cent	mole per cent
B4	28	295	35.6		331	89.3	10.7		100.1	-0.1
B5	7	296	38.1		304	88.6	11.4		91.0	9.0
A4	7	296	55.5		223	84.3	15.7		63.4	36.6
B6	15	297	24.1		117.6	92.5	7.5		36.6	63.4
B3	1	297	8.8			97.5	2.5			100
B10	14	297	8.4			97.6	2.4			100

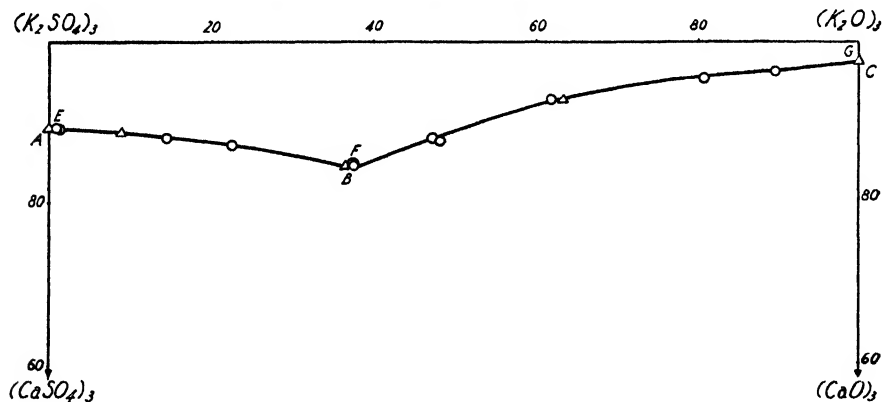


FIG. 2. Quinary system: projections of boundary curves from $\text{Al}_2(\text{SO}_4)_3\text{--Al}_2\text{O}_3$ edge. $\text{CaSO}_4 \cdot 2\text{H}_2\text{O--C}_3\text{A} \cdot 3\text{CaSO}_4 \cdot 32\text{H}_2\text{O}$ (EF); $\text{Ca}(\text{OH})_2\text{--C}_3\text{A} \cdot 3\text{CaSO}_4 \cdot 32\text{H}_2\text{O}$ (FG).

Quaternary system: solubility curves. $\text{CaSO}_4 \cdot 2\text{H}_2\text{O}$ (AB); $\text{Ca}(\text{OH})_2$ (BC).

examined, except to trace the continuation of the $\text{Al}_2\text{O}_3\text{aq.}$ boundary curve some distance within this area. The equilibria within the area $(\text{K}_2\text{O})_3\text{--Al}_2\text{O}_3\text{--}(\text{K}_2\text{SO}_4)_3$ consist entirely of the solubility curve for hydrated alumina. From previous work it is to be expected that the position of this curve will depend on the extent to which crystal aggregation has proceeded in the hydrated alumina. In the present investigation the position of the curve has been determined for (a)

alumina gel freshly precipitated in the cold (with one exception actually in the mix examined), using a 10-min. shaking period only, followed by immediate filtration; (b) a crystalline hydrated alumina using similar mixes to those employed in (a), but with a shaking period of 24 hr. during which the initially formed gel is converted into a characteristic crystalline product. The mixes were in general prepared from various combinations of potassium sulfate, potas-

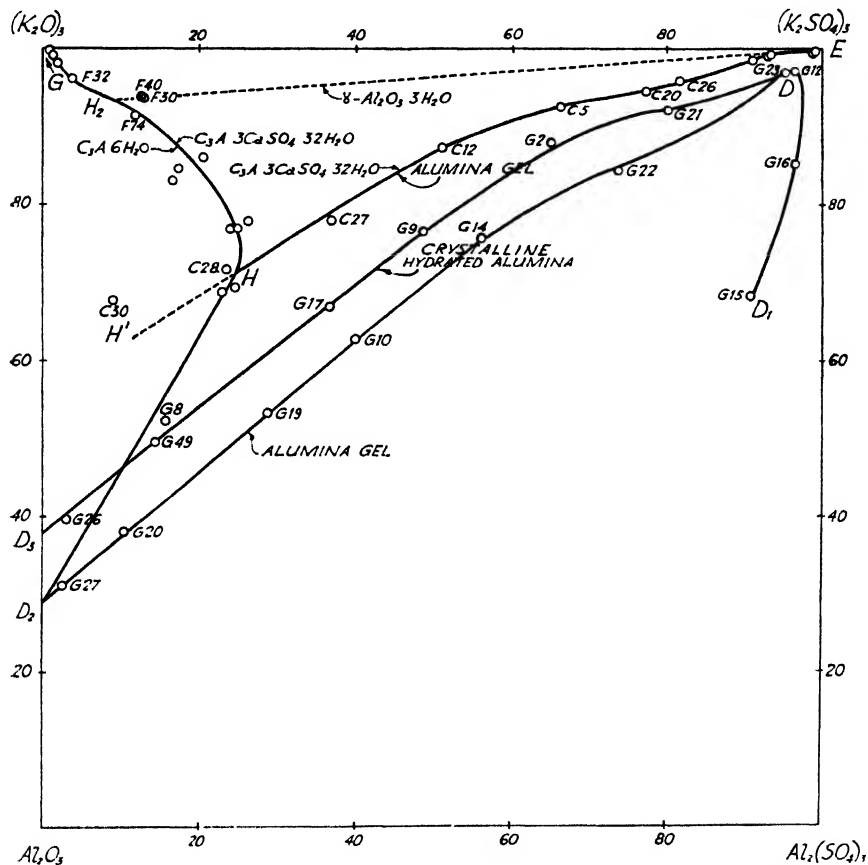


FIG. 3. Quinary system: projections of boundary curves from $(\text{CaO})_2$ - $(\text{CaSO}_4)_2$ edge. $\text{C}_3\text{A} \cdot 6\text{H}_2\text{O}$ - $\text{C}_3\text{A} \cdot 3\text{CaSO}_4 \cdot 32\text{H}_2\text{O}$ (GH); alumina gel- $\text{C}_3\text{A} \cdot 3\text{CaSO}_4 \cdot 32\text{H}_2\text{O}$ (EHH¹).

Quaternary system: solubility curves. Crystalline hydrated alumina (DD₂); alumina gel (D₁DD₂).

sium hydroxide, and a solution of aluminum in potassium hydroxide. These were made up to give 125 g. of solution containing the equivalent of 1 per cent KOH, and aluminum sulfate was added. In two cases, alumina gel precipitated in the cold from aluminum sulfate and potassium hydroxide and well washed was also used. In the case of the (α) series, before the addition of aluminum sulfate the mix was first allowed to stand in the thermostat until at 25°C., and

vigorously shaken after adding the finely powdered material. Under these conditions the unstable equilibrium is reached almost immediately. Data for both curves D_1DD_2 and DD_3 are given in table 2, and plotted in figure 3. (This figure also contains the projections from the $(CaO)_8-(CaSO_4)_3$ edge on to the face $Al_2O_3-(K_2O)_3-(K_2SO_4)_3-Al_2(SO_4)_3$ of the boundary curves $C_3A \cdot 6H_2O-C_3A \cdot 3CaSO_4 \cdot 32H_2O$ and $Al_2O_3 aq.-C_3A \cdot 3CaSO_4 \cdot 32H_2O$, which will be dealt with later). As regards the solid phases obtained along the two curves, microscopic examination

TABLE 2
The quaternary system $Al_2O_3-(K_2O)_3-(K_2SO_4)_3-Al_2(SO_4)_3-H_2O$
Solubility curve D_1D_2 : $Al_2O_3 aq.$
Solubility curve D_1D_3 : crystalline hydrated alumina

NO.	TIME SHAKEN	GRAM-MOLES $\times 10^4$ PER 1000 G. OF SOLUTION				POSITIVE COMPONENTS = 100 PER CENT			NEGATIVE COMPONENTS = 100 PER CENT	
		(K ₂ O) ₃	(CaO) ₃	Al ₂ O ₃	(SO ₂) ₃	(K ₂ O) ₃	(CaO) ₃	Al ₂ O ₃	(SO ₂) ₃	(H ₂ O) ₃
Solubility curve DDD ₂ : Al ₂ O ₃ aq.										
						mole per cent	mole per cent	mole per cent	mole per cent	mole per cent
G15	1 day	294		136	390	68.3		31.7	91.7	9.3
G16	1 day	295		51.3	334	85.2		14.8	96.5	3.5
G23	1 day	295		8.1	291	97.3		2.7	95.5	4.5
G12	10 min.	295		8.6	293	97.2		2.8	96.5	3.5
G22	10 min.	295		54.6	258	84.4		15.6	73.8	26.2
G14	10 min.	295		93.8	218	75.8		24.2	56.1	43.9
G10	10 min.	294		176	187	62.5		37.5	39.8	60.2
G19	10 min.	295		259	159	53.2		46.8	28.7	71.3
G20	10 min.	295		480	80.5	38.1		61.9	10.4	89.6
G27	10 min.	297		661	22.3	31.0		69.0	2.3	97.7
Solubility curve D ₁ D ₃ : crystalline hydrated alumina										
	days									
G21	1	295		25.6	257	92.0		8.0	80.1	19.9
G2	1	294		40.4	217	87.9		12.1	64.9	35.1
G9	1	294		90.0	187	76.5		23.5	48.7	51.3
G17	1	295		146	161	66.8		33.2	36.6	63.4
G49	1	295		301	86	49.5		50.5	14.4	85.6
G26	1	301		461	22.7	39.5		60.5	3.0	97.0

showed that mixes G15, G16, G12, and G23 (along D_1D), in all of which little or no potassium aluminate is present, yielded typical alumina gel in horny masses of refractive index 1.460 (after drying *in vacuo* over saturated ammonium sulfate solution). Along the alumina gel curve D_1DD_2 , from G22 into regions of increasing potassium aluminate content, a tendency was observed for the gel to become more powdery in character. In G22, the index was unaltered at 1.460, in G14 and G10 it had risen slightly to 1.465, while in G19 and G20 the value was 1.495. For mix G27, however, where rather more solid phase was present, the

value was 1.480. It is apparent that with increasing content of potassium aluminate in the system, the change alumina gel \rightarrow crystalline hydrated alumina is accelerated. With the short shaking periods employed, however, the curve obtained is substantially that for the freshly precipitated gel. Along the crystalline hydrated alumina curve DD_3 from mix G21 into regions of increasing potassium aluminate content, examination showed that the gel had been converted into a crystalline form. Mixes G21 and G2 contained masses of tiny birefringent crystals of mean index 1.555 ± 0.003 , while mixes G9, G17, G8, G49, and G26 contained typical birefringent crystals with indices 1.555, 1.575. It is evident from the data given that there is a considerable decrease in the solubility of the crystalline hydrated alumina here formed as compared with the gel initially precipitated, and it seems clear that with longer periods of shaking gradual conversion to the α - and γ -forms of $\text{Al}_2\text{O}_3 \cdot 3\text{H}_2\text{O}$ (the latter form has indices $\alpha = \beta = 1.566$, $\gamma = 1.587$) is to be expected with still further decreases in the equilibrium content of alumina in solution. There is a corresponding shift of the whole curve DD_3 towards the $(\text{K}_2\text{O})_3$ corner. The curve DD_3 , though it is for convenience termed the "crystalline hydrated alumina" curve, is not the equilibrium curve with respect to the most stable form of hydrated alumina, gibbsite. From the alumina gel curve a short extrapolation to D_2 yields the solubility of fresh alumina gel in a 1 per cent KOH solution: 7.4 g. Al_2O_3 per 1000 g. of solution. This is highly unstable and the solubility is soon reduced by conversion of the gel to a crystalline form. Thus the form present at the stage represented by curve (b) gives a solubility (by extrapolation to D_3) of only 4.7 g. Al_2O_3 per 1000 g. of solution.

Some tests made in the case of one initial mix composition to determine the Al_2O_3 content of the solution after various times of shaking gave the following results in grams of Al_2O_3 per 1000 g. of solution: 10 min., 4.91 (G20); 8 hr., 3.66; 24 hr., 3.07 (G49); 48 hr., 2.93; 168 hr., 2.70 (G51). The data fall on a smooth curve and show that after 24 hr. there is only a relatively slow fall in the Al_2O_3 concentration. To determine the water content of the hydrated alumina solid phase, in two cases, after 24 hr. (G49) and 168 hr. (G51), the solid phase (dried *in vacuo* over saturated ammonium sulfate solution) was ignited at 1000°C . The loss on ignition, 37.6 per cent in both cases, corresponds to a molar ratio $\text{H}_2\text{O}/\text{Al}_2\text{O}_3 = 3.4$.

The quaternary system $(\text{CaSO}_4)_3\text{-Al}_2(\text{SO}_4)_3\text{-(K}_2\text{SO}_4)_3\text{-H}_2\text{O}$

A portion only of the solubility curve for $\text{CaSO}_4 \cdot 2\text{H}_2\text{O}$ has been traced, using mixes of potassium sulfate, aluminium sulfate, and calcium sulfate. Data are given in table 3 and plotted in figure 4.

The quaternary system $(\text{CaO})_3\text{-Al}_2\text{O}_3\text{-(K}_2\text{O})_3\text{-H}_2\text{O}$

In this modification of the ternary system $\text{CaO-Al}_2\text{O}_3\text{-H}_2\text{O}$, we are concerned for the present essentially with the $\text{C}_3\text{A} \cdot 6\text{H}_2\text{O}$ solubility curve. The alumina gel curve for practical purposes disappears, since the $\text{C}_3\text{A} \cdot 6\text{H}_2\text{O}$ curve becomes eventually practically coincident with the Al_2O_3 axis. The data (table 4) were

obtained by shaking 0.300 g. $C_3A \cdot 6H_2O$ with potassium hydroxide (with and without dissolved aluminum) and calcium hydroxide. The $C_3A \cdot 6H_2O$ used was

TABLE 3
The quaternary system $(CaSO_4)_3-Al_2(SO_4)_3-(K_2SO_4)_3-H_2O$
Solubility curve AI: $CaSO_4 \cdot 2H_2O$

NO.	TIME SHAKEN	GRAM-MOLES $\times 10^4$ PER 1000 G. OF SOLUTION				POSITIVE COMPONENTS = 100 PER CENT			NEGATIVE COMPONENTS = 100 PER CENT	
		$(K_2O)_2$	$(CaO)_2$	Al_2O_3	$(SO_3)_2$	$(K_2O)_2$	$(CaO)_2$	Al_2O_3	$(SO_3)_2$	$(H_2O)_2$
	days					mole per cent	mole per cent	mole per cent	mole per cent	mole per cent
I2.....	28	294	35.6	12.6	342	85.9	10.4	3.6	100	
I1.....	28	294	36.1	43.5	373	78.8	9.6	11.6	100	
I5.....	28	293	36.1	86.1	412	70.6	8.7	20.7	99.3	0.7

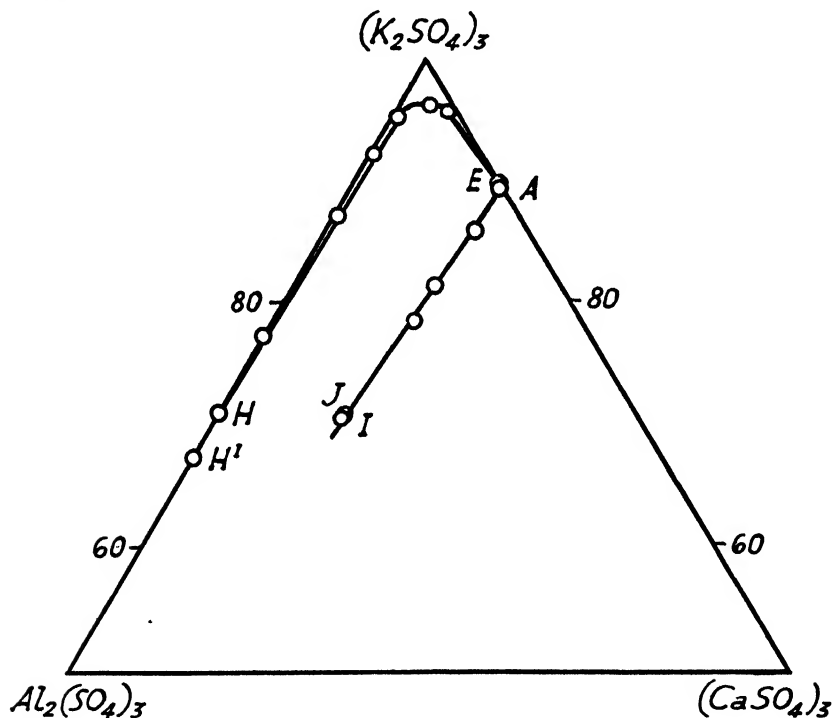


FIG. 4. Quaternary system: solubility curve. $CaSO_4 \cdot 2H_2O$ (AI).

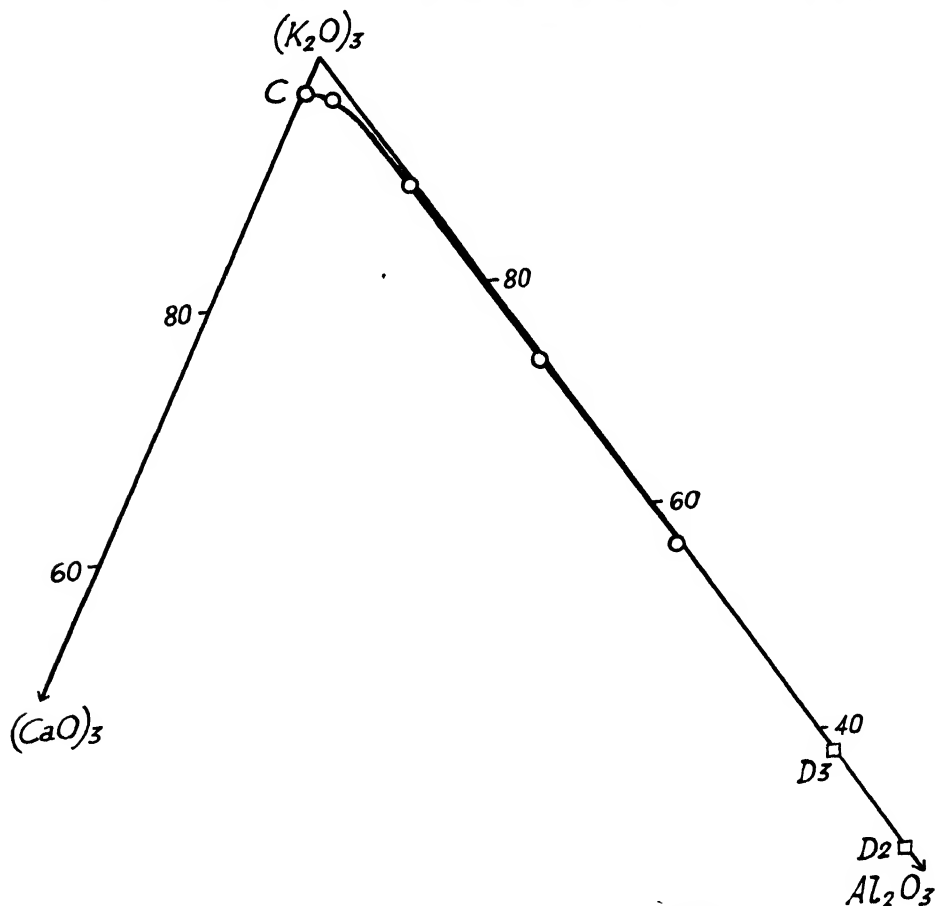
Quinary system: projection of boundary curves. $Al_2O_3 \text{ aq.} - C_3A \cdot 3CaSO_4 \cdot 32H_2O$ (EHH'); $Al_2O_3 \text{ aq.} - CaSO_4 \cdot 2H_2O$ (EJ).

that obtained by the method of Travers and Zahabi (15) and employed in previous work. It contained a small amount of the birefringent hexagonal plate form. The data are plotted in figure 5a. A comparison is given in figure 6

TABLE 4

The quaternary system $(\text{CaO})_3-\text{Al}_2\text{O}_3-(\text{K}_2\text{O})_3-\text{H}_2\text{O}$ Invariant point C: $\text{C}_3\text{A} \cdot 6\text{H}_2\text{O}-\text{Ca}(\text{OH})_2$ (mix J6)Solubility curve D_2C : $\text{C}_3\text{A} \cdot 6\text{H}_2\text{O}$ (other mixes)

NO.	TIME SHAKEN	GRAM-MOLES $\times 10^4$ PER 1000 G. OF SOLUTION				POSITIVE COMPONENTS = 100 PER CENT			NEGATIVE COMPONENTS = 100 PER CENT	
		$(\text{K}_2\text{O})_3$	$(\text{CaO})_3$	Al_2O_3	$(\text{SO}_3)_3$	$(\text{K}_2\text{O})_3$	$(\text{CaO})_3$	Al_2O_3	$(\text{SO}_3)_3$	$(\text{H}_2\text{O})_3$
	days					mole per cent	mole per cent	mole per cent	mole per cent	mole per cent
J6.	7	298	8.7	0.5		97.0	2.8	0.15		100
J1	7	298	4.1	8.1		96.1	1.3	2.6		100
J4.	7	298	0.55	38.1		88.5	0.2	11.3		100
J3.	7	299	0.45	110		73.0	0.1	26.9		100
J2	7	301	0.3	231		56.6	0.05	43.4		100

FIG. 5a. Quaternary system: solubility curve. $\text{C}_3\text{A} \cdot 6\text{H}_2\text{O}$ (D_2C)

with the $\text{CaO-Al}_2\text{O}_3\text{-H}_2\text{O}$ system as determined for alumina gel by Lea and Bessey (11). While the alumina gel curve is virtually absent, it must be recognized that for the crystalline product a short curve exists. With decrease in solubility this curve moves down the Al_2O_3 axis of figure 6, terminating in the minimum solubility values for $\gamma\text{-Al}_2\text{O}_3\cdot 3\text{H}_2\text{O}$. The position of this latter curve is tentatively shown in the figure at D_4D_5 . It may well fall below this. For Al_2O_3 concentrations greater than that corresponding to the invariant point $\gamma\text{-Al}_2\text{O}_3\cdot 3\text{H}_2\text{O-C}_3\text{A}\cdot 6\text{H}_2\text{O}$, the $\text{C}_3\text{A}\cdot 6\text{H}_2\text{O}$ curve is metastable. The invariant

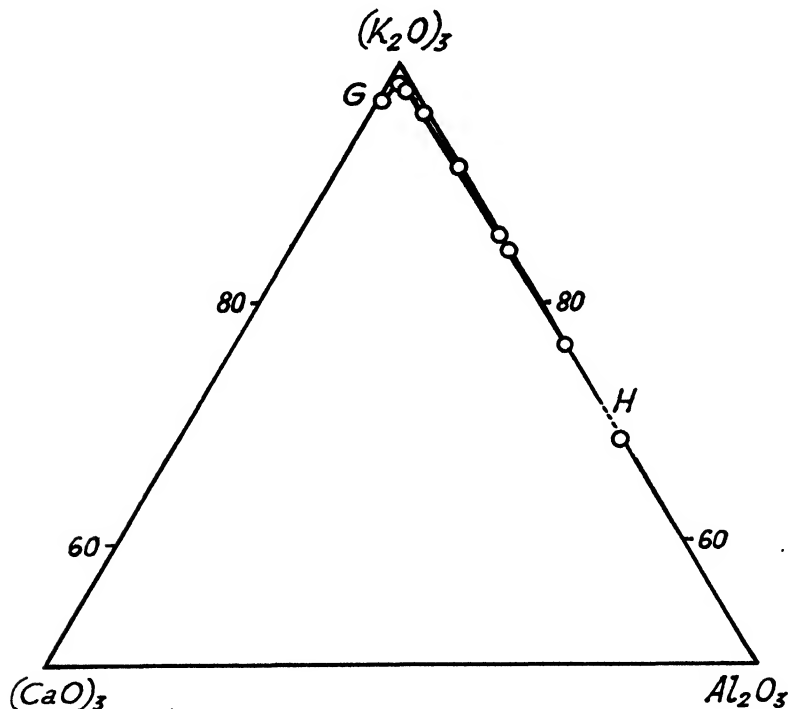


Fig. 5b. Quinary system: projection of boundary curves. $\text{C}_3\text{A}\cdot 6\text{H}_2\text{O-C}_3\text{A}\cdot 3\text{CaSO}_4\cdot 32\text{H}_2\text{O}$ (GH).

point $\text{C}_3\text{A}\cdot 6\text{H}_2\text{O-Ca(OH)}_2$ is experimentally coincident with the solubility of Ca(OH)_2 in 1 per cent KOH solution, and the same letter C is therefore used to denote both.

II. THE QUINARY SYSTEM

The following boundary curves and invariant points have been determined within the quinary system:

(a) Boundary curves:

- (1) $\text{Al}_2\text{O}_3\text{aq.}-\text{C}_3\text{A}\cdot 3\text{CaSO}_4\cdot 32\text{H}_2\text{O}$ (EH) and its unstable prolongation to H^1 (figures 3, 4, 8)

- (2) $\text{CaSO}_4 \cdot 2\text{H}_2\text{O}-\text{C}_3\text{A} \cdot 3\text{CaSO}_4 \cdot 32\text{H}_2\text{O}$ (EF) (figures 2, 8)
 (3) $\text{Ca}(\text{OH})_2-\text{C}_3\text{A} \cdot 3\text{CaSO}_4 \cdot 32\text{H}_2\text{O}$ (FG) (figures 2, 8)
 (4) $\text{C}_3\text{A} \cdot 6\text{H}_2\text{O}-\text{C}_3\text{A} \cdot 3\text{CaSO}_4 \cdot 32\text{H}_2\text{O}$ (GH) (figures 5b, 8)

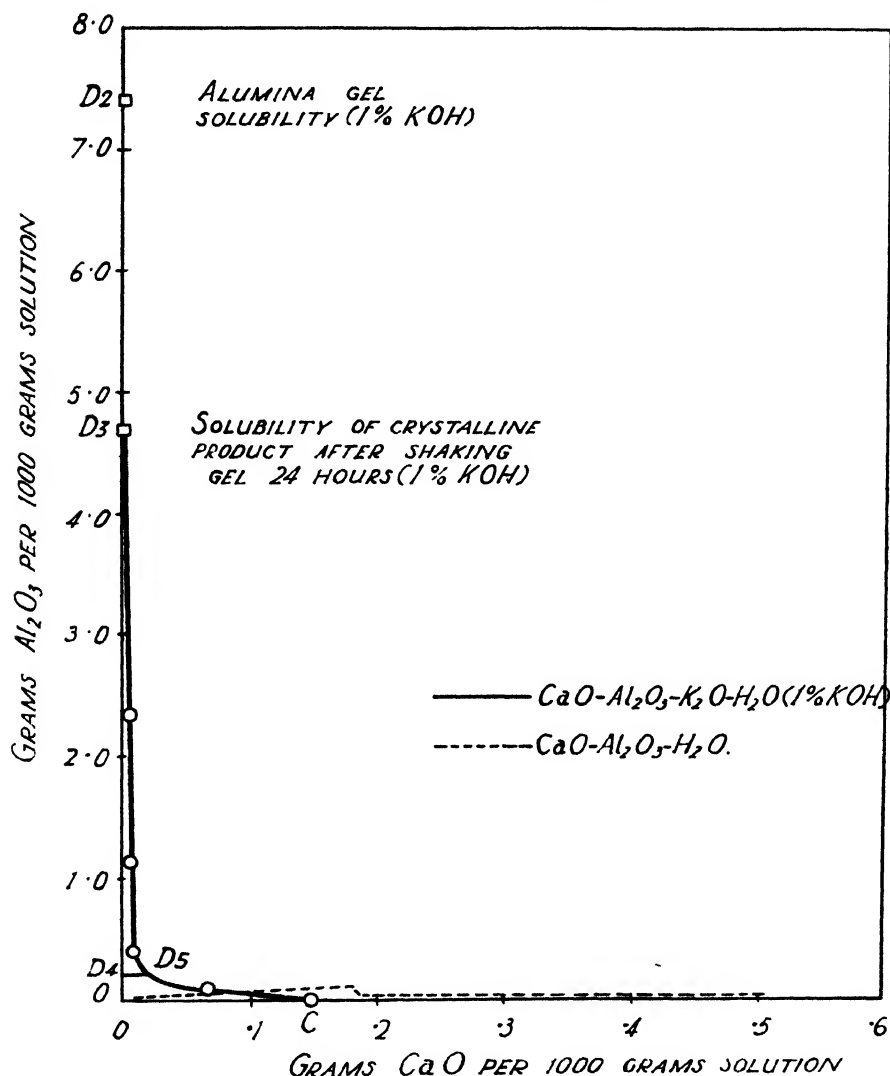


Fig. 6. Comparison at 25°C . of systems $\text{CaO}-\text{Al}_2\text{O}_3-\text{K}_2\text{O}-\text{H}_2\text{O}$ (1 per cent KOH) and $\text{CaO}-\text{Al}_2\text{O}_3-\text{H}_2\text{O}$.

(b) Invariant points:

- (1) $\text{CaSO}_4 \cdot 2\text{H}_2\text{O}-\text{Al}_2\text{O}_3\text{aq.}-\text{C}_3\text{A} \cdot 3\text{CaSO}_4 \cdot 32\text{H}_2\text{O}$ (E) (figures 2, 4, 8)
 (2) $\text{CaSO}_4 \cdot 2\text{H}_2\text{O}-\text{Ca}(\text{OH})_2-\text{C}_3\text{A} \cdot 3\text{CaSO}_4 \cdot 32\text{H}_2\text{O}$ (F) (figures 2, 8)
 (3) $\text{Ca}(\text{OH})_2-\text{C}_3\text{A} \cdot 6\text{H}_2\text{O}-\text{C}_3\text{A} \cdot 3\text{CaSO}_4 \cdot 32\text{H}_2\text{O}$ (G) (figures 2, 5b, 8)
 (4) $\text{C}_3\text{A} \cdot 3\text{CaSO}_4 \cdot 32\text{H}_2\text{O}-\text{C}_3\text{A} \cdot 6\text{H}_2\text{O}-\text{Al}_2\text{O}_3\text{aq.}$ (H) (figures 3, 4, 5b, 8)

The isothermal invariant point $\text{CaSO}_4 \cdot 2\text{H}_2\text{O} - \text{Al}_2\text{O}_3\text{aq.} - \text{C}_3\text{A} \cdot 3\text{CaSO}_4 \cdot 32\text{H}_2\text{O}$ (E) (figures 2, 4, 8)

The data are given in table 6 (mixes A25, A26). The invariant point was determined with suitable mixes of lime solution, aluminum sulfate, potassium sulfate, and calcium sulfate. As in the quaternary system, the alumina gel occurred as small rounded isotropic grains, refractive index 1.53.

TABLE 5
Boundary curve JE: $\text{CaSO}_4 \cdot 2\text{H}_2\text{O} - \text{Al}_2\text{O}_3\text{aq.}$

NO.	TIME SHAKEN	GRAM-MOLES $\times 10^4$ PER 1000 G. OF SOLUTION				POSITIVE COMPONENTS = 100 PER CENT			NEGATIVE COMPONENTS = 100 PER CENT	
		(K ₂ O) ₁	(CaO) ₁	Al ₂ O ₃	(SO ₃) ₁	(K ₂ O) ₂	(CaO) ₂	Al ₂ O ₃	(SO ₃) ₂	(H ₂ O) ₂
	days					mole per cent	mole per cent	mole per cent	mole per cent	mole per cent
I7.....	7	293	36.0	31.9	355	81.2	10.0	8.8	98.4	1.6
I8.....	7	292	35.9	83.6	397	71.0	8.7	20.3	96.2	3.5

TABLE 6
Invariant point E: $\text{CaSO}_4 \cdot 2\text{H}_2\text{O} - \text{Al}_2\text{O}_3\text{aq.} - \text{C}_3\text{A} \cdot 3\text{CaSO}_4 \cdot 32\text{H}_2\text{O}$ (mixes A25, A26)
Boundary curve EHH: $\text{Al}_2\text{O}_3\text{aq.} - \text{C}_3\text{A} \cdot 3\text{CaSO}_4 \cdot 32\text{H}_2\text{O}$ (other mixes)

NO.	TIME SHAKEN	GRAM-MOLES $\times 10^4$ PER 1000 G. OF SOLUTION				POSITIVE COMPONENTS = 100 PER CENT			NEGATIVE COMPONENTS = 100 PER CENT	
		(K ₂ O) ₁	(CaO) ₁	Al ₂ O ₃	(SO ₃) ₁	(K ₂ O) ₂	(CaO) ₂	Al ₂ O ₃	(SO ₃) ₂	(H ₂ O) ₂
	days					mole per cent	mole per cent	mole per cent	mole per cent	mole per cent
A25.....	7	295	35.5	1.7	329	88.8	10.7	0.5	99.0	1.0
A26.....	28	295	35.7	0.9	329	89.0	10.8	0.25	99.2	0.8
C11.....	28	296	11.3	2.05	289	95.7	3.65	0.65	93.4	6.6
C17.....	7	295	6.5	4.95	279	96.3	2.1	1.6	91.0	9.0
C26.....	7	294	1.5	12.5	255	94.3	0.5	4.0	81.7	18.3
C5.....	7	294	0.8	23.8	212	92.4	0.25	7.4	66.6	33.4
O12.....	28	292	0.7	43.0	171	87.2	0.2	12.6	51.0	49.0
C27.....	7	297		85.6	141	77.6		22.4	36.8	63.2
C28.....	7	297		117	97	71.7		28.3	23.5	76.5
C30.....	7	297		142	39.5	67.6		32.4	9.0	91.0

The boundary curve $\text{CaSO}_4 \cdot 2\text{H}_2\text{O} - \text{C}_3\text{A} \cdot 3\text{CaSO}_4 \cdot 32\text{H}_2\text{O}$ (EF) (figures 2, 8)

The boundary curve $\text{Ca}(\text{OH})_2 - \text{C}_3\text{A} \cdot 3\text{CaSO}_4 \cdot 32\text{H}_2\text{O}$ (FG) (figures 2, 8)

The invariant point $\text{CaSO}_4 \cdot 2\text{H}_2\text{O} - \text{Ca}(\text{OH})_2 - \text{C}_3\text{A} \cdot 3\text{CaSO}_4 \cdot 32\text{H}_2\text{O}$ (F) (figures 2, 8)

The boundary curves are shown in figure 2 as a projection on to the face $(\text{CaO})_3 - (\text{K}_2\text{O})_3 - (\text{K}_2\text{SO}_4)_3 - (\text{CaSO}_4)_3$ of the prism from the $\text{Al}_2\text{O}_3 - \text{Al}_2(\text{SO}_4)_3$ edge, and in figure 8 as a projection on to the base as described previously. The data (table 7) were obtained with mixes involving lime, calcium sulfate, potassium sulfate, aluminum sulfate, and potassium hydroxide in suitable proportions.

$\text{C}_3\text{A} \cdot 3\text{CaSO}_4 \cdot 32\text{H}_2\text{O}$ is formed by reaction between aluminum sulfate and lime. While the $\text{C}_3\text{A} \cdot 3\text{CaSO}_4 \cdot 32\text{H}_2\text{O}$ obtained was on the whole satisfactory in showing characteristic form, occasionally the form was poor and the needles small, tending to occur as groups showing a mottled appearance. This is apparently to be ascribed to the alkali present and the correspondingly small solubility of

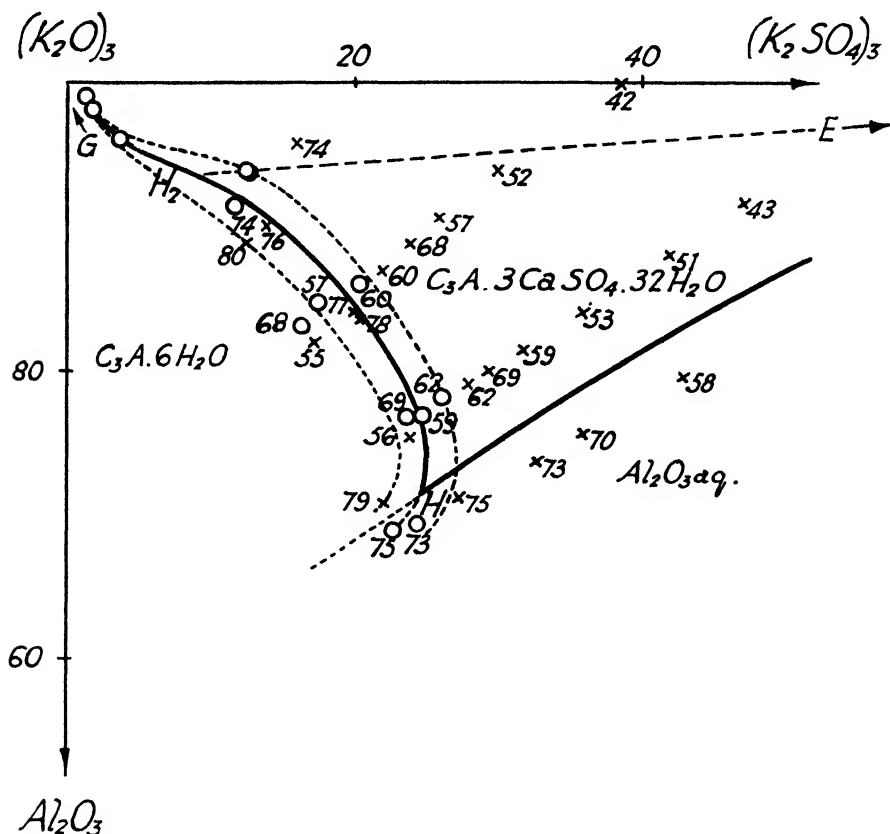


FIG. 7. Determination of boundary curve $\text{C}_3\text{A} \cdot 6\text{H}_2\text{O}-\text{C}_3\text{A} \cdot 3\text{CaSO}_4 \cdot 32\text{H}_2\text{O}$ within metastable region H_2H .

lime, but it does not appear that the size and form of the crystals deteriorates with increase in alkali content.

The invariant point $\text{Ca}(\text{OH})_2-\text{C}_3\text{A} \cdot 3\text{CaSO}_4 \cdot 32\text{H}_2\text{O}-\text{C}_3\text{A} \cdot 6\text{H}_2\text{O}$ (G) (figures 2, 5b, 8)

This point was obtained in two ways: (1) from a suitable mix of potassium hydroxide, lime, and aluminum sulfate, with the addition of $\text{C}_3\text{A} \cdot 6\text{H}_2\text{O}$ and crystalline $\text{Ca}(\text{OH})_2$ (table 8, mixes A11, A22); (2) from a mix of potassium hydroxide and calcium sulfate solution, with the addition of $\text{C}_3\text{A} \cdot 6\text{H}_2\text{O}$ and $\text{Ca}(\text{OH})_2$ (table 8, mix F15).

The boundary curve $\text{Al}_2\text{O}_3\text{aq.}-\text{C}_3\text{A}\cdot 3\text{CaSO}_4\cdot 32\text{H}_2\text{O}$ (EHH¹) (figures 3, 4, 8)

The curve is shown in figure 3 as a projection on to the face $\text{Al}_2\text{O}_3-(\text{K}_2\text{O})_3-(\text{K}_2\text{SO}_4)_3-\text{Al}_2(\text{SO}_4)_3$ of the prism from the $(\text{CaO})_3-(\text{CaSO}_4)_3$ edge, and in figure 8 as a projection on to the base. Points C4, C11, C17, C26, C20, C5 were obtained as follows: First a mix of lime solution and aluminum sulfate was shaken for 1

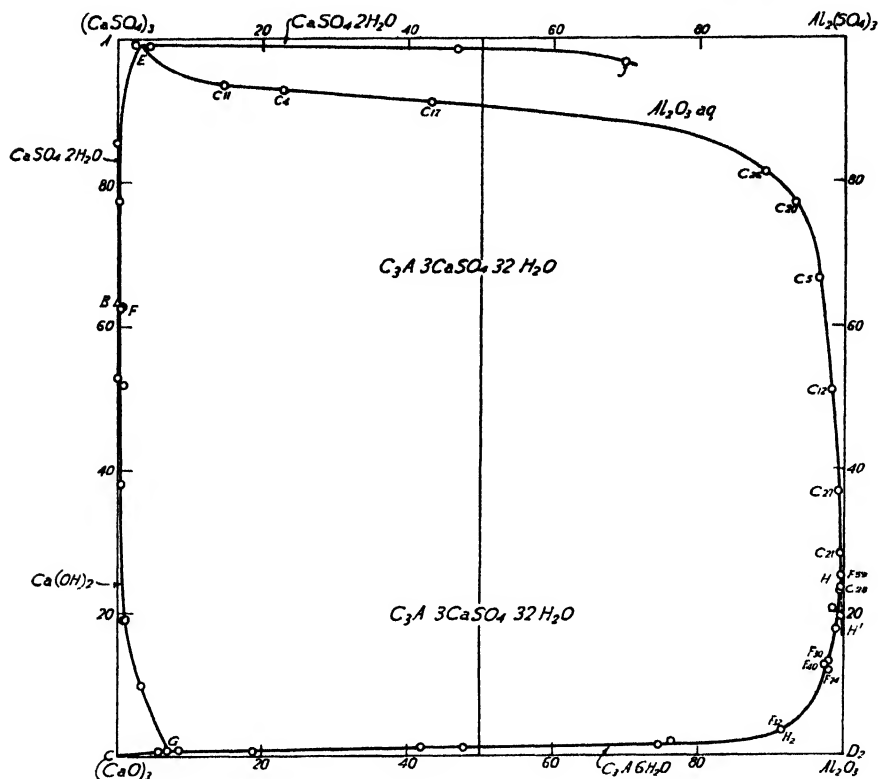


FIG. 8. Quinary system $\text{CaO}-\text{Al}_2\text{O}_3-\text{CaSO}_4-\text{K}_2\text{O}-\text{H}_2\text{O}$ (1 per cent KOH): projection on base of space figure.

$\text{Al}_2\text{O}_3\text{aq.}-\text{C}_3\text{A}\cdot 3\text{CaSO}_4\cdot 32\text{H}_2\text{O}$ (EHH¹) $\text{CaSO}_4\cdot 2\text{H}_2\text{O}-\text{C}_3\text{A}\cdot 3\text{CaSO}_4\cdot 32\text{H}_2\text{O}$ (EF)

$\text{Al}_2\text{O}_3\text{aq.}-\text{C}_3\text{A}\cdot 6\text{H}_2\text{O}$ (HD₂) $\text{CaSO}_4\cdot 2\text{H}_2\text{O}-\text{Ca}(\text{OH})_2$ (BF)

$\text{Al}_2\text{O}_3\text{aq.}-\text{CaSO}_4\cdot 2\text{H}_2\text{O}$ (EJ) $\text{Ca}(\text{OH})_2-\text{C}_3\text{A}\cdot 3\text{CaSO}_4\cdot 32\text{H}_2\text{O}$ (FG)

$\text{Ca}(\text{OH})_2-\text{C}_3\text{A}\cdot 6\text{H}_2\text{O}$ (GC)

$\text{C}_3\text{A}\cdot 6\text{H}_2\text{O}-\text{C}_3\text{A}\cdot 3\text{CaSO}_4\cdot 32\text{H}_2\text{O}$ (GH)

day, giving a $\text{C}_3\text{A}\cdot 3\text{CaSO}_4\cdot 32\text{H}_2\text{O}$ -lime water mix. To this was added suitable proportions of potassium sulfate, potassium hydroxide, and aluminum sulfate, and the resulting mix shaken, usually for 7 days. From mix C12 and on into regions of lower K_2SO_4 content, it was necessary to add increasing amounts of precipitated alumina gel to the initial mix. In general, the method of preparation was as follows: An initial 1-day mix was first prepared as described above. Varying amounts of alumina gel (precipitated at room temperature from alu-

minum sulfate and lime solutions) were then added, and the mix shaken with the necessary amount of alkali (equivalent to 1 per cent KOH) for half an hour.

TABLE 7

Boundary curve EF: $\text{CaSO}_4 \cdot 2\text{H}_2\text{O-C}_3\text{A} \cdot 3\text{CaSO}_4 \cdot 32\text{H}_2\text{O}$ (mixes A5, A19)

Invariant point F: $\text{CaSO}_4 \cdot 2\text{H}_2\text{O-Ca(OH)}_2\text{-C}_3\text{A} \cdot 3\text{CaSO}_4 \cdot 32\text{H}_2\text{O}$ (mixes A12, A24)

Boundary curve FG: $\text{Ca(OH)}_2\text{-C}_3\text{A} \cdot 3\text{CaSO}_4 \cdot 32\text{H}_2\text{O}$ (mixes A16, A8, A15)

NO.	TIME SHAKEN	GRAM-MOLES $\times 10^4$ PER 1000 G. OF SOLUTION				POSITIVE COMPONENTS = 100 PER CENT			NEGATIVE COMPONENTS = 100 PER CENT	
		(K ₂ O) ₂	(CaO) ₂	Al ₂ O ₃	(SO ₃) ₂	(K ₂ O) ₂	(CaO) ₂	Al ₂ O ₃	(SO ₃) ₂	(H ₂ O) ₂
	days					mole per cent	mole per cent	mole per cent	mole per cent	mole per cent
A5	7	297	41.2	0	289	87.8	12.2	0.0	85.5	14.5
A19	7	297	44.4	0.15	264	87.1	13.0	0.05	77.3	22.7
A12	7	297	54.7	0.3	220	84.4	15.5	0.1	62.5	37.5
A24	28	297	55.3	0.15	220	84.3	15.7	0.05	62.4	37.6
A16	28	297	42.6	0.4	176	87.4	12.5	0.1	51.7	48.3
A8	7	297	24.2	0.1	122	92.5	7.5	0.05	38.0	62.0
A15	28	297	13.7	0.15	59.5	95.5	4.5	0.05	19.2	80.8

TABLE 8

Invariant point G: $\text{Ca(OH)}_2\text{-C}_3\text{A} \cdot 3\text{CaSO}_4 \cdot 32\text{H}_2\text{O-C}_3\text{A} \cdot 6\text{H}_2\text{O}$ (mixes A11, A22, F15)

Boundary curve GH: $\text{C}_3\text{A} \cdot 3\text{CaSO}_4 \cdot 32\text{H}_2\text{O-C}_3\text{A} \cdot 6\text{H}_2\text{O}$ (other mixes)

NO.	TIME SHAKEN	GRAM-MOLES $\times 10^4$ PER 1000 G. OF SOLUTION				POSITIVE COMPONENTS = 100 PER CENT			NEGATIVE COMPONENTS = 100 PER CENT	
		(K ₂ O) ₂	(CaO) ₂	Al ₂ O ₃	(SO ₃) ₂	(K ₂ O) ₂	(CaO) ₂	Al ₂ O ₃	(SO ₃) ₂	(H ₂ O) ₂
	days					mole per cent	mole per cent	mole per cent	mole per cent	mole per cent
A11	7	297	8.7	0.8	2.6	96.9	2.8	0.25	0.85	99.2
A22	28	297	9.0	0.55	2.1	96.9	2.9	0.2	0.7	99.3
F15	28	297	8.6	0.65	2.1	96.9	2.8	0.2	0.7	99.3
F45	28	297	3.1	2.25	3.5	98.2	1.0	0.75	1.2	98.8
F39	28	297	1.8	5.8	5.6	97.5	0.6	1.9	1.8	98.2
F32	7	297	1.1	12.0	10.8	95.7	0.4	3.9	3.5	96.5
F40	28	297	0.5	19.5	39.8	93.7	0.15	6.15	12.6	87.4
F74	7	297	0.6	27.5	38.2	91.3	0.2	8.5	11.8	88.2
F57	7	297	0.4	54.3	1.5	84.5	0.1	15.4	17.5	82.5
F60	7	297	0.7	49.0	71.0	85.7	0.2	14.1	20.5	79.5
F59	7	297		89.0	96.0	76.9		23.1	24.9	75.1
F75	7	297		134.5	98.0	68.8		31.2	22.8	77.2

Finally, varying amounts of aluminum sulfate were added and the mix shaken, usually for 7 days. The data are given in table 6. The solid phase consisted of $\text{C}_3\text{A} \cdot 3\text{CaSO}_4 \cdot 32\text{H}_2\text{O}$ and an alumina gel phase consisting of rounded or ir-

regularly shaped material, isotropic, and with refractive index 1.525–1.530. It may be noted that in contrast to the hydrated alumina curve of the quaternary system $\text{Al}_2\text{O}_3\text{--}(\text{K}_2\text{O})_3\text{--}(\text{K}_2\text{SO}_4)_3\text{--}\text{Al}_2(\text{SO}_4)_3\text{--H}_2\text{O}$, the hydrated alumina phase was still present as an isotropic gel. The presence of lime in the initial mix appears effectively to inhibit the formation of a crystalline phase. While the boundary curve has been drawn as a straight line between points C27 and C28, the disposition of the various points in the more alkaline region suggests that the curve may bend upwards, slightly concave to the $(\text{K}_2\text{O})_3\text{--}(\text{K}_2\text{SO}_4)_3$ edge in figure 3.

For comparison, a rough indication of the expected position of a stable $\gamma\text{-Al}_2\text{O}_3\cdot 3\text{H}_2\text{O}\text{--C}_3\text{A}\cdot 3\text{CaSO}_4\cdot 32\text{H}_2\text{O}$ boundary curve is given by the broken line EH_2 in figure 3. The actual position remains to be determined.

The invariant point $\text{C}_3\text{A}\cdot 3\text{CaSO}_4\cdot 32\text{H}_2\text{O}\text{--C}_3\text{A}\cdot 6\text{H}_2\text{O}\text{--Al}_2\text{O}_3\text{aq. (H)}$ (figures 3, 4, 5b, 8)

Theoretically it is to be expected that this invariant point may be attained with suitable mixes of $\text{C}_3\text{A}\cdot 6\text{H}_2\text{O}$ and various combinations of alumina gel, aluminum sulfate, lime, calcium sulfate, and alkali. However, the addition of 1 g. of $\text{C}_3\text{A}\cdot 6\text{H}_2\text{O}$ to a mix made up as for C28 on the $\text{Al}_2\text{O}_3\text{aq.}\text{--C}_3\text{A}\cdot 3\text{CaSO}_4\cdot 32\text{H}_2\text{O}$ boundary curve resulted after 7 days' shaking in complete conversion of the $\text{C}_3\text{A}\cdot 6\text{H}_2\text{O}$, the solid phases found being $\text{Al}_2\text{O}_3\text{aq.}$ and $\text{C}_3\text{A}\cdot 3\text{CaSO}_4\cdot 32\text{H}_2\text{O}$. The equilibrium solution composition is shown at C30. The invariant point may be indirectly determined by the intersection of the boundary curves $\text{Al}_2\text{O}_3\text{aq.}\text{--C}_3\text{A}\cdot 3\text{CaSO}_4\cdot 32\text{H}_2\text{O}$ and $\text{C}_3\text{A}\cdot 6\text{H}_2\text{O}\text{--C}_3\text{A}\cdot 3\text{CaSO}_4\cdot 32\text{H}_2\text{O}$ at H. The invariant point composition in grams per 1000 g. of solution is $\text{CaO} = \text{nil}$, $\text{Al}_2\text{O}_3 = 1.21$, $\text{SO}_3 = 2.43$ (1 per cent KOH).

The boundary curve $\text{C}_3\text{A}\cdot 3\text{CaSO}_4\cdot 32\text{H}_2\text{O}\text{--C}_3\text{A}\cdot 6\text{H}_2\text{O}$ (GH) (figures 5b, 8)

This curve is shown projected on to the $(\text{K}_2\text{O})_3\text{--}(\text{CaO})_3\text{--Al}_2\text{O}_3$ face in figure 5b, on to the face $\text{Al}_2\text{O}_3\text{--}(\text{K}_2\text{O})_3\text{--}(\text{K}_2\text{SO}_4)_3\text{--Al}_2(\text{SO}_4)_3$ in figure 3, and on to the base of the prism in figure 8. Selected data are given in table 8. The curve was obtained by means of mixes of 0.300 g. of $\text{C}_3\text{A}\cdot 6\text{H}_2\text{O}$ and 125 g. of solution containing varying amounts of potassium sulfate and potassium hydroxide together with added crystalline $\text{Ca}(\text{OH})_2$ in that portion of the curve lying between the invariant point G and points F30, F40 (figure 3), and aluminum sulfate in that lying between points F30, F40, and the invariant point H. It seems probable that these two portions of the curve correspond approximately to stable and metastable equilibria, respectively, since the fundamentally stable curve $\text{C}_3\text{A}\cdot 3\text{CaSO}_4\cdot 32\text{H}_2\text{O}\text{--}\gamma\text{-Al}_2\text{O}_3\cdot 3\text{H}_2\text{O}$ probably cuts the $\text{C}_3\text{A}\cdot 6\text{H}_2\text{O}\text{--C}_3\text{A}\cdot 3\text{CaSO}_4\cdot 32\text{H}_2\text{O}$ curve in the neighborhood of F30, F40. Formation of $\text{C}_3\text{A}\cdot 3\text{CaSO}_4\cdot 32\text{H}_2\text{O}$ may occur in different ways, depending on the initial composition of the mix, thus:

- (1) $\text{C}_3\text{A}\cdot 6\text{H}_2\text{O} + 3\text{Ca}(\text{OH})_2 + 3\text{K}_2\text{SO}_4 \longrightarrow \text{C}_3\text{A}\cdot 3\text{CaSO}_4\cdot 32\text{H}_2\text{O} + 6\text{KOH}$
- (2) $2\text{C}_3\text{A}\cdot 6\text{H}_2\text{O} + 3\text{K}_2\text{SO}_4 \longrightarrow \text{C}_3\text{A}\cdot 3\text{CaSO}_4\cdot 32\text{H}_2\text{O} + 6\text{KOH} + \text{A}$
- (3) $2\text{C}_3\text{A}\cdot 6\text{H}_2\text{O} + \text{Al}_2(\text{SO}_4)_3 \longrightarrow \text{C}_3\text{A}\cdot 3\text{CaSO}_4\cdot 32\text{H}_2\text{O} + \text{A}$

It was found that the partial reaction of the $\text{C}_3\text{A}\cdot 6\text{H}_2\text{O}$ removed entirely the proportion of hexagonal plate form of $\text{C}_3\text{A}\cdot \text{aq.}$ present in the initial material, as

shown by the disappearance of birefringent "needles," this form evidently reacting, as is to be expected, more easily than the cubic $\text{C}_3\text{A} \cdot 6\text{H}_2\text{O}$. The position of that portion of the curve lying between point F32 and the invariant point H was found difficult to define precisely. The cause of this appears to be that in this region the fields for both $\text{C}_3\text{A} \cdot 6\text{H}_2\text{O}$ and $\text{C}_3\text{A} \cdot 3\text{CaSO}_4 \cdot 32\text{H}_2\text{O}$ lie practically in the $\text{Al}_2\text{O}_3\text{-(K}_2\text{O)}_3\text{-(K}_2\text{SO}_4)_3\text{-Al}_2(\text{SO}_4)_3$ face, the CaO content of the equilibrium solutions being very small. Since these fields are practically in the same plane in this region and there is, therefore, no abrupt change in the concentrations of the components on passing from one field to the other, it is not surprising that there is a lack of definiteness in the position of the boundary curve. (A parallel to this may exist in a ternary system. In the case of the solubility curves for two compounds A and B meeting in an invariant point P, these may meet at widely different angles or may be virtually in the same straight line or curve. In other words, there is no abrupt change in the concentrations of the components. Just as for the boundary curve above, the position of P may be expected to be difficult to determine precisely.) The procedure adopted within this region is illustrated in figure 7. Parallel series of mixes were made up and shaken for 7 days. Initial concentrations are shown by crosses. The 7-day period was found sufficient to reach equilibrium. The initial concentrations were made up to correspond with the direction of the change in solution concentrations during the conversion of $\text{C}_3\text{A} \cdot 6\text{H}_2\text{O}$ to $\text{C}_3\text{A} \cdot 3\text{CaSO}_4 \cdot 32\text{H}_2\text{O}$. Microscopic examination showed—proceeding towards the $(\text{K}_2\text{O})_3\text{-Al}_2\text{O}_3$ edge—either nearly complete conversion of $\text{C}_3\text{A} \cdot 6\text{H}_2\text{O}$ (mixes 42, 52; 43, 51, 53; 58, 70), or partial conversion (mixes 57, 58, 60; 59, 69, 62; 73, 75), or no formation of $\text{C}_3\text{A} \cdot 3\text{CaSO}_4 \cdot 32\text{H}_2\text{O}$ (mixes 77, 78, 55; 56; 79). The small amount of $\text{C}_3\text{A} \cdot 6\text{H}_2\text{O}$ remaining in mixes where it is clear that theoretically complete conversion should be effected is apparently due to the formation of a protective coating around a small proportion of the grains. Such a coating might arise either by a direct formation of $\text{C}_3\text{A} \cdot 3\text{CaSO}_4 \cdot 32\text{H}_2\text{O}$ on the surface of the grains, or by the formation of a skin of CaCO_3 by reaction with traces of carbonate in the potassium hydroxide used. It may be noted that in the reaction of crystalline $\text{Al}_2\text{O}_3 \cdot 3\text{H}_2\text{O}$ with lime and calcium sulfate solutions, it has previously been found that an inhibiting coating, apparently of $\text{C}_3\text{A} \cdot 3\text{CaSO}_4 \cdot 32\text{H}_2\text{O}$, is formed. Analysis of those mixes showing partial conversion of $\text{C}_3\text{A} \cdot 6\text{H}_2\text{O}$ yielded the points shown by the circles in the figure. These lie within a band of concentrations enclosed by the dotted lines, and it seems that for the reason given the originally sharply demarcated boundary curve has now become diffuse. Of the other numbered mixes shown, 74 gave a partial conversion to $\text{C}_3\text{A} \cdot 3\text{CaSO}_4 \cdot 32\text{H}_2\text{O}$, while 76 and 80 showed the presence of traces of $\text{C}_3\text{A} \cdot 3\text{CaSO}_4 \cdot 32\text{H}_2\text{O}$. Mixes 80, 78, and 79 were originally made up with an additional small quantity of calcium sulfate corresponding to 0.0205 g. CaSO_4 per 1000 g. of solution. The purpose of this was to react with any traces of carbonate present in the potassium hydroxide used before the $\text{C}_3\text{A} \cdot 6\text{H}_2\text{O}$ was added, and hence to guard against the possibility of a protective carbonate film forming over the $\text{C}_3\text{A} \cdot 6\text{H}_2\text{O}$ grains. The approximate position of the boundary between the two fields is shown by the full line in figure 7, meeting the boundary

curve $\text{Al}_2\text{O}_3\text{aq.}-\text{C}_3\text{A}\cdot 3\text{CaSO}_4\cdot 32\text{H}_2\text{O}$ in the invariant point H. It will be clear that this invariant point also cannot be precisely defined.

The space figure and the basal projection

The spacial relations of the various curves are shown in figure 1. The curves and invariant points given are as follows:

I. The quaternary systems:

- (i) System $\text{H}_2\text{O}-(\text{CaO})_3-\text{Al}_2\text{O}_3-(\text{K}_2\text{O})_3$
 D_2 = solubility of $\text{Al}_2\text{O}_3\text{aq.}$ (fresh gel) in 1 per cent KOH solution
 D_2C = $\text{C}_3\text{A}\cdot 6\text{H}_2\text{O}$
 C = solubility of $\text{Ca}(\text{OH})_2$ in 1 per cent KOH solution
- (ii) System $\text{H}_2\text{O}-(\text{CaO})_3-(\text{CaSO}_4)_3-(\text{K}_2\text{SO}_4)_3-(\text{K}_2\text{O})_3$
 AB = $\text{CaSO}_4\cdot 2\text{H}_2\text{O}$
 BC = $\text{Ca}(\text{OH})_2$
- (iii) System $\text{H}_2\text{O}-\text{Al}_2\text{O}_3-\text{Al}_2(\text{SO}_4)_3-(\text{K}_2\text{SO}_4)_3-(\text{K}_2\text{O})_3$
 D_2D_1 = $\text{Al}_2\text{O}_3\text{aq.}$ (fresh gel)
 DD_3 = crystalline hydrated alumina (not shown in figure 1; see figure 3)
- (iv) System $\text{H}_2\text{O}-(\text{CaSO}_4)_3-\text{Al}_2(\text{SO}_4)_3-(\text{K}_2\text{SO}_4)_3$
 A = solubility of $\text{CaSO}_4\cdot 2\text{H}_2\text{O}$ in K_2SO_4 solution (\equiv 1 per cent KOH)
 AI = $\text{CaSO}_4\cdot 2\text{H}_2\text{O}$

II. The quinary systems:

(i) Boundary curves:

- JE = $\text{CaSO}_4\cdot 2\text{H}_2\text{O}-\text{Al}_2\text{O}_3\text{aq.}$ (gel)
- EH = $\text{Al}_2\text{O}_3\text{aq.}-\text{C}_3\text{A}\cdot 3\text{CaSO}_4\cdot 32\text{H}_2\text{O}$
- HH^1 = unstable prolongation of EH
- EF = $\text{CaSO}_4\cdot 2\text{H}_2\text{O}-\text{C}_3\text{A}\cdot 3\text{CaSO}_4\cdot 32\text{H}_2\text{O}$
- BF = $\text{CaSO}_4\cdot 2\text{H}_2\text{O}-\text{Ca}(\text{OH})_2$
- FG = $\text{Ca}(\text{OH})_2-\text{C}_3\text{A}\cdot 3\text{CaSO}_4\cdot 32\text{H}_2\text{O}$
- GC = $\text{Ca}(\text{OH})_2-\text{C}_3\text{A}\cdot 6\text{H}_2\text{O}$
- GH = $\text{C}_3\text{A}\cdot 6\text{H}_2\text{O}-\text{C}_3\text{A}\cdot 3\text{CaSO}_4\cdot 32\text{H}_2\text{O}$
- HD_2 = $\text{C}_3\text{A}\cdot 6\text{H}_2\text{O}-\text{Al}_2\text{O}_3\text{aq.}$ (gel)

(ii) Invariant points:

- E = $\text{CaSO}_4\cdot 2\text{H}_2\text{O}-\text{Al}_2\text{O}_3\text{aq.}-\text{C}_3\text{A}\cdot 3\text{CaSO}_4\cdot 32\text{H}_2\text{O}$
- F = $\text{CaSO}_4\cdot 2\text{H}_2\text{O}-\text{Ca}(\text{OH})_2-\text{C}_3\text{A}\cdot 3\text{CaSO}_4\cdot 32\text{H}_2\text{O}$
- G = $\text{Ca}(\text{OH})_2-\text{C}_3\text{A}\cdot 6\text{H}_2\text{O}-\text{C}_3\text{A}\cdot 3\text{CaSO}_4\cdot 32\text{H}_2\text{O}$
- H = $\text{C}_3\text{A}\cdot 3\text{CaSO}_4\cdot 32\text{H}_2\text{O}-\text{C}_3\text{A}\cdot 6\text{H}_2\text{O}-\text{Al}_2\text{O}_3\text{aq.}$

The projection on to the base of the prism by means of lines drawn through the edge $(\text{K}_2\text{O})_3-(\text{K}_2\text{SO}_4)_3$ parallel to the triangular end-faces is shown in figure 8. Invariant point compositions are given in table 9.

DISCUSSION

The present paper establishes those equilibria curves in the system $\text{CaO}-\text{Al}_2\text{O}_3-\text{CaSO}_4-\text{K}_2\text{O}-\text{H}_2\text{O}$ (1 per cent KOH) at 25°C. of special interest in the

chemistry of cement, on parallel lines to those used in the first study of the quaternary system $\text{CaO-Al}_2\text{O}_3\text{-CaSO}_4\text{-H}_2\text{O}$ at 25°C . (8). Thus only the alumina gel phase equilibria have been primarily considered, the fundamentally stable equilibria with $\gamma\text{-Al}_2\text{O}_3\cdot 3\text{H}_2\text{O}$ being left for future examination.

The presence of alkali, with the correspondingly much increased solubility of alumina and the much decreased solubility of lime, causes considerable modification in the solution compositions as compared with the quaternary equilibria. Nevertheless the compound $\text{C}_3\text{A}\cdot 3\text{CaSO}_4\cdot 32\text{H}_2\text{O}$ is the only quaternary stable solid phase obtained. Comparing the present system with the system $\text{CaO-Al}_2\text{O}_3\text{-CaSO}_4\text{-H}_2\text{O}$, it is clear that the boundary curve $\text{C}_3\text{A}\cdot 6\text{H}_2\text{O-C}_3\text{A}\cdot 3\text{CaSO}_4\cdot 32\text{H}_2\text{O}$ now traced is not fundamentally stable throughout its length, but must meet a fundamentally stable curve $\gamma\text{-Al}_2\text{O}_3\cdot 3\text{H}_2\text{O-C}_3\text{A}\cdot 3\text{CaSO}_4\cdot 32\text{H}_2\text{O}$ in a stable invariant point. From this latter curve a metastable extension of the

TABLE 9
Invariant point compositions

INVARIANT POINT		GRAM-MOLES $\times 10^4$ PER 1000 G. OF SOLUTION				POSITIVE COMPONENTS = 100 PER CENT			NEGATIVE COMPONENTS = 100 PER CENT	
		(K ₂ O) ₂	(CaO) ₂	Al ₂ O ₃	(SO ₃) ₂	(K ₂ O) ₂	(CaO) ₂	Al ₂ O ₃	(SO ₃) ₂	(H ₂ O) ₂
						mole per cent	mole per cent	mole per cent	mole per cent	mole per cent
E	$\text{CaSO}_4\cdot 2\text{H}_2\text{O-Al}_2\text{O}_3\text{aq.-C}_3\text{A}\cdot 3\text{CaSO}_4\cdot 32\text{H}_2\text{O}$	295	35.6	1.3	329	88.8	10.8	0.4	99.1	0.9
F	$\text{CaSO}_4\cdot 2\text{H}_2\text{O-Ca(OH)}_2\text{-C}_3\text{A}\cdot 3\text{CaSO}_4\cdot 32\text{H}_2\text{O}$	297	55.0	0.2	220	84.4	15.6	0.1	62.4	37.6
G	$\text{Ca(OH)}_2\text{-C}_3\text{A}\cdot 6\text{H}_2\text{O-C}_3\text{A}\cdot 3\text{CaSO}_4\cdot 32\text{H}_2\text{O}$	297	8.8	0.65	2.2	96.9	2.8	0.2	0.7	99.3
H	$\text{C}_3\text{A}\cdot 3\text{CaSO}_4\cdot 32\text{H}_2\text{O-C}_3\text{A}\cdot 6\text{H}_2\text{O-Al}_2\text{O}_3\text{aq.}$	297		119	101.5	71.4		28.6	24.4	75.6
B	$\text{CaSO}_4\cdot 2\text{H}_2\text{O-Ca(OH)}_2$	296	55.5		223	84.3	15.7		63.4	36.6
C	$\text{C}_3\text{A}\cdot 6\text{H}_2\text{O-Ca(OH)}_2$	298	8.7	0.5		97.0	2.8	0.15		100

$\text{C}_3\text{A}\cdot 3\text{CaSO}_4\cdot 32\text{H}_2\text{O}$ field proceeds, bounded by the metastable prolongation of the $\text{C}_3\text{A}\cdot 6\text{H}_2\text{O-C}_3\text{A}\cdot 3\text{CaSO}_4\cdot 32\text{H}_2\text{O}$ curve and the curve $\text{Al}_2\text{O}_3\text{aq.-C}_3\text{A}\cdot 3\text{CaSO}_4\cdot 32\text{H}_2\text{O}$, found in the present work. To make this quite clear, reference should be made to figure 3a in the previous work (9) dealing with the quaternary system. In this figure it is seen that part of the $\text{C}_3\text{A}\cdot 3\text{CaSO}_4\cdot 32\text{H}_2\text{O}$ field is a metastable extension bounded by the $\text{Al}_2\text{O}_3\text{aq.-C}_3\text{A}\cdot 3\text{CaSO}_4\cdot 32\text{H}_2\text{O}$ curve, part of the $\text{C}_3\text{A}\cdot 6\text{H}_2\text{O-C}_3\text{A}\cdot 3\text{CaSO}_4\cdot 32\text{H}_2\text{O}$ curve (metastable), and the stable $\text{A}\cdot 3\text{H}_2\text{O-C}_3\text{A}\cdot 3\text{CaSO}_4\cdot 32\text{H}_2\text{O}$ curve. The invariant point II corresponds to the similar invariant point H in the quaternary system. It has previously been shown (9) that in the quaternary system solid solution equilibria exist in the metastable region near the $\text{H}_2\text{O-Al}_2\text{O}_3\text{-CaO}$ face, involving high concentrations of Al_2O_3 or CaO or both, and that this solid solution has, over a range, a composition approximating to $\text{C}_3\text{A}\cdot \text{CaSO}_4\cdot 12\text{H}_2\text{O}$, i.e., corresponding to the so-called low sul-

fate form of calcium sulfoaluminate. It is probable that in the present system somewhat similar solid solution equilibria exist within a volume contained in the angle made by the $(K_2O)_3-Al_2O_3$ edge and the faces $(K_2O)_3-(CaO)_3-Al_2O_3$ and $(K_2O)_3-Al_2O_3-Al_2(SO_4)_3-K_2(SO_4)_3$, close to the latter face. This is confirmed by the formation of a solid phase approximating to the refractive index of and formula for the solid phase $C_3A \cdot CaSO_4 \cdot 12H_2O$, from a mix of aluminum-potassium hydroxide and calcium sulfate solutions (1 per cent KOH). The precise conditions for the formation of such solid solutions, however, remain to be determined, probably in conjunction with the equilibria involving crystalline $Al_2O_3 \cdot 3H_2O$. It will be clear from the present work that the presence of alkali, and the consequent relative ease of formation of crystalline hydrated alumina, make the determination of the equilibria with the crystalline hydrated alumina rather than alumina gel of special importance.

A point of interest, however, in this connection is that in the presence of lime, as in the mixes determining the boundary curve $Al_2O_3 aq.-C_3A \cdot 3CaSO_4 \cdot 32H_2O$, the initially precipitated alumina gel is still present as gel after 7 days or longer, although in the quaternary system $H_2O-Al_2O_3-(K_2O)_3-(K_2SO_4)_3-Al_2(SO_4)_3$ in the absence of lime, there is a rapid transition to the crystalline state.

Application of the equilibria relations found in the present work to the conditions existing in a setting Portland cement can be made as follows: The work of Stein (13), Hänsel, Steinherz, and Wagner (5), Hein (6), Roller (12), Assarsson (1), and Forsén (4) has shown that a short time after mixing a gypsum-containing Portland cement with water to give a mix of approximately normal consistence, the liquid phase consists essentially of a mixed alkali sulfate-alkali hydroxide solution. Table 10 gives typical analyses of the liquid phase obtained by several authors, using different Portland cements. In every case the solution contains much free alkali hydroxide. The total alkali concentration, expressed as the KOH equivalent, amounts in grams of KOH per liter to 7.5, 14.6, 21.0, 21.3, 13.7, and 11.2, respectively (from left to right of table 10). Expressed in terms of NaOH, the corresponding amounts are, in grams per liter, 5.4, 10.5, 15.0, 9.8, and 8.0. The maximum concentration of the alkali component, expressed as KOH, thus varies in practice from about 0.75 per cent to 2 per cent. In some quite recent work by Kalousek, Jumper, and Tregoning (10), twelve commercial Portland cement clinkers (i.e., with no added gypsum), finely ground, mixed with 35 per cent water for 2.5 min. and filtered under pressure, gave after 7 min. (including time for mixing and filtration) values for the alkali concentration up to 22.3 g. KOH per liter and up to 3.86 g. NaOH per liter. Amounts varying between 1 per cent and 58 per cent of the total KOH dissolved within this period, and there was a straight-line relationship between dissolved KOH and SO_3 corresponding to a molar ratio $K_2O/SO_3 = 2.1$. It was concluded that the readily soluble part is K_2SO_4 , and the disappearance of SO_3 was attributed to formation of $C_3A \cdot 3CaSO_4 \cdot 32H_2O$. K_2SO_4 could not be positively identified by microscopic examination, though according to W. C. Taylor (14) in a later paper, recent microscopic examinations of commercial clinkers have revealed the presence of K_2SO_4 in many cases. Returning to Portland cement proper (with

added gypsum), the liquid phase is saturated with $\text{Ca}(\text{OH})_2$ and $\text{CaSO}_4 \cdot 2\text{H}_2\text{O}$, and in contact with these solid phases, as well as the remaining cement constituents. If no calcium aluminate constituent were present, the equilibrium would thus be essentially that of the invariant point B (figure 1) in the quaternary system $(\text{CaO})_3-(\text{CaSO}_4)_3-(\text{K}_2\text{SO}_4)_3-(\text{K}_2\text{O})_3-\text{H}_2\text{O}$. In the presence of the calcium aluminate constituents of the clinker, however, formation of $\text{C}_3\text{A} \cdot 3\text{CaSO}_4 \cdot 32\text{H}_2\text{O}$ must occur and the equilibrium will be that of the invariant point F (figure 1) in the quinary system. This equilibrium will persist so long as solid $\text{CaSO}_4 \cdot 2\text{H}_2\text{O}$ remains for reaction with the calcium aluminates. The liquid phase composition will thus remain substantially unaltered for some time. Thus

TABLE 10

The composition of the liquid phase in Portland cement-water mixes

AUTHOR.	ROLLER		HÄNSEL, STEINHERZ, AND WAGNER			STEIN				FORSÉN		
Per cent mixing water ...	26.0	24.2	24.5	45	45	27*				60	60	60
Time after gauging.	15 min.	15 min.	15 min.	5 min.	5 min.	10 min.	1 hr.	2 hr.	3 hr.	2 min.	10 min.	2 hr.
K^+ , equivalents per liter	0.110	0.231	0.292	0.348	0.226	0.2†	0.2†	0.2†	0.2†	0.121		
Na^+ , equivalents per liter	0.024	0.030	0.083	0.033	0.018							
$\frac{1}{2}\text{Ca}^{++}$, equivalents per liter	0.041	0.037	0.038	0.0355	0.0365	0.0345	0.0345	0.033	0.0355	0.042	0.043	0.038
$\frac{1}{2}\text{SO}_4^{--}$, equivalents per liter	0.098	0.182	0.271	0.286	0.162	0.138	0.130	0.137	0.134	0.073	0.073	0.075
OH^- , equivalents per liter	0.073	0.103	0.115	0.122	0.096	0.058	0.069	0.069	0.069	0.082	0.092	0.084
Al_2O_3 , grams per liter	0.0015	0.001	0.001	0.030†	0.036†	0.112	0.064	0.064	0.064			

* Actually reported as "normal consistency", corresponding to 23-30 per cent water.

† No analysis. Approximate value assuming SO_4^{--} present wholly as K_2SO_4 and OH^- wholly as KOH . Real value must be less than this.

‡ R_2O_3 .

Hänsel, Steinherz, and Wagner (5) found only a small change in the liquid phase composition between 5 and 60 min. for a Portland cement shaken with 45 per cent water, and Stein's and Forsén's data (table 10) show little change during periods varying from 2 min. to 3 hr.

Since the amount of the calcium aluminate compounds in Portland cement exceeds the amount of $\text{CaSO}_4 \cdot 2\text{H}_2\text{O}$ for $\text{C}_3\text{A} \cdot 3\text{CaSO}_4 \cdot 32\text{H}_2\text{O}$ formation, it must be concluded that the equilibrium will eventually move along the boundary curve $\text{Ca}(\text{OH})_2-\text{C}_3\text{A} \cdot 3\text{CaSO}_4 \cdot 32\text{H}_2\text{O}$ in the quinary system towards the invariant point G. At G, for stable equilibrium, formation of $\text{C}_3\text{A} \cdot 6\text{H}_2\text{O}$ should occur. From analogy with behavior in the quaternary system $\text{CaO}-\text{Al}_2\text{O}_3-\text{CaSO}_4-\text{H}_2\text{O}$, how-

ever, it seems probable that the fundamentally stable phase will not appear, at any rate for a considerable time, and that the equilibria will pass into a metastable region where formation of a solid solution phase of general formula $x\text{CaO} \cdot y\text{Al}_2\text{O}_3 \cdot z\text{CaSO}_4 \cdot \text{aq.}$ commences, and an appropriate metastable equilibrium is set up. This is as far as it is possible on the basis of the present work to trace the changing conditions in the liquid phase during the setting of an alkali-containing Portland cement. It is hoped that later the limits of solid solution formation may be established.

SUMMARY

As a further contribution to the study of the reactions occurring in the setting and hardening of Portland cements and the disintegration of such cements on exposure to sulfate waters, an investigation has been made of the quinary system $\text{CaO}-\text{Al}_2\text{O}_3-\text{CaSO}_4-\text{K}_2\text{O}-\text{H}_2\text{O}$ (1 per cent KOH) at 25°C . As compared with the system $\text{CaO}-\text{Al}_2\text{O}_3-\text{CaSO}_4-\text{H}_2\text{O}$ at 25°C ., in spite of the considerable modifications in solution compositions, the compound $\text{C}_3\text{A} \cdot 3\text{CaSO}_4 \cdot 32\text{H}_2\text{O}$ is still the only quaternary stable solid phase. Solid solution equilibria and equilibria with crystalline $\text{Al}_2\text{O}_3 \cdot 3\text{H}_2\text{O}$ require further study. The application of the equilibria relations found in the present work to the conditions existing in a setting Portland cement is discussed.

The investigations described in this paper were carried out at the Building Research Station of the Department of Scientific and Industrial Research, and the paper is published by permission of the Director of Building Research.

REFERENCES

- (1) ASSARSSON, G.: *Zement* **23**, 15 (1934).
- (2) CAMERON, F. K., AND BREAZEALE, J. F.: *J. Phys. Chem.* **8**, 335 (1904).
- (3) D'ANS, J., AND SCHREINER, O.: *Z. anorg. Chem.* **67**, 437 (1910).
- (4) FORSÉN, L.: Symposium on the Chemistry of Cements, Stockholm, 1938, p. 298.
- (5) HÄNSEL, P., STEINHERZ, R., AND WAGNER, C. L.: *Zement* **20**, 1064 (1931).
- (6) HEIN, H.: *Tonind. Ztg.* **56**, 203 (1932).
- (7) HEROLD, I.: *Z. Elektrochem.* **11**, 417 (1905).
- (8) JONES, F. E.: *Trans. Faraday Soc.* **35**, 1484 (1939).
- (9) JONES, F. E.: *J. Phys. Chem.* **48**, 311 (1944).
- (10) KALOUSEK, G. L., JUMPER, C. H., AND TREGONING, J. J.: *Rock Products* **44**, 52 (1941).
- (11) LEA, F. M., AND BESSEY, G. E.: Private communication.
- (12) ROLLER, P. S.: *Ind. Eng. Chem.* **26**, 669 (1934).
- (13) STEIN, S.: *Zement* **19**, 240 (1930).
- (14) TAYLOR, W. C.: *J. Res. Natl. Bur. Standards* **27**, 311 (1941).
- (15) TRAVERS, A., AND ZAHABI, H.: *Compt. rend.* **205**, 1407 (1937).

THE QUINARY SYSTEM $\text{CaO-Al}_2\text{O}_3\text{-CaSO}_4\text{-Na}_2\text{O-H}_2\text{O}$ (1 PER CENT NaOH) AT 25°C .

F. E. JONES

*Building Research Station, Garston, Watford, Herts, England**Received May 27, 1944*

The writer has previously described the system $\text{CaO-Al}_2\text{O}_3\text{-CaSO}_4\text{-K}_2\text{O-H}_2\text{O}$ (1 per cent KOH) at 25°C . (3). The present purpose is to describe a corresponding investigation, using NaOH instead of KOH . For a discussion of the alkali systems and their significance in cement chemistry, reference should be made to the previous paper.

The quinary system is represented graphically in figure 1 (for explanation, see the previous paper). It involves the following quaternary systems:

- (1) $(\text{CaO})_3\text{-(CaSO}_4)_3\text{-Al}_2(\text{SO}_4)_3\text{-Al}_2\text{O}_3\text{-H}_2\text{O}$
- (2) $(\text{CaO})_3\text{-(CaSO}_4)_3\text{-(Na}_2\text{SO}_4)_3\text{-(Na}_2\text{O})_3\text{-H}_2\text{O}$
- (3) $\text{Al}_2\text{O}_3\text{-(Na}_2\text{O})_3\text{-(Na}_2\text{SO}_4)_3\text{-Al}_2(\text{SO}_4)_3\text{-H}_2\text{O}$
- (4) $(\text{CaSO}_4)_3\text{-Al}_2(\text{SO}_4)_3\text{-(Na}_2\text{SO}_4)_3\text{-H}_2\text{O}$
- (5) $(\text{CaO})_3\text{-Al}_2\text{O}_3\text{-(Na}_2\text{O})_3\text{-H}_2\text{O}$

As in the corresponding K_2O system, no data appear to be available in the literature on the quaternary systems (2) and (5) and the necessary amount of work has therefore been carried out. Experimental methods and materials were similar to those previously used. As before, there was no evidence of any change in the optical properties of the solid phases obtained to suggest the taking up of alkali. Since analysis of solid phases for alkali in the K_2O system had shown very little K_2O , it was considered unnecessary to carry out such analyses in the present system.

RESULTS

I. THE QUATERNARY SYSTEM

The quaternary system $(\text{CaO})_3\text{-(CaSO}_4)_3\text{-(Na}_2\text{SO}_4)_3\text{-(Na}_2\text{O})_3\text{-H}_2\text{O}$

The solubility of $\text{CaSO}_4 \cdot 2\text{H}_2\text{O}$ in sodium sulfate solution (Na_2SO_4 concentration equivalent to 1 per cent NaOH), of crystalline Ca(OH)_2 in 1 per cent NaOH solution, the invariant point $\text{Ca(OH)}_2\text{-CaSO}_4 \cdot 2\text{H}_2\text{O}$, and the solubility curves for $\text{CaSO}_4 \cdot 2\text{H}_2\text{O}$ and Ca(OH)_2 have been determined. Interpolation of Cameron and Breazeale's data (1) for the solubility of $\text{CaSO}_4 \cdot 2\text{H}_2\text{O}$ in sodium sulfate yields a value in agreement with the present result: 1.395 g. CaSO_4 per 1000 g. of solution (17.8 g. Na_2SO_4 per 1000 g. of solution = 1 per cent NaOH). It may here be noted that the ternary system $\text{CaSO}_4\text{-Na}_2\text{SO}_4\text{-H}_2\text{O}$ at 25°C . differs from the corresponding system $\text{CaSO}_4\text{-K}_2\text{SO}_4\text{-H}_2\text{O}$ in that no double salt is formed. The solubility of Ca(OH)_2 in 1 per cent NaOH amounts to 0.089 g. CaO per 1000 g. of solution. Data are given in table 1 and plotted in figure 2, using triangular symbols. The projections of the corresponding boundary

curves in the quinary system, involving $C_3A \cdot 3CaSO_4 \cdot 32H_2O$ as additional solid phase, are also plotted in this figure. As in the K_2O system, they are coincident with the quaternary system solubility curves.

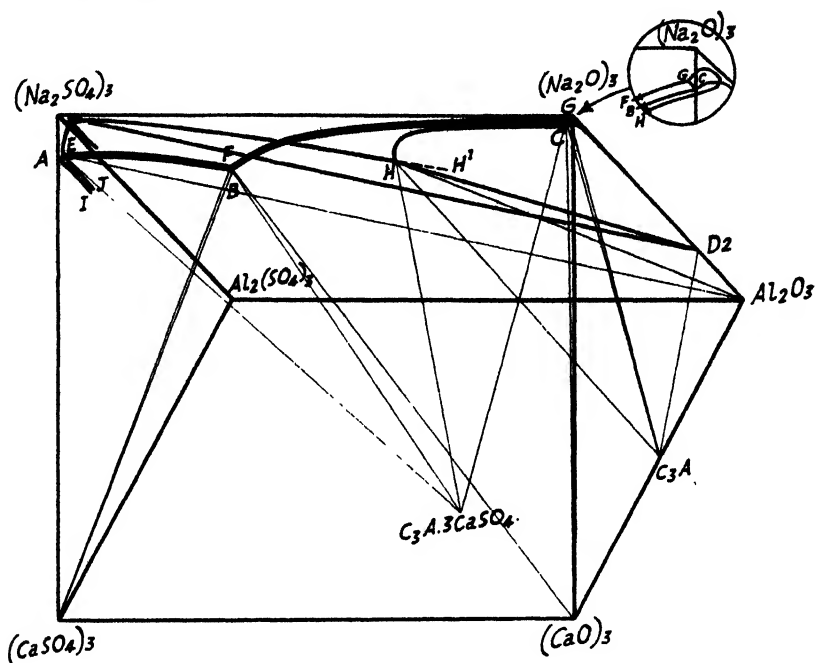


FIG. 1. Quinary system $CaO-Al_2O_3-CaSO_4-Na_2O-H_2O$ (1 per cent $NaOH$) at $25^\circ C$.

TABLE 1

The system $H_2O-(CaO)_3-(CaSO_4)_3-(Na_2SO_4)_3-(Na_2O)_3$

Solubility curve AB: $CaSO_4 \cdot 2H_2O$

Invariant point B: $CaSO_4 \cdot 2H_2O-Ca(OH)_2$ (mix B8)

Solubility curve BC: $Ca(OH)_2$

NO.	TIME SHAKEN	GRAM-MOLES $\times 10^4$ PER 1000 G. OF SOLUTION				POSITIVE COMPONENTS = 100 PER CENT			NEGATIVE COMPONENTS = 100 PER CENT	
		$(Na_2O)_3$	$(CaO)_3$	Al_2O_3	$(SO_3)_3$	$(Na_2O)_3$	$(CaO)_3$	Al_2O_3	$(SO_3)_3$	$(H_2O)_3$
						mole per cent	mole per cent	mole per cent	mole per cent	mole per cent
B7.....	28	417	34.2		449	92.4	7.6		99.5	0.5
B8.	28	413	51.3		313	89.0	11.0		67.5	32.5
B9.....	28	417	15.3		167	96.5	3.5		38.7	61.3
B11.....	7	417	5.3			98.8	1.2			100

The quaternary system $Al_2O_3-(Na_2O)_3-(Na_2SO_4)_3-Al_2(SO_4)_3-H_2O$

The general procedure followed was as in the corresponding K_2O system. As before, the equilibrium consists entirely of the solubility curve for hydrated alumina. Three positions of the curve have been determined: (a) alumina gel freshly

precipitated at 25°C ., using a 10-min. shaking period; (b) as (a), but shaking for 24 hr., during which time a crystalline product is formed; (c) as (a), but shaking for 7 days. Data for the three curves are given in table 2 and plotted in figure 3.

The fall in the Al_2O_3 concentration with time of shaking is shown in figure 4 for four different series of mixes. In each series the mixes were of the same initial composition. The curves shown indicate that while at 24 hr. the rate of fall is still high, after 7 days it is either very small or apparent equilibrium has been reached. None of the curves shown involve mixes in which precipitated alumina gel was used in preparing the initial mix. For mixes G53 and G45 (figure 3) such addition was necessary in order to reach the required high initial concentration of Al_2O_3 . Similarly to the K_2O system, the gel was precipitated in the cold by adding a solution of aluminum in sodium hydroxide to a dilute solution of aluminum sulfate. In both these cases there was not a smooth fall in the Al_2O_3 concentration with increase in the time of shaking, as in the results

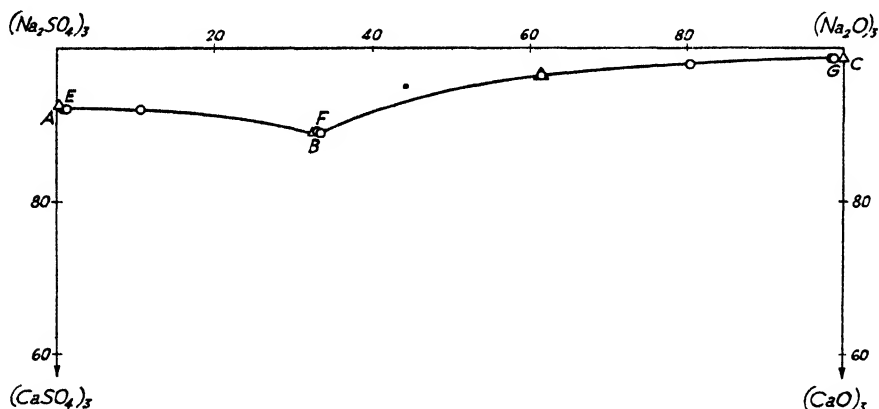


FIG. 2. Quinary system: projections of boundary curves from $\text{Al}_2(\text{SO}_4)_3\text{-Al}_2\text{O}_3$ edge. $\text{CaSO}_4\cdot 2\text{H}_2\text{O-C}_3\text{A}\cdot 3\text{CaSO}_4\cdot 32\text{H}_2\text{O}$ (EF); $\text{Ca}(\text{OH})_2\text{-C}_3\text{A}\cdot 3\text{CaSO}_4\cdot 32\text{H}_2\text{O}$ (FG).

Quaternary system: solubility curves. $\text{CaSO}_4\cdot 2\text{H}_2\text{O}$ (AB); $\text{Ca}(\text{OH})_2$ (BC).

described above. The fall was both variable and considerably greater. Thus G42, a similar mix to G45, but shaken for 1 day, lies much above the 1-day curve DD_3 , while G57 and G65, both similar to G53 but shaken for 7 days, lie much above the extrapolated portion of the 7-day curve, DD_4 . This behavior was accompanied by more or less precipitation of crystalline hydrated alumina on the walls of the tube. It seems likely that in the higher alkali concentrations there is at any rate partial conversion of the hydrated alumina to a more stable and less soluble form. It is evident that although an apparent equilibrium has been reached in the less alkaline mixes after 7 days' shaking, the crystalline hydrated alumina phase must nevertheless be unstable with respect to α - and γ - $\text{Al}_2\text{O}_3\cdot 3\text{H}_2\text{O}$. In two cases, G39 (24 hr.) and G60 (168 hr.), the loss on ignition was determined and found to correspond to the molar ratios $\text{H}_2\text{O}/\text{Al}_2\text{O}_3 = 3.38$ and 3.22, respectively. Both mixes were of the same initial composition. Microscopic examination of the solid phases obtained along the three hydrated

alumina curves showed that they were essentially similar to those obtained in the K_2O system. The alumina gel curve D_1DD_2 (10 min. shaking) was associated with irregular isotropic grains of refractive index 1.460. In one case, G53, the index was 1.47 ± 0.01 , and in two cases, G31 and G45, there was slight indefinite

TABLE 2

The system $H_2O-Al_2O_3-(Na_2O)_2-(Na_2SO_4)_2-Al_2(SO_4)_3$

Solubility curve (a) D_1D_2 : Al_2O_3 aq. (gel)

Solubility curve (b) DD_3 : crystalline hydrated alumina (24 hr.)

Solubility curve (c) DD_4 : crystalline hydrated alumina (7 days)

NO.	TIME SHAKEN	GRAM-MOLES $\times 10^4$ PER 1000 G. OF SOLUTION				POSITIVE COMPONENTS = 100 PER CENT			NEGATIVE COMPONENTS = 100 PER CENT	
		(Na ₂ O) ₂	(CaO) ₂	Al ₂ O ₃	(SO ₃) ₂	(Na ₂ O) ₂	(CaO) ₂	Al ₂ O ₃	(SO ₃) ₂	(H ₂ O) ₂
(a) Solid phase: Al ₂ O ₃ aq. (gel)										
						mole per cent	mole per cent	mole per cent	mole per cent	mole per cent
G28.....	1 day	417		192	564	68.5		31.5	92.6	7.4
G29.....	1 day	417		61	466	87.2		12.8	97.5	2.5
G40.....	10 min.	417		3.4	408	99.2		0.8	97.0	3.0
G31.....	10 min.	417		119	364	77.8		22.2	67.9	32.1
G32.....	10 min.	417		266	310	61.0		39.0	45.4	54.6
G35.....	10 min.	417		436	248	48.9		51.1	29.1	70.9
G36.....	10 min.	417		661	175	38.7		61.3	16.3	83.7
G53.....	10 min.	417		956	49.6	30.4		69.6	3.6	96.4
G45.....	10 min.	417		1011	8.4	29.2		70.8	0.6	99.4
(b) Solid phase: crystalline hydrated alumina (24 hr.)										
	days									
G37.....	1	417		0.2	410	100			98.3	1.7
G33.....	1	417		67.4	369	86.3		13.7	76.1	23.9
G34.....	1	417		148	315	73.8		26.2	55.7	44.3
G38.....	1	417		275	262	60.3		39.7	37.9	62.1
G39.....	1	417		383	197	52.1		47.9	24.6	75.4
(c) Solid phase: crystalline hydrated alumina (7 days)										
G67.....	7	417		54.6	369	88.4		11.6	78.2	21.8
G70.....	7	417		104.5	317	79.9		20.1	60.8	39.2
G66.....	7	417		191	262	68.6		31.4	43.1	56.9
G60.....	7	417		275	194	60.2		39.8	28.1	71.9

birefringence. As in the K_2O system the solid phase was more powdery in character in the more alkaline media. Along the 24-hr. curve DD_3 it was found that while G37 showed relatively little change—though there was slight birefringence and the refractive index had risen to 1.495—the remaining solid phases consisted of small plates or needles (plates on edge) with positive elongation,

showing slight birefringence and in general with refractive indices lying between 1.545 and 1.565. In G56, where small spherulitic clusters of plates were observed, the index was approximately 1.575. After 7 days' shaking the index of the crystalline product had risen to a value of 1.570 ± 0.005 . $\gamma\text{-Al}_2\text{O}_3 \cdot 3\text{H}_2\text{O}$ has indices $\alpha = \beta = 1.566$, $\gamma = 1.587$.

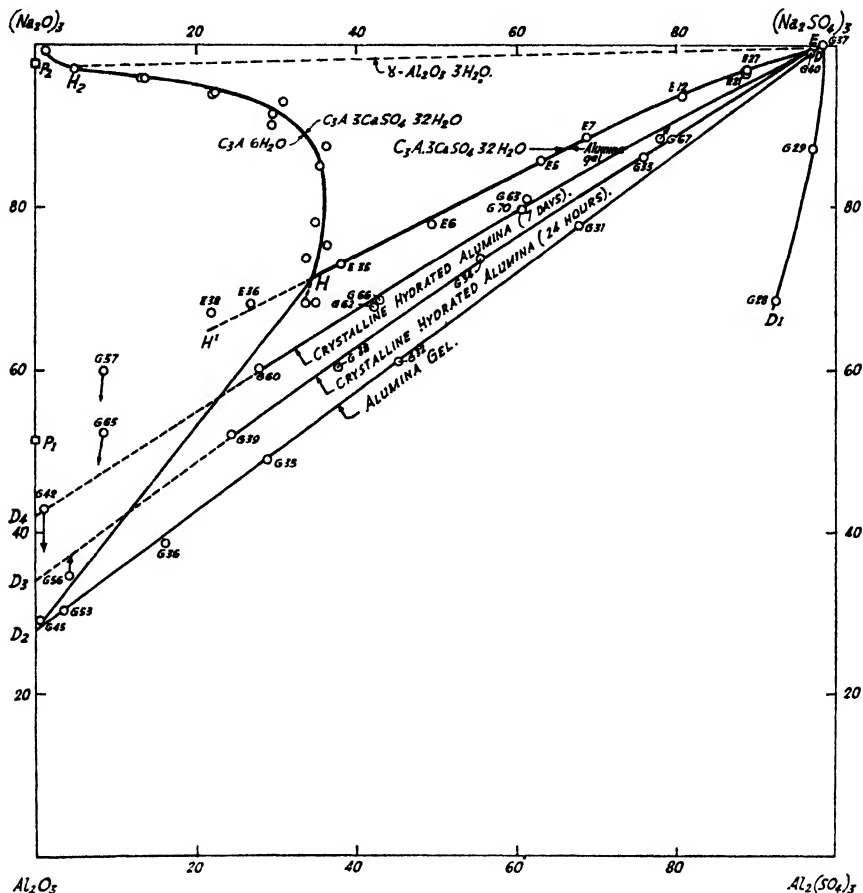


FIG. 3. Quinary system: projections of boundary curves from $(\text{CaO})_3$ -(CaSO_4)₃ edge. $\text{C}_3\text{A} \cdot 6\text{H}_2\text{O}$ - $\text{C}_3\text{A} \cdot 3\text{CaSO}_4 \cdot 32\text{H}_2\text{O}$ (GH); alumina gel- $\text{C}_3\text{A} \cdot 3\text{CaSO}_4 \cdot 32\text{H}_2\text{O}$ (EHH¹).

Quaternary system: solubility curves. Crystalline hydrated alumina (DD₃, DD₄); alumina gel (D₁DD₂).

Goudriaan (2) has examined the system $\text{Na}_2\text{O}-\text{Al}_2\text{O}_3-\text{H}_2\text{O}$ at 30°C. By shaking hydrated alumina prepared in three ways with sodium hydroxide solutions of various concentrations for 1 to 2 months, three different solubility curves were obtained by this author. Alumina gel prepared by adding ammonia to aluminum sulfate solution and drying at 130–140°C. sufficiently to give a composition $\text{Al}(\text{OH})_3$ showed the highest solubilities. Interpolation of Goudriaan's

data gives for a 1 per cent sodium hydroxide solution a value of roughly 4.0 g. Al_2O_3 per 1000 g. of solution, corresponding to point P_1 on the $(\text{Na}_2\text{O})_s\text{-Al}_2\text{O}_3$ edge in figure 3. This point represents a possible termination of a curve of the same type as those obtained in the present work, but at much longer periods of shaking. It may be noted that Goudriaan in many cases found the solubility dropping much below the maximum values of the solubility curve, in agreement with the behavior described above. By shaking the dried gel with 0.5 to 2 N sodium hydroxide for about 2 months, a crystalline hydrated alumina was ob-

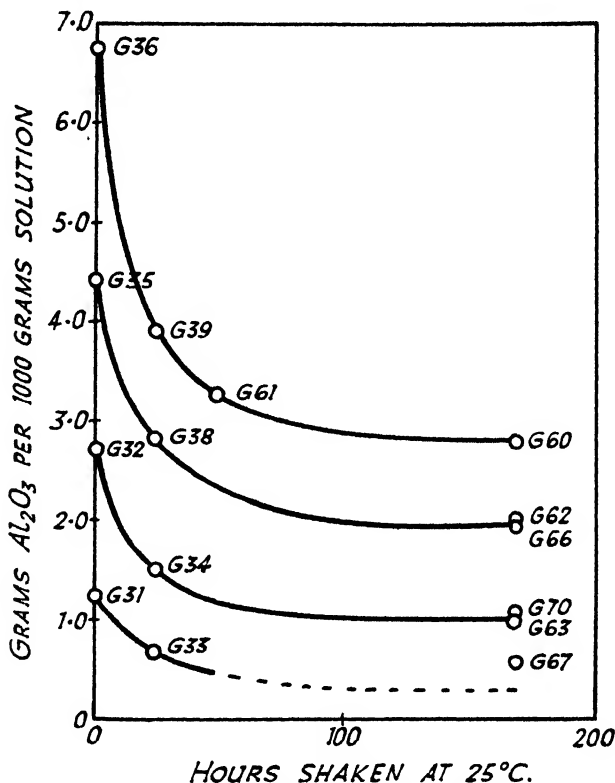


FIG. 4. Fall in Al_2O_3 concentration in solution during change $\text{Al}_2\text{O}_3\text{aq. (gel)} \rightarrow \text{Al}_2\text{O}_3\text{aq. (crystalline)}$.

tained by Goudriaan in the form of small needles or plates and of composition $\text{Al}_2\text{O}_3 \cdot 3\text{H}_2\text{O}$. The solubility of this product was determined in the same way, and was found to be very low compared to that of the original gel. What relation this product bears to $\alpha\text{-Al}_2\text{O}_3 \cdot 3\text{H}_2\text{O}$ ("bayerite") or $\gamma\text{-Al}_2\text{O}_3 \cdot 3\text{H}_2\text{O}$ ("gibbsite" or "hydrargillite") is not known. At a concentration corresponding to 5.5 per cent Na_2O , Goudriaan found a concentration of 0.08 per cent Al_2O_3 with higher Al_2O_3 values at higher alkali concentrations. Assuming tentatively by interpolation a concentration of 0.01 per cent Al_2O_3 at 0.775 per cent Na_2O (1 per cent NaOH), the solution composition corresponds to point P_2 on the

$(\text{Na}_2\text{O})_3-\text{Al}_2\text{O}_3$ edge in figure 3. This gives an approximate terminal point for a stable crystalline hydrated alumina curve in the system $\text{Al}_2\text{O}_3-(\text{Na}_2\text{O})_3-(\text{Na}_2\text{SO}_4)_3-\text{Al}_2(\text{SO}_4)_3-\text{H}_2\text{O}$.

TABLE 3
The system $\text{H}_2\text{O}-(\text{CaSO}_4)_3-\text{Al}_2(\text{SO}_4)_3-(\text{Na}_2\text{SO}_4)_3$
Solubility curve AI: $\text{CaSO}_4 \cdot 2\text{H}_2\text{O}$

NO.	TIME SHAKEN	GRAM-MOLES $\times 10^4$ PER 1000 G. OF SOLUTION				POSITIVE COMPONENTS = 100 PER CENT			NEGATIVE COMPONENTS = 100 PER CENT	
		$(\text{Na}_2\text{O})_3$	$(\text{CaO})_3$	Al_2O_3	$(\text{SO}_3)_3$	$(\text{Na}_2\text{O})_3$	$(\text{CaO})_3$	Al_2O_3	$(\text{SO}_3)_3$	$(\text{H}_2\text{O})_3$
	days					mole per cent	mole per cent	mole per cent	mole per cent	mole per cent
B7.....	28	417	34.2		449	92.4	7.6		99.5	0.5
I3.....	28	417	34.7	43.7	490	84.2	7.0	8.8	99.0	1.0
I4.....	28	412	34.5	84.7	529	75.7	6.7	16.6	99.6	0.4

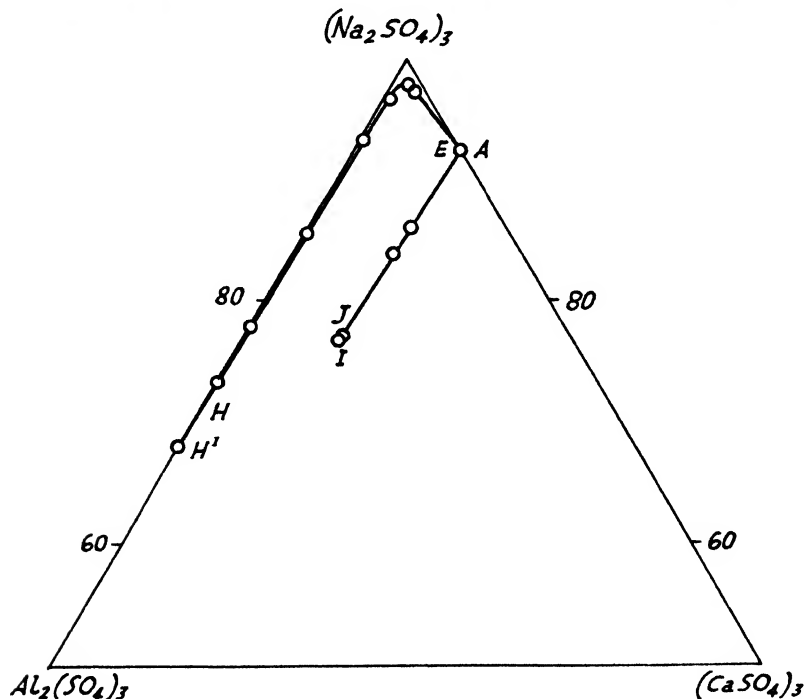


FIG. 5. Quaternary system: solubility curve. $\text{CaSO}_4 \cdot 2\text{H}_2\text{O}$ (AI).
Quinary system: projection of boundary curves. $\text{Al}_2\text{O}_3\text{aq.}-\text{C}_2\text{A} \cdot 3\text{CaSO}_4 \cdot 32\text{H}_2\text{O}$ (EHH¹);
 $\text{Al}_2\text{O}_3\text{aq.}-\text{CaSO}_4 \cdot 2\text{H}_2\text{O}$ (EJ).

The quaternary system $(\text{CaSO}_4)_3-\text{Al}_2(\text{SO}_4)_3-(\text{Na}_2\text{SO}_4)_3-\text{H}_2\text{O}$

Part of the solubility curve for $\text{CaSO}_4 \cdot 2\text{H}_2\text{O}$ has been traced, as for the K_2O system. Data are given in table 3 and plotted in figure 5.

The quaternary system $(\text{CaO})_3\text{-Al}_2\text{O}_3\text{-(Na}_2\text{O)}_3\text{-H}_2\text{O}$

Precisely the same considerations apply as in the corresponding K_2O system, to which reference should be made. The data (table 4) are plotted in figure 6a. A comparison with the $\text{CaO-Al}_2\text{O}_3\text{-H}_2\text{O}$ system is given in figure 7.

TABLE 4

The system $\text{H}_2\text{O-(CaO)}_3\text{-Al}_2\text{O}_3\text{-(Na}_2\text{O)}_3$

Invariant point C: $\text{C}_3\text{A}\cdot 6\text{H}_2\text{O-Ca(OH)}_2$ (mix J12)

Solubility curve D_2C : $\text{C}_3\text{A}\cdot 6\text{H}_2\text{O}$ (other mixes)

NO.	TIME SHAKEN	GRAM-MOLES $\times 10^4$ PER 1000 G. OF SOLUTION				POSITIVE COMPONENTS = 100 PER CENT			NEGATIVE COMPONENTS = 100 PER CENT	
		$(\text{Na}_2\text{O})_3$	$(\text{CaO})_3$	Al_2O_3	$(\text{SO}_3)_3$	$(\text{Na}_2\text{O})_3$	$(\text{CaO})_3$	Al_2O_3	$(\text{SO}_3)_3$	$(\text{H}_2\text{O})_3$
	days					mole per cent	mole per cent	mole per cent	mole per cent	mole per cent
J12.....	7	417	5.2	1.5		98.4	1.25	0.35		100
J7.....	7	417	2.55	7.65		97.6	0.6	1.8		100
J11.....	7	417	0.65	29.8		93.1	0.15	6.7		100
J10.....	7	417	0.65	105		79.8	0.1	20.1		100
J9.....	7	417	0.5	314		57.0	0.05	43.0		100
J8.....	7	417	0.5	649		39.1	0.05	60.9		100

II. THE QUINARY SYSTEM

The following boundary curves and invariant points have been determined within the quinary system:

(a) Boundary curves:

- (1) $\text{Al}_2\text{O}_3\text{aq.-C}_3\text{A}\cdot 3\text{CaSO}_4\cdot 32\text{H}_2\text{O}$ (EH) and unstable prolongation to H^1 (figures 3, 5, 9)
- (2) $\text{CaSO}_4\cdot 2\text{H}_2\text{O-C}_3\text{A}\cdot 3\text{CaSO}_4\cdot 32\text{H}_2\text{O}$ (EF) (figures 2, 9)
- (3) $\text{Ca(OH)}_2\text{-C}_3\text{A}\cdot 3\text{CaSO}_4\cdot 32\text{H}_2\text{O}$ (FG) (figures 2, 9)
- (4) $\text{C}_3\text{A}\cdot 6\text{H}_2\text{O-C}_3\text{A}\cdot 3\text{CaSO}_4\cdot 32\text{H}_2\text{O}$ (GH) (figures 3, 6b, 9)

(b) Invariant points:

- (1) $\text{CaSO}_4\cdot 2\text{H}_2\text{O-Al}_2\text{O}_3\text{aq.-C}_3\text{A}\cdot 3\text{CaSO}_4\cdot 32\text{H}_2\text{O}$ (F) (figures 3, 5, 9)
- (2) $\text{CaSO}_4\cdot 2\text{H}_2\text{O-Ca(OH)}_2\text{-C}_3\text{A}\cdot 3\text{CaSO}_4\cdot 32\text{H}_2\text{O}$ (F) (figures 2, 9)
- (3) $\text{Ca(OH)}_2\text{-C}_3\text{A}\cdot 6\text{H}_2\text{O-C}_3\text{A}\cdot 3\text{CaSO}_4\cdot 32\text{H}_2\text{O}$ (G) (figures 2, 6b, 9)
- (4) $\text{C}_3\text{A}\cdot 3\text{CaSO}_4\cdot 32\text{H}_2\text{O-C}_3\text{A}\cdot 6\text{H}_2\text{O-Al}_2\text{O}_3\text{aq.}$ (H) (figures 3, 5, 6b, 9)

The isothermal invariant point $\text{CaSO}_4\cdot 2\text{H}_2\text{O-Al}_2\text{O}_3\text{aq.-C}_3\text{A}\cdot 3\text{CaSO}_4\cdot 32\text{H}_2\text{O}$ (E) (figures 3, 5, 9)

The data are given in table 6 (mixes D14, D15). The alumina gel occurred as small rounded isotropic grains, refractive index 1.525.

The boundary curve $\text{CaSO}_4\cdot 2\text{H}_2\text{O-C}_3\text{A}\cdot 3\text{CaSO}_4\cdot 32\text{H}_2\text{O}$ (EF) (figures 2, 9)

The boundary curve $\text{Ca(OH)}_2\text{-C}_3\text{A}\cdot 3\text{CaSO}_4\cdot 32\text{H}_2\text{O}$ (FG) (figures 2, 9)

The invariant point $\text{CaSO}_4\cdot 2\text{H}_2\text{O-Ca(OH)}_2\text{-C}_3\text{A}\cdot 3\text{CaSO}_4\cdot 32\text{H}_2\text{O}$ (F) (figures 2, 9)

The boundary curves are shown in figure 2 as a projection on to the face $(\text{CaO})_3\text{-(Na}_2\text{O)}_3\text{-(Na}_2\text{SO}_4)_3\text{-(CaSO}_4)_3$ from the $\text{Al}_2\text{O}_3\text{-Al}_2(\text{SO}_4)_3$ edge, and in

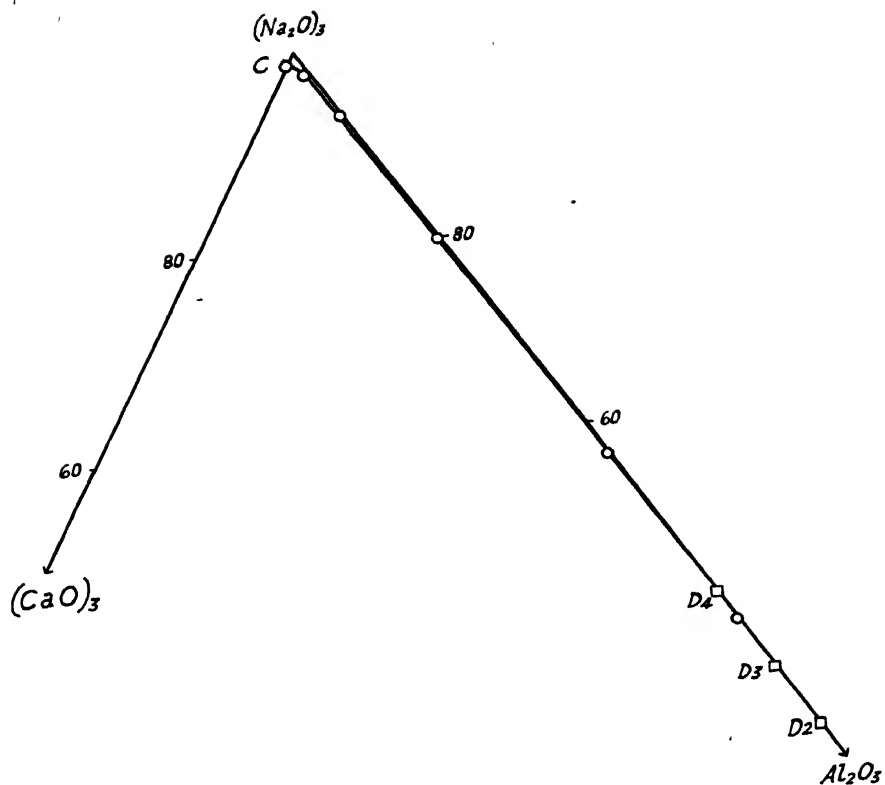


FIG. 6a. Quaternary system: solubility curve. $C_3A \cdot 6H_2O$ (D_2C)

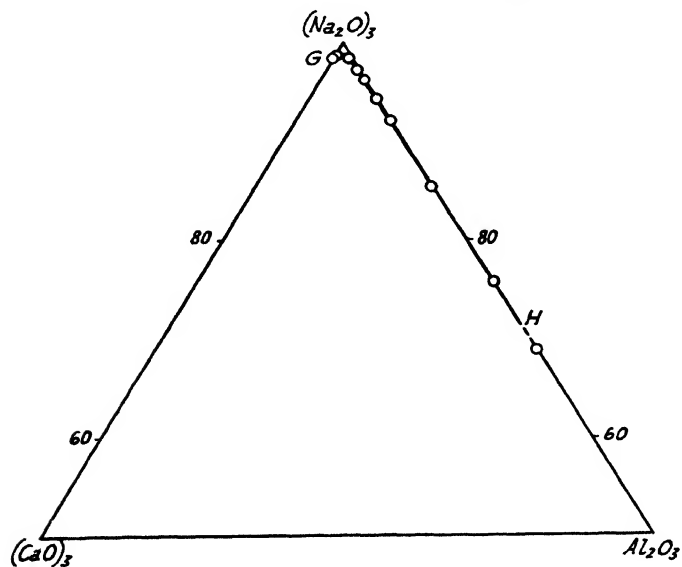


FIG. 6b. Quinary system: projection of boundary curve.
 $C_3A \cdot 6H_2O$ - $C_3A \cdot 3CaSO_4 \cdot 32H_2O$ (GH).

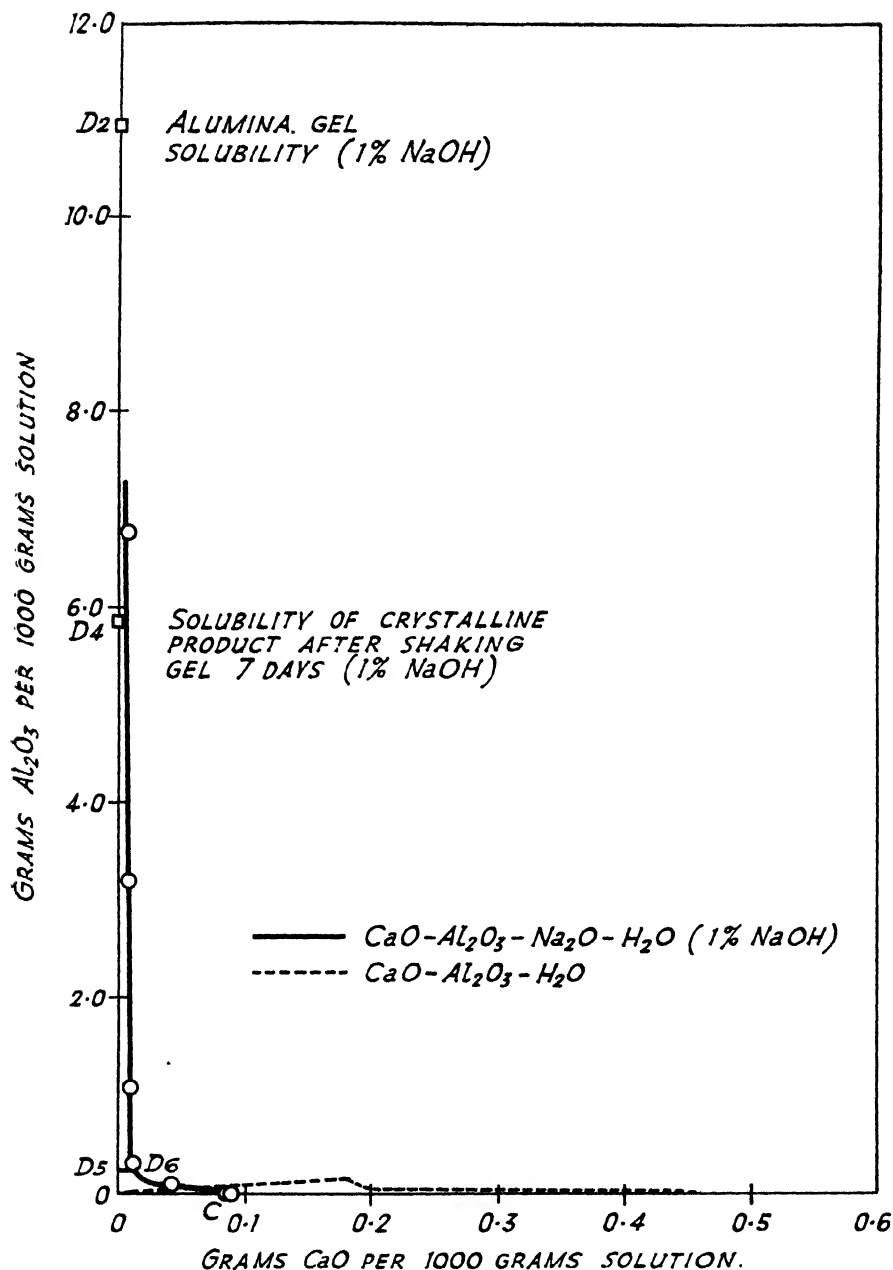


FIG. 7. Comparison at 25°C. of systems $CaO-Al_2O_3-Na_2O-H_2O$ (1 per cent NaOH) and $CaO-Al_2O_3-H_2O$.

figure 9 as a projection on to the base. Mixes were prepared as in the K_2O system. Data are given in table 7. The $C_3A \cdot 3CaSO_4 \cdot 32H_2O$ present in the solid phase was in general well formed.

The invariant point $\text{Ca}(\text{OH})_2-\text{C}_3\text{A} \cdot 3\text{CaSO}_4 \cdot 32\text{H}_2\text{O}-\text{C}_3\text{A} \cdot 6\text{H}_2\text{O}$ (G) (figures 2, 6b, 9)

This point was obtained from a suitable mix of sodium hydroxide and sodium sulfate solution, with the addition of $\text{C}_3\text{A} \cdot 6\text{H}_2\text{O}$ and crystalline $\text{Ca}(\text{OH})_2$ (table 8, mixes H1, H11).

TABLE 5

The quinary system $\text{H}_2\text{O}-(\text{CaO})_3-(\text{CaSO}_4)_3-\text{Al}_2(\text{SO}_4)_3-\text{Al}_2\text{O}_3-(\text{Na}_2\text{SO}_4)_3-(\text{Na}_2\text{O})_3$

Boundary curve JE: $\text{CaSO}_4 \cdot 2\text{H}_2\text{O}-\text{Al}_2\text{O}_3\text{aq.}$

NO.	TIME SHAKEN	GRAM-MOLES $\times 10^4$ PER 1000 G. OF SOLUTION				POSITIVE COMPONENTS = 100 PER CENT			NEGATIVE COMPONENTS = 100 PER CENT	
		$(\text{Na}_2\text{O})_3$	$(\text{CaO})_3$	Al_2O_3	$(\text{SO}_3)_3$	$(\text{Na}_2\text{O})_3$	$(\text{CaO})_3$	Al_2O_3	$(\text{SO}_3)_3$	$(\text{H}_2\text{O})_3$
						mole per cent	mole per cent	mole per cent	mole per cent	mole per cent
I9	7	417	34.5	31.1	474	86.4	7.1	6.5	1.8	98.2
I10.	7	417	34.7	83.5	514	77.9	6.5	15.6	4.0	96.0

TABLE 6

The quinary system $\text{H}_2\text{O}-(\text{CaO})_3-(\text{CaSO}_4)_3-\text{Al}_2(\text{SO}_4)_3-\text{Al}_2\text{O}_3-(\text{Na}_2\text{SO}_4)_3-(\text{Na}_2\text{O})_3$

Invariant point E: $\text{CaSO}_4 \cdot 2\text{H}_2\text{O}-\text{Al}_2\text{O}_3\text{aq.}-\text{C}_3\text{A} \cdot 3\text{CaSO}_4 \cdot 32\text{H}_2\text{O}$ (mixes D14, D15)

Boundary curve EHH¹: $\text{Al}_2\text{O}_3\text{aq.}-\text{C}_3\text{A} \cdot 3\text{CaSO}_4 \cdot 32\text{H}_2\text{O}$ (other mixes)

NO.	TIME SHAKEN	GRAM-MOLES $\times 10^4$ PER 1000 G. OF SOLUTION				POSITIVE COMPONENTS = 100 PER CENT			NEGATIVE COMPONENTS = 100 PER CENT	
		$(\text{Na}_2\text{O})_3$	$(\text{CaO})_3$	Al_2O_3	$(\text{SO}_3)_3$	$(\text{Na}_2\text{O})_3$	$(\text{CaO})_3$	Al_2O_3	$(\text{SO}_3)_3$	$(\text{H}_2\text{O})_3$
						mole per cent	mole per cent	mole per cent	mole per cent	mole per cent
D14 ..	7	417	33.7	1.55	447	92.2	7.5	0.35	98.8	1.2
D15 ..	28	417	34.1	1.30	451	92.2	7.6	0.3	99.7	0.3
E25 ..	28	417	7.4	3.2	415	97.6	1.7	0.7	97.1	2.9
E26 ..	28	417	4.4	4.3	415	98.0	1.0	1.0	97.5	2.5
E27 ..	28	417	1.5	12.6	382	96.9	0.35	2.9	88.8	11.2
E12 ..	7	417	1.4	27.7	360	93.5	0.3	6.2	80.8	19.2
E5	7	417	0.5	68.6	307	85.7	0.1	14.1	63.2	36.9
E6 ..	7	417	0.4	117.8	265	77.9	0.1	22.0	49.5	50.5
E35 ..	7	417		152	217	73.3		26.7	38.2	61.8
E36 ..	7	417	0.2	194	165	68.3	0.05	31.7	27.0	73.0

The boundary curve $\text{Al}_2\text{O}_3\text{aq.}-\text{C}_3\text{A} \cdot 3\text{CaSO}_4 \cdot 32\text{H}_2\text{O}$ (EHH) (figures 3, 5, 9)

The curve is shown in figure 3 as a projection on to the face $\text{Al}_2\text{O}_3-(\text{Na}_2\text{O})_3-(\text{Na}_2\text{SO}_4)_3-\text{Al}_2(\text{SO}_4)_3$ of the prism from the $(\text{CaO})_3-(\text{CaSO}_4)_3$ edge, and in figure 9 as a projection on to the base. The curve was traced a short way beyond the invariant point with $\text{C}_3\text{A} \cdot 6\text{H}_2\text{O}$. Mixes were prepared as in the K_2O system. In the Al_2O_3 -rich mixes E6, E35, E36, it was necessary to add increasing amounts of precipitated alumina gel to the initial mix. The gel was precipitated by the addition of an aluminum sulfate solution to a saturated lime solution. As before, the added gel was dissolved in the mix before adding aluminum sulfate. The latter addition results in direct precipitation of fresh gel within the mix.

As in the K_2O system, the final hydrated alumina phase present with the $C_3A \cdot 3CaSO_4 \cdot 32H_2O$ consisted of rounded or irregularly shaped isotropic material with refractive index 1.525–1.530, no change to a crystalline phase occurring.

TABLE 7

The quinary system $H_2O-(CaO)_2-(CaSO_4)_2-Al_2(SO_4)_3-Al_2O_3-(Na_2SO_4)_2-(Na_2O)_2$

Boundary curve EF: $CaSO_4 \cdot 2H_2O-C_3A \cdot CaSO_4 \cdot 32H_2O$ (mix D1)

Invariant point F: $CaSO_4 \cdot 2H_2O-Ca(OH)_2-C_3A \cdot 3CaSO_4 \cdot 32H_2O$ (mixes D8, D10)

Boundary curve FG: $Ca(OH)_2-C_3A \cdot 3CaSO_4 \cdot 32H_2O$ (mixes D11, D12, D13)

NO.	TIME SHAKEN	GRAM-MOLES $\times 10^4$ PER 1000 G. OF SOLUTION				POSITIVE COMPONENTS = 100 PER CENT			NEGATIVE COMPONENTS = 100 PER CENT	
		$(Na_2O)_2$	$(CaO)_2$	Al_2O_3	$(SO_3)_2$	$(Na_2O)_2$	$(CaO)_2$	Al_2O_3	$(SO_3)_2$	$(H_2O)_2$
						mole per cent	mole per cent	mole per cent	mole per cent	mole per cent
D1.....	7	417	37.3	0.1	406	91.9	8.2		89.5	10.6
D8.....	7	417	51.1	0.4	314	89.1	10.9	0.1	67.1	33.0
D10.....	28	417	51.4	0.15	312	89.1	11.0		66.6	33.4
D11.....	28	417	15.3	0.1	168	96.5	3.5		38.8	61.2
D12.....	28	417	8.7	0.25	83.7	98.0	2.05	0.05	19.7	80.3
D13.....	28	417	5.7	0.5	6.0	98.6	1.35	0.15	1.4	98.6

TABLE 8

The quinary system $H_2O-(CaO)_2-(CaSO_4)_2-Al_2(SO_4)_3-Al_2O_3-(Na_2SO_4)_2-(Na_2O)_2$

Invariant point G: $Ca(OH)_2-C_3A \cdot 3CaSO_4 \cdot 32H_2O-C_3A \cdot 6H_2O$ (H1, H11)

Boundary curve GH: $C_3A \cdot 3CaSO_4 \cdot 32H_2O-C_3A \cdot 6H_2O$ (other mixes)

NO.	TIME SHAKEN	GRAM-MOLES $\times 10^4$ PER 1000 G. OF SOLUTION				POSITIVE COMPONENTS = 100 PER CENT			NEGATIVE COMPONENTS = 100 PER CENT	
		$(Na_2O)_2$	$(CaO)_2$	Al_2O_3	$(SO_3)_2$	$(Na_2O)_2$	$(CaO)_2$	Al_2O_3	$(SO_3)_2$	$(H_2O)_2$
						mole per cent	mole per cent	mole per cent	mole per cent	mole per cent
H1.....	7	417	5.5	1.25	3.2	98.6	1.3	0.3	0.75	99.25
H11.....	28	417	5.4	0.85	3.1	98.7	1.3	0.2	0.75	99.25
H6.....	7	417	3.55	1.7	5.2	98.8	0.85	0.4	1.2	98.8
H2.....	7	417	2.85	2.45	5.95	98.8	0.7	0.6	1.4	98.6
H10.....	28	417	1.5	6.3	10.3	98.3	0.35	1.5	2.4	97.6
H9.....	14	417	0.85	12.05	21.2	97.0	0.2	2.8	4.9	95.1
H13.....	28	417	0.5	17.4	60.6	95.9	0.1	4.0	13.9	86.1
H52.....	7	417	0.5	25.7	99	94.1	0.1	5.8	22.4	77.6
H41.....	7	417		37.2	135	91.8		8.2	29.8	70.2
H68.....	7	417		72	174	85.2		14.8	35.7	64.3
H47.....	7	417		135	202	75.5		24.5	36.5	63.5
H70.....	7	417		192	206	68.4		31.6	33.8	66.2

Data are given in table 6. For comparison, a possible position for the stable $\gamma-Al_2O_3 \cdot 3H_2O-C_3A \cdot 3CaSO_4 \cdot 32H_2O$ curve is shown by the broken line EH₂ in figure 3.

The invariant point $\text{C}_3\text{A} \cdot 3\text{CaSO}_4 \cdot 32\text{H}_2\text{O}-\text{C}_3\text{A} \cdot 6\text{H}_2\text{O}-\text{Al}_2\text{O}_3\text{aq.}$ (H) (figures 3, 5, 6b, 9)

The addition of $\text{C}_3\text{A} \cdot 6\text{H}_2\text{O}$ to a suitable mix designed (in the absence of $\text{C}_3\text{A} \cdot 6\text{H}_2\text{O}$) to yield an equilibrium solution on the boundary curve $\text{Al}_2\text{O}_3\text{aq.}-\text{C}_3\text{A} \cdot 3\text{CaSO}_4 \cdot 32\text{H}_2\text{O}$ resulted in complete conversion of the $\text{C}_3\text{A} \cdot 6\text{H}_2\text{O}$. Thus E38 is a mix of the initial composition of E35 (figure 3) but with the addition of 1 g. $\text{C}_3\text{A} \cdot 6\text{H}_2\text{O}$. Only $\text{Al}_2\text{O}_3\text{aq.}$ and $\text{C}_3\text{A} \cdot 3\text{CaSO}_4 \cdot 32\text{H}_2\text{O}$ were found after 7 days shaking. The invariant point is indirectly obtained by the intersection of the appropriate boundary curves at H. This gives an invariant point composition in grams per 1000 g. of solution of $\text{CaO} = \text{nil}$, $\text{Al}_2\text{O}_3 = 1.72$, $\text{SO}_3 = 4.85$ (1 per cent NaOH).

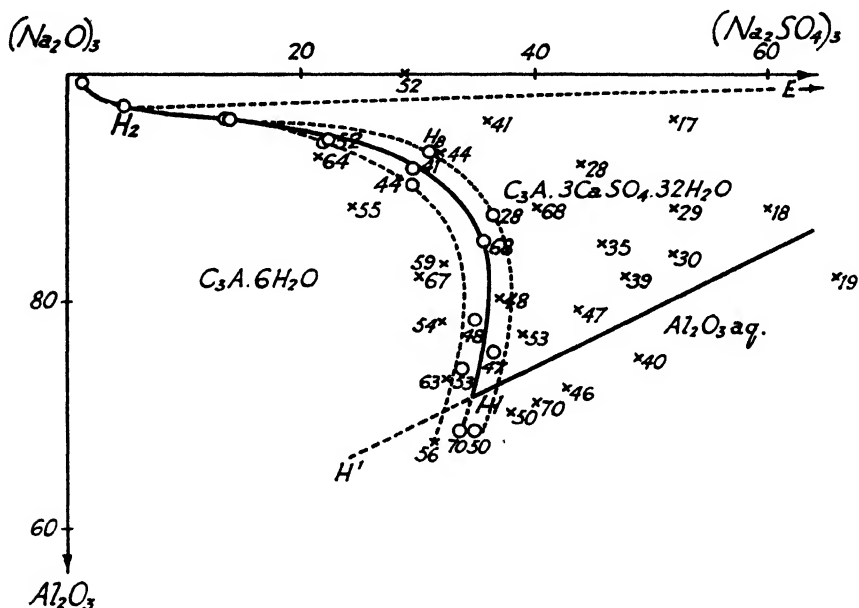


FIG. 8. Determination of boundary curve $\text{C}_3\text{A} \cdot 6\text{H}_2\text{O}-\text{C}_3\text{A} \cdot 3\text{CaSO}_4 \cdot 32\text{H}_2\text{O}$ within metastable region H_2H .

The boundary curve $\text{C}_3\text{A} \cdot 3\text{CaSO}_4 \cdot 32\text{H}_2\text{O}-\text{C}_3\text{A} \cdot 6\text{H}_2\text{O}$ (GH) (figures 3, 6b, 9)

This curve is shown projected on to the face $(\text{Na}_2\text{O})_3-(\text{CaO})_3-\text{Al}_2\text{O}_3$ in figure 6b, on to the face $\text{Al}_2\text{O}_3-(\text{Na}_2\text{O})_3-(\text{Na}_2\text{SO}_4)_3-\text{Al}_2(\text{SO}_4)_3$ in figure 3, and on to the base of the prism in figure 9. Selected data are given in table 8. The curve was obtained by means of mixes of 0.300 g. $\text{C}_3\text{A} \cdot 6\text{H}_2\text{O}$ and 125 g. of solution containing varying amounts of sodium sulfate and sodium hydroxide, together with added crystalline calcium hydroxide in that portion of the curve lying between the invariant point G and point H8 (figure 8) and aluminum sulfate plus small additions of calcium sulfate (at a rate varying from 0.0205 to 0.123 g. CaSO_4 per 1000 g. solution) in that portion of the curve lying between point 52 and the invariant point H. As in the case of the K_2O system, the latter part of the curve,

which is evidently a metastable prolongation of the stable $C_2A \cdot 3CaSO_4 \cdot 32H_2O$ — $C_3A \cdot 6H_2O$ boundary curve beyond a stable invariant point with crystalline γ - $Al_2O_3 \cdot 3H_2O$, cannot be defined sharply. It was determined as illustrated in figure 8, the general procedure being that used previously. As before, mixes were shaken for 7 days. The initial compositions are shown by crosses. In

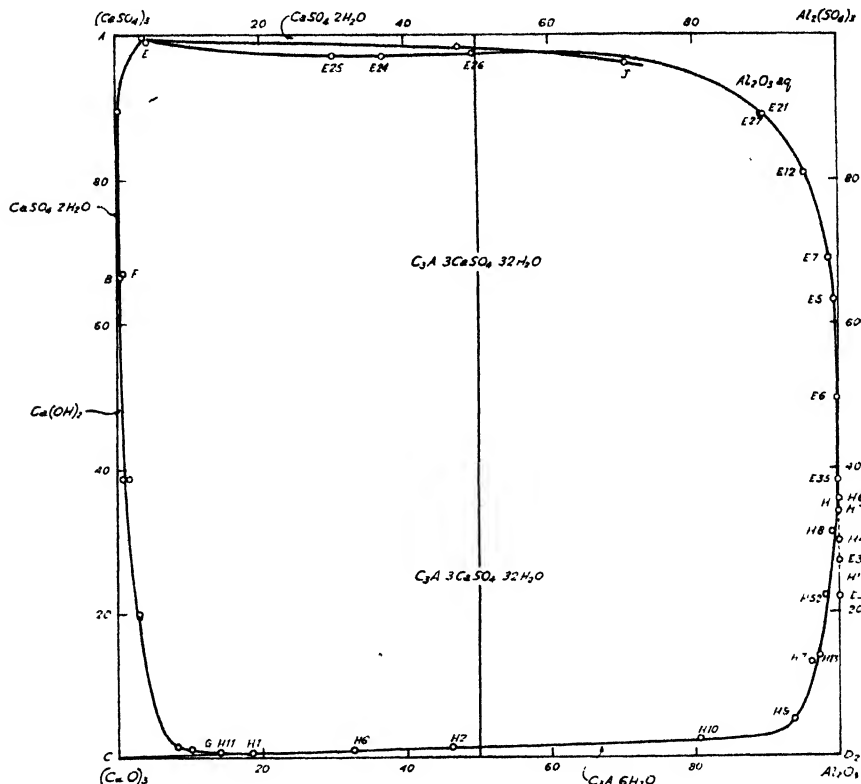


FIG. 9. Quinary system $CaO-Al_2O_3-CaSO_4-Na_2O-H_2O$ (1 per cent $NaOH$). Projection on base of space figure.

$Al_2O_3aq-C_3A \cdot 3CaSO_4 \cdot 32H_2O$ (EHH')

$Al_2O_3aq-C_3A \cdot 6H_2O$ (HD₂)
 $Al_2O_3aq-CaSO_4 \cdot 2H_2O$ (EJ)

$CaSO_4 \cdot 2H_2O-C_2A \cdot 3CaSO_4 \cdot 32H_2O$ (EF)

$CaSO_4 \cdot 2H_2O-Ca(OH)_2$ (BF)
 $Ca(OH)_2-C_2A \cdot 3CaSO_4 \cdot 32H_2O$ (FG)

$Ca(OH)_2-C_2A \cdot 6H_2O$ (GC)
 $C_2A \cdot 6H_2O-C_3A \cdot 3CaSO_4 \cdot 32H_2O$ (GH)

the case of those mixes containing a small addition of calcium sulfate, the true position is slightly behind the face shown.

Microscopic examination showed—proceeding towards the $(Na_2O)_3-Al_2O_3$ edge—either nearly complete conversion of $C_3A \cdot 6H_2O$ (mixes 17; 29, 35; 18, 30, 39; 19, 40, 46), or partial conversion (mixes 52, 64; 41, 44; 28, 68; 48; 47, 53; 70, 50), or no formation of $C_3A \cdot 3CaSO_4 \cdot 32H_2O$ (mixes 64; 49, 55; 59, 67; 54; 63; 56). Small amounts of residual $C_3A \cdot 6H_2O$ are ascribed to the formation of a

protective coating, either of $\text{C}_3\text{A} \cdot 3\text{CaSO}_4 \cdot 32\text{H}_2\text{O}$ or of CaCO_3 . In some few mixes, not shown in the figure, it was found that the reaction was stopped soon after commencement of $\text{C}_3\text{A} \cdot 3\text{CaSO}_4 \cdot 32\text{H}_2\text{O}$ formation. To guard against the possibility of carbonated impurity in the sodium hydroxide used being responsible for preventing reaction, small amounts of calcium sulfate solution were added in the remaining mixes. Those showing partial conversion gave, on analysis of the equilibrium solutions, the distribution of points shown, lying within the dotted lines. Of the mixes listed as not forming $\text{C}_3\text{A} \cdot 3\text{CaSO}_4 \cdot 32\text{H}_2\text{O}$ and therefore lying in the $\text{C}_3\text{A} \cdot 6\text{H}_2\text{O}$ field, 59 and 67 actually contained traces. The mean position of the boundary is shown by the full line, meeting the boundary curve $\text{Al}_2\text{O}_3\text{aq-C}_3\text{A} \cdot 3\text{CaSO}_4 \cdot 32\text{H}_2\text{O}$ in the invariant point H.

TABLE 9
Invariant point compositions

	INVARIANT POINT	GRAM MOLES $\times 10^4$ PER = 1000 G. OF SOLUTION				POSITIVE COMPONENTS = 100 PER CENT			NEGATIVE COMPONENTS = 100 PER CENT	
		(Na_2O) ₂	(CaO) ₂	Al_2O_3	(SO_3) ₂	(Na_2O) ₂	(CaO) ₂	Al_2O_3	(SO_3) ₂	(H_2O) ₂
						mole per cent	mole per cent	mole per cent	mole per cent	mole per cent
E . .	$\text{CaSO}_4 \cdot 2\text{H}_2\text{O-Al}_2\text{O}_3\text{aq-}$ $\text{C}_3\text{A} \cdot 3\text{CaSO}_4 \cdot 32\text{H}_2\text{O}$	417	33.9	1.40	449	92.2	7.55	0.3	99.2	0.8
F ..	$\text{CaSO}_4 \cdot 2\text{H}_2\text{O-Ca(OH)}_2\text{-}$ $\text{C}_3\text{A} \cdot 3\text{CaSO}_4 \cdot 32\text{H}_2\text{O}$	417	51.3	0.25	313	89.1	11.0	0.05	66.8	33.2
G.....	$\text{Ca(OH)}_2\text{-C}_3\text{A} \cdot 6\text{H}_2\text{O-}$ $\text{C}_3\text{A} \cdot 3\text{CaSO}_4 \cdot 32\text{H}_2\text{O}$	417	5.4	0.85	3.1	98.7	1.3	0.2	0.75	99.25
H.....	$\text{C}_3\text{A} \cdot 3\text{CaSO}_4 \cdot 32\text{H}_2\text{O-}$ $\text{C}_3\text{A} \cdot 6\text{H}_2\text{O-Al}_2\text{O}_3\text{aq.}$	417		168	202	71.3		28.7	34.6	65.4
B	$\text{CaSO}_4 \cdot 2\text{H}_2\text{O-Ca(OH)}_2$	413	51.3		313	89.0	11.0		67.5	32.5
C	$\text{C}_3\text{A} \cdot 6\text{H}_2\text{O-Ca(OH)}_2$	417	5.2	1.5		98.4	1.25	0.35		100

The space figure and the basal projection

The spacial relations of the various curves are shown in figure 1. The curves and invariant points given are as listed in the work on the K_2O system, with appropriate substitution of Na_2O for K_2O . The projection on to the base of the prism by means of lines drawn through the edge $(\text{Na}_2\text{O})_3\text{-(Na}_2\text{SO}_4)_3$ parallel to the triangular end faces is shown in figure 9. Invariant point compositions are given in table 9.

DISCUSSION

The results now obtained confirm the behavior found in the corresponding K_2O system. The spacial relations of the various boundary curves are similar, though differences naturally arise in the relative positions which are to be related to the substitution of sodium for potassium and to the increase in molecular concentration of the alkali from 0.0297 gram-moles of $(\text{K}_2\text{O})_3$ to 0.0417 gram-

moles of $(\text{Na}_2\text{O})_3$ per 1000 g. of solution. As in the K_2O system, the fundamentally stable equilibria with $\text{Al}_2\text{O}_3 \cdot 3\text{H}_2\text{O}$ have been left for future examination, as have the conditions of formation of metastable solid solutions which probably exist. A discussion has been given in the previous paper on the application of the equilibria relations to the conditions existing in a setting Portland cement. This applies also to the present work.

Since the foregoing paper was written, the writer has seen a discussion by Kalousek (4) in which reference is made to a recent dissertation by this author on the system $\text{CaO}-\text{Al}_2\text{O}_3-\text{SO}_3-\text{Na}_2\text{O}-\text{H}_2\text{O}$ at 25°C . (5). The latter publication has not been seen by the writer, but in the former it is stated that the work "indicated that the stable sulfate bearing compounds (in the presence of NaOH) are members of a solid solution series having $3\text{CaO} \cdot \text{Al}_2\text{O}_3 \cdot \text{CaSO}_4 \cdot 12\text{H}_2\text{O}$ and $3\text{CaO} \cdot \text{Al}_2\text{O}_3 \cdot \text{Ca}(\text{OH})_2 \cdot 12\text{H}_2\text{O}$ as end members". The results of the present work however indicate that for alkali concentrations equivalent to 1 per cent NaOH (and 1 per cent KOH also) the compound $3\text{CaO} \cdot \text{Al}_2\text{O}_3 \cdot 3\text{CaSO}_4 \cdot 32\text{H}_2\text{O}$ is the only stable sulfate phase and suggest that solid solutions will occur as metastable phases as in the quaternary system. In this system the low-sulfate form $3\text{CaO} \cdot \text{Al}_2\text{O}_3 \cdot \text{CaSO}_4 \cdot 12\text{H}_2\text{O}$ was found to occur as a terminal component in a solid solution series $3\text{CaO} \cdot \text{Al}_2\text{O}_3 \cdot \text{CaSO}_4 \cdot 12\text{H}_2\text{O} + 3\text{CaO} \cdot \text{Al}_2\text{O}_3 \cdot \text{Ca}(\text{OH})_2 \cdot 12\text{H}_2\text{O}$.

SUMMARY

As a further contribution to the study of the reactions occurring in the setting and hardening of Portland cements, and the disintegration of cements on exposure to sulfate waters, a study has been made of the quinary system $\text{CaO}-\text{Al}_2\text{O}_3-\text{CaSO}_4-\text{Na}_2\text{O}-\text{H}_2\text{O}$ (1 per cent NaOH) at 25°C . The results are similar to those already found for the corresponding 1 per cent KOH system.

The investigations described in this paper were carried out at the Building Research Station of the Department of Scientific and Industrial Research, and the paper is published by permission of the Director of Building Research.

REFERENCES

- (1) CAMERON, F. K., AND BREAZEALE, J. F.: *J. Phys. Chem.* **8**, 335 (1904).
- (2) GOUDRIAAN, F.: *Rec. trav. chim.* **41**, 82 (1922).
- (3) JONES, F. E.: *Trans. Faraday Soc.* **35**, 1484 (1939).
- (4) KALOUSEK, G. L.: *Am. Concrete Inst.* **12** (Proceedings **37**), 692 (1941).
- (5) KALOUSEK, G. L.: Dissertation, University of Maryland, 1941.

OBSERVATIONS ON THE RARE EARTHS. LI¹AN ELECTROMETRIC STUDY OF THE PRECIPITATION OF TRIVALENT HYDROUS
RARE EARTH OXIDES OR HYDROXIDESTHERALD MOELLER AND HOWARD E. KREMERS²*Noyes Chemical Laboratory, University of Illinois, Urbana, Illinois**Received June 29, 1944*

INTRODUCTION

Theoretical considerations based upon the more or less steady decrease in the molecular volumes of isomorphous compounds of the trivalent rare earth elements, or in the radii of the trivalent ions themselves, with increase in atomic numbers indicate a corresponding decrease in basicity in this series of elements (23). Experimental data obtained in a variety of fashions agree well with this prediction (22), but many of the methods used have been indirect. Probably the most useful comparisons are those based upon the properties of the hydrous oxides or hydroxides themselves, but in most instances such data as are available depend upon results obtained with rare earth mixtures rather than with the individual elements.

It has already been shown (6) that the basicities of the rare earth elements can be compared in terms of the solubility-product constants for the hydrous hydroxides, but data are available only for the elements lanthanum, praseodymium, neodymium, samarium, gadolinium, dysprosium, and yttrium (6). Furthermore, basicity comparisons can also be made in terms of the pH values at which the hydrous oxides or hydroxides precipitate (4).

Since both of these types of data can be obtained from electrometric titrations of metal salt solutions with alkalis (3), it seemed logical to approach the problem in this fashion. The rare earth elements have thus far been only incompletely investigated in this manner. Thus, Hildebrand (8) found praseodymium and neodymium chloride solutions to yield precipitates in pH ranges close to 7, whereas the corresponding nitrate solutions gave precipitates at pH values below 4, a difference which has been ascribed to catalytic reduction of the nitrate ion at the hydrogen electrode employed (2). Britton (2), working with a hydrogen electrode in solutions approximately 0.01 *M* in rare earth ions, investigated the effects of sodium hydroxide upon salts of the cerium earths (lanthanum through samarium) and yttrium. A similar investigation, based upon results obtained with a glass electrode, was carried out by Bowles and Partridge (1) upon approximately 0.01 *M* lanthanum, cerous, ceric, praseodymium, neodymium, ytterbium, and thorium salt solutions. Some additional measurements upon 0.03 *M* lanthanum chloride solutions (21) and upon approximately 0.005 *N* lanthanum, cerous, and yttrium salt solutions (18) have been reported.

¹ For the preceding communication in this series, see Moeller and Kremers: *J. Am. Chem. Soc.* **66**, 307 (1944).

² Present address: Lindsay Light and Chemical Company, West Chicago, Illinois.

Inasmuch as in all these investigations except the last two (18, 21) no data upon solubility-product constants have been presented, and inasmuch as data upon the yttrium earths are almost entirely lacking, a comprehensive study of the series was indicated. This paper presents data obtained by the electrometric method for twelve of the rare earth elements, including yttrium, for nitrate, sulfate, and acetate solutions. These data serve the triple purposes of checking the effects of anions, evaluating the precipitation pH values and the solubility-product con-

TABLE 1
Rare earth materials employed

OXIDE	DESIGNATION	COMPOSITION	SOURCE
Y ₂ O ₃	YT-17	Atomic weight purity	Reference 9
La ₂ O ₃	LA-24	Atomic weight purity	Reference 10
CeO ₂		Chemically pure	Ignition of G. F. Smith Chemical Co. hexanitrate ammonium cerate
Pr ₆ O ₁₁	PR-21	Less than 1% Nd ₂ O ₃	Unknown
Nd ₂ O ₃	ND-34	Atomic weight purity	Unknown
Sm ₂ O ₃	SM-19	Atomic weight purity	Reference 19
Eu ₂ O ₃		Atomic weight purity	Ignition of oxalate prepared by McCoy (14)
Gd ₂ O ₃	GD-5	Atomic weight purity	Fraction Gd-7 (reference 17)
Er ₂ O ₃	ER-34-2d	96% Er ₂ O ₃ , 4% Y ₂ O ₃	Reference 16
Tm ₂ O ₃	TM-5-R3	78% Tm ₂ O ₃ , 11% Lu ₂ O ₃ , <1% Yb ₂ O ₃	Extraction of Yb from Tm-Yb fractions with sodium amalgam (reference 13)
Yb ₂ O ₃	YB-1-a	Less than 0.1% other rare earths	Reference 20
Lu ₂ O ₃	LU-4-R11	95% Lu ₂ O ₃ , 4% Tm ₂ O ₃ , <0.3% Yb ₂ O ₃	Extraction of Yb from Yb-Lu fractions with sodium amalgam (reference 13)

stants, and indicating the basicity order and relative basicities of the hydrous oxides or hydroxides.

EXPERIMENTAL

A. Materials

The rare earth materials used were the best available in this laboratory. Data concerning the sources and degrees of purity of the oxides employed are summarized in table 1. From these highly purified rare earth oxides solutions of the nitrates, sulfates, and acetates were prepared by dissolving weighed quantities of the oxides in the appropriate acids, evaporating to dryness to remove excess acids, taking up the residues in distilled water, and diluting. Cerous acetate was prepared from cerous carbonate, and hydrogen peroxide was used to reduce ceric nitrate and ceric sulfate.

All other chemicals were of reagent quality. Solutions of sodium hydroxide were standardized against primary standard potassium acid phthalate and were protected from carbon dioxide.

B. Titration procedure

Forty-milliliter portions of rare earth nitrate, sulfate, and acetate solutions (approximately 0.1 *M* in rare earth ions, R^{+++}) were titrated with 0.1 *N* carbonate-free sodium hydroxide in a thermostat controlled to $25^{\circ}\text{C.} \pm 0.5^{\circ}$ (15), the changes in pH being followed with a Beckman Laboratory Model G pH Meter, the glass electrode of which had been calibrated with a 0.05 *M* potassium acid phthalate buffer. The solutions were stirred mechanically, and atmospheric carbon dioxide was excluded by bubbling nitrogen through the solutions. Oxidation of cerous compounds was prevented by covering the aqueous salt solutions with 3-cm. layers of neutral petroleum ether.

Since complete equilibrium, as indicated by a constant pH reading after the addition of an increment of alkali, was attained only very slowly and since relative values were desired, all titrations were performed as follows: After neutralization of traces of free acid, sodium hydroxide was added in 0.3-ml. increments to a mole ratio of added alkali to rare earth ion initially present (OH^-/R^{+++}) of 0.2 to 0.3. Then 1.5- to 2.0-ml. increments of alkali were added. Each pH measurement was made 10 min. after the addition of the alkali, any change in pH after this time interval being quite small.

RESULTS AND DISCUSSION

Titration data for rare earth nitrate, sulfate, and acetate solutions are plotted in figures 1, 2, and 3, respectively. Although the horizontal or precipitation regions of the curves for all the elements studied lie within a rather narrow pH interval, definite differences are distinguishable, and there is a rather steady decrease in the pH range in which this region falls as one proceeds by increasing atomic numbers from lanthanum to lutecium. The position of yttrium between gadolinium and erbium is in agreement with predictions based upon size relationships (23). The anomalous shapes of the curves for praseodymium nitrate and acetate are unexplained, since the praseodymium material used was of high quality.

Summarized in table 2 are data for precipitation pH values. Since it was not always easy to determine exactly when precipitates first formed, pH data at the mole ratio $\text{OH}^-/R^{+++} = 0.4$ are also included. At this mole ratio, precipitation was proceeding uniformly, and these data thus serve well for comparisons among the several rare earth elements. For purposes of comparison, such other data (with references) as have been reported on the pH values at precipitation incidence are included. The agreement is reasonably good.

The data in table 2 are perhaps best considered in their relation to the radii of the trivalent ions, the calculated values (7) for which have also been listed. It is apparent that decrease in pH either at incidence of precipitation or at mole ratio $\text{OH}^-/R^{+++} = 0.4$ closely parallels decrease in ionic radius. The position of

yttrium, which would be anomalous from the point of view of atomic number considerations, is then perfectly justifiable.

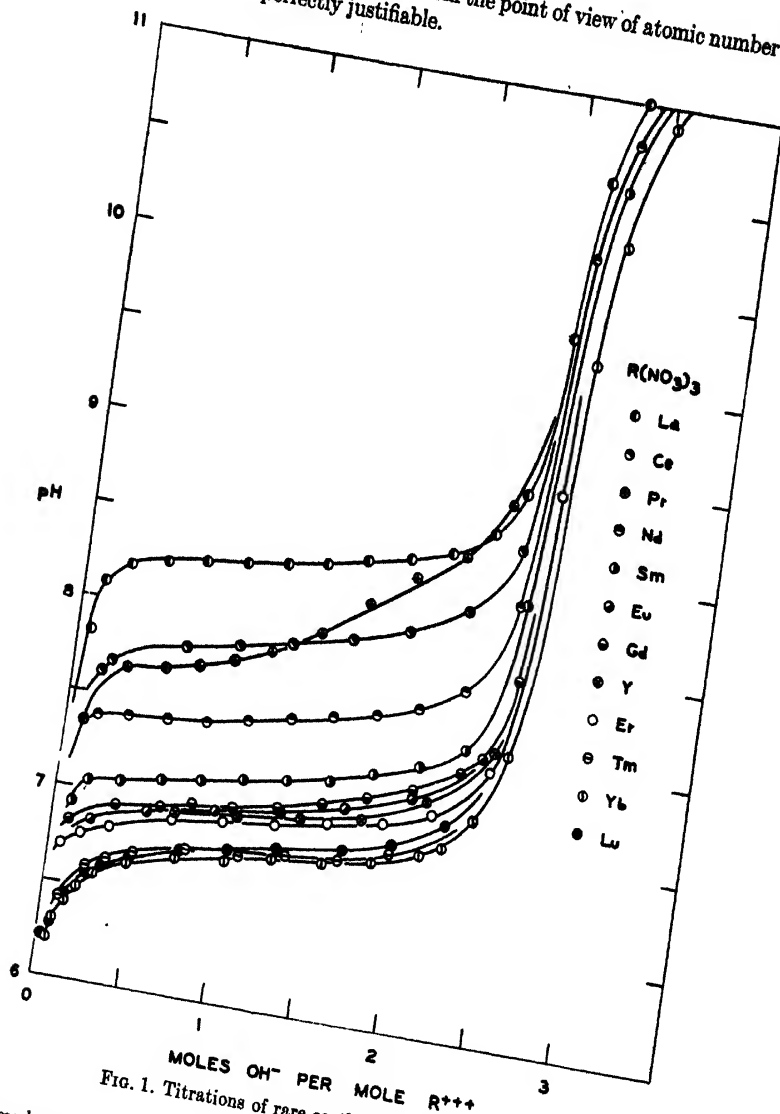


Fig. 1. Titrations of rare earth nitrate solutions

It seems logical to conclude then, on the basis of precipitation pH data, that the basicities of the rare earth elements decrease fairly regularly in the series lanthanum to lutecium, yttrium occupying a position commensurate with its ionic radius. That an arrangement of the hydrous oxides and hydroxides in the

order of decreasing precipitation pH values actually corresponds to the order of decreasing basicities has been questioned (4). However, the precipitation pH is

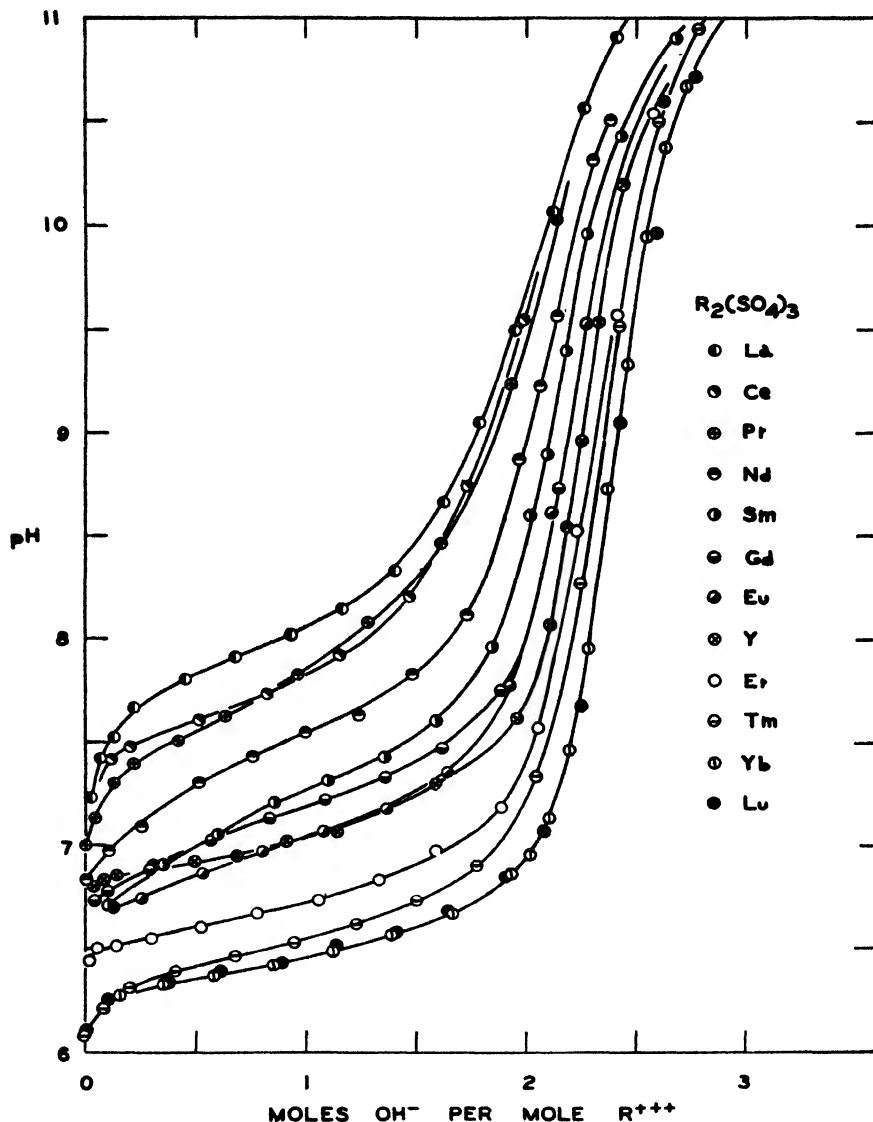
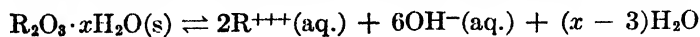
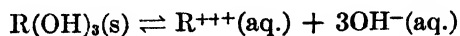


FIG. 2. Titrations of rare earth sulfate solutions

a measure of the hydroxyl-ion concentrations (or activities) in the equilibria



and



and must, therefore, be a measure of the extent to which the hydroxyl ion is lost by the hydrous oxide or hydroxide, or in other words of the basicity.

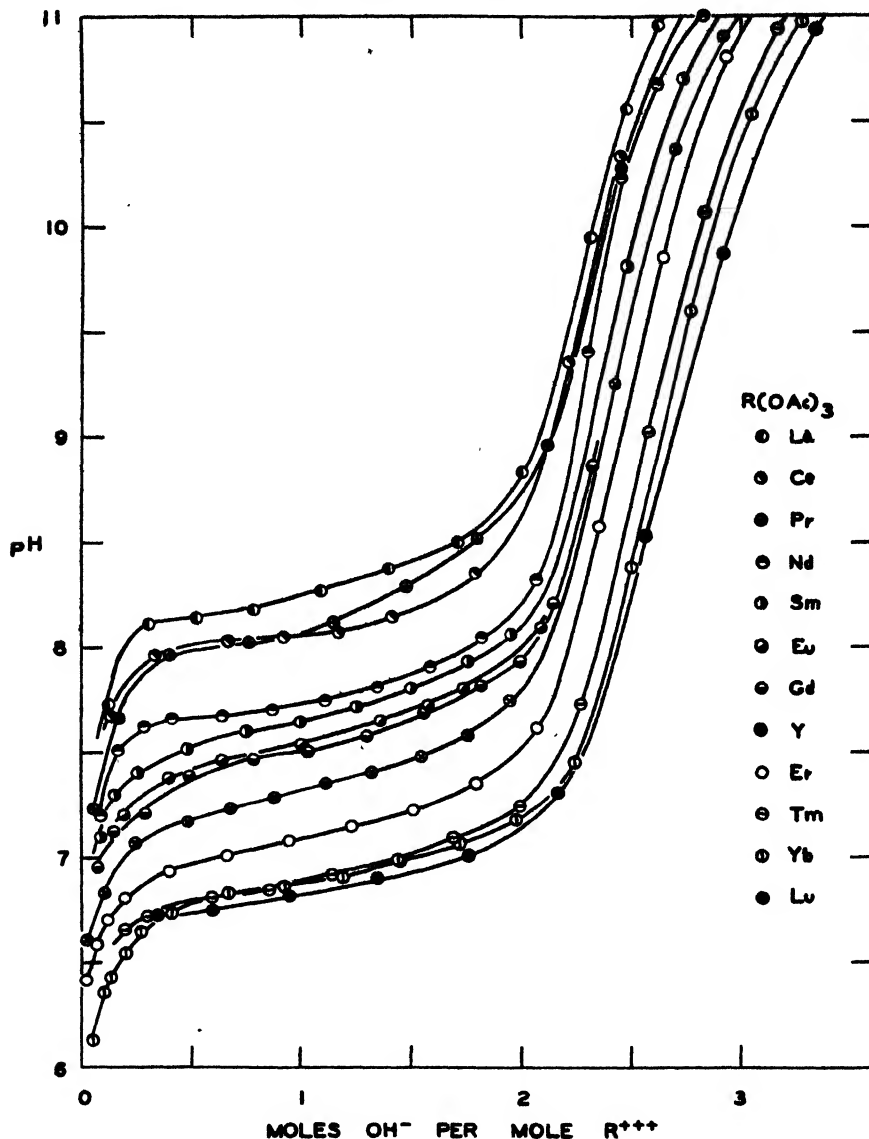


FIG. 3. Titrations of rare earth acetate solutions

Precipitation generally occurred at a higher pH value with an acetate than with the corresponding nitrate or sulfate. This is indicative of slightly reduced concentrations of rare earth ion in acetate solutions and is due to coordination between the rare earth and acetate ions. Since the precipitation regions of the ace-

tate curves are in relatively higher pH ranges for the rare earth ions of smaller size than are those of the nitrate and sulfate curves, it is apparent that an increase in coordinating tendency toward the acetate parallels a decrease in ion size.

In all instances, the titration curves rise steeply before the theoretical 3 OH⁻ to 1 R⁺⁺⁺ mole ratio is attained. This suggests the formation of basic salts during the precipitation processes (2, 18). For the individual rare earth ions, there is little significant difference in the tendency toward basic nitrate formation, but

TABLE 2
Precipitation pH values

RARE EARTH (R)	ATOMIC NUM- BER	RADIUS OF R ⁺⁺⁺ Å.	pH								
			This investigation						Other investigations		
			At precipitation incidence			At OH ⁻ /R ⁺⁺⁺ = 0.4			At precipitation incidence		
			NO ₃ ⁻	SO ₄ ⁻⁻	C ₂ H ₃ O ₂ ⁻	NO ₃ ⁻	SO ₄ ⁻⁻	C ₂ H ₃ O ₂ ⁻	NO ₃ ⁻	SO ₄ ⁻⁻	Cl ⁻
La. . . .	57	1.00	7.82	7.41	7.93	8.23	7.78	8.13	8.35 (2) 8.71 (18)	7.61 (1)	8.03 (1)
Ce . . .	58	0.94	7.60	7.35	7.77	7.76	7.56	7.99	8.1 (18)	7.07 (1)	7.41 (2)
Pr . . .	59	0.91	7.35	7.17	7.66	7.67	7.50	7.96		6.98 (1)	7.05 (2)
Nd . . .	60	0.90	7.31	6.95	7.59	7.40	7.23	7.65	7.00 (2)	6.73 (1)	7.02 (2) 7.40 (1)
Sm . . .	62	0.87	6.92	6.70	7.40	7.08	6.93	7.48			6.83 (2)
Eu . . .	63	0.87	6.82	6.68	7.18	6.90	6.82	7.37			
Gd . . .	64	0.86	6.83	6.75	7.10	6.94	6.95	7.31			
Y . . .	39	0.83	6.95	6.83	6.83	6.90	6.90	7.15	7.39 (18)		6.78 (2)
Er . . .	68	0.82	6.76	6.50	6.59	6.84	6.58	6.93			
Tm . . .	69	0.81	6.40	6.21	6.53	6.70	6.38	6.77			
Yb . . .	70	0.79	6.30	6.18	6.50	6.65	6.32	6.73		6.16 (1)	
Lu . . .	71	0.79	6.30	6.18	6.46	6.63	6.32	6.73			

with sulfates and acetates the major inflections occur at lower OH⁻/R⁺⁺⁺ ratios as one proceeds from lutecium to lanthanum, a trend which is also apparent in the data of other investigators (1, 2). Since the smallest ions in the series should form basic salts the most extensively, such a trend is not unexpected.

That basic salts did form was further indicated by the slowness with which equilibria were established in the precipitation regions. In these regions, the addition of each increment of alkali caused the observed pH to rise to a maximum. The pH then decreased slowly and gradually approached a reasonably constant value. Apparently, basic salts were first precipitated and then reacted with more hydroxyl ions from the solutions. This phenomenon was most pronounced with yttrium and may account for the apparently anomalous placing of yttrium along with samarium in some basicity series (22).

TABLE 3
Solubility products and solubilities for hydrous rare earth hydroxides at 25°C.

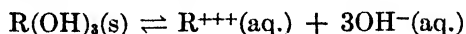
RARE EARTH	OXIDE IN 40 ML.	NITRATE SOLUTIONS		SULFATE SOLUTIONS		ACETATE SOLUTIONS		AVERAGE OF SOLUBILITY PRODUCTS	AVERAGE OF SOLUBILITIES $\times 10^6$
		K	$S \times 10^6$	K	$S \times 10^6$	K	$S \times 10^6$		
	grams		gram-moles per liter		gram-moles per liter		gram-moles per liter		gram-moles per liter
La.....	0.1108	1.1×10^{-19}	8.0	7.7×10^{-20}	7.3	1.1×10^{-19}	8.0	1.0×10^{-19}	7.8
	0.1085								
	0.1100								
Ce.....	0.1033	7.0×10^{-21}	4.0	2.2×10^{-20}	5.3	1.8×10^{-20}	5.1	1.5×10^{-20}	4.8
	0.1035								
	0.0860								
Pr.....	0.1048	8.4×10^{-21}	4.2	3.0×10^{-20}	5.8	4.3×10^{-20}	6.3	2.7×10^{-20}	5.4
	0.1011								
	0.1084								
Nd.....	0.1093	3.1×10^{-22}	1.8	2.6×10^{-21}	3.1	2.8×10^{-21}	3.2	1.9×10^{-21}	2.7
	0.1083								
	0.1108								
Sm.....	0.1113	4.6×10^{-23}	1.1	6.0×10^{-22}	2.2	1.4×10^{-21}	2.7	6.8×10^{-22}	2.0
	0.1096								
	0.1092								
Eu.....	0.0985	1.3×10^{-23}	0.8	2.9×10^{-23}	1.0	1.0×10^{-21}	2.5	3.4×10^{-23}	1.4
	0.0987								
	0.0998								
Gd.....	0.1123	1.8×10^{-23}	0.9	7.8×10^{-23}	1.3	5.4×10^{-23}	2.1	2.1×10^{-22}	1.4
	0.1073								
	0.1092								
Y.....	0.0877	1.4×10^{-23}	0.9	3.8×10^{-23}	1.1	1.9×10^{-23}	1.6	8.1×10^{-23}	1.2
	0.0894								
	0.0869								
Er.....	0.1016	7.5×10^{-24}	0.7	2.7×10^{-24}	0.6	3.0×10^{-23}	1.0	1.3×10^{-23}	0.8
	0.1088								
	0.1038								
Tm.....	0.1038	3.0×10^{-24}	0.6	8.3×10^{-25}	0.4	6.2×10^{-24}	0.7	3.3×10^{-24}	0.6
	0.1097								
	0.1062								
Yb.....	0.1117	2.2×10^{-24}	0.5	3.0×10^{-25}	0.3	6.2×10^{-24}	0.7	2.9×10^{-24}	0.5
	0.1158								
	0.1167								
Lu.....	0.1104	3.9×10^{-24}	0.6	3.1×10^{-25}	0.3	3.4×10^{-24}	0.6	2.5×10^{-24}	0.5
	0.1200								
	0.2000								

Evaluation of solubility-product constants from electrometric titration data is dependent upon a knowledge of the compositions of the precipitates ultimately produced and an assumption that the compositions of these precipitates remain essentially the same throughout the titrations (3). Even though precipitation from lanthanum salt solutions appears to be complete before the theoretical 3 OH⁻ to 1 La⁺⁺⁺ mole ratio is attained, dehydration experiments have shown the precipitate to be hydrous lanthanum hydroxide (11). Similar experiments show that praseodymium and neodymium form hydrous hydroxides, while samarium and yttrium yield hydrous oxides (25). Although corresponding data are not available for the remaining earths, at least some appear to form hydroxides (24). Therefore, for purposes of calculation, it seemed not unreasonable to assume that the precipitates formed during the titrations were hydrous hydroxides. This has been done.

On this basis, the solubility-product constants were calculated from pH values and rare earth ion concentrations at OH⁻/R⁺⁺⁺ mole ratios of 0.6, 1.2, and 1.5, the ion product of water at 25°C. being taken as 1×10^{-14} and the concentrations being corrected for the volumes of added alkali. In table 3 are recorded the average solubility-product constants (K) based upon the values at the three stated mole ratios. Given also are the average water solubilities (S) calculated from the average solubility-product constants by means of the relation $S = \sqrt[3]{K/27}$. In addition, values are given for the overall average solubility-product constant and water solubility for each hydroxide. These data represent averages of all data available for the individual materials.

Because of the anomalous shapes of the titration curves for its salts, the solubility product and solubility for praseodymium hydroxide are excessively high and this element is out of line with the others. The other values in table 3 agree well with the few available from other investigations. Thus Oka (18) found the following values for the average solubility products for the freshly precipitated hydroxides at 25°C.: La, 4.3×10^{-19} ; Ce (III), 0.87×10^{-20} ; Y, 5.2×10^{-22} . Working at 18°C., Sadolin (21) obtained a value of 1.2×10^{-19} for the solubility-product constant for freshly precipitated lanthanum hydroxide. Aged lanthanum hydroxide gave a constant of 1.1×10^{-21} (21), a value agreeing well with 0.91×10^{-21} reported for the aged hydroxide at 25°C. (12). Busch (5) obtained values for the water solubilities of the sesquioxides of lanthanum, praseodymium, neodymium, yttrium, and erbium of the order of 10^{-6} gram-mole per liter.

The almost steady decrease in the magnitudes of the solubility-product constants and water solubilities as listed in table 3 parallels the decrease in ionic radii as listed in table 2. Inasmuch as both the solubility product and the solubility are measures of the extent to which the equilibrium



is displaced for a particular hydroxide, it is apparent that they are also measures of relative basicities.

On this basis, as well as on the basis of precipitation pH values, one can then conclude that basicity in the trivalent hydrous hydroxides of the rare earth ele-

ments decreases with decrease in ionic size of the constituent metal, yttrium occupying a position between gadolinium and erbium which is in accord with the

TABLE 4
Relative basicities of rare earth hydroxides

RATIO	RATIO OF SOLUBILITY PRODUCTS		RATIO OF IONIC RADII
	This investigation	Endres' investigation (6)	
La:Y	1235	1300	1.21
Ce:Y	185		1.13
Pr:Y	333	80	1.10
Nd:Y	23.5	47	1.09
Sm:Y	8.4		1.05
Eu:Y	4.2		1.05
Gd:Y	2.6	3.4	1.04
Dy:Y		0.5	1.01
Y:Y	1.0	1.0	1.00
Er:Y	0.16		0.99
Tm:Y	0.041		0.98
Yb:Y	0.036		0.95
Lu:Y	0.031		0.95

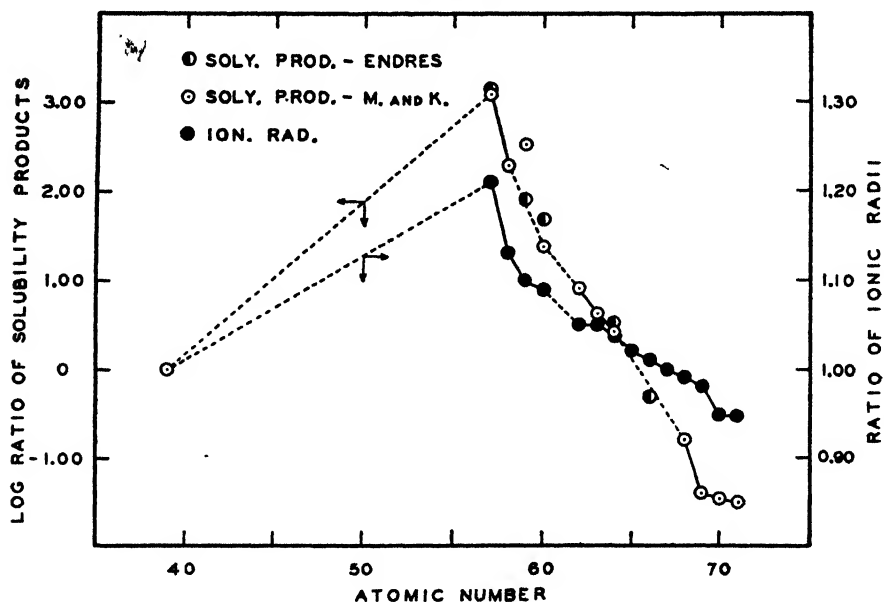


FIG. 4. Relative basicities and ionic radii

relative size of its cation. Independent confirmation of published basicity arrangements (22) is thereby offered.

If one assumes with Endres (6) that the relative basicities of the hydroxides

stand in the same ratio as their solubility-product constants, one can then evaluate these relative basicities from the data in table 3. Basing these calculations upon yttrium hydroxide as a standard, one thus obtains the values listed in table 4. Included also are the corresponding values given by Endres (6), as well as the ratios of the ionic radii of the trivalent ions to the yttrium ion. Agreement between the values obtained in this investigation and those of Endres is good, and the decrease in relative basicities parallels the decrease in the ratios of the ionic radii. The anomalously high value for the basicity of praseodymium hydroxide is again traceable to peculiarities in the titration curves.

Inasmuch as Endres (6) pointed out that plots of both the logarithms of the ratios of the solubility-product constants and the ratios of the corresponding ionic radii against atomic numbers gave similar curves, this approach has been carried out in figure 4. Since the similarities in trend are so apparent, Endres' conclusions as to the relations between basicities and ionic sizes (6) can be considered substantiated.

Consideration of the precipitation pH values and the solubilities of the hydrous hydroxides indicates that only in the separation of lanthanum from the other trivalent rare earth elements can basic precipitation take place with any reasonable degree of efficiency. Furthermore, separations of the elements samarium, europium, and gadolinium and of the elements thulium, ytterbium, and lutecium cannot be effectively carried out in this manner. These indications are in accord with experimental observations. The data given in figures 1, 2, and 3 suggest that, of the anions studied, nitrates are preferable for separations of the cerium earth metals by basic precipitation, acetates are preferable for corresponding separations of the terbium earths, and sulfates are preferable for the yttrium earths. Further investigations along these lines are indicated.

SUMMARY

1. Electrometric titration data for nitrate, sulfate, and acetate solutions of twelve of the rare earth elements, including yttrium, indicate decreases in the basicities of the hydrous oxides or hydroxides which parallel decreases in the radii of the trivalent cations.
2. The basicity of yttrium hydroxide is between those of gadolinium and erbium hydroxides, in accordance with size relationships.
3. Calculation of the solubility-product constants and water solubilities has been carried out on the assumption that all precipitates are hydrous hydroxides.
4. A numerical evaluation of relative basicities based upon solubility-product constants is given.

REFERENCES

- (1) BOWLES AND PARTRIDGE: *Ind. Eng. Chem., Anal. Ed.* **9**, 124 (1937).
- (2) BRITTON: *J. Chem. Soc.* **127**, 2142 (1925).
- (3) BRITTON: *Hydrogen Ions*, Vol. II, 3rd edition, p. 41. Chapman and Hall, Ltd., London (1942).
- (4) BRITTON: *Reference 3*, p. 79.
- (5) BUSCH: *Z. anorg. allgem. Chem.* **161**, 161 (1927).

- (6) ENDRES: *Z. anorg. allgem. Chem.* **205**, 321 (1932).
- (7) GRIMM AND WOLFF: *Z. physik. Chem.* **119**, 254 (1926).
- (8) HILDEBRAND: *J. Am. Chem. Soc.* **35**, 847 (1913).
- (9) HOPKINS AND BALKE: *J. Am. Chem. Soc.* **38**, 2332 (1916).
- (10) HOPKINS AND DRIGGS: *J. Am. Chem. Soc.* **44**, 1927 (1922).
- (11) HÜTTIG AND KANTOR: *Z. anorg. allgem. Chem.* **202**, 421 (1931).
- (12) KOLTHOFF AND ELMQUIST: *J. Am. Chem. Soc.* **53**, 1217 (1931).
- (13) KREMERS: Doctoral Dissertation, University of Illinois, 1944.
- (14) MCCOY: *J. Am. Chem. Soc.* **59**, 1131 (1937).
- (15) MOELLER: *J. Am. Chem. Soc.* **63**, 2625 (1941).
- (16) MOELLER AND KREMERS: *J. Am. Chem. Soc.* **66**, 307 (1944).
- (17) NAESER AND HOPKINS: *J. Am. Chem. Soc.* **57**, 2183 (1935).
- (18) OKA: *J. Chem. Soc. Japan* **59**, 971 (1938).
- (19) OWENS, BALKE, AND KREMERS: *J. Am. Chem. Soc.* **42**, 515 (1920).
- (20) PEARCE AND NAESER WITH HOPKINS: *Trans. Am. Electrochem. Soc.* **69**, 557 (1936).
- (21) SADOLIN: *Z. anorg. allgem. Chem.* **160**, 133 (1927).
- (22) SHERWOOD WITH HOPKINS: *J. Am. Chem. Soc.* **55**, 3117 (1933).
- (23) VON HEVESY: *Die seltenen Erden vom Standpunkte des Atombaues*, pp. 16-30. Verlag von Julius Springer, Berlin (1927).
- (24) WALDEN: *Handbuch der allgemeinen Chemie*, Band IX, "Hydroxyde und Oxydhydrate," (Fricke und Hüttig), pp. 114-129. Akademische Verlagsgesellschaft m.b.h., Leipzig (1937).
- (25) WEISER AND MILLIGAN: *J. Phys. Chem.* **42**, 673 (1938).

CATION EXCHANGE AT HIGH pH

RAYMOND NELSON AND HAROLD F. WALTON

Department of Chemistry, Northwestern University, Evanston, Illinois

Received July 10, 1944

It was found by one of the authors (4) that the uptake of calcium ions from a calcium salt solution by the carbonaceous cation exchanger Zeo-Karb rose continuously with pH and showed no signs of levelling off at the highest pH recorded. It was suggested (private communication from Professor John A. Bishop) that the increased uptake in alkaline solution might be due to absorption of an ion, CaOH^+ , similar to the ZnOH^+ postulated by Elgaby and Jenny (1) to explain their results on ion exchange in bentonite. To test this suggestion, measurements have been made on the uptake of potassium ions, which can form no such complex cations, by Zeo-Karb from solutions of pH 3.8 to 12.5. Again an almost linear increase of uptake with pH was found, rising at high pH to over 4 milliequivalents per gram.

This abnormal ion-exchange capacity in alkaline solutions may have some utility,—for example, in the absorption of heavy metals as metal-ammonia complex ions. Tests were therefore made to determine the uptake of nickel, copper, and zinc from ammoniacal salt solutions, and to find whether the metal was absorbed as an ammonia complex or as the free ion.

EXPERIMENTAL

Material

The cation exchanger was the sulfuric acid-treated coal sold as "Zeo-Karb." It was ground, screened to 40-80 mesh, washed thoroughly with concentrated hydrochloric acid and water, and then air dried. The moisture content was found by heating a weighed sample to 110°C. It was the same batch used in previous experiments (4).

Potassium exchange tests

Half-gram samples of Zeo-Karb were shaken overnight at room temperature with 200 cc. of a solution which was $N/10$ in potassium ion, and made up from potassium acetate and acetic acid, potassium acetate and potassium hydroxide, or potassium hydroxide and boric acid. After shaking, the pH of the solution was measured electrometrically; then the Zeo-Karb was separated and ashed in a platinum crucible. The ash was fused with a little sodium carbonate, the mass dissolved, and the potassium determined gravimetrically as the dipicrylamine salt (3).

Metal-ammonia exchange tests

Half-gram samples of Zeo-Karb were shaken overnight with 200 cc. of a solution which was $M/20$ in metal sulfate and contained varying quantities of ammonia. Runs were also made in which no ammonia was added. After shaking, the pH of the solution was found as before, and the Zeo-Karb separated and ashed in a porcelain dish. The ash was evaporated to fumes with concentrated sulfuric acid, then taken up in water and the solution analyzed. Nickel was determined by electrodeposition, and also by dimethylglyoxime; copper was determined by thiosulfate titration; zinc was estimated gravimetrically with 8-hydroxyquinoline.

To determine whether the metal was taken into the Zeo-Karb as an ammonia complex ion, a bed of Zeo-Karb was set up in a 20-mm. diameter tube, the Zeo-Karb having first been treated with sodium bicarbonate to raise its pH. An ammoniacal solution $M/20$ in the metal sulfate was passed until the bed was saturated. It was then washed, and $N/2$ sulfuric acid was passed until no more metal ions could be displaced. The effluent was analyzed for metal and for ammonium, the latter by the distillation method.

RESULTS

The potassium exchange

The potassium uptake is plotted against pH in figure 1. For comparison, the curve for calcium previously obtained is included. In both cases, potassium as well as calcium, the exchange increases almost linearly with pH, suggesting that the increasing calcium exchange is not due to the absorption of CaOH^+ . The continued increase in exchange up to pH 12.5 indicates that Zeo-Karb contains extremely weak acidic groups with dissociation constant of the order of 10^{-13} .

These are probably phenolic hydroxyls, whose acidity is depressed by the presence of sulfonate or carboxylate radicals in the same molecule.

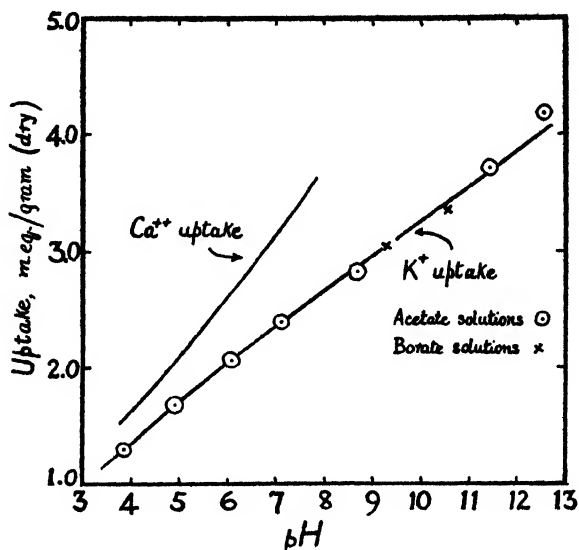


FIG. 1. Calcium and potassium uptake *versus* pH

TABLE 1
Shaking tests

0.5-g. of exchanger (dry basis) containing no cations but H^{+} was shaken with 200 cc. of a solution $M/20$ in metal ion

METAL (CONCENTRATION, 0.05 M)	TOTAL NH_3 ADDED	pH	METAL UPTAKE
	<i>moles per liter</i>		<i>millimoles per gram</i>
Ni	0.00	2.75	0.66
	0.0057	4.00	0.85
	0.77	10.75	2.16
	3.36	11.55	1.97
Cu	0.00	2.68	1.02
	0.32	10.20	2.36
	0.49	10.50	2.21
	2.92	11.60	2.03
Zn	0.00	2.75	1.04
	0.36	10.75	1.91
	3.03	11.20	2.50

Metal-ammonia exchanges

These results are presented in table 1. As expected, the exchange is much greater in ammoniacal than in acid solution, being as much as 5 milliequivalents per gram in one case. This is probably near the saturation value for this ion

exchanger. If this is so, it is not surprising that the differences in uptake of the three metals in ammoniacal solution are so small. Nickel is absorbed less than the others in acid solution.

The results of the percolation experiments designed to find the nature of the cation taken into the Zeo-Karb are given in table 2. It appears that copper is absorbed principally as $\text{Cu}(\text{NH}_3)_2^{++}$, nickel as $\text{Ni}(\text{NH}_3)_4^{++}$, and zinc as a complex or complexes of intermediate composition. The uptake of copper as $\text{Cu}(\text{NH}_3)_2^{++}$ by a resinous exchanger from an ammoniacal solution has been reported previously (2).

TABLE 2
Percolation tests

An ammoniacal solution of the metal sulfate, $M/20$ in metal ion, was passed through a bed of exchanger, which was then "regenerated" with $M/2$ sulfuric acid; analysis of the effluent from this regeneration is given below

METAL	EXCHANGER (DRY BASIS)	EFFLUENT FRACTION	METAL	NH_3 OR NH_4^+	RATIO NH_3 :METAL
	<i>grams</i>	<i>cc.</i>	<i>millimoles</i>	<i>millimoles</i>	
Ni	11.3*	0-60	8.53	41.5	3.82:1
		60-120	8.96	30.3	
		120-280	1.85	2.0	
		Total	19.34	73.8	
Cu	24.3	0-120	14.6†	83.6	2.16:1
		120-220	21.9	47.5	
		220-570	30.8	14.5	
		Total	67.3	145.6	
Zn	10.7*	Total (0-400)	18.25	58.0	3.22:1

* A different batch of Zeo-Karb was used in these tests from that used in the other experiments reported in this paper.

† A small amount of cuprous ion was detected in this portion of the effluent.

It is interesting that the effluent at the beginning of the sulfuric acid regeneration is strongly ammoniacal despite the acid influent. It might be added that a slight amount of reduction of cupric to cuprous ion took place when the Zeo-Karb containing cupric ammine ions stood for 5 days; this might be expected if the exchanger contains phenolic compounds.

CONCLUSION

In sulfuric acid-treated coal there seem to be a good many acidic groups having a very low dissociation constant, since at pH 10 to 12 the cation-exchange capacity is about twice as great as in weakly acid or neutral solutions. This extra exchange capacity can be utilized with heavy metals if these form ammonia complexes. A practical process to recover or separate such metals at high pH might be worked out if the ammonia used to form and stabilize the complex ions could be recovered.

This investigation was supported by a grant from the Abbott Fund of Northwestern University. The Zeo-Karb was furnished by the Permutit Company.

REFERENCES

- (1) ELGABY AND JENNY: *J. Phys. Chem.* **47**, 399 (1943).
- (2) I. G. FARBENINDUSTRIE A-G.: French patent 818,428 (1937); British patent 489,437 (1938); GRIESSBACH: Beihefte zu der Zeitschrift des Vereins² Deutscher Chemiker, Nr. 31 (1939).
- (3) KOLTHOFF: *Ind. Eng. Chem., Anal. Ed.* **11**, 94 (1939).
- (4) WALTON: *J. Phys. Chem.* **47**, 371 (1943).

VISCOSITY AND RIGIDITY OF STRUCTURAL SUSPENSIONS¹

PAUL S. ROLLER² AND C. KERBY STODDARD³

Bureau of Mines, U. S. Department of Agriculture, College Park, Maryland

Received July 17, 1944

A structural suspension, which consists in the resting state of a rigid network of particles enclosing the liquid medium, possesses a comparatively high viscosity and one that varies characteristically with the rate of shear. In interpreting the flow, concepts of yield value, plasticity, pseudoplasticity, consistency, etc., have been advanced. These designations we regard as unnecessary or inappropriate, reserving as sufficiently descriptive of the flow only the property of structural viscosity. It is the object of this paper to analyze the rigidity and viscous flow of structural suspensions, using in part original data on bentonite suspensions, and to offer a basic method of interpretation.

The occurrence of structural suspensions is wide, and structure may be present at surprisingly small concentrations. The degree of rigidity of a suspension may be measured by placing it in the annular space of two concentric cylinders and noting the torque on the inner cylinder for a given angular displacement of the outer one. In this manner Schwedoff (42) early determined the modulus of rigidity of a sol containing 0.5 per cent gelatin. Hatschek and Jane (22) made similar determinations for gelatin and other organic sols at concentrations down to 0.15 per cent. Michaud (31) determined the modulus of rigidity of gelatin

¹ Presented at the 102nd Meeting of the American Chemical Society, Atlantic City, New Jersey, September 11, 1941. Published by permission of the Director, Bureau of Mines, U. S. Department of the Interior.

² Senior Chemist, Bureau of Mines, College Park, Maryland.

³ Bureau of Mines-University of Maryland Cooperative Fellow; now Associate Technologist, Bureau of Mines, Boulder City, Colorado. The procedure and experimental results referred to in this paper are given in detail in a dissertation, "The Fluid Characteristics of Bentonite Suspensions," submitted by the junior author to the University of Maryland in partial fulfillment of the requirements for the degree of Doctor of Philosophy, June, 1941.

sols at a concentration as low as 0.05 per cent by noting the displacement in a capillary tube at various pressures. The modulus of rigidity of a copper ferrocyanide sol containing 0.035 per cent of suspended solids was measured by McDowell and Usher (30). By a magnetic displacement method, Freundlich and coworkers (17) detected elasticity in a number of sols at concentrations down to 0.1 per cent.

CHARACTER OF THE VISCOUS FLOW OF STRUCTURAL SUSPENSIONS

During structural viscous flow the rigid structure is broken, and flow takes place as a composite of liquid suspension and undecomposed structure. The pattern of flow in a concentric cylinder or Couette viscometer⁴ is shown in figure 1.

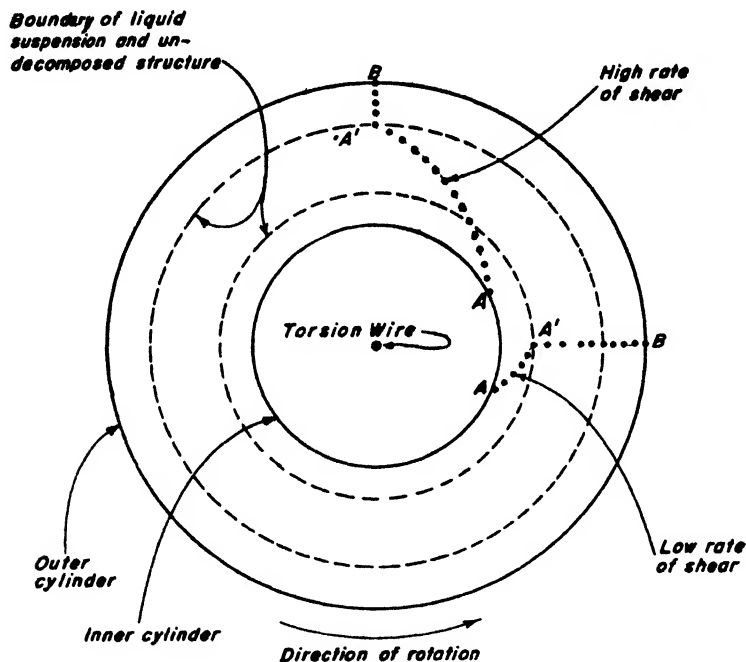


FIG. 1. Flow of a structural suspension in a Couette viscometer

A radial filament of coal dust was placed on the surface of a structural 7 per cent bentonite suspension. During rotation of the outer cylinder at a constant rate, $A'B$ remained radial, proving that the structure was intact within these limits; however, AA' was disposed along a curve, with A and A' becoming relatively more and more displaced with time. The suspension between A and A' was therefore in a liquid state, undergoing differential or laminar viscous flow. Measurements by Richardson (40) of the velocity distribution in a clay suspension showed that the flattened velocity gradient became more extended the

⁴ The measurements reported in this paper were actually carried out in a concentric tapered cylinder viscometer (after Goodeve (18)).

lower the rate of rotation. This condition is represented in figure 1, which shows the increase in undecomposed structure $A'B$ with decrease in rate of shear.

Ungar (48) describes a result similar to that in figure 1 for a clay suspension. Von Muralt and Edsall (49) measured the extinction angle of a myosin sol during rotation and at a certain radial distance found a sharp transition from an angle of 45° to an angle of 61° – 63° , indicating the presence of an annulus of structure adjacent to that of liquid suspension.

The character of the flow of a structural suspension in a capillary is shown in figure 2, based upon the observations of Pichot and Dupin (38), who determined

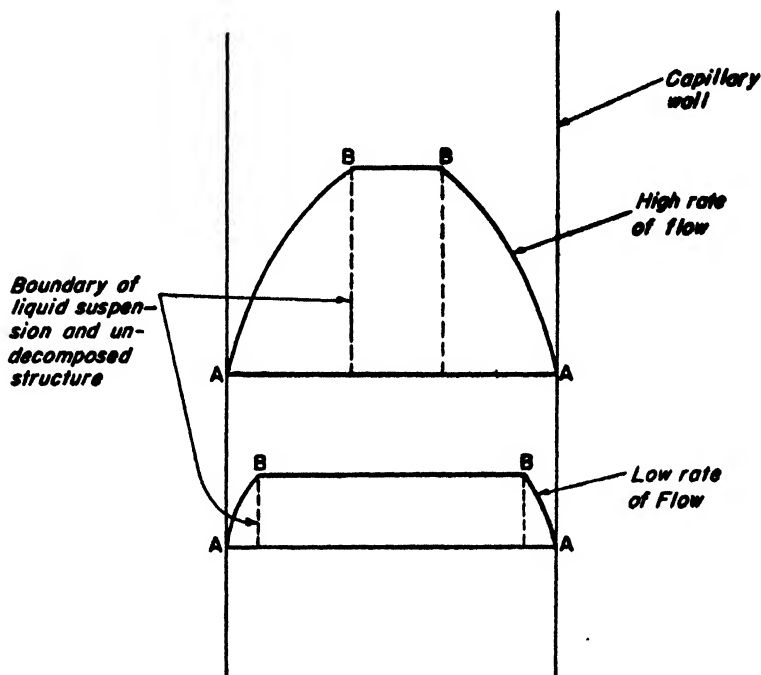


FIG. 2. Flow of a structural suspension in a capillary

the velocity of flow at different radial distances by chronophotographic measurement of illuminated specks of metal suspended in a gelatin sol. The velocity is constant across the center from B to B , corresponding to the flow of an undecomposed core of structure; from B to a point A at the wall, a parabolic velocity gradient exists corresponding to liquid suspension in laminar flow. Scott-Blair and Crowther (44) observed that the lower the rate of flow, the greater the central core in the flow of bentonite suspensions. This condition is represented in figure 2 by the increase in undecomposed structure BB with decrease in rate of flow. Kroepelin (29) made pitot-tube measurements of the flow of a gelatin sol in a capillary. His curve of velocities is not completely flattened at the center as in figure 2, a result which is probably due to disturbance of the stream lines during measurement.

The separation of a structural suspension into concentric annuli of liquid suspension and undecomposed structure during viscous flow and the progressive decrease in the proportion of structure with increase in flow are theoretically to be expected. The origin of the effect is the radial gradient of shear stress. To show the relations quantitatively, the basic equations (36) of laminar viscous flow of a liquid, which are applicable also to a liquid suspension in the absence of structure, are made use of. For a Couette viscometer,

$$T = 4\pi\eta_0 l \frac{a_1^2 r^2}{r^2 - a_1^2} \omega \quad (1)$$

where T is the torque on the liquid suspension at radial distance r , ω the angular rate of rotation at r , η_0 the viscosity, a_1 the radius of the inner cylinder, a_2 that of the outer cylinder, and l the length of the cylinder. The shear stress at r is given by

$$S = T/2\pi r^2 l \quad (2)$$

Substituting from equation 2 into equation 1, one obtains:

$$S = 2\eta_0 \frac{a_1^2}{r^2 - a_1^2} \omega \quad (3)$$

Equation 3 shows that the shear stress varies systematically from point to point, tending to exceed the breaking stress of the suspension in its structural state for small values of r . At a certain value of r equal to r_b , S is equal to S_b , the breaking strength of the suspension. For values of r less than r_b , the suspension is therefore in a liquid state; for values of r greater than r_b , the suspension is structurally rigid and rotates as a whole at a velocity ω equal to that at r_b . Letting $S = S_b$ and $r = r_b$ in equation 3, it is seen that when $\omega = 0$, then $r_b = a_1$, so that the suspension is entirely rigid. At a sufficiently high value of ω , $r_b = a_2$, and the suspension then possesses no rigid structure.

For a capillary,

$$v = \frac{p(a^2 - r^2)}{4\eta_0 l} \quad (4)$$

where v is the velocity of the suspension at radial distance r , p the pressure, a the radius of the capillary, and l the length of the capillary. The shear stress at radial distance r is given by

$$S = \frac{pr}{2l} \quad (5)$$

Substituting from equation 5 into equation 4, one obtains:

$$v = \frac{S(a^2 - r^2)}{2\eta_0 r} \quad (6)$$

Let S in equation 6 equal S_b , and correspondingly r equals r_b . When $v = 0$, then $r_b = a$, and structure is intact up to the wall of the capillary. For any

value of $v > 0$, r_b has a value less than a , so that the suspension is in a liquid state from the wall to the particular value of r_b , while its structure is intact from the particular value of r_b to the center. At $v = \infty$, $r_b = 0$, and the suspension is then entirely liquid. It may be noted that although $v = \infty$ at $r_b = 0$, the volume rate of flow, which is given by $\int_{r=0}^{r=a} v 2\pi r dr$, is finite.

RIGIDITY AND VISCOUS FLOW

In addition to the cited measurements of elasticity, the breaking strength of structural suspensions has also been determined, as for starches (7), bentonites (15, 24), and asphalts (46). We have similarly measured in a Couette viscometer the breaking strength as well as elasticity of a structural bentonite suspension.

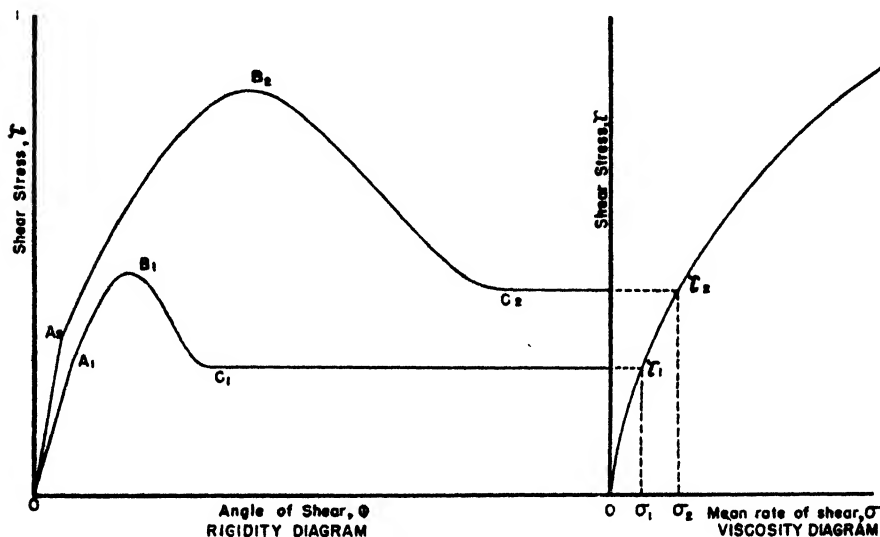


FIG. 3. Relation between rigidity and viscosity of a structural suspension

The outer cylinder was rotated at a constant rate, and the angular displacement, φ , or difference in angle between the inner cylinder and outer cylinder, was noted against the shear stress, τ , at the inner cylinder. The constant angular rate of rotation of the outer cylinder is proportional to the mean rate of shear, σ . The results obtained are represented in the rigidity diagram to the left in figure 3. The linear distance OA_2 comprises the elastic range. At A_2 yield occurs, and at B_2 breaking of the suspension. The break occurs at the wall of the inner cylinder and proceeds out to a radial distance r less than the diameter of the outer cylinder, whose value depends upon the mean rate of shear. As the break spreads outward, forming an increasing inner annulus of liquid suspension, the shear stress drops along B_2C_2 . At C_2 the shear stress becomes constant at a value τ_2 , which is the viscous resistance at the mean rate of shear σ_2 . The viscous resistance of the suspension is that of the liquefied part extending from the inner cylinder to

the radial distance r . As shown in the viscosity diagram to the right in figure 3, τ_2, σ_2 represents a point on the viscosity curve of the structural suspension.

At a lower mean rate of shear σ_1 , curve $OA_1B_1C_1$ is obtained. A_1 is lower than A_2 and B_1 lower than B_2 owing to relaxation of stress. C_1 is lower than C_2 because of the smaller viscous resistance at the lower rate of shear. Accordingly, the point represented by τ_1, σ_1 falls below the point τ_2, σ_2 in the viscosity diagram for the suspension.

For a capillary, exactly the same results apply, the variables corresponding to shear stress, angle of shear, and mean rate of shear being, respectively, pressure, relative linear displacement, and volume rate of flow.

Although the development of a constant shear stress corresponding to C_2 or C_1 has previously been noted (15, 24, 46), the interpretation given in figure 3, according to which the constant shear stress is recognized as a viscous resistance and is explicitly represented as a point in a viscosity diagram adjoined to a rigidity diagram, does not seem to have been previously made.

At very low mean rates of shear, the line $C_2\tau_2$ or $C_1\tau_1$ in figure 3 instead of being smooth was irregular, as observed also by Hobson (24). It might be supposed that this effect is "due to a periodic recovery and loss of structure." However, in accordance with the principles of dynamic equilibrium, one would expect under constant rotation a fixed ratio of liquid suspension to undecomposed structure, and correspondingly a steady shear stress as for high rates of shear. It is probable that the irregularity is due to vibrations which at very low rates of shear are of the order of magnitude of the shear stress due to viscous resistance. If the vibrations are periodic, the observed shear stress will be similarly periodic. The extreme sensitivity of structural suspensions to outside disturbances has been emphasized by McDowell and Usher (30).

EQUILIBRIUM DURING STRUCTURAL VISCOUS FLOW

The presence of undecomposed structure adjacent to liquid suspension raises the question of the reproducibility of results in measuring the viscosity of a structural suspension. In this connection, an 8 per cent bentonite suspension was highly agitated to yield a fluid suspension and then placed in a Couette viscometer. The variation of shear stress with time was noted for the suspension after it had been allowed to set for 18 hr. to a gel, and also after zero set while still fluid. The results at a low and a high mean rate of shear are shown in figure 4. For the gel with 18-hr. set, the shear stress decreased from a high value initially to a much smaller, nearly steady value after 30 min.; for the fluid suspension with zero set, the initial shear stress was comparatively low and decreased slightly to a steady value in less than 5 min.

At lesser concentrations of bentonite a steady value of the shear stress was in all instances reached in a relatively shorter time.

As indicated in figure 4, there appeared in general to be a slight hysteresis, so that the steady shear stress for suspensions at all concentrations between 2 per cent and 8 per cent after 18-hr. set was somewhat greater than for those with zero set. However, the difference was not too great and for all practical purposes

the steady values may be considered as equilibrium values. This conclusion is illustrated in figure 5, in which the steady values of the shear stress have been

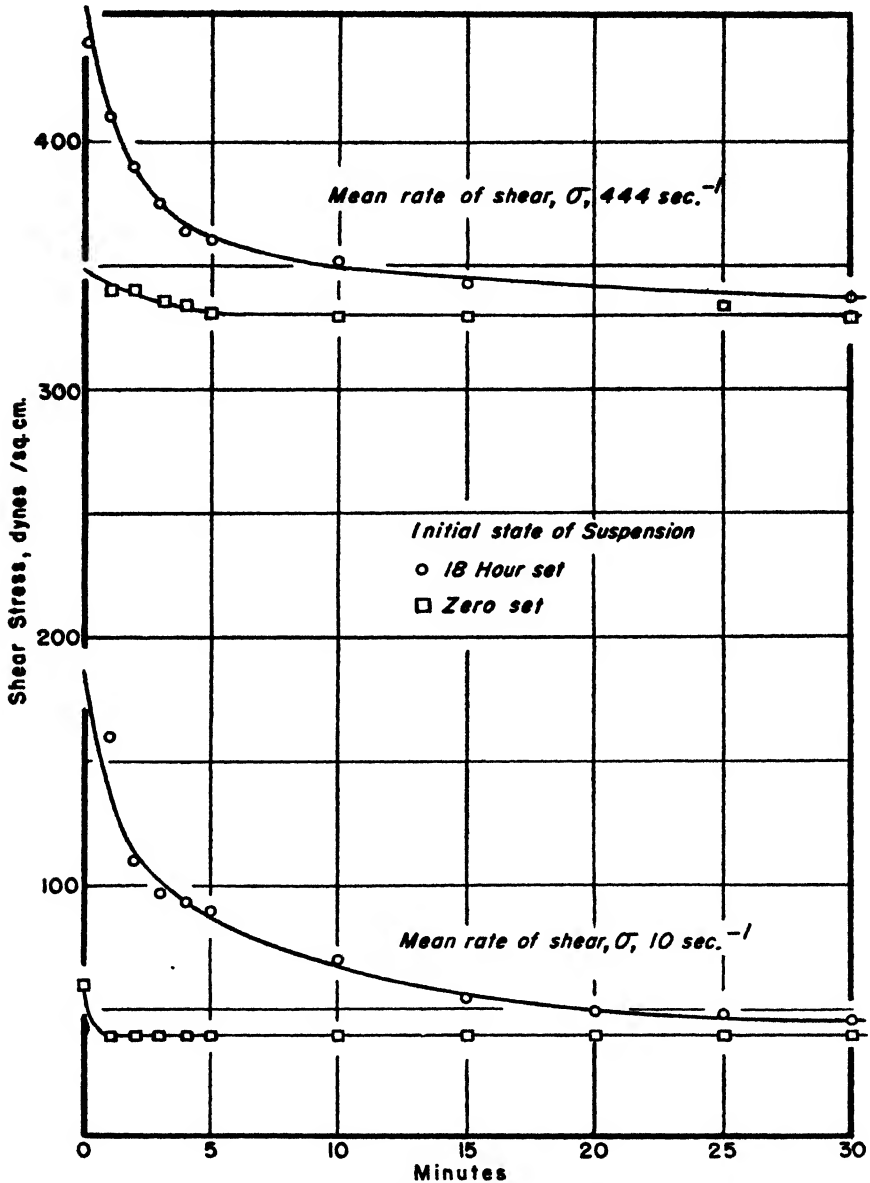


FIG. 4. Approach to equilibrium for a highly structural suspension (8 per cent bentonite)

plotted against mean rate of shear for the 8 per cent bentonite suspension under the conditions of 18-hr. set, 1-hr. set, and zero set. The points fall on the same curve within a spread of a few per cent.

For asphalt suspensions, the steady shear stress seemed also to be independent of the initial state (46).

In view of the length of time required to arrive at a steady value of the shear stress for the set suspensions, a capillary tube or analogous viscometer that does not allow elimination from the measured result of the stresses due to rigidity will give proportionately erroneous values for the structural viscosity. The results in figure 4 indicate that the error may be largely avoided if the suspension is initially stirred and measurement of the viscosity immediately started.

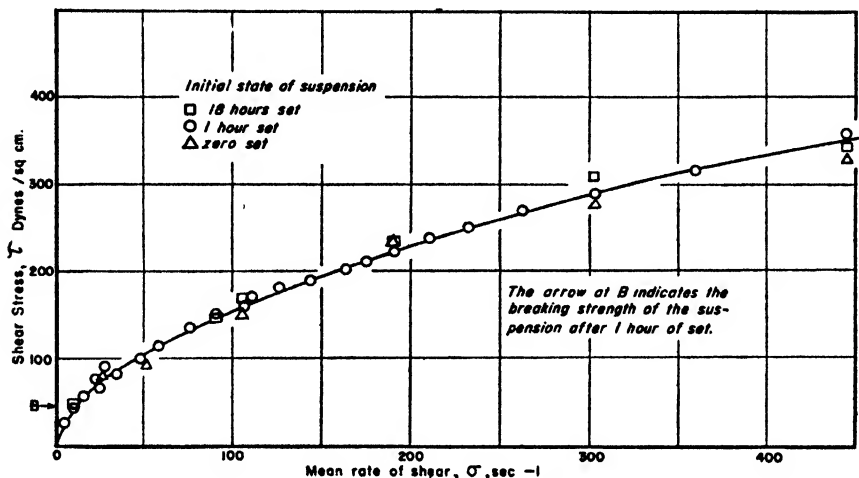


Fig. 5. Equilibrium viscosity diagram for a highly structural suspension (8 per cent bentonite)

CONDITIONS AT HIGH RATE OF SHEAR

As the mean rate of shear is increased, the proportion of liquid suspension increases relative to undecomposed structure. In view of this fact, the viscosity decreases with increase in rate of shear, which is an invariable result for structural suspensions. At a sufficiently high rate of shear, the suspension is entirely liquefied and becomes equivalent to a simple suspension having discrete particles. The viscosity is then at a minimum and remains constant with increase in rate of shear. At still higher rates, turbulent flow as defined by the Reynolds number sets in, and the apparent viscosity increases with increase in rate of shear.

The above sequence of changes was first reported by Ostwald (33, 34) and was represented by him in the curves of figure 6 for the viscosity, or the shear stress, against mean rate of shear. In this figure, OA represents the range of structural viscous flow, AB the range of laminar viscous flow and constant viscosity, and BC the range of turbulent flow.

The attainment of constant viscosity at sufficiently high rates of shear has been experimentally observed for numerous suspensions, both inorganic and organic, as of clays (8, 32), amalgams (27), soaps (35), paraffins (45), nitrocellulose (37), and gelatin and other organic compounds (34).

The attainment of constant viscosity depends greatly on the strength of structure, and therefore on the concentration. For a 1 per cent bentonite suspension, the viscosity was almost immediately constant; for a 2 per cent suspension it became constant at σ equal to about 250 sec^{-1} ; while for a 4 per cent suspension it was still decreasing markedly at σ equal to 450 sec^{-1} .

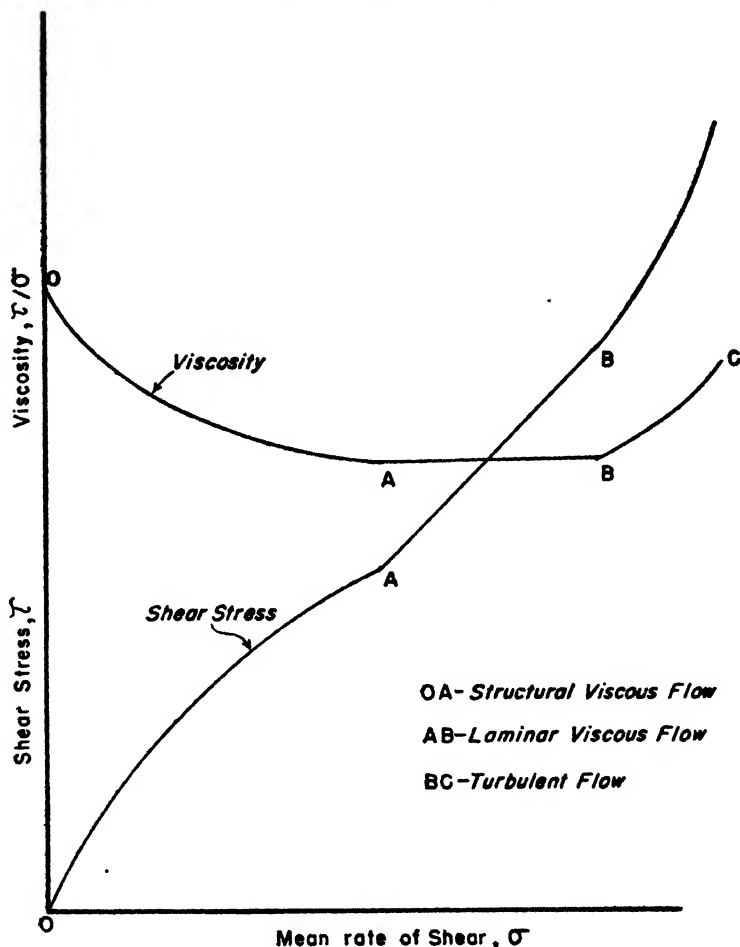


FIG. 6. Modes of flow for a structural suspension (after Ostwald (31))

CONSTANT VISCOSITY AND THE EINSTEIN EQUATION

Since a structural suspension is then equivalent to a simple suspension having discrete particles, application of the Einstein equation (12) to structural suspensions is warranted at constant viscosity. The equation, which has been verified for simple suspensions at a concentration by volume up to about 3 per cent (13), is

$$\eta = \eta_0(1 + k\phi) \quad (7)$$

where η is the viscosity of the suspension, η_0 the viscosity of the liquid, k the Einstein factor (which is theoretically equal to 2.5), and 100ϕ the per cent concentration by volume. The theoretical value of 2.5 for the Einstein factor applies to rigid spheres; it may be greater than 2.5, owing to absorption of liquid by molecular or crystallite micelles (28) resulting in a greater volume concentration than nominally present, to mutual interference of flow by the micelles at intrinsic high concentrations, to electrophoretic charge on the particles, or to asymmetry of the particles particularly under conditions of disorientation.

Equation 7 shows that the viscosity of the suspension depends directly on the viscosity of the liquid. On the other hand, at low rates of shear the viscosity depends mostly on the degree of structure. As an example, the viscosity of lubricating greases was at low rates determined mainly by the amount and kind of soap, but at high rates of shear the viscosity of different greases was in the order of the viscosity of the oils (2, 5).

In equation 7 the viscosity is linearly dependent on the concentration of the suspended solid. Structural viscosity, however, varies in general with a high power of the concentration. Phillipoff and Hess (37) found it to be the eighth power for structural suspensions of 0.05 per cent to 1.0 per cent trinitrocotton in butyl acetate at low rates of shear approaching zero. At high rates of shear in the range of constant viscosity, the latter varied exactly as the first power of the concentration, in agreement with the Einstein equation. The Einstein factor in the range of constant viscosity was indicated to be 245.

The factor for structural suspensions of starch in a solution of carbon tetrachloride and toluene at a concentration of 2 to 6 per cent by volume is indicated from the results of Hatschek and Jane (23) to be of the order of 5 to 10 in the range of constant viscosity.

Hankinson and Briggs (20) observed that sodium caseinate in water possessed structural viscosity even at low concentrations but that the effect was eliminated and the viscosity became constant at a pressure of 30 cm. of mercury or greater. Freshly prepared sols of calcium caseinate possessed no structure. In the range of constant viscosity, after correction for the electroviscous effect, the Einstein factor was 8.0 for sodium caseinate and 3.2 for calcium caseinate. Assuming the true factor to be the theoretical one of 2.5, it was calculated that the micellar absorption of liquid was 7.4 g. of water per gram of sodium caseinate and 2.4 g. of water per gram of calcium caseinate.

Eirich, Margaretha, and Bunzl (14) determined the viscosity of silk particles (40 to 47 microns in diameter and having a length to width ratio of 5/1, 11/1, 17/1, and 23/1) suspended in a liquid of equal density, consisting of tetrachloroethane and olive oil. With a capillary viscometer, the viscosity of a 1 per cent suspension decreased with increase in mean rate of shear by a two- to three-fold factor, becoming approximately constant at high rates of shear. The authors state that there was no coagulation, so that the decrease in viscosity is apparently due to progressive orientation of the elongated particles in the direction of the stream lines. The value for the Einstein factor at approximately constant viscosity is given in table 1. In this table the directly measured values are recorded,

omitting a correction for inertia effects that raised the values somewhat. The Einstein factor varies from 2.0 to 3.4 for an increase in l/d of from 5/1 to 23/1. This trend might have been diminished if higher rates of shear had been employed. The results show that in the range of constant viscosity the Einstein factor approaches the theoretical value of 2.5 for highly asymmetric particles.

Jeffery (26) showed that the Einstein factor should lie between 2.0 and 2.5 for ellipsoids oriented so that the dissipation of energy is least, i.e., in the direction of the stream lines.

For suspensions of proteins consisting of elongated particles the results were quite different from those for silk particles. Boehm and Signer (6) found that sols of egg albumin (ovalbumin), for which the ratio of length to width is about 5 (9), gave an extinction angle of 90° throughout, indicating that the particles were fully oriented at all rates of shear. The viscosity decreased with increase

TABLE 1

Einstein factor for a 1 per cent suspension of silk particles at approximately constant viscosity (from Eirich, Margaretha, and Bunzl (14))

RATIO, LENGTH TO DIAMETER	EINSTEIN FACTOR
5/1	2.0
11/1	2.4
17/1	2.9
23/1	3.4

in rate of shear, and at a concentration of 0.2 per cent a constant value was reached at the highest rates. The Einstein factor was then 150. This high factor is apparently due not to asymmetry, since orientation was complete, but rather to other influences, such as micellar swelling, mutual interference of swelled particles, etc., which need further study.

The viscosity of myosin sols was found by Edsall and Mehl (11) to decrease with increase in rate of shear. At the lowest concentration of 0.171 per cent, constant viscosity was attained at the highest rates of shear. The Einstein factor was then 340. The authors inferred that, owing to the low rotary diffusion constant of myosin, the particles were highly oriented in the direction of the stream lines. Therefore, as for egg albumin, asymmetry is apparently not a cause of the high Einstein factor for myosin.

CONDITIONS AT ZERO RATE OF SHEAR

In view of the rigidity of a structural suspension, it is natural to assume that at zero rate of shear a finite breaking stress would exist. Accordingly, common representations (3, 25, 43) of the viscosity curve for a structural suspension are those shown in curves a and b of figure 7. In these representations the curve of shear stress against mean rate of shear is presumed to intersect the axis of shear stress, giving rise to a "yield value" for the suspension whose magnitude is given by the height of the intercept OP_2 or OP_1 on the axis. Ostwald (33)

and Hatschek (21) disputed the representations a and b in figure 7, claiming that the curve actually bent toward the origin of axes at very low rates of shear, as in curve c of figure 7. The same bending toward a zero shear stress is also shown in figure 5 by the highly structural 8 per cent bentonite suspension.

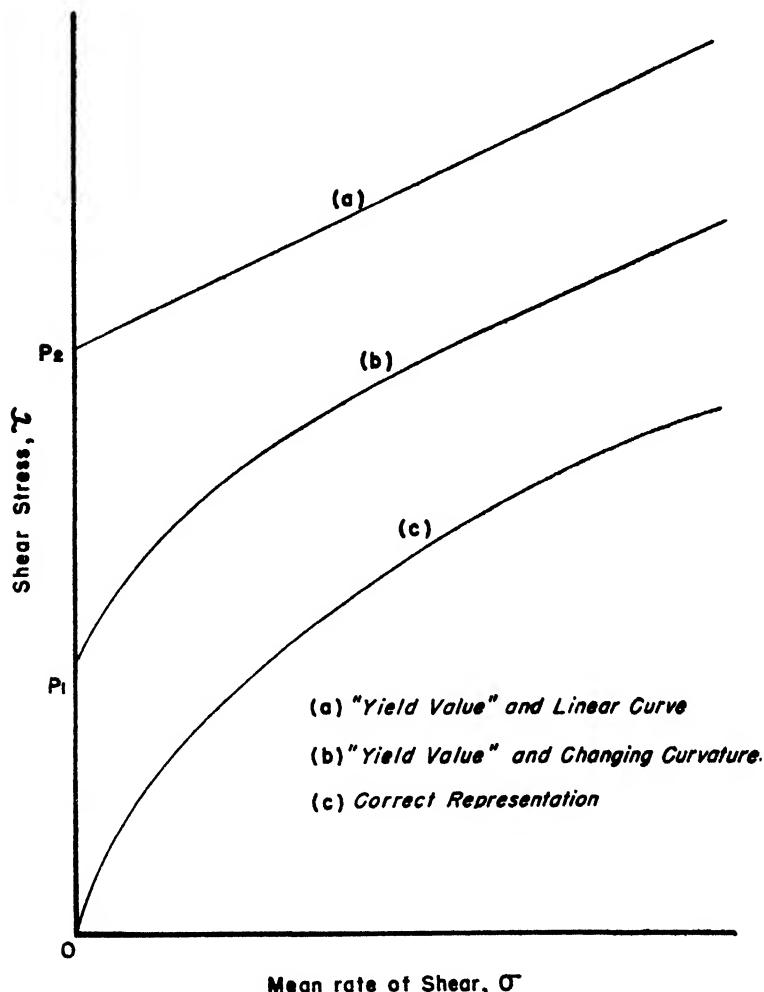


FIG. 7. Illustrating concept of "yield value" in a viscosity diagram for a structural suspension

The breaking strength of this suspension, determined as in the rigidity diagram of figure 3 at a low mean rate of displacement of 0.033 sec.^{-1} , was 50 dynes per square centimeter after 1-hr. set. It is marked in figure 5 by point B. The directly measured breaking strength exceeds observed values of the viscous shear stress in figure 5, and cannot be represented as an intersection of the viscosity curve with the shear axis.

The intersection for curves a and b in figure 7 is due to a broad extrapolation of the main part of the viscosity curve. In order to account for the actual trend toward zero shear stress, proponents of the yield value theory have suggested the phenomenon of "slip" or "plug flow" (4, 19, 44). However, it is evident that these expressions merely denominate the normal and theoretically expected annular separation of a structural suspension into liquid suspension and undecomposed structure, and are no defense against the observed trend toward zero shear stress.

In addition to the experimental evidence, it may be shown also theoretically that the viscosity curve of a structural suspension has to end in the origin of coordinates. It is to be noted that the variable, rate of shear, implies the application of an indefinitely increasing angular displacement or strain. Therefore, for all values of σ the structural suspension must be in a broken state consisting in part of liquid suspension. Only viscous resistance has to be overcome, so that at an infinitesimal rate of shear, the shear stress is infinitesimal; in the limit of zero rate of shear the shear stress is zero. This result does not deny the existence of a finite breaking strength. It merely implies that, as previously suggested (41), rigidity cannot be determined with σ as variable, but only with the angular displacement φ as variable.

It may be proved that, while the shear stress is zero, a unique condition does hold for structural suspensions at zero rate of shear, which is that the viscosity is infinite. For a Couette viscometer, η_0 in equation 3 is the viscosity of the liquid suspension which is in contact with undecomposed structure. The measured viscosity is S/ω . As ω decreases, the proportion of liquid suspension relative to undecomposed structure decreases, and r approaches closer and closer to a_1 . In the limit of $\omega = 0$, $r = a_1$, so that by equation 3 the viscosity S/ω is infinite.

For a capillary, the volume rate of flow of liquid suspension and undecomposed structure is given by

$$q = \int_r^a v 2\pi r \, dr + v_r \pi r^2 \quad (8)$$

where q is the volume rate of flow, and v_r , which is the velocity of the liquid at the radial boundary r of liquid suspension and undecomposed structure, is also the velocity of the core. Substituting from equation 4 into 8, one obtains on integration and rearrangement,

$$p = 8\eta_0 q / \pi (a^4 - r^4) \quad (9)$$

The measured viscosity is equal to p/q . For $q = 0$, and therefore $r = a$, the viscosity by equation 9 is infinite.

The conditions $\tau = 0$, $\sigma = 0$ and $(\tau/\sigma)_{\sigma=0} = \infty$ taken together require that the following relation should hold: $\left(\frac{d\tau}{d\sigma}\right)_{\sigma=0} = \infty$. Accordingly, in a plot of τ against σ , the ordinate of axes is tangent to the curve at the origin.

A simple function which satisfies the necessary conditions of zero shear stress

and infinite viscosity at zero rate of shear is that suggested independently by Ostwald (33) and deWaele (10). It is

$$\tau = k\sigma^n \quad (10)$$

where k and n are constants, and $n < 1$.

Equation 10 has been verified for many structural suspensions, as of bentonite (1), kaolin (32), paint (10, 50), starch (16, 39, 47), and various organic compounds (33, 34). We have found it to apply accurately also to the present series of bentonite suspensions with the viscosity measured at equilibrium. In table 2 are given the values of k and n for different concentrations between 2 per cent and 8 per cent by weight. As the concentration increases, k increases very rapidly. The increase in viscosity with concentration was much less, only about a third to a tenth that of k , depending on the mean rate of shear. The breaking strength, however, according to preliminary measurements, appeared to increase at a rate of the order of that of k .

TABLE 2

Values of constants k and n for bentonite suspensions with the viscosity measured at equilibrium

WEIGHT PER CENT	10^3k	n
2	2.3	0.98
4	26.9	0.77
6	141	0.71
8	1250	0.55

The factors which determine the strength of structural suspensions are those which influence the mutual attraction of the suspended particles or micelles: namely, intrinsic attractive force, electrophoretic potential, solvation, and particle size and shape. An experimental test of certain of these factors with reference to the mutual attraction of the particles in concentrated suspension has previously been made (41).

SUMMARY

The relation between viscosity and rigidity of structural suspensions is analyzed, employing in part original data for bentonite suspensions, and a basic interpretation is offered.

The occurrence of structural suspensions is wide, and rigidity may be present in suspensions containing less than 0.1 per cent solids. During structural viscous flow, the structure is broken and the suspension consists of a concentrically disposed composite of liquid suspension and undecomposed residue. The transition of a structural suspension from its rigid state during rest to its broken state during viscous flow is analyzed.

It is indicated that equilibrium values for the structural viscosity may be closely realized.

At a sufficiently high mean rate of shear, the structure is completely de-

composed, and the viscosity, hitherto decreasing with increase in rate of shear, becomes constant. At constant viscosity, the structural suspension is equivalent to a simple suspension having discrete particles. The application of the Einstein equation to structural suspensions in the range of constant viscosity is discussed, and several examples are given, including suspensions of asymmetric particles.

At zero rate of shear, the shear stress for a structural suspension is shown experimentally and theoretically to be zero. Although a breaking strength exists, it may be determined only with angular displacement as variable. It cannot be measured with mean rate of shear as variable, and any result obtained in this way is necessarily fictitious. It is proved that at zero rate of shear a singular condition does exist for a structural suspension which is that the viscosity is infinite.

The Ostwald-deWaele power equation for structural suspensions satisfies the necessary boundary conditions of zero shear stress and infinite viscosity, and its application is considered.

REFERENCES

- (1) AMBROSE, H. A., AND LOOMIS, A. G.: *Physics* **4**, 265 (1933).
- (2) ARVESON, M. H.: *Ind. Eng. Chem.* **24**, 71 (1932).
- (3) BINGHAM, E. C.: *Fluidity and Plasticity*. McGraw-Hill Book Company, Inc., New York (1922).
- (4) BINGHAM, E. C., AND GREEN, H.: *Proc. Am. Soc. Testing Materials* **19**, 641 (1919).
- (5) BLOTT, J. F. T., AND SAMUEL, D. L.: *Ind. Eng. Chem.* **32**, 68 (1940).
- (6) BOEHM, G., AND SIGNER, R.: *Helv. Chim. Acta* **14**, 1370 (1931).
- (7) BRIMHALL, B., AND HIXON, R. M.: *Ind. Eng. Chem., Anal. Ed.* **11**, 358 (1939).
- (8) BURKE, W. H.: *Trans. Am. Inst. Mining Met. Engrs.* **114**, 53 (1935).
- (9) COHN, E. J., AND EDSALL, J. T.: *Proteins, Amino Acids and Peptides*. Reinhold Publishing Corporation, New York (1943).
- (10) DE WAELE, A.: *J. Oil Colour Chem. Assoc.* **6**, 33 (1923).
- (11) EDSALL, J. T., AND MEHL, J. W.: *J. Biol. Chem.* **133**, 409 (1940).
- (12) EINSTEIN, A.: *Ann. Physik* **19**, 289 (1906); **34**, 591 (1911).
- (13) EIRICH, F., BUNZL, M., AND MARGARETHA, H.: *Kolloid-Z.* **74**, 276 (1936).
- (14) EIRICH, F., BUNZL, M., AND MARGARETHA, H.: *Kolloid-Z.* **75**, 20 (1936).
- (15) EVANS, P., AND REID, A.: *Trans. Mining Geol. Inst. India* **32**, 1 (1936).
- (16) FARROW, F. D., AND LOWE, G. M.: *J. Textile Inst.* **14**, 414T (1923).
- (17) FREUNDLICH, H., AND SEIFRITZ, W.: *Z. physik. Chem.* **104**, 233 (1923).
- (18) GOODEVE, C. F.: *J. Sci. Instruments* **16**, 19 (1939).
- (19) GREEN, H.: *Proc. Am. Soc. Testing Materials* **20**, 451 (1920).
- (20) HANKINSON, C. L., AND BRIGGS, D. R.: *J. Phys. Chem.* **45**, 943 (1941).
- (21) HATSCHEK, K.: *Viscosity of Liquids*, p. 209. Bell & Sons, London (1928).
- (22) HATSCHEK, K., AND JANE, R. S.: *Kolloid-Z.* **39**, 300 (1926).
- (23) HATSCHEK, K., AND JANE, R. S.: *Kolloid-Z.* **40**, 53 (1926).
- (24) HOBSON, G. D.: *J. Inst. Petroleum Tech.* **26**, 533 (1940).
- (25) HOUWINK, R.: *Elasticity, Plasticity and Structure of Matter*. University Press, Cambridge (1937).
- (26) JEFFERY, G. B.: *Proc. Roy. Soc. (London)* **A102**, 163 (1923).
- (27) KÖHLER, R.: *Kolloid-Z.* **64**, 200 (1933).
- (28) KRAEMER, E. O., AND WILLIAMSON, R. V.: *J. Rheol.* **1**, 76 (1929).
- (29) KROEPFELIN, H.: *Z. physik. Chem.* **84**, 291 (1930).
- (30) McDOWELL, C. M., AND USHER, F. L.: *Proc. Roy. Soc. (London)* **A131**, 409, 564 (1931).

- (31) MICHAUD, M. F.: *Compt. rend.* **174**, 1282 (1922).
- (32) NISHIKAWA, K.: *Kolloid-Z.* **33**, 328 (1926).
- (33) OSTWALD, Wo.: *Kolloid-Z.* **36**, 99 (1925); **47**, 176 (1929).
- (34) OSTWALD, Wo., AND AUERBACH, R.: *Kolloid-Z.* **38**, 261 (1926).
- (35) OSTWALD, Wo., AND RIEDEL, R.: *Kolloid-Z.* **70**, 67 (1935).
- (36) PAGE, L.: *Introduction to Theoretical Physics*, p. 228. D. Van Nostrand Company, New York (1928).
- (37) PHILLIPPOFF, W., AND HESS, K.: *Z. physik. Chem.* **B31**, 237 (1936).
- (38) PICHOT, M., AND DUPIN, P.: *Compt. rend.* **192**, 1079 (1931).
- (39) PORTER, A. W., AND RAO, P. A. M.: *Trans. Faraday Soc.* **23**, 312 (1927).
- (40) RICHARDSON, E. G.: *J. Australian Inst. Agr. Sci.* **23**, 176 (1933).
- (41) ROLLER, P. S.: *J. Phys. Chem.* **43**, 460 (1939).
- (42) SCHWEDOFF, T.: *J. Phys.* **8**, 341 (1889).
- (43) SCOTT-BLAIR, G. W.: *Industrial Rheology*, The Blakiston Company, Philadelphia (1938).
- (44) SCOTT-BLAIR, G. W., AND CROWTHER, E. M.: *J. Phys. Chem.* **33**, 321 (1929).
- (45) SIBREE, J. O.: *Trans. Faraday Soc.* **26**, 26 (1931).
- (46) TRAXLER, R. N., ROMBERG, J. W., AND SCHWEYER, H. E.: *Ind. Eng. Chem., Anal. Ed.* **14**, 340 (1942).
- (47) TSUDA, S.: *Kolloid-Z.* **45**, 325 (1928).
- (48) UNGAR, G.: *Kolloid-Z.* **71**, 16 (1935).
- (49) VON MURALT, A. L., AND EDSALL, J. T.: *J. Biol. Chem.* **89**, 315 (1930).
- (50) WILLIAMSON, R. V.: *Ind. Eng. Chem.* **21**, 1108 (1929).

COMMUNICATION TO THE EDITOR

ON THE DEFINITION OF A CRYSTAL¹

Under the above title in the March, 1944, issue of *The Journal of Physical Chemistry*, page 95, G. Antonoff points out that many authors of textbooks of physical chemistry mention "isotropic crystals" and that from a crystallographer's point of view there can be no "isotropic crystal", because a crystal is defined by the crystallographer as "a homogeneous *anisotropic* body having the natural shape of a polyhedron." With the above statements I heartily agree. In fact, the above definition is in agreement with the following definition found in most chemical dictionaries for the term isotropic, "having similar physical properties in all directions." Certainly crystals do not have *all* similar physical properties in all directions and therefore in strict accordance with this definition there cannot be an isotropic crystal.

What has not been pointed out, however, is that the term "isotropic crystal", now in common use in textbooks of physical chemistry, is used in reference to only the optical properties and not to all physical properties. Crystals belonging to the cubic or regular system, such as sodium chloride, have the same optical properties in all directions and therefore in a restricted sense of the word are isotropic crystals. As long as this restricted definition is understood, the use of

¹ Received August, 1944.

the term seems justified for the purpose. This reasoning seems all the more valid when it is realized that we also have the term "amorphous" to indicate non-crystallized material.

A. C. SHUMAN.

Central Laboratories
General Foods Corporation
Hoboken, New Jersey

NEW BOOKS

Plant Viruses and Virus Diseases. By F. C. BAWDEN. Second edition. xi + 294 pp.; 48 illustrations. Waltham, Massachusetts: Chronica Botanica Co., 1944. Price: \$4.75.

This is the second and revised edition of Bawden's book, which was first published in 1939. It will be welcomed as the only up-to-date publication bringing together information regarding the pathology, symptomology, serology, and chemistry of plant viruses. The author is chiefly concerned with those virus diseases which have been studied most extensively, and the discussion is limited largely to studies made since 1930.

The chemist will be especially interested in the five chapters on the preparation and properties of purified virus proteins. The author is well qualified to discuss this particular phase of virus research, because many of the important contributions in this field have originated in his own laboratory.

It is a well-recognized fact that the application of physical-chemical methods to the study of plant viruses during the past decade has resulted in a remarkable increase in our understanding of the nature of these rather unique substances. On the other hand, the virus proteins have benefited the study of physical chemistry by providing suitable materials for studying those phenomena relating to viscosity, sedimentation, diffusion, and the optical properties of anisotropic flow.

Chapters 8, 9, and 11 deal with the methods of preparation and the properties of purified virus proteins. Chapter 10, on the optical properties of virus proteins, is presented in a thorough and interesting manner. Chapter 12 discusses studies on the determination of the particle sizes of viruses by such methods as ultrafiltration, diffusion, viscosity, sedimentation, and ultramicroscopy. The author takes the viewpoint that the molecular weight of tobacco mosaic virus has not been established conclusively. This conclusion seems to be well founded in view of the available evidence showing interaction and aggregation of virus particles in solution. In the final chapter, on the nature of viruses, the author points out that it is impossible to determine whether or not viruses are living entities because the distinctions between animate and inanimate matter are not clearly defined.

The book is well written and the illustrations are especially good. The reviewer regards this book as a valuable contribution to the study of plant viruses and virus diseases.

CLAUDE H. HILLS.

Systematic Inorganic Chemistry of the Fifth- and Sixth-Group Nonmetallic Elements. By DON M. YOST AND HORACE RUSSELL, JR., California Institute of Technology. xx + 423 pp. New York: Prentice-Hall, Inc., 1944. Price: \$6.00.

It has been a great pleasure to become acquainted with this book and to note the modern and even revolutionary treatment of topics in an advanced course in inorganic chemistry. The authors state, in their preface, "From these considerations it is evident that any discussion of a chemical element or compound is complete only when the spectroscopic, structural, thermodynamic, chemical kinetic, and nuclear properties have been consid-

ered. In addition to these more modern aspects of the subject, due consideration must be given to the older, humbler, but nevertheless important, chemical facts that one finds in simple experiments with test tubes, beakers and flasks."

As the part of the title given in smaller print will indicate, this book discusses the properties of nitrogen and phosphorus of the fifth group, of oxygen, sulfur, selenium, and tellurium of the sixth group, and of many of their compounds, including oxides, oxyacids, halides, sulfides, and hydrides.

In order to give the readers of *This Journal* an adequate idea of the character of this book, the reviewer offers a summary of the treatment of nitrogen.

After describing several methods of preparing nitrogen, the authors discuss its physical properties. From the fact that its magnetic susceptibility is negative, the conclusion is drawn that in its ground state the nitrogen molecule has no resultant angular momentum. The existence of alternating intensities in the rotational spectrum can be used to show that the nuclear spin quantum number is one. There is a mention of the number of symmetric and antisymmetric nuclear spin functions which leads (using Pauli's principle) to the conclusion that the nitrogen nucleus must consist of an even number of fundamental particles; thus the nucleus could consist of 7 protons and 7 neutrons, but not of 14 protons and 7 electrons nor of 14 neutrons and 7 positrons. There is a discussion of why in practice we do not observe specific heat behavior analogous to that of ortho- and para-hydrogen.

Reference is made to the ratio of N^{14} to N^{15} in ordinary nitrogen and the use of the heavier isotope in biochemical studies.

The authors give formulas for calculating the rotational and vibrational energy states. They note the N-N internuclear distance, the dissociation energy at 0°K. and at 291°K.

Table 1 lists many of the physical constants of nitrogen, including melting point, boiling point, transition temperature (α to β) and the corresponding ΔH values; also equations giving the vapor pressure of solid and of liquid, the surface tension of liquid, the density of liquid, the weight of one liter of $N_2(g)$ at standard conditions, and critical data. Included are heat capacity data for solid, liquid, and gas, the entropy (experimental and spectroscopic) at 77.32°K. and at 298.1°K., and equations for the viscosity of the gas. Values of pV for N_2 at temperatures from -100°C. to 400°C. and at pressures ranging from 1 atm. to 1000 atm. are presented in Table 2.

Included in the tabulated physical properties of nitrogen is its solubility in water at 0°, 20°, 30°, 50°, and 100°C.

Under the heading of chemical properties of nitrogen, the authors discuss its adsorption by charcoal, its reaction with a number of metals and compounds at higher temperatures, the hydrolysis of nitrides of the metals, and the preparation and properties of "active" nitrogen. They include a free energy equation for the formation of HCN(g) from C, H_2 , and N_2 .

Chapter I contains also a treatment of the oxides and sulfides of nitrogen, their formation, and their physical and chemical properties. Aside from data analogous to those already referred to in the discussion of elementary nitrogen, equilibrium constants and rate constants are here presented in considerable detail. ΔH and ΔF values are given for reactions whenever they are known with sufficient accuracy.

It will be clear from the foregoing summary that the authors of this book believe that students of some degree of maturity who desire to become acquainted with the properties of an element or of its compounds are justified in wanting to have at their disposal all the appropriate resources of modern chemistry and physics. The reviewer thinks that the authors have done a very good job in the field to which they limited themselves. An equally skillful application of their method of treatment to other elements would certainly be welcomed.

In a somewhat hurried reading of this book, the reviewer has found few statements that he would criticize adversely. However, he would like to call attention to the remarks on p. 103 about amine sulfonic acid. Referring to experiments reported in 1896 and in 1901, the authors state that "conductivity measurements show the percentage ionization

to be 98% at 0.001 m and 79% at 0.03 m at 25°." These percentages are undoubtedly conductance ratios and not, as the authors of this book certainly know, measures of the degree of ionization.

A few typographical errors have been noticed. Thus on page 182, ΔH for the heat of formation of P_2O_{10} is negative and not positive; on page 257, ΔE and ΔH for the dissociation of O_2 should be positive and not negative.

Altogether this excellent book can be recommended enthusiastically to the attention of all teachers and students of chemistry.

F. H. MACDOUGALL.

Infrared Spectroscopy: Industrial Applications and Bibliography. By R. B. BARNES, R. C. GORE, U. LIDDELL, AND V. Z. WILLIAMS. vi + 236 pp.; 11 figures; 363 infrared transmission curves. New York: Reinhold Publishing Corporation, 1944. Price: \$2.25.

The purpose of this volume, and the limitations of it, are adequately stated in the preface: "This work is presented as a partial answer to the increasing demand for information concerning the industrial applications of infrared spectroscopy. It is not claimed that this material represents a complete survey of the field or its literature or the ultimate in infrared techniques. Rather, the applications and the results discussed are based entirely on work done in this laboratory in order that a unified picture of a typical infrared research program could be available to those who may be interested." It will surprise no one who is acquainted with Dr. Barnes's long experience in infrared spectroscopy and in the industrial application of this tool, to learn that he and his fellow-authors have turned out an excellent book for this purpose. The volume discusses, rather briefly, the applications of infrared spectroscopy, the experimental equipment and techniques involved, the elementary theory needed to understand the tool, and its present status in the industrial field. Both the advantages and the limitations of infrared spectroscopy are presented clearly.

The book should appeal to the reader who is ignorant of infrared technique and applications, but who wishes to gain some knowledge of them in order that he may appreciate the possibilities of this research tool. The volume can be heartily recommended to this group.

The infrared spectroscopist who is already familiar with the field will find no new material in the text; he will, however, profit from, and perhaps find stimuli in, the discussion of the various applications of infrared spectroscopy. The "library of reference curves"—363 infrared transmission curves of various organic materials—is of value for preliminary study of the spectra of particular compounds, characteristic bands of particular functional groups, and the like; its value is limited by the fact that the curves cover only the region from 5 to 12 μ (in many cases only from 5 to 10 μ), by the absence of any numerical values for the band frequencies, and by the fact that the appearance of a given infrared band does, alas, vary with the instrument used to study it. The bibliography of 2701 references is perhaps the most valuable feature of the book to the specialist in the field.

The material in the volume, with the important exception of the bibliography, was previously published in *Industrial and Engineering Chemistry (Analytical Edition)*; its publication in book form is a distinct service to those working in and those considering the application of infrared spectroscopy.

BRYCE L. CRAWFORD, JR.

SUBJECT INDEX

- Acetic acid-*p*-toluidine system, 85
 Acid, Brönsted-Lowry definition of, 51
 Lewis definition of, 51
 Adsorption analysis of colorless compounds, 179
 on solid surfaces, relation to contact angles, 120
 Agents, surface-active, effect on dispersions of calcium carbonate in xylene, 134
 Alkyl sulfonic acids, diffusion of, 237
 Aluminum halides, fused, electrochemistry of, 259, 268
 oxide-calcium oxide-calcium sulfate-potassium oxide-water system, 356
 oxide-calcium oxide-calcium sulfate-sodium oxide-water system, 379
 oxide-calcium oxide-calcium sulfate-water system, 311
 Antonoff's rule, 75, 158
- Base, Brönsted-Lowry definition of, 51
 Lewis definition of, 51
 Benzene-butyl alcohol-water system, 241
 Boundary tension, measurement by the pendent-drop method, 168
- Calcium carbonate, dispersions in xylene, effect of surface-active agents upon, 134
 Cancer, protective colloids in diagnosis of, 187
 Carbon, colloidal dispersion in xylene, 125
 Cation exchange at high pH, 406
 Cluster formation in the adsorbed state, 195
 Colloids, protective, in cancer, 187
 Complex ions, formation in copper (II) salt solutions containing chloride ions, 111
 Contact angles, relation to adsorption on solid surfaces, 120
 Crystal, definition of, 95, 425
 Cupric salt solutions, complex-ion formation in, 111
- Densities of liquids, effect of change in temperature on, 80
 Detergent-egg albumin complex, 12
 Diffusion of large molecules, 237
- Egg albumin-detergent complex, 12
 Electrochemistry of baths of fused aluminum halides. III, 259; IV, 268
- Electrodes, membrane, uses and limitations of, 67
 Electrokinetics. XXVI, 1
 Electroviscosity data for β -lactoglobulin systems, 1
 Ergot, separation from rye, 203
 Ethylene, oxidation to ethylene oxide, 290
 oxide, preparation from ethylene by catalytic oxidation, 290
- Flotation, physical chemistry of. X, 203
 Foam formation in organic liquids, 141
 stability of soap solutions, 280
 Force constant, relation to interatomic distance of a diatomic linkage, 295
- Gases, viscosity of, variation with temperature, 23
- Ions, microscopic, relative free energies and dissociation constants of, 101
 Iron compounds, cathodic and anodic deposits of, 21
- β -Lactoglobulin systems, electroviscosity effect in, 1
 Laurylsulfonic acid, migration data for, 62
 Light, absorption in soap solutions, 89
 Linkage, diatomic, relation of force constant to interatomic distance of, 295
 Liquids, densities of, changes with temperature, 80
 organic, formation of foam in, 141
- Magnesium selenate-selenic acid-water system, 174
 tungstate phosphor, 303
 Membrane electrodes, uses of, 67
 Metals, molten, distribution equilibria with molten salts, 159
 Methyl iodide, reaction with silver perchlorate, kinetics of, 224
 Molecules, large, diffusion of, 237
- Oil, separation from the surface of water, 173
 Oleic acid, separation from stearic acid by adsorption analysis, 179
- Particle-size distribution, determination by centrifugal sedimentation, 246
 Phase transitions in the adsorbed state, 195
 Phosphor, magnesium tungstate, 303

- Rare earths, hydrous hydroxides of, precipitation of, electrometric study of, 395
hydrous oxides of, precipitation of, electrometric study of, 395
Rye, separation of ergot from, 203
- Salts, molten, distribution equilibria with molten metals, 159
- Sedimentation, centrifugal, in determination of particle-size distribution, 246
- Silver perchlorate, reaction with methyl iodide, kinetics of, 224
- Soap solutions, absorption of light in, 89
solutions, foam stability of, 280
- Soaps of pure fatty acids, foam stability of solutions of, 280
- Sodium alcohol sulfates, minima in surface tension-concentration curves of solutions of, 57
palmitate, preparation of single crystals of, 154
stearate, preparation of single crystals of, 154
- Stearic acid, separation from oleic acid by adsorption analysis, 179
- Sulfamates, aqueous solutions of, viscosity of, 165
- Sulfamic acid, aqueous solutions of, viscosity of, 165
- Suspensions, structural, rigidity of, 410
structural, viscosity of, 410
- System acetic acid-*p*-toluidine, 85
benzene-butyl alcohol-water, 241
calcium oxide-aluminum oxide-calcium sulfate-potassium oxide-water, 356
calcium oxide-aluminum oxide-calcium sulfate-sodium oxide-water, 379
calcium oxide-aluminum oxide-calcium sulfate-water, 311
magnesium selenate-selenic acid-water at 30°C., 174
- Trichloroethylene, heat of vaporization of, 47
vapor pressure of, 47
- Vapors, viscosity of, variation with temperature, 23
- Viscosity, mixture law for, 76
of gases, variation with temperature, 23

AUTHOR INDEX

- ANTONOFF, GEORGE. On the definition of a crystal, 95
 Densities of liquids and their temperature changes, 80
 On the separation of oil from the surface of water, 173
 On some compounds of iron deposited on both poles simultaneously, 21
- BRIGGS, D. R., AND HANIG, MARTIN. Electrokinetics. XXVI. The electroviscous effect. III. In β -lactoglobulin systems. An interpretation of the meaning of K_F values obtained from electroviscosity data, 1
- BROWN, CALLAWAY. Particle-size distributions by centrifugal sedimentation, 246
- CASSEL, HANS M. Cluster formation and phase transitions in the adsorbed state, 195
- CUPPLES, H. L. Note on Antonoff's so-called rule, 75
- DAMERELL, V. R., AND MATTSO, RAYMOND. Effect of surface-active agents upon dispersions of calcium carbonate in xylene, 134
- AND URBANIC, A. A study of the colloidal system carbon dispersed in xylene, 125
- DE BRETTEVILLE, A., JR., AND RYER, F. V. A method of growing single crystals of sodium stearate and sodium palmitate, 154
- DUTTON, HERBERT J. Adsorption analysis of colorless compounds: method and application to the resolution of stearic and oleic acids, 179
- FONDA, GORTON R. The magnesium tungstate phosphor, 303
- FOX, WILLIAM. On Harkins' "final spreading coefficient" and Antonoff's rule, 158
- FURUKAWA, H., AND KING, G. BROOKS. The system magnesium selenate-selenic acid-water at 30°C., 174
- HANIG, MARTIN. See Briggs, D. R.
- HEYMANN, E., MARTIN, R. J. L., AND MULLICAHY, M. F. R. Note on the interpretation of distribution equilibria between molten metals and molten salts, 159
- HILL, TERRELL L. Relative free energies and dissociation constants of microscopic ions, 101
- IREDALE, T. See Redies, M. F.
- JONES, F. E. The quaternary system $\text{CaO}-\text{Al}_2\text{O}_3-\text{CaSO}_4-\text{H}_2\text{O}$ at 25°C. Equilibria with crystalline $\text{Al}_2\text{O}_3 \cdot 3\text{H}_2\text{O}$, alumina gel, and solid solution, 311
 The quinary system $\text{CaO}-\text{Al}_2\text{O}_3-\text{CaSO}_4-\text{Na}_2\text{O}-\text{H}_2\text{O}$ (1 per cent NaOH) at 25°C., 379
 The quinary system $\text{CaO}-\text{Al}_2\text{O}_3-\text{CaSO}_4-\text{K}_2\text{O}-\text{H}_2\text{O}$ (1 per cent KOH) at 25°C., 356
- KING, E. GRAY. Foam formation in organic liquids, 141
- KING, G. BROOKS. See Furukawa, H.
- KOLTHOFF, I. M. The Lewis and the Brönsted-Lowry definitions of acids and bases, 51
- KOOB, ROBERT P. See Lucasse, Walter W.
- KOTTLER, F. The mixture law for viscosity, 76
- KREMERS, HOWARD E. See Moeller, Therald
- LICHT, WILLIAM, JR., AND STECHERT, DIETRICH G. The variation of the viscosity of gases and vapors with temperature, 23
- LIVINGSTON, H. K. Contact angles and adsorption on solid surfaces, 120
- LUCASSE, WALTER W., KOOB, ROBERT P., AND MILLER, JOHN G. The solid-liquid phase equilibria of the system *p*-toluidine-acetic acid, 85
- MARSHALL, C. E. The uses and limitations of membrane electrodes, 67
- MARTIN, R. J. L. See Heymann, E.
- MATTSO, RAYMOND. See Damerell, V. R.
- MCBAIN, M. E. LAING. Absorption of light in soap solutions, 89
 Diffusion of the lower alkyl sulfonic acids and some large molecules, 237
- MCDONALD, HUGH J. The vapor pressure and heat of vaporization of trichloroethylene, 47

- MILES, GILBERT D., AND ROSS, JOHN. Foam stability of solutions of soaps of pure fatty acids, 280
- AND SHEDLOVSKY, LEO. Minima in surface tension-concentration curves of solutions of sodium alcohol sulfates, 57
- MILLER, JOHN G. *See* Lucasse, Walter W.
- MOELLER, THERALD. An application of the method of continuous variations to complex-ion formation in copper (II) salt solutions containing chloride ion, 111
- AND KREMERS, HOWARD E. Observations on the rare earths. LI. An electro-metric study of the precipitation of trivalent hydrous rare earth oxides or hydroxides, 395
- MULCAHY, M. F. R. *See* Heymann, E.
- MUNRO, L. A. Protective colloids in cancer, 187
- NELSON, RAYMOND, AND WALTON, HAROLD F. Cation exchange at high pH, 406
- OPPENHEIMER, HANS. *See* Reyerson, L. H.
- PALMER, K. J. The structure of an egg albumin-detergent complex, 12
- PLANTE, ENID C., AND SUTHERLAND, K. L. The physical chemistry of flotation. X. The separation of ergot from rye, 203
- REDIES, M. F., AND IREDALE, T. The kinetics of the reaction between silver perchlorate and methyl iodide, 224
- REYERSON, L. H., AND OPPENHEIMER, HANS. The catalytic oxidation of ethylene to ethylene oxide, 290
- ROLLER, PAUL S., AND STODDARD, C. KERBY. Viscosity and rigidity of structural suspensions, 410
- ROSS, JOHN. *See* Miles, Gilbert D.
- RYER, F. V. *See* de Bretteville, A., Jr.
- SCHMELZLE, A. F., AND WESTFALL, J. E. The relative viscosity of aqueous solutions of sulfamic acid and of some of its salts at 25°C., 165
- SHEDLOVSKY, LEO. *See* Miles, Gilbert D.
- SHUMAN, A. C. On the definition of a crystal, 425
- SMITH, GRANT W. The measurement of boundary tension by the pendent-drop method. II. Hydrocarbons, 168
- STECHELT, DIETRICH G. *See* Licht, William, Jr.
- STODDARD, C. Kerby. *See* Roller, Paul S.
- STRANDSKOV, CARL V. *See* Washburn, E. Roger
- SUTHERLAND, K. L. *See* Plante, Enid C.
- URBANIC, A. *See* Damerell, V. R.
- VAN RYSELBERGHE, PIERRE. Discussion and interpretation of the migration data of laurylsulfonic acid in aqueous solution, 62
- VERDIECK, RALPH G., AND YNTEMA, L. F. The electrochemistry of baths of fused aluminum halides. IV, 268
- WALTON, HAROLD F. *See* Nelson, Raymond
- WASHBURN, E. ROGER, AND STRANDSKOV, CARL V. The ternary system *n*-butyl alcohol-benzene-water at 25°C. and 35°C., 241
- WEHRMANN, RALPH, AND YNTEMA, L. F. The electrochemistry of baths of fused aluminum halides. III. Bromide baths, 259
- WESTFALL, J. E. *See* Schmelzle, A. F.
- WU, C. K., AND YANG, CHANG-TSING. The relation between the force constant and the interatomic distance of a diatomic linkage, 295
- YANG, CHANG-TSING. *See* Wu, C. K.
- YNTEMA, L. F. *See* Verdieck, Ralph G.
See Wehrmann, Ralph

INDEX TO NEW BOOKS

- ABRAMSON, HAROLD A., MOYER, LAURENCE S., AND GORIN, MANUEL H. *Electrophoresis of Proteins and the Chemistry of Cell Surfaces*, 161
- Abridged Scientific Publications from the Kodak Research Laboratories, 231
- BARNES, R. B., GORE, R. C., LIDDELL, U., AND WILLIAMS, V. Z. *Infrared Spectroscopy: Industrial Applications and Bibliography*, 428
- BAWDEN, F. C. *Plant Viruses and Virus Diseases*, 426
- BULL, HENRY B. *Physical Biochemistry*, 100
- COURANT, R., AND HILBERT, D. *Methoden der mathematischen Physik*, 162
- CREIGHTON, H. JERMAIN. *Principles and Applications of Electrochemistry. Volume I. Principles*, 233
- EPHRAIM, F. A *Textbook of Inorganic Chemistry* (English edition by P. C. L. Thorne and E. R. Roberts), 307
- GORE, R. C. *See Barnes, R. B.*
- GORIN, MANUEL H. *See Abramson, Harold A.*
- HARNED, HERBERT S., AND OWEN, BENTON B. *The Physical Chemistry of Electrolytic Solutions*, 231
- HARRIS, MILTON, AND MACK, H. (Editors). *Natural and Synthetic Fibers*, 309
- HILBERT, D. *See Courant, R.*
- HOUGEN, OLAF A., AND WATSON, KENNETH M. *Chemical Process Principles. Part One: Material and Energy Balances*, 232
- JACOBS, MORRIS B. *War Gases: Their Identification and Decontamination*, 66
- KOEHLER, W. A. *Principles and Applications of Electrochemistry. Volume II. Applications*, 233
- KOLTHOFF, I. M., AND SANDELL, E. B. *Textbook of Quantitative Inorganic Analysis*, 98
- AND STENGER, V. A. *Volumetric Analysis*, 97
- LANGE, NORBERT ADOLPH (Editor). *Lange's Handbook of Chemistry*, 308
- LIDDELL, U. *See Barnes, R. B.*
- MACK, H. *See Harris, Milton*
- MONDOLFO, LUCIO F. *Metallography of Aluminum Alloys*, 98
- MOYER, LAURENCE S. *See Abramson, Harold A.*
- NORD, F. F., AND WERKMAN, C. H. (Editors) *Advances in Enzymology and Related Subjects of Biochemistry, Vol. III*, 96
- OWEN, BENTON B. *See Harned, Herbert S.*
- Papers Presented at the Second Conference on the Corrosion of Metals, 99
- POWERS, PAUL O. *Synthetic Resins and Rubbers*, 232
- PRINGSHEIM, PETER, AND VOGEL, MARCEL. *Luminescence of Liquids and Solids and its Practical Applications*, 163
- REED, CHARLES ELI. *Chemical Engineering*, 231
- RUSSELL, HORACE, JR. *See Yost, Don M.*
- SANDELL, E. B. *See Kolthoff, I. M.*
- SCHOENGOLD, MORRIS D. *Encyclopedia of Substitutes and Synthetics*, 66
- SELWOOD, P. W. *Magnetochemistry*, 234
- STENGER, V. A. *See Kolthoff, I. M.*
- STRANATHAN, J. D. *The "Particles" of Modern Physics*, 99
- THOMPSON, MAURICE DE KAY. *The Total and Free Energies of Formation of the Oxides of Thirty-two Metals*, 309
- VOGEL, MARCEL. *See Pringsheim, Peter*
- WATSON, KENNETH M. *See Hougen, Olaf A.*
- WERKMAN, C. H. *See Nord, F. F.*
- WILLIAMS, V. Z. *See Barnes, R. B.*
- YOST, DON M., AND RUSSELL, HORACE, JR. *Systematic Inorganic Chemistry of the Fifth- and Sixth-Group Nonmetallic Elements*, 426

L. A. R. L. 75.

INDIAN AGRICULTURAL RESEARCH
INSTITUTE LIBRARY,
NEW DELHI.

[illegible]

MGIPC-S5-38 AR/54-7.7.54-7,000.